NON-INVASIVE ASSESSMENT OF THE TEAR FILM AND THE OCULAR SURFACE: EFFECT OF CONTACT LENSES

Programa de Doctorado en Optometría y Ciencias de la Visión

Doctorando:

José Vicente García Marqués

Directores:

Alejandro Cerviño Expósito

Santiago García Lázaro

Valencia, Junio de 2022

NON-INVASIVE ASSESSMENT OF THE TEAR FILM AND THE OCULAR SURFACE: EFFECT OF CONTACT LENSES

Memoria presentada por

JOSÉ VICENTE GARCÍA MARQUÉS

para optar al grado de

DOCTOR en OPTOMETRÍA Y CIENCIAS DE LA VISIÓN

2022

La investigación que dio lugar a la escritura de esta tesis fue financiada mediante un contrato FPI predoctoral del programa “Atracció de Talent” de la Universidad de Valencia concedido a José Vicente García Marqués (UV-INV_PREDOC18F2-886420).

VNIVERSITAT DE VALÈNCIA

DECLARACIÓN

Ninguna parte de este trabajo ha sido presentada para optar a ningún otro grado ni titulación, ni en esta ni en otra universidad o institución educativa o de investigación.

El Prof. Alejandro Cerviño Expósito, Catedrático de la Universidad de Valencia y el Dr. Santiago García Lázaro, Profesor Titular de la Universidad de Valencia

CERTIFICAN que la presente memoria "NON-INVASIVE ASSESSMENT OF THE TEAR FILM AND THE OCULAR SURFACE: EFFECT OF CONTACT LENSES" resume el trabajo de investigación de D. José Vicente García Marqués, bajo su dirección y supervisión, y constituye su Tesis Doctoral para optar al Grado de Doctor en Optometría y Ciencias de la Visión.

Y para que así conste, y en cumplimiento de la legislación vigente, firman el presente certificado en Valencia, a mayo de dos mil veintidós.

Fdo. Alejandro Cerviño Expósito Fdo. Santiago García Lázaro

A mis padres,

Carmen y Quino

A mis abuelos,

Salva, Visantico, Carmen e Isabel

“The only way to do great work is to love what you do”

Steve Jobs

“In order to succeed, your desire for success should be greater than your fear of failure”

Bill Cosby

“Believe you can and you're halfway there”

Theodore Roosevelt

“Success is the sum of small efforts, repeated day in and day out”

Robert Collier

“Move out of your comfort zone. You can only grow if you are willing to feel awkward and uncomfortable when you try something new “

Brian Tracy

AGRADECIMIENTOS

Después de mucho trabajo y esfuerzo elaborando la presente tesis doctoral, debo agradecer a todas las personas que de una manera u otra han estado apoyándome en este bonito y duro camino.

En primer lugar, me gustaría dar las gracias a mis directores de tesis Alejandro Cerviño Expósito y Santiago García Lázaro. Por vuestros consejos y por haberme guiado y apoyado a lo largo de estos años. Gracias también por darme la oportunidad de formar parte de este gran equipo. Siempre estaré agradecido.

Al Profesor Robert Montés Micó porque gracias a él empecé esta andadura y decidí adentrarme en el mundo de la investigación. Gracias por creer en mí desde los inicios, cuando estudiaba el grado, y apoyarme siempre que he necesitado cualquier cosa.

A mis compañeros de viaje del Grupo de Investigación en Optometría: Noelia, Cristian, Dani, Edouard, Izabela, Vicent y Teresa. Sois unas personas maravillosas y habéis sido un gran apoyo para mí. En especial me gustaría dar las gracias a Dani por las innumerables horas ayudándome con Matlab, has sido un pilar fundamental en la elaboración de la presente tesis doctoral. Gracias, amigo.

A Noelia y a Cristian por formar el mejor equipo de compañeros que me podría haber tocado. Más que compañeros, sois amigos. Hemos trabajado duro, nos hemos ayudado mutuamente, nos hemos reído, hemos aguantado buenos y no tan buenos

momentos, y siempre hemos estado apoyándonos. Gracias por vuestra infinita ayuda a lo largo de estos años.

A José Manuel González Méijome y todo el equipo del CEORLab de la Universidade do Minho. Sois todos unas increíbles personas y no pude tener más suerte conociéndoos en la estancia. Gracias por integrarme tan bien en vuestro equipo y darme la oportunidad de formar parte de él en las dos estancias que realicé, las cuales me hicieron enamorarme de Portugal y de sus bellísimas personas. El trabajo realizado allí, claramente ha enriquecido esta tesis doctoral y mi estancia allí me ha enriquecido a mí como persona. Millones de gracias, José Manuel, por el trabajo realizado, por transmitirme tu pasión por la investigación y por apoyarme en todo.

A María José Luque y José Juan Esteve, por siempre estar dispuestos a ayudarme desinteresadamente cuando he tenido cualquier duda. Y en general a todos los compañeros de la universidad que en algún momento me han brindado una sonrisa por los pasillos, con los ojos en estos últimos años de pandemia, o se han preocupado por cómo llevaba la tesis.

A Carlos, por tu apoyo en la recta final de esta tesis. A mis amigas y amigos, tanto de mi pueblo como los que conocí en Portugal, por ayudarme a desconectar del trabajo, lo cual es muy necesario. Por preguntarme por mis estudios, animarme a seguir adelante, por aguantar mis explicaciones sin entender muy bien de qué estaba hablando, y por estar presentes en los buenos y malos momentos. Habéis sido un gran apoyo todos y cada uno de vosotros. Poca gente puede decir que tiene unos amigos tan buenos como los míos. Somos afortunados. No hace falta nombraros, sabéis quienes sois.

También me gustaría agradecer a todas las personas que me han “prestado” sus ojos para hacer las medidas de la presente tesis doctoral. Gracias por vuestro tiempo y paciencia.

Para terminar, gracias a mi familia. En especial a mis padres Carmen y Quino, por apoyarme siempre, educarme, cuidarme, hacerme creer que podía con todo, por inculcarme que con trabajo, esfuerzo y creyendo en lo que hago puedo conseguir todo lo que me proponga en la vida. Sois un gran ejemplo a seguir para mí. Os quiero muchísimo. Y a ti, mamá, ojalá algún día llegar a ser la mitad de buena persona y buen profesional que tú eres. Eres mi patrón a seguir. También mencionar a mi hermano Julián, gracias por todo. Y a mis abuelos Salva, Visantico, Carmen e Isabel por siempre creer en mí y por vuestro apoyo incondicional. Os quiero. Gracias abuelo Salva porqué sé que me has guiado en innumerables ocasiones a lo largo de esta aventura.

La elaboración de la presente tesis no ha sido un camino de rosas, no obstante ha sido una experiencia bonita y única de superación personal, que me ha hecho crecer tanto personal como profesionalmente, de la cual me siento muy orgulloso y feliz por el resultado obtenido. Este mérito no es solo mío, es también de todos y cada uno de vosotros.

INDEX OF CONTENTS

RESUMEN

RESUMEN

El diagnóstico y tratamiento del síndrome del ojo seco es un reto debido al carácter multifactorial de la enfermedad y la falta de un test clínico "gold standard". Además, la falta de correlación entre los signos y síntomas de la enfermedad del ojo seco, la falta de correlación entre métricas, su baja repetibilidad, su carácter invasivo y su relativa objetividad dificulta el estudio de la película lagrimal y el diagnóstico de la enfermedad del ojo seco.

En el *Capítulo 1* del presente trabajo se describen las características principales de la película lagrimal y la enfermedad del ojo seco, y se realiza una revisión bibliográfica sobre técnicas no invasivas de análisis de la película lagrimal y la superficie ocular. Las técnicas de imagen no invasivas tienen un alto potencial a explotar en el estudio de la película lagrimal y del síndrome del ojo seco. El análisis no invasivo de la superficie ocular permite a los clínicos evaluarla bajo condiciones más naturales, evitando el lagrimeo reflejo y la desestabilización de la película lagrimal. Generalmente, estas técnicas son más precisas, repetibles y objetivas que las invasivas. Por lo tanto, técnicas no invasivas deberían ser consideradas para evaluar la película lagrimal y la superficie ocular frente a técnicas invasivas para conseguir una mayor capacidad diagnóstica y manejo de los pacientes con sequedad ocular.

Aunque existen muchas técnicas de imagen de análisis de la película lagrimal, este es todavía un campo de estudio que necesita más investigación y que tiene un alto potencial para ser explorado. Por lo tanto, es necesario el desarrollo de nuevos métodos no invasivos y objetivos para evaluar la película lagrimal, siendo necesarios

más estudios para mejorar la correlación de estas métricas con hallazgos clínicos en pacientes con sequedad ocular.

El *Capítulo 2* está enfocado en la justificación y objetivos de la presente tesis doctoral. Debido a la incidencia y morbilidad a la alza del síndrome del ojo seco, es de vital importancia mejorar el diagnóstico temprano de esta patología para proporcionar un mejor tratamiento de la enfermedad. El diagnóstico de la enfermedad del ojo seco es todavía un reto y son necesarias pruebas clínicas objetivas con buena sensibilidad y especificidad, repetibilidad, que sean fáciles de realizar y adecuadas para la práctica clínica. Por lo tanto, nuevas métricas objetivas son todavía requeridas para proporcionar nuevos hallazgos en el análisis de la película lagrimal. Así, el Tear Film and Ocular Surface Society Dry Eye Workshop II Diagnostic Methodology Report reconoció la necesidad de desarrollar nuevas métricas no invasivas, objetivas y tan automáticas como sea posible para evaluar la película lagrimal y la superficie ocular.

La presente tesis doctoral tiene como objetivo 1) Estudiar los factores de riesgo de la enfermedad del ojo seco, la repetibilidad de algunas métricas actuales de análisis de la superficie ocular, y la eficacia de la aplicación de bolsas térmicas; 2) Desarrollar y validar nuevas métricas para evaluar la superficie ocular y la película lagrimal de una manera no invasiva y tan objetiva como sea posible; y 3) evaluar el efecto de diferentes lentes de contacto, lágrima artificial, parpadeos y el uso del ordenador en la superficie ocular y en las métricas desarrolladas en la presente tesis doctoral.

El *Capítulo 3* describe la metodología general de los estudios realizados en la presente tesis doctoral. La superficie ocular y la película lagrimal fueron analizadas

mediante diferentes dispositivos: El Keratograph 5M, el osmolarímetro TearLab, el aberrómetro IRX3, el Medmont E 300, el Cobra fundus camera y el Light Disturbance Analyzer. Además, los síntomas oculares fueron evaluados mediante los cuestionarios Ocular Surface Disease Index y el 5-item Dry Ey Questionnaire. Diferentes métricas no invasivas basadas en el procesamiento de imágenes fueron desarrolladas mediante Matlab© R2018a. Finalmente, estas nuevas métricas fueron aplicadas a sujetos adaptados con lentes de contacto.

En el *Capítulo 4* se estudiaron los factores de riesgos sistémicos, ambientales y del estilo de vida de la enfermedad del ojo seco, debido a la influencia del carácter etiológico multifactorial de la enfermedad en su diagnóstico. Este es un estudio transversal en 120 participantes caucásicos con edades comprendidas entre 18 y 89 años (47.0 ± 22.8 años). Diferentes variables fueron obtenidas en una única sesión clínica: historia médica, información sobre las condiciones ambientales y el estilo de vida, el cuestionario Ocular Surface Disease Index, el cuestionario 5-item Dry Eye Questionnaire, el tiempo de ruptura lagrimal no invasivo, la osmolaridad y la tinción de la superficie ocular. El diagnóstico de la enferemedad del ojo seco se llevó a cabo de acuerdo con el criterio descrito por el Tear Film and Ocular Surface Society Dry Eye Workshop II Diagnostic Methodology Report. Un modelo de regresión logística multivariado fue construido incluyendo las variables con un p-valor inferior a 0.15 en el análisis univariado.

Se obtuvo una prevalencia de 57.7 % para la enfermedad del ojo seco. No se encontraron diferencias en la edad entre aquellos sujetos sanos y con el síndrome del ojo seco ($p = 0.243$). Sin embargo, el grupo con la enfermedad del ojo seco tenía más

mujeres (p = 0.008). La regresión logística univariada identificó los siguientes parámetros como potenciales factores de riesgo para la enfermedad del ojo seco: Sexo femenino, horas de sueño al día, menopausia, ansiedad, enfermedades sistémicas reumatológicas, ansiolíticos, tomar medicación diariamente, cirugía ocular, dieta de pobre calidad, ingerir una cantidad mayor de ultraprocesados en la dieta, no beber café y horas de exposición al aire acondicionado por día. La regresión logística multivariada reveló que las horas de sueño al día, la menopausia y el uso de ansiolíticos estaban independientemente asociados con la enfermedad del ojo seco ($p \leq 0.026$). Para concluir, la enfermedad del ojo seco está asociada con factores de riesgos sistémicos, ambientales y del estilo de vida. Estos hallazgos son útiles para identificar potenciales factores de riesgo modificables, en conjunto con los tratamientos convenciones para la enfermedad del ojo seco.

Debido a la relevancia del tiempo de ruptura lagrimal no invasivo en el diagnóstico de la enfermedad del ojo seco, el *Capítulo 5* tiene como objetivo evaluar la repetibilidad intraexaminador del tiempo de ruptura lagrimal no invasivo utilizando el Oculus Keratograph 5M, el cual es una de las herramientas más utilizadas para la evaluación objetiva de la película lagrimal. 80 sujetos sanos con edades comprendidas entre 30 y 89 años participaron en el presente estudio. Las medidas fueron clasificadas de acuerdo con la edad, el sexo y la presencia o no de síndrome del ojo seco. La repetibilidad de las medidas fue evaluada a través de la desviación estándar entre las medidas en cada sujeto, el coeficiente de repetibilidad y el coeficiente de variación. Además, el método de regresión Passing-Bablok fue aplicado. Los coeficientes de repetibilidad mostraron una baja repetibilidad en las medidas de todos los grupos, con

valores entre 3.57 y 7.14; 9.90 y 19.79; y 51.90 y 65.49, para cada coeficiente, respectivamente. No se encontraron diferencias estadísticamente significativas en el tiempo de ruptura lagrimal no invasivo entre los sujetos sanos y con la enfermedad del ojo seco ($p = 0.188$). Los grupos con más riesgo de desarrollar sequedad ocular tenían una mejor repetibilidad. La regresión Passing-Bablok también confirmó una falta de acuerdo entre el valor máximo y mínimo del tiempo de ruptura lagrimal no invasivo. Para concluir, el tiempo de ruptura lagrimal no invasivo tiene una baja repetibilidad intraexaminador incluso considerando el sexo, la edad o el diagnóstico del ojo seco. Sin embargo, no solo esta baja repetibilidad es debida al dispositivo, sino que también es debida a la variabilidad intrínseca de la película lagrimal.

Debido al hecho de que el enrojecimiento ocular es un importante signo a tener en cuenta en algunas enfermedades inflamatorias y a la relación entre el enrojecimiento ocular y la enfermedad del ojo seco, el *Capítulo 6* tiene como objetivo evaluar la repetibilidad intraexaminador de las medidas de enrojecimiento de la superficie ocular obtenidas mediante el Oculus Keratograph 5M. Setenta y ocho ojos derechos de 78 voluntarios sanos con edades comprendidas entre 18 y 79 años participaron en el presente estudio. El enrojecimiento de la conjuntiva bulbar fue medido tres veces consecutivas en el mismo ojo. El enrojecimiento fue clasificado automáticamente por el dispositivo dependiendo de la zona evaluada: temporal bulbar, nasal bulbar, temporal limbal, nasal limbal y total. La repetibilidad fue evaluada para cada métrica a través del cálculo de la desviación estándar entre las medidas en cada sujeto, el coeficiente de repetibilidad y el coeficiente de variación. Además, el

método de regresión Passing-Bablok fue aplicado. Un p-valor inferior a 0.05 fue definido como estadísticamente significativo.

Los coeficientes de repetibilidad revelaron una repetibilidad aceptable en todas las métricas. El método de regresión Passing-Bablok también confirmó el buen grado de acuerdo entre la medida máxima y mínima de enrojecimiento bulbar para cada métrica. La repetibilidad más alta fue conseguida en el enrojecimiento bulbar total con una pendiente de 1; por lo tanto, solo errores sistemáticos causados por el intercepto podrían alterar los resultados. En el resto de las métricas, la repetibilidad fue peor cuando el enrojecimiento ocular era mayor pero, incluso en estos casos, la repetibilidad fue aceptable. El análisis de Friedman mostró diferencias estadísticamente significativas entre la tercera medida y las primeras dos, siendo la tercera ligeramente más elevada. Sin embargo, estas diferencias no pueden considerarse clínicamente significativas. Finalmente, las medidas bulbares obtuvieron valores clínicamente más elevados que las limbales; el enrojecimiento bulbar total fue clínicamente más elevado que los valores limbales; y los valores nasales fueron clínicamente mayores que los temporales. Como conclusión se obtuvo que el Keratograph 5M es un dispositivo útil y repetible para evaluar el enrojecimiento ocular. Todas las medidas proporcionaron valores objetivos con una repetibilidad aceptable, lo cual podría ayudar a los clínicos en el diagnóstico y tratamiento de diferentes patologías relacionadas con la inflamación de la superficie ocular, como el síndrome del ojo seco o la uveítis.

Debido a que el Keratograph 5M es una de las herramientas más utilizadas para la evaluación objetiva de la superficie ocular, conocer su utilidad en el seguimiento de

algunos tratamientos es relevante. Por lo tanto, el *Capítulo 7* tiene como objetivo evaluar la asociación entre la aplicación de las bolsas térmicas MGDRx EyeBags y los signos y síntomas de la superficie ocular en sujetos jóvenes y mayores. Treinta voluntarios jóvenes con edades comprendidas entre 18 y 31 años (23.95 ± 3.94 años) y treinta sujetos mayores con edades comprendidas entre 61 y 90 años (77.97 ± 8.11 años) participaron en este estudio. Distintos parámetros de la superficie ocular fueron evaluados mediante el Oculus Keratograph 5M, siguiendo las recomendaciones del Tear Film and Ocular Surface Dry Eye Workshop II Diagnostic Methodology Report. Solo los sujetos que tenían una puntuación positiva en uno de los cuestionarios y el tiempo de ruptura lagrimal no invasivo inferior a 10 segundos fueron incluidos en el estudio. Después de la aplicación de las bolsas térmicas en ambos ojos, diariamente y durante dos semanas, el protocolo fue realizado de nuevo. Los sujetos fueron instruidos a realizar un masaje palpebral inmediatamente después de la aplicación de las bolsas térmicas. El grado de cumplimiento del tratamiento y el grado de mejora fueron también evaluados.

El grupo joven mostró una mejora del tiempo de ruptura lagrimal no invasivo, la capa lipídica, el porcentaje de pérdida de las glándulas de meibomio en el párpado superior y en los síntomas de sequedad ocular durante las dos semanas de tratamiento. Mejoras en la calidad del meibum, la obstrucción de las glándulas, la puntuación de telangiectasias, y en los síntomas de ojo seco fueron encontradas en el grupo de mayor edad. El ANOVA mixto reveló mejor tiempo de ruptura lagrimal no invasivo y capa lipídica en los sujetos jóvenes. A pesar de que el cumplimiento del tratamiento fue mayor en los sujetos mayores que en los jóvenes ($p = 0.002$), no se

encontraron diferencias estadísticamente significativas en la mejora subjetiva entre grupos (p = 0.097). Para concluir, los síntomas de sequedad ocular mejoraron después de la aplicación de las bolsas térmicas, mientras que el tiempo de ruptura lagrimal no invasivo y la capa lipídica mejoraron solo en el grupo de sujetos jóvenes.

El Tear Film and Ocular Surface Dry Eye Workshop II Diagnostic Methodology Report reconoció la necesidad de desarrollar nuevas métrica no invasivas y tan objetivas como sea posible para evaluar la película lagrimal y la superficie ocular. Por ello, el *Capítulo 8* está enfocado en el desarrollo de nuevas métricas para evaluar la película lagrimal y la superficie ocular de una forma no invasiva y objetiva. En la primera parte de este capítulo (*Capítulo 8.1*) se desarrolla un método para evaluar la visibilidad de las glándulas de meibomio a partir del análisis de los valores de intensidad de gris de los píxeles de las meibografías obtenidas a través de meibografía infrarroja de no contacto. El *Capítulo 8.1.1* tiene como objetivo desarrollar este nuevo método semiautomático para analizar la visibilidad de las glándulas de meibomio cuantitativamente. 112 voluntarios sanos con edades comprendidas entre 18 y 90 años (48.3 ± 27.5 años) participaron en el presente estudio. Las meibografías fueron obtenidas del párpado superior de los sujetos mediante el Oculus Keratograph 5M y se clasificaron en 3 grupos: Grupo 1 = Sujetos con buena visibilidad subjetiva de las glándulas y una pérdida de las glándulas < 1/3 del área total de las glándulas de meibomio; Grupo 2 = Sujetos con baja visibilidad subjetiva de las glándulas y una pérdida de las glándulas < 1/3 del área total de las glándulas de meibomio; y Grupo 3 = Sujetos con baja visibilidad subjetiva de las glándulas y una pérdida de las glándulas > 1/3 del área total de las glándulas de meibomio. Las nuevas métricas basadas en la

visibilidad de las glándulas de meibomio fueron calculadas y posteriormente comparadas entre grupos. Correlaciones de Rho Spearman fueron utilizadas para evaluar las correlaciones entre cada métrica y el porcentaje de pérdida de las glándulas de meibomio con la muestra completa y después de excluir el grupo 2. Un p-valor inferior a 0.05 fue definido como estadísticamente significativo.

Cincuenta y seis sujetos fueron clasificados en el grupo 1 (24.5 ± 9.6 años), 19 en el grupo 2 (69.2 ± 21.3 años) y 37 en el grupo 3 (73.6 ± 13.7 años). No se encontraron diferencias estadísticamente significativas entre el grupo 1 y el 2 en el porcentaje de pérdida de glándulas de meibomio. Todas las métricas, excepto la entropía, mostraron una visibilidad mayor de las glándulas de meibomio en el grupo 1 que en los otros dos grupos. Se encontraron correlaciones moderadas estadísticamente significativas para todas las métricas, con excepción de la entropía. Las correlaciones fueron más fuertes después de excluir el grupo 2 del análisis. Como conclusión se obtuvo que el método propuesto es útil para evaluar la visibilidad de las glándulas de meibomio de una forma objetiva y repetible, lo cual podría ayudar a los clínicos a mejorar el diagnóstico de la disfunción de las glándulas de meibomio y el seguimiento de sus tratamientos.

En el *Capítulo 8.1.2*, se analiza la capacidad diagnóstica de estas nuevas métricas relacionadas con la visibilidad de las glándulas para detectar la disfunción de las glándulas de meibomio, así como sus correlaciones con otros signos clínicos y síntomas de la enfermedad el ojo seco y la disfunción de las glándulas de meibomio. 112 voluntarios sanos (48.3 ± 27.5 años) participaron en el presente estudio. Distintos parámetros de la superficie ocular fueron evaluados mediante el Oculus Keratograph 5M. Los sujetos fueron clasificados de acuerdo con la presencia o ausencia de

disfunción de las glándulas de meibomio. Las nuevas métricas basadas en la visibilidad de las glándulas de meibomio fueron calculadas y posteriormente comparadas entre grupos. La capacidad diagnóstica de distintos parámetros de la superficie ocular y de las métricas basadas en la visibilidad de las glándulas fue estudiada a través de curvas de la característica operativa del receptor. Un modelo de regresión logística fue utilizado para obtener una curva combinada de las métricas con la capacidad diagnostica más elevada.

Diferencias estadísticamente significativas fueron encontradas entre los grupos para todos los parámetros de la superficie ocular evaluados y las nuevas métricas basadas en la visibilidad de las glándulas de meibomio, excepto para el primer tiempo de ruptura lagrimal no invasivo y la expresibilidad de las glándulas. Las nuevas métricas relacionadas con la visibilidad de las glándulas mostraron una sensibilidad y especificidad superior que las métricas actuales cuando su capacidad diagnostica se evalúo sin ninguna combinación. La capacidad diagnóstica aumentó cuando las nuevas métricas desarrolladas se incorporaron a la regresión logística conjuntamente con el porcentaje de pérdida de glándulas de meibomio, la altura del menisco lagrimal, los síntomas de sequedad ocular y la puntuación de anormalidad en el margen palpebral ($p < 0.001$). La combinación de la mediana de la intensidad de los pixeles de los valores de gris de la meibografía con las métricas que se acaban de mencionar consiguió el área bajo la curva más elevada (0.99), y una excelente sensibilidad (1.00) y especificidad (0.93). Para concluir, las nuevas métricas basadas en la visibilidad de las glándulas de meibomio tienen más poder diagnóstico para la disfunción de las glándulas de meibomio que las métricas actuales y pueden servir como una

herramienta complementaria para apoyar en el diagnostico de la disfunción de las glándulas de meibomio.

En el *Capítulo 8.2*, se desarrolla un método para evaluar la propagación y la dinámica de la película lagrimal a través del seguimiento de las partículas en suspensión en la película lagrimal después del parpadeo. Se evaluaron distintos parámetros de la superficie ocular y se grabó un video de la propagación de las partículas en suspensión en la película lagrimal después de un parpadeo espontáneo en 81 voluntarios sanos (43.7 ± 27.0 años) utilizando el Oculus Keratograph 5M. El software desarrollado automáticamente descomponía el video en "frames" para posteriormente seguir la posición de las partículas manualmente durante 1.75 segundos después del parpadeo. Las siguientes métricas relacionadas con la dinámica de la película lagrimal fueron automáticamente calculadas: media, mediana, máxima y mínima velocidad de las partículas, la velocidad en diferentes intervalos de tiempo después del parpadeo y el tiempo transcurrido hasta que la velocidad de las partículas decrece hasta < 1.20 mm/segundo. La repetibilidad de cada métrica basada en la dinámica de la película lagrimal, y sus correlaciones con signos y síntomas de sequedad ocular fueron analizadas. Se realizó también una regresión logística binomial para evaluar la predictibilidad de las nuevas métricas para diferentes parámetros oculares.

La repetibilidad tendió a ser inferior justo después del parpadeo (variabilidad de 12.24 %), mientras que las métricas a partir de 0.5 segundos tenían una repetibilidad aceptables (variabilidad por debajo del 10 %). Las nuevas métricas basadas en la dinámica de la película lagrimal estaban positivamente correlacionadas con el tiempo de ruptura lagrimal no invasivo y negativamente con la pérdida de glándulas de

meibomio. La regresión logística binomial reveló que las métricas basadas en la dinámica de la película lagrimal pueden predecir el tiempo de ruptura lagrimal no invasivo. Sin embargo, no se encontró una asociación estadísticamente significativa con la pérdida de glándulas de meibomio. Esto significa que una mayor velocidad de propagación de las partículas en suspensión en la película lagrimal después del parpadeo está relacionada con un tiempo de ruptura lagrimal más largo. La métrica llamada "tiempo transcurrido hasta que la velocidad de las partículas decrece hasta < 1.20 mm/segundo" puede ser considerada la mejor métrica para evaluar la calidad de la película lagrimal, debido a que estaba más fuertemente correlacionada con el tiempo de ruptura lagrimal no invasivo ($r = 0.42$, $p = 0.004$), estaba más fuertemente asociada en la regresión logística binomial con el tiempo de ruptura lagrimal y mostró una buena repetibilidad (variabilidad = 5.49 %). Como conclusión se obtuvo que las nuevas métricas desarrolladas basadas en la dinámica de la película lagrimal son parámetros emergentes que pueden servir para evaluar la homeostasis de la película lagrimal e indirectamente evaluar la calidad de la película lagrimal en condiciones naturales con una repetibilidad aceptable.

En el *Capítulo 8.3*, se desarrolla un método para evaluar el espesor de la capa lipídica a través del análisis de los valores de intensidad de gris de los píxeles del disco de Plácido reflejado en la película lagrimal. Distintos parámetros de la superficie ocular fueron evaluados utilizando el Oculus Keratograph 5M en 94 voluntarios sanos (43.8 ± 26.8 años). La capa lipídica de los sujetos fue subjetivamente gradada en 4 grupos utilizando una escala de gradación basada en la interferometría. Las nuevas métricas basadas en la intensidad de las imágenes del disco de Plácido fueron calculadas y

comparadas entre grupos. La repetibilidad de las nuevas métricas y su capacidad diagnostica fue analizada mediante curvas de la característica operativa del receptor. El nivel de acuerdo entre la nueva herramienta objetiva desarrollada y las escalas subjetivas ya existentes fue analizado mediante la precisión, el índice Kappa y el F-measure.

La intensidad media de los píxeles, la intensidad mediana y la energía relativa 5.33 segundos después del parpadeo consiguieron el mejor rendimiento, con una correlación con el espesor de la capa lipídica entre $r = 0.655$ y 0.674 ($p < 0.001$), sensibilidad entre 0.92 y 0.94, especificidad entre 0.79 y 0.81, área bajo la curva entre 0.89 y 0.91, precisión entre 0.76 y 0.77, índice Kappa de 0.77 y F-measure entre 0.86 y 0.87. Para concluir, el análisis de los valores de intensidad de gris del disco de Plácido puede ser utilizado como una herramienta objetiva para evaluar el espesor de la capa lipídica. Estas nuevas métricas podrían ser incorporadas en una batería de tests clínicos como un método fácil, repetible, objetivo y accesible para mejorar la detección y seguimiento de la enfermedad del ojo seco y la disfunción de las glándulas de meibomio.

Debido al hecho de que las lentes de contacto impactan la homeostasis de la superficie ocular, el *Capítulo 9* está enfocado en el efecto de las lentes de contacto en la película lagrimal y la superficie ocular. En este capítulo se usan las métricas actuales y las métricas desarrolladas en la presente tesis doctoral para evaluar la película lagrimal y la superficie ocular. El *Capítulo 9.1* tiene como objetivo evaluar el efecto a corto plazo de una lente de contacto para doble foco en la película lagrimal, el rendimiento visual y la calidad óptica, en comparación con una lente de contacto

monofocal hecha del mismo material. El *Capítulo 9.1.1* está enfocado en el rendimiento visual, la calidad óptica y la distorsión lumínica a corto plazo de estas lentes de contacto. Este es un estudio aleatorio, transversal y doble ciego. 28 voluntarios sanos y miopes entre 18 y 32 años (23.5 ± 4.1 años) participaron en este estudio. El ojo dominante sensorial para la visión lejana fue evaluado. La refracción, la agudeza visual mejor corregida y las aberraciones para una pupila de 3 y 5 mm fueron medidas en la medida basal (sin lente de contacto in situ). Los sujetos fueron binocularmente adaptados en un orden aleatorio con uno de estos dos diseños de lentes de contacto: una lente de contacto de doble foco y otra monofocal, ambas hechas de omafilcon A. El cuestionario Quality of Vision, la sobrerefracción, la agudeza visual mejor corregida, la estereopsis a 40 cm, la sensibilidad al contraste mejor corregida fotópica y mesópica, la distorsión lumínica y las aberraciones fueron evaluados 25 minutos después de la inserción de la lente de contacto. Diferencias entre los grupos fueron estudiadas y un p-valor inferior a 0.05 fue definido como estadísticamente significativo.

La esfera y el cilindro medios fueron -1.36 ± 1.04 D (con un rango desde -6.00 a -0.25 D) y -0.23 ± 0.30 D (con un rango desde -0.75 a 0.00 D), respectivamente. No se encontraron diferencias estadísticamente significativas en la agudeza visual mejor corregida y la estereopsis entre la medida basal, la lente de doble foco y la monofocal. La sensibilidad al contraste fotópica y mesópica fueron inferiores en la lente de contacto de doble foco en todas las frecuencias, con la excepción de la sensibilidad al contraste mesópica en 18 ciclos por grado ($p = 0.234$). Las aberraciones de alto orden y el tamaño y la irregularidad de la distorsión lumínica fueron mayores en la lente de

contacto de doble foco ($p < 0.001$). No se encontraron diferencias estadísticamente significativas en las aberraciones de alto orden entre la medida basal y la lente monofocal in situ para ambos diámetros pupilares. El cuestionario Quality of Vision reveló valores más bajos en las puntuaciones de la frecuencia, severidad y molestia con la lente monofocal que con la de doble foco ($p < 0.001$). Para concluir, la lente de contacto de doble foco disminuyó las puntuaciones de calidad visual psicofísicas y psicométricas a corto plazo en condiciones de baja iluminación, en comparación con una lente de contacto monofocal del mismo material. Sin embargo, la agudeza visual y la estereopsis no estaban afectadas por el diseño de la lente.

La segunda parte de este capítulo (*Capítulo 9.1.2*) está enfocada en el efecto a corto plazo de estas lentes en la estabilidad de la película lagrimal pre-lente y en el confort. Este estudio aleatorio, doble ciego y transversal fue realizado en 28 voluntarios sanos y miopes con edad comprendidas entre 18 y 32 años (23.5 ± 4.1 años). Solo uno de los ojos, escogido al azar, fue evaluado. La visión de lejos y la refracción fueron evaluadas en la medida basal. Cada lente de contacto (monofocal y de doble foco) fue aleatoriamente adaptada en ambos ojos. Una escala visual analógica entre 0 y 10 fue utilizada para evaluar el confort general, el físico y el visual. El índice Tear Film Surface Quality, la área del Tear Film Surface Quality y el tiempo de ruptura lagrimal automático fueron obtenidos mediante el Medmont E 300 en la medida basal (ojo sin lente de contacto) y 25 minutos después de la inserción de cada lente.

La esfera y el cilindro de la refracción de los sujetos fue -1.36 ± 1.04 D (rango: -6.00 a -0.25 D) and -0.23 ± 0.30 D (rango: -0.75 a 0.00 D). El índice Tear Film Surface

Quality y el área del Tear Film Surface Quality fueron inferiores (película lagrimal más estable) en la medida basal que en ambas lente de contacto ($p < 0.025$). La lente de doble foco mostró una estabilidad de la película lagrimal pre-lente inferior que la lente monofocal (valores más elevados en el índice Tear Film Surface Quality y en el área del Tear Film Surface Quality). El tiempo de ruptura lagrimal automático fue más elevado en la medida basal que con cada lente de contacto, pero no mostró diferencias significativas entre ambas lentes de contacto. Las escalas visual analógicas revelaron puntuaciones estadísticamente mejores en la lente de contacto monofocal que en la de doble foco para el confort general (0.77 ± 1.14 frente a 3.12 ± 2.79), físico (0.96 ± 1.46 frente a 2.19 ± 2.45) y el visual (1.27 ± 1.66 frente a 3.92 ± 2.04). Para concluir, una ligera disminución de la estabilidad de la película lagrimal pre-lente a corto plazo fue encontrada en la lente de contacto de doble foco en comparación con una lente monofocal, potencialmente contribuyendo al deterioro del rendimiento visual y confort en la lente de contacto de doble foco.

El *Capítulo 9.2* va un paso más allá comparando la agudeza visual, la calidad óptica, la distorsión lumínica, confort y la estabilidad de la película lágrima pre-lente a corto plazo entre dos lentes de contacto prototipo de doble foco para el control de la miopía, hechas con el mismo material. El estudio tiene como objetivo evaluar si los distintos parámetros son influenciados por el diferente diseño óptico de las dos lentes de contacto de doble foco. 28 sujetos con miopía (23.49 ± 4.07 años) fueron incluidos en este estudio aleatorio, doble ciego y transversal. La refracción, la agudeza visual mejor corregida, las aberraciones y la estabilidad de la película lagrimal (Medmont E 300) fueron evaluadas en la medida basal. Los sujetos fueron binocularmente

adaptados con dos lentes de contacto de doble foco (aleatoriamente) y solo el ojo dominante sensorial fue evaluado. Las lentes tenían el mismo material con dos zonas internas de distinto diámetro: 2.1 mm (diseño S) y 4.0 mm (diseño M). El confort visual y físico, la sobrerefracción, la agudeza visual mejor corregida, la estereopsis a 40 cm, la sensibilidad al contraste fotópica y mesópica mejor corregida, el tamaño y la forma de la distorsión lumínica, las aberraciones, la calidad visual subjetiva (cuestionario Quality of Vision) y la estabilidad de la película lagrimal pre-lente fueron evaluados en ambas lentes.

Ambas lentes de contacto decrecieron la agudeza visual y la estabilidad de la película lagrimal y indujeron mayores niveles de aberraciones de alto orden en comparación con la medida basal. Sin embargo, la agudeza visual y la sensibilidad al contraste fotópica estaban dentro de los valores normales para la edad de los sujetos. Con respecto a la comparación de ambas lentes, el diseño M produjo mejor sensibilidad al contraste fotópica en la frecuencia espacial de 18 ciclos por grado ($p < 0.001$) y una menor distorsión lumínica ($p < 0.017$). Sin embargo, las aberraciones de alto orden fueron menores en el diseño S ($p = 0.015$). No se encontraron diferencias estadísticamente significativas entre las dos lentes de contacto en el cuestionario Quality of Vision y en la estabilidad de la película lagrimal pre-lente. Como conclusión se obtuvo que ambas lentes de contacto de doble foco producían un rendimiento visual aceptable en condiciones fotópicas. La lente de contacto con el diámetro central medio (4.0 mm) inducía una mejor sensibilidad al contraste en las altas frecuencias y una distorsión lumínica menor, mientras que la lente de contacto con el diámetro central más pequeño (2.1 mm) producía menores niveles de aberraciones de alto

orden para un diámetro pupilar de 5 mm. Ambas lentes de contacto producían el mismo confort visual subjetivo.

En el *Capítulo 9.3* se evalúa la distorsión lumínica relacionada con cambios en la estabilidad de la película lagrimal, con el objetivo de validar el dispositivo Light Disturbance Analyzer como una herramienta fiable y útil para evaluar cambios relacionados con la calidad óptica inducidos por la película lagrimal. Así, la distorsión lumínica, la estabilidad de la película lagrimal y las aberraciones corneales fueron evaluadas bajo diferentes condiciones: Diferentes patrones de parpadeo, con y sin lágrima artificial, y con una lente de contacto monofocal y otra de doble foco. Cuarenta voluntarios sanos y miopes con edades entre 19 y 38 años (26.6 ± 5.1 años) participaron en el presente estudio aleatorio, doble ciego y transversal. El ojo dominante sensorial para visión lejana fue evaluado. La refracción y la agudeza visual mejor corregida fueron evaluadas en la medida basal (sin lente de contacto). En la primera visita, la distorsión lumínica (evaluada con el Light Disturbance Analyzer) y la estabilidad de la película lagrimal y las aberraciones corneales (Medmont E 300) fueron medidas con diferentes patrones de parpadeo en un orden aleatorio: Parpadeo natural, parpadeo cada 6 segundos y parpadeo cada 12 segundos. Las medidas se repitieron con lágrima artificial. En la segunda visita, los sujetos fueron adaptados binocularmente con cada diseño de lente de contacto en un orden aleatorio: La lente de doble foco y la monofocal. La sobrerefracción y la agudeza visual mejor corregida fueron evaluadas 25 minutos después de la inserción de las lentes de contacto. La distorsión lumínica, la estabilidad de la película lagrimal y las aberraciones corneales

fueron estudiadas para cada lente de contacto, con cada patrón de parpadeo, con y sin lágrima artificial.

La distorsión lumínica fue mayor en el patrón de parpadeo con baja frecuencia ($p < 0.034$) cuando los sujetos estaban adaptados con las lentes de contacto debido a que ambas lentes decrecían la estabilidad de la película lagrimal ($p < 0.001$). Se observaron mejoras estadísticamente significativas en la distorsión lumínica y la estabilidad de la película lagrimal después de instilar lágrima artificial (sin lente de contacto) para el patrón de parpadeo con baja frecuencia y con ambas lentes de contacto. La lente de contacto de doble foco proporcionada una menor estabilidad de la película lagrimal ($p < 0.008$) y una mayor distorsión lumínica ($p < 0.001$) que la monofocal en todos los patrones de parpadeo. A pesar de la mejora en la estabilidad lagrimal ($p < 0.001$) y la distorsión lumínica ($p < 0.008$) con la lente de doble foco después de instilar lágrima artificial, esta lente producía una menor estabilidad lagrimal y mayor distorsión lumínica que la medida basal (sin lente de contacto) y la lente de contacto monofocal. Como conclusión, el patrón de parpadeo con menor frecuencia y las lentes de contacto incrementaron la distorsión lumínica, debido al hecho de que la estabilidad de la película lagrimal disminuyó. Monitorear el parpadeo o la lágrima artificial podrían ayudar a disminuir la distorsión lumínica y podrían ser una buena opción en el manejo de sujetos con tiempos de ruptura lagrimal cortos o con frecuencias de parpadeo bajas, como por ejemplo en usuarios de lentes de contacto que utilicen dispositivos electrónicos. La medida de la distorsión lumínica podría ayudar en la evaluación y el manejo de sujetos con síntomas de sequedad ocular, así como en la evaluación in-vivo de la humectabilidad de la lente.

En el *Capítulo 9.4*, el método desarrollado en el *Capítulo 8.1* es aplicado a usuarios de lentes esclerales para evaluar la pérdida de glándulas de meibomio y la visibilidad de ellas después de un año de porte de lentes esclerales. Se obtuvo meibografía infrarroja del parpado superior mediante el Cobra fundus camera en 43 voluntarios (34.2 ± 10.1 años). Las meibografías fueron clasificadas en 3 grupos: Grupo 1 = buena visibilidad subjetiva de las glándulas y una pérdida de las glándulas de meibomio < 1/3 del área total; Grupo 2 = baja visibilidad subjetiva de las glándulas y una pérdida de las glándulas de meibomio < 1/3 del área total; y Grupo 3 = baja visibilidad subjetiva de las glándulas y una pérdida de las glándulas de meibomio > 1/3 del área total. Se calcularon las métricas basadas en la visibilidad de las glándulas de meibomio a través de un método previamente desarrollado a partir del análisis de la intensidad del nivel de gris de los pixeles de las meibografías. La repetibilidad de estas nuevas métricas y sus correlaciones con el grado de pérdida de glándulas de meibomio fueron analizadas. Las meibografías y los síntomas oculares fueron de nuevo evaluados después de 1 año de porte de lentes esclerales en 29 sujetos.

El porcentaje de pérdida de glándulas de meibomio no fue estadísticamente significativo entre los grupos 1 y 2 ($p = 0.464$). Sin embargo, el grupo 1 mostró mayores niveles de intensidad del nivel de gris que los otros dos grupos. Se encontraron correlaciones estadísticamente significativas entre las métricas basadas en la visibilidad de las glándulas y el porcentaje de pérdida de éstas. La repetibilidad fue aceptable para todas las métricas, el coeficiente de variación obteniendo valores entre 0.52 y 3.18. Mientras que los síntomas oculares disminuyeron después del porte de lentes de contacto esclerales ($p < 0.001$), no se encontraron diferencias

estadísticamente significativas en el porcentaje de pérdida de glándulas de meibomio ($p = 0.157$) y la visibilidad de las glándulas ($p > 0.217$). Para concluir, el método propuesto puede evaluar la visibilidad de las glándulas de meibomio de una manera objetiva y repetible. Las lentes esclerales parecen no afectar adversamente a la pérdida de glándulas de meibomio ni a su visibilidad mientras que podrían mejorar los síntomas de sequedad ocular después de un año de porte. Estos resultados preliminares deberían ser confirmados con un grupo control.

En el *Capítulo 9.5*, se evalúa el efecto del porte de lentes de contacto blandas y su duración de porte en la película lagrimal y las glándulas de meibomio. El método desarrollado en el *Capítulo 8.1* es aplicado a usuarios de lentes de contacto blandas para evaluar la pérdida de las glándulas de meibomio y la visibilidad de éstas. Treinta voluntarios no usuarios de lentes de contacto (22.5 ± 2.3 años) y 34 usuarios de lentes de contacto blandas a largo plazo (23.8 ± 2.2 años) participaron en el presente estudio. Se evaluó la superficie ocular de los participante mediante el Oculus Keratograph 5M en el siguiente orden: Ocular Surface Disease Index, 5-item Dry Eye Questionnaire, el enrojecimiento de la conjuntiva bulbar, la altura del menisco lagrimal, el tiempo de ruptura lagrimal no invasivo y se obtuvo una meibografía del parpado superior de los sujetos. Se preguntó a los usuarios de lentes de contacto sobre sus hábitos de uso de las lentes, incluyendo los años de porte de las lentes y las horas de porte semanales. La visibilidad de las glándulas de meibomio fue evaluada mediante un método previamente desarrollado basado en el análisis de la intensidad de los valores de gris de los pixeles de las meibografías.

El grupo portador de lentes de contacto mostró un mayor grado de pérdida de glándulas de meibomio ($p < 0.001$) y valores más bajos en las métricas relacionadas con la visibilidad de las glándulas ($p < 0.022$). No se encontraron diferencias en el Ocular Surface Disease Index, 5-item Dry Eye Questionnaire, la altura del menisco lagrimal, el enrojecimiento de la conjuntiva bulbar y en el tiempo de ruptura lagrimal no invasivo. La regresión logística binomial reveló que la pérdida de glándulas de meibomio estaba independientemente asociada con el uso de lentes de contacto ($p = 0.006$). Cuando la pérdida de las glándulas de meibomio fue excluida del análisis, la energía relativa de la intensidad de los pixeles de las meibografías mostró estar independientemente asociada con el uso de lentes de contacto ($p = 0.005$). Además, horas más prolongadas de uso de las lentes de contacto estaban asociadas con mayores síntomas de sequedad ocular y la entropía de las meibografías ($p < 0.029$), la cual podría ser una medida de la tortuosidad de las glándulas. Una reducción en el tiempo de ruptura lagrimal no invasivo estaba independientemente asociada con el uso de lentes de contacto durante 8 años o más ($p = 0.030$). Para concluir, la pérdida de glándulas de meibomio fue mayor y la visibilidad de éstas menor en usuarios de lentes de contacto blandas a largo plazo en comparación con sujetos no usuarios de lentes de contacto. Las nuevas métricas basadas en la visibilidad de las glándulas de meibomio podrían ayudar a evaluar el seguimiento de las glándulas de meibomio en usuarios de lentes de contacto blandas de una manera rápida y objetiva.

En el *Capítulo 9.6*, se evalúa el efecto del uso del ordenador, el uso de lentes de contacto y de lágrimas artificiales en las métricas actuales y las desarrolladas en la presente tesis doctoral en los *Capítulos 8.2 y 8.3*. Se estudia si estas nuevas métricas

son capaces de detectar cambios en la película lagrimal y en la superficie ocular de una forma no invasiva y objetiva, lo cual podría ayudar a validar todavía más estas métricas. 84 voluntarios sanos con edades entre 18 y 27 años (22.4 ± 2.6 años) participaron en el presente estudio. Se evaluó la respuesta de la superficie ocular y la película lagrimal a (1) el uso del ordenador, (2) lentes de contacto y (3) la instilación de lágrima artificial durante el uso del ordenador con las lentes de contacto. Para ello se utilizaron las métricas actuales y las desarrolladas en la presente tesis doctoral. Las métricas actuales incluyeron el cuestionario Ocular Surface Disease Index, el 5-item Dry Eye Questionnaire, el enrojecimiento de la conjuntiva bulbar, la altura del menisco lagrimal y el tiempo de ruptura de la película lagrimal no invasivo. Una de las nuevas métricas consistía en la medida del espesor de la capa lipídica obtenido a partir de la intensidad del disco de Plácido reflejado en la película lagrimal, mientras que la otra en la medida de la velocidad de propagación de las partículas en suspensión en la película lagrimal después del parpadeo.

Después de la tarea de lectura con el ordenador, se encontró un incremento en los síntomas de sequedad ocular, una mayor altura del menisco lagrimal y un mayor enrojecimiento de la conjuntiva bulbar. Además, se encontraron valores inferiores en las métricas relacionadas con la intensidad del disco de Plácido reflejado y en las métricas relacionadas con la velocidad de las partículas en suspensión en la película lagrimal ($p < 0.036$). Cuando las lentes de contacto fueron adaptadas, se encontró una altura del menisco lagrimal inferior, un menor tiempo de ruptura lagrimal no invasivo, menor moda de la intensidad de los pixeles del disco de Plácido, menor valor mínimo de la intensidad de los píxeles, y una menor velocidad de propagación de las partículas

en suspensión en la película lagrimal ($p < 0.044$). El ANOVA mixto reveló que la lágrima artificial tenía un efecto significativo en disminuir el impacto del ordenador en el cuestionario Ocular Surface Disease Index, el 5-item Dry Eye Questionnaire, el tiempo de ruptura lagrimal no invasivo, las métricas relacionadas con la intensidad del disco de Plácido y las métricas relacionadas con la velocidad de las partículas en suspensión en la película lagrimal ($p < 0.033$). Como conclusión, el uso del ordenador y de las lentes de contacto empeoraron los signos y síntomas de sequedad ocular, incluyendo las nuevas métricas desarrolladas en la presente tesis doctoral. La lágrima artificial ayudó a reducir el efecto de las lentes de contacto y el ordenador en las métricas actuales y las recientemente desarrolladas. Los métodos recientemente desarrollados para evaluar la película lagrimal pueden utilizarse como una herramienta útil para detectar cambios en la película lagrimal ocasionados por diferentes situaciones que alteran la superficie ocular.

Finalmente, en el *Capítulo 10*, se exponen las conclusiones generales de la presente tesis doctoral y se plantean futuras líneas de investigación. A pesar de que existe una gran variedad de técnicas disponibles para evaluar la película lagrimal, algunas de ellas presentan una repetibilidad, sensibilidad y especificidad limitadas. Además, algunas de ellas no son objetivas o son invasivas, lo cual ocasiona que la evaluación de la película lagrimal sea difícil y el diagnostico del síndrome del ojo seco un reto. Por ello, técnicas no invasivas de análisis lagrimal deberían ser consideradas para evaluar la película lagrimal y la superficie ocular frente a técnicas más invasivas, para así alcanzar un mayor poder diagnóstico y un mejor manejo de los pacientes con síndrome del ojo seco.

Las métricas desarrolladas en la presente tesis doctoral pueden ayudar a evaluar la película lagrimal de una forma no invasiva, objetiva y repetible. Estas nuevas métricas podrían ser incluidas en una batería de tests clínicos como métodos fáciles, repetibles y objetivos que pueden mejorar la evaluación de la película lagrimal, lo cual podría mejorar la detección y el seguimiento de enfermedades como el síndrome del ojo seco y la disfunción de las glándulas de meibomio. Además, estas métricas son capaces de evaluar cambios en la superficie ocular y la película lagrimal debidos al uso de lentes de contacto.

Aunque las métricas desarrolladas en la presente tesis doctoral son capaces de evaluar la película lagrimal y la superficie ocular, este es el primer paso en el proceso de desarrollo de estas métricas. Son necesarios más estudios que evalúen el rendimiento de las nuevas métricas desarrolladas en sujetos diagnosticados de síndrome del ojo seco o disfunción de las glándulas de meibomio, y establecer valores de corte basados en la edad de los sujetos. Sin embargo, aunque estos resultados son preliminares, son motivadores, y el presente trabajo podría ser la base para futuros estudios.

ABSTRACT

ABSTRACT

The diagnosis and management of dry eye disease is a challenge because of the multifactorial character of the disease and the lack of a gold standard test. Furthermore, the lack of correlation between signs and symptoms of dry eye disease, the lack of correlation between techniques, their low repeatability, their invasiveness and their relative objectivity challenge the assessment of the tear film and the diagnosis of dry eye disease.

In *Chapter 1* of the present work, the characteristics of the tear film and dry eye disease are described and a literature review about non-invasive techniques to assess the tear film and the ocular surface is performed. Non-invasive imaging techniques have a high potential in the assessment of tear film and dry eye disease. The non-invasive analysis of the ocular surface allows clinicians to assess it under more natural conditions, avoiding reflex tearing and tear film destabilization. Generally, they are more accurate, repeatable and objective than invasive ones. Therefore, non-invasive techniques should be considered to assess the tear film and the ocular surface in front of invasive techniques to achieve a higher diagnostic capability and management of dry eye disease subjects.

Although many imaging techniques exist to assess the tear film, this is a field that needs further research and which has a high potential to be explored. Therefore, it is necessary to develop new non-invasive and objective methods to evaluate the tear

film and further studies are needed to improve the correlation of these techniques with clinical findings in dry eye patients.

Chapter 2 is focused on the justification and objectives of the present work. Due to the growing incidence of dry eye disease and morbidity, improving the timely diagnosis to provide a better diagnosis and treatment of the disease is vital. Dry eye disease diagnosis is still challenging and there is a lack of objective tests with good sensitivity and specificity, repeatability, ease of performance, and suitability for clinical practice settings. Therefore, new objective metrics are still required to provide new insights into tear film assessment. Thus, the Tear Film and Ocular Surface Society Dry Eye Workshop II Diagnostic Methodology report recognized the need of developing new non-invasive, objective and as automatic as possible metrics to assess the tear film and the ocular surface.

The present study aims 1) To study the risk factors for dry eye disease, the repeatability of some current metrics for the assessment of the ocular surface, and the efficacy of a thermal eyebag application; 2) To develop and validate new metrics to assess the tear film and the ocular surface in a non-invasive and as objective as possible way. The repeatability and diagnostic capability of new metrics will be assessed; and 3) To assess the effect of contact lenses, artificial tears, blinking and computer use on the ocular surface and the newly developed metrics.

Chapter 3 describes the general methodology of the studies performed in this work. The ocular surface and the tear film were assessed using different devices: the

Keratograph 5M, the TearLab osmolarity system, the IRX3 aberrometer, the Medmont E 300, the Cobra fundus camera and the Light Disturbance Analyzer. The assessment of ocular symptoms was assessed by means of the Ocular Surface Disease Index questionnaire and the 5-item Dry Eye Questionnaire. Different non-invasive metrics based on image processing were developed using Matlab© R2018a software. Finally, these newly developed metrics were applied to subjects fitted with contact lenses.

Systemic, environmental and lifestyle risk factors for dry eye disease are studied in *Chapter 4*; due to the influence of the multifactorial aetiology of dry eye disease in its diagnosis. A cross-sectional study was performed on 120 Caucasian participants aged between 18 and 89 years (47.0 ± 22.8 years). Medical history, information regarding environmental conditions and lifestyle, Ocular Surface Disease Index, Dry Eye Questionnaire-5, non-Invasive (Oculus Keratograph 5M) breakup time, tear film osmolarity and ocular surface staining parameters were assessed in a single clinical session to allow dry eye disease diagnosis based on the guidelines of the Tear Film and Ocular Surface Society Dry Eye Workshop II Diagnostic Methodology Report. A multivariate logistic regression model was constructed including those variables with a p-value less than 0.15 in the univariate analysis.

A prevalence of 57.7 % for dry eye disease was found. No age differences were found between those with and without dry eye disease ($p = 0.243$). Nevertheless, the dry eye disease group had more females ($p = 0.008$). The univariate logistic regression identified as potential risk factors for dry eye disease the following: female sex, sleep hours per day, menopause, anxiety, systemic rheumatologic disease, use of anxiolytics,

daily medication, ocular surgery, poor diet quality, more ultra-processed food in the diet, not drinking caffeine and hours of exposure to air conditioning per day. Multivariate logistic regression revealed that hours of sleep per day, menopause and use of anxiolytics were independently associated with dry eye disease ($p \leq 0.026$ for all). To conclude, dry eye disease is associated with systemic, environmental and lifestyle risk factors. These findings are useful to identify potentially modifiable risk factors, in addition to conventional treatments for dry eye disease.

Due to the relevance of non-invasive keratograph break-up time in the diagnosis of dry eye disease, *Chapter 5* aims to assess the intraexaminer repeatability of non-invasive keratograph break-up time using the Oculus Keratograph 5M, which is one of the most common tools used to objectively assess the tear film. 80 healthy volunteers aged between 30 and 89 years participated. Measurements were classified according to age, sex and the presence or not of dry eye disease. Repeatability was evaluated by the calculation of within-subject standard deviation, coefficient of repeatability and coefficient of variation. Moreover, the Passing-Bablok regression method was applied. Repeatability coefficients showed low repeatability in all groups with values between 3.57 and 7.14; 9.90 and 19.79; and 51.90 and 65.49, for each coefficient, respectively. No statistically significant differences were found in the non-invasive keratograph break-up time measurements between healthy and dry eye disease patients ($p = 0.188$). Groups with more dry eye disease risk had better repeatability. Passing-Bablok regression also confirmed a lack of agreement between the maximum and minimum non-invasive keratograph break-up time measurement. Overall, non-invasive keratograph break-up time measurement has low intraexaminer repeatability even

when considering sex, age and dry eye disease diagnosis. Nevertheless, not only is this low repeatability due to the device, but also it is largely due to the intrinsic variability of the tear film.

As ocular redness is an important sign to take into account in some inflammatory diseases and the relationship between ocular redness and dry eye disease, *Chapter 6* aims to assess the intraexaminer repeatability of ocular redness measurements obtained using the Oculus Keratograph 5M. Seventy-eight right eyes of 78 healthy volunteers aged between 18 and 79 years participated in this study. Bulbar redness was measured three consecutive times in the same eye. Redness was classified automatically by the device depending on the zone: temporal bulbar, nasal bulbar, temporal limbal, nasal limbal and total bulbar redness. Repeatability was evaluated for each metric by the calculation of within-subject standard deviation, coefficient of variation and coefficient of repeatability. Furthermore, the Passing-Bablok regression method was applied. A p-value less than 0.05 was defined as statistically significant.

Repeatability coefficients revealed acceptable repeatability in all metrics. Passing-Bablok regression also confirmed the good grade of agreement between the maximum and minimum bulbar redness measurement for each metric. The highest repeatability was achieved in total bulbar redness since the slope was 1; therefore only systematic errors caused by the intercept might alter the results. In the other metrics, the repeatability was poorer when the ocular redness was higher. Even in these cases, the repeatability was acceptable. Friedman's analysis showed statistical differences between the third measurement and the first two, being the third slightly higher.

However, these differences were not considered clinically significant. Finally, bulbar measurements had clinical higher values than limbal ones, total redness was clinically higher than limbal measurements, and nasal measurements were clinically higher than temporal. To conclude, Keratograph 5M is a useful and repeatable device to assess ocular surface redness. All bulbar redness metrics provide objective values with acceptable repeatability, which might help clinicians in the diagnosis and treatment of different pathologies related to ocular surface inflammation, such as dry eye disease or uveitis.

Since the Keratograph 5M is one of the most common tools used to objectively assess the ocular surface, knowing its usefulness in the follow-up of some treatments is relevant. Therefore, *Chapter 7* aims to evaluate the association between the application of MGDRx thermal EyeBags and ocular surface signs and symptoms in young and aged subjects. Thirty young volunteers aged between 18 and 31 years old (23.95 ± 3.94 years) and thirty aged subjects aged between 61 and 90 years old (77.97 ± 8.11 years) participated in this study. Ocular surface parameters were assessed using the Oculus Keratograph 5M, following the guidelines of the Tear Film and Ocular Surface Dry Eye Workshop II Diagnostic Methodology Report. Only subjects who had a positive score in almost one questionnaire and a first non-invasive keratograph break-up time lower than 10 seconds were included in the study. After thermal bag self-application in both eyes every day for 2 weeks, the protocol was carried out again. Lid massage was performed after lid warming. Compliance and degree of improvement were also assessed. The young group showed an improvement in non-invasive keratograph break-up time, lipid layer, upper eyelid gland drop-out percentage and dry

eye symptoms over the two week treatment period. Improvements in meibum quality, gland obstruction, telangiectasia scores, and dry eye symptoms were found in aged subjects. Mixed ANOVA revealed better non-invasive keratograph break-up time and lipid layer values in young subjects. Despite the treatment compliance being statistically higher in the aged group than in the younger one ($p = 0.002$), there were no significant differences in subjective improvement between groups ($p = 0.097$). Overall, dry eye-related symptoms were improved after thermal bag application, while non-invasive keratograph break-up time and lipid layer thickness were only improved in young subjects.

The Tear Film and Ocular Surface Dry Eye Workshop II Diagnostic Methodology Report recognized the need of developing new non-invasive and as objective as possible metrics to assess the tear film and the ocular surface. *Chapter 8* is focused on the development of new metrics to assess the tear film and the ocular surface in a non-invasive and objective way. In the first part of this chapter (*Chapter 8.1*), a method to assess meibomian gland visibility is developed from the analysis of grey pixel intensity values of meibographies obtained through non-contact infrared meibography. *Chapter 8.1.1* aims to develop a new objective semiautomatic method for analysing meibomian glands' visibility quantitatively. 112 healthy volunteers aged between 18 and 90 years (48.29 ± 27.46 years) participated in this study. Infrared meibography was obtained from the right upper eyelid through Oculus Keratograph 5M. Meibographies were classified into 3 groups: Group 1 = Patients with good subjective glands visibility and a gland drop-out percentage < 1/3 of the total meibomian gland area; Group 2 = Patients with low subjective glands visibility and a

gland drop-out < 1/3; and Group 3 = Patients with low subjective glands visibility and a gland drop-out > 1/3. New metrics based on the visibility of the meibomian glands were calculated and later compared between groups. Rho Spearman test was used to assess the correlation between each metric, and Meibomian gland drop-out percentage with the entire sample and after excluding group 2. A p-value less than 0.05 was defined as statistically significant.

Fifty-six subjects were classified in group 1 (24.48 ± 9.62 years), 19 in group 2 (69.16 ± 21.30 years) and 37 in group 3 (73.59 ± 13.70 years). No statistically significant differences were found between groups 1 and 2 in drop-out percentage. All metrics, except entropy, showed higher meibomian gland visibility in Group 1 than in the other two groups. Moderate correlations were statistically significant for all metrics with the exception of entropy. Correlations were higher after excluding the group 2. To conclude, the proposed method is able to assess meibomian gland visibility in an objective and repeatable way, which might help clinicians enhance meibomian gland dysfunction diagnosis and follow-up treatment.

In *Chapter 8.1.2*, the diagnostic capability of these new gland visibility metrics for meibomian gland dysfunction is assessed, as well as their correlations with other clinical signs and symptoms of dry eye disease and meibomian gland dysfunction. 112 healthy volunteers (48.3 ± 27.5 years) were enrolled in this study. Ocular surface parameters were measured using the Oculus Keratograph 5M. Subjects were classified according to the presence or absence of meibomian gland dysfunction. New metrics based on the visibility of the meibomian glands were calculated and later compared

between groups. The diagnostic ability of ocular surface parameters and gland visibility metrics was studied through receiver operating characteristics curves. Logistic regression was used to obtain the combined receiver operating characteristics curve of the metrics with the best diagnostic ability.

Statistically significant differences were found between groups for all ocular surface parameters and new gland visibility metrics, except for the first non-invasive keratograph break-up time and gland expressibility. New gland visibility metrics showed higher sensitivity and specificity than current single metrics when their diagnostic ability was assessed without any combination. The diagnostic capability increased when gland visibility metrics were incorporated into the logistic regression analysis together with gland drop-out percentage, tear meniscus height, dry eye symptoms and lid margin abnormality score ($p < 0.001$). The combination of median pixels intensity of meibography grey values with the aforementioned ocular surface metrics achieved the highest area under the curve (0.99), along with excellent sensitivity (1.00) and specificity (0.93). Overall, new meibomian gland visibility metrics are more powerful to diagnose meibomian gland dysfunction than current single metrics and can serve as a complementary tool for supporting the diagnosis of meibomian gland dysfunction.

In *Chapter 8.2*, a method to assess tear film spread and dynamics is developed by tracking the tear film particles post-blink. Ocular surface parameters and the recording of tear film particles' spreading post-blink were assessed in eighty-one healthy volunteers (43.7 ± 27.0 years) using the Oculus Keratograph 5M. The developed

software automatically decomposed the video into frames to manually track particles' position for 1.75 seconds after a blink. The following tear film-dynamic metrics were automatically calculated: mean, median, maximum and minimum particles' speed at different times after blinking and the time for particle speed to decrease to < 1.20 mm/second. The repeatability of each tear film-dynamic metric and its correlations with ocular surface signs and symptoms were analyzed. Binomial logistic regression was performed to assess the predictability of new metrics to ocular parameters.

Repeatability tended to be lower just after blinking (variability of 12.24 %), whereas the metrics from 0.5 seconds onwards had acceptable repeatability (variability below 10 %). Tear film-dynamic metrics correlated positively with non-invasive keratograph break-up time while negatively with meibomian gland drop-out. Binomial logistic regression analysis revealed that tear film-dynamic metrics were able to predict non-invasive keratograph break-up time. Nevertheless, no statistically significant association was found with gland drop-out. This means that higher particle speed is related to larger non-invasive keratograph break-up time. The metric "time for particle speed to decrease to < 1.20 mm/second" can be considered the best metric to assess the quality of the tear film, since it was more strongly correlated with non-invasive keratograph break-up time ($r = 0.42$, $p = 0.004$), it was more strongly associated in the binomial logistic regression analysis with non-invasive keratograph break-up time and showed good repeatability (variability = 5.49 %). To conclude, tear film-dynamic metrics are emerging homeostasis parameters for assessing indirectly the tear film quality in natural conditions with acceptable repeatability.

In *Chapter 8.3*, a method to objectively assess the lipid layer thickness is developed through the analysis of grey intensity values obtained from the Placido disk pattern reflected onto the tear film. Ocular surface parameters were measured using Oculus Keratograph 5M in 94 healthy volunteers (43.8 ± 26.8 years). Subjects' lipid layer thickness was subjectively classified into 4 groups using an interferometry-based grading scale. New metrics based on the intensity of the Placido disk images were calculated and compared between groups. The repeatability of the new metrics and their diagnostic ability was analyzed through receiver operating characteristics curves. The level of agreement between the new objective tool and the existing subjective classification scale was analyzed by means of accuracy, weighted Kappa index and F-measure.

Mean pixels intensity, median pixels intensity and relative energy at 5.33 seconds after blinking achieved the highest performance, with a correlation with a lipid layer thickness between $r = 0.655$ and 0.674 ($p < 0.001$), sensitivity between 0.92 and 0.94, specificity between 0.79 and 0.81, area under the receiver operating characteristics curve between 0.89 and 0.91, accuracy between 0.76 and 0.77, weighted Kappa index of 0.77 and F-measure between 0.86 and 0.87. To conclude, the analysis of grey intensity values in videokeratography can be used as an objective tool to assess lipid layer thickness. These new metrics could be included in a battery of clinical tests as an easy, repeatable, objective and accessible method to improve the detection and monitoring of dry eye disease and meibomian gland dysfunction.

Since contact lens wear impacts the ocular surface homeostasis, *Chapter 9* is focused on the effect of contact lenses on the tear film and the ocular surface. Current and newly developed metrics are used to assess the ocular surface and the tear film. *Chapter 9.1* aims to assess the short-term effect of a dual-focus contact lens design on the tear film, visual performance and optical quality, compared to a single-vision contact lens design built with the same material. *Chapter 9.1.1* is focused on the short-term light disturbance, optical quality and visual performance of these contact lenses. This is a randomized, double-masked, crossover study. Twenty-eight healthy, myopic volunteers aged between 18 and 32 years (23.5 ± 4.1 years) participated in this study. Sensory dominant eye for distance vision was determined. Refraction, best-corrected visual acuity and aberrations for 3 mm and 5 mm pupil diameter were acquired at baseline (without a contact lens in situ). Subjects were binocularly fitted in random order with each of two contact lens designs: dual-focus and single-vision, both made of omafilcon A material. Quality of Vision questionnaire, over-refraction, best-corrected visual acuity, stereopsis at 40 cm, best-corrected photopic and mesopic contrast sensitivity, light disturbance and aberrations were assessed 25 minutes after contact lens insertion. Differences between groups for each metric were analysed. A p-value less than 0.05 was defined as statistically significant.

Mean sphere and cylinder were -1.36 ± 1.04 D (range: -6.00 to -0.25 D) and -0.23 ± 0.30 D (range: -0.75 to 0.00 D), respectively. There were no statistically significant differences in best-corrected visual acuity and stereopsis between baseline, dual-focus and single-vision contact lens wear conditions. Photopic and mesopic contrast sensitivities were lower for the dual-focus contact lens at all frequencies, with the

exception of mesopic contrast sensitivity at 18 cycles per degree ($p = 0.234$). High order aberrations and light disturbance size and irregularity were higher for the dual-focus contact lens ($p < 0.001$). No differences were found in high order aberrations between baseline and with the single-vision contact lens in situ for both pupil diameters. Quality of Vision scores also revealed lower frequency, severity and bothersome scores with the single-vision contact lens than with the dual-focus contact lens ($p < 0.001$). Overall, the dual-focus contact lens design decreases the psychophysical and psychometric visual quality scores in the short-term under dim-light conditions when compared to a single-vision contact lens design with the same material. Visual acuity and stereopsis were not affected by lens design.

The second part of this chapter (*Chapter 9.1.2*) is focused on the short-term effect of these contact lenses on the pre-lens tear film stability and comfort. This randomized, double-masked, crossover study was performed on twenty-eight healthy, myopic volunteers aged between 18 and 32 years (23.5 ± 4.1 years). Only one randomly chosen eye was assessed. Distance vision and refraction were evaluated at baseline. Each contact lens type (monofocal and dual-focus) was randomly fitted, always in both eyes. A visual analogue scale between 0 and 10 was used to assess general comfort, physical comfort and visual comfort. Tear Film Surface Quality index, Tear Film Surface Quality area and auto Tear Break-Up Time were obtained using Medmont E-300 at baseline (naked eye condition) and 25 minutes after each contact lens insertion.

Refractive sphere and cylinder were respectively -1.36 ± 1.04 D (ranging from -6.00 to -0.25 D) and -0.23 ± 0.30 D (ranging from -0.75 to 0.00 D). Tear Film Surface Quality and Tear Film Surface Quality area were lower (meaning more stable tear film) at baseline when compared with both contact lens types ($p < 0.025$). Higher pre-lens tear instability (larger Tear Film Surface Quality and Tear Film Surface Quality area values) was found with the dual-focus than with the monofocal lens. Auto Tear Break-Up Time was higher at baseline than with each of the contact lenses, without statistically significant differences between both contact lens types. Visual analogue scales revealed statistically significant better scores in the monofocal contact lens than in the dual-focus contact lens for general (0.77 ± 1.14 vs 3.12 ± 2.79), physical (0.96 ± 1.46 vs 2.19 ± 2.45) and visual comfort (1.27 ± 1.66 vs 3.92 ± 2.04). To conclude, a slight reduction in short-term pre-lens tear film stability was found in the dual-focus design in comparison with the monofocal lens, potentially contributing to the deterioration of visual performance and comfort during dual-focus contact lens wear.

Chapter 9.2 goes one step further by comparing short-term visual quality, optical quality, light disturbance, comfort and tear film stability between two dual-focus prototype contact lenses for myopia control made from the same material. It aims to assess whether parameters are influenced by the different optical designs of two dual-focus contact lenses. Twenty-eight subjects (23.49 ± 4.07 years) with myopia were included in this randomized, double-masked, crossover study. Refraction, best-corrected visual acuity, wavefront aberrations and tear film stability (Medmont E 300) were measured at baseline. Subjects were then binocularly fitted with two dual-focus contact lenses (randomly) and only the sensorial dominant eye was assessed. Lenses

had the same material with two varying inner zone diameters of 2.1 mm (S design) and 4.0 mm (M design). Visual and physical comfort, over-refraction, best-corrected visual acuity, stereopsis at 40 cm, best-corrected photopic and mesopic contrast sensitivity, size and shape of light disturbance, wavefront aberrations, subjective quality of vision (Quality of Vision Questionnaire) and tear film stability were measured for both lenses.

Both contact lens designs decreased visual acuity and tear film stability, and induced higher levels of higher-order aberrations in comparison to baseline. Nevertheless, visual acuity and photopic contrast sensitivity were within normal values for the subjects' age. Regarding comparisons between lenses, the M design promoted better photopic contrast sensitivity in the spatial frequency of 18 cycles per degree ($p < 0.001$) and a better light disturbance ($p < 0.017$). However, higher-order aberrations were better in S design ($p = 0.015$). No statistically significant differences were found between the two contact lenses in Quality of Vision scores and tear film stability. Overall, both dual-focus contact lenses provided an acceptable visual performance under photopic conditions. The contact lens with medium central diameter of 4.0 mm induced better contrast sensitivity at high frequencies and lower light disturbance size, while the smaller central diameter contact lens of 2.1 mm induced lower levels of higher-order aberrations for a 5 mm pupil diameter. Both diameters promoted the same subjective visual comfort.

Chapter 9.3 assesses the light disturbance related to changes in the tear film stability parameters to validate the Light Disturbance Analyzer device as a reliable and useful tool to assess the optical quality-related changes induced by the tear film. Thus,

light disturbance, tear film stability and corneal aberrations were evaluated under different conditions: Different blinking patterns, with and without artificial tears, and with a single-vision and a dual-focus contact lens. Forty healthy, myopic volunteers aged between 19 and 38 years (26.6 ± 5.1 years) were recruited to participate in this randomized, double-masked, crossover study. The sensory dominant eye for distance vision was examined. Refraction and best-corrected visual acuity were assessed at baseline (without contact lens). In the first visit, light disturbance (measured with Light Disturbance Analyzer) and the tear film stability and corneal aberrations (Medmont E 300 Corneal Topographer) were assessed with different blinking patterns in random order: Blinking naturally, blinking every 6 seconds and blinking every 12 seconds. Measurements were repeated with artificial tears. In the second visit, subjects were binocularly fitted in random order with each contact lens design: Dual-focus and single-vision. Over-refraction and best-corrected visual acuity were assessed 25 minutes after contact lens insertion. Light disturbance, tear film stability and corneal aberrations were assessed for each contact lens with each blinking pattern without and with artificial tears.

Light vision disturbance was higher with the slowest blinking rate ($p < 0.034$) when subjects wear contact lenses since both contact lenses decreased tear stability ($p < 0.001$). Statistically significant improvements in light disturbance and tear film were observed after the instillation of artificial tears in the naked eye for delayed blinking and with both contact lenses tested. The dual-focus contact lens provided greater tear film instability ($p < 0.008$) and light disturbance ($p < 0.001$) than single-vision contact lens in all blinking patterns. Despite the improved tear film stability ($p < 0.001$) and

light disturbance ($p < 0.008$) in the dual-focus contact lens after the instillation of artificial tears, this lens showed higher destabilization of the tear film and disturbance phenomena than the naked eye and single-vision contact lens. Overall, delayed blinking and contact lens wear increased light disturbance due to tear film instability. Monitoring blinking or artificial tears use might decrease the light disturbance and could be an option to manage subjects with short break-up time or with lower blinking rates such as computer users with contact lenses. Light disturbance measurement might help in the assessment and management of subjects with dry eye disease symptoms, as well as in the in-vivo assessment of lens wettability.

In *Chapter 9.4*, the method developed in *Chapter 8.1* is applied to scleral lens wearers to assess the meibomian gland drop-out and visibility after one year of lens wear. Infrared meibography was obtained from the upper eyelid using the Cobra fundus camera in forty-three volunteers (34.2 ± 10.1 years). Meibographies were classified into 3 groups: Group 1 = good subjective gland visibility and gland drop-out < 1/3 of the total area; Group 2 = low visibility and gland drop-out < 1/3; and Group 3 = low visibility and gland drop-out > 1/3. Meibomian gland visibility metrics were then calculated using the developed method from the pixel intensity values of meibographies. The repeatability of new metrics and their correlations with gland drop-out were assessed. Meibographies and ocular symptoms were also assessed after 1 year of scleral lens wear in 29 subjects.

Gland drop-out percentage was not statistically different between groups 1 and 2 ($p = 0.464$). Nevertheless, group 1 showed higher grey pixel intensity values than the

other groups. Statistically significant correlations were found between gland visibility metrics and gland drop-out percentage. Repeatability was acceptable for all metrics, with the coefficient of variation achieving values between 0.52 and 3.18. While ocular symptoms decreased with scleral lens wear ($p < 0.001$), no statistically significant differences were found in gland drop-out percentage ($p = 0.157$) and gland visibility metrics ($p > 0.217$). To conclude, the proposed method can assess meibomian gland visibility in an objective and repeatable way. Scleral lens wear appears to not adversely affect meibomian gland drop-out and visibility while might improve dry eye symptoms after one year of lens wear. These preliminary results should be confirmed with a control group.

In *Chapter 9.5*, the effect of soft contact lens wear and duration on the tear film and meibomian glands is assessed. The method developed in *Chapter 8.1* is applied to soft contact lens wearers to assess the meibomian gland drop-out and visibility. Thirty non-contact lens wearers (22.5 ± 2.3 years) and twenty-four long-term soft contact lens wearers (23.8 ± 2.2 years) participated in this study. The ocular surface of participants was assessed using the Oculus Keratograph 5M in the following order: Ocular Surface Disease Index, 5-item Dry Eye Questionnaire, bulbar redness, tear meniscus height, non-invasive keratograph break-up time and upper eyelid meibography. Contact lens users were surveyed on their wearing habits, including years of contact lens wear and hours of contact lens wear per week. Meibomian gland visibility was assessed using a previously developed method based on the analysis of pixel intensity values of meibographies.

The contact lens group showed a statistically higher gland drop-out ($p < 0.001$) and lower values in gland visibility metrics ($p < 0.022$). No differences were found in Ocular Surface Disease Index, 5-item Dry Eye Questionnaire, tear meniscus height, bulbar redness and non-invasive keratograph break-up time. Binomial logistic regression revealed that gland drop-out was independently associated with contact lens wear ($p = 0.006$). When gland drop-out was excluded from the analysis, relative energy of pixel intensity values showed an independent association with the use of contact lenses ($p = 0.005$). Prolonged hours of contact lens wear was associated with higher dry eye symptoms and entropy of meibomian glands ($p < 0.029$), which might be a measurement of gland tortuosity. A reduction in non-invasive keratograph break-up time was independently associated with the use of contact lenses for 8 years or more ($p = 0.030$). Overall, gland drop-out was higher and gland visibility lower in long-term soft contact lens wearers in comparison with non-contact lens wearers. New gland visibility metrics might help to assess the follow-up of meibomian glands in soft contact lens wearers quickly and objectively.

In *Chapter 9.6*, the effect of computer use, contact lens wear and artificial tears on new metrics developed in *Chapters 8.2 and 8.3* and current ones are assessed. It is studied whether these new metrics are able to detect changes in the tear film and the ocular surface in a non-invasive and objective way, which might help to further validate these metrics. Eighty-four healthy volunteers ranging in age from 18 to 27 years (22.4 ± 2.6 years) participated in this study. The ocular surface and tear film response to (1) the use of a computer, (2) contact lens insertion and (3) tear film instillation during computer use with contact lenses were assessed using current and

novel metrics. Current metrics included the Ocular Surface Disease Index questionnaire, 5-item Dry Eye Questionnaire, bulbar redness, tear meniscus height and non-invasive keratograph break-up time. Novel metrics included the measurement of the lipid layer thickness obtained from the intensity of the reflected Placido disk and the measurement of the speed of tear film particles post-blink.

Higher dry eye symptoms, tear meniscus height and bulbar redness; and lower values in metrics related to the intensity of the reflected Placido disk pattern and in metrics related to particle speed after blinking were found after the computer reading task ($p < 0.036$). When a contact lens was fitted, lower tear meniscus height, non-invasive keratograph break-up time, mode pixel intensity, minimum pixel intensity of the reflected Placido disk pattern, and particle speed metrics were obtained ($p < 0.044$). Mixed ANOVA revealed that artificial tears had a significant effect in ameliorating the effect of computer reading on the Ocular Surface Disease Index questionnaire, 5-item Dry Eye Questionnaire, non-invasive keratograph break-up time, metrics related to the intensity of the reflected Placido disk pattern and metrics related to particle speed after blinking ($p < 0.033$). Overall, computer use and contact lens wear worsened dry eye signs and symptoms, including novel ocular surface metrics. Artificial tears help in ameliorating the effect of contact lens wear and computer use on current and novel metrics. Newly developed methods can serve as a tool to detect changes in the tear film triggered by different ocular surface-disturbing conditions.

Finally, in *Chapter 10*, the general conclusions and further research lines are exposed. Despite many techniques being available to assess the tear film, some of them have limited repeatability, sensitivity and specificity. Moreover, some of them are non-objective or invasive, which makes the assessment of the tear film challenging and the diagnosis of dry eye disease difficult. Non-invasive imaging techniques should be considered to assess the tear film and the ocular surface and should prevail over invasive ones to achieve greater diagnostic capability and better management of individuals with dry eye disease.

The metrics developed in the present work can help assess the tear film and the ocular surface in a non-invasive, objective and repeatable manner. These new metrics could be included in a battery of clinical tests as easy, repeatable and objective methods to improve the assessment of the tear film, which could enhance the detection and monitoring of dry eye disease and meibomian gland dysfunction. Moreover, these metrics are capable of assessing the changes in the ocular surface and the tear film due to contact lens wear.

Although newly developed metrics are able to assess the tear film and the ocular surface; this is the first step in developing these metrics. Further research is needed to assess the performance of these metrics in subjects diagnosed with dry eye disease or meibomian gland dysfunction, and to establish cut-off values based on the age of the subjects. Nonetheless, although these results are preliminary, they are highly encouraging, and this study could be the basis for future works.

ACRONYMS

µm: Microns

ADDE: Aqueous Deficient Dry Eye

BFC: Best-Fit Circle

BUT: Break-Up Time

CoR: Coefficient of Repeatability

CoV: Coefficient of Variation

DED: Dry Eye Disease

DEQ-5: 5-item Dry Eye Questionnaire

EDE: Evaporative Dry Eye

ICU: Interferometric Color Units

IQR: Interquartile Range

LDA: Light Disturbance Analyzer

LDI: Light Disturbance Index

LED: Light-Emitting Diode

LIPCOF: Lid Parallel Conjunctival Folds

MGD: Meibomian Gland Dysfunction

mm: Millimeters

MTF: Modulation Transfer Function

NIBUT: Non-Invasive Break-Up Time

NIKBUT: Non-Invasive Keratograph Break-Up Time

OCT: Optical Coherence Tomography

OQAS: Optical Quality Analysis System

OSDI: Ocular Surface Disease Index

OSI: Ocular Scatter Index

OST: Ocular Surface Temperature

PSF: Point Spread Function

QoV: Quality of Vision

RMS: Root Mean Square

ROC: Receiver Operating Characteristic

ROI: Region Of Interest

SD: Standard Deviation

Sw: Within-Subject Standard Deviation

TFOS DEWS: Tear Film and Ocular Surface Dry Eye WorkShop

TFSQ: Tear Film Surface Quality

TMA: Tear Meniscus Area

TMD: Tear Meniscus Depth

TMH: Tear Meniscus Height

TMR: Tear Meniscus Radius

TMV: Tear Meniscus Volume

LIST OF FIGURES

LIST OF TABLES

Table 9.6.4. *Analysis of the interaction between the time (pre-task versus post-task) and the condition (computer versus computer + contact lens + artificial tears) for each dependent variable through a mixed ANOVA.*

CHAPTER 1: Introduction

1. INTRODUCTION

1.1 The tear film

The tear film is a complex structure that covers the ocular surface of the eye and forms a metastable covering between blinks (Lemp, 2008; Willcox et al., 2017). It is composed of many substances including lipids, proteins, mucins and electrolytes (Willcox et al., 2017). The tear film performs different functions related to the health of the ocular surface, providing mechanical and defensive functions against the environment. For instance, the tear film removes the waste, has bactericide properties, reduces tension forces and maintains a regular optical surface, clear vision, corneal health, transparency, nutrition and lubrication of the ocular surface (Willcox et al., 2017). Thus, having a proper lacrimal quality and quantity is vital for having a healthy and functional ocular surface (Craig et al., 2017; Willcox et al., 2017).

The tear film is formed after a blink, which redistributes the tears over the ocular surface from three compartments: the fornix, the tear menisci and the preocular tear film, which has a thickness of around 2-5.5 µm (Stern et al., 1998; King-Smith et al., 2000; King-Smith et al., 2004; Chen et al., 2010). During the inter blink time, the tear film becomes thinner due to evaporation and breaks-up until the next blink occurs (Craig and Tomlinson, 1997; Bron et al., 2004; Nichols, Mitchell and King-Smith, 2005; Lemp, 2008; King-Smith et al., 2009; Peng et al., 2014a; Peng et al., 2014b;). Finally, tears are drainage towards the lacrimal fossa by upper and lower canaliculi, lacrimal points, sacs and ducts (Doane, 1981; Klein et al., 1998).

1.1.1 The lacrimal function unit

The lacrimal function unit is the mechanism through which the eye maintains the homeostasis of the tear film. It is a set of structures that have the function of regulating the production, distributing and clearing the tears to meet ocular surface demands, resulting in maintaining the tear film homeostasis (Bron et al., 2017). Through the lacrimal function unit, sensory receptors monitor the ocular surface, send afferent signals to the central nervous system and send efferent impulses to the secretory glands and cells to modulate the tear film secretion and local immunity (Stern al., 2004; Lemp, 2008; Foulks and Pflugfelder, 2014; Belmonte et al., 2017).

The fifth cranial nerve also called the trigeminal nerve and its terminal branches innervate the ocular surface and contiguous areas of the upper and lower eyelids. Corneal nerves send different afferent inputs to the brain such as pain (polymodal nociceptor), temperature (cold thermoceptor) and mechanical sensation (mechano-nociceptor) (Belmonte et al., 2017; Bron et al., 2017). These signals cause the stimulation of the lacrimal glands, conjunctival goblet cells and meibomian glands as a response to the inputs, which generates an efferent loop modulated by the parasympathetic nervous system to adapt the needs of the ocular surface against the environment (Bron et al., 2017).

1.1.2 Composition of the tear film

Traditionally, the tear film has been thought to consist of three discrete layers: a mucin layer covering the corneal and conjunctival cells, an intermediate aqueous layer and a lipid layer, which is the outermost layer and covers the aqueous layer (Holly and

Lemp, 1977; Willcox et al., 2017). However, currently, it is widely accepted that the tear film is a complex structure in which the aqueous and mucous layers are mixed. Thus, the tear film is composed of a glycocalyx covering the corneal surface and a mucoaqueous-gel with a gradient of mucin content decreasing from the epithelium to the aqueous layer (Dilly, 1994; Arntz-Bustos and Durán-de-la-Colina, 2004; Stern et al., 2004; Cher, 2008; Craig et al., 2017; Willcox et al., 2017).

1.1.2.1 The tear film lipid layer

The lipid layer is secreted by Meibomian glands (Bron and Tiffany, 1998; Korb, 2002; Kunnen et al., 2016; Willcox et al., 2017) and is the thinnest layer of the tear film. Its mean thickness is 40nm (King-Smith, Hinel and Nichols, 2010) and it is composed of a multi-layered model, which consist of an external non-polar hydrophobic lipid layer in contact with the external environment (waxes, cholesterol esters and triglycerides) and an internal polar lipid layer ((0-acyl)-w-hydroxy fatty acids and phospholipids) (Bron and Tiffany, 2004; Bron et al., 2004; King-Smith, Hinel and Nichols, 2010; Millar and Schuett, 2015; Cwiklik, 2016, Willcox et al., 2017).

The lipid layer interacts with the mucoaqueous layer, retarding the evaporation of the aqueous layer and increasing the stability and spreading of the tear film between blinks (Lemp, 2008; Willcox et al., 2017). However, the role of the lipid layer in preventing evaporation is controversial. Nowadays it is believed that not only is the lipid layer that contributes to avoiding the evaporation and collapse of the tear film, but rather the interaction of all the tear film layers, salts and proteins. Moreover, the lipid layer also provides a smooth optical surface and reduces surface tension (Miller,

1969; Willcox et al., 2017). Further studies are needed to better understand the role of the tear film lipid layer.

1.1.2.2 The tear film aqueous layer

The aqueous layer is the thickest layer of the tear film, having a thickness higher than 98 % of the tear film (7 μm) (Craig et al., 2017). It is secreted by the main lacrimal glands and the accessory glands of Krause and Wolfring, with soluble mucins secreted by the goblet cells in the conjunctiva (Dartt, 2002; Harriet and Kuonen, 2004; Ubels et al., 2012; Willcox et al., 2017). The aqueous layer is also composed of proteins, metabolites, enzymes, electrolytes, antibacterial proteins (lysozyme and lactoferrin), nutrients (glucose, glycogen and oxygen) and proteins to protect the eye against pathogens (albumin, immunoglobulin, lipocalin, fibroblast grow factor and nerve growth factor). The aqueous layer has different functions such as nutrition, cleaning the debris, maintaining epithelial hydration and it also has a bacteriostatic function (Willcox et al., 2017).

1.1.2.3 The tear film mucin layer

The mucin layer is the innermost layer of the tear film and is secreted by the goblet cells, located in the conjunctival epithelium (Gipson, 2007; Willcox et al. 2017). The mucin layer is composed of immunoglobulins, urea, salts, leukocytes, glucose and enzymes (Nichols, Chiappino and Dawson, 1985). Mucins are high molecular glycoproteins that play the role of protection against pathogens, lubrication and hydration of the ocular surface, reduction of frictional forces, clear waste and debris and it acts as a barrier formation. The mucin layer also converts the epithelial surface

into a hydrophilic surface (Mantelli and Argüeso, 2008; Stephens and McNamara, 2015; Willcox et al., 2017).

There are different types of mucins: transmembrane mucins and secretory mucins (Willcox et al., 2017). Transmembrane mucins are produced by the conjunctival cells and are mainly placed at the apex of the ocular mucosal epithelial cells. They have anti-adhesive properties and play the role of clearing debris and preventing the adhesion of foreign bodies and pathogens. They also play a role in the stabilization of the tear film (Mantelli and Argüeso, 2008; Govindarajan and Gipson, 2010; Willcox et al., 2017). Moreover, membrane-associated mucins secrete glycocalyx, which creates a barrier for epithelial integrity (Gipson, Hori and Argüeso, 2004; Blalock et al., 2007; Lemp, 2008; Willcox et al., 2017).

Secretory mucins can be subclassified into large gel-forming mucins and small soluble mucins (or non-gel forming mucins). Gel-forming mucins are secreted by the conjunctival goblet cells and have the function of trapping and removing cellular debris. They also have antimicrobial functions, reduces the stress during blinking and acts as a scaffold for cytokines (Gipson, Hori and Argüeso, 2004; Lemp, 2008; Mantelli and Argüeso, 2008; Willcox et al., 2017). Finally, soluble mucins are primarily secreted by the lacrimal gland and conjunctival cells and have an antibacterial function (Bobek and Situ, 2003; Jumblatt et al., 2003; Lemp, 2008; Gipson, Hori and Argüeso, 2004; Willcox et al., 2017).

1.2 Dry eye disease

1.2.1 Definition

Dry eye disease (DED) is a pathology in increasing prevalence, which severely affects the integrity of the eye, optical quality and patients' quality of life (Lemp, 2008; Montés-Micó et al., 2010a; Paulsen et al. 2014; Craig et al., 2017). It is recognized as a growing worldwide public health problem, one of the most frequent reasons for seeking eye care and a very common cause of ophthalmologic visits (Lemp, 2008; Deschamps et al., 2013; Craig et al., 2017).

In the year 2017, the report of the Tear Film and Ocular Surface Society Dry Eye Workshop II (TFOS DEWS II) defined the disease as "*a multifactorial disease of the ocular surface characterized by a loss of homeostasis of the tear film, and accompanied by ocular symptoms, in which tear film instability and hyperosmolarity, ocular surface inflammation and damage, and neurosensory abnormalities play etiological roles*" (Craig et al., 2017).

The definition recognized symptoms as the central feature of the disease and their presence is necessary to diagnose it. Moreover, the definition also covered the aetiology of the disease, such as tear instability, hyperosmolarity, neurosensory abnormalities, and ocular surface inflammation and damage (Craig et al., 2017).

The authors of the TFOS DEWS II Definition and Classification Report (Craig et al., 2017) also recognized the multifactorial character of the disease, in which the main cause is the loss of homeostasis of the tear film. The multifactorial character of the disease challenges clinicians, making the collaboration between professions vital in the assessment of DED (Remeseiro et al., 2016; Craig et al., 2017). Thus, several risk factors

have been identified to be associated with DED such as age, sex, hormones, lifestyle, environment, medical history, systemic and topical medications, ocular surgery or contact lens wear (Yang et al., 2015; Stapleton et al., 2017; Wang et al., 2020; Wang et al., 2021).

1.2.2 Epidemiology

TFOS DEWS II Epidemiology Report argued that DED has a prevalence between 5 and 50 % (Stapleton et al., 2017). The authors reported that prevalence based on signs alone was generally higher and more variable than the prevalence based on symptoms, reaching up to 75 % in some populations. This wide range of prevalence is due to the different populations studied, diagnostic methods, geography, age, sex and the lack of a global consensus between studies in the criterion of diagnosis (Stapleton et al., 2017; Wang et al., 2020).

The prevalence of the disease is increasing due to the rise of refractive surgeries, the ageing of the population and the increasing use of contact lenses and visual displays (Bron et al., 2017; Stapleton et al., 2017). Likewise, the current lifestyle exposes millions of people in the world to artificial environments with low humidity and high airflow, which can increase tears evaporation and intensify the signs and symptoms of DED (Alex et al., 2013; Tesón et al., 2013; López-Miguel et al., 2014; Bron et al., 2017; Stapleton et al., 2017).

The literature revealed that consistent risk factors for DED were ageing, female sex (although differences between sexes generally become significant only with increasing age due to hormonal changes), Asian race, Meibomian Gland Dysfunction (MGD), connective tissue diseases, Sjögren syndrome, androgen deficiency, computer

use, contact lens wear, hormone replacement therapy, hematopoietic stem cell transplantation, medication such as antihistamines, antidepressants, anxiolytics or isotretinoin, and factors related to the environment such as pollution, low humidity or sick building syndrome. Nevertheless, very few of the current studies included young patients in the analysis (Stapleton et al., 2017).

Also, the TFOS DEWS II Epidemiology Report (Stapleton et al., 2017) highlighted that some of the listed risk factors are still probable or inconclusive, and there is still no clear evidence that most of them induce DED: refractive surgery, diabetes, rosacea, viral infection, thyroid disease, psychiatric conditions, pterygium, low fatty acids intake, allergic conjunctivitis, Hispanic ethnicity, menopause, acne, sarcoidosis, smoking, alcohol, pregnancy, Demodex infestation, botulinum toxin injection and medications such as anticholinergics, diuretics, beta-blockers, multivitamins or oral contraceptive (Yao et al., 2011; Stapleton et al., 2017).

Furthermore, most of the published studies have differences in the methodology adopted and in the criterion followed to diagnose DED, which makes their direct comparison and the building of global conclusions challenging (Stapleton et al., 2017; Wolffsohn et al., 2017; Wang et al., 2020; Wang et al., 2021). In the report (Stapleton et al., 2017), the authors argued that there is still a considerable lack of information about risk factors for DED and that the implementation of studies to assess such factors in different geographic regions is required. Thus, further studies following the recommendation of the TFOS DEWS II Diagnostic Methodology Report (Wolffsohn et al., 2017) are needed to assess the prevalence and risk factors for DED.

There are only two studies (Wang et al., 2020; Wang et al., 2021) that have assessed DED risk factors following the TFOS DEWS II guidelines for the diagnosis of DED. Authors found that age, East Asian ethnicity, migraine headaches, systemic rheumatologic disease, thyroid disease, use of antidepressant medication, oral contraceptive therapy, digital screen exposure and reduced caffeine consumption were factors independently associated with DED.

1.2.3 Symptoms and quality of life

The main symptoms of DED are visual disturbances, blurry vision, ocular discomfort, damage of the ocular surface, feeling of grit in the eyes, foreign body sensation, photophobia and, paradoxically, excessive tearing in some cases (Craig et al., 2017). Different studies have also demonstrated that DED patients have also decreased quality of life (Yao et al., 2011; Paulsen et al., 2014; Mertzanis et al., 2015; Craig et al., 2017), and psychological problems such as anxiety, stress or depression (Labbé et al., 2013; Hallak, Tibrewal and Jain, 2015). DED patients can also suffer from ocular fatigue and difficulties in reading and driving at night (Lemp, 2008). Moreover, the high cost of the treatment and the work productivity losses cause a highly negative socioeconomic impact (Clegg et al., 2006; Uchino et al., 2014; Craig et al., 2017).

1.2.4 Dry eye disease classification

The purpose of dry eye classification is to guide the diagnosis and follow-up of DED patients through appropriate treatments. DED can be classified as aqueous deficient dry eye (ADDE), which may or may not be associated with Sjögren syndrome; and

evaporative dry eye (EDE), which is more frequent and can be subclassified as intrinsic or extrinsic (Yao et al., 2011; Craig et al., 2017; Wolffsohn et al., 2017).

However, the TFOS DEWS II Definition and Classification Report (Craig et al., 2017) argued that this classification has some issues. The authors of the report preferred to remove any perception of exclusivity in the DED classification because ADDE and EDE are merged in advanced stages of the disease, being both types a continuum instead of separate subtypes. For instance, ADDE causes tear film thickness reduction, which affects tear film lipid layer spreading and might cause EDE. Likewise, severe EDE might cause afferent corneal nerve impairment, which could reduce the sensitivity of the ocular surface and cause ADDE (Bron et al., 2017; Stapleton et al., 2017). Moreover, other conditions can be confounded with DED. For that reason, the TFOS DEWS II Definition and Classification Report defined DED as the presence of signs and symptoms of dry eye (*Figure 1.1*) (Craig et al., 2017).

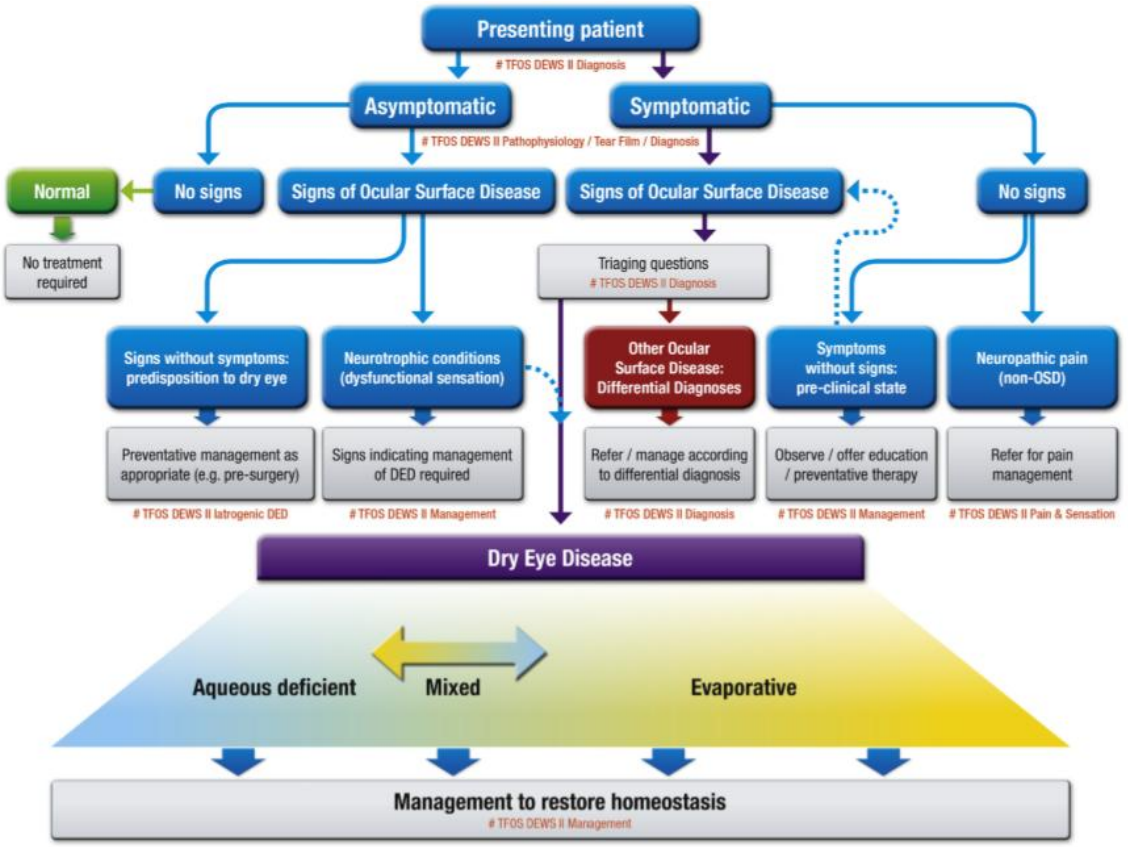

Fig. 1.1. *Classification of dry eye disease (Craig et al., 2017).*

The DED definition recognizes the necessity of dry eye symptoms and associated ocular surface signs in making a diagnosis (Craig et al., 2017; Wolffsohn et al., 2017). Symptoms without signs could be due to neuropathic pain, which is caused by an injury or a disease in the somatosensory system. This is an important distinction in the diagnosis because the required pain management falls outside the scope of DED therapy (Craig et al., 2017; Belmonte et al., 2017; Wolffsohn et al., 2017). Besides, symptoms without signs might also mean a pre-clinical dry eye state. In this case, the clinician can educate the patient to identify modifiable risk factors of DED, use ergonomics and preventive therapy. On the other hand, the presence of signs without symptoms could be due to reduced corneal sensitivity (neurotrophic conditions).

Corneal nerve damage secondary to DED is recognized to reduce corneal sensitivity and this can mask discomfort. Finally, signs without symptoms could also be a predisposition to DED, in which preventive management is appropriate (Craig et al., 2017).

1.2.5 Pathophysiology

The lacrimal function unit is constantly dealing with external factors that can jeopardize the tear film homeostasis and cause an inflammatory cascade. Tear hyperosmolarity along with tear instability have been recognized to be the main drivers of DED (Bron et al., 2017).

Tear hyperosmolarity cannot occur without evaporation. Actually, both subtypes of DED can be considered evaporative since evaporation is present in both of them. In ADDE, tear hyperosmolarity results when lacrimal secretion is reduced and the evaporation is normal; while in EDE, hyperosmolarity is caused by excessive evaporation of the tear film (Bron et al., 2017).

Evaporation increases the solute concentration of the tear film, which causes hyperosmolarity. This leads to surface desiccation and a chain of inflammatory events, which is an entry point into a vicious circle that aggravates the DED state. Any aetiology of DED has one or more entry points into the vicious circle (*Figure 1.2*) (Bron et al., 2017).

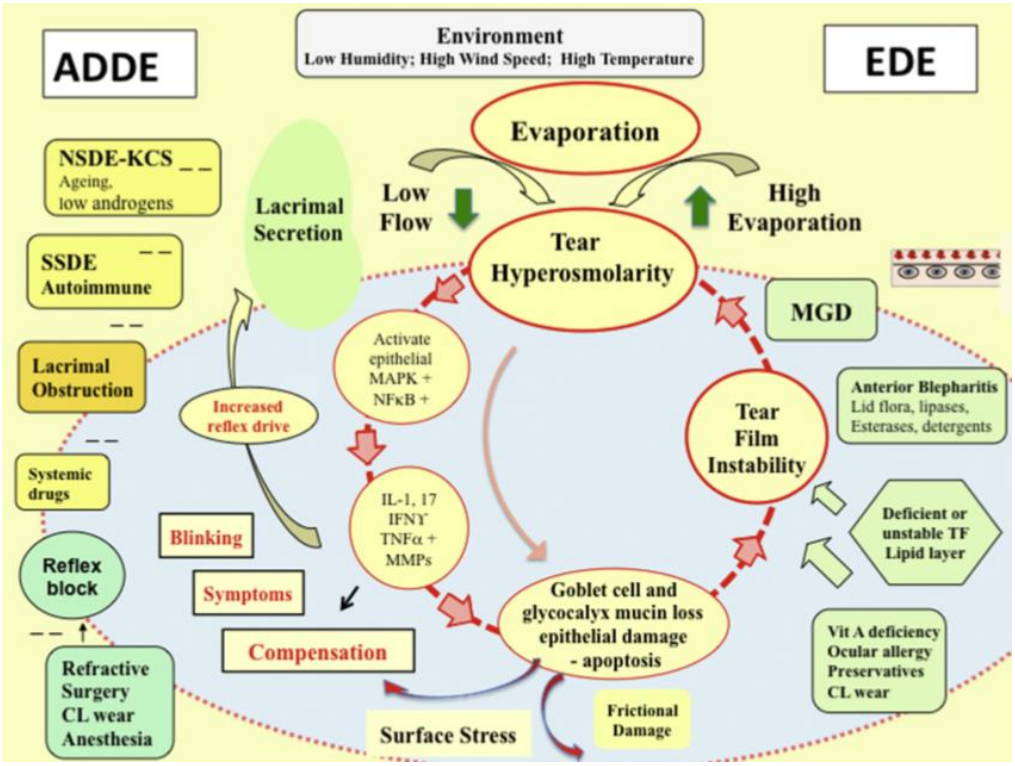

Fig. 1.2. *The vicious circle of DED (Bron, 2015; Bron et al., 2017).*

Hyperosmolarity is considered the hallmark of the disease. Tear hyperosmolarity stimulates a cascade of events in epithelial cells of the eye, involving MAP kinases, NF-$_{K}$B signalling pathways and inflammatory cytokines (IL-1, IL-1α, IL-1β), tumour necrosis factor-α and proteases, such as MMP9 (Gupta et al., 1996; Li et al., 2001; Li et al., 2006; Chotikavanich et al., 2009; Chen et al., 2011b; Zhang et al., 2012; Stern, Schaumburg and Pflugfelder, 2013; Coursey et al., 2014; Bonaccorsi et al., 2015; Bron et al., 2017). These inflammatory mediators, together with hyperosmolarity, lead to a reduced expression of the glycocalyx mucins, disrupt the epithelial corneal barrier, and cause cell stress and damage of the ocular surface. All of this causes apoptosis of epithelial cells. Damage is reinforced by inflammatory mediators from activated T-cells, recruited to the ocular surface. Cell apoptosis aggravates the vicious circle due to the

loss of cells that secrete lacrimal compounds. Moreover, when a cell dies more inflammatory cells are generated.

Goblet cell loss is a feature of every form of DED because it reduces the levels of MUC5AC (Bron et al., 2017). Likewise, altered expression of glycocalyx mucins causes ocular surface staining and alters ocular surface wetting, leading to instability of the tear film and early tear film break-up. This aggravates hyperosmolarity and completes the vicious circle. The treatment of the disease should be focused on breaking the vicious circle to restore the tear film stability and ocular surface health (Bron et al., 2017).

The alteration of the tear film increases friction between eyelids and the ocular surface. Frictional damage stimulates corneal nerve endings and mechano-nociceptors, which cause symptoms of discomfort, increased blink rate, and increased lacrimal secretion due to compensatory reflex (Bron et al., 2017). This also secrets neuropeptides, which leads to neurogenic inflammation, nerve growth factor liberation and promotes nerve regeneration (Baudouin et al., 2017; Bron et al., 2017). Moreover, the evaporation of the tear film causes cooling in the ocular surface, which causes discomfort through the activation of cold thermoceptors. They increase the lacrimal secretion and blinking rate (Nakamori et al., 1997; Wu et al., 2014b; Belmonte et al., 2017; Bron et al., 2017;). However, prolonged stress can cause the loss of corneal sensitivity, which can modify the composition of the tear film (Bron et al., 2017).

Tear film instability can also be initiated without the prior existence of hyperosmolarity. As reported in the Epidemiology section, a wide range of environmental, lifestyle or medical conditions can trigger inflammatory cascades leading to DED. For instance, some of the conditions that can cause tear instability are xerophthalmia, ocular allergy, topical preservative use or contact lens wear. EDE can be caused by a deficient or unstable lipid layer, MGD or eyelid pathologies like anterior blepharitis. Besides, low tear secretion in ADDE can be caused by a sensory reflex block, which can be initiated by trigeminal nerve damage in refractive surgery, contact lens wear, topical anaesthetics or systemic drugs such as antihistamines, beta-blockers, antispasmodics, diuretics and some psychotropic drugs. Other causes may include a lacrimal obstruction, which can occur in any form of cicatricial conjunctival diseases such as trachoma, erythema multiforme, graft-versus-host disease and chemical burns. Inflammatory infiltration of the lacrimal gland is the most common cause of ADDE, which causes both acinar and ductal epithelial cell dysfunction and neurosecretory block (Bron et al., 2017; Stapleton et al., 2017). Despite these different entry points to the vicious circle, all of them share a common inflammatory pathway leading to ocular surface damage.

1.2.6 Dry eye disease diagnosis

DED diagnosis is still challenging due to its multifactorial aetiology, the lack of a gold standard metric and the low agreement between DED signs and symptoms (Nichols, Mitchell and Zadnik, 2004; Bartlett et al., 2015; Geerling et al., 2017; Wolffsohn et al., 2017). DED diagnosis is even more challenging in the early stages of DED due to the poor repeatability of diagnostic tests (Sullivan et al., 2012b), low

diagnostic capability (high rates of false positives and false negatives) (Tomlinson et al., 2006; Sullivan, 2014) and the influence of external factors in the tear film metrics (Savini et al., 2008). Nowadays, DED diagnosis is based on a combination of symptoms described by the patient and a battery of clinical tests. However, the majority of these tests are inconsistent and they do not agree with each other (Craig et al., 2017; Wolffsohn et al., 2017). At the same time, this complicates the development of new methods, metrics or markers because there is no test of reference to correctly diagnose the disease (Wolffsohn et al., 2017).

The TFOS DEWS II Diagnostic Methodology Report (Wolffsohn et al., 2017) recommended a diagnostic approach to diagnose DED (*Table 1.1*). First of all, it is important to exclude cases that can be confused with DED through different triaging questions. Evaluation of risk factors is also important. In the report, authors argued that a subject is classified as DED when has symptoms of dryness in at least one questionnaire (Dry Eye Questionnaire-5 (DEQ-5) ≥ 6 or Ocular Surface Disease Index (OSDI) ≥ 13) and at least a sign of loss of the tear film homeostasis (hyperosmolarity, low Non-Invasive Break-Up Time (NIBUT) or ocular surface staining). The typical staining of DED is punctate epitheliopathy.

Further examinations could be carried out to classify the DED. Thus, meibography, tear volume measurements or lipid layer metrics can be used to classify the DED into ADDE, EDE or mixed DED. In this way, clinicians can determine the severity of the disease and where the DED falls on the spectrum between ADDE and EDE. It is important to take into account that the diagnostic tests should be performed from the

less to the most invasive so that tear film is not destabilized and to avoid reflex tearing (Wolffsohn et al., 2017).

Table 1.1. *Diagnosis of dry eye disease according to the TFOS DEWS II Diagnostic Methodology Report (Wolffsohn et al., 2017).*

Diagnosis			Criterion
DED	OSDI ≥ 13 /o/ DEQ-5 ≥ 6	+ at least 1	• NIBUT < 10 seconds • Osmolarity ≥ 308 mOsm/L in either eye • Interocular osmolarity difference > 8 mOsm/L • Corneal staining > 5 spots • Conjunctival staining > 9 spots • Lid margin staining ≥ 2 mm length y ≥ 25 % width
ADDE	Criterion of DED	+	• TMH ≤ 0.20 mm
EDE	Criterion of DED	+	• Abnormal lipid layer • MGD

(Where ADDE: Aqueous Deficient Dry Eye; DED: Dry Eye Disease; DEQ-5: Dry Eye Questionnaire-5; EDE: Evaporative Dry Eye; MGD: Meibomian Gland Dysfunction; mOsm/L: milliosmoles per litre; NIBUT: Non-Invasive Break-Up Time; OSDI: Ocular Surface Disease Index; and TMH: Tear Meniscus Height)

1.3 Imaging techniques to assess the tear film

There are different tests to assess the tear film. However, there is a lack of correlation between them, which makes the diagnosis of DED difficult (Lemp, 2008; Sullivan et al., 2012b; Zhang et al., 2012). Besides, the tear film is highly dynamic and may be influenced by many internal and external factors (Wang, Palakuru and Aquavella, 2008).

The techniques can be divided into invasive and non-invasive, and in turn into objective and subjective. Subjective techniques depend on the examiner's ability, which might increase the variability and reproducibility of results (Kottaiyan et al., 2012). Likewise, invasive techniques can disturb the tear film, induce reflex tearing and

alter the results of the test. Thus, invasive tests such as the Schirmer tests, Break-Up Time (BUT) using fluorescein, or fluorescein-stain Tear Meniscus Height (TMH) measurements are limited by their invasive nature (Hosaka et al., 2011; Wolffsohn et al., 2017).

In light of the above, the TFOS DEWS II Diagnostic Methodology Report recommended the use of non-invasive and as objective as possible techniques to assess the tear film (Wolffsohn et al., 2017). New image systems that evaluate the anterior segment of the eye in a non-invasive way, such as corneal topographers, optical coherence tomography (OCT) systems or confocal microscopes, have high potential in this field (Lemp, 2008; Palakuru, Wang and Aquavella, 2008; Yuan et al., 2010; Varikooty, Keir and Simpson, 2012; Celik et al., 2013; Fukuda et al., 2013; Foulks and Pflugfelder, 2014; Abdelfattah et al., 2015; Ji et al., 2017; Wolffsohn et al., 2017; Llorens-Quintana., 2018; Llorens-Quintana., 2019a).

Thus, the development of ocular imaging systems has improved the repeatability, objectivity and diagnostic ability of the tests to detect DED (Goto et al., 2004a; Chan et al., 2017; Wolffsohn et al., 2017). However, the cost is a common drawback of these new technologies (McGinnigle, Naroo and Eperjesi, 2012). *Table 1.2* shows the benefits and drawbacks of invasive techniques in comparison with non-invasive imaging techniques to assess the tear film (Goto et al., 2004a; Hosaka et al., 2011; Kottaiyan et al., 2012; McGinnigle, Naroo and Eperjesi, 2012; Foulks and Pflugfelder, 2014; Chan et al., 2017; Wolffsohn et al., 2017).

Table 1.2. *Advantages and disadvantages of invasive techniques in comparison with non-invasive imaging techniques to assess the tear film.*

Invasive techniques		Non-invasive techniques	
Advantages	Disadvantages	Advantages	Disadvantages
Cheaper cost	Invasiveness	Non-invasiveness	More expensive
Availability in any clinic	Less patient-friendly	More patient-friendly	It is not always available in any clinic
	They might destabilize the tear film – Unreal measurement	Measure the tear film under more real conditions	
	Poor repeatability and reproducibility	Higher repeatability and reproducibility	
	Generally, more time to perform the technique	Generally, testing is faster	
	Generally, depends more on the examiner's ability	Generally, depend less on the examiner's ability (if the device has software)	

Techniques to assess the tear film can be divided into two types depending on whether they assess the quantity or the quality of the tear film.

1.3.1 Imaging techniques to assess the quantity of the tear film

1.3.1.1 Tear meniscus measurements

Tear meniscus is a concave reservoir of tears at the lower and upper eyelid margins from which the tear film is formed after a blink. The majority of tears are contained in the tear meniscus; therefore, their quantitative assessment is the most direct method to assess the tear film volume (Tiffany, 2006; McGinnigle, Naroo and Eperjesi, 2012; Wolffsohn et al., 2017).

Tear meniscus can be measured by a slit-lamp, reflective meniscometry, pachymetry, corneal topography devices, interferometers or OCT (Oguz, Yokoi and Kinoshita, 2000; Yokoi et al., 2004; Johnson and Murphy, 2005; Santodomingo-Rubido, Wolffsohn and Gilmartin, 2006a; Uchida et al., 2007; Wang, Palakuru and Aquavella,

2008; Zhou et al., 2009). Generally, non-invasive meniscometry techniques are quick and useful ways to assess the quantity of tear film, especially OCT. These techniques may be useful in the development of new diagnostic metrics, which would be less invasive, quicker, and more reliable to detect DED and help in the evaluation of the efficacy of treatments (Wang, Palakuru Aquavella, 2008; Yuan et al., 2010; Zhang et al., 2011; Czajkowski et al., 2012; Kottaiyan et al., 2012; Tung et al., 2012; Fukuda et al., 2013; Werkmeister et al., 2013; Foulks and Pflugfelder, 2014; Akiyama, Usui and Yamagami, 2015; Eroglu, Karalezli and Dursun, 2016; Bai and Nichols, 2017; Chan et al., 2017; Gumus and Pflugfelder, 2017; Thulasi and Djalilian, 2017).

1.3.1.1.1 Slit-lamp

The assessment of the tear meniscus using a slit-lamp is the most accessible tool for clinicians; nevertheless, this is a very subjective method and depends on the clinician´s ability (Fodor et al., 2010; Arita et al., 2020). A graticule can be placed to increase its objectivity and to quantify the TMH (Santodomingo-Rubido, Wolffsohn and Gilmartin, 2006a; Hosaka et al., 2011; Imamura et al., 2017; Alshammeri et al., 2019). Imamura et al. (2017) found that TMH measured with slit-lamp and a graticule was lower than when it was measured using swept-source optical coherence tomography. However, both methods were highly reproducible and repeatable.

The distance between the darkest edge of the lower eyelid and the upper limit of the tear meniscus is the absolute TMH; while the distance between the darkest edge of the lower eyelid and the brightest reflex of the tear meniscus is the relative TMH

(Santodomingo-Rubido, Wolffsohn and Gilmartin, 2006a). One study found significant differences between both metrics ($p < 0.0001$) (García-Resúa et al., 2009).

Likewise, a camera can be attached to a slit-lamp, which allows the measurement of pixels in the image to subsequently convert these values to millimetres (Doughty, Laiquzzaman and Button, 2001). Some authors have also instilled fluorescein to increase the contrast of the tear meniscus. Nonetheless, fluorescein can disrupt the tear film and increase the TMH (Patel et al., 1985; Lekhanont et al., 2019). Lam et al. (2019) found that applying fluorescein through a strip might overestimate TMH 0.03 mm. However, applying fluorescein at the bulbar or palpebral conjunctiva did not affect TMH.

1.3.1.1.2 Reflective meniscometry

Earlier, reflective meniscometry was used to quantitatively measure the Tear Meniscus Radius (TMR) in a non-invasive way using a videomeniscometer. This method is based on the specular reflection of a target onto the central tear meniscus. The target has a series of horizontal stripes (4 blacks and 5 white stripes). The specularly reflected image is recorded by a digital video recorder, allowing the measurement of TMR through the concave mirror formula (Yokoi et al., 1999; Oguz, Yokoi and Kinoshita, 2000; Yokoi et al., 2004; Yokoi et al., 2017). For instance, Oguz, Yokoi and Kinoshita (2000) assessed the tear meniscus using a videomeniscometer and found a significant positive correlation between TMR and TMH. Yokoi et al. (2004) found that TMR increased with the volume of the artificial drop instilled.

1.3.1.1.3 Pachymetry

Pachymetry also allows measuring non-invasively the TMH, although this method is less widely used. A pachymeter is attached to a slit-lamp and it provides two images. In this way, TMH is measured by aligning the superior part of the first image with the lower part of the second image. Thus, the angular separation between them is directly proportional to TMH (Johnson and Murphy, 2005).

1.3.1.1.4 Corneal topography systems

Some corneal topographers also include a tool that allows assessing the TMH in an objective and non-invasive way (Choi et al., 2018; Xie et al., 2018; Zang et al., 2018; Kim et al., 2019; Wang et al., 2019b; Lee et al., 2020b; Li et al., 2020a; Li et al., 2020b; Llorens-Quintana, Garaszczuk and Szczesna-Iskander, 2020; Talens-Estarelles et al., 2020; Yuan et al., 2020; Chen et al., 2021; Duong et al., 2021; Li et al., 2021). The measurement is similar to the measurement with a slit-lamp using a photograph. Examiner has to delineate the tear meniscus borders and the software calculates the height of the tear meniscus (Figure 1.3). It has some advantages like a short evaluation time and the use of infrared light. This prevents reflex tearing, eliminates the need for calibration of magnification and the use of fluorescein (Baek, Doh and Chung, 2015).

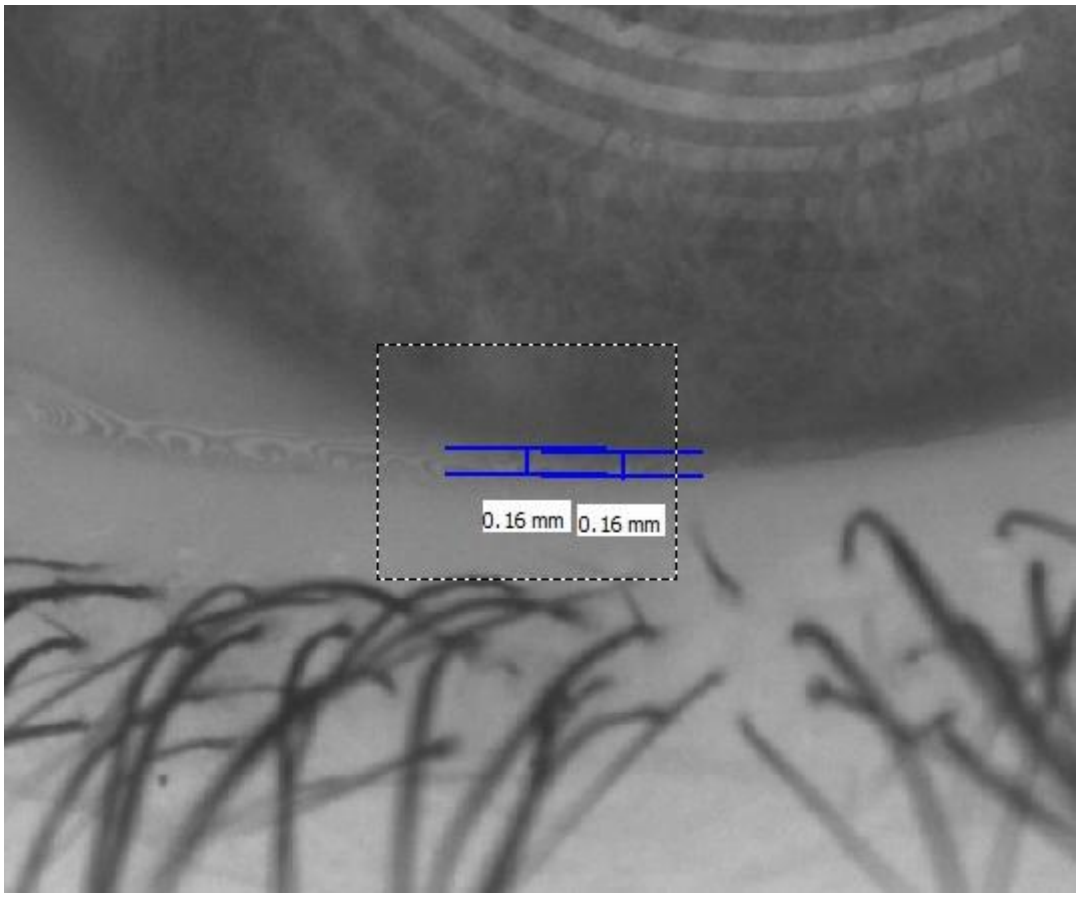

Fig. 1.3. *Measurement of the tear meniscus height using a videokeratograph.*

Some authors have found differences in TMH between healthy and DED subjects (Koh et al., 2016; Kim et al., 2019; Wang et al., 2019b) and between symptomatic and asymptomatic contact lens wearers (Siddireddy et al., 2018a) using corneal topographers. This suggests that this technique can be used by clinicians to non-invasively assess the tear meniscus to help in DED diagnosis. Moreover, TMH was correlated with dry eye symptoms, BUT using fluorescein, Schirmer test and corneal staining (Baek, Doh and Chung, 2015; Siddireddy et al., 2018a). Nevertheless, Zang et al. (2018) did not find significant differences in TMH between Sjögren syndrome subjects and non-Sjögren syndrome ADDE subjects. Likewise, Kim et al., 2019 neither found differences in TMH between controls and MGD patients.

Corneal topographers have also been useful to assess the effect on tear meniscus of contact lenses (Siddireddy et al., 2018a; García-Montero et al., 2019a; García-Montero et al., 2019b; Wang et al., 2019a; Llorens-Quintana, Garaszczuk and Szczesna-Iskander, 2020; Martínez-Alberquilla et al., 2020; Duong et al., 2021), blinking (Kim et al., 2020), diseases (He et al., 2018; Zang et al., 2018), treatments (Ren et al., 2018; Ge et al., 2020; Li et al., 2020a; Wu et al., 2020b; Chen et al., 2021), visual displays (Choi et al., 2018; Golebiowski et al., 2020; Talens-Estarelles et al., 2020) or surgical procedures (Zhong et al., 2018; Recchioni et al., 2020) (*Table 1.3*).

Topographic devices have been compared with OCT in the tear meniscus measurement (*Table 1.4*). Thus, Baek, Doh and Chung (2015) found lower values of TMH when it was measured with a videokeratograph than with OCT (23.8 % lower); however, a correlation between both devices was found ($r^2 = 0.359$). These differences might be because OCT has higher resolution and provides cross-sectional images, which allows more accurate measurements. Moreover, the nature of both techniques and imaging processing was different. Images also suffer from fan and optical distortions. The sagittal image provided by OCT can also affect the results. Besides, the shorter time of examination and infrared light used in videokeratographs can eliminate reflex tearing leading to differences between devices (Ortiz et al., 2011; Arriola-Villalobos et al., 2015; Baek, Doh and Chung, 2015). Conversely, Arriola-Villalobos et al. (2015) did not find statistical differences between both devices in TMH ($p=0.35$), but the correlation between devices was poor. Additionally, Lam et al. (2019) also reported that the Keratograph 5M and OCT provided similar TMH results.

Table 1.3. *Results reported by different authors regarding the use of corneal topographers to assess the effect on tear meniscus of contact lenses, diseases, treatments, visual displays and surgical procedures.*

Study	Sample	Age (mean ± SD) years	Technique	Tear meniscus measurements (mean ± SD)	Main findings
García-Montero et al. (2019a)	15 subjects	24.1±2.2	Keratograph 5M	TMH Baseline Lotrafilcon A: 0.27±0.12 mm Samfilcon A: 0.30±0.08 mm Comfilcon A: 0.28±0.11 mm Filcom V3: 0.30±0.12 mm TMH 15 days Lotrafilcon A: 0.25±0.08 Samfilcon A: 0.29±0.08 Comfilcon A: 0.24±0.06 Filcom V3: 0.29±0.06	-TMH did not change for any CL over 15 days
He et al. (2018)	120 subjects (120 eyes): 44 diabetics <5 years, 40 diabetics between 5-10 years, 36 >10 years and 40 healthy.	Control: 64.88±7.04 <5 years: 64.75±8.20 5-10 years: 65.03±7.14 >10 years: 66.11±7.44	Keratograph 5M	TMH Control: 0.23±0.06 mm TMH <5 years: 0.23±0.05 mm TMH 5-10 years: 0.21±0.07 mm TMH >10 years: 0.18±0.06 mm	-TMH was shorter in long-term type 2 diabetes
Wang et al. (2019a)	59 myopic subjects (59 eyes)	12.03±2.31	Keratograph 5M	TMH baseline: 0.22±0.06 mm TMH 1 month: 0.25±0.05 mm TMH 6 months: 0.24±0.06 mm TMH 24 months: 0.24±0.04 mm	-Overnight orthokeratology affected TMH
Chen et al. (2021)	100 MGD subjects (100 eyes) (35 had a combined therapy)	45.10±4.81	Keratograph 5M	(Median (IQR)) TMH baseline: 0.19(0.15,0.24) TMH 1 month: 0.20(0.15,0.22) TMH 3 months: 0.22(0.16,0.23)	-Although the combination of meibomian gland expression and intense pulsed light had a synergistic effect, no changes were found in TMH
Li et al. (2020a)	25 hyposecretory MGD subjects (25 eyes) and 25 obstructive MGD subjects (25 eyes)	Hyposecretory MGD: 32.6±10.26 Obstructive MGD: 37.2±11.74	Keratograph 5M	TMH Hyposecretory Baseline: 0.19±0.09 mm 8 weeks: 0.22±0.09 mm TMH Obstructive Baseline: 0.19±0.11 mm 8 weeks: 0.28±0.11 mm	-TMH increased in both groups after treatment -Thermal pulsation LipiFlow was effective for both MGD types -The therapeutic effect was higher in the obstructive MGD group
Llorens-Quintana, Garaszczuk and Szczesna-Iskander (2020)	41 CL wearers (41 eyes)	Experienced: 24±5 Unexperienced: 25±4	Keratograph 5M	TMH Baseline: 0.24±0.05 mm TMH 12 months: 0.23±0.06 mm	-No differences were wound in CL wearers between baseline and 12 months in TMH

(continuation)					
Study	Sample	Age (mean ± SD) years	Technique	Tear meniscus measurements (mean ± SD)	Main findings
Choi et al. (2018)	50 smartphone 30 controls	Smartphone: 23.52±2.92 Controls: 26.70±2.98	Keratograph 5M	TMH smartphone: 0.20±0.05 mm TMH controls: 0.21±0.05mm	-TMH did not show statistically significant differences between groups
Ge et al. (2020)	25 patients with conventional cataract surgery (25 eyes) and 22 with optimal pulsed technology (22 eyes)	Conventional: 65.8±8.1 Pulsed: 63.48±8.47	Keratograph 5M	Meiboscore (Median (IQR)) Conventional group Baseline: 0.18±0.03 mm 3 months: 0.20±0.02 mm Optical pulsed treatment group Baseline: 0.18±0.31 mm 3 months: 0.19±0.02 mm	-There were significant differences in TMH before and 3 months after surgery in the optical pulsed treatment group -Cataract surgery aggravated MGD
Recchioni et al. (2020)	16 LASIK subjects (16 eyes) and 13 SMILE subjects (13 eyes)	LASIK: 32.6±9.1 SMILE: 32.2±5.3	Keratograph 5M	TMH Pre-LASIK: 0.32±0.13 Post-LASIK: 0.22±0.09 Pre-SMILE: 0.30±0.07 Post-SMILE: 0.33±0.08	-LASIK caused a significant decrease in TMH in comparison with SMILE
Wu et al. (2020)	62 MGD subjects (124 eyes) (29 subjects in the optimal IPL group and 33 in the regulated IPL)	Optimal: 48.72±13.99 Regulated: 54.79±14.79	Keratograph 5M	(Median (IQR)) TMH Baseline Optimal: 0.19(0.08) mm TMH Baseline Regulated: 0.17(0.09) mm TMH 3 months Optimal: 0.22(0.04) mm TMH 3 months Regulated: 0.19(0.04) mm	-IPL has clinical value in the treatment of MGD; however, no differences were found in TMH

(Where CL: Contact Lens; IPL: Intense Pulsed Light; IQR: Interquartile range; LASIK: Laser-Assisted In Situ Keratomileusis; MGD: Meibomian Gland Dysfunction; SD: Standard Deviation; SMILE: Small Incision Lenticule Extraction; TMH: Tear Meniscus Height)

Table 1.4. *Comparison of corneal topography systems with OCT in the tear meniscus assessment.*

Study	Sample	Age (mean ± SD) years	Technique	Tear meniscus height (mean ± SD)	Main findings
Baek, Doh and Chung (2015)	64 ADDE patients (64 eyes)	62.3±13.5	Fourier-domain OCT (RTVue-100) and Keratograph 5M	OCT examiner 1: 0.308±0.136 mm OCT examiner 2: 0.308±0.129 mm K5M examiner 1: 0.233±0.077 mm K5M examiner2: 0.230±0.074 mm	-Keratograph values tended to be lower -TMH measured with Keratograph was correlated with TMH measured with OCT
Arriola-Villalobos et al. (2015)	29 eyes of healthy patients	34.28±9.24	Keratograph 5M and Spectralis Fourier-domain OCT	K5M observer 1: 240.34±67.16 and 235.52±59.50 µm K5M observer 2: 237.24±81.15 and 233.10±69.65 µm OCT observer 1: 246.10±75.16 and 239.86±68.83 µm OCT observer 2: 243.55±69.92 and 243.41±73.13 µm	-No statistical differences were found between devices -The correlation between devices was poor -Fourier-domain OCT was more reliable
Lam et al. (2019)	41 healthy subjects (41 eyes)	21.2±1.3	CASIA SS-1000 OCT and Keratograph 5M	TMH baseline K5M: 0.248±0.053 mm TMH baseline OCT: 0.254±0.051 mm TMH bulbar K5M: 0.274±0.067 mm TMH bulbar OCT: 0.277±0.058 mm TMH palpebral K5M: 0.264±0.063 mm TMH palpebral OCT: 0.268±0.061 mm	-The Keratograph and OCT provided similar TMH results -Applying fluorescein through a strip might overestimate TMH (0.03 mm) -Applying fluorescein at bulbar or palpebral conjunctiva did not affect TMH

(Where ADDE: Aqueous Deficient Dry Eye; OCT: Optical Coherence Tomography; SD: Standard Deviation; TMH: Tear Meniscus Height)

Regarding the repeatability of TMH using topographic devices, Tian et al. (2016) found acceptable repeatability and reproducibility of TMH using a videokeratograph. However, TMH was less reliable in DED patients. Baek, Doh and Chung (2015) also found good repeatability and reliability in the TMH measurement using a

videokeratograph and OCT. García-Montero et al. (2019b) found that TMH measured with the Keratograph 5M had excellent repeatability before and after contact lens wear. Nonetheless, Arriola-Villalobos et al. (2015) found that the repeatability and reproducibility of a videokeratograph were poor in the tear meniscus measurements, concluding by saying that Fourier-domain OCT was more reliable than videokeratograph in the measurement of lower TMH. Further studies are needed to better understand the agreement between both devices. *Table 1.5* shows the main results of the studies that assessed the repeatability of TMH using corneal topography devices.

Table 1.5. *Results of main studies that assessed the repeatability of TMH using corneal topography devices.*

Study	Type of repeatability	S_w	CoV (%)	CoR	ICC
Tian et al. (2016)	Intraexaminer		Healthy: 18.89 DED: 15.96	Healthy: 0.14 mm DED: 0.11 mm	Healthy: 0.84 DED: 0.76
	Interexaminer		Healthy: 19.76 DED: 16.08	Healthy: 0.14 mm DED: 0.11 mm	-
Baek, Doh and Chung (2015)	Intraexaminer	Examiner 1: 0.015 mm Examiner 2: 0.015 mm	Examiner 1: 6.43 Examiner 2: 6.53	Examiner 1: 0.041 mm Examiner 2: 0.042 mm	Examiner 1: 0.987 Examiner 2: 0.986
	Interexaminer	0.0129 mm	5.58	0.0358 mm	0.985
García-Montero et al. (2019b)	Intraexaminer	Baseline: 0.02 mm 8 hours CL: 0.02 mm	Baseline: 8.03 8 hours CL: 9.22	Baseline: 0.06 mm 8 hours CL: 0.06 mm	Baseline: 0.95 8 hours CL: 0.90
Arriola-Villalobos et al. (2015)	Intraexaminer	49.32 µm	21	136.62 µm	0.79
	Interexaminer	58.13 µm	0.24	161.02 µm	0.70

(Where CL: Contact Lens; CoR: Repeatability Coefficient; CoV: Coefficient of Variation; DED: Dry Eye Disease; ICC: Intraclass Correlation Coefficient; S_w: within-subject standard deviation)

1.3.1.1.5 Interferometers

Interferometers also allow imaging of the tear meniscus non-invasively when the clinician focuses on the lower lid margin. It can be measured subjectively or by analysing the image using software (Uchida et al., 2007; Fodor et al., 2010; Hosaka et al., 2011; Pena-Verdeal et al., 2016; Tong and Teng, 2018; Arita and Fukuoka, 2020). Some authors (Uchida et al., 2007; Hosaka et al, 2011) have found lower TMH in subjects with DED in comparison to controls using interferometers. Moreover, Uchida et al. (2007) used an interferometer to assess the effect on tear meniscus of punctual occlusion in Sjögren syndrome subjects.

Regarding repeatability and agreement with other devices, Pena-Verdeal et al. (2016) found that TMH measured using an interferometer and ImageJ tool had low interobserver variability. Moreover, interferometer meniscus values had good concordance with a subjective grading scale. Fodor et al. (2010) claimed that TMH measured with slit-lamp could be reliable, but the measurement with Tearscope was more repeatable. Regarding the diagnostic capability, Yamaguchi et al. (2016) found a sensitivity of 0.84 and a specificity of 0.91 with a cut-off value of 0.22 mm with the interferometer DR-1α. Moreover, Arita et al. (2019) found a sensitivity of 0.73 and a specificity of 0.75 with a cut-off value of 180 μm, using the same interferometer.

1.3.1.1.6 Optical coherence tomography

Anterior segment OCT is the most important advance and the most promising technique in the assessment of the tear meniscus (Gumus and Pflugfelder, 2013; Gumus and Pflugfelder, 2017). OCT is an optical non-invasive device, which allows

obtaining high-resolution, cross-sectional images by low coherence interference of the waves. OCT analyses the light reflected on different structures of the eye, including the tear film, and obtains high-resolution images of the tear meniscus in real-time and under natural conditions (Fukuda et al., 2013).

OCT creates images through the compilation of A-scans. An A-scan provides information about the depth of the sample, while a B-scan (cross-sectional tomography) is obtained by linear addition of A-scans and provides two-dimensional images. Different B-scans form C-scans, which are three-dimensional images (Cerviño, García-Lázaro and Montés-Micó, 2011; Zhang et al., 2011; Czajkowski et al., 2012).

A real-time anterior segment OCT with a light of 1310 nm wavelength and 60 nm bandwidth is the most commonly used in the tear film assessment. These devices use a high wavelength to provide higher penetration of the light in the tissues. Thus, short-wavelength systems provide higher axial resolution, while long-wavelength systems provide deeper penetration but the lower resolution (Ibrahim et al., 2010a; Cerviño, García-Lázaro and Montés-Micó, 2011; Zhang et al., 2011; Czajkowski et al., 2012; Kottaiyan et al., 2012; Lin and Yiu, 2014; Akiyama, Usui and Yamagami, 2015; Raj, Dhasmana and Nagpal, 2016; Tukenmez-Dikmen et al., 2016; Bai and Nichols, 2017; Chan et al., 2017; Gumus and Pflugfelder, 2017; Thulasi and Djalilian, 2017; Situ et al., 2020).

Tear meniscus parameters measured with OCT: OCT allows the measurement of different quantitative parameters related to the tear meniscus such as TMH, TMR, Tear Meniscus Area (TMA), Tear Meniscus Depth (TMD) and Tear Meniscus Volume (TMV).

Several studies have demonstrated that these metrics are good predictors of the tear volume (Savini, Barboni and Zanini, 2006; Wang et al., 2006; Palakuru, Wang and Aquavella, 2007; Palakuru, Wang and Aquavella, 2008; Wang, Palakuru and Aquavella, 2008; Ibrahim et al., 2010a; Fukuda et al., 2013; Hong et al., 2013; Lin and Yiu, 2014; Tukenmez-Dikmen et al., 2016).

TMR is calculated considering that the tear meniscus is a part of a circle; while TMV can be calculated by multiplying TMA and inferior eyelid length, assuming that the tear meniscus was uniform across the entire eyelid (Mainstone, Bruce and Golding, 1996). As the eyelids are curved, a correction factor of 1.294 was suggested by Tiffany, Todd and Baker (1998). That is to say: TMV = TMA x Inferior lid length x 1.294. *Figure 1.4* shows a cross-sectional image of the tear meniscus using OCT.

In the light of the above, OCT proves to be the most complete technique because it allows clinicians to measure all tear meniscus parameters (TMH, TMA, TMR, TMD and TMV), while reflective meniscometry only allows measuring TMR, and topography devices, slit-lamp and interferometers TMH. Raj et al. (2016) did not find a significant correlation between TMH obtained using OCT and a slit-lamp. This lack of correlation can be because TMH using slit-lamp is less accurate and the meniscus is not visualised in a cross-section, which causes the measurement to be more challenging.

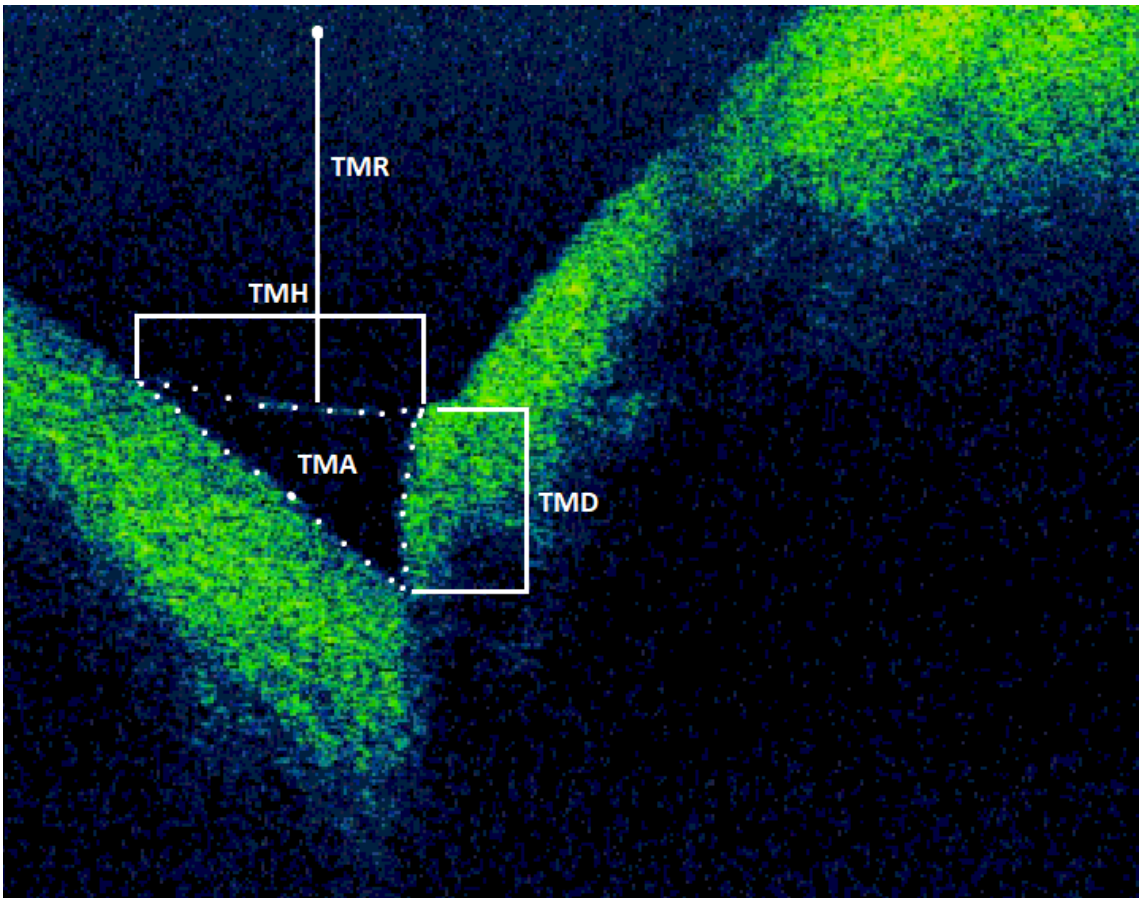

Fig. 1.4. *Tear meniscus imaged through a slit-lamp, Fourier-domain OCT (TMA=Tear Meniscus Area, TMD=Tear Meniscus Depth, TMH=Tear Meniscus Height, and TMR=Tear Meniscus Radius).*

OCT in the diagnosis of DED: Some authors have demonstrated that OCT is a useful technique to quantify the tear film meniscus due to its high resolution, good accuracy, non-invasiveness, acceptable repeatability and good sensitivity and specificity to diagnose DED (Savini, Barboni and Zanini, 2006; Wang et al., 2006; Palakuru, Wang and Aquavella, 2007; Wang, Palakuru and Aquavella, 2008; Zhou et al., 2009; Ibrahim et al., 2010a; Yuan et al., 2010; Tittler et al., 2011; Zhang et al., 2011; Czajkowski et al., 2012; Qiu et al., 2012; Fukuda et al., 2013; Hong et al., 2013; Canan et al., 2014; Lin and Yiu, 2014; Akiyama, Usui and Yamagami, 2015; Baek, Doh and Chung, 2015; Arriola-

Villalobos et al., 2015; Chan et al., 2015; Eroglu, Karalezli and Dursun, 2016; Koh et al., 2016; Tukenmez-Dikmen et al., 2016; Arriola-Villalobos et al., 2017; Ruiz-Alcocer et al., 2018; Shinzawa et al., 2018; Singh et al., 2019). Nonetheless, the accuracy in DED diagnosis is higher in severe DED patients; thus, it is more challenging to detect mild DED stages (Zhang et al., 2011; Czajkowski et al., 2012; Eroglu, Karalezli and Dursun, 2016). *Table 1.6* shows a summary of the sensitivity and specificity of tear meniscus measurements through OCT. Moreover, *Table 1.7* shows the main studies that evaluated the repeatability of OCT in tear meniscus measurements.

OCT has the disadvantage of being a partially subjective method because it depends on the ability of the examiner to delineate tear meniscus margins. Despite being partially subjective, Arriola-Villalobos et al. (2017) found an excellent intra-observer and intersession repeatability in the measurement of lower TMH with swept-source OCT.

Several authors have found that the best predictive metric to diagnose DED is TMA (Wang et al., 2009; Ibrahim et al., 2010a; Czajkowski et al., 2012; Akiyama, Usui and Yamagami, 2015; Chan et al., 2015; Raj, Dhasmana and Nagpal, 2016; Eroglu, Karalezli and Dursun, 2016; Garaszczuk et al., 2018). For instance, Czajkowski et al. (2012) showed that TMA and TMH displayed good sensitivity and specificity, but these values were lower for TMD. Akiyama, Usui and Yamagami (2015) found that swept-source OCT had good inter-grader repeatability and inter-image repeatability in DED patients. TMA, TMH and TMV had good sensitivity and specificity, being TMA the most accurate metric.

Table 1.6. *Sensitivity and specificity found by different authors in the tear meniscus measurement through OCT.*

Study	Sample	Age (mean ± SD) years	Technique	Parameter	Cut-off value	Sensitivity	Specificity
Ibrahim et al. (2010a)	24 eyes of DED patient and 27 eyes of control patients	DED: 63.14±13.4 Control: 56.04±14.22	Visante Time-Domain OCT	Lower TMH	<0.25 mm	0.83	0.68
Akiyama, Usui and Yamagami (2015)	26 eyes of healthy Japanese patients and 24 of DED Japanese patients	43.3±13.7	Swept-source OCT	Lower TMH	191µm	0.67	0.88
				Lower TMA	12360 μm^2	0.62	0.92
				Lower TMV	0.0473 mm^3	0.63	0.81
Czajkowski et al. (2012)	50 eyes of patients with Schirmer >10 mm 25 between 5-10 mm and 36 <5 mm	34.35±11.17	Spectral-domain OCT	Lower TMH		0.81	0.89
				Lower TMA		0.86	0.85
				Lower TMD		0.78	0.83
Eroglu, Karalezli and Dursun (2016)	104 eyes of acne rosacea patients and 104 of healthy patients	Acne rosacea: 38.37±12.37 Control: 38.24±11.53	Fourier-domain OCT	Lower TMH		0.76	0.69
				Lower TMA		0.78	0.71
				Lower TMD		0.74	0.63
Singh et al. (2019)	30 DED subjects (60 eyes) and 30 controls (60 eyes)	DED: 36.43±11.80 Controls: 32.47±9.70	Fourier-domain OCT (RTVue)	Lower TMH	204.96 µm	0.98	0.97
				Lower TMD	190 µm	0.97	0.95
Shinzawa et al. (2018)	22 DED subjects (44 eyes) and 28 controls (49 eyes)	DED: 58.3±14.0 Controls: 56.1±15.3	CASIA SS-1000 OCT	Lower TMH	0.197 mm	0.74	0.78
				Lower TMA	0.020 mm^2	0.81	0.67

(Where DED: Dry Eye Disease; OCT: Optical Coherence Tomography; SD: Standard Deviation; TMH: Tear Meniscus Height; TMA: Tear Meniscus Area; TMR: Tear Meniscus Radius; TMV: Tear Meniscus Volume; and TMD: Tear Meniscus Depth)

Table 1.7. *Main studies that assessed the repeatability of OCT in the measurement of the tear meniscus.*

Study	Technique	Metric	S_w	CoV (%)	CoR	ICC
Akiyama, Usui and Yamagami (2015)	Swept-source OCT (SS-1000)	Upper TMH		Interimage: 34.9 Intergrader: 21.2		Interimage: 85.5 Intergrader: 96.4
		Lower TMH		Interimage: 23.9 Intergrader: 14.5		Interimage: 90.9 Intergrader: 94.8
		Upper TMA		Interimage: 51.1 Intergrader: 27.3		Interimage: 81.6 Intergrader: 84.0
		Lower TMA		Interimage: 45.5 Intergrader: 29.4		Interimage: 83.8 Intergrader: 81.3
		TMV		Interimage: 29.4 Intergrader: 30.8		Interimage: 84.7 Intergrader: 82.5
Eroglu, Karalezli and Dursun (2016)	Fourier-domain OCT (RTVue)	TMH				<u>Rosacea</u> Intraobserver: 0.93 Interobserver: 0.94 <u>Control group</u> Intraobserver: 0.90 Interobserver: 0.92
		TMD				<u>Rosacea</u> Intraobserver: 0.92 Interobserver: 0.93 <u>Control group</u> Intraobserver: 0.93 Interobserver: 0.94
		TMA				<u>Rosacea</u> Intraobserver: 0.96 Interobserver: 0.96 <u>Control group</u> Intraobserver: 0.95 Interobserver: 0.93
Zhou et al. (2009)	Fourier-domain OCT (RTVue)	TMH		Between visits: 17.5		Between visits: 0.605
		TMD		Between visits: 18.0		Between visits: 0.558
		TMA		Between visits: 35.5		Between visits: 0.567
Baek, Doh and Chung (2015)	Fourier-domain OCT (RTVue-100)	TMH	Intraexaminer 1: 0.021 mm Intraexaminer 2: 0.021 mm Interexaminer: 0.0155 mm	Intraexaminer 1: 6.9 Intraexaminer 2: 6.82 Interexaminer: 5.05	Intraexaminer 1: 0.059 mm Intraexaminer 2: 0.058 mm Interexaminer: 0.043 mm	Intraexaminer 1: 0.992 Intraexaminer 2: 0.991 Interexaminer: 0.993
Arriola-Villalobos et al. (2015)	Spectralis Fourier-domain OCT	TMH	Intraexaminer: 26.48 µm Interexaminer: 29.16 µm	Intraexaminer: 10.9 Interexaminer: 0.12	Intraexaminer: 73.35 µm Interexaminer: 80.77 µm	Intraexaminer: 0.93 Interexaminer: 0.92

(continuation)						
Study	Technique	Metric	S_w	CoV (%)	CoR	ICC
Arriola-Villalobos et al. (2017)	Triton Swept-Source OCT and Spectralis Fourier-domain OCT	TMH	Triton Intraobserver: 50.77 µm Interobserver: 17.31 µm Spectralis Interobserver: 30.43 µm	Triton Intraobserver: 18.8 Interobserver: 6.4 Spectralis Interobserver: 10.8	Triton Intraobserver: 140.63 µm Interobserver: 47.95 µm Spectralis Interobserver: 84.29 µm	Triton Intraobserver: 0.82 Interobserver: 0.98 Spectralis Interobserver: 0.90
Fukuda et al. (2013)	Swept-source OCT (SS-1000)	Upper TMH		Interimage: 25.0 Intergrader: 19.4		Interimage: 69.4 Intergrader: 96.6
		Lower TMH		Interimage: 19.7 Intergrader: 10.7		Interimage: 78.3 Intergrader: 97.6
		Upper TMA		Interimage: 34.4 Intergrader: 28.4		Interimage: 63.8 Intergrader: 95.1
		Lower TMA		Interimage: 36.8 Intergrader: 18.9		Interimage: 83.2 Intergrader: 97.0
		TMV		Interimage: 34.7 Intergrader: 18.9		Interimage: 71.3 Intergrader: 96.9
Tittlet et al. (2011)	Fourier-Domain OCT	TMH		Between grader: 12.1 Between image: 17.1		99.0
		TMD		Between grader: 15.7 Between image: 13.4		
		TMA		Between grader: 19.5 Between image: 35.4		

(Where CoR: Repeatability Coefficient; CoV: Coefficient of Variation; ICC: Intraclass Correlation Coefficient; S_w: within-subject standard deviation; TMH: Tear Meniscus Height; TMA: Tear Meniscus Area; TMR: Tear Meniscus Radius; TMV: Tear Meniscus Volume; and TMD: Tear Meniscus Depth)

Furthermore, some authors (Wang, Palakuru and Aquavella, 2008; Ibrahim et al., 2010a; Czajkowski et al., 2012; Eroglu, Karalezli and Dursun, 2016; Tukenmez-Dikmen et al., 2016; Singh et al., 2019; Ulusoy, Işık-Ulusoy and Kıvanç, 2019) have found that tear meniscus measurements using OCT were positively correlated with TMH using slit-lamp, strip meniscometry, Schirmer test and BUT; and inversely correlated with ocular surface staining and OSDI score.

OCT has also been useful to evaluate the influence on tear meniscus of some diseases (Eroglu, Karalezli and Dursun, 2016; Poh et al., 2017; Cardigos et al., 2018; Işık-Ulusoy and Kıvanç, 2019), treatments (Palakuru, Wang and Aquavella, 2008; García-Lázaro et al., 2011; Pérez-Bartolomé et al., 2017; Carracedo et al., 2018; Karadenız Ugurlu, Altın Ekın and Aytogan, 2019; Yang et al., 2019; Altin Ekin, Karadeniz Ugurlu and Kahraman, 2020; Karaca, Özek and Evren Kemer, 2020; Ozek, Karaca and Evren Kemer, 2020; Rocha-de-Lossada et al., 2020; Yeter, Koçak and Eser-Ozturk, 2020), contact lenses (García-Lázaro et al., 2012; Ruiz-Alcocer et al., 2018; Lafosse et al., 2018), surgical procedures (Tao et al., 2010; Shaaban and Badran, 2018) or video display terminals (Doguizi et al., 2019) (*Table 1.8*).

Comparisons between OCT devices: There are different types of OCT such as time-domain, Fourier-domain and swept-source OCT (Cerviño, García-Lázaro and Montés-Micó, 2011; Zhang et al., 2011; Czajkowski et al., 2012). The development of Fourier-domain OCT improved the optical resolution and velocity of scans, in comparison with time-domain OCT. Various authors have found that this technique has higher intra- and inter-observer repeatability than previous OCT instruments in TMH and TMA measurements (Keech et al., 2009; Savini et al., 2009; Zhou et al., 2009; Chan et al., 2015; Canan et al., 2014; Chan et al., 2017).

Table 1.8. *Results reported by different authors regarding the use of OCT to assess the effect on tear meniscus of contact lenses, diseases, treatments, visual displays and surgical procedures.*

Study	Sample	Age (mean ± SD) years	Technique	Tear meniscus measurements (mean ± SD)	Main findings
García-Lázaro et al. (2012)	20 contact lens wearers (20 eyes)	24.7±3.5	Fourier-domain OCT (Copernicus)	TMV With CL: 1.71±1.56µL Without CL: 1.35±1.18µL	-Without significant differences in TMV between contact lenses -Fourier-domain OCT provides useful measurements of tear volume
Tao et al. (2010)	28 post-LASIK subjects (28 eyes) and 35 controls (35 eyes)	Post-LASIK: 23.3±4.2 Controls: 22.9±3.7	Real-time OCT prototype	TMH controls: 240±53 µm TMH pre: 205±32 µm TMH 1 month: 180±23 µm TMA controls: 20054±6700 μm^2 TMA pre: 15669±4246 μm^2 TMA 1 month: 12832±2952 μm^2 TMV controls: 0.69±0.23 µL TMV pre: 0.54±0.15 µL TMV 1 month: 0.44±0.10 µL	-Tear meniscus parameters were lower 1 month after surgery
Eroglu, Karalezli and Dursun (2016)	104 acne rosacea patients (104 eyes) and 104 healthy (104 eyes)	Acne rosacea: 38.37±12.37 Controls: 38.24±11.53	Fourier-domain OCT (RTVue)	TMH acne rosacea: 247.70±22.54 µm TMH controls: 297.33±48.16 µm TMA acne rosacea: 19500±3256.5 μm^2 TMA controls: 27490±7724.69 μm^2 TMD acne rosacea: 270.87±25.19 µm TMD controls: 308.32±37.65 µm	-Significant lower values in acne rosacea group
García-Lázaro et al. (2011)	20 DED subjects (20 eyes)	57.5±8.4	Fourier-domain OCT (Copernicus)	TMV baseline: 0.38±0.10 µL TMV post-eyedrop: 0.94±0.22 µL TMV 10 min post: 0.57±0.13 µL	-Higher TMV values 10 minutes after eye drop instillation.
Palakuru, Wang and Aquavella (2008)	21 healthy subjects (21 eyes)	32.1±8.7	Real-time slit-lamp OCT	Tear film volume (Approximately) After eyedrops Before blink: 25.0±-- µl After blink: 22.0±-- µl Before closure: 23.0±-- µl 5 minutes after eyedrops Before blink: 3.5±-- µl After blink: 3.4±-- µl Before closure: 3.5±-- µl	-Immediately after the instillation of eyedrops, TMV increased -Blinking plays an essential role in the distribution and removal of instilled tears
Carracedo et al. (2018)	23 healthy subjects (23 eyes)	23.57±2.56	Fourier-domain OCT (iVue)	Saline solution TMH baseline: 255.11±67.75 µm TMH 1 minute: 379.68±159.23 µm TMD baseline: 178.90±46.69 µm TMD 1 minute: 254.68±95.69 µm Ocudry 0.1 % TMH baseline: 301.48±144.49 µm TMH 1 minute: 461.89±150.19 µm TMD baseline: 207.48±83.41 µm TMD 1 minute: 314.58±81.84 µm	-TMH and TMD significantly increased after the instillation of eyedrops

(continuation)

Study	Sample	Age (mean ± SD) years	Technique	Tear meniscus measurements (mean ± SD)	Main findings
Karaca, Özek and Evren Kemer (2020)	122 subjects with mild to moderate DED (122 eyes) (56 receiver eyedrops 1 and 66 eyedrops 2)	Eyedrops 1: 52.5±13.2 Eyedrops 2: 53.4±11.4	Triton Swept-Source OCT	<u>TMH</u> Eyedrop1 baseline: 237.4±85.6 µm Eyedrop1 240 mins: 246.5±76.3 µm Eyedrop2 baseline: 242.8±75.3 µm Eyedrop2 240 mins: 241.7±44.7 µm <u>TMD</u> Eyedrop1 baseline: 164.4±55.5 µm Eyedrop1 240 mins: 162.7±49.4 µm Eyedrop2 baseline: 159.3±55.1 µm Eyedrop2 240 mins: 167.8±32.3 µm	-Hyaluronic acid 0.3 % remained on the ocular surface for a longer time.
Ruiz-Alcocer et al. (2018)	20 subjects (20 eyes)	28.7±4.2	Slit-lamp Scan-1 OCT	<u>TMA</u> 20 mins Delefilcon A: 0.014±0.007mm^2 8 hours Delefilcon A: 0.013±0.006mm^2 20 mins Stenfilcon A: 0.011±0.004mm^2 8 hours Stenfilcon A: 0.011±0.004mm^2 20 mins Nesofilcon A: 0.013±0.007mm^2 8 hours Nesofilcon A: 0.011±0.006mm^2	-No differences were found in TMA as a function of the contact lens measured on time of use
Doguizi et al. (2019)	53 high video display users (53 eyes) and 49 low video display users (49 eyes)	High use: 38.9±5.5 Low use: 37.8±5.8	Spectralis Fourier-domain OCT	<u>TMH High use</u> 300.1±7.7µm <u>TMH Low use</u> 311.9±9.1µm <u>TMA High use</u> 0.023±0.005mm^2 <u>TMA Low use</u> 0.028±0.004mm^2	-Lower TMH and TMA was found in high video display users -OCT is an effective tool to assess the tear meniscus in video display users
Shaaban and Badran (2018)	45 healthy subjects (90 eyes) (15 subjects in each group)	Femtosecond: 31.1±8.9 SMILE: 30.0±6.1	Cirrus HD-model 5000 Fourier-Domain OCT	<u>TMH</u> Femtosecond pre: 0.255±0.032 µm Femtosecond 6 months: 0.245±0.036 µm SMILE pre: 0.255±0.022 µm SMILE 6 months: 0.251±0.021 µm <u>TMD</u> Femtosecond pre: 0.183±0.017 µm Femtosecond 6 months: 0.177±0.017 µm SMILE pre: 0.166±0.018 µm SMILE 6 months: 0.161±0.015 µm	-TMH was statistically significant between surgeries at 1 week and 1 month -No differences were found in TMH at 3 and 6 months -TMH recovered earlier in SMILE than in LASIK surgery

(continuation)					
Study	Sample	Age (mean ± SD) years	Technique	Tear meniscus measurements (mean ± SD)	Main findings
Rocha-de-Losada et al. (2020)	17 subjects (34 eyes)	61.05±11.43	Triton Swept-Source OCT	TMH 0.1% Baseline: 279.94±120.94µm TMH 0.1% 10 mins: 511.00±493.68µm TMH 0.2% Baseline: 266.35±123.66µm TMH 0.2% 10 mins: 563.71±420.58µm TMA 0.1% Baseline: 27484.30±23950.03µm^2 TMA 0.1% 10 mins: 108119.90±207908.54µm^2 TMA 0.2% Baseline: 28428.79±28610.06µm^2 TMA 0.2% 10 mins: 111480.00±138104.30µm^2	-0.2% sodium hyaluronate achieved better TMH and TMA at 1 and 3 minutes, but there were no differences after 10 minutes
Karadenız Ugurlu, Altın Ekın and Aytogan (2019)	32 subjects with unilateral canalicular repair (32 eyes)	32.8±21.3	Cirrus Fourier-Domain OCT	TMH: 283.7±127.1µm TMD: 235.2±85.4µm TMA: 29829.2±19801µm	-OCT is a quick, objective and quantitative tool to measure tear meniscus parameters in subjects with canalicular laceration repair
Ulusoy, Işık-Ulusoy and Kıvanç (2019)	40 subjects with depression (40 eyes), 35 with anxiety (35 eyes) and 37 healthy (37 eyes)	Depression: 38.8±10.6 Anxiety: 40.7±14.8 Controls: 39.4±6.1	Fourier-domain OCT (RTVue-100)	TMH Depression: 215.28±55.7 µm TMH Anxiety: 198.82±48.09 µm TMH Controls: 465.29±183.25 µm TMD Depression: 149.1±35.41 µm TMD Anxiety: 125.68±29.72 µm TMD Controls: 260.97±91.06 µm TMA Depression: 0.01±0.005 mm^2 TMA Anxiety: 0.01±0.004 mm^2 TMA Controls: 0.11±0.02 mm^2	-TMD, TMH and TMA were lower in anxiety and depression groups, and they were correlated with conventional tests -DED was related to anxiety and depression

*(Where DED: Dry Eye Disease; LASIK: Laser-Assisted In Situ Keratomileusis; OCT: Optical Coherence Tomography; SD: Standard Deviation; SMILE: Small Incision Lenticule Extraction; TMH: Tear Meniscus Height; TMA: Tear Meniscus Area; TMR: Tear Meniscus Radius; TMV: Tear Meniscus Volume; and TMD: Tear Meniscus Depth) * In the cases where "approximately" is written, studies showed the results in a figure, instead of a numerical value.*

For instance, Zhou et al. (2009) found higher reproducibility in TMA, TMH and TMD with Fourier-domain OCT than other previous time-domain OCTs. Chan et al. (2015) found that TMH and TMA had higher intra-rater repeatability when measured using Fourier-domain OCT (Cirrus) than time-domain OCT (Visante). They did not find differences between devices for lower TMH, but TMA was higher in Visante ($p=0.0002$) by a difference of 10.223 μm^2. Moreover, the inter-device agreement was poor, being both devices not interchangeable. Keech et al. (2009) found lower tear meniscus values with time-domain OCT in comparison with Fourier-domain OCT ($p < 0.001$). These differences found between devices might be because Fourier-domain OCT has higher resolution, which improves image analysis within and between examiners. Furthermore, this device is faster than time-domain OCT, which allows measuring the tear meniscus in more natural conditions. Higher acquisition times can increase the evaporation, or cause reflex tearing.

Swept-source OCT has also been compared with other OCT techniques. Arriola-Villalobos et al. (2017) found poor agreement in TMH measurement between Fourier-domain OCT and swept-source OCT. This difference can be because swept-source OCT provides better resolution and faster capture time. This causes more accurate and reliable measurements since the examiner has to delineate the tear meniscus margins (Keech et al., 2009; Arriola-Villalobos et al., 2017). *Table 1.9* shows the main studies that compared OCT devices.

Table 1.9. *Results reported by different authors regarding the comparison of OCT devices.*

Study	Sample	Age (mean ± SD) years	Technique	Tear meniscus measurements (mean ± SD)	Main findings
Keech et al. (2009)	50 healthy subjects (50 eyes)	33.2±-- (Range: 19 to 62)	Fourier-domain OCT (RTVue-100) and Time-domain OCT (OCT2)	TMH Fourier-domain module short: 0.354±0.163 mm Fourier-domain module long: 0.345±0167mm Time-domain: 0.280±0.139 mm	-Significant differences between Fourier-domain OCT and Time-domain OCT -Time-domain OCT showed lower tear meniscus values
Chan et al. (2015)	20 healthy subjects (20 eyes)	Median: 22 (Range: 21 to 60)	Visante Time-Domain OCT and Cirrus Fourier-Domain OCT	TMH Visante upper: 324±103 µm Cirrus upper: 282±73 µm TMA Visante upper: 35218±19595 μm^2 Cirrus upper: 21058±8551 μm^2	-No significant differences between devices for TMH -TMA was significantly lower in Fourier-domain OCT -Fourier-domain OCT was more intra- and inter-rater repeatable than time-domain OCT for TMH and TMA
Arriola-Villalobos et al. (2017)	27 healthy subjects (27 eyes)	30.4±8.3	Triton Swept-Source OCT and Spectralis Fourier-domain OCT	TMH Triton observer 1: 266.3±89.9 µm and 272.8±76.4 µm Triton observer 2: 276±98.4 µm and 280.9±84.4 µm Spectralis observer 1: 291.4±78 µm Spectralis observer 2: 269.3±84.7 µm	-A low agreement was found between devices

(Where OCT: Optical Coherence Tomography; SD: Standard Deviation; TMH: Tear Meniscus Height; TMA: Tear Meniscus Area)

Comparisons between upper and lower meniscus: OCT also has the benefit of allowing the examination of the upper and lower tear menisci simultaneously (Wang et al., 2006; Palakuru, Wang and Aquavella, 2008; Wang, Palakuru and Aquavella, 2008; Zhang et al., 2011; Fukuda et al., 2013; Foulks and Pflugfelder, 2014; Lin and Yiu, 2014). Wang et al. (2006) did not find differences between upper and lower TMA, TMR and

TMH. Fukuda et al. (2013) found that measurements in the lower tear meniscus were more repeatable and accurate than in the upper. This might be because focusing on the upper tear meniscus is more challenging.

Tear film thickness measurement with OCT: Generally, OCT does not have enough axial resolution to measure the tear film thickness. The highest axial resolution of OCT systems is 3 µm, but a resolution better than 2 µm to measure the tear film is needed. Axial resolution is inversely proportional to bandwidth, while numerical aperture determines the lateral resolution (King-Smith et al., 2004; Kottaiyan et al., 2012; Bai and Nichols, 2017; Gumus and Pflugfelder, 2017).

In some studies, authors have built a customized OCT device to increase the resolution and measure the tear film thickness (Wang et al., 2006; Palakuru, Wang and Aquavella, 2007; Wang et al., 2009; Chen et al., 2010; Kottaiyan et al., 2012; Werkmeister et al., 2013; Dos Santos et al., 2015; Bai and Nichols, 2017). Generally, these customized devices use a lower wavelength to provide higher resolution (around 800 nm). Authors have found that the tear film thickness ranged from 2 to 5.5 µm using OCT (Chen et al., 2010; Kottaiyan et al., 2012; Dos Santos et al., 2015; Willcox et al., 2017). This device also allows the study of the tear film pre- and post-contact lens wear (Wang et al., 2009; Chen et al., 2010; García-Lázaro et al., 2012). Werkmeister et al. (2013) found high reproducibility and an intra-class correlation coefficient of 0.97 in the precorneal tear film thickness measurement using ultrahigh-resolution, Fourier-domain OCT. Dos Santos et al. (2015) also found that central tear film thickness measurement was precise and repeatable with a variation coefficient of 0.65.

1.3.2 Imaging techniques to assess the quality of the tear film

1.3.2.1 NIBUT

Tear film BUT was first introduced by Norn (Norn, 1969). The technique consists of placing sodium fluorescein into the eye and measuring the time until a dry spot appears and the tear film breaks, while the patient avoids blinking (Goto et al., 2004a; Yao et al., 2011; Sweeney, Millar and Raju, 2013). BUT higher than 10 seconds means normal tear film stability, while a time lower than 5 seconds is related to an unstable tear film (Goto et al., 2004a; Yao et al., 2011). It has been demonstrated that BUT is useful to assess the stability of the tear film and to diagnose DED and MGD (Goto et al., 2004b; Geerling et al., 2017). Thus, Goto et al. (2004b) found a sensitivity and specificity of 75 % and 60 %, respectively, to categorise dry eye symptoms through BUT.

Nevertheless, the technique has poor reproducibility since results may be influenced by many factors such as the amount, concentration and pH of fluorescein applied; partial blinking, illumination techniques, the interval between instillation of the dye and examination, and the examiner's ability (Mengher et al., 1985; Cho et al., 1992; Goto et al., 2004a). Furthermore, the instillation of fluorescein can disturb and destabilize the tear film, or even cause reflex tearing. Thus, some authors have found lower values when BUT is measured using fluorescein (Wang, Palakuru and Aquavella, 2008; McGinnigle, Naroo and Eperjesi, 2012).

Given the drawbacks of BUT, other non-invasive techniques have been developed to assess tear film stability. Generally, these devices analyse the tear film from the reflection of ring mires or a grid pattern (earlier with keratometry) into the pre-corneal

tear film layer. Some studies have found more quick and extensive pattern distortion in subjects with tear dysfunction, which is correlated with the severity of corneal epithelial disease (Gumus et al., 2011; Hong et al., 2013; Foulks and Pflugfelder, 2014; Thulasi and Dialilian, 2017).

The available devices use different reflective patterns. For instance, keratometers use mires and a dark background; modified keratometers use an HIR-CAL grill and a dark background; manual keratoscope use the Loveridge grill and a dark background; and some interferometers, topographic devices and videokeratographs use a Placido disk (Best, Drury and Wolffsohn, 2012; Asharlous et al., 2015; Wolffsohn et al., 2017).

1.3.2.1.1 Keratometers

Keratometers can be used to assess tear film stability. This device represents the beginnings of NIBUT. Currently, it is still used because it is more clinically accessible than other devices due to its cost. Asharlous et al. (2015) compared the evaluation of tear stability with Javal-Schiotz keratometer (tear deformation time) and invasively with fluorescein. They found that values obtained with keratometers were higher because fluorescein destabilized the tear film, concluding that non-invasive techniques are preferable. However, despite keratometers having the advantage of being non-invasive, they only allow the assessment of the 3 central millimetres of the corneal apex. This issue may also cause higher NIBUT values because they assess fewer corneal points.

1.3.2.1.2 Corneal topography systems

Nowadays, corneal topography systems are widely used than keratometers in a clinical setting for measuring NIBUT, in this case called Non-Invasive Keratograph Break-Up Time (NIKBUT). *Table 1.10* shows a summary of the advantages and disadvantages of keratometers in comparison with corneal topography devices in NIKBUT measurements.

Table 1.10. *Advantages and disadvantages of keratometers and corneal topography devices in NIBUT measurement.*

Keratometers		Corneal topography devices	
Advantages	Disadvantages	Advantages	Disadvantages
Non-invasiveness	Partially subjective	Non-invasiveness	Cost
Patient-friendly	Analyse a small corneal region	Patient-friendly	
		If they include software, they will be more objective.	
		The software can detect non-visually apparent alterations	
		More data points analysed	
		Saves images for future examinations	
		If they use infrared light, less reflex tearing	

The devices use the specular reflection of a pattern into the tear film. The pattern can be a rectangular grid or concentric rings (Placido disk) such as in videokeratography systems. In this way, NIKBUT can be subjectively measured, observing the reflected pattern and measuring the time until the first deformation of the pattern appears. On the other hand, it can also be measured using software that analyses the changes in the reflected pattern in an objective way (Best, Drury and Wolffsohn, 2012; McGinnigle, Naroo and Eperjesi, 2012; Foulks and Pflugfelder, 2014).

These devices have the advantage of assessing more corneal data points, and software can detect alterations that may not be visually apparent for the examiner (Best, Drury and Wolffsohn, 2012; McGinnigle, Naroo and Eperjesi, 2012; Foulks and Pflugfelder, 2014). Likewise, it allows a comprehensive analysis and data can be easily stored for future records and comparison purposes. Besides, images can also be used to improve communication with patients (Best, Drury and Wolffsohn, 2012).

Generally, videokeratographs use the distortion of a ring pattern to analyse the surface regularity index and the surface asymmetry index. The tear surface is used as a convex mirror and the virtual image of the reflected pattern is analysed (King-Smith, Begley and Braun, 2018). That is to say, the device uses the error between the measured surface and its parametric model to obtain the result. It allows the measurement of BUT and break-up area. Thus, the interval of time in seconds following a complete blink to the first variation of the pattern is called NIKBUT. Besides, the devices that use infrared light prevents reflex tearing (Goto et al., 2004a; McGinnigle, Naroo and Eperjesi, 2012; Sweeney, Millar and Raju, 2013; Jiang et al., 2014; Lin and Yiu, 2014; Ramos et al., 2014; Ramos et al., 2015; Ring et al., 2015; Bhandari et al., 2016; Chan et al., 2017; Geerling et al., 2017; Wolffsohn et al., 2017). *Figure 1.5* shows an example of the NIKBUT measurement using a commercially available videokeratograph called Oculus Keratograph 5M.

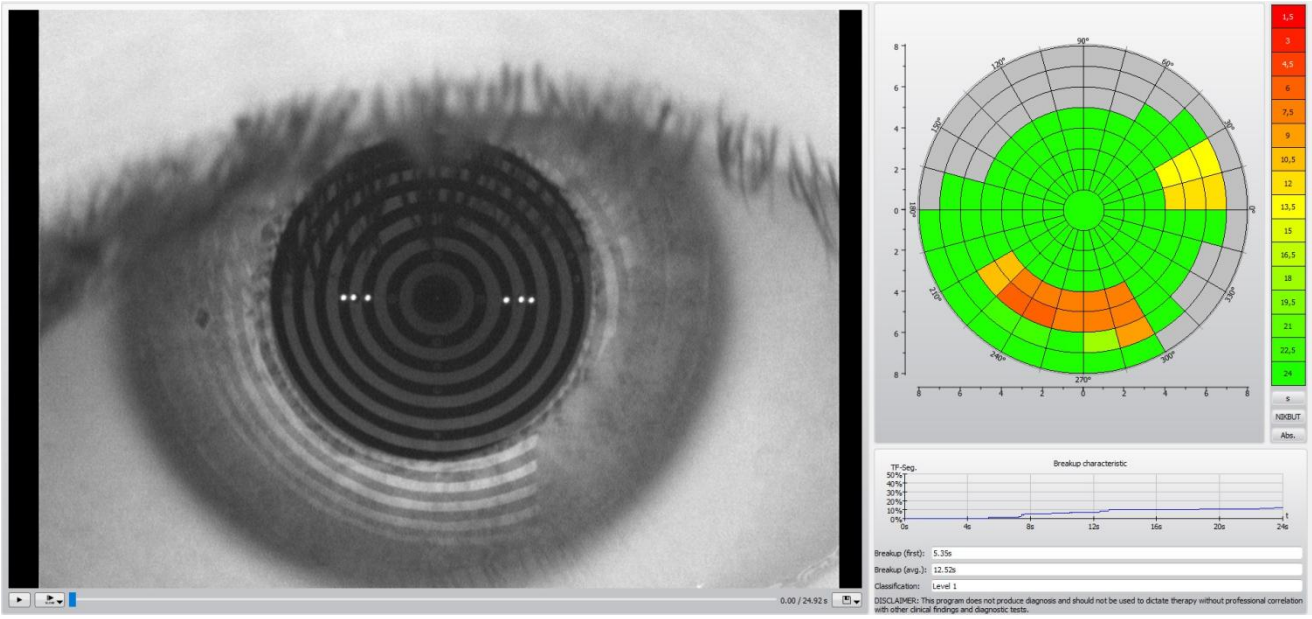

Fig. 1.5. *NIKBUT measurement through a commercially available videokeratograph (Oculus Keratograph 5M). Left: Placido disk rings reflected onto the tear film surface. Right: Break-up map of the tear film (warm colours indicate an earlier break-up of the tear film in that area).*

Some authors (Koh et al., 2016; Wang et al., 2016; Wang and Craig, 2018; Zang et al., 2018; Kim et al., 2019; Tong, Teo and Lee, 2019) have found shorter NIKBUT in DED subjects in comparison with controls (*Table 1.11*). Thus, the differences found between DED and healthy patients in this technique can be used by clinicians in the diagnosis of the disease.

Table 1.11. *NIKBUT results obtained by authors using corneal topographers.*

Study	Sample	Age (mean ± SD) years	Technique	NIKBUT (s) (mean ± SD)	Main findings
Koh et al. (2016)	49 ADDE subjects (49 eyes) 31 healthy subjects (31 eyes)	ADDE: 57.9±12.5 Controls: 37.7±9.8	Keratograph 5M	ADDE: 4.59±1.25 Controls: 9.71±6.68	-Significantly lower NIKBUT in the ADDE group
Wang et al. (2016)	47 DED subjects (47 eyes) 201 healthy subjects (201 eyes)	DED: 12.45±1.54 Controls: 11.75±1.95	Keratograph 5M	DED: 6.32±2.49 Controls: 13.14±3.67	-Significantly lower NIKBUT in the DED group
Kim et al. (2019)	250 DED subjects (250 eyes) (23 ADDE, 95 MGD and 132 ADDE/MGD) and 55 healthy subjects (55 eyes)	ADDE: 35.4±12.7 MGD: 48.1±16.7 ADDE/MGD: 51.2±13.6 Controls: 29.5±9.8	Keratograph 5M	ADDE: 7.88±3.61 MGD: 4.30±2.88 ADDE/MGD: 7.23±3.69 Controls: 4.71±2.44	-NIKBUT and the location and pattern of NIKBUT were different between controls and DED subtypes
Zang et al. (2018)	22 Sjögren syndrome subjects (22 eyes) and 22 non-Sjögren syndrome ADDE subjects (22 eyes)	Sjögren syndrome: 50.1±11.8 Non-Sjögren syndrome: 49.6±11.7	Keratograph 5M	Median (IQR) Sjögren syndrome: 3.8 (2.7-5.2) Non-Sjögren syndrome: 6.3 (3.7-8.9)	-Non-Sjögren syndrome subjects had higher NIKBUT

(Where ADDE: Aqueous Deficient Dry Eye; BUT: Break-Up Time; DED: Dry Eye Disease; IQR: Interquartile Range; MGD: Meibomian Gland Dysfunction; NIKBUT: Non-Invasive Keratograph Break-Up Time; SD: Standard Deviation)

It has been widely reported that corneal topographic devices can be used as a non-invasive, reproducible and objective method with acceptable sensitivity and specificity to assess the stability of the tear film (Goto et al., 2004a; McGinnigle, Naroo and Eperjesi, 2012; Sweeney, Millar and Raju, 2013; Lin and Yiu, 2014; Ramos et al., 2014; Downie, 2015; Ramos et al., 2015; Koh et al., 2016; Chan et al., 2017; Geerling et

al., 2017; Wolffsohn et al., 2017; Lee et al., 2020b). *Table 1.12* shows the diagnostic capability of NIKBUT to diagnose DED found by different authors. Generally, they claim that a cut-off value of around 10 seconds can be used to detect DED (Mengher et al., 1985; Goto et al., 2004a; Hong et al., 2013; Downie, 2015; Bhandari et al., 2016; Wolffsohn et al., 2017). Moreover, this cut-off value has been also recommended by the TFOS DEWS II Diagnostic Methodology Report (Wolffsohn et al., 2017).

Some studies (Goto et al., 2004a; Hong et al., 2013; Jiang et al., 2014; Bhandari et al., 2016) have compared NIKBUT values with the conventional BUT technique and have found that NIKBUT was shorter when is measured using a videokeratograph. The instillation of the fluorescein can destabilize the tear film and cause lower BUT. However, in these studies, lower values have been found with a videokeratograph because authors compared BUT with fluorescein and a videokeratograph device with software. Thus, the software evaluates more data points and might detect non-visually apparent small tear film changes (Goto et al., 2004a; Hong et al., 2013; Jiang et al., 2014). It might be also possible that topographic devices measure a change of the curvature in the tear film, rather than the disruption of the tear film (Goto et al., 2004a). Nonetheless, two studies (Lan et al., 2014; Wang and Craig, 2018) found longer BUT with Keratograph 5M than with fluorescein. This might be explained since BUT was measured with controlled volumes of fluorescein (Lan et al., 2014). Recently, Ozulken et al. (2020) found a strong correlation between NIBUT and BUT using fluorescein, which suggests that NIBUT allows obtaining similar values than BUT with fluorescein but with the advantage of not destabilizing the tear film and being more

objective. Downie (2015) confirmed that the non-invasive analysis of the tear film stability showed better repeatability than the measurement using fluorescein.

Wang and Craig (2018) claimed that NIKBUT using Keratograph 5M had a higher diagnostic capability to diagnose DED than BUT using fluorescein. Goto et al. (2004a) also reported that in comparison with BUT with fluorescein, videokeratography had significantly higher sensitivity in evaluating tear stability, whereas the specificity was similar. In contrast, Yeh, Graham and Lin (2015) did not find differences in sensitivity and specificity of NIKBUT, BUT with fluorescein and osmolarity to diagnose moderate to severe DED; and Zhang et al. (2011) found that NIBUT and BUT using fluorescein were both sensitive methods to diagnose mild office dry eye. A value lower than 5 seconds was more appropriate for the diagnosis of mild dry eye using BUT with fluorescein, while a value lower than 10 seconds is preferred using NIBUT.

Tear Film Surface Quality (TFSQ) is another previously validated parameter, which is related to tear film stability (Alonso-Caneiro, Iskander and Collins, 2009). It has also been proven that this parameter can discern between dry eye and healthy eyes (Downie, 2015). TFSQ also analyses the structure of the reflected Placido disk pattern onto the tear film. To calculate TFSQ at 300 radial points, the software analyses the variability of the pattern over time by using the approach of the block-feature (Alonso-Caneiro, Iskander and Collins, 2009). Local TFSQ in a specific point is calculated as the standard deviations of the radial distances to the next innermost ring for n = 8 points on either side of the analysis point. TFSQ ranges from 0 to 1 and a value of ≥ 0.30 is considered as a destabilized tear film (Alonso-Caneiro, Iskander and Collins, 2009; Downie, 2015).

Table 1.12. *Sensitivity and specificity found by different authors in the assessment of NIKBUT through corneal topographic devices.*

Study	Sample	Age (mean ± SD) years	Technique	Metric	Cut-off value	Sensitivity	Specificity
Yamaguchi et al. (2016)	64 subjects (108 eyes)	50.0±21.1	Tomey RT-7000 Auto Refractor-Keratometer	NIBUT	< 5 seconds	0.78	0.70
Gumus et al. (2011)	45 subjects (45 eyes)	48.2±16.5	Tomey RT-7000 Auto Refractor-Keratometer	NIBUT	< 5 seconds	0.82	0.60
Yeh, Graham and Lin (2015)	137 subjects (274 eyes)	28.10±13.11	Carl Zeiss Humphrey Atlas Corneal Topography System	NIKBUT	11 seconds	0.72 (moderate-severe)	0.52 (moderate-severe)
Bhandari et al. (2016)	25 DED subjects (25 eyes) 25 healthy subjects (25 eyes)	DED: 42.64±14.12 Controls: 48.32±15.1	Video-keratograph Optikon Keratron Scout	NIKBUT	6.2 seconds	0.86	0.81
Hong et al. (2013)	44 DED subjects (44 eyes) and 41 healthy subjects (41 eyes)	DED: 41.4±2.9 Controls: 34.7±2.8	Keratograph 4	NIKBUT	≤2.65 seconds	0.84	0.76
Wang and Craig (2018)	37 DED subjects (37 eyes) and 37 healthy subjects (37 eyes)	DED: 24±4 Controls: 23±4	Keratograph 5M	NIKBUT	≤ 9 seconds	0.68	0.70
Downie (2015)	28 DED subjects (28 eyes) and 17 healthy subjects (17 eyes)	DED: 41.2±14.4 Controls: 45.5±14.6	Medmont E300	TFSQ	12.1 seconds	0.82	0.94
Mengher et al. (1985)	33 DED subjects (65 eyes) and 66 healthy subjects (132 eyes)	DED: 65 Controls: 65	-	NIKBUT	10 seconds	0.82	0.86
Kim et al. (2019)	250 DED subjects (250 eyes) (23 ADDE, 95 MGD and 132 ADDE/MGD) and 55 healthy subjects (55 eyes)	ADDE: 35.4±12.7 MGD: 48.1±16.7 ADDE/MGD: 51.2±13.6 Controls: 29.5±9.8	Keratograph 5M	NIKBUT	4.84 seconds	0.56	0.76

(Where ADDE: Aqueous Deficient Dry Eye; DED: Dry Eye Disease; MGD: Meibomian Gland Dysfunction; NIBUT: Non-Invasive Break-Up Time; NIKBUT: Non-Invasive Keratograph Break-Up Time; SD: Standard Deviation; TFSQ: Tear Film Surface Quality)

There is some controversy in the repeatability of the technique since some studies reported that it is acceptable, while other ones claim that it is limited (Hong et al., 2013; Cox, Nichols and Nichols, 2015; Bhandari et al., 2016; Markoulli et al., 2017; Fernández et al., 2018; Wang and Craig, 2018; Bandlitz et al., 2019a; Dutta et al., 2019; García-Montero et al., 2019b). *Table 1.13* shows the main studies that have evaluated the repeatability of topography devices in the assessment of NIKBUT.

Fernández et al., (2018), Markoulli et al. (2017) and Cox, Nichols and Nichols (2015) found poor repeatability and between-visit agreement. They found more variability in repeated measures at high NIKBUT values. Therefore, the repeatability was better at lower NIKBUT values. Conversely, Dutta et al. (2019) found moderate reproducibility (CoR = 11.9) and García-Montero et al. (2019b) found that intrarater repeatability remained stable when three measurements were performed after contact lens wear. However, the repeatability decreased during contact lens wear.

Different authors have demonstrated that corneal topographic devices are also useful to assess the effect on tear stability of contact lenses (Llorens-Quintana et al., 2018; Mousavi et al., 2018; Vidal-Rohr et al., 2018; García-Montero et al., 2019b; Wang et al., 2019a; Martínez-Alberquilla et al., 2020), some diseases (He et al., 2018; Wang et al., 2019c), treatments (Ren et al., 2018; Seo et al., 2018; Li et al., 2020a; Nosch, Joos and Job, 2020; Chen et al., 2021), visual displays (Choi et al., 2018) or surgical procedures (Goto et al., 2004a; Jiang et al., 2014; Recchioni et al.,2020) (*Table 1.14*).

Table 1.13. *Results of main studies that assessed the repeatability of NIKBUT using corneal topography devices.*

Study	Type of repeatability	S_w	CoV (%)	CoR	ICC
Downie (2015)	Intraexaminer		9.4		
Markoulli et al. (2017)	Intraexaminer			11.37 seconds	
Tian et al. (2016)	Intraexaminer		Healthy: 26.10 DED: 23.54	Healthy: 5.24 seconds DED: 3.76 seconds	Healthy: 0.75 DED: 0.82
	Interexaminer		Healthy: 20.30 DED: 21.85	Healthy: 4.13 seconds DED: 3.55 seconds	-
Cox, Nichols and Nichols (2015)	Between visit				0.53
Fernández et al. (2018)	Intraexaminer		Healthy: 23.54 DED: 26.10		
García-Montero et al. (2019b)	Intrarater	4.61 seconds	43.66	12.77 seconds	0.57
Dutta et al., (2019)	Intervisit			11.9 seconds	

(Where CoR: Repeatability Coefficient; CoV: Coefficient of Variation; DED: Dry Eye Disease; ICC: Intraclass Correlation Coefficient; S_w: within-subject standard deviation)

In light of the above, this is a useful, quick, reliable, patient-friendly, objective and non-invasive technique to detect and monitor DED, and to differentiate among different degrees of severity of the disease (Hong et al., 2013; Jiang et al., 2014; Bhandari et al., 2016; Koh et al., 2016; Markoulli et al., 2017; Choi et al., 2018; He et al., 2018; Llorens-Quintana et al., 2018; Markoulli et al., 2018; Mousavi et al., 2018; Ren et al., 2018; Seo et al., 2018; Vidal-Rohr et al., 2018; Wang and Craig, 2018; García-Montero et al., 2019b; Itokawa et al., 2020; Li et al., 2020a; Li et al., 2020b; Martínez-Alberquilla et al., 2020; Nosch, Joos and Job, 2020; Ozulken et al., 2020; Robin et al., 2019; Tong, Teo and Lee, 2019; Wang et al., 2019a; Wang et al., 2019c; Recchioni et al., 2020; Wu et al., 2020b; Chen et al., 2021). Nevertheless, the technique is not

perfect and further effort should be focused on the improvement of the tear stability analysis to increase its repeatability and diagnostic capability.

Table 1.14. *Results reported by different authors regarding the use of corneal topographers to assess the effect on NIKBUT of contact lenses, diseases, treatments, visual displays and surgical procedures.*

Study	Sample	Age (mean ± SD) years	Technique	NIKBUT (s) (mean ± SD)	Main findings
Mousavi et al. (2018)	46 CL wearers (92 eyes)	25.5±4.3	Keratograph 5M	Silicone hydrogel: 8 Hydrogel: 7 *Medians approximately	-NIKBUT provided additional information of interest during CL fitting -No differences in NIKBUT between lenses
Vidal-Rohr et al. (2018)	19 CL wearers (19 eyes)	21.6±1.7	Keratograph 5M	Uncoated lenses: 5.86±3.28 Coated lenses: 7.10±3.95	-Coating lenses increased the stability of the pre-lens tear film
Jiang et al. (2014)	86 subjects with cataract and DED (86 eyes)	68±10	Keratograph 4	2.21±0.23	-NIKBUT assessment is useful for preoperative evaluation of the tear film in subjects with cataract
Goto et al. (2004a)	34 subjects (64 eyes)	30.4±11.2	Videokeratography software for a topographic modelling system	Pre-LASIK: 6.42±1.76 Post-LASIK: 3.48±1.69	-Tear film stability can be useful for screening LASIK candidates -Tear film stability was worse post-LASIK
Nosch, Joos and Job (2020)	36 subjects (36 eyes)	32.3±16.1	Keratograph 5M	Before spray: 7.7±1.7 After spray: 11.6±4.6	-Longer NIKBUT after treatment
Seo et al. (2018)	17 rosacea-MGD subjects (17 eyes)	Median: 64 (IQR: 57-68)	Keratograph 5M	Median: 3.0 (IQR: 2.5-5.9)	-NIKBUT improved after intense pulsed light treatment but it was not maintained at 6 and 12 months after treatment
Martínez-Alberquilla et al. (2020)	15 extended focus CL wearers (15 eyes) and 15 conventional multifocal CL wearers (15 eyes)	53.7±5.3	Keratograph 5M	Baseline extended focus: 9.31±7.17 Baseline conventional: 8.32±6.15 Day 15 extended focus: 7.83±5.75 Day 15 conventional: 8.02±5.87	-None of the CL caused significant changes in NIKBUT
He et al. (2018)	120 subjects (120 eyes): 44 diabetics <5 years, 40 diabetics between 5-10 years, 36 >10 years and 40 healthy.	Control: 64.88±7.04 <5 years: 64.75±8.20 5-10 years: 65.03±7.14 >10 years: 66.11±7.44	Keratograph 5M	Control: 6.86±2.20 <5 years: 6.76±2.24 5-10 years: 6.25±2.53 >10 years: 5.13±1.77	-NIKBUT is shorter in long-term type 2 diabetes

(continuation)					
Study	Sample	Age (mean ± SD) years	Technique	NIKBUT (s) (mean ± SD)	Main findings
Wang et al. (2019a)	59 myopic subjects (59 eyes)	12.03±2.31	Keratograph 5M	Baseline: 11.03±5.53 1 month: 12.49±7.20 6 months: 11.10±6.35 24 months: 11.73±5.33	-Overnight orthokeratology affected NIKBUT
Wang et al. (2019c)	78 subjects with lupus erythematosus (78 eyes)	37±11	Keratograph 5M	9.12±5.97	-Lupus erythematosus is associated with higher tear film instability and DED
Chen et al. (2021)	100 MGD subjects (100 eyes) (35 had a combined therapy)	45.10±4.81	Keratograph 5M	Pre-treatment: 6.68±5.39 1 month: 6.50±3.50 3 month: 5.89±3.22	-Although the combination of meibomian gland expression and intense pulsed light had a synergistic effect, no changes were found in NIKBUT
Li et al. (2020a)	25 hyposecretory MGD subjects (25 eyes) and 25 obstructive MGD subjects (25 eyes)	Hyposecretory MGD: 32.6±10.26 Obstructive MGD: 37.2±11.74	Keratograph 5M	Hyposecretory: Baseline: 3.17±1.40 8 weeks: 3.77±1.27 Obstructive: Baseline: 3.22±1.47 8 weeks: 8.13±2.05	-Thermal pulsation LipiFlow was effective for both MGD types -The therapeutic effect was higher in the obstructive MGD group
Choi et al. (2018)	50 subjects in the smartphone group (50 eyes) and 30 controls (30 eyes)	Smartphone group: 25.52±2.92 Controls: 26.70±2.98	Keratograph 5M	Smartphone group: 10.26±6.13 Controls: 11.84±6.97	-Smartphone use could aggravate dry eye symptoms and increase tear film instability
Ren et al. (2018)	22 DED subjects (22 eyes)	26.554.85	Keratograph 5M	Baseline: 3.49±0.97 5 min: 10.20±7.21 30 min: 6.06±2.85 60 min: 6.34±3.69	-Temporary use of warming moist chamber goggle was able to relieve ocular discomfort and increase NIKBUT
Recchioni et al. (2020)	16 LASIK subjects (16 eyes) and 13 SMILE subjects (13 eyes)	LASIK: 32.6±9.1 SMILE: 32.2±5.3	Keratograph 5M	Pre-LASIK: 11.3±5.7 Post-LASIK: 6.7±3.6 Pre-SMILE: 10.2±5.4 Post-SMILE: 9.8±4.6	-LASIK caused a significant decrease in NIKBUT in comparison with SMILE

(Where CL: Contact Lens; DED: Dry Eye Disease; IQR: Interquartile Range; LASIK: Laser Assisted In Situ Keratomileusis; MGD: Meibomian Gland Dysfunction; NIKBUT: Non-Invasive Keratograph Break-Up Time; SD: Standard Deviation; SMILE: Small Incision

*Lenticule Extraction) * In the cases where "approximately" is written, studies showed the results in a figure, instead of a numerical value.*

1.3.2.1.3 Interferometers

Apart from the measurement of the lipid layer, some interferometers also allow assessing NIBUT (Wang, Palakuru and Aquavella, 2008; Hosaka et al., 2011; Pult, Purslow and Murphy, 2011; Zhang et al., 2011; Jones and Nischal, 2013; Guillon et al., 2016; Nosch et al., 2016; Wang et al., 2017; Pult et al., 2018b; Tong and Teng, 2018; Garzón, López-Alemany and Gené-Sampedro, 2019; Guillon et al., 2019a; Guillon et al., 2019b; Vigo et al., 2020). Interferometers are also based on the reflection of a pattern onto de tear film to assess BUT. It has also been reported that these devices have an acceptable diagnostic capability (*Table 1.15*) (Pult, Purslow and Murphy, 2011; Zhang et al., 2011).

Nichols et al. (2002b) reported that BUT using fluorescein was shorter than NIBUT using an interferometer. Some authors have found that NIBUT measured with the Tearscope interferometer was longer than NIBUT measured with the Keratograph 5M (Best, Drury and Wolffsohn, 2012, Markoulli et al., 2017; Tong and Teng, 2018). This might be explained as Tearscope measurements are more subjective and the technique depends on the examiner´s ability. Moreover, the keratograph is more sensitive to small tear film changes and analyses more data points of the ocular surface (Best, Drury and Wolffsohn, 2012; Tong and Teng, 2018). In addition, Markoulli et al. (2017) found that both devices were not interchangeable. They also found that the subjectivity of the Tearscope Plus limited its repeatability and detracts from its utility

in comparison with more objective devices. Conversely, Bandlitz et al. (2019a) did not find differences in NIBUT between Tearscope Plus, Polaris, EasyTear and Keratograph 5M, despite the last being objective. Moreover, the repeatability in the measurement of NIBUT was reasonable for all of them. Regarding the repeatability of NIBUT using interferometers, some authors have found it to be acceptable (Nichols et al., 2002b; Bandlitz et al., 2019a; Markoulli et al., 2017). For instance, Markoulli et al. (2017) found a coefficient of repeatability of 15 using the Tearscope Plus.

Table 1.15. *Sensitivity and specificity found by different authors in the assessment of NIBUT through interferometers.*

Study	Sample	Age (mean ± SD) years	Technique	Metric	Cut-off value	Sensitivity	Specificity
Zhang et al. (2011)	20 mild self-reported DED subjects (20 eyes), 20 moderate-severe self-reported DED (20 eyes) and 20 healthy subjects (20 eyes)	Mild: 27.2±3.6 Moderate to severe: 27.8±5.6 Controls: 28.6±5.7	Keeler Tearscope	NIBUT	< 9.7 seconds	0.90	0.50
Pult, Purslow and Murphy (2011)	47 healthy (47 eyes)	Median: 35 Range; 19-70	Tearscope Plus	NIBUT	10 seconds	0.80	0.93

(Where DED: Dry Eye Disease; NIBUT: Non-Invasive Break-Up Time; SD: Standard Deviation)

Furthermore, different authors have demonstrated that interferometers are also useful to assess the effect on tear stability of contact lenses (Guillon et al., 2016; Guillon et al., 2019a; Guillon et al., 2019b) and blinking (Nosch et al., 2016) (*Table 1.16*).

Table 1.16. *Results reported by different authors regarding the use of interferometers to assess the effect of contact lenses and blinking on NIBUT.*

Study	Sample	Age (mean ± SD) years	Technique	NIBUT (s) (mean ± SD)	Main findings
Guillon et al. (2016)	202 CL wearers (202 eyes)	29.5±9.4	Tearscope Plus	Low OSDI: 5.99±6.65 High OSDI: 4.70±4.85	-CL wearers with DED symptoms had shorter NIBUT
Nosch et al. (2016)	42 subjects (42 eyes)	27.76±5.36	Tearscope Plus	38.58±28.62	-Blink rate and NIBUT were negatively correlated -Central corneal sensitivity threshold and NIBUT were positively correlated
Guillon et al. (2019a)	32 delefilcon A CL wearers (32 eyes) and 32 somofilcon A CL wearers (32 eyes)	Delefilcon A: 34.3±9.5 Somofilcon A: 33.4±10.1	Tearscope	Delefilcon A: 9.2±11.1 Somofilcon A: 6.2±5.7	-Differences in NIBUT between lenses
Guillon et al. (2019b)	202 CL wearers (404 eyes) and 133 non-CL wearers (266 eyes)	CL wearers: 29.5±9.4 Non-CL wearers: 37.3±12.9	Tearscope Plus	CL wearers: 5.12±5.37 Non-CL wearers: 9.05±8.21	-Shorter NIBUT in CL wearers

(Where CL: Contact Lens; DED: Dry Eye Disease; NIBUT: Non-Invasive Break-Up Time; OSDI: Ocular Surface Disease Index; SD: Standard Deviation).

1.3.2.1.4 Other techniques

Other techniques to assess the stability of the tear film non-invasively are less used. For instance, assessing the movement of the particles in the tear film have been used to measure the upward spread and stability of the tear film (Owens and Phillips, 2001; Varikooty, Keir and Simpson, 2012; Sweeney, Millar and Raju, 2013; Lin and Yiu, 2014; Lai et al., 2019). Moreover, tear film stability can also be measured using interferometry, retroillumination, thermography, aberrometry or defocus microscopy.

Interferometry can be used to measure BUT through the thickness of the tear film. Thus a thinning of the tear film indicates a break-up. On the other hand, defocus microscopy measures the BUT through the focus or defocus of the tear film. Thus, the break-up zone is shown as a rough and concave surface. In this way, break-up areas appear brighter because they have a concave surface (Agero et al., 2003). Finally, retroillumination is based on the assessment of optical aberrations through the analysis of the light reflected on the retina. In this case, changes in the intensity of the reflected light can be used as a measure of the tear film stability (Liu et al., 2010; King-Smith, Begley and Braun, 2018).

1.3.2.2 Optical quality measurements

The tear film is the most anterior refractive surface of the eye and has a high impact on maintaining the optical quality of the eye due to the large difference in the refractive index between the tear film and air (Montés-Micó et al., 2010a; Denoyer, Rabut and Baudouin, 2012; Kottaiyan et al., 2012; Ring et al., 2015; Tan et al., 2015a; Koh, Higashiura and Maeda, 2016; Chan et al., 2017). Local changes in the tear film thickness or regularity, such as variations in tear break-up, will induce aberrations, which in turn will reduce retinal image quality (Tutt et al., 2000; Sweeney, Millar and Raju, 2013; Lin and Yiu, 2014). For that reason, the assessment of the optical quality has become a tool to indirectly detect and monitor DED in an objective and non-invasive way, which has the advantage of assessing the tear film stability in real time. Furthermore, a decrease in the optical quality can negatively affect the quality of life of DED patients (Deschamps et al., 2013).

There are different ways to evaluate the optical quality of the eye. Formerly, optical quality was measured by quantifying vessels' contrast in the retina or by retroillumination (Tutt et al., 2000; Himebaugh et al., 2003; Benito et al., 2019). Tutt et al. (2000) and Benito et al. (2019) confirmed that retroillumination may be a useful technique to non-invasively analyse the optical quality of the tear film. In this method, the plane of the camera is conjugated to the tear film, which allows obtaining quantitative values related to changes in the tear film stability (Tutt et al., 2000; Liu et al., 2010; Montés-Micó et al., 2010a). Moreover, the optical quality can also be measured by using aberrometers, corneal topography systems or double-pass systems.

1.3.2.2.1 Aberrometers

Wavefront sensing Hartmann-Shack aberrometer is one of the most common tools to assess the optical quality of the eye (Thibos and Hong, 1999). Hartmann-Shack wavefront sensor consists of a square array of 1024 lenslets. The device uses a laser beam that is directed to the eye, it is reflected onto the retina and returns. The reflected wavefront is subdivided into different small wavefronts by the array of lenslets. Thus, each lenslet samples a small part of the incident wavefront and focuses the light on a charge-coupled device, which allows recording the wavefront for being described by polynomials of Zernike (Thibos and Hong, 1999; McGinnigle, Naroo and Eperjesi, 2012; Tung et al., 2012; Ring et al., 2015; García-Marqués et al., 2016).

Aberrometers allow a dynamic assessment of the aberrations created by the eye, as a measurement of the tear film instability and break-up. Two types of aberrations can be distinguished: lower-order aberrations that correspond to the refraction, and

higher-order aberrations. Thus, tear film instability is reported to increase corneal higher-order aberrations after blinking (Ferrer-Blasco et al., 2009).

Several authors have also reported that DED patients have higher levels of aberrations (more Root Mean Square (RMS) values) than healthy patients (Koh et al., 2008b; Liu et al., 2010; Montés-Micó et al., 2010b; Denoyer, Rabut and Baudouin, 2012; Kottaiyan et al., 2012; McGinnigle, Naroo and Eperjesi, 2012; Tung et al., 2012; Deschamps et al., 2013; Lin and Yiu, 2014; McGinnigle, Eperjesi and Naroo, 2014; Ring et al., 2015; Koh, Higashiura and Maeda, 2016; Chan et al., 2017; Wolffsohn et al., 2017; King-Smith, Begley and Braun, 2018; Montani, Murphy and Patel, 2018; Monaco and Casalino, 2020). Moreover, low optical quality is related to increased signs and symptoms in OSDI, which suggests that the measurement of aberrations can help to assess DED (Denoyer, Rabut and Baudouin, 2012).

The technique has also been used to evaluate the efficacy of treatments (*Table 1.17*) (Tung et al., 2012; McGinnigle, Eperjesi and Naroo, 2014; Montani, Murphy and Patel, 2018; Monaco and Casalino, 2020). Tung et al. (2012) found that some components of artificial tears initially reduced the visual quality. Similarly, McGinnigle, Eperjesi and Naroo (2014) found that immediately after the instillation of hypromellose drops total higher-order aberrations increased in healthy and DED patients. Likewise, the drops caused a reduction in the Strehl ratio in healthy and dry eye patients.

Finally, wavefront sensors can be combined with topographic devices to achieve a better assessment of the tear film stability. For instance, Kottaiyan et al. (2012) combined a high-resolution wavefront sensor with a Placido disk. They confirmed that

this combination allows a better assessment of the tear film and the ocular surface since it allows quantifying NIBUT and its impact on visual quality at the same time.

Table 1.17. *Results reported by different authors regarding the use of aberrometers and corneal topography systems to assess the effect of treatments on the quality of vision.*

Study	Sample	Age (mean ± SD) years	Technique	Total ocular HOA RMS (µm) (mean ± SD)	Main findings
McGinnigle, Eperjesi and Naroo (2014)	24 DED subjects (24 eyes) and 24 healthy subjects (24 eyes)	DED: 25.7±7 Controls: 24.2±8	Aberrometer and corneal topographer Nidek OPD-Scan III	5mm DED: Baseline: 0.237±0.078 After 1 hour of drops instillation: 0.243±0.062 CONTROLS: Baseline: 0.218±0.079 After 1 hour of drops instillation: 0.213±0.075	-Immediately after the instillation, higher-order aberrations increased and the Strehl ratio reduced
Koh et al. (2008b)	7 DED subjects without superficial punctate keratopathy (7 eyes) and 13 with keratocon-junctivitis sicca (13 eyes)	Without: 45.8±10.3 With: 51.3±3.4	Hartmann-Shack wavefront aberrometer (Topcon)	4 mm Without: 0.139±-- With: 0.241±--	-Significantly lower HOAs in patients without superficial punctate keratopathy.
Montani, Murphy and Patel (2018)	50 subjects (100 eyes)	33.2±11.0	Placido disk topographer + Hartmann-Shack wavefront aberrometer	The value of the total HOA was not reported	-Artificial tears reduced HOA and meibomian gland expression increased HOA

(Where DED: Dry Eye Disease; HOA: Higher-Order Aberrations; RMS: Root Mean Square; SD: Standard Deviation).

1.3.2.2.2 Corneal topography systems

Aberrometers obtains the wavefront of the total eye. Thus, tear film aberrations are mixed with eye aberrations. To solve this issue, corneal topography systems can be used to measure the aberrations of the air-tear film interface (Guirao and Artal, 2000; Montés-Micó et al., 2004; Montés-Micó, Alió and Charman, 2005a; Ferrer-Blasco et al., 2009; Montés-Micó et al., 2010b; Ruiz-Alcocer et al., 2018; Hovanesian et al., 2019; Lafosse et al., 2019; Lorente-Velázquez et al., 2019; Yildirim, Ozsaygili and Kucuk, 2020; Gao et al., 2021). Different authors have found lower optical quality in subjects with dry eye and low BUT (*Table 1.18*). In a previous report (Guirao and Artal, 2000), the authors obtained the corneal shape elevation map and fitted it to a Zernike polynomial expansion. They found that videokeratography allowed clinicians to measure the corneal wavefront aberrations with an accuracy of 0.05-0.2 μm for a pupil diameter of 4-6 mm.

Optical quality has also been used to assess BUT as the measurement in seconds from blinking until the aberrations increase. Mihashi et al. (2006) found that BUT measured using fluorescein caused lower values than BUT measured through wavefront aberrations as well as BUT measured through the distortion of Placido disk. As explained before, these differences between methods can be due to the fact that fluorescein can destabilize the tear film. In two different studies (Montés-Micó et al., 2004; Montés-Micó, Alió and Charman, 2005a), authors evaluated the optical quality of the tear film through corneal elevation maps. They found that RMS was correlated with tear film BUT. Thus, RMS in DED patients was minimal at 2.9±0.4 seconds as compared to 6.1±0.5 seconds in healthy patients. Montés-Micó et al. (2010b) also

found a decrease in corneal higher-order aberrations after the instillation of artificial tears into eyes with pupils of 3.0 mm and 5.5 mm of diameter ($p < 0.01$). The reduction was maintained ten minutes after the instillation ($p < 0.02$). This is because eye drops increased the regularity of the tear film, which in turn decreased high-order aberrations.

Table 1.18. *Optical quality results obtained by authors.*

Study	Sample	Age (mean ± SD) years	Technique	Corneal HOA RMS (μm) (mean ± SD)	Main findings
Montés-Micó, Alió and Charman (2005a)	13 DED subjects (13 eyes)	DED: 45.3±5	Tomey TMS-2N topography system	7mm (Approximately) 1 s after blink: 1.28±--μm 4 s: 1.09±-- 6 s: 1.19±-- 8 s: 1.4±-- 10 s: 1.6±-- 14 s: 1.79±--	-RMS in DED patients was minimal at 2.9±0.4 seconds -Dynamic changes in optical aberrations may provide an objective method for the DED diagnosis
Montés-Micó et al. (2004)	15 healthy patients (15 eyes)	Healthy: 26±1.7	Tomey TMS-2N topography system	7mm (Approximately) 1 second after blink: 1.12±-- 4 s: 0.98±-- 6 s: 0.70±-- 8 s: 0.86±-- 10 s: 1.17±-- 14 s: 1.41±--	-RMS in healthy patients was minimal at 6.1±0.5 seconds.

*(Where DED: Dry Eye Disease; HOA: Higher-Order Aberrations; RMS: Root Mean Square; SD: Standard Deviation). * In the cases where "approximately" is written, studies showed the results in a figure, instead of a numerical value.*

In addition, Ferrer-Blasco et al. (2009) also studied the air-tear film interface Modulation Transfer Function (MTF) by fitting videokeratographic data with Zernike polynomials using software. They found that air-tear film MTF had the highest values at 6-7 seconds after blinking. Strehl ratio had the greatest value at 6.2±0.4 seconds after blinking and it was correlated with BUT using fluorescein, which suggests that

MTF and Strehl ratio can also be used as tools to examine optical quality changes of the tear film. Finally, the technique has also been successfully used to evaluate the efficacy of treatments and the performance of contact lenses (Table 1.19).

Table 1.19. *Results reported by different authors regarding the use of aberrometers and corneal topography systems to assess the effect on the quality of vision of treatment and contact lenses.*

Study	Sample	Age (mean ± SD) years	Technique	Corneal HOA RMS (μm) (mean ± SD)	Main findings
Montés-Micó et al. (2010b)	20 mild to moderate DED subjects (40 eyes)	57.5±8.4	Computerized video Topography system PCT 200 (corneal elevation maps)	Baseline: 3mm: 0.29±-- 5mm: 0.38±-- 10 minutes after instillation: 3mm: 0.14±-- 5mm: 0.2±--	-Corneal aberrations and corneal PSF improved significantly after eye drop instillation
Ruiz-Alcocer et al. (2018)	20 subjects (20 eyes) (A: Nesofilcon A; B: Delefilcon A; and C: Stenfilcon A)	28.7±4.2	ATLAS 9000 Corneal Topographer	4.5mm (Approximately) A Baseline: 0.43±-- A 8 hours: 0.42±-- B Baseline: 0.43±-- B 8 hours:0.42±-- C Baseline:0.43±-- C 8 hours:0.42±--	-No significant differences were found between lenses in optical quality
Lorente-Velázquez et al. (2019)	20 presbyopic (20 eyes) and non-presbyopic subjects (30 eyes) (A: Monofocal; B: Multifocal with high addition; and C: Multifocal with low addition)	Presbyopic: 53.94±7.57 Non-presbyopic: 27.00±5.97	Pentacam rotating Scheimpflug system	4.5 mm (Approximately) A Baseline: 0.39±-- A 8 hours: 0.44±-- B Baseline: 0.54±-- B 8 hours:0.57±-- C Baseline:0.50±-- C 8 hours:0.52±--	-No significant changes were found in HOA for the wearing time of CLs
Hovanesian et al. (2019)	83 subjects (83 eyes)	71.3±11.6	Zeiss Atlas topographer	6mm Pre: 0.37±0.29 Post: 0.21±0.13	-Lifitegrast decreased HOA
Gao et al. (2021)	25 DED subjects (25 eyes)	45.95±15.90	OPD Scan III aberrometer	Pre: 0.50±0.05 Post: 0.41±0.04	-Optical quality improved after DED treatment
Lafosse et al. (2019)	40 presbyopic subjects (40 eyes)	50.0±4.4	ATLAS 9000 Corneal Topographer	6mm Baseline: 0.38±0.21 20 min: 0.61±0.44 8 hours: 0.64±0.41	-Statistical significant differences were found between baseline and 20 minutes, and baseline and 8 hours of CL wearing

(continuation)					
Study	Sample	Age (mean ± SD) years	Technique	Corneal HOA RMS (μm) (mean ± SD)	Main findings
Yildirim, Ozsaygili and Kucuk (2020)	76 DED subjects (76 eyes) (26 in Group 1: 1.5 mg/mL sodium hyaluronate; 24 in Group 2: 2.0 mg/mL sodium hyaluronate; 26 in Group 3: trehalosa and sodium hyaluronate)	Group 1: 50.13±14.0 Group 2: 49.92±10.98 Group 3: 45.16±12.98	Pentacam rotating Scheimpflug system	Group 1 pre: 0.71±0.28 Group 1 post: 0.53±0.12 Group 2 pre: 0.58±0.16 Group 2 post: 0.51±0.11 Group 3 pre: 0.51±0.14 Group 3 post: 0.46±0.16	-The tree artificial tears decreased corneal aberrations

(Where CL: Contact Lens; DED: Dry Eye Disease; HOA: Higher-Order Aberrations; PSF: Point Spread Function; RMS: Root Mean Square; SD: Standard Deviation). In the cases where "approximately" is written, studies showed the results in a figure, instead of a numerical value.*

1.3.2.2.3 Double-pass systems

The measurement of higher-order aberrations is useful to assess optical quality changes in DED, but it does not evaluate the influence of scattering, which might overestimate the optical quality (Chan et al., 2017). Contrary, double-pass systems allow measuring scattering that causes light dispersion. Thus, this is a joint measurement of aberrations and light scatter.

Double-pass systems used a collimated diode laser, which enters the pupil and is reflected on the retina; the beam returns and is recorded by a charge-coupled device camera. Thus, it records the images of a point source projected on the retina and assesses the spread of this point after passing through the eye, which allows the measurement of the Ocular Scatter Index (OSI), MTF and the Strehl ratio. OSI measures

the amount of light scattered, while MTF characterizes the image degradation caused by an optical system depending on the frequency; and the Strehl ratio measures the quality of an optical system through the ratio of the peak of the Point Spread Function (PSF) of an optical system and the peak of the PSF of a perfect system (Benito, 2011; Koh et al., 2014b; Tan et al., 2015a; Chan et al., 2017).

Some authors have found that double pass systems are sensitive in the early diagnosis of DED, being the light scatter higher in DED subjects (*Table 1.20*) (Benito, 2011; Díaz-Valle et al., 2012; Kobashi et al., 2013; Habay et al., 2014; Tan et al., 2015a; Yu et al., 2016; Fernández et al., 2018; Herbaut et al., 2018; Benito et al., 2019; Gouvea et al., 2019; Xi, Qin and Bao, 2019; Ye et al., 2019; D'Souza et al., 2020; Mencucci et al., 2020; Passi et al., 2020; Wu et al., 2020a; Gao et al., 2021). For instance, Habay et al. (2014) found that OSI and the OSI standard deviation were higher in more advanced stages of the disease. The Standard Deviation (SD) represents optical quality changes; therefore, more severe DED patients had more variations and lower optical quality.

Moreover, double-pass systems have also been used to assess the inter-blink optical quality, as an indirect measurement of NIBUT. Yu et al. (2016) reported that OSI was more sensitive compared with BUT using fluorescein. Kobashi et al. (2013) did not find differences in MTF cut-off frequency, Strehl ratio and OSI over a period of 10 seconds in healthy patients. However, these parameters were altered in patients with short BUT. The repeatability of this metric in the tear film stability assessment has also been studied. Fernández et al. (2018) found that Optical Quality Analysis System (OQAS) had better intra-session repeatability in the measurement of tear film stability than a corneal topographer device.

Table 1.20. *Optical quality results obtained by authors.*

Study	Sample	Age (mean ± SD) years	Technique	MTF cut-off frequency (cpd) (mean ± SD)	Main findings
Kobashi et al. (2013)	20 subjects with short BUT (20 eyes) and 20 healthy subjects (20 eyes)	Short BUT: 31.6±4.1 Controls: 31.2±3.8	OQAS double-pass system	SHORT BUT Initial: 27.2±7.9 10 s after blink: 13.2±6.1 CONTROLS Initial: 31.6±9.0 10 s: 27.3±7.1	-Optical quality deteriorated with time in the group with short BUT -Short BUT group had greater deterioration in optical quality after the blink
Xi, Qin and Bao (2019)	35 DED subjects with short BUT (35 eyes) and 43 healthy subjects (43 eyes)	DED: 31.31±6.44 Controls: 29.02±5.37	OQAS double-pass system	DED: 26.340±8.460 Controls: 34.695±8.609	-MTF cut-off frequency was significantly lower in the short BUT subjects in the early stage of the disease -Tear film instability in short BUT DED subjects affected the optical quality
Study	Sample	Age (mean ± SD) years	Technique	Strehl ratio (mean ± SD)	Results
Kobashi et al. (2013)	20 subjects with short BUT (20 eyes) and 20 healthy subjects (20 eyes)	Short BUT: 31.6±4.1 Controls: 31.2±3.8	OQAS double-pass system	SHORT BUT Initial: 0.17±0.04 10 s after blink: 0.09±0.03 CONTROLS Initial: 0.19±0.05 10 s: 0.17±0.03	-Optical quality deteriorated with time in the group with short BUT -Short BUT group had greater deterioration in optical quality after the blink
Xi, Qin and Bao (2019)	35 DED subjects with short BUT (35 eyes) and 43 healthy subjects (43 eyes)	DED: 31.31±6.44 Controls: 29.02±5.37	OQAS double-pass system	DED: 0.149±0.039 Controls: 0.201±0.051	-The Strehl ratio was significantly lower in the short BUT subjects in the early stage of the disease -Tear film instability in short BUT DED subjects affected the optical quality
Study	Sample	Age (mean ± SD) years	Technique	OSI (mean ± SD)	Results
Tan C et al. (2015)	28 mild DED subjects (28 eyes), 28 severe DED subjects (28 eyes) and 35 controls (35 eyes)	Mild DED: 41.82±13.85 Severe DED: 45.82±11.46 Controls: 43.29±18.93	OQAS double-pass system	Mild DED: ΔOSI: 0.240±0.452 Severe DED: ΔOSI: 0.518±0.692 Controls: ΔOSI: -0.004±0.293	-DED subjects had higher OSI -The double-pass system allowed monitoring the dynamic changes in the tear film
Habay et al. (2014)	8 stage 1 DED subjects (8 eyes), 21 stage 2 subjects (21 eyes), 22 stage 3 subjects (22 eyes) and 4 stage 4 subjects (4 eyes)	Stage 1: 63±7.4 Stage 2: 63.2±10.9 Stage 3: 64.5±9.7 Stage 4: 67.6±9	OQAS double-pass system	Stage 1: 6.6±3.2 Stage 2: 16.9±4.6 Stage 3: 29.2±3.7 Stage 4: 41±5.1	-Higher severity stages had lower optical quality (more OSI).

(continuation)					
Study	Sample	Age (mean ± SD) years	Technique	OSI (mean ± SD)	Results
Kobashi et al. (2013)	20 subjects with short BUT (20 eyes) and 20 healthy subjects (20 eyes)	Short BUT: 31.6±4.1 Controls: 31.2±3.8	OQAS double-pass system	SHORT BUT Initial: 1.1±0.4 10 s after blink: 2.5±0.7 CONTROLS Initial: 0.9±0.5 10 seconds: 1.3±0.7	-Optical quality deteriorated with time in the group with short BUT -Short BUT group had greater deterioration in optical quality after the blink
Xi, Qin and Bao (2019)	35 DED subjects with short BUT (35 eyes) and 43 healthy subjects (43 eyes)	DED: 31.31±6.44 Controls: 29.02±5.37	OQAS double-pass system	DED: 1.206±0.688 Controls: 0.637±0.285	-OSI was significantly higher in the short BUT subjects in the early stage of the disease -Tear film instability in short BUT DED subjects affected the optical quality
Herbaut et al.(2018)	72 DED subjects (136 eyes)	49.2±17.3	OQAS double-pass system	1.9±1.55	-OSI was correlated with BUT, Oxford score, the Van Bijsterveld score, Schirmer test and OSDI -The OQAS system might be useful to assess visual function in DED subjects
Ye et al. (2019)	25 ADDE (25 eyes), 25 MGD (25 eyes) and 25 healthy subjects (25 eyes)	ADDE: 43.12±18.27 DED: 43.12±18.27 Controls: 43.12±18.27	OQAS double-pass system	ADDE: 1.554±0.058 DED: 2.386±0.118 Controls: 0.431±0.017	-Both ADDE and MGD had an increased OSI in comparison with controls -MGD subjects had significantly altered the optical quality in comparison with ADDE subjects
D'Souza et al. (2020)	25 DED (50 eyes) and 25 healthy subjects (50 eyes)	Range: 25-40 years	OQAS double-pass system	DED: 9.50±-- Controls: 0.69±--	-DED subjects had lower quality of vision and higher optical scatter
Gouvea et al. (2019)	66 DED (66 eyes) and 44 healthy subjects (44 eyes)	DED: 60.48±13.24 Controls: 44.51±8.06	OQAS double-pass system	DED: 4.29±4.07 Controls: 1.88±2.04	-DED had a higher OSI -Tear film instability can be objectively assessed by dynamic changes un OSI over 20 seconds
Wu et al. (2020a)	39 DED (39 eyes) and 62 healthy subjects (62 eyes)	DED: 24.9±4.6 Controls: 25.3±3.4	OQAS double-pass system	DED: 1.33±0.68 Controls: 1.17±0.76	-No statistical differences were found in OSI between groups. Nevertheless, non-ascending and ascending correlation coefficients between OSI and time of DED subjects reflect different stability of the tear film

(Where ADDE: Aqueous Deficient Dry Eye; BUT: Break-Up Time; cpd: cycles per degree; DED: Dry Eye Disease; MGD: Meibomian Gland Dysfunction; MTF: Modulation Transfer Function; OQAS: Optical Quality Analysis System; OSI: Ocular Scatter Index; SD: Standard Deviation).

Herbaut et al.(2018) confirmed that OSI was correlated with dry eye symptoms and signs, which suggests that the OQAS double-pass system can help in the understanding of DED patients' complaints about the visual quality and it could be used in the objective assessment of DED severity and follow-up.

In addition, double pass systems have also been used to assess the effectiveness and follow-up of treatments, contact lenses, the study of blinking, or the effect of visual displays (*Table 1.21*). For instance, Diaz-Valle D et al. (2012) analysed the light scattering through OQAS and found that OSI decreased after the instillation of eyedrops ($p < 0.001$, 45 minutes; $p < 0.01$, 60 minutes). García-Montero et al. (2019c) found that OSI increased only under the condition of low blink ratio after wearing silicone hydrogel contact lenses for 15 days.

Scheimpflug imaging has also been used to assess the ocular forward light scattering and corneal backward light scattering, which has been demonstrated to be higher in DED patients (Koh et al., 2014b). In this way, Koh et al. (2014b) found that DED patients had more intraocular forward light scattering and corneal backward light scattering. Furthermore, as expected, DED patients with superficial punctate keratopathy had higher anterior and total corneal backward light scattering since the cornea is less transparent. Nevertheless, Asena et al. (2017) did not find differences in the mean corneal peak densitometry and volume before and after DED therapy.

These studies confirm that optical quality systems provide a reliable assessment of the tear film stability, especially in patients with mild DED in whom the disease is more difficult to diagnose.

Table 1.21. *Results reported by different authors regarding the use of double-pass systems to assess the effect on the quality of vision of treatments, contact lenses, blinking and visual displays.*

Study	Sample	Age (mean ± SD) years	Technique	MTF cut-off frequency (cpd) (mean ± SD)	Main findings
Ferrer-Blasco T et al. (2009)	14 eyes of healthy, young patients	25±1.3	Tomey TMS-2N topography system (corneal elevation maps)	Authors provided the figures of the MTF in the air-tear film interface	-The best optical quality was achieved 6 seconds after the blink -MTF is a useful metric for optical quality assessment of tear film changes
Bettach et al. (2021)	41 subjects (41 eyes)	32.1±10.6	OQAS double-pass system (HD Analyzer)	Before reading task: 39.53±8.23 After reading task: 38.42±9.73	-A reading task on a smartphone affected tear film stability and OSI. Nevertheless, the MTF cut-off was not altered
Gao et al. (2021)	25 DED subjects (25 eyes)	45.95±15.90	OQAS double-pass system	Pre: 23.88±2.16 Post: 30.87±2.08	-Optical quality improved after DED treatment
Study	Sample	Age (mean ± SD) years	Technique	Strehl ratio (mean ± SD)	Results
Ferrer-Blasco et al. (2009)	14 eyes of healthy, young patients	25±1.3	Tomey TMS-2N topography system (corneal elevation maps)	Air-tear film interface optical quality (Approximately) <u>3mm:</u> 2 s after blink: 0.49±-- 6s: 0.63±-- 10s: 0.49±-- 15s: 0.31±--	-The best optical quality was achieved 6 seconds after the blink -The Strehl ratio is a useful metric for optical quality assessment of tear film changes
Bettach et al. (2021)	41 subjects (41 eyes)	32.1±10.6	OQAS double-pass system (HD Analyzer)	Before reading task: 0.24±0.15 After reading task: 0.21±0.05	-A reading task on a smartphone affected tear film stability and OSI. Nevertheless, the MTF cut-off was not altered
Gao et al. (2021)	25 DED subjects (25 eyes)	45.95±15.90	OQAS double-pass system	Pre: 0.14±0.01 Post: 0.17±0.01	-Optical quality improved after DED treatment
Study	Sample	Age (mean ± SD) years	Technique	OSI (mean ± SD)	Results
Diaz-Valle et al. (2012)	25 DED subjects (25 eyes) and 10 healthy subjects (10 eyes)	DED: 39.2±10.7 Controls 31.1±11.4	OQAS double-pass system	DED: 20 s after blinking: 4.7±2.7 Controls: 20 s without blinking: 1.6±0.4	-OSI was significantly higher in the DED group -The instillation of eye drops improved OSI -OSI was correlated with Schirmer test, OSDI, BUT using fluorescein and corneal staining score

(continuation)					
Study	Sample	Age (mean ± SD) years	Technique	OSI (mean ± SD)	Results
Yu et al. (2016)	32 DED subjects (32 eyes) and 109 asymptomatic subjects (109 eyes)	DED: 24.8±5.3 Asymptomatic: 24.6±4.2	OQAS double-pass system	DED: 1.41±0.88 Asymptomatic: 1.05±0.63	-There were variations in OSI after the blink even in asymptomatic subjects -The double-pass system has potential to detect the preclinical phase of DED
García-Montero et al. (2019c)	15 subjects (15 eyes)	24.1±2.2 (CL A: Lotrafilcon B; CL B: Samfilcon A; CL C: Comfilcon A; and CL D: Filcom V3)	OQAS double-pass system (HD Analyzer)	Low blink ratio A Day 0: 0.83±0.46 A Day 15: 1.84±1.64 B Day 0: 0.79±0.26 B Day 15: 1.88±1.98 C Day 0: 1.02±0.60 C Day 15: 2.23±2.44 D Day 0: 0.66±0.16 D Day 15: 1.10±0.43 High blink ratio A Day 0: 0.66±0.26 A Day 15: 0.93±0.61 B Day 0: 0.79±0.22 B Day 15: 1.15±0.58 C Day 0: 0.70±0.34 C Day 15: 1.15±0.76 D Day 0: 0.64±0.16 D Day 15: 1.01±0.67	-OSI increased over time for all CLs in low blink rate -Tear film optical quality decreased only for the lowest blink ratio after wearing silicone hydrogel CLs
Bettach et al. (2021)	41 subjects (41 eyes)	32.1±10.6	OQAS double-pass system (HD Analyzer)	Before reading task: 0.57±0.25 After reading task: 0.68±0.36	-A reading task on a smartphone affected tear film stability and the optical quality
Passi et al. (2020)	21 DED subjects (33 eyes)	64.8±14.9	OQAS double-pass system (HD Analyzer)	Pre: 2.08±1.70 Post: 1.78±1.39	-Optical quality after intranasal neurostimulator improved optical quality
Study	Sample	Age (mean ± SD) years	Technique	OSI (mean ± SD)	Results
Mencucci et al. (2020)	60 subjects (60 eyes) (30 novel injectable intracameral solution and 30 anaesthetic drops)	Novel: 73±7 Anaesthetic: 74±8	OQAS double-pass system	(Approximately) Novel Day 1: 1.85±-- Day 5: 1.52±-- Day 15: 1.25±-- Anaesthetic Day 1: 1.90±-- Day 5: 1.70±-- Day 15: 1.68±--	-Novel injectable intracameral solution cause better optical quality and tear film stability after cataract surgery
Gao et al. (2021)	25 DED subjects (25 eyes)	45.95±15.90	OQAS double-pass system	Pre: 3.58±0.69 Post: 2.11±0.49	-Optical quality improved after DED treatment

(continuation)					
Study	Sample	Age (mean ± SD) years	Technique	OSI (mean ± SD)	Results
Vandermeer, Chamy and Pisella (2018)	19 DED subjects (19 eyes with artificial tears and 19 with normal saline)	67±13.5	OQAS double-pass system	Artificial tears pre: 1.607±1.109 Artificial tears post: 1.507±0.985 Normal saline pre: 1.917±1.478 Normal saline pre: 1.693±1.317	-Artificial tear allowed better stabilization of the tear film and a significant improvement in the optical quality in comparison to normal saline

(Where BUT: Break-Up Time; CL: Contact Lens; cpd: cycles per degree; DED: Dry Eye Disease; MTF: Modulation Transfer Function; OQAS: Optical Quality Analisys System; OSDI: Ocular Surface Disease Index; OSI: Ocular Scatter Index; SD: Standard Deviation).

** In the cases where "approximately" is written, studies showed the results in a figure, instead of a numerical value.*

1.3.2.3 Lipid layer thickness assessment

The assessment of the lipid layer thickness is essential due to the role that it plays in maintaining the stability of the tear film. The lipid layer thickness can be non-invasively evaluated using interferometry, which allows clinicians to carry out both a qualitative and a quantitative assessment of the lipid layer (Arita, Fukuoka and Morishige, 2017b). It has been reported that interferometry provides clinical information about DED and MGD (Arita, Fukuoka and Morishige, 2017a) and it allows clinicians to monitor the condition of the lipid layer (Geerling et al., 2017; Arita, Fukuoka and Morishige, 2017c; Park et al., 2018).

This technique is based on the analysis of the fringe interference pattern caused by the interaction of waves. Lipid layer interferences are caused by differences in the optical path of the waves reflected on the air-lipids and lipids-aqueous layer interfaces

(King-Smith et al., 2004; Montés-Micó et al., 2010a; Hosaka et al., 2011; Szczesna, 2011; McGinnigle, Naroo and Eperjesi, 2012; Sweeney, Millar and Raju, 2013; Lin and Yiu, 2014; Ring et al., 2015; Arita, Fukuoka and Morishige, 2017a; Arita, Fukuoka and Morishige, 2017b; Arita, Fukuoka and Morishige, 2017c; Bai and Nichols, 2017; Chan et al., 2017; Geerling et al., 2017; Park et al., 2018). Constructive interference occurs when two waves interfere in-phase and generate a bright fringe, whilst destructive interference occurs when two waves interfere out-phase and a dark fringe is generated (Hosaka et al., 2011; Sharma and Oliver, 2018). Due to the polychromatism of light, a colour pattern is created in the thickest lipid layer thicknesses (Bai and Nichols, 2017).

A white or grey wave-pattern is observed in normal subjects, whereas a dark pattern is characteristic of DED and hyposecretory MGD (Arita, Fukuoka and Morishige, 2017c). The Guillon-Keeler system describes the following patterns: open meshwork (13-53 nm), closed meshwork (13-50 nm), wave/flow (50-70 nm), amorphous (80-90 nm), colour fringes (90-180 nm) and globular (>200 nm) (Isenberg et al., 2003). On the other hand, the Yokoi scheme is more commonly used and it has five grades: grade 1 (greyish and uniform), grade 2 (greyish and non-uniform), grade 3 (few colours but non-uniform), grade 4 (very colourful but non-uniform) and grade 5 (exposed cornea from absent of lipid layer) (Guillon et al., 1997; Eom et al., 2013; Ring et al., 2015).

In addition, interferometry has also been used to assess the whole tear film thickness (Wolffsohn et al., 2017). In this case, the reflection of the waves is caused on the surface of the tear film and the interface between the tear film and the cornea.

1.3.2.3.1 Specular reflection using a slit-lamp

Different interferometry techniques exist to evaluate the tear film lipid layer stability, but the cheapest technique is the specular reflection using a slit-lamp (Yokoi, Takehisa and Kinoshita, 1996; Wolffsohn et al., 2017). In this technique, clinicians observe the interference pattern of the tear film and subjectively classify it into a grade. Yokoi, Takehisa and Kinoshita (1996) found that despite the repeatability of this technique being influenced by the examiner's ability; results were highly correlated with DED severity. Neverthelessbi, it had a high degree of intra and inter-observer variability and clinicians need more time to carry it out. To solve this issue, some authors developed computer-based analysis systems to assess and classify interferometric patterns in an automatic way, which provides more objectivity, good accuracy, precision, sensitivity and specificity (Remeseiro et al., 2014a; Remeseiro et al., 2016).

1.3.2.3.2 Interferometers

The tear film can also be measured through interferometers, which are portable devices that are usually coupled with a slit-lamp. Not only are interferometers able to assess the lipid layer, but most of them also allow the evaluation of other tear film parameters, such as NIBUT and TMH (Ring et al., 2015; Arita, Fukuoka and Morishige, 2017b; Wolffsohn et al., 2017).

Different studies have demonstrated the utility of interferometry in diagnosis and grading of DED and MGD in different populations (Nichols et al., 2002b; Yokoi et al., 2008; Hosaka et al., 2011; Eom et al., 2013; Jones and Nischal, 2013; Menzies et al.,

2015; Zhao, Tan and Tong, 2015; Aragona et al., 2017; Park et al., 2018; Chou, Fan and Lin, 2019; Hwang, Lee and Chung, 2019; Jie et al., 2019; Arita and Fukuoka, 2020; Li et al., 2020b; Zhang et al., 2020a; Zhang et al., 2020b). They have found statistical thinner lipid layer thickness in DED subjects than in controls (*Table 1.22*) (Yokoi et al., 2008; Hosaka et al., 2011; Jones and Nischal, 2013; Menzies et al., 2015; Chou, Fan and Lin, 2019; Hwang, Lee and Chung, 2019; Zhang et al., 2020a; Zhang et al., 2020b). Moreover, lipid layer thickness measured using interferometers have found to be directly correlated with BUT and meibomian gland secretion; and inversely correlated with DED symptoms, osmolarity, meibomian glands drop-out, ocular surface staining and Schirmer test (Nichols et al., 2002b; Jones and Nischal, 2013; Chou, Fan and Lin, 2019; Hwang, Lee and Chung, 2019; Jie et al., 2019; Tong, Teo and Lee, 2019; Lee et al., 2020c; Li et al., 2020b; Zhang et al., 2020a; Weng et al., 2021). This suggests that interferometry might be a useful tool in understanding the pathophysiology of DED (Hwang, Lee and Chung, 2019).

Main tear interferometers which are commercially available are Tearscope, Tearscope Plus, Tearscope 2, Lipiscanner, LipiView and DR-1 interferometer (Goto and Tseng, 2003; Yokoi et al., 2008; García-Resúa et al., 2014; Rohit et al., 2014; Menzies et al., 2015; Ring et al., 2015; Zhao, Tan and Tong, 2015; Aragona et al., 2017; Arita, Fukuoka and Morishige, 2017b; Rohit, Willcox and Stapleton, 2017; Wolffsohn et al., 2017; Arita et al., 2018; Itokawa et al., 2018; Park and Baek, 2018; Cho et al., 2019; Chou, Fan and Lin, 2019; Garzón, López-Alemany and Gené-Sampedro, 2019; Jie et al., 2019; Kang et al., 2019; Lee et al., 2019; Tong, Teo and Lee, 2019; Wong et al., 2019a; Arita and Fukuoka, 2020; Fan et al., 2020; Kaido et al., 2020; Lim, Han and Tong, 2020;

Simsek et al., 2020; Zhang et al., 2020b; Lee, Hyon and Jeon, 2021; Weng et al., 2021). Generally, they also depend on the examiner's ability to classify the interference pattern, which might decrease the repeatability of the method (*Table 1.23*) (García-Resúa et al., 2014). García-Resúa et al. (2014) found poor intra- e inter-observer repeatability in the lipid layer thickness measurement with Tearscope Plus. Thus, misinterpretations may appear even in the same observer. Nevertheless, Nichols et al. (2002b) found that Tearscope Plus had moderate to substantial within and between examiners' agreement in the lipid layer assessment.

On the other hand, LipiView overcomes this issue since it allows quantifying the lipid layer thickness automatically using a broad-band white light source in 20 seconds (Eom et al., 2013; Finis et al., 2013; Menzies et al., 2015; Ring et al., 2015; Zhao, Tan and Tong, 2015; Kim et al., 2016; Arita, Fukuoka and Morishige, 2017b; Markoulli et al., 2018; Park and Baek, 2018; Park, Kim and Baek, 2018; Chou, Fan and Lin, 2019; Hwang, Lee and Chung, 2019; Jie et al., 2019; Kang et al., 2019; Lee et al., 2019; Tong, Teo and Lee, 2019; Wong et al., 2019a; Arita and Fukuoka, 2020; Li et al., 2020b; Lim, Han and Tong, 2020; Zhang et al., 2020b; Kang et al., 2021; Lee, Hyon and Jeon, 2021; Weng et al., 2021). This device quantifies the thickness in Interferometric Color Units (ICU) by analysing specular reflections. 1 ICU is approximately 1 nm (Finis et al., 2013; Ring et al., 2015; Arita, Fukuoka and Morishige, 2017b; Chan et al., 2017). The automatic measurement provides more objective, repeatable and standardized results since they depend less on the examiner's ability (Eom et al., 2013; Zhao, Tan and Tong, 2015; Markoulli et al., 2017). Thus, Eom et al. (2013) found that the LipiView interferometer had excellent intra-observer reliability.

Table 1.22. *Lipid layer thickness results using interferometers obtained by authors.*

Study	Sample	Age (mean ± SD) years	Device	Lipid layer pattern or Lipid layer thickness (mean ± SD)	Main findings
Nichols et al. (2002b)	40 subjects (40 eyes)	31.6±11.0	Tearscope Plus	(Guillon: Range 1-5) Real time examiner: Grade (0-1): 13 subjects Grade (2): 15 Grade (3-5): 12 Digital examiner: Grade (0-1): 22 subjects Grade (2): 7 Grade (3-5): 11	- Higher NIBUTs for both examiners were associated with thicker tear film interference patterns
Hosaka et al. (2011)	28 ADDE (28 eyes) and 14 healthy subjects (14 eyes)	ADDE: 62.2±11.4 Controls: 27.1±6.1	Quore MSPA1100 and DR-1 interferometer	Tear film thickness ADDE: 2.0±1.5 µm Controls: 6.0±2.4 µm (Yokoi: Range 1-5) ADDE: 3.4±0.9 score Controls: 2.0±0.7 score	-ADDE had significant lower tear film thickness.
Eom et al. (2013)	30 obstructive MGD (30 eyes) and 25 healthy subjects (25 eyes)	MGD: 46.1±11.6 Controls: 30.4±6.9	LipiView interferometer	MGD: 54.2±17.9 ICU Controls: 65.0±19.1 ICU	-Lipid layer thickness was significantly lower in MGD subjects -Lipid layer thickness was negatively correlated with upper and lower meibomian gland drop-out
Chou, Fan and Lin (2019)	115 subjects (229 eyes)	60.5±13.6	LipiView interferometer	71.2±-- nm	-Lipid layer thickness was inversely correlated to DED symptoms -Lipid layer thickness was inversely correlated to the Schirmer test -Subjects with lipid layer thickness < 69 nm were more likely to have DED symptoms
Weng et al. (2021)	143 young (143 eyes), 304 middle age subjects (304 eyes) and 228 elderly subjects (228 years)	Young: 32.0±5.9 Middle: 52.1±5.7 Elderly: 68.5±6.3	LipiView interferometer	Young: 50.5±15.9 nm Middle: 52.4±14.1 nm Elderly: 57.1±16.0 nm	-DED symptoms were negatively correlated with lipid layer thickness -Young DED subjects had thinner lipid layer thickness
Jie et al. (2019)	29 subjects (29 eyes)	62±12.30	LipiView interferometer	67.42±21.17 nm	-Lipid layer thickness was negatively correlated with tear osmolarity
Zhang et al. (2020a)	31 night medical staff (62 eyes) and 31 controls (59 eyes)	Night: 26.55±3.15 Controls: 21.91±4.33	LipiView II interferometer	Night: 55.02±21.17 ICU Controls: 72.76±21.62 ICU	-Lipid layer thickness was thinner in night shift medical staff -Lipid layer thickness was negatively correlated with DED symptoms

(continuation)					
Study	Sample	Age (mean ± SD) years	Device	Lipid layer pattern or Lipid layer thickness (mean ± SD)	Main findings
Kim et al. (2016)	43 subjects (43 eyes)	65.0±13.8	LipiView interferometer	Baseline: 66.95±19.09 ICU 1 month: 60.60±20.99 ICU 3 months: 66.67±20.42 ICU	-Lipid layer thickness was positively correlated with BUT. -Lipid layer thickness was negatively correlated with DED symptoms, ocular surface staining, and meibum quality score
Hwang, Lee and Chung (2019)	30 Sjögren syndrome DED (30 eyes) and 30 non-Sjögren syndrome DED subjects (30 eyes)	Sjögren: 50.8±9.8 Non-Sjögren: 55.3±15.0	LipiView II interferometer	Sjögren: 72.3±31.2 nm Non-Sjögren: 84.7±20.2 nm	-Maximum lipid layer thickness was thinner in the Sjögren syndrome DED group -Lipid layer thickness was negatively correlated meibomian glands drop-out and conjunctival staining scores in the Sjögren syndrome group
Menzies et al. (2015)	11 Sjögren syndrome (11 eyes) and 10 healthy subjects (10 eyes)	Sjögren: 56.0±9.1 Controls: 58.5±4.7	Tearscope Plus	Median (IQR) Sjögren: 15 (15-15) nm Controls: 60 (45-100) nm	-Sjögren syndrome group had thinner lipid layer thickness
Tong, Teo and Lee (2019)	120 subjects (120 eyes)	61.0±13.8	LipiView interferometer	66.2±24.5 nm	-Low NIBUT in inferior peripheral locations is associated with a thin lipid layer thickness

(Where ADDE: Aqueous Deficient Dry Eye; DED: Dry Eye Disease; ICU: Interferometric Color Units; MGD: Meibomian Gland Dysfunction; NIBUT: Non-Invasive Break-Up Time; SD: Standard Deviation).

Table 1.23. *Results of main studies that assessed the repeatability of lipid layer thickness using interferometers.*

Study	Type of repeatability	Device	Cohen's kappa	CoR
Markoulli et al. (2017)	Intraexaminer	LipiView		20.9 nm
		Tearscope		90.2 nm
Zhao, Tan and Tong (2015)	Intraexaminer	LipiView		16 nm
	Interexaminer			13 nm
García-Resúa et al. (2014)	Intraexaminer	Tearscope	Examiner 1: 0.770 Examiner 2: 0.812	
	Interexaminer		Examiner 1: 0.615 Examiner 2: 0.633	
Dutta et al. (2019)	Intraexaminer	LipiView		42.4 nm

(Where CoR: Repeatability Coefficient).

Moreover, it has been reported that LipiView has a sensitivity of 65.8 % and a specificity of 63.4 % with a cut-off value of 75nm of lipid layer thickness in the diagnosis of MGD (Finis et al., 2013). Zhao, Tan and Tong (2015) found that the limits of agreement for inter- and intra-observer results were similar, which suggests that the repeatability of LipiView is independent of its examiner. In addition, Markoulli et al. (2017) found significantly higher lipid layer thickness with Tearscope Plus in comparison to LipiView. Thus, both devices were not interchangeable due to the subjectivity of the Tearscope Plus, which limits its repeatability and detracts from its utility in comparison with more objective devices.

Recently, IDRA ocular surface analyzer has been developed. It allows performing automatic interferometry through the analysis of the interference colours from the lipid layer. It determines the average, maximum and minimum lipid layer thickness according to the scale of Guillon (Lee et al., 2020a). Lee et al. (2020a) did not find significant differences between IDRA and LipiView in the lipid layer thickness assessment.

Finally, lateral shearing interferometry relies on illumination with a helium-neon laser to obtain the data, which are processed using Fourier transform analysis. This allows clinicians to evaluate tear film surface irregularities and their relationship to the break-up of the lipid layer (Szczesna, 2011; Szczesna-Iskander, 2014; Szczesna-Iskander, 2018). Szczesna-Iskander et al. (2014) compared the pre-lens tear film quality of two contact lenses through this interferometric technique and found a reduction in pre-lens tear film quality in both contact lenses. However, water gradient silicone hydrogel lenses had less impact on the tear film. The same author (Szczesna, 2011)

claimed that this method can help to assess the tear film on soft contact lenses in a non-invasive way.

In addition, interferometers have also been used to assess the effectiveness and follow-up of treatments and surgical procedures, and the effect of some diseases on the lipid layer (*Table 1.24*) (Rohit et al., 2014; Kim et al., 2016; Rohit, Willcox and Stapleton, 2017; Arita et al., 2018; Itokawa et al., 2018; Markoulli et al., 2018; Park, Kim and Baek, 2018; Szegedi et al., 2018; Kang et al., 2019; Lee et al., 2019; Wong et al., 2019a; Arita and Fukuoka, 2020; Kaido et al., 2020; Lim, Han and Tong, 2020; Zhang et al., 2020b; Kang et al., 2021).

Table 1.24. *Results reported by different authors regarding the use of interferometers to assess the effect on the lipid layer of treatments, surgical procedures and diseases.*

Study	Sample	Age (mean ± SD) years	Device	Lipid layer pattern or Lipid layer thickness (mean ± SD)	Main findings
Wong et al. (2019a)	20 subjects (20 eyes with treatment and contralateral eyes used as controls)	Median: 63.5 (range 48-76)	LipiView interferometer	Treated baseline: 70.4±25.5 nm Treated 30 days: 68.5±24.8 nm Non-treated baseline: 71.4±22.3 Non-treated 30 days: 68.3±23.7	-Lipid layer thickness did not improve after treatment with eyelid wipes
Aragona et al. (2017)	66 psoriasis (66 eyes) and 30 healthy subjects (30 eyes)	Psoriasis: 50.7±13.1 Controls: 45.6±16.3	Tearscope Plus	(Guillon: Range 1-5) Psoriasis: 2.7±1.9 Controls: 4.7±1.8	-Subjects with psoriasis had altered lipid layer thickness
Kang et al. (2019)	124 DED subjects (124 eyes)	28.92±6.33	LipiView interferometer	Baseline: 61.50±2.57 nm After diquafosol eye drops: 73.27±2.67 nm	-Topical instillation of diquafosol increased lipid layer thickness in DED subjects with MGD

(continuation)					
Study	Sample	Age (mean ± SD) years	Device	Lipid layer pattern or Lipid layer thickness (mean ± SD)	Main findings
Park and Baek (2018)	98 thyroid eye disease (98 eyes) and 62 DED subjects (62 eyes)	Thyroid: 45.8±12.4 Controls: 48.3±11.3	LipiView Interferometer	Thyroid: 78.64±22.11 nm Controls: 78.47±23.94 nm	-No statistically significant differences were found between controls and subjects with thyroid eye disease in lipid layer thickness
Zhang et al. (2020b)	31 diabetic cataracts (31 eyes) and 38 age-related cataract subjects (38 eyes)	Diabetic: 71.0±10.7 Controls: 65.2±11.0	LipiView II interferometer	Diabetic before: 65.7±23.3 nm Diabetic after: 51.3±17.1 nm Controls before: 67.1±23.4 nm Controls after: 60.2±21.1 nm	-Lipid layer thickness was correlated with the duration of diabetes mellitus and was significantly thinner after cataract surgery
Kim et al. (2016)	43 subjects (43 eyes)	65.0±13.8	LipiView interferometer	Baseline: 66.95±19.09 ICU 1 month: 60.60±20.99 ICU 3 months: 66.67±20.42 ICU	-Lipid layer thickness was thinner 1 month after cataract surgery
Arita and Fukuoka (2020)	36 MGD with posterior blepharitis subjects (36 eyes) (16 azithromycin and 20 preservative-free artificial drops)	Azithromycin: 60.1±17.9 Controls: 61.9±12.2	LipiView interferometer	Azithromycin class 0: 19% Azithromycin class 1: 38% Azithromycin class 2: 44% Controls class 0: 25% Controls class 1: 25% Controls class 2: 50%	-Azithromycin improved lipid layer thickness after treatment
Fan et al. (2020)	64 MGD subjects (36.09±11.13)	36.09±11.13	DR-1 interferometer	(Yokoi: Range 1-5) Baseline: 3.61±0.5 score Post: 1.93±1.25 score	-Lipid layer thickness improved after intense pulsed light treatment
Lee et al. (2019)	30 unilateral normal-tension glaucoma subjects (60 eyes)	61.33±11.75	LipiView interferometer	Glaucoma eye: 64.83±16.50 Normal eye: 77.26±17.81	-Eyes with long-term glaucoma medications had thinner lipid layer thickness
Kang et al. (2021)	41 subjects (41 eyes) (A: 21 cyclosporine A and 20 carboxymethyl cellulose	A: 63.43±12.09 B: 68.45±8.83	LipiView interferometer	Pre A: 77.67±21.71 Post A: 81.57±18.45 Pre B: 75.80±20.56 Post B: 71.45±19.64	-Treatment with 0.05% cyclosporine A is effective after cataract surgery to improve lipid layer thickness

(continuation)					
Study	Sample	Age (mean ± SD) years	Device	Lipid layer pattern or Lipid layer thickness (mean ± SD)	Main findings
Lee, Hyon and Jeon (2021)	102 DED subjects (201 eyes)	56.38±11.78	LipiView II interferometer	77.86±22.66	-Eyes with corneal erosions had significantly higher lipid layer thickness
Rohit, Willcox and Stapleton (2017)	40 contact lens wearers (40 eyes)	26±9	Tearscope	(Guillon: Range 1-5) Baseline: 3.0±1.0 Day 14 lipid: 3.0±1.0 Day 14 placebo: 2.0±1.0	-Lipid drops did not change lipid layer thickness -Placebo drops decreased lipid layer thickness
Park, Kim and Baek (2018)	17 subjects after chemotherapy (34 eyes)	62.4±14.82	LipiView interferometer	Mean: 34.5 (Range: 20-89) nm	-Lipid layer thickness in subjects after chemotherapy was under the normal value
Kaido et al. (2020)	17 contact lens wearers (17 eyes)	36.8±8.3	DR-1 interferometer	(2 patterns: 1=grayish monochromatic and 2=multicolour band) With CL 1: 8 subjects 2: 9 subjects After CL 1: 17 subjects 2: 0 subjects	-CL decreased lipid layer thickness
Markoulli et al. (2018)	20 subjects (40 eyes)	20.7±1.7	LipiView interferometer	Visit 1 right eye: 55.4±13.6 nm Visit 2 right eye: 61.9±18.2 nm Visit 3 right eye: 57.2±22.7 nm Visit 1 left eye: 59.2±15.5 nm Visit 2 left eye: 65.1±21.3 nm Visit 3 left eye: 54.9±16.8 nm	-Eyedrops increased lipid layer thickness for 15 minutes
Simsek et al. (2020)	22 subjects drinking alcohol (44 eyes) and 22 subjects drinking water (44 eyes)	Alcohol: 35.3±-- Water: 37.5±--	DR-1 interferometer	(Yokoi: Range 1-5) The lipid layer showed mixed colour indicating dry eye in the alcohol group	-Lipid layer was altered 12 hours after alcohol intake

(Where CL: Contact Lens; DED: Dry Eye Disease; ICU: Interferometric Color Units; MGD: Meibomian Gland Dysfunction; SD: Standard Deviation).

1.3.2.3.3 Other techniques

Other techniques have also been developed to measure the lipid layer thickness. For instance, Ellipsometry has advantages in front of the use of coloured interference patterns to assess the lipid layer thickness. It measures the degree of phase shift as light is reflected from a surface film, which increases sensitivity over a reflection measurement. It allows the measurement of the lipid refractive index and the lipid layer thickness (Kottaiyan et al., 2012; Glasgow, 2019).

Finally, topographic devices, such as Keratograph 5M, have also incorporated software to analyse the tear film, which allows the recording of the pattern. However, generally, they also need that clinicians classify subjectively the lipid layer interference patterns (Markoulli et al., 2017; Li et al., 2019; Kim et al., 2021).

1.3.2.4 Infrared thermography

Infrared thermography is a non-invasive technique, which measures the amount of infrared radiation emitted from the ocular surface and periorbital skin by using a long-wave infrared thermal camera (Chan et al., 2017). It has been reported that the normal corneal temperature calculated using thermography is between 35.4 ± 0.1ºC and 34.01 ± 0.64ºC (Tan, Ng and Acharya, 2011). Purslow et al.(211) found that the Ocular Surface Temperature (OST) was mainly due to the tear film. Thus, changes in the temperature of the ocular surface can also help clinicians in understanding ocular physiology and in DED diagnosis since evaporation of tear film causes the ocular surface cooling rate to be faster in DED patients than in controls (*Table 1.25*) (Ring et

al., 2015; Versura et al., 2015; Zhang et al., 2015; Abreau et al., 2016; Yamaguchi et al., 2016; Matteoli et al., 2020).

Table 1.25. *Results reported by different authors through thermography.*

Study	Sample	Age (mean ± SD) years	Device	Results (mean ± SD)	Main findings
Abreau et al. (2016)	10 subjects (10 eyes) in each group: controls, Sjögren syndrome, EDE and ADDE	SS: 51.8±13.83 EDE: 48.4±13.12 ADDE: 46.1±13.67 Controls: 50.1±12.25	Non-invasive infrared thermal camera (Thermovision A40)	OST in 9 mm diameter in the central cornea over 5 seconds Controls: 34.95±0.60 ºC SS: 34.29±0.57 ºC EDE:34.36±0.60 ºC ADDE: 33.95±1.11 ºC	-All DED types had significantly lower ocular surface temperatures than controls
Kawali (2013)	Patients with ocular inflammation (1 eye with MGD-keratitis)	35 years	Non-contact thermographic camera FLIR P620	The authors provided the thermography maps	-MGD-keratitis patient had a low corneal temperature
Nosch et al. (2016)	42 healthy subjects (42 eyes)	27.76±5.36	Self-calibrating thermal infrared camera (FLIR A310)	2 seconds after 5 natural blinks Minimum OST central cornea: 34.98±0.68 ºC Minimum OST inferior cornea: 35.11±0.74 ºC	-Interactions between OST, corneal sensitivity, NIBUT and blink frequency
Matteoli et al. (2020)	220 healthy subjects (220 eyes) (112 male and 108 female)	Male: 45.7±19.9 Female: 44.4±17.6	Non-contact infrared thermography camera (FLIR 320 A)	OST nasal cantus ºC Male: 35.78±0.49 Female: 35.68±0.49 OST central cornea ºC Male: 35.00±0.48 Female: 34.93±0.46 OST temporal cantus ºC Male: 35.15±0.44 Female: 35.23±0.48	-OST measured in five different regions was different -The nasal cantus was the hottest region and the central cornea the coolest -OST was inversely correlated with age
Yamaguchi et al. (2016)	30 DED subjects (30 eyes) and 30 healthy (30 subjects)	DED: 52.9±17.1 Controls: 42.7±17.0	Ocular surface termographer (TOMEY Corp)	-	-The decrease of temperature in DED subjects was higher than in controls at 10 seconds after blinking -OST was correlated with NIBUT

(Where ADDE: Aqueous Deficient Dry Eye; DED: Dry Eye Disease; EDE: Evaporative Dry Eye; MGD: Meibomian Gland Dysfunction; NIBUT: Non-Invasive Break-Up Time; OST: Ocular Surface Temperature; SD: Standard Deviation; SS: Sjögren Syndrome).

For instance, Abreau et al. (2016) compared the temperatures of the eyelid, the ocular surface and the periorbital skin between Sjögren syndrome, ADDE and EDE patients and found that ADDE patients had the lowest mean initial OST in each region than controls, EDE and Sjögren syndrome subjects, whilst the healthy group had the highest. Moreover, Versura et al. (2015) found a relationship between the sensation of discomfort and low corneal temperatures in DED patients. In addition, Tan, Sanjay and Morgan (2016b) reported that the best detectors of DED were the absolute temperature of extreme nasal conjunctiva 5 and 10 seconds after eye-opening.

Several authors have claimed that thermography is a non-invasive, easy, quick, reproducible and repeatable technique with acceptable sensitivity and specificity, which could be used as a clinical diagnostic tool to differentiate and grade the severity of DED (*Table 1.26*) (Kamao et al., 2011; Kottaiyan et al., 2012; Kawali, 2013; Li et al., 2015b; Ring et al., 2015; Zhang et al., 2015; Abreau et al., 2016; Tan, Sanjay and Morgan, 2016a; Tan, Sanjay and Morgan, 2016b; Yamaguchi et al., 2016; Matteoli et al., 2017; Su et al., 2017; Wolffsohn et al., 2017; Itokawa et al., 2018; Konieczka et al., 2018; García-Porta et al., 2019; Konieczka et al., 2019; García-Montero et al., 2019a; Minatel-Riguetto et al., 2019; Kremers, Hohberger and Bergua, 2020; Matteoli et al., 2020; Németh et al., 2020; Su and Chang, 2021). Thus, Su et al. (2011) found acceptable sensitivity (0.84) and specificity (0.83) in the diagnosis of DED using a custom-designed infrared thermal image system. In this case, they combined two parameters to diagnose the disease: the temperature difference value which was the change of temperature after blinking and the compactness value which was the degree of tear film stability over 6 seconds eye-open period. In addition, Tan, Sanjay and

Morgan (2016a) found that NEC infrared thermo-tracer TH 9260 had acceptable repeatability in assessing OST in healthy and DED patients.

Table 1.26. *Sensitivity and specificity found by different authors in the assessment of ocular temperature through thermography.*

Study	Sample	Age (mean ± SD) years	Technique	Metric	Cut-off value	Sensitivity	Specificity	Area under the curve
Su and Chang (2021)	195 subjects (195 eyes)	42.2±16.2	IT-85 video-thermographer	OST	3 seconds	0.87	0.8	
Su et al. (2016)	42 DED subjects (42 eyes) and 31 controls (31 eyes)	DED: 54±9 Control:35±12	Customized ocular surface thermography device (IT-85)	OST	4 seconds	0.80	0.89	0.88
Tan, Sanjay and Morgan (2016b)	62 DED subjects (62 eyes) and 63 controls (63 eyes)	DED: 48±10 Controls: 49±7	Thermography in real time with an infrared thermo tracer	Nasal conjunctiva OST 5 seconds after blinking	34.7 ºC	0.87	0.51	
				Nasal conjunctiva OST 10 seconds after blinking	34.5 ºC	0.78	0.62	
Kamao et al. (2011)	30 DED subjects (30 eyes) and 30 of controls (30 eyes)	DED: 52.9±17.1 Controls: 42.7±17.0	Ocular surface termographer (TOMEY)	OST 10 seconds after blinking in the central cornea	0.13 ºC	0.83	0.80	
Yamaguchi et al. (2016)	30 DED subjects (30 eyes) and 30 healthy (30 subjects)	DED: 52.9±17.1 Controls: 42.7±17.0	Ocular surface termographer (TOMEY Corp)	OST	0.13 ºC	0.83	0.80	0.86
					0.11 ºC	0.80	0.73	

(Where DED: Dry Eye Disease; OST: Ocular Surface Temperature; SD: Standard Deviation).

Moreover, due to the relationship between tear film instability, tear film evaporation and ocular surface cooling; thermography can also be used as an index of

tear film stability to non-invasively measure the tear film BUT. For instance, Su et al. (2016) developed a technique based on thermography to measure thermal BUT area and time. They defined the thermal BUT as the first of three dots showing a temperature reduction of 0.2 ºC and found that DED patients had lower thermal BUT ($p < 0.001$) and a faster increase in the thermal break-up area. In addition, they reported acceptable sensitivity and specificity of thermal BUT. It has been reported that thermal NIBUT and OST were correlated with age, BUT with fluorescein, NIBUT, corneal sensitivity and blink rate (Li et al., 2015b; Nosch et al., 2016; Su et al., 2016; Yamaguchi et al., 2016; Matteoli et al., 2020).

Thermography has also been proved to be helpful for MGD diagnosis and its follow-up (Kawali, 2013; Zhang et al., 2015; Su et al., 2017). For instance, Kawali (2013) reported low corneal temperatures in one MGD-keratitis patient. Zhang et al. (2015) found that MGD patients had both higher initial temperature ($p < 0.022$) and higher asymptotic temperature ($p < 0.007$) than ADDE patients. In another study (Su et al., 2017), subjects with MGD had higher eyelid temperature than in controls due to the accumulation of inflammatory molecules in the eyelid margin and a sensitivity and specificity of 0.90 and 0.88 in the nasal side was reported.

Thermography has also been used to provide indirect information about the influence of contact lenses (Itokawa et al., 2018; García-Montero et al., 2019a), diseases (García-Porta et al., 2019; Minatel-Riguetto et al., 2019; Németh et al., 2020), drugs (Konieczka et al., 2019) and therapies (Konieczka et al., 2019; Kremers, Hohberger and Bergua, 2020) on OST (Table 1.27). All of the above studies confirm

that this technique is a useful method to assess the tear film to help in the diagnosis of DED and MGD (Kottaiyan et al., 2012; Su et al., 2017).

Table 1.27. *Results reported by different authors regarding the use of thermography to assess the effect on the ocular surface temperature of treatments, contact lenses, diseases and drugs.*

Study	Sample	Age (mean ± SD) years	Device	Results (mean ± SD)	Main findings
García-Montero et al. (2019a)	15 subjects	24.1±2.2	Non-contact infrared thermography camera (FLIR A325)	OST (ºC) Baseline Lotrafilcon A: 35.13±0.99 Samfilcon A: 35.31±0.65 Comfilcon A: 34.82±1.12 Filcom V3: 35.16±0.91 OST (ºC) 15 days Lotrafilcon A: 34.83±1.08 Samfilcon A: 34.91±0.92 Comfilcon A: 34.47±1.35 Filcom V3: 35.01±1.23	-OST did not change for any CL over 15 days -CL wear did not impact ocular surface over 15 days, except for ocular surface staining
Németh et al. (2020)	90 subjects with keratoconus (179 eyes) and 41 controls (82 eyes)	Keratoconus: 36.1±12.5 Controls: 36.4±12.8	TG-1000 ocular surface thermographer	OST (ºC) Central Keratoconus: 34.3±0.6 Controls: 34.3±0.7	-Thermography was not altered in subjects with keratoconus -OSDI was higher in the keratoconus group -OST was not correlated with OSDI
Minatel-Riguetto et al. (2019)	136 subjects with Graves' disease (136 eyes) and 62 healthy (62 eyes)	Graves > 3: 53 (15-68) Graves <3: 48 (19-80) Graves without ophthalmopathy: 49.5 (16-80) Controls: 48 (15-80)	Non-contact infrared thermography camera (FLIR ONE)	(Median (IQR)) OST caruncles (ºC) Graves > 3: 38.4 (37-39.6) Graves <3: 36.05 (34.85-37.5) Graves without ophthalmopathy: 36.13 (34.3-37.4) Controls: 36.13 (34.35-37.35) OST eyelids (ºC) Graves > 3: 38 (37.3-38.55) Graves <3: 36.08 (34.75-36.95) Graves without ophthalmopathy: 36.28 (33.3-37.15) Controls: 36.05 (34.35-37.2)	-Infrared thermography is an objective tool to assess inflammation in Graves ophthalmopathy

(continuation)					
Study	Sample	Age (mean ± SD) years	Device	Results (mean ± SD)	Main findings
Itokawa et al. (2018)	20 CL wearers (20 eyes)	34.4±4.1	TG-1000 ocular surface thermographer	Differences in OST with and without CLs Delefilcon A: 0.15±0.33 Etafilcon A PVP: 0.22±0.33 Etafilcon A: 0.46±0.33 Polymacon: 0.50±0.35	-Changes in OST over soft CLs was related to tear film stability -Infrared thermography can be used as a non-invasive tool to assess tear film stability in CL wearers
Konieczka et al. (2019)	40 healthy subjects (80 eyes)	Range: 19-47	TG-1000 ocular surface thermographer	-	-Brimonidine reduced central corneal temperature 0.5ªC -Latanoprost did not affect the corneal temperature
García-Porta et al. (2019)	21 glaucoma subjects (21 eyes) and 19 healthy (19 eyes)	Glaucoma: 19 Controls: 19	Long-wave infrared thermal camera (Therm-App)	(Median-approximately) OST eyelid ºC Glaucoma: 35.35 Controls: 35.85 OST central ºC Glaucoma: 36.05 Controls: 36.4 OST peripheral ºC Glaucoma: 36.6 Controls: 36.7	-Tear film stability and changes in ocular blood play a key role in temperature in patients with glaucoma

(Where CL: Contact Lens; IQR: Interquartile Range; OSDI: Ocular Surface Disease Index; OST: Ocular Surface Temperature; SD: Standard Deviation).

1.4 Imaging techniques to assess the meibomian glands

In the definition and classification report of the international workshop on MGD, MGD was defined as "a chronic, diffuse abnormality of the meibomian glands, commonly characterized by terminal duct obstruction and/or qualitative/quantitative changes in the glandular secretion. This may result in alteration of the tear film, symptoms of eye irritation, clinically apparent inflammation, and ocular surface disease" (Nelson et al., 2011). Generally, MGD is associated with skin disease and it is positively correlated with ageing (Bron et al., 2017).

MGD is the main cause of evaporative DED and it is characterized by altered meibomian gland secretions, tear film instability, dry eye symptoms, and ocular

surface staining. Thus, the assessment of meibomian glands is essential in the diagnosis of DED related to MGD since these glands secrete meibum which contributes to the lipid layer of the tear film (Arita et al., 2008; McGinnigle, Naroo and Eperjesi, 2012; Eom et al., 2013; Lin and Yiu, 2014; Koh et al., 2016; Arita, Fukuoka and Morishige, 2017a; Arita, Fukuoka and Morishige, 2017b; Arita, Fukuoka and Morishige, 2017c; Bron et al., 2017; Wolffsohn et al., 2017; Yoo et al., 2017b).

MGD can be classified as hyposecretory or hypersecretory (Arita et al., 2008; McGinnigle, Naroo and Eperjesi, 2012; Eom et al., 2013; Lin and Yiu, 2014; Koh et al., 2016; Arita, Fukuoka and Morishige, 2017a; Arita, Fukuoka and Morishige, 2017b; Arita, Fukuoka and Morishige, 2017c; Bron et al., 2017; Yoo et al., 2017b). The hypersecretory type is uncommon and it is known as meibomian seborrhoea, which can be associated with seborrhoeic dermatitis or rosacea. On the other hand, hyposecretory MGD is more common and is caused by low meibum delivery or obstruction of meibomian glands. Furthermore, it can be divided into non-cicatricial MGD or cicatricial MGD, depending on the mechanism that causes low meibum delivery (Bron et al., 2017). *Figure 1.6* summarizes the aetiology and physiopathology of the disease.

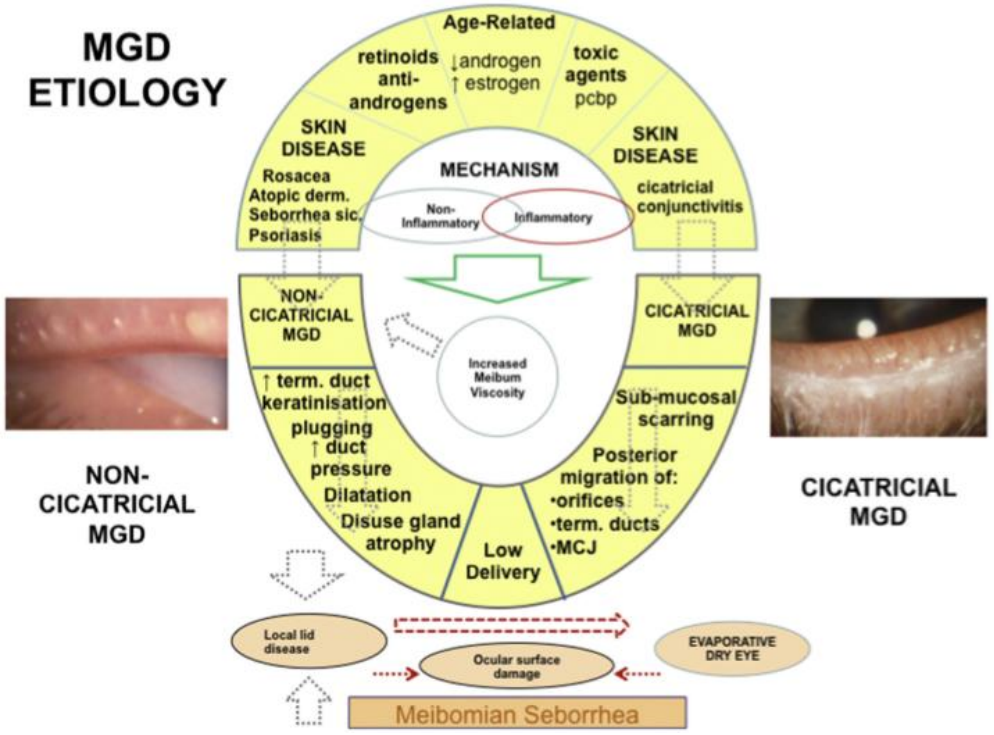

Fig. 1.6. *A summary of the aetiology and pathophysiology of MGD (Bron et al., 2017).*

The analysis of both the structure and function of the meibomian glands is vital to diagnose MGD. Meibometry is a technique that assesses the function of meibomian glands by using plastic tape to blot the central lower lid margin. The lipid blot changes the optical density and can be measured using a photometer (Chew et al., 1993; Lin and Yiu, 2014). Thus, infrared spectroscopy has been used to study human meibum secretion, which has the advantage of not being necessary preparation or the extraction of lipids (Borchman, Yappert and Foulks, 2010). On the other hand, meibography assesses the structure of meibomian glands, which is a valuable method to assess the structure of the glands (Lin and Yiu, 2014; Arita, Fukuoka and Morishige, 2017a). Nevertheless, meibomian glands structure cannot be used as a single method to diagnose MGD, and its results should be combined with other signs and symptoms to improve the diagnosis (Chan et al., 2017).

Different imaging techniques are available to image the meibomian glands, such as non-contact infrared meibography, confocal microscopy or OCT (Yoo et al., 2017b; Villani and Arita, 2019; Villani et al., 2020). A summary of the advantages and disadvantages of the imaging techniques to assess meibomian glands is shown in *Table 1.28*.

Table 1.28. *Summary of advantages and disadvantages of the different imaging techniques to assess the meibomian glands (Ibrahim et al., 2010b; Hwang et al., 2013;* Yoo et al., 2017a; *Yoo et al., 2017b).*

Technique	Advantages	Disadvantages
Non-contact infrared meibography	All meibomian glands are shown in one image	No depth analysis
	Quicker	It provides a more general analysis
		Errors due to the light intensity
		Disagreement between images due to changes in the quality
OCT meibography	Better field of view than confocal microscopy, but worse than non-contact infrared meibography (4.3mm x 4.3mm)	All meibomian glands are not shown in one image
	Depth analysis allows clinicians to obtain 3D images	Motion artefacts occur during the examination
	High resolution	More time to acquire 3D images
	Allows the detailed evaluation of acini and ducts	
Confocal microscopy	High resolution	Lower field of view (400µm x 400µm)
	Allows the evaluation of acinar density, diameter, inflammation and secretion reflectivity	All meibomian glands are not shown in one image
		Partially invasive (anaesthesia)
		Requires a learning curve to obtain images of high quality

1.4.1 Non-contact infrared meibography

Early meibography systems imaged the meibomian gland structure through the illumination of the tarsal plate from the skin side and were thereby able to detect abnormalities in gland morphology (Mathers, Daley and Verdick, 1994; Nichols et al., 2005; Yokoi et al., 2007; Arita, Fukuoka and Morishige, 2017c). However, these systems were invasive and involved contact, which had some disadvantages such as

discomfort, pain, heat sensation and limited area of view (Yokoi et al., 2007; Arita, Fukuoka and Morishige, 2017c). These problems were overcome with the use of meiboscopy, which is a technique that uses transillumination to observe the meibomian glands.

Currently, non-contact meibography systems have been developed and are the most widely used technique to assess meibomian glands structure since they allow clinicians to observe meibomian glands across the entire eyelid without contact (Molinari and Tapie, 1982; Arita et al., 2008; Arita, Fukuoka and Morishige, 2017a). Thus, non-contact infrared meibography is a technique used to obtain two-dimensional images of the meibomian gland structure by retroillumination using infrared light.

The image is obtained by adding an infrared transmitting filter and an infrared-sensitive camera to detect infrared light using a slit-lamp (Arita et al., 2008; Eom et al., 2013; Kim et al., 2015; Liang et al., 2015; Arita, Fukuoka and Morishige, 2017b; Arita, Fukuoka and Morishige, 2017c; Yoo et al., 2017b; Geerling et al., 2017; Karaca et al., 2019; Lekhanont et al., 2019; Arita and Fukuoka, 2020; Pondelis et al., 2020; Ha et al., 2021). Thus, meibomian glands are detected as areas of high reflectivity while gland drop-out is detected as areas of low reflectivity. Furthermore, it also has the advantage that the required observation time is short. Likewise, despite not being non-invasive, since it needs eyelid eversion, patients experience minimal discomfort. Contrary, it has the drawback of not providing information about depth (Hwang et al., 2013) because the infrared non-contact meibography systems usually use a shorter wavelength (800-940 nm) than OCT (1300 nm), which limits its penetration in the palpebral conjunctiva.

Other devices such as videoqueratographs or interferometers have also incorporated non-contact infrared meibography (Arita et al., 2013; Koh et al., 2016; Wang et al., 2016; Kang et al., 2017; Yin et al., 2017; Yoo et al., 2017b; El Ameen et al., 2018; He et al., 2018; Li et al., 2018; Park et al., 2018; Park and Baek, 2018; Portela et al., 2018; Randon et al., 2018; Seo et al., 2018; Siddireddy et al., 2018a; Zang et al., 2018; Ağın et al., 2019; Al-Hayouti et al., 2019; Dereli-Can and Kara, 2019; Guarnieri et al., 2019; Rico-del-Viejo et al., 2019; Ruan et al., 2019; Shrestha et al., 2019; Wang et al., 2019a; Wong et al., 2019b; Yu, 2019; Altin Ekin, Karadeniz Ugurlu and Kahraman, 2020; Garduño et al., 2020; Garza-Leon et al., 2020; Ge et al., 2020; Gjerdrum et al., 2020; Guo et al., 2020; Lee et al., 2020a; Lee et al., 2020b; Li et al., 2020a; Li et al., 2020b; Li et al., 2020c; Llorens-Quintana, Garaszczuk and Szczesna-Iskander, 2020; Recchioni et al., 2020; Wu et al., 2020b; Bilkhu et al., 2021; Chen et al., 2021; Dikmetas, Kocabeyoglu and Mocan, 2021; Kang et al., 2021; Weng et al., 2021). Moreover, some of them include software to automatically enhance the contrast of meibographies (Rico-del-Viejo et al., 2019; Llorens-Quintana, Garaszczuk and Szczesna-Iskander, 2020). *Figure 1.7* shows a meibography obtained with a videokeratograph through non-contact infrared meibography before and after contrast enhancement.

Lee et al. (2020a) found statistically lower gland drop-out values with LipiView II than when it was measured with IDRA ocular surface analyzer. These differences could be due to differences between the instruments' everting eyelids (IDRA uses a simple plastic everter while LipiView II uses a light-emitting lid everter). Likewise, the surface lighting with LipiView II is less, providing a clearer image of the meibomian gland shape. Similarly, Garduño et al. (2020) found statistically significant differences

between Antares and Cobra topographers in meibomian gland drop-out. This could be due to differences in image quality between both devices. However, no differences were found in DED subjects, which suggest that both devices can be used interchangeably in DED subjects.

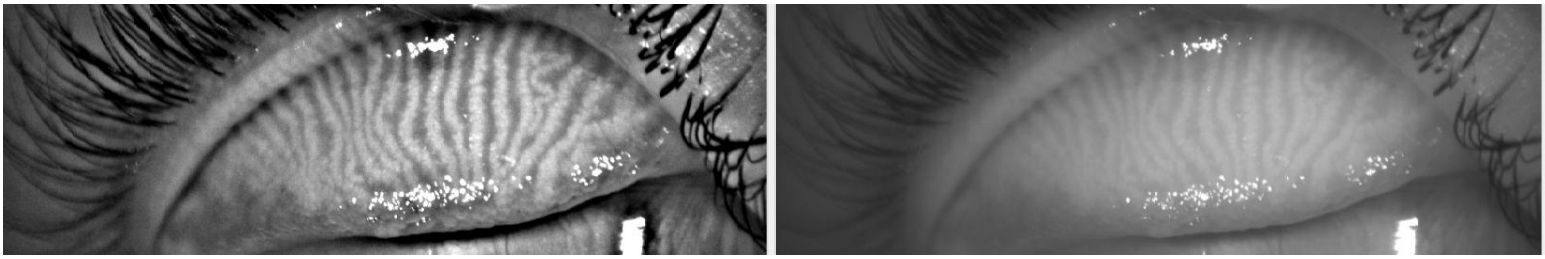

Fig. 1.7. *Meibography obtained using a non-contact infrared meibography system of a commercially available videoqueratograph (Oculus Keratograph 5M). Left: Meibography with contrast enhancement. Right: Meibography without contrast enhancement.*

Infrared imaging has been proven to be a quick and patient-friendly tool to help in the diagnosis and treatment of MGD and it provides information about the morphology, drop-out of meibomian glands or other acini abnormalities such as shortening, dilatation and distortion (Arita et al., 2008; Pult, Riede-Pult and Nichols, 2012; Eom et al., 2013; Kim et al., 2015; Liang et al., 2015; Koh et al., 2016; Wang et al., 2016; Chan et al., 2017; Arita, Fukuoka and Morishige, 2017a; Arita, Fukuoka and Morishige, 2017b; Geerling et al., 2017; Kang et al., 2017; Thulasi and Djalilian, 2017; Yoo et al., 2017b; Park et al., 2018; Park and Baek, 2018; Portela et al., 2018; Zang et al., 2018; Al-Hayouti et al., 2019; Karaca et al., 2019; Pondelis et al., 2020). Several studies have found alterations in meibomian glands in MGD and DED patients (*Table 1.29*) and significant correlations have been found between meibomian glands loss and

tear film parameters such as the lipid layer pattern, NIBUT and OSDI (Pult, Riede-Pult and Nichols, 2012).

Table 1.29. *Results reported by different authors regarding the assessment of meibomian glands through non-contact infrared meibography.*

Study	Sample	Age (mean ± SD) years	Device	Results (mean ± SD)	Main findings
Koh et al. (2016)	49 ADDE (49 eyes) and 31 healthy subjects (31 eyes)	DED: 57.9±12.5 Controls: 37.7±9.8	Keratograph 5M	Meiboscore Arita DED upper eyelid: 1.06±0.92 DED lower eyelid: 0.65±0.90 Controls upper eyelid: 0.32±0.54 Controls lower eyelid: 0.19±0.54	-Significant higher meiboscore in ADDE subjects
Wang et al. (2016)	47 DED subjects (47 eyes) 201 healthy subjects (201 eyes)	DED: 12.45±1.54 Controls: 11.75±1.95	Keratograph 5M	Meiboscore Arita DED: 3.21±1.02 CONTROL: 0.61±0.65	-Significant higher meiboscore in the DED group
Arita et al. (2008)	236 eyes of healthy subjects (236 eyes)	41.2±23.1	Non-contact infrared meibography system (Slit-lamp + infrared transmitting filter IR-83 + infrared charge-coupled camera)	Meiboscore Arita (Approximately) 0-9 years: 0.20±-- 10-19 years: 0.60±-- 20-29 years: 0.75±-- 30-39 years: 1.05±-- 40-49 years: 1.00±-- 50-59 years: 1.35±-- 60-69 years: 1.85±-- 70-79 years: 1.35±-- ≥80 years: 1.90±--	-A positive correlation was found between meiboscore and age, and between meiboscore and lid margin abnormality score
Eom et al. (2013)	30 obstructive MGD (30 eyes) and 25 healthy subjects (25 eyes)	MGD: 46.1±11.6 Controls: 30.4±6.9	BG-4M Non-Contact Meibography System (Topcon)	Gland drop-out (%) MGD upper eyelid: 19.4±14.6 Controls upper eyelid: 8.1±4.4 MGD lower eyelid: 25.2±17.5 Controls lower eyelid: 10.2±6.2	-MGD had a significantly higher percentage of drop-out
Kim et al. (2015)	51 Grave's Orbipathy (51 eyes) and 31 healthy subjects (31 eyes)	Grave´s: 42.35±12.80 Controls: 45.45±16.73	BG-4M Non-Contact Meibography System (Topcon)	Meiboscore Arita Grave´s Orbipathy: 1.67±1.58 Control: 1.03±1.08	-Significant lower meiboscore in the control group -Significant negative correlation between meiboscore and BUT

(continuation)

Study	Sample	Age (mean ± SD) years	Device	Results (mean ± SD)	Main findings
Weng et al. (2021)	143 young (143 eyes), 304 middle age subjects (304 eyes) and 228 elderly subjects (228 years)	Young: 32.0±5.9 Middle: 52.1±5.7 Elderly: 68.5±6.3	LipiView interferometer	Meiboscore Pult Young: 2.1±1.3 Middle: 2.5±1.2 Elderly: 2.9±1.3	-Elderly DED subjects had higher meibomian gland drop-out
Rico-del-Viejo et al. (2019)	161 subjects (161 eyes)	42±17	Keratograph 5M	Meiboscore Arita Upper eyelid Grade 0: 57 subjects Grade 1: 67 subjects Grade 2: 25 subjects Grade 3: 7 subjects Lower eyelid Grade 0: 47 subjects Grade 1: 83 subjects Grade 2: 23 subjects Grade 3: 3 subjects	-Meibomian gland drop-out higher than 50% was accompanied by signs -Age was a relevant factor when assessing meibomian gland drop-out -Statistically significant differences were found between meibomian gland loss groups in osmolarity, bulbar redness and ocular surface staining
Bilkhu et al. (2021)	15 MGD subjects (15 eyes)	31.6±13.1	Keratograph 5M	-	-Length is the key functional morphology feature of lower eyelid meibomian glands -Gland length was negatively correlated with gland expression and tortuosity scores, but not with width
Ha et al. (2021)	141 DED subjects (141 eyes)	54.8±14.6	Slit-lamp biomicroscope with an infrared transmitting filter (R-72) and an infrared camera	-	-Lid margin abnormalities were associated with meibomian gland drop-out
Kang et al. (2017)	31 Sjögren syndrome subjects (31 eyes), 30 non-Sjögren syndrome DED (30 eyes) and 35 healthy (35 eyes)	Sjögren: 54.65±14.46 Non-Sjögren: 56.53±15.25 Controls: 58.43±10.81	Keratograph 5M	Meiboscore Arita (Approximately) Sjögren: 4.5±-- Non-Sjögren: 3.5±-- Controls: 0.5±--	-Sjögren syndrome and non-Sjögren DED subjects had higher meiboscore and meibomian gland impairment than controls -Sjögren syndrome subjects had higher meiboscore than non-Sjögren patients
Li et al. (2020b)	209 subjects (209 eyes) (Young: 77, Middle: 52, and Older: 80)	All: 49.68±18.33 Median (IQR) Young: 29 (8) Middle: 51 (7.75) Older: 66 (13)	Keratograph 5M	Gland drop-out (%) (Median (IQR)) All: 32 (12) nm Young: 32 (11) nm Middle: 32 (13) nm Older: 30 (13) nm	-Gland drop-out was inversely correlated with lipid layer thickness

(continuation)					
Study	Sample	Age (mean ± SD) years	Device	Results (mean ± SD)	Main findings
Zang et al. (2018)	22 Sjögren syndrome subjects (22 eyes) and 22 non-Sjögren syndrome ADDE(22 eyes)	Sjögren: 50.1±11.8 Non-Sjögren: 49.6±11.7	LipiView II interferometer	Meiboscore Arita Upper eyelid Sjögren Grade 0: 4.5% Grade 1: 31.9% Grade 2: 54.5% Grade 3: 9.1% Upper eyelid non-Sjögren Grade 0: 13.3% Grade 1: 77.3% Grade 2: 9.1% Grade 3: 0%	-Sjögren syndrome subjects had more severe meibomian gland drop-out in the upper eyelid

*(Where ADDE: Aqueous Deficient Dry Eye; BUT: Break-Up Time; DED: Dry Eye Disease; IQR: Interquartile Range; MGD: Meibomian Gland Dysfunction; SD: Standard Deviation).*In the cases where "approximately" is written, it is because the studies did not show the numerical value. They only showed the results in a figure.*

Meibographies can be graded into different scale categories depending on the structure, morphology and gland drop-out. For instance, Arita et al. (2008) proposed a meiboscore grading scale to quantify the degree of meibomian gland drop-out. The scale ranged from 0 to 3 where a higher score represents higher meibomian gland loss (0 = No loss of meibomian glands; 1 = gland drop-out < 1/3 of the total gland area; 2 = grand drop-out between 1/3 and 2/3; and 3 = gland drop-out > 2/3) (Arita et al., 2008; Chan et al., 2017). The same author (Arita et al., 2008) found a positive correlation between age and meiboscore; as well as between the meiboscore and lid margin abnormality. Nevertheless, this method has the drawback of being partially subjective and depends on the examiner's ability. In addition, meibographies can only be graded into a few categories, making the difference between meibography grades too high.

This makes the method less accurate and less precise because within one group there may be meibographies with a wide range of variability (Arita et al., 2008). Furthermore, there are other grading scales, which difficult the comparison between studies.

To minimize the influence of the observer in the classification of meibographies, some softwares have been developed to automatically classify them according to different alterations of the glands such as gland drop-out, shortening, visibility, dilation or distortion (Pult and Riede-Pult, 2011a; Koh et al., 2012; Celik et al., 2013; Eom et al., 2013; Pult and Riede-Pult, 2013; Koprowski et al., 2016; Thulasi and Djalilian, 2017; Llorens-Quintana et al., 2019a). Thus, meibographies can be processed and analysed to obtain continuous numerical values, which increase the objectivity and repeatability of measurements (*Table 1.30*). For instance, some authors (Pult, Riede-Pult and Nichols, 2012; Eom et al., 2013; Kim et al., 2015; Koh et al., 2016; Wang et al., 2016; Thulasi and Djalilian, 2017; Zang et al., 2018; Garduño et al., 2020; Garza-Leon et al., 2020; Wu et al., 2020b; Bilkhu et al., 2021) have used ImageJ tool, Phoenix software or Matlab to assess meibographies in an objective way. For instance, Eom et al. (2013) found that the ImageJ tool had excellent intra-observer and inter-observer reliability in the glands drop-out assessment. Moreover, the diagnostic capability of meiboscore has also been studied and has been reported to be acceptable (*Table 1.31*).

Table 1.30. *Results of main studies that assessed the repeatability of meibomian glands assessment using non-contact infrared meibography.*

Study	Type of repeatability	Device	S_w	CoV (%)	CoR	ICC
Eom et al. (2013)	Intraexaminer	BG-4M Non-Contact Meibography System (Topcon)				0.875
	Interexaminer					0.801
Garza-Leon et al. (2020)	Intraexaminer	Antares	Phoenix: 2.54 ImageJ: 2.94	Phoenix: 11.85 ImageJ: 10.88		Phoenix: 0.989 ImageJ: 0.988

(Where CoR: Repeatability Coefficient; CoV: Coefficient of Variation; ICC: Intraclass Correlation Coefficient; S_w: within-subject standard deviation).

Table 1.31. *Sensitivity and specificity found by different authors in the assessment of meibomian glands through non-contact infrared meibography to diagnose MGD.*

Study	Sample	Age (mean ± SD) years	Metric	Cut-off value	Sensitivity	Specificity	Area under the curve
Arita et al. (2009b)	53 subjects (53 eyes)	71.4±10.0	Meiboscore				0.92
Yin and Gong (2019)	47 subjects (47 eyes)	39.2±11.1	Meiboscore	1 score	0.94	0.96	0.95
Adil et al. (2019)	487 subjects (487 eyes)	35.1±16.4	Meiboscore	0.5 score	0.97	0.85	
Finis et al. (2014)	128 subjects (128 eyes)	57.0±17.0	Meiboscore	4 score	0.28	0.80	
Giannaccare et al. (2018)	149 subjects (149 eyes)	53.4±15.5	Gland loss	20 %	0.60	0.61	0.60
Koprowski, Tian and Olczyk (2017)	57 subjects (57 eyes)	-	The area occupied by the glands in an automatic algorithm	-	0.99	0.97	
Xiao et al. (2020)	447 subjects (447 eyes)	42.1±15.1	Meiboscore	1.5 score	0.93	0.97	0.98
			Gland loss	-			0.98

(Where SD: Standard Deviation)

Some authors have compared the results obtained with different devices to assess meibomian glands (*Table 1.32*). Despite using the ImageJ tool to assess gland drop-out,

Wong et al. (2019b) found statistically lower values in meiboscore and gland drop-out percentage with LipiView II in comparison with Keratograph 5M, which suggests that both devices should not be used interchangeably to assess meibomian gland drop-out. Authors argued that this is caused by differences in the amount of eyelid that was typically everted and differences in image quality between devices. In addition, Garza-Leon et al. (2020) found that ImageJ and Phoenix programs had good repeatability in the measurement of meibomian gland loss. However, their results were not interchangeable since statistically differences were found between them.

Non-contact infrared meibography has also been used to assess the effect of treatments and contact lenses (Yin et al., 2017; Li et al., 2018; Ruan et al., 2019; Wang et al., 2019a; Altin Ekin, Karadeniz Ugurlu and Kahraman, 2020; Arita and Fukuoka, 2020; Guo et al., 2020; Li et al., 2020a; Li et al., 2020c; Llorens-Quintana, Garaszczuk and Szczesna-Iskander, 2020; Pondelis et al., 2020; Wu et al., 2020b; Chen et al., 2021), pathologies (He et al., 2018; Portela et al., 2018; Karaca et al., 2019, Lekhanont et al., 2019; Shrestha et al., 2019; Dikmetas, Kocabeyoglu and Mocan, 2021) and surgical procedures (El Ameen et al., 2018; Ge et al., 2020; Gjerdrum et al., 2020; Lee et al., 2020a) on meibomian glands (*Table 1.33)*.

Table 1.32. *Studies that compared the results obtained with different devices to assess meibomian glands.*

Study	Sample	Age (mean ± SD) years	Device	Results (mean ± SD)	Main findings
Wong et al. (2019b)	20 subjects (20 eyes)	36.6±13.1	LipiView II interferometer and Keratograph 5M	Meiboscore Arita LipiView: 1.43±0.78 Keratograph: 1.90±0.81 Gland drop-out (%) LipiView: 31.5 Keratograph: 43.4	-Statistically significant differences in meiboscore and drop-out percentage were found between LipiView II and Keratograph 5M -LipiView II showed lower values in meiboscore and gland drop-out percentage using ImageJ
Lee et al. (2020a)	47 subjects (47 eyes)	56.77±14.47	LipiView II interferometer IDRA ocular surface analyzer	Gland drop-out (%) LipiView II: 36.51±17.53 nm IDRA: 45.36±21.87 nm	-The gland drop-out percentage was statistically significantly lower in the LipiView II than in the IDRA interferometer
Lee et al. (2020c)	33 subjects (33 eyes)	61.5±10.6	Antares topographer and LipiView	Gland drop-out (%) LipiView: 16.1±11.8 Antares: 21.4±16.3	-A positive significant correlation was found between gland drop-out using Antares and LipiView
Garduño et al. (2020)	80 subjects (80 eyes)	36.93±18.34	Antares topographer Cobra topographer	Gland drop-out (%) Antares upper eyelid: 18.97±0.78 Antares lower eyelid: 20.24±0.71 Cobra upper eyelid: 17.89±0.77 Cobra lower eyelid: 21.24±0.95	-Statistically significant differences in upper gland drop-out were found between both topographers -Measurements were similar in DED subjects, which suggests that both devices are interchangeable
Lee et al. (2020b)	33 subjects (33 eyes)	61.5±10.6	LipiView II interferometer and Antares topographer	Gland drop-out (%) LipiView: 16.1±11.8 Antares: 21.4±16.3	-Antares topographer is useful in DED diagnosis and meibomian glands assessment -Gland drop-out measured with both devices was correlated

(Where DED: Dry Eye Disease; SD: Standard Deviation).

Table 1.33. *Results reported by different authors regarding the use of non-contact infrared meibography to assess the effect on the meibomian glands of treatments, contact lenses, diseases and surgical procedures.*

Study	Sample	Age (mean ± SD) years	Device	Results (mean ± SD)	Main findings
Park et al. (2018)	30 thyroid eye disease subjects (30 eyes)	42.9±11.8	LipiView interferometer	Meiboscore Arita Upper eyelid: 1.17±0.75 Lower eyelid: 0.70±0.65	-MGD may also be a cause of DED in thyroid eye disease subjects
Seo et al. (2018)	17 rosacea-MGD subjects (17 eyes)	Median: 64 (IQR: 57-68)	Keratograph 5M	Meiboscore Arita Grade 2: 13 subjects Grade 3: 4 subjects	-Meibomian gland parameters improved after intense pulsed light treatment
Karaca et al. (2019)	36 subjects with severe sleep apnea (36 eyes) and 24 with primary snoring or mild sleep apnea (24 eyes)	Severe: 50.8±8.3 Mild: 47.9±10.5	Slit-lamp biomicroscope (SL-D701) with DC-4 digital camera and BG-5 background illuminator	Meiboscore Arita Total meiboscore severe: 2.8±2.3 Total meiboscore mild: 1.1±2.2 Morphological alterations Severe: 86.1 % Mild: 45.8 %	-Morphological changes (duct distortion, thinning and dilatation) and gland drop-out were higher in subjects with severe obstructive sleep apnea
Ağın et al. (2019)	50 chronic smokers (50 eyes) and 50 non-smokers (50 eyes)	Smokers: 31.46±5.72 Controls: 31.66±10.65	Scheimpflug camera-Placido topography device (Sirius)	Meiboscore Pult Smokers: 3.22±1.18 Controls: 1.48±1.12	-Smokers showed decreased meiboscore
Wang et al. (2019a)	59 myopic subjects (59 eyes)	12.03±2.31	Keratograph 5M	Baseline: 0.68±0.51 1 month: 0.68±0.51 6 months: 0.68±0.51 24 months: 0.68±0.51	-Overnight orthokeratology did not affect meibomian glands drop-out
Pondelis et al. (2020)	15 DED subjects (30 subjects)	53.26±17.33	Infrared meibography (RTVUE XR)	Perimeter pre-stimulation: 235.94±51.38 µm Perimeter post-stimulation: 222.21±47.72 µm Area pre-stimulation: 2187.60±635.88 μm^2 Area post-stimulation: 1933.20±538.55 μm^2	-Infrared meibography can be used to detect changes in the meibomian gland area and perimeter -Meibomian gland area and perimeter were reduced after intranasal stimulation

(continuation)

Study	Sample	Age (mean ± SD) years	Device	Results (mean ± SD)	Main findings
He et al. (2018)	120 subjects (120 eyes): 44 diabetic <5 years, 40 diabetic between 5-10 years, 36 >10 years and 40 healthy.	Control: 64.88±7.04 <5 years: 64.75±8.20 5-10 years: 65.03±7.14 >10 years: 66.11±7.44	Keratograph 5M	Meiboscore Arita Control: 3.15±1.09 <5 years: 3.13±1.08 5-10 years: 3.53±1.05 >10 years: 4.25±1.14	-Meiboscore in the 1 years diabetic group was significantly higher than in the other three groups
Park and Baek (2018)	98 thyroid eye disease (98 eyes) and 62 DED subjects (62 eyes)	Thyroid: 45.8±12.4 Controls: 48.3±11.3	LipiView Interferometer	Meiboscore Arita Thyroid: 1.21±0.76 Controls: 0.94±0.71	-Meibomian gland loss in the upper eyelid was higher in DED subjects with thyroid disease
Shrestha et al. (2019)	16 patients with Stevens-Johnson Syndrome (16 eyes)	32.0±14.3	Keratograph 5M	Meiboscore Arita 3.6±1.9	-Meiboscore was correlated with Stevens-Johnson Syndrome
Cui et al. (2020)	49 MGD subjects (49 eyes) and 54 healthy (54 eyes)	MGD: 51.16±12.97 Controls: 46.35±14.4	Keratograph 5M	Maximal duct diameter (μm) MGD: 120.22±27.92 Controls: 100.96±20.30	-MGD subjects had more diversified orifices and larger terminal duct diameters, while duct diameter was decreased in MGD subjects after gland massage
Chen et al. (2021)	100 MGD subjects (100 eyes) (35 had a combined therapy)	45.10±4.81	Keratograph 5M	Gland drop-out (%) Upper eyelid Pre-treatment: 33±15 1 month: 33±13 3 month: 32±12 Lower eyelid (Median (IQR)) Pre-treatment: 21 (17,25) 1 month: 15 (11,25) 3 month: 18 (13,23)	-Lower meibomian gland drop-out was reduced at 1 and 3 months in the combined therapy
Arita and Fukuoka (2020)	36 MGD with posterior blepharitis subjects (36 eyes) (16 azithromycin and 20 preservative-free drops)	Azithromycin: 60.1±17.9 Controls: 61.9±12.2	Non-contact meibography system (Topcon)	Meiboscore Arita Azithromycin: 3.2±1.8 Controls class: 4.2±1.5	-No differences were found in meiboscore between groups

(continuation)					
Study	Sample	Age (mean ± SD) years	Device	Results (mean ± SD)	Main findings
El Ameen et al. (2018)	30 who underwent cataract surgery (30 eyes)	Men: 73.5±9.4 Women: 78.9±4.7	Keratograph 5M	Gland drop-out (%) Upper eyelid Pre: 28.8±14.9 Upper eyelid 1 month: 32.5±14.9 Upper eyelid 3 months: 35.8±17 Lower eyelid Pre: 22.7±18.9 Lower eyelid 1 month: 23.8±19.7 Lower eyelid 3 months: 25.8±20.9	-Meibomian gland loss was significantly higher in the upper eyelid 1 and 3 months after cataract surgery
Lekhanont et al. (2019)	32 subjects with Stevens-Johnson syndrome (64 eyes)	42.2±17.7	Non-contact infrared meibography system mounted on a slit-lamp biomicroscope (Topcon DC-4)	Meiboscore Arita Upper eyelid: 2.7±0.8 Lower eyelid: 2.5±0.9	-Stevens-Johnson syndrome is associated with obstructive MGD
Portela et al. (2018)	30 glaucoma subjects (30 eyes) and 27 controls (27 eyes)	Glaucoma: 71.33±11.50 Controls: 68.96±6.48	Keratograph 5M	Meiboscore Pult Glaucoma: 2.34±1.01 Controls: 1.52±0.64	-Significant higher meiboscore was found in glaucoma subjects
Li et al. (2020a)	25 hyposecretory MGD subjects (25 eyes) and 25 obstructive MGD subjects (25 eyes)	Hyposecretory MGD: 32.6±10.26 Obstructive MGD: 37.2±11.74	LipiView II interferometer	Meiboscore Arita Upper eyelid hyposecretory: 52% grade 1, 44% grade 2, and 4% grade 3 Upper eyelid obstructive: 64% grade 1 and 36% grade 2	-Meibomian gland loss did not improve during the 12 week follow-up period -Thermal Pulsation LipiFlow is effective for both obstructive and hyposecretory MGD
Altin Ekin, Karadeniz Ugurlu and Kahraman (2020)	55 subjects with a unilateral ocular prosthesis (110 eyes)	44.7±17.5	Scheimpflug camera-Placido topography device (Sirius)	<u>Total meiboscore Arita</u> Prosthetic: 3.9±1.8 Control: 5.1±1.6 <u>Total gland drop-out (%)</u> Prosthetic: 71.8±36.5 Control: 112.8±44.9	-Ocular prosthesis is related to MGD and higher meiboscore and gland drop-out

(continuation)					
Study	Sample	Age (mean ± SD) years	Device	Results (mean ± SD)	Main findings
Llorens-Quintana, Garaszczuk and Szczesna-Iskander (2020)	33 experienced CL wearers (33 eyes) and 8 unexperienced (8 eyes)	Experienced: 24±5 Unexperienced: 25±4	Keratograph 5M	<u>Gland atrophy (%)</u> Experienced: 23.9±10.7 Unexperienced: 13.6±9.1 <u>Gland length (mm)</u> Experienced: 2.9±0.6 Unexperienced: 3.6±0.7 <u>Gland width (mm)</u> Experienced: 0.5±0.1 Unexperienced: 0.5±0.1 <u>Irregularity (%)</u> Experienced: 25.8±14.5 Unexperienced: 26.6±8.6	-Significant differences were found between groups for gland atrophy and length -CL wear impacted meibomian gland morphology
Gjerdrum et al. (2020)	94 subjects with laser vision correction (LVC), 80 with implantable collamer lens (ICL) and 83 controls	LVC: 41.3±6.3 ICL: 40.8±8.8 Controls: 41.2±8.1	Keratograph 5M	Meiboscore Arita LVC: 0.5±0.7 ICL: 0.3±0.5 Controls: 0.4±0.7	-No significant differences were found between surgical procedures for meiboscore
Ge et al. (2020)	25 patients with conventional cataract surgery (25 eyes) and 22 with optimal pulsed technology (22 eyes)	Conventional: 65.8±8.1 Pulsed: 63.48±8.47	Keratograph 5M	Meiboscore (Median (IQR)) Conventional group Baseline: 1 (1,2) 3 months: 1 (1,2) Optical pulsed treatment group Baseline: 1 (1,2) 3 months: 1 (1,1)	-There were significant differences in meiboscore before and 3 months after surgery in the optical pulsed treatment group -Cataract surgery aggravated MGD
Recchioni et al. (2020)	16 LASIK subjects (16 eyes) and 13 SMILE subjects (13 eyes)	LASIK: 32.6±9.1 SMILE: 32.2±5.3	Keratograph 5M	Meiboscore Pre-LASIK: 2±2 Post-LASIK: 2±2 Pre-SMILE: 1±1 Post-SMILE: 1±1	-No differences were found in meiboscore after LASIK and SMILE surgery
Dikmetas, Kocabeyoglu and Mocan (2021)	22 graft-versus-host DED subjects (22 eyes) and 28 healthy (28 eyes)	Graft: 29.6±12.6 Controls: 26.9±13.5	Scheimpflug camera-Placido topography device (Sirius)	Meiboscore Pult Graft: 2.9±1.1 Controls: 0.7±0.4	-Subjects with graft-versus-host disease had worse meiboscore

(continuation)					
Study	Sample	Age (mean ± SD) years	Device	Results (mean ± SD)	Main findings
Wu et al. (2020b)	62 MGD subjects (124 eyes) (29 subjects in the optimal IPL group and 33 in the regulated IPL)	Optimal: 48.72±13.99 Regulated: 54.79±14.79	Keratograph 5M	Gland drop out (%) (Median (IQR)) Baseline Optimal: 29(9) Baseline Regulated: 30(8) 3 months Optimal: 27(4) 3 months Regulated: 30(0)	-IPL has clinical value in the treatment of MGD -Optimal IPL was more effective

(Where CL: Contact Lens; IPL: Intense Pulsed Light; IQR: Interquartile Range; LASIK: Laser-Assisted In Situ Keratomileusis; MGD: Meibomian Gland Dysfunction; SD: Standard Deviation; SMILE: Small Incision Lenticule Extraction).

1.4.2 Optical coherence tomography

In-vivo 3D images of meibomian glands using OCT was first introduced by Hwang et al. (2013), who developed a Fourier-domain OCT system based on a high-speed, wavelength-swept laser with a spectral bandwidth of 100 nm and a centre wavelength of 1310 nm. Usually, a long wavelength is used to increase the penetration of the light in the tissues. Nevertheless, longer wavelengths cause less image resolution. This device allowed examiners to obtain 3-dimensional images of the meibomian glands by reconstructing tomograms with an axial resolution of 5 µm and a lateral resolution of 13 µm in the air (Hwang et al., 2013; Gumus and Pflugfelder, 2017; Yoo et al., 2017b; Kheirkhah et al., 2018).

OCT imaging has the advantage of providing more detailed information of acini and ducts in the deep layer, data about depth, and enhanced visibility compared with

infrared meibography, which has a shorter penetration depth. Likewise, OCT meibography also allows examiners to obtain 3D images and to identify the nerve plexus of capillaries between or behind the meibomian glands. However, OCT meibography has also some limitations to consider. It cannot cover the entire area of meibomian glands in the eyelids and data processing for rendering three-dimensional images requires a longer time than infrared meibography (Hwang et al., 2013; Liang et al., 2015; Yoo et al., 2017a; Yoo et al., 2017b; Kheirkhah et al., 2018; Al-Hayouti et al., 2019; Cui et al., 2020).

This was studied by Yoo et al. (2017a), who compared infrared meibography with swept-source OCT and found a slight disagreement between both devices. Authors found a percentage of disagreement between devices of 49.45 % for gland drop-out. They claimed that meibomian glands drop-out detected with infrared meibography should be carefully interpreted, OCT being useful to confirm the information found with infrared meibography. Some studies have found this technique useful to assess the structure of meibomian glands to help in the diagnosis of MGD (Hwang et al., 2013; Liang et al., 2015). Moreover, it has been reported that mean length was correlated with DED symptoms and mean width with BUT (Liang et al., 2015).

1.4.3 Confocal microscopy

Meibomian glands can also be assessed using confocal microscopy, which also has different advantages in comparison with infrared meibography. It can be used to analyse acinar density, acinar length and diameter, secretion, reflectivity and inflammation. Nonetheless, both OCT and confocal microscopy are less automated (Kobayashi, Yoshita and Sugiyama, 2005; Villani et al., 2013b; Liang et al., 2015; Chan

et al., 2017; Gumus and Pflugfelder, 2017; Thulasi and Djalilian, 2017). Confocal microscopy allows obtaining high-resolution images with depth selectivity of different ocular surface structures through the analysis of the light reflected on tissues. Thus, changes in the refractive index provide information to recognise inter- and intra-cellular details (Montés-Micó, 2011). However, the technique has the limitation of having a small visual field due to high magnifications (Kottaiyan et al., 2012).

It focuses the light source and the objective lens on the small area of interest, the focal volume of which is defined by the numerical aperture, magnification and working distance from the objective lens. Thus, it eliminates the light that comes from other points of the sample. This provides a resolution similar to histological analysis. Images are acquired point-by-point and reconstructed using a computer program, allowing three-dimensional reconstructions of topologically complex objects (Minsky, 1988; Wakamatsu et al., 2009; Montés-Micó, 2011; McGinnigle, Naroo and Eperjesi, 2012; Chan et al., 2017).

It is usually performed in the centre of the cornea and requires the use of anaesthesia and a coupling agent between the applanating lens and the patients' cornea. Therefore this technique is invasive, but its invasiveness does not alter the results since it does not analyse the tear film, but it assesses physical changes on meibomian glands or in the ocular surface (Zhang et al., 2011; McGinnigle, Naroo and Eperjesi, 2012). Nevertheless, it has also been previously used to study the tear film thickness (Bai and Nichols, 2017).

There are several confocal microscopes. Some of them use a confocal slit principal, such as ConfoScan 4; whereas, in tandem scanning microscopes, images are captured using a rotating Nipkow disc. Other instruments, such as the Rostock Cornea Module-HRT use a laser, generating high-contrast and high-quality images with the greatest resolution (Erie, McLaren and Patel, 2009; Shaheen, Bakir and Jain, 2014, Baek, Doh and Chung, 2015).

Different authors have assessed meibomian glands through confocal microscopy and have found differences between healthy and subjects with MGD (*Table 1.34*) (Ibrahim et al., 2012; Villani et al., 2013a; Villani et al., 2013b; Randon et al., 2018; Cheng et al., 2019; Yu, 2019; Vagge et al., 2020), and between healthy and DED subjects (Ban et al., 2011; Villani et al., 2011a), which suggests that the tool can be helpful in the assessment of these diseases. For instance, Villani et al. (2013b) found that MGD patients had a low acinar density and more secretion reflectivity, high acini diameter and orifices. In addition, Ban et al. (2011) found that meibomian gland acinar unit density, gland longest diameter and gland shortest diameter were lower and shorter in patients with DED associated with chronic graft-versus-host disease when measured using confocal microscopy. Villani et al. (2011a) found that Sjögren's Syndrome patients had more periglandular inflammation, higher secretion reflectivity and more drop-out than controls. However, they had higher acinar density and smaller diameters than MGD patients.

Randon et al. (2018) found a strong correlation between in vivo confocal microscopy score and infrared meibography with Keratograph 5M in the assessment of meibomian glands, and they concluded by saying that in vivo confocal microscopy

classification can help to understand patients' symptoms and enhance MGD treatment.

Table 1.34. *Results reported by different authors regarding the assessment of meibomian glands through confocal microscopy.*

Study	Sample	Age (mean ± SD) years	Device	Results (mean ± SD)	Main findings
Villani et al. (2013b)	30 eyes of 15 SSDE I patients, 30 of 15 NSSDE, 30 of 15 MGD and 30 of 15 controls.	SSDE: 52.1±15.4 NSSDE: 56.3±9.8 MGD: 55.3±7.3 CONTROLS: 45.2±15.9	Confocal microscope HRT II Corneal Rostock Module	<u>Acini density (acini/mm^2)</u> SSDE: 146±62 NSSDE: 128±43 MGD: 64±33 Controls: 121±45 <u>Acini diameter (µm)</u> SSDE: 46±25 NSSDE: 57±28 MGD: 94±36 Controls: 49±12 <u>Orifice diameter (µm):</u> SSDE: 29±6 NSSDE: 31±4 MGD: 48±7 Controls: 32±5 <u>Secretion reflectivity:</u> SSDE: 1.7±0.6 NSSDE: 1.5±-- MGD: 3.3±0.7 Controls: 1.1±0.7	-MGD patients had the worst values -Laser scanning confocal microscopy is able to provide in vivo, non-invasive and high-resolution images of the ocular surface
Ban et al. (2011)	9 DED associated with chronic graft-versus-host disease (17 eyes) and 8 non-DED hematopoietic stem cell transplantation subjects (16 eyes)	(Median) DED: 50.5 (Range 38-57) Controls: 47.0 (Range 26-62)	Heidelberg Retina Tomograph II-Rostick Cornea Module	<u>Acinar unit density:</u> DED: 57.8±38.3 glands/mm^2 Controls: 88.8±26.6 glands/mm^2 <u>Gland acinar longest diameter:</u> DED: 37.3±24.4 µm Controls: 60.4±11.8 µm <u>Acinar shortest diameter:</u> DED: 17.7±11.8 µm Controls: 26.6±6.03 µm	-Lower and shorter values in the DED group

(Continuation)					
Study	Sample	Age (mean ± SD) years	Device	Results (mean ± SD)	Main findings
Randon et al. (2018)	100 MGD subjects (100 eyes) and 15 healthy (15 eyes)	52±20	Keratograph 5M and Heidelberg Retina Tomograph II-Rostick Cornea Module	Meiboscore Arita 1.3±0.9	-In vivo confocal microscopy classification can help in understanding the symptoms of subjects and enhance MGD treatment -In vivo confocal microscopy score was correlated with the meibography score

(Where DED: Dry Eye Disease; MGD: Meibomian Gland Dysfunction; NSSDE: Non-Sjögren Syndrome Dry Eye; SD: Standard Deviation; SSDE: Sjögren Syndrome Dry Eye).

Confocal microscopy has also proven to be useful to evaluate the effect of some treatments, diseases and contact lenses on meibomian glands (*Table 1.35*) (Matsumoto et al., 2009; Villani et al., 2011b; Agnifili et al., 2013; Villani et al., 2015; Yin et al., 2017; Agnifili et al., 2018; Siddireddy et al., 2018a; Agnifili et al., 2019; Li et al., 2020c; Vagge et al., 2020). Nevertheless, Zhou and Robertson (2018) claimed that in vivo confocal microscopy was unable to obtain images from meibomian glands in the eyelid margin due to light attenuation in that tissue. Therefore, this might be a field with further research to improve the technique.

Table 1.35. *Results reported by different authors regarding the use of confocal microscopy to assess the effect on the meibomian glands of treatments, contact lenses and diseases.*

Study	Sample	Age (mean ± SD) years	Device	Results (mean ± SD)	Main findings
Villani et al. (2011b)	20 CL wearers (20 eyes) and 20 controls (20 eyes)	CL: 25±3.2 Controls: 25±3.5	Heidelberg Retina Tomograph II-Rostick Cornea Module	<u>Acinar unit diameter</u> CL: 36.5±8 µm Control: 45±9 µm <u>Acinar unit density</u> CL: 129±48 units/mm^2 Control: 119±22 units/mm^2 <u>Glandular orifices diameter</u> CL: 44±16 µm Control: 33±7 µm	-Altered values in CL wearers
Siddireddy et al. (2018a)	30 CL wearers (30 eyes)	Median (IQR) Symptomatic: 23 (13) Asymptomatic: 23 (16)	Keratograph 5M and Heidelberg Retina Tomograph II-Rostick Cornea Module	<u>Meiboscore Arita</u> Symptomatic: 1±1 Asymptomatic: 0±0 <u>Acini secretion reflectivity</u> Symptomatic: 3±1 Asymptomatic: 1±1	-Meibomian acini reflectivity was higher in symptomatic CL wearers
Yu (2019)	132 diabetes mellitus (132 eyes) and 100 control subjects(100 eyes)	Diabetes: 60.18±7.59 Controls: 60.27±7.59	Keratograph 5M and Heidelberg Retina Tomograph II-Rostick Cornea Module	<u>Acinar unit density</u> Diabetes: 79.42±24.68 U/mm^2 Controls: 115.38±19.05 U/mm^2 <u>Acinar longest diameter</u> Diabetes: 91.21±22.35 µm Controls: 58.01±14.99 µm <u>Acinar shortest diameter</u> Diabetes: 45.87±11.68 µm Controls: 31.34±34 µm	-Meiboscore and gland drop-out was higher in the diabetes mellitus group -Confocal microscopy revealed alterations in acinar cells (expansion, atrophy and fibrosis), decreased density of acinar units, deposition of lipids and infiltration of inflammatory cells

(continuation)					
Study	Sample	Age (mean ± SD) years	Device	Results (mean ± SD)	Main findings
Yin et al. (2017)	18 MGD subjects with IPL treatment (18 eyes) and 17 MGD with eyelid hygiene (17 eyes)	IPL: 41.56±9.67 Hygiene: 40.76±13.93	Keratograph 5M and Heidelberg Retina Tomograph II-Rostick Cornea Module	<u>Gland drop-out (%)</u> IPL pre: 45.72±12.93 IPL post: 40.28±13.15 Hygiene pre: 39.27±13.65 Hygiene post: 35.22±11.93 <u>Acinar longest diameter</u> IPL pre: 101.89±21.44 IPL post: 84.67±20.25 Hygiene pre: 98.0±29.01 Hygiene post: 97.86±25.39 <u>Acinar unit density</u> IPL pre: 91.50±37.42 IPL post: 113.11±40.12 Hygiene pre: 88.57±34.24 Hygiene post: 103.71±27.43 <u>Inflammatory cells</u> IPL pre: 44.44 % IPL post: 16.67% Hygiene pre: 50 % Hygiene post: 50%	-Meibomian gland drop-out improved in both groups -Meibomian gland microstructure indexes were improved only in the IPL group
Li et al. (2020c)	23 subjects treated with a conservative method for chalazion (23 eyelids) and 35 treated with surgery (44 eyelids)	Conservative: 32.39±13.43 Surgery: 32.86±14.64	Keratograph 5M and Heidelberg Retina Tomograph 3 with the Rostock Cornea Module	Gland drop-out (%) (Median (IQR)) Conservative: 14.64 (10.33,25.77) Surgery: 14.84 (11.31,21.81)	-Chalazion caused meibomian gland loss -A hot compress improved meibomian gland function

(continuation)					
Study	Sample	Age (mean ± SD) years	Device	Results (mean ± SD)	Main findings
Vagge et al. (2020)	21 Graves ophthalmopathy subjects (21 eyes) and 24 healthy (24 eyes)	Graves: 44.2±9.9 Controls: 39.8±10.7	Heidelberg Retina Tomograph 3 with the Rostock Cornea Module	Acinar unit density (U/mm^2) Graves: 24.5±8.1 Controls: 34.2±7.5 Total lumen area (μm^2) Graves: 3104.7±1713.3 Controls: 1393.8±448.0 Acinar longest diameter (µm) Graves: 94.4±21.2 Controls: 64.3±10.1 Acinar shortest diameter (µm) Graves: 46.6±15.3 Controls: 42.2±12.3	-Significant differences were found between groups for all meibomian gland features -In vivo confocal microscopy allowed to assess distinctive features of meibomian glands in subjects with Graves ophthalmopathy

(Where CL: Contact Lens; IPL: Intense Pulsed Light; IQR: Interquartile Range; SD: Standard Deviation).

1.5 Imaging techniques to assess physical changes on the ocular surface

1.5.1 Assessment of physical changes through confocal microscopy

Apart from helping in the assessment of meibomian glands, in vivo confocal microscopy can also be a device that allows assessing corneal and conjunctival cell changes related to DED (Erie, McLaren and Patel, 2009; Bron et al., 2017). Thus, it has been reported that confocal microscopy is a tool that can help in the early DED diagnosis and monitoring, and in evaluating the influence of treatments on the ocular surface (Kobayashi, Yoshita and Sugiyama, 2005; Villani et al., 2007; Wakamatsu et al., 2009; Wakamatsu et al., 2010; Villani et al., 2011a; Villani et al., 2011b; Zhang et al., 2011; McGinnigle, Naroo and Eperjesi, 2012; Villani et al., 2013b; Lin and Yiu, 2014; Liu et al., 2017; López-De La Rosa et al., 2017; Cardigos et al., 2018; Labetoulle et al., 2018; Lee et al., 2018; Matsumoto and Ibrahim, 2018; Qazi et al., 2018; López-De La Rosa et

al., 2019a; Lafiti et al., 2020; Liu et al., 2020; Matsumoto et al., 2020; Wei et al., 2020; Aggarwal et al., 2021).

Authors have found higher inflammatory cell density in DED and MGD subjects. Higher inflammatory cell density was negatively correlated with tear film quantity and stability; and positively correlated with dry eye symptoms and ocular surface staining (Wakamatsu et al., 2009; Wakamatsu et al., 2010; López-De La Rosa et al., 2017; Qazi et al., 2018; Liu et al., 2020; Matsumoto et al., 2020; Aggarwal et al., 2021). Aggarwal et al. (2021) found a correlation between corneal immune dendritiform cell density and severity of DED. It has also been reported that DED and MGD subjects had a loss in goblet cells (Agnifili et al., 2018), lower conjunctival epithelial cell densities (Wakamatsu et al., 2010; Matsumoto et al., 2020) and lower superficial, intermediate and basal epithelial cells in the layers of the cornea (Villani et al., 2007; Villani et al., 2011b; Zhang et al., 2011; Lee et al., 2018; Matsumoto et al., 2020). Villani et al. (2013b) found reduced epithelial cell densities in all tissues except in eyelid margins in subjects with Sjögren syndrome, non-Sjögren DED and MGD in comparison with controls. Similarly, Dogan, Gurdal and Arslan (2018) found that contact lens subjects with discomfort had higher dritiform cells, with indicates intensified inflammation of the cornea. Moreover, Zhang et al. (2011) concluded that confocal microscopy can be used for non-invasive impression cytology (Wakamatsu et al., 2010). In-vivo confocal microscopy imaging is less invasive and as effective as impression cytology; nevertheless, it has not been widely used in clinical practice and its predictive ability is unknown in DED diagnosis (Kojima et al., 2010; Wolffsohn et al., 2017).

Eye surface damage in DED also causes losing corneal nerves and increasing tortuosity (Bron et al., 2017; Liu et al., 2017; Cardigos et al., 2018; Matsumoto and Ibrahim, 2018; Qazi et al., 2018; Lyu et al., 2019; Lafiti et al., 2020; Liu et al., 2020; Ma et al., 2020; Matsumoto et al., 2020; Wei et al., 2020; Dermer et al., 2021; Patel et al., 2021). Corneal nerves assessment is essential because they play a relevant role in the blink reflex, wound healing and tear secretion (Shaheen, Bakir and Jain, 2014; Belmonte et al., 2017). Villani et al. (2007) found that corneal thickness in Sjögren syndrome patients was higher than in controls, and they had a lower number of subbasal nerves, and higher nerve tortuosity. The same author (Villani et al., 2013b) found that subjects with Sjögren syndrome, non-Sjögren DED and MGD had fewer sub-basal nerve plexi fibers and more bead density than controls ($p < 0.001$). Sub-basal dendritic cell density was higher in the Sjögren syndrome and MGD groups ($p < 0.01$). Zhang et al. (2011) also found that the grade of sub-basal nerve tortuosity was significantly higher in the moderate to severe dry eye group compared with the control group ($p < 0.01$), but there was no significant difference between mild dry eye and the control groups ($p > 0.05$).

In summary, confocal microscopy allows clinicians to obtain valuable information about physical changes in the ocular surface to diagnose DED, such as cell densities, inflammatory cells or sub-basal corneal nerves alteration (Chan et al., 2017).

1.5.2 Assessment of physical changes through optical coherence tomography

OCT can also be used as a device to assess ocular surface changes related to DED. For instance, OCT has been used to evaluate Lid Parallel Conjunctival Folds (LIPCOF), conjunctivochalasis, map 3-dimensional corneal epithelial thickness and to assess the

structure of Meibomian glands (Lin and Yiu, 2014; Poh et al., 2017; Thulasi and Djalilian, 2017; Bandlitz et al., 2019b; Kheirkhah et al., 2019; Gumus and Pflugfelder, 2021). Gumus and Pflugfelder (2013) found that conjunctivochalasis may disrupt tear distribution along the lower lid. Thus, Fourier domain-OCT was reported to be a useful, objective and quantitative technique to assess conjunctivochalasis.

Regarding the assessment of LIPCOF with OCT, results were correlated with slit-lamp evaluation. Thus, this technique may allow a more detailed and objective method of assessment of this condition in the future and can be useful in DED due to the correlation between dry eye and the presence of LIPCOF (McGinnigle, Naroo and Eperjesi, 2012). Moreover, Gumus and Pflugfelder (2021) found that ADDE patients had lower bulbar conjunctival epithelial thickness than controls and EDE patients, especially in the temporal region, but the difference was not statistically significant. Subjects with DED and conjunctivochalasis had lower bulbar conjunctival epithelial thickness in temporal and inferior regions in comparison with DED subjects without conjunctivochalasis.

Finally, the device has been found to have good repeatability. Sella et al. (2019) found that iVue Fourier-domain OCT provided good repeatability and reproducibility in the measurement of epithelial thickness in normal and DED subjects. Moreover, Ma et al. (2018) also found excellent repeatability and reproducibility for corneal thickness and epithelial thickness in DED and healthy subjects.

1.5.3 Bulbar redness assessment

Ocular redness is the principal sign of ocular surface inflammation (Kilduff and Luis, 2016), being inflammation crucial for the inclusion of a patient in the DED definition (Craig et al., 2017). Conjunctival redness can be assessed using a slit-lamp or a pen torch. However, it is quite subjective since it involves image-based grading scales (Papas, 2000; Wolffsohn and Purslow, 2003; Wolffsohn, 2004; Peterson and Wolffsohn, 2007; Peterson and Wolffsohn, 2009; Schulze, Hutchings and Simpson, 2011; Amparo et al., 2013; Baudouin et al., 2015; Downie, Keller and Vingrys, 2015; Wu et al., 2015; Tauste et al., 2017; Wolffsohn et al., 2017; Albietz and Schmid, 2018; Macchi et al., 2018; Sapkota, Franco and Lira, 2018; Sorbara et al., 2018; Beshtawi et al., 2019; Mann et al., 2019; Debarun and Wolffsohn, 2021). Due to the fact that these scales depends on the examiners' ability; objective and quantitative image analysis methods have been developed to quantify bulbar redness (Papas, 2000; Wolffsohn, 2004; Peterson and Wolffsohn, 2007; Peterson and Wolffsohn, 2009; Amparo et al., 2013; Baudouin et al., 2015; Downie, Keller and Vingrys, 2015; Wu et al., 2015; Wolffsohn et al., 2017).

Some corneal topographers such as Oculus Keratograph 5M allow clinicians assessing bulbar redness in an objective, automated and non-invasive way (Wu et al., 2015; Pérez-Bartolomé et al., 2017; Wolffsohn et al., 2017; Pérez-Bartolomé et al., 2018; Xie et al., 2018; García-Montero et al., 2019a; Lorente-Velázquez et al., 2019; Rico-del-Viejo et al., 2019; Wang et al., 2019a; Cheng et al., 2020; Mylla-Bosso et al., 2020; Talens-Estarelles et al., 2020). They include software that enables the evaluation of ocular redness in a continuous score. Thus, clinicians are able to grade redness

accurately, instead of choosing between two categories of a grading scale when an intermediate score is needed (Pérez-Bartolomé et al., 2018).

Generally, topography systems use white light illumination and conjunctiva must be properly focused (Wu et al., 2015; Pérez-Bartolomé et al., 2017; Pérez-Bartolomé et al., 2018). The software automatically detects bulbar conjunctival boundaries and excludes the iris and the eyelids from the analysis. Thus, bulbar redness is calculated through the ratio between conjunctival vessels (red pixels) and sclera (white pixels) (Best, Drury and Wolffsohn, 2012; Downie, Keller and Vingrys, 2015; Wu et al., 2015; Pérez-Bartolomé et al., 2017; Pérez-Bartolomé et al., 2018; Xie et al., 2018; García-Montero et al., 2019a; Lorente-Velázquez et al., 2019; Rico-del-Viejo et al., 2019; Cheng et al., 2020; Mylla-Bosso et al., 2020; Talens-Estarelles et al., 2020). Ocular redness is classified between bulbar and limbal; and temporal and nasal (*Figure 1.8*). Furthermore, a total measurement of the global bulbar redness is also calculated (Wu et al., 2015; Wolffsohn et al., 2017; Pérez-Bartolomé et al., 2018; García-Montero et al., 2019a).

Some authors have found higher ocular redness in DED and MGD subjects (Srinivasan et al., 2008; Abelson, Lane and Maffei, 2010; Rodriguez et al., 2013; Rico-del-Viejo et al., 2019). Nevertheless, the repeatability of these devices in some measurements is still unclear (Hong et al., 2013; Best, Drury and Wolffsohn, 2015; Wu et al., 2015; Tian et al., 2016; Pérez-Bartolomé et al., 2017; Fernández et al., 2018; Pérez-Bartolomé et al., 2018; Vidal-Rohr et al., 2018). Wu et al. (2015) found that the bulbar redness score had the highest reproducibility in comparison with other grading scales (Institute for Eye Research, Efron and Validated Bulbar Redness). Conversely,

Pérez-Bartolomé et al. (2018) found poor agreement between objective and subjective techniques. They concluded by saying that Keratograph 5M overestimates the scores in comparison with subjective grading scales. Schulze et al. (2021) found that although Keratograph 5M and a subjective grading scale were both sensitive to assess changes in bulbar redness, statistically significant differences in bulbar redness between DED and controls were found only in the subjective grading scale. Authors also argued that Keratograph 5M may underestimate bulbar redness (Downie, Keller and Vingrys, 2015; Schulze et al., 2021). This might be due to the visible areas that are being assessed. Thus, the Keratograph 5M evaluates ocular redness from a front view, which causes a less area of analysis in comparison with slit-lamp examination. Finally, in some cases, the algorithm was not able to properly assess the conjunctival redness since it includes parts of the surrounding skin in the analysis. Further research is needed to clarify this lack of agreement between studies.

The analysis of bulbar redness has also been proven to be useful to assess the influence of contact lenses (Tauste et al., 2017; Sapkota, Franco and Lira, 2018; Xie et al., 2018; García-Montero et al., 2019a; Lorente-Velázquez et al., 2019; Debarun and Wolffsohn, 2021), some medications (Pérez-Bartolomé et al., 2017; Albietz and Schmid, 2018; Cheng et al., 2020; Mylla-Bosso et al., 2020), and visual displays (Talens-Estarelles et al., 2020; Talens-Estarelles et al., 2021a) on the ocular surface inflammation.

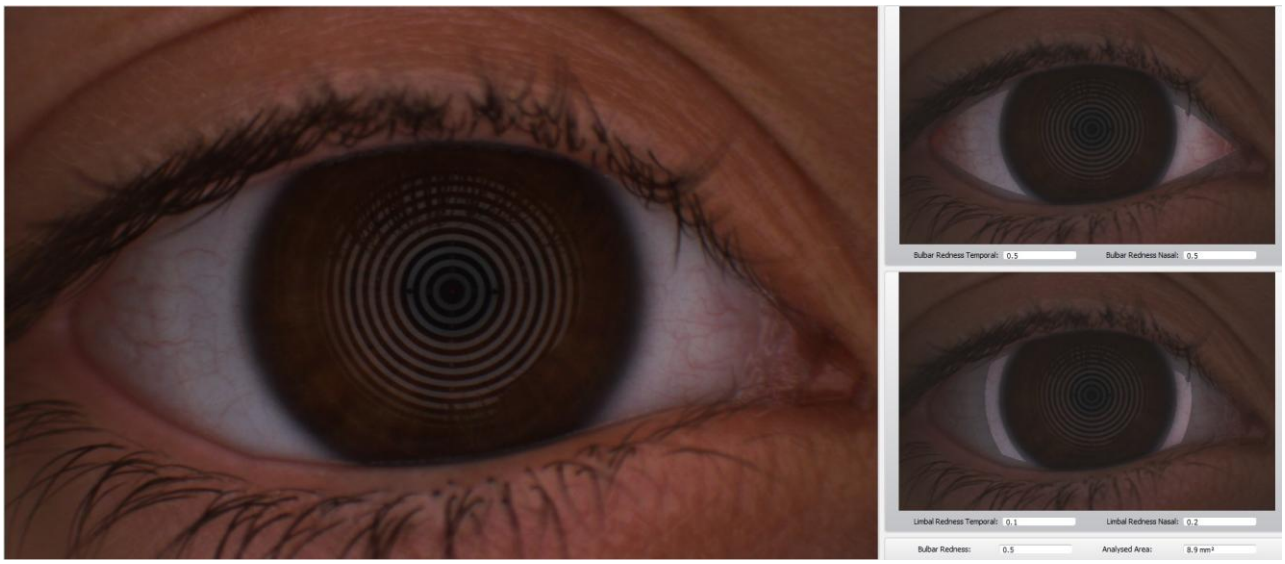

Fig. 1.8. *Measurement of the ocular redness using a videokeratograph.*

1.6 Impact of contact lenses on the tear film and the ocular surface

Iatrogenic disease is known as an adverse clinical condition in which a disease is a result of a medical treatment. Tear film can be altered by several iatrogenic conditions. For instance, contact lens wear has been reported to be associated with DED (Gomes et al., 2017; Stapleton et al., 2017). The increasing number of contact lens wearers has highlighted the need of studying iatrogenic dry eye (Gomes et al., 2017).

Contact lens wear impacts the ocular surface homeostasis (Stapleton et al., 2006; Stapleton et al., 2017). Approximately, 50 % of contact lens wearers suffer from dryness and ocular discomfort, both problems being the major causes of contact lens intolerances (Doughty et al., 1997; Young et al., 2002; Dumbleton et al., 2013a; Llorens-Quintana et al., 2018). Nevertheless the authors of the TFOS DEWS II Iatrogenic Report argued that it is largely reliant upon symptoms because they can be confounded by overlap with that of discomfort during contact lens wear and for which

the cause is multifactorial (Dumbleton et al., 2013a; Gomes et al., 2017). Dryness, discomfort, tearing, itching, hyperaemia and/or blurred vision are common signals and symptoms related to dry eye that are reported by contact lens wearers (Montés-Micó et al., 2004; Ferrer-Blasco et al., 2009; Ruiz-Pomeda et al., 2018a; Lafosse et al., 2019).

Contact lens discomfort was defined as "a condition characterized by episodic or persistent adverse ocular sensations related to lens wear, either with or without visual disturbance, resulting from reduced compatibility between the contact lens and the ocular environment, which can lead to decreased wearing time and discontinuation of contact lens wear" (Nichols et al., 2013b; Koh, 2020). Dry eye in contact lens wearers has been identified as a growing public health issue (Pili et al., 2014; Gomes et al., 2017). Two definitions of dryness associated to contact lens wear have been proposed: CL-induced dry eye and CL-associated dry eye (Pult, Murphy and Purslow, 2009; Gomes et al., 2017; Alzahrani et al., 2018). The first one is related to the presence of signs and symptoms during contact lens wear, which did not exist before contact lens wear. The second one is also related to the presence of signs and symptoms, but they could be the consequence of a pre-existing dry eye before contact lens wear (Pult, Murphy and Purslow, 2009; Gomes et al., 2017; Alzahrani et al., 2018).

Several studies have found that signs and symptoms of ocular dryness were more prevalent in contact lens wearers (Viso, Rodríguez-Ares and Gude, 2009; Han et al., 2011; Uchino et al., 2011; Dumbleton et al., 2013a; Uchino et al., 2013; Paulsen et al., 2014; Vehof et al., 2014; Tan et al., 2015b; Yang et al., 2015; Stapleton et al., 2017; Kojima, 2018; Li et al., 2018; McMonnies, 2018; Rico-del-Viejo et al., 2018; Wang and Craig, 2019; Willcox, 2019; Kaido et al., 2020; Koh, 2020; Kobia-Acquah et al., 2021a;

Kobia-Acquah et al., 2021b). Likewise, the TFOS DEWS II Epidemiology Report recognized contact lens wear as a consistent risk factor for DED (Stapleton et al., 2017). However, other studies did not find an association with DED (Schaumberg et al., 2003; Galor et al., 2012; Wang et al., 2020).

In light of the above, tear film assessment is essential in contact lens wearers (Dumbleton et al., 2013a; Llorens-Quintana et al., 2018; Mousavi et al., 2018; Lafosse et al., 2019) because contact lenses induce biophysical and biochemical changes in the tear film (Mann and Tighe, 2013; Gomes et al., 2017; Llorens-Quintana et al., 2018; Sorbara et al., 2018; Willcox, 2019; Read et al., 2020). When a contact lens is inserted into the eye, tear film destabilizes (Foulks et al., 2013) because the contact lens divides the tear film into two layers: pre-lens and post-lens tear film. The pre-lens tear film is constituted by a lipid layer and a reduced aqueous layer with approximately 2µm, whilst the post-lens tear film consists of an aqueous layer and a mucin layer. The pre-lens tear film plays a key role in visual quality, comfort, lubrication and hydration of the contact lens front surface. It also facilitates palpebral interaction with the contact lens surface and provides a smooth optical surface. Thus, the assessment of the pre-lens tear film will be crucial in contact lens wearers to understand the symptoms related to ocular dryness (Fabber et al., 1991; Korb, Greiner and Glonek, 1996; Szczesna-Iskander et al., 2012; Tyagi et al., 2012; Dumbleton et al 2013b; Llorens-Quintana et al., 2018; Guillon et al., 2019b; Itokawa et al., 2020; Marx, Eckstein and Sickenberger, 2020).

The division of the tear film will differ depending on the characteristics of each subject, as well as the characteristics of the contact lens such as its design and its

material (Dumbleton et al., 2013a). Moreover, when a contact lens is inserted into the eye, corneal sensitivity decreases; which might reduce tear secretion through the reflex sensory loop (Dumbleton et al., 2013a).

Insufficient tear distribution, increased friction, tear evaporation, tear instability and contact lens dewetting are the main proposed mechanisms that cause dryness associated to contact lens wear (Nichols and Sinnott, 2006; Szczesna-Iskander and Iskander, 2014; Kojima, 2018; Llorens-Quintana et al., 2018; Vidal-Rohr et al., 2018; Kolbe et al., 2019; Koh, 2020). Several studies reported that contact lens wear caused a decrease in tear kinetics (Faber et al., 1991; Nichols and King-Smith, 2004; Nichols and Sinnott, 2006; Guillon and Maissa, 2008; Szczesna-Iskander et al., 2012; Tyagi et al., 2012; Guillon et al., 2016; Guillon et al., 2019b; Kaido et al., 2020), tear stability and BUT (Santodomingo-Rubido, Wolffsohn and Gilmartin, 2006b; Dogan, Gurdal and Arslan, 2018; Itokawa et al., 2018; Llorens-Quintana et al., 2018; Moro et al., 2018; Stahl and Jalbert, 2018; Siddireddy et al., 2018b; Vidal-Rohr et al., 2018; Guillon et al., 2019b; Walther, Subbaraman and Jones, 2019; Yucekul et al., 2019; Gu et al., 2020b; Itokawa et al., 2020), lipid layer thickness (Yokoi et al., 2008; Gomes et al., 2017), optical quality (Vidal-Rohr et al., 2018; García-Montero et al., 2019c; Kolbe et al., 2019), less goblet cell densitiy (Colorado et al., 2016), tear meniscus parameters (Chen et al., 2011a; Lafosse et al., 2018; Siddireddy et al., 2018a; Gu et al., 2020b), and an increase in tear evaporation (Kojima et al., 2011; Gomes et al., 2017), discomfort and dry eye symptoms (Dogan, Gurdal and Arslan, 2018; Sapkota, Franco and Lira, 2018; Siddireddy et al., 2018a; Siddireddy et al., 2018b; Sorbara et al., 2018; Stahl and Jalbert, 2018; Vidal-Rohr et al., 2018; Yucekul et al., 2019; Kaido et al., 2020; Situ et al.,

2020; Jeon and Park, 2021). It has also been reported to increase tear osmolarity (Nichols and Sinott, 2006; Stahl and Jalbert, 2018; López-De La Rosa et al., 2019b) and ocular surface staining (Fonn, Peterson and Woods, 2010; Li et al., 2018; Sapkota, Franco and Lira, 2018; Siddireddy et al., 2018a; Stahl and Jalbert, 2018; Muntz et al., 2020); and to alter bulbar redness and ocular surface inflammation (López-De La Rosa et al., 2017; McMonnies, 2018; Sapkota, Franco and Lira, 2018; Tauste et al., 2017; Dogan, Gurdal and Arslan, 2018; Siddireddy et al., 2018b; Gad et al., 2019; López-De La Rosa et al., 2019b; Alghamdi, Markoulli and Papas, 2020; Liu et al., 2020) and meibomian gland drop-out, morphology and secretions (Siddireddy et al., 2018a; Siddireddy et al., 2018b; Pucker et al., 2019b; Gu et al., 2020a; Gu et al., 2020b; Llorens-Quintana, Garaszczuk and Szczesna-Iskander, 2020; Pucker and Tichenor, 2020; Uçakhan and Arslanturk-Eren, 2019), especially in high water content contact lenses (Nichols and Sinnott, 2006; Szczesna-Iskander, 2014; García-Montero et al., 2019c; Lafosse et al., 2019; Lorente-Velázquez et al. 2019). Ocular redness is related to oxygen transmissibility of contact lens materials and it is a sign of ocular surface inflammation and hypoxia (Papas et al., 1997; Fonn, Peterson and Woods, 2010; García-Montero et al., 2019a).

In contrast to these studies, García-Montero et al. (2019a) did not find significant changes in the ocular surface parameters over 15 days of use of a monthly silicone hydrogel contact lens. Ruiz-Pomeda et al. (2018a) did not report significant changes in osmolarity over 24-months in the dual-focus lens; and García-Montero et al. (2019a) neither found differences in tear film stability, TMH and limbal and bulbar redness after 15 days of silicone hydrogel contact lens wear.

The use of daily disposable contact lenses (Lazón-de la Jara et al., 2013), lenses with internal wetting agents (Peterson et al., 2006), and reducing wearing time or ceasing contact lens wear (Santodomingo-Rubido, Barrado-Navascués and Rubido-Crespo, 2010; Tan, Ng and Acharya, 2011) can help to solve discomfort in contact lens wearers. Vidal-Rohr et al. (2018) found that enhancing the physical properties of contact lenses improved comfort. However, the effect of contact lens properties on the tear film is still unclear and further controlled studies are required (Kojima, 2018).

Hydrogels with lower water content have higher lens hydration (Martín, 1995; Vidal-Rohr et al., 2018), providing a better lens comfort (Efron et al., 1986; Young, 1996; Vidal-Rohr et al., 2018) than other materials with higher water content. Silicone increases oxygen permeability; however, it compromises lens wettability (Vidal-Rohr et al., 2018). Choosing a silicone hydrogel contact lens can also help to maintain the homeostasis of the tear film and the ocular surface (Guillon et al., 2018; García-Montero et al., 2019a; Guillon et al., 2019a). Conversely, Ruiz-Alcocer et al. (2018) did not find significant differences between a hydrogel and two silicone hydrogel contact lenses in osmolarity, TMA, central corneal thickness and corneal aberrations. Another study compared the performance of silicone hydrogel daily disposable with hydrogel daily disposable contact lenses (Diec, Tilia and Thomas, 2018; Koh, 2020). They did not find a difference in discomfort between lenses. However, hydrogel lenses caused more limbal redness and silicone hydrogel lenses caused more conjunctival staining and indentation. Thus, the choice between silicone hydrogel and hydrogel contact lenses is controversial and it depends on the individual eye (Koh, 2020). Overall, despite the development of new materials and contact lenses with a short replacement, tear film

alterations and discomfort in contact lens wearers remains a common reason for contact lens wear ceasing (Chalmers, 2014; Chen et al., 2017; McMonnies, 2018).

1.7 Conclusions

In light of the above, the diagnosis and management of DED is a challenge because of the multifactorial character of the disease and the lack of a gold standard test. Moreover, the lack of correlation between signs and symptoms for DED, the lack of correlation between techniques, their low repeatability, their invasiveness and their relative objectivity challenges the assessment of the tear film and the diagnosis of DED.

The development of new diagnostic methods would allow a better assessment, monitoring and control of dry eye patients; and therefore, a better evaluation of treatments for this disease. Imaging techniques have a high potential in this field due to their non-invasiveness. Thus, they can provide an accurate, repeatable, objective and quick measurement of the tear film in a non-invasive way, which allows clinicians to assess the tear film in more natural conditions and without disturbing the tear film. Although many imaging techniques exist to assess the tear film, this is a field that needs further research and which has a high potential to be explored. Therefore, it is necessary to develop new non-invasive and objective methods to evaluate the tear film and further studies are needed to improve the correlation of these techniques with clinical findings in dry eye patients.

CHAPTER 2: Justification

2. JUSTIFICATION

2.1 Current situation

The tear film plays an essential role in the maintenance of the ocular surface health and the optical quality of the eye (Montés-Micó et al., 2010a). An altered tear film can lead to DED, which is a multifactorial disease that induces discomfort symptoms, visual alterations and ocular surface damage (Craig et al., 2017). DED has become a public health issue worldwide because of its high impact on the healthcare system (Brown, 2009; Mizuno, Yamada and Shigeyasu, 2012; Farrand et al., 2016; Stapleton et al., 2017). Moreover, it has also been reported to cause a high economic burden (Clegg et al., 2006; Yu, Asche and Fairchild, 2011; Mizuno, Yamada and Shigeyasu, 2012; Farrand et al., 2016; McDonald et al., 2016; Stapleton et al., 2017). The cost of DED patients also affects global productivity due to the need for treatment and office visits (Clegg et al., 2006; Yu, Asche and Fairchild, 2011). For instance, Mizuno, Yamada and Shigeyasu (2012) claimed that the annual cost in 2010 for each DED patient was USD $323±219 for drugs, USD $165±101 for healthcare, and USD $530±384 for punctal plug placement. Furthermore, a recent study found that the annual cost for DED treatment was USD $783 per patient, with a total cost of USD $3840 milions (Yu, Asche and Fairchild, 2011).

Apart from the economic cost, DED also has a social impact. Different studies have demonstrated that DED subjects have a reduced quality of life (Mertzanis et al., 2005; Paulsen et al., 2014) and a higher chance to have stress, anxiety or depression (Labbé et al., 2013; Hallak, Tibrewal and Jain, 2015). Moreover, subjects diagnosed with DED

find challenging the performance of common tasks such as reading, performing work activities, using the computer, driving or watching the television (Alex et al., 2013).

The prevalence of DED is increasing due to the current lifestyle of the population. Thus, factors such as the increasing cases of refractive surgery, the use of contact lenses and computers are associated with DED (Stapleton et al., 2017). Likewise, the increasing cases of environments with low humidity or with air-conditioned can also be behind the increase of DED prevalence because of tears evaporation (Alex et al., 2013; Tesón et al., 2013; López-Miguel et al., 2014).

Nowadays, the diagnosis of DED is based on a combination of signs and symptoms. Nevertheless, DED diagnosis is still challenging due to its multifactorial aetiology, the lack of a gold standard metric, the low agreement between DED signs and symptoms and the lack of an objective and quantitative method with high repeatability and sufficient diagnostic capability (Wolffsohn et al., 2017). DED diagnosis is still more difficult in the early or mild stages of the disease due to the lack of objective tests with good sensitivity and specificity, repeatability, ease of performance, and suitability for clinical practice settings (Wolffsohn et al., 2017). In this way, subjective assessments depend on the ability of the examiner to detect alterations (Arita et al., 2009b; Tomlinson et al., 2011; Pult and Riede-Pult, 2013; Wolffsohn et al., 2017), which may lead to a decrease in repeatability and agreement between clinicians (Nichols et al., 2005). Therefore, new objective metrics are still required to provide new insights into tear film assessment (Abdelfattah et al., 2015; Ji et al., 2017; Wolfsohn et al., 2017; King-Smith et al., 2018).

New non-invasive methods have been developed recently to enhance tear film and ocular surface analysis without destabilizing it (Varikooty, Keir and Simpson, 2012; Celik et al., 2013; Abdelfattah et al., 2015; Ji et al., 2017; Wolfsohn et al., 2017; King-Smith et al., 2018; Llorens-Quintana et al., 2018; Lai et al., 2019; Llorens-Quintana, Szczesna-Iskander and Iskander, 2019; Llorens-Quintana et al., 2019a; Llorens-Quintana et al., 2020). In addition, the TFOS DEWS II Diagnostic Methodology report recognized the need of developing new non-invasive, objective and as automatic as possible metrics to assess the tear film and the ocular surface (Wolffsohn et al., 2017).

Overall, due to the growing incidence of DED and morbidity, improving the timely diagnosis to provide a better diagnosis and treatment of the disease is vital. Thus, the development of new metrics that could be used as tear film homeostasis markers is essential to improve the assessment of DED. Image processing has been reported to be a field with high potential to exploit (Arita et al., 2013; Celik et al., 2013; Koprowski et al., 2016; Geerling et al., 2017; Llorens-Quintana et al., 2019a).

2.2 Hypothesis and objectives

Due to the influence of DED on the health and the quality of life of subjects, the effect of DED on the economy, the abovementioned issues found in the assessment of the tear film and the need of developing new methods to assess the tear film non-invasively and objectively; the present work aims to develop new metrics to assess the tear film and the ocular surface in a non-invasive and as objective as possible way.

The main goals of the study are as follow:

1. To study the risk factors for DED, the repeatability of some current metrics for the assessment of the ocular surface, and the efficacy of a thermal eyebag application.

1.1 To study systemic, environmental and lifestyle DED risk factors in a Mediterranean Caucasian population.

1.2 To assess the repeatability of NIKBUT obtained using the Oculus Keratograph 5M.

1.3 To assess the repeatability of bulbar redness obtained using the Oculus Keratograph 5M.

1.4 To assess the effect of MGDRx eyebag application on the ocular surface of young and older subjects with dry eye symptoms.

2. To develop and validate new metrics to assess the tear film and the ocular surface in a non-invasive and as objective as possible way. The repeatability and diagnostic capability of new metrics will be assessed.

2.1 To develop and validate new quantitative metrics to assess meibomian glands visibility objectively.

2.2 To develop and assess the performance of an analysis method to measure in vivo the spreading speed of tear film particles post-blink.

2.3 To develop and validate a novel method to objectively assess the lipid layer through the analysis of grey intensity values obtained from the Placido disk pattern reflected onto the tear film.

3. To assess the effect of contact lenses, artificial tears, blinking and computer use on the ocular surface and the newly developed metrics.

3.1 To assess the short-term effect of dual-focus design on pre-lens tear film stability, optical quality and visual performance in comparison with a single-vision contact lens of the same material.

3.2 To assess the short-term effect of two different dual-focus designs on pre-lens tear film stability, optical quality and visual performance.

3.3 To assess dry eye symptoms and meibomian gland alterations in scleral lens wearers after one year of lens wear.

3.4 To assess the light disturbance related to changes in the tear film stability parameters.

3.5 To assess the effect of soft contact lens wear and duration on meibomian glands, the tear film and ocular surface parameters.

3.6 To assess the effect of computer use, contact lenses and artificial tears on the newly developed metrics and current ones.

Contact lens wear and computer use have been identified as potential risk factors for DED according to the TFOS DEWS II Epidemiology Report (Stapleton et al., 2017). Moreover, the instillation of artificial tears is generally accepted as one of the main management strategies for DED (Jones et al., 2017). Therefore, the hypothesis is that new metrics are able to detect changes in the tear film and the ocular surface in a non-invasive and objective way. This might help to validate the metrics and find clinical

applications for them such as the assessment of the ocular surface in contact lens wearers, computer users or in subjects under artificial tears treatment.

CHAPTER 3: General methodology

3. GENERAL METHODOLOGY

3.1 General design and ethical considerations of the studies

To implement this doctoral thesis, a wide range of ocular surface measurements have been taken to develop new metrics to assess the tear film and the ocular surface and to validate them. The population studied consisted of students or staff from the University of Valencia. Participants had no prior history of ocular complications, injury or disease in the last three months. To evaluate various ocular surface stages, no exclusion based on the state of the meibomian glands or the tear film of subjects was made. Thus, inclusion and exclusion criteria were not restrictive and they depended on the purpose of each study; therefore, they will be mentioned in each chapter of the thesis. The present study followed the tenets of the Declaration of Helsinki and was approved by the Ethics Committee of the University of Valencia. Written consent of each subject was obtained after the explanation of the purpose and the protocol of the study.

The present work was divided into 3 parts: 1) Development of new metrics to assess the tear film and the ocular surface; 2) Validation of the developed metrics; and 3) Application of the new metrics to subjects fitted with contact lenses. Metrics were developed using Matlab© R2018a software (MathWorks, Natick, MA) and the procedure will be explained in each chapter of the present work. The protocol was prepared considering the cost limits of the project.

3.2 Measurements and devices

This section describes the technical information of the devices used for data

collection. Measurements were taken in the following research centres: 1) University of Valencia, Optometry Research Group (GIO) and 2) University of Minho, Clinical and Experimental Optometry Research Laboratory (CEORLab).

The most appropriate ocular measures to fulfil the definition of DED were chosen, based on the literature review and the practical experience. Thus, DED was defined according to the TFOS DEWS II Diagnostic Methodology Report criterion (Wolffsohn et al., 2017). Despite non-invasive tests preventing the tear film from destabilizing, it is important to proceed from the least to the most invasive measurement since some alteration of blinking or bright illumination can alter the results (Wolffsohn et al., 2017). Evaluation sheets were prepared following this rule. The order in which each measurement was taken is specified in each chapter of the present work; however, this was the general order used: subjective questionnaires, bulbar redness, TMH, lipid layer thickness, NIKBUT, tear film osmolarity, ocular surface staining and non-contact infrared meibography.

Generally, the time of each visit was estimated to be around 45 minutes. Availability of the laboratory, national and academic holidays and weekends also were considered. Moreover, all measurements were taken by the same experienced researcher and laboratory temperature (°C) and humidity (%) were monitored with a thermo-hygrometry device (C3121, Comet, Czech Republic).

3.2.1 Ocular symptoms assessment

The TFOS DEWS II Diagnostic Methodology Report recommended the use of the OSDI and DEQ-5 questionnaires to assess dry eye symptoms and to diagnose DED (Wolffsohn et al., 2017). In this study, a combination of both questionnaires was used to assess ocular

symptoms. Questionnaires were self-administered by the participants.

3.2.1.1 OSDI

OSDI questionnaire is the most commonly used tool for the dry eye symptoms assessment (Wolffsohn et al. 2017). Originally it was developed by the Outcomes Research Group at Allergan Inc (Irvine, California) (Walt et al., 1997) and is a 12-item questionnaire designed to assess the frequency in which symptoms related to dry eye appeared and their impact on vision-related tasks. Thus, each frequency is attributed with a score: 4) All the time; 3) Most of the time; 2) Half of the time; 1) Some of the time; and 0) None of the time. Dry eye symptoms can be quantified by using these scores. Moreover, it includes questions regarding the "last week period" to assess the impact on the quality of life of dry eye (Stevenson, Tauber and Reis, 2000; Russo, Bouchard and Galasso, 2007; Chang et al., 2009; Yüksel et al., 2010). The questionnaire was previously validated for the diagnosis of DED (Özcura, Aydin and Helvaci, 2007).

Questions are separated into three groups: 1) Physical symptoms, which are 5 questions that include light sensitivity, gritty eyes, pain or sore in eyes, blurred vision and poor vision; 2) Daily activities, which are 4 questions that include reading, driving at night, working with a computer or bank machine and watching the television; and 3) Environmental factors, which are 3 questions that include windy conditions, low humidity and areas with air-conditioned. The OSDI ranges from 0 to 100, with higher scores representing higher symptoms. The score is calculated as OSDI = [(Sum of all scores for each question answered) × 100] / [(total number of questions answered) × 4]. The total score allows the classification of subjects as normal if they have a score between 0 and 12, mild DED if they have a score between 13 and 22, moderate DED if

they have a score between 23 and 32, and severe DED if they have a score between 33 and 100 (Schiffman, 2000; Simpson et al., 2008; Dougherty, Nichols and Nichols, 2011; Wolffsohn et al., 2017). OSDI test is attached in *Appendix A*.

3.2.1.2 DEQ-5

DEQ-5 is a 5-item questionnaire to assess dry eye symptoms. It is a shortened version of the DEQ developed by Begley et al. (2002). Questions are related to the severity and frequency of eye discomfort, dryness and tearing (Chalmers, Begley and Caffery, 2010; Wolffsohn et al., 2017). Frequency questions are scored as 0) Never; 1) Rarely; 2) Sometimes; 3) Frequently; and 4) Constantly. Moreover, severity questions are scored from 0 to 5, where 0 means “Never have it”, 1 “Not all intense” and 5 “Very intense”. DEQ-5 scores range from 0 to 22 with higher scores representing higher symptoms. The total score is calculated as the sum of the scores of each question. A score between 6 and 11 represents mild to moderate ocular symptoms, and values > 12 means severe ocular symptoms (Chalmers, Begley and Caffery, 2010). DEQ-5 is attached in *Appendix B*.

3.2.2 Keratograph 5M

The ocular surface was assessed using the Keratograph 5M (K5 M; Oculus GmbH, Wetzlar, Germany), which is a videokeratograph that can be used with white light or infrared light (880 nm) and allows the non-invasive measurement of TMH, NIKBUT, bulbar redness, lipid layer thickness and the assessment of the meibomian glands using the meiboscan. *Figure 3.1* shows a picture of the device.

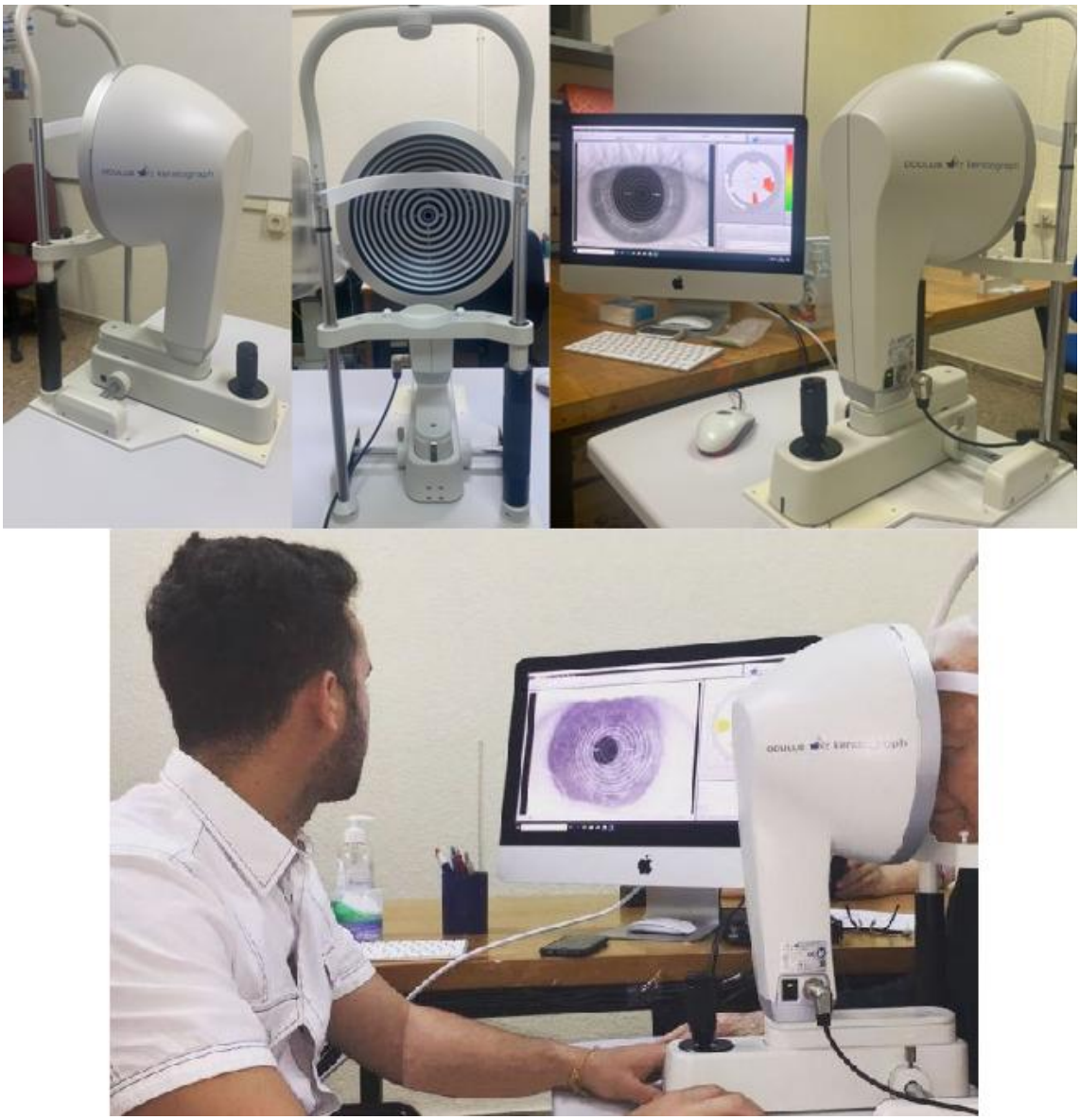

Fig. 3.1. *The Keratograph 5M.*

3.2.2.1 Tear meniscus height

A picture of the lower TMH was obtained using infrared light with the Keratograph 5M. It was measured using digital callipers as the distance between the lower eyelid margin and the upper limit of the reflective zone in the centre of the eyelid. The measurement was taken immediately post-blink in primary gaze (*Figure 3.2*) (Wolffsohn et al., 2017).

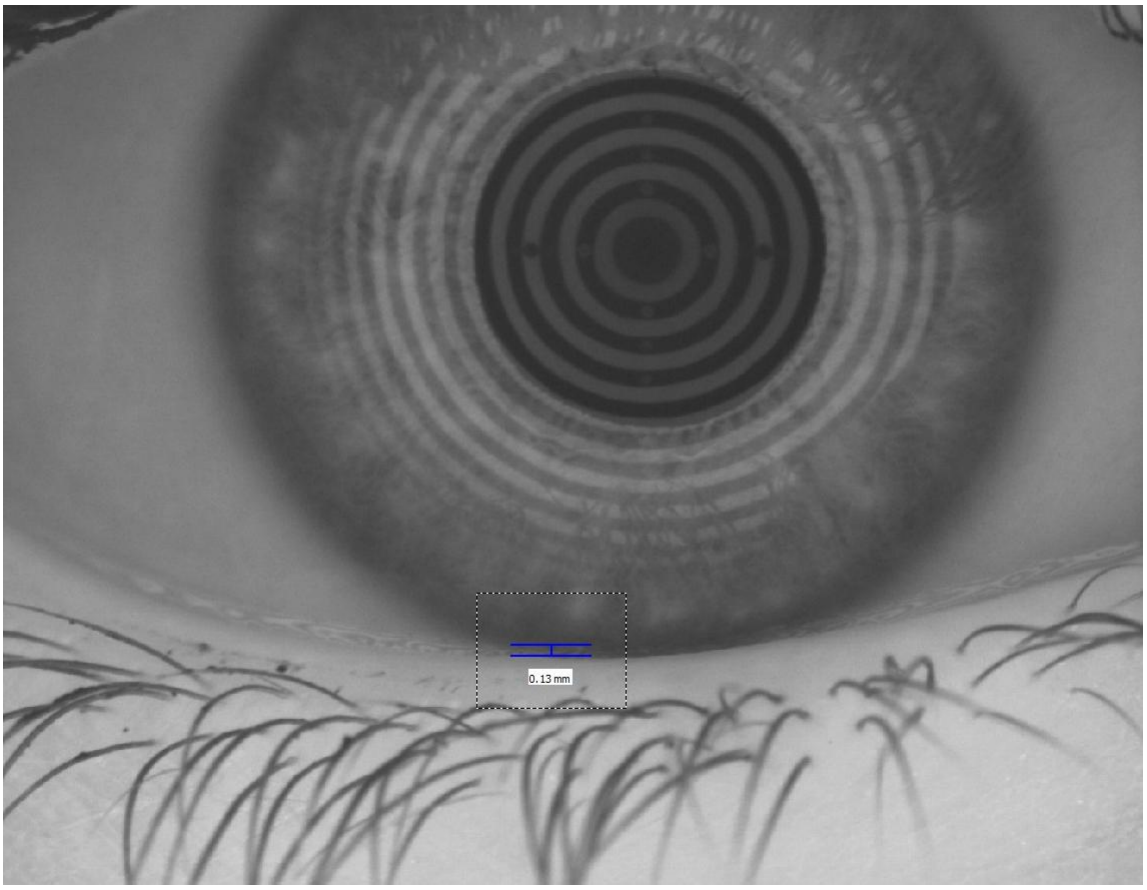

Fig. 3.2. *Example of the measurement of the lower TMH in primary gaze.*

3.2.2.2 NIKBUT

NIKBUT was measured according to the manufacturer's instructions. Infrared light was used and subjects were asked to perform two consecutive blinks and focus on the light fixation target during the measurement. The video recording of the Placido disk pattern started automatically after two blinks. Break-ups were automatically detected by the Keratograph 5M and appeared on a polar-type grid representing the corneal area (*Figure 3.3*). NIKBUT was measured three consecutive times. Measurements were taken every three minutes to allow the stabilization of the tear film between evaluations (Wolffsohn et al., 2017). The software automatically calculated two measurements: the first NIKBUT and the average/mean NIKBUT. The first NIKBUT was

the moment of the first break-up of the tear film, whilst the average NIKBUT was the average time of all break-ups (Wolffsohn et al., 2017).

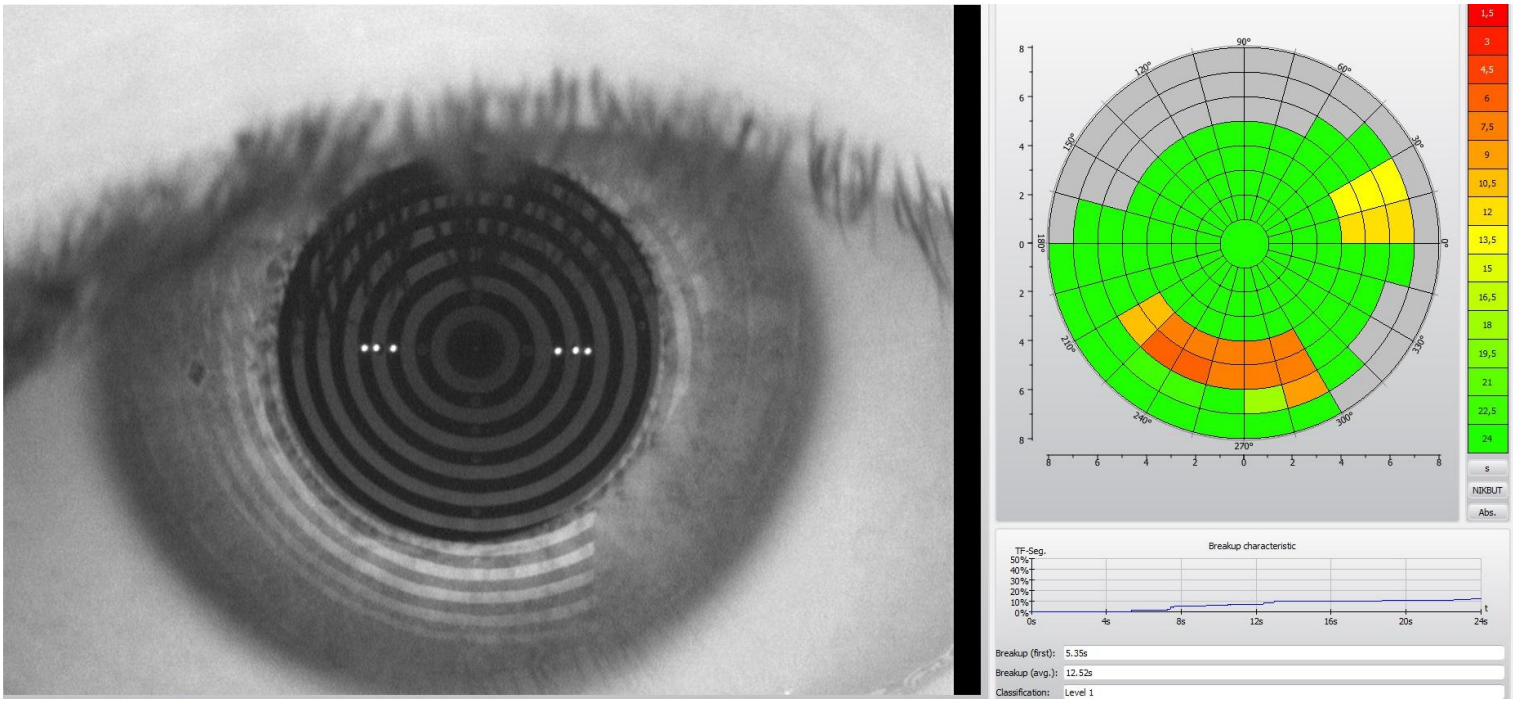

Fig. 3.3. *Example of the measurement of the NIKBUT.*

3.2.2.3 Lipid layer thickness

The lipid layer was assessed using the Keratograph 5M with a magnification of ×1.4, which enables the observation of subtle changes in the interference pattern and the debris floating over the surface of the tear film. Once the lipid layer was properly focused, the interference pattern was recorded using white light (*Figure 3.4*). Subjects were advised to look at the central focusing spot of the device and blink freely. The lipid layer pattern was classified into 4 groups using a standardized grading scale (Guillon, 1998b; Tomlinson et al., 2011; Wang et al., 2015): 1 = open meshwork (13-15 nm); 2 = closed meshwork (30-50 nm); 3 = wave (50-80 nm); and 4 = color fringe (90-140 nm).

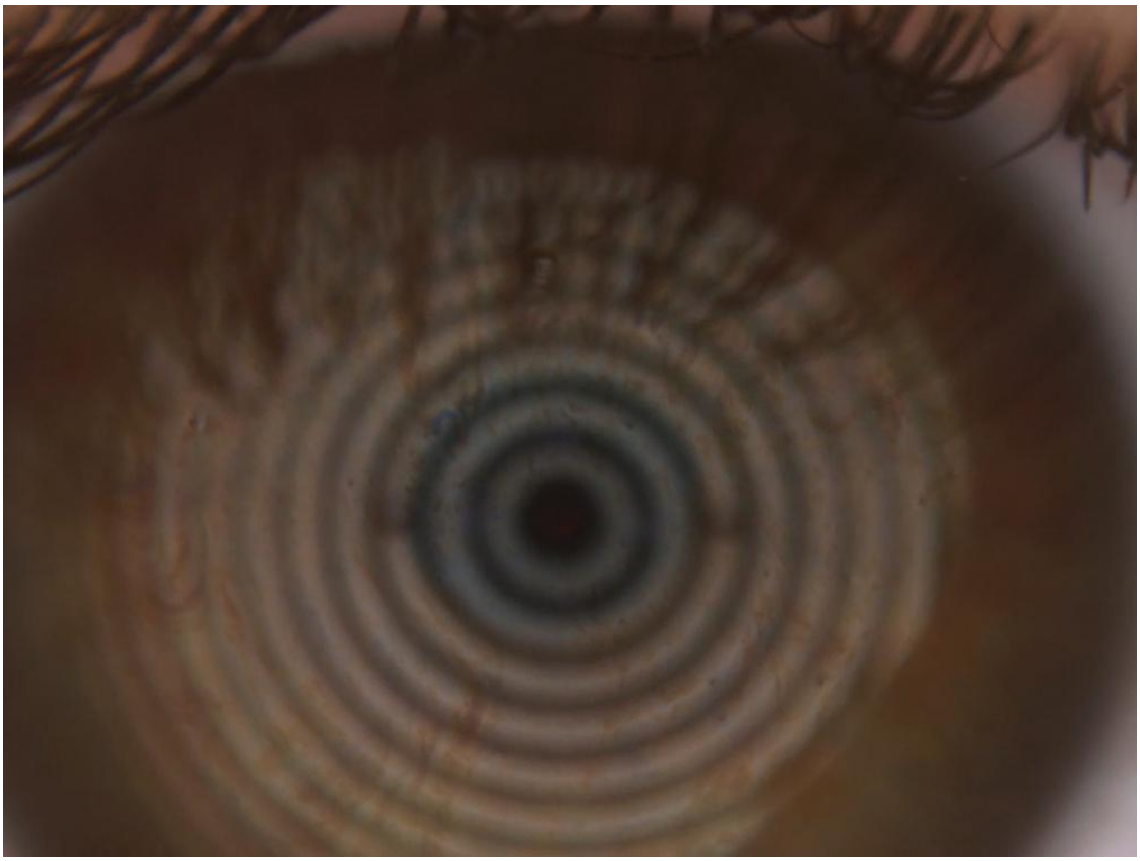

Fig. 3.4. *Example of the visualization of the lipid layer that is used to measure its thickness.*

3.2.2.4 Ocular redness

The R-Scan function of the Keratograph 5M was used to assess the ocular redness. White light illumination is used to acquire bulbar redness measurement (Wu et al., 2015; Pérez-Bartolomé et al., 2017; Pérez-Bartolomé et al., 2018). Conjunctiva must be properly focused, and once the grey disc of the device covered the iris, the picture was taken. A keratograph image of 1156 X 873 pixels and at 96 dpi was created and displayed on a computer screen. Ocular redness was evaluated three consecutive times, and an averaged value was calculated. The software automatically detected the bulbar and limbal conjunctiva and obtained the ratio between conjunctival vessels (red

pixels) and sclera (white pixels) with an accuracy of 0.1 units (*Figure 3.5*). It calculated five different metrics: bulbar redness nasal, bulbar redness temporal, limbal redness nasal, limbal redness temporal and total bulbar redness. Total bulbar redness score ranged from 0.0 to 4.0 (Wu et al., 2015; Koprowski, Tian and Olczyk, 2017).

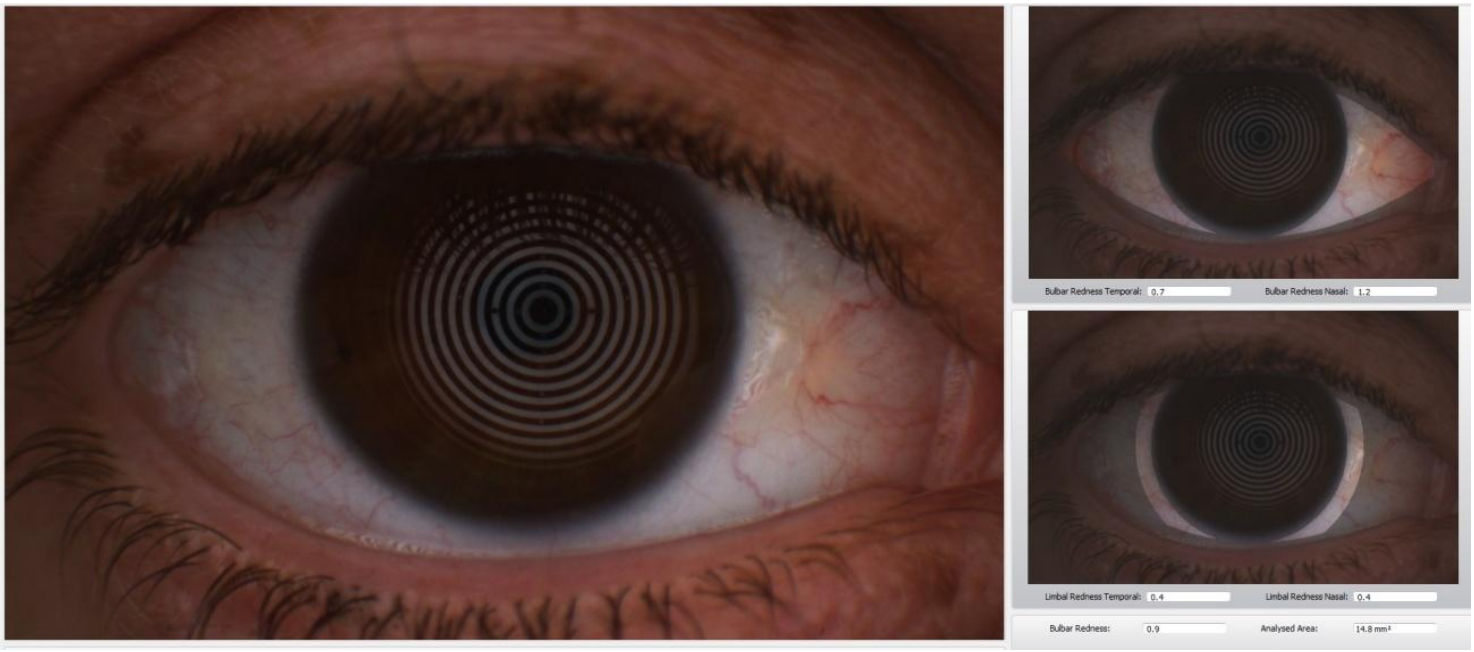

Fig. 3.5. *Example of the measurement of the ocular redness. On the left, the ocular surface is shown. On the right top, the bulbar redness temporal and nasal are measured, whilst on the right bottom, the limbal redness temporal and nasal are measured.*

3.2.2.5 Ocular surface staining

Ocular surface staining was evaluated using the Keratograph 5M with fluorescein strips for the assessment of the cornea (*Figure 3.6 left*), and with lissamine strips for the assessment of the conjunctiva (*Figure 3.6 right*) and eyelid margins. TFOS DEWS II recommendations were followed in the protocol (Wolffsohn et al., 2017). The Fluo-Imaging tool of the Keratograph 5M was used to assess the fluorescein staining. The

strip was applied onto the outer canthus to avoid ocular surface damage (Mooi et al., 2017). The recommendations of Peterson, Wolffsohn and Fowler (2006) were followed to optimize the visualization of the staining. Thus, a period between 1-3 minutes was established between the instillation of the dye and the assessment of the ocular surface. Subjects were asked to look at the red central dot of the device. The red target was focused and a picture of the central ocular surface was obtained. To assess the conjunctival staining, subjects were asked to look up and down, and then look left and right. Moreover, the lid wiper was recorded using the Imaging tool of the Keratograph 5M after eyelid eversion. After pictures from the ocular surface were obtained, the number of corneal and conjunctival spots was recorded (Wolffsohn et al., 2017). Positive lid wiper epitheliopathy was defined as a lid margin staining ≥ 2 mm in length and/or ≥ 25 % of sagittal width (excluding Marx's line) (Wolffsohn et al., 2017).

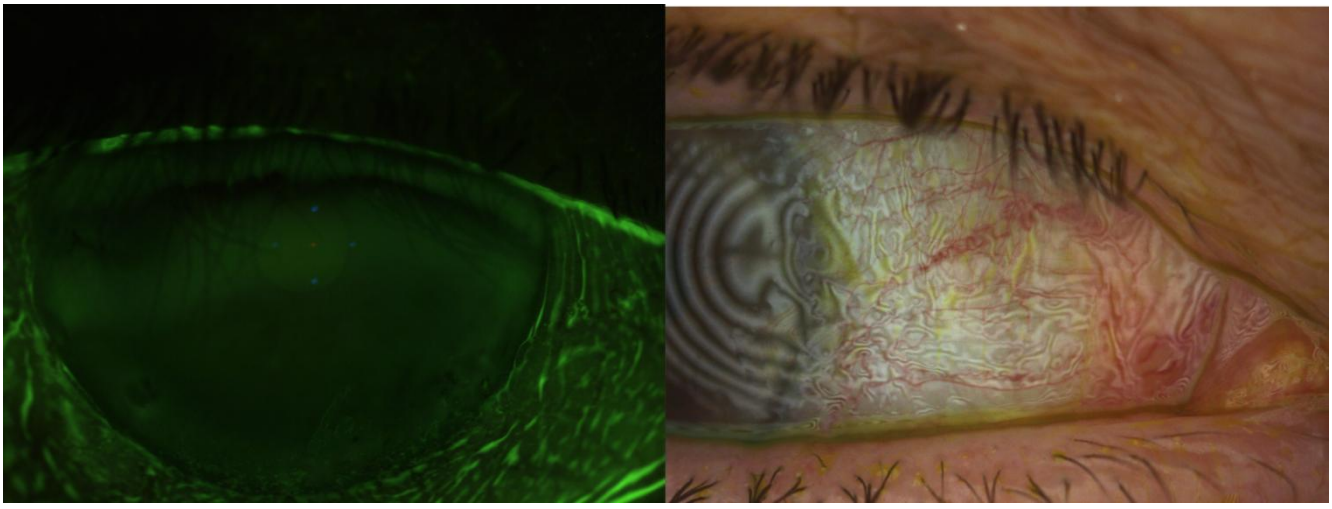

Fig. 3.6. *Example of the images that are used for the assessment of the corneal staining with fluorescein strips (left) and the assessment of conjunctival staining with lissamine strips (right).*

3.2.2.6 Meibography

Meibomian gland morphology was captured by non-contact infrared meibography using the Meibo-Scan tool (Meibography Single Image) of the Keratograph 5M after eyelid eversion. Default settings were used with a magnification of x0.5. Images were stored automatically for further processing. Meiboscore was graded according to the scale of Arita et al. (2009b) and Arita, Fukuoka and Morishige (2017c): 0 = No gland loss; 1 = loss < 1/3 of the total gland area; 2 = loss between 1/3 and 2/3; 3 = loss > 2/3. Moreover, gland drop-out percentage was calculated by using the Polygon selection tool of the Image J tool (Wayne Rasband, National Institutes of Health, Bethesda, MD) as the ratio between the eyelid area and gland loss area (*Figure 3.7*) (Pult, Riede-Pult and Nichols, 2012).

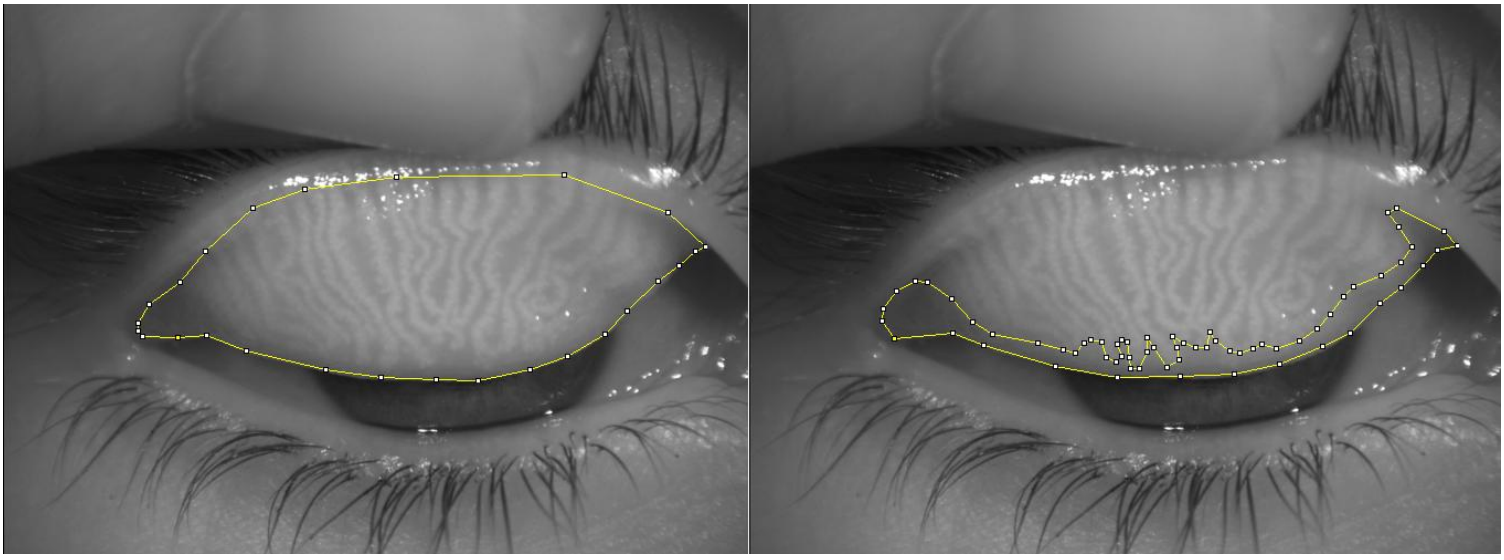

Fig. 3.7. *Example of the assessment of meibomian gland drop-out using the Image J tool. Left: Selection of the entire eyelid area; Right: Selection of the gland drop-out area.*

3.2.3 TearLab osmolarity system

Tear film osmometry was performed in both eyes using the TearLab Osmolarity device (TearLab Corporation, San Diego, CA, USA) from 50 nL tear samples collected from the lower tear meniscus (*Figure 3.8*). The device calculates the osmolarity through electrical impedance in the inferior-lateral tear meniscus. An electronic check card is used every morning to ensure the accuracy of the measurements. The device and the test cards were stored in the laboratory in which the measurements were conducted, to ensure them being at the same temperature as the environment, and the same pen was used in all subjects. Once the osmolarity was measured in each eye, the interocular difference in osmolarity was calculated (Wolffsohn et al., 2017).

Fig. 3.8. *TearLab osmolarity system.*

3.2.4 IRX3

Ocular aberrations were measured with a high-density Hartmann-Shack Aberrometer (irx3^{TM}, Imagine Eyes, Orsay, France) for pupil diameters of 3 mm and 5 mm. RMS of lower-order aberrations, higher-order aberrations up to 9th order and total aberrations were analyzed and expressed as Zernike polynomials (*Figure 3.9*).

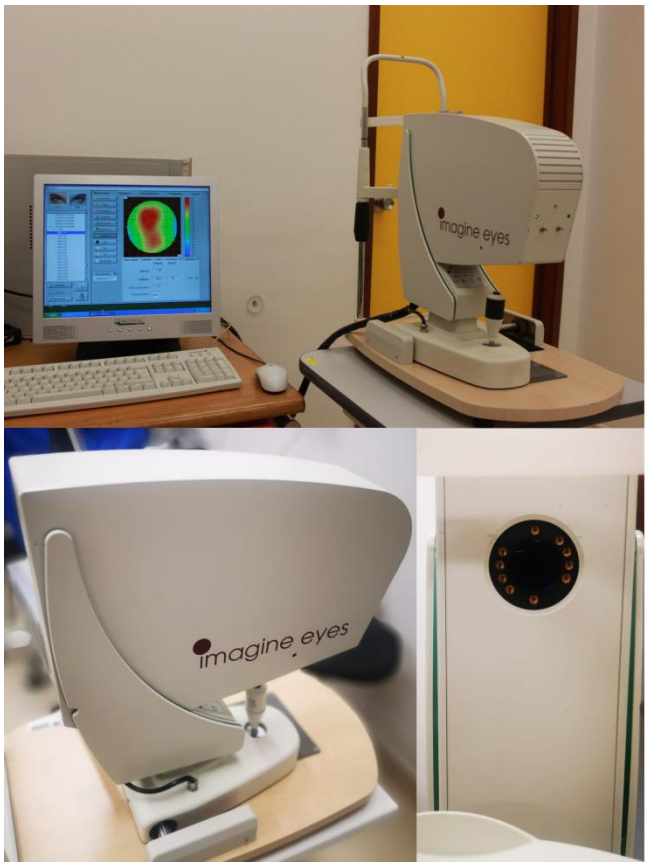

Fig. 3.9. *IRX3.*

3.2.5 Medmont E 300

Medmont E 300 6.1 version (Medmont Pty., Ltd, Melbourne, Australia) was used to measure the TFSQ and corneal aberrations. *Figure 3.10* shows a picture of the device.

Fig. 3.10. *Medmont E 300.*

3.2.5.1 Tear Film Surface Quality

TFSQ is a previously validated algorithm, which is directly related to tear film stability (Alonso-Caneiro, Iskander and Collins, 2009). It was evaluated using Medmont E 300. As NIKBUT, TFSQ is based on the analysis of the structure of the reflected Placido disk pattern onto the tear film. Subjects were instructed to focus on the centre of the innermost ring, blink twice and then suppress blinking. Measurements were carried out three consecutive times and mean and median were calculated for each metric. The software automatically calculates TFSQ at 300 radial points using the

approach of the block-feature reported by Alonso-Caneiro, Iskander and Collins (2009). Local TFSQ at a given point is assessed by analysing the standard deviations of the radial distances to the next innermost ring for n=8 point on either side of the analysis point. TFSQ values range from 0 to 1, and a local value ≥ 0.30 corresponds to a destabilized tear film. Thus, higher TFSQ scores represent a less regular tear film (Alonso-Caneiro, Iskander and Collins, 2009; Downie, 2015). Moreover, TFSQ area is the percentage of the tear film area with a TFSQ value higher than 0.30, while auto Tear Break-Up Time is the time in seconds in which the TFSQ area is at least 5.0 % in two consecutive images (Alonso-Caneiro, Iskander and Collins, 2009; Downie, 2015). *Figure 3.11* shows an example of measurement.

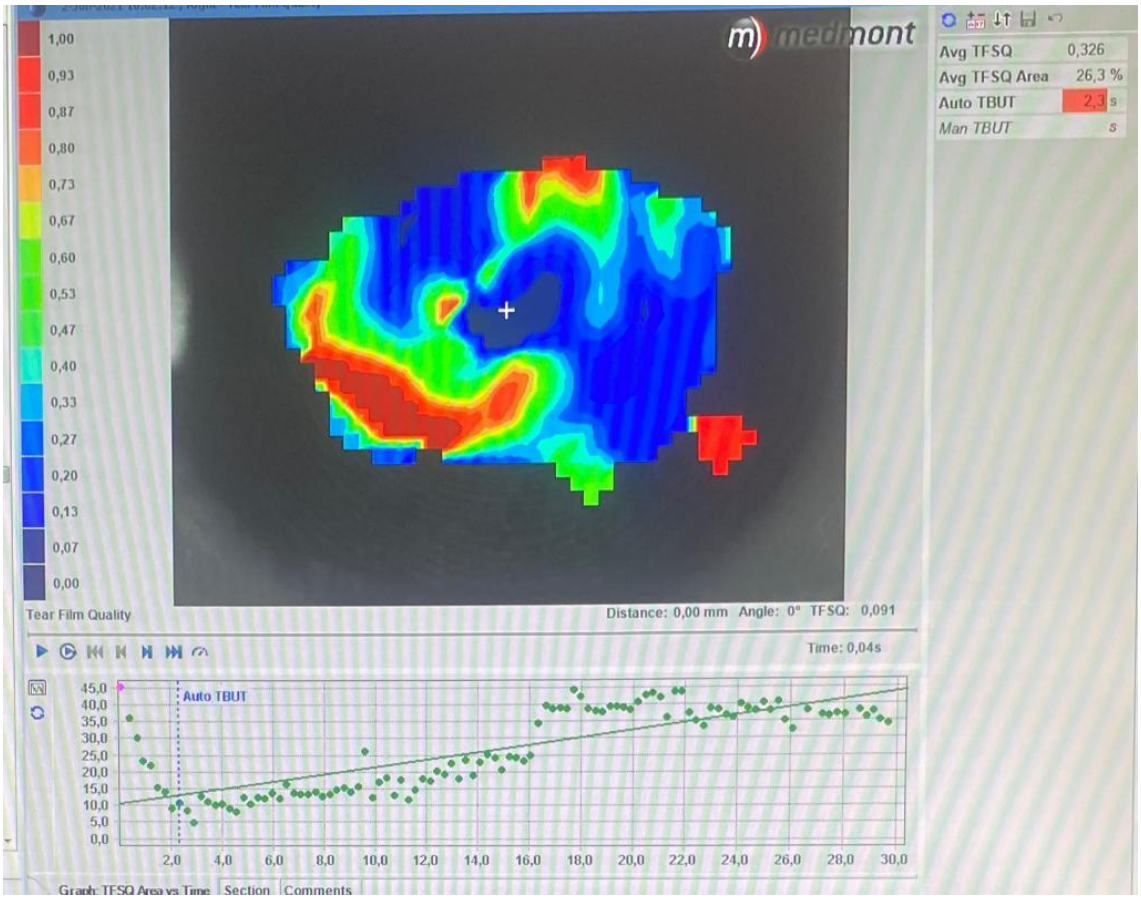

Fig. 3.11. *Example of the measurement of TFSQ, TFSQ area and TBUT using the Medmont E 300.*

3.2.5.2 Corneal aberrations

Corneal aberrations were assessed using Medmont E 300. The device assessed the structure of the reflected Placido disk pattern onto the cornea. Thus, corneal aberrations were calculated until the 4th order and expressed as Zernike polynomials. RMS of higher-order aberrations, spherical aberration, vertical coma and horizontal coma were analyzed. *Figure 3.12* shows an example of measurement.

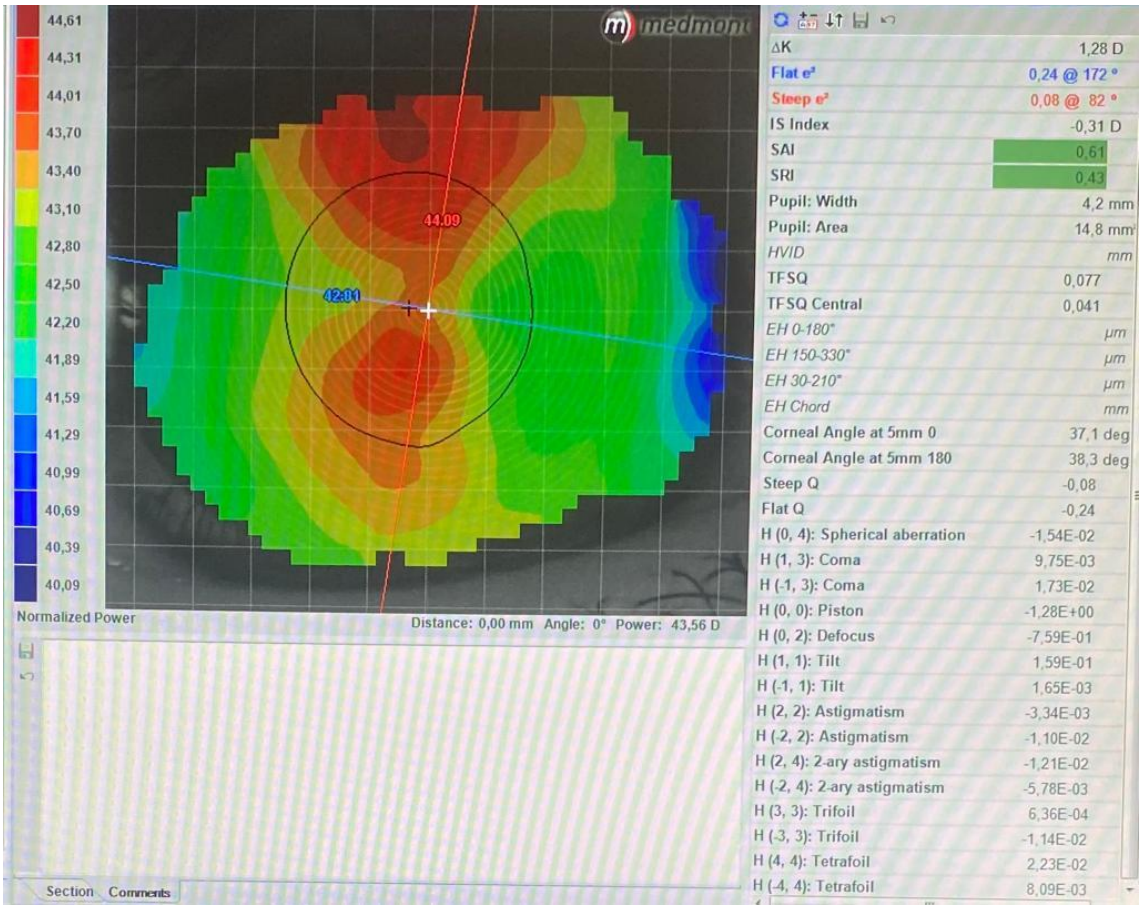

Fig. 3.12. *Example of the measurement of corneal aberrations using the Medmont E 300.*

3.2.6 Cobra Fundus Camera

Apart from the use of the Keratograph 5M to obtain meibographies, Cobra fundus camera (CSO, Scandicci, Firenze, Italy) was also used to perform non-contact infrared meibography in the upper eyelid (*Figure 3.13*). Gland drop-out percentage was also calculated by using the Image J tool as the ratio between the eyelid area and gland loss area, as previously described (Pult, Riede-Pult and Nichols, 2012).

Fig. 3.13. *Cobra fundus camera.*

3.2.7 Light Disturbance Analyzer

Light Disturbance Analyzer (LDA, CEORLab, Portugal) was used to evaluate the

light disturbance monocularly. LDA is a prototype device to assess the size and shape of the light disturbance surrounding a central bright light source. It consists of a central 5 mm white Light-Emitting Diode (LED) surrounded by 240 small, white LEDs of 1 mm divided into 24 semimeridians with an angular separation of 15 degrees and covering an area of 10 degrees at a 2 meters examination distance. A detailed description of the system, light sources and acquisition procedure has been previously reported (Linhares et al., 2013). In the present work, semimeridians with an angular separation of 30 degrees were assessed to reduce the time of examination. LDA measured 3 times each meridian and the final value was the mean of the three measurements. Whether the SD along each meridian was above 20%, the device automatically repeated the measurement to ensure consistency.

Software calculated different metrics related to the size and regularity of the light disturbance. Disturbance area was the sum of the areas of semimeridians assessed, in mm^2. Light Disturbance Index (LDI) was the ratio of the area of points missed by the subject and the total area explored, expressed as a percentage (%). Best-Fit Circle (BFC) radius was the circle that best fits the disturbance area, expressed in millimetres. The deviation of the obtained polygonal shape from the BFC was called BFC irregularity. The SD of BFC irregularity measured the asymmetry of the actual limits of the disturbance from the perfect circular shape of the BFC and indicated the light disturbance irregularity. Further details on these parameters can be found in previous reports (Ferreira-Neves et al., 2015; Fernandes et al., 2018). *Figure 3.14* shows a picture of the device and *Figure 3.15* a picture of the results obtained with the LDA.

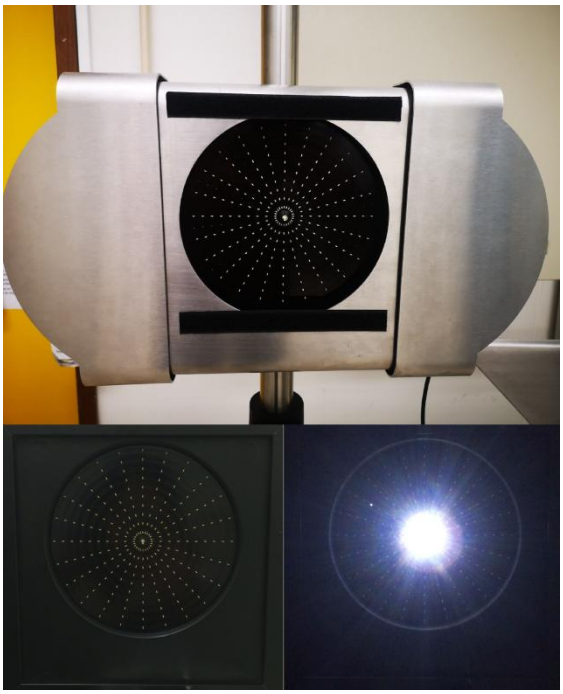

Fig. 3.14. *Light disturbance analyzer.*

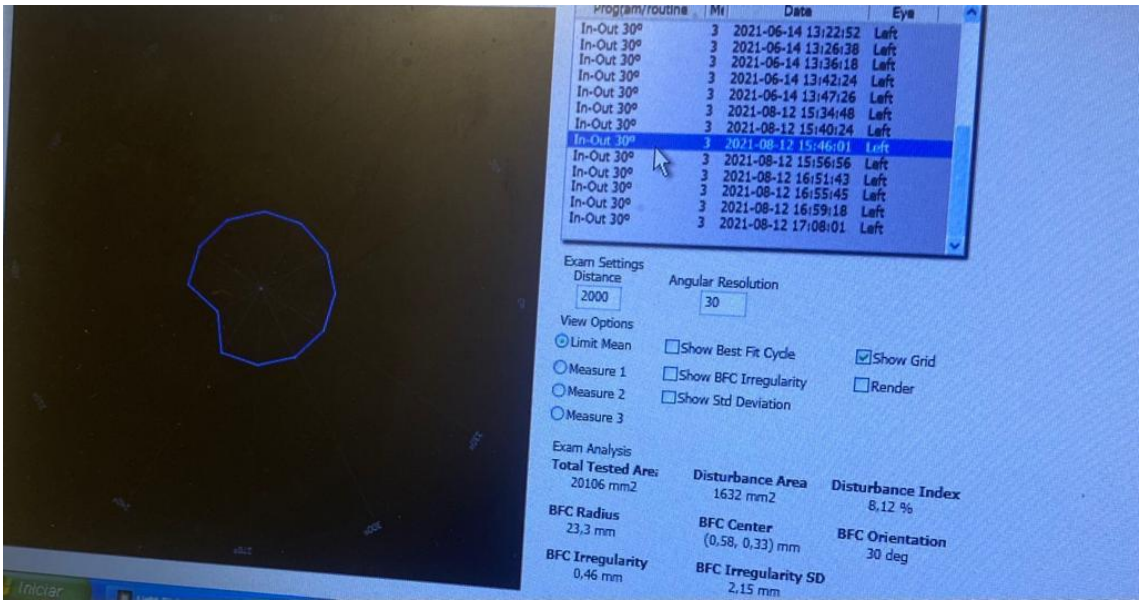

Fig. 3.15. *Results obtained with the LDA.*

3.2.8 Over-refraction, visual acuity and stereopsis

An open field binocular autorefractor (Grand Seiko Autorefractometer WAM-5500, Grand Seiko Co., Ltd., Hiroshima, Japan) was used to objectively assess the over-

refraction while subjects were wearing contact lenses. It was subjectively adjusted with spheres, using the end-point criterion of maximum plus for the best visual acuity (Ferreira-Neves et al., 2015). Distance best-corrected photopic visual acuity was assessed using the Logarithmic Visual Acuity Chart "2000" (Precision Vision, USA). Moreover, the Randot Stereo Test (Stereo Optical Company Inc, Chicago, IL) was used to measure stereopsis at 40 cm.

3.2.9 Contrast sensitivity

Best-corrected photopic and mesopic contrast sensitivity were measured using Vision Contrast Test System VCTS 6500 (Vistech Consultants, Dayton, OH) at 3 meters. Luminance was manually adjusted by the examiner using a dim light.

3.2.10 Quality of Vision questionnaire

Quality of Vision (QoV) questionnaire (McAlinden, Pesudovs and Moore, 2010; Fernandes et al., 2018) was used to assess the subjective quality of vision of subjects while wearing contact lenses. The questionnaire consists of 10 questions about visual symptoms such as glare, haloes, starburst, hazy vision, blurred vision, distortion, double or multiple images, fluctuation in vision, focusing difficulties and difficulty in depth perception. Moreover, seven questions had a photographic image to help in defining the visual symptom. The questionnaire was Rasch-scaled (0-100 scale) based on the frequency, severity and bothersomeness of symptoms. Higher scores indicate the worse quality of vision (McAlinden, Pesudovs and Moore, 2010; Fernandes et al., 2018). QoV questionnaire is attached in *Appendix C*.

3.3 Application of the developed metrics to contact lens wearers

The methodological procedure as well as the contact lens type and fitting will be explained in each chapter of the present work. In all of them, contact lens fit included contact lens centration, corneal coverage, blink movement and push-up test with slit-lamp.

3.4 Statistical analysis

The data analysis was performed using Excel (version 2016, Microsoft Corporation, Redmond, WA, USA) and SPSS statistical software (version 26.0, IBM Corp., Armonk, NY, USA). In this section, the main statistical procedures are explained in a general way. The specific methods used to analyse the data will be exposed in each chapter according to the variable assessed.

3.4.1 Sample size

The sample size was not calculated a priori due to the large number of parameters assessed and the need to take first the measurements to be analysed using the developed software to obtain the new metrics developed. Therefore, a post-hoc statistical power calculation was carried out using the G*Power 3.1 software. More details about the statistical power calculation can be found in each chapter.

3.4.2 Descriptive statistics

Results were shown as the mean ± SD, as the median and interquartile range, as confidence intervals or as the number and percentage of participants, depending on the parameter assessed in each study.

3.4.3 Assessment of sample distribution

Normality distribution for each group was assessed via the Kolmogorov-Smirnov test or the Shapiro-Wilk test, depending on the number of subjects in each sample. The Shapiro-Wilk test was used when the sample was up to 50 subjects and the Kolmogorov-Smirnov test when the sample size was larger than 50 subjects. A p-value of less than 0.05 was considered statistically significant. Q-Q plots were also run in the normality analysis, showing the plots near the diagonal when the sample is normally distributed.

3.4.4 Differences between two groups

To assess differences between two independent groups the t-test for independent groups or Mann-Whitney U test was used, depending on the data distribution. T-test was used when groups followed a normal distribution. Moreover, the homogeneity of the variances was checked by means of Levene's test. When variables did not follow a normal distribution or were ordinal, the Mann-Whitney U test was used.

To assess differences between two related groups the paired t-test or Wilcoxon signed-rank test was used, depending on sample distribution. T-test was used when groups followed a normal distribution. When variables did not follow a normal distribution or were ordinal, the Wilcoxon signed-rank test was used.

The Chi-Square test was used to assess the association of two categorical variables (ordinal or nominal). In this case, a contingency table was created to obtain the frequency in which the variables were associated. A p-value of less than 0.05 was considered statistically significant.

3.4.5 Correlation between variables

The correlation between variables was assessed using the correlation coefficient of Pearson and the Rho Spearman coefficient. Bivariates correlations were obtained and a p-value of less than 0.05 was defined as statistically significant. When variables were normally distributed the coefficient of Pearson was used, otherwise the Rho Spearman coefficient was the non-parametric option. The Rho Spearman coefficient was also used for ordinal variables.

3.4.6 Repeated ANOVA

Repeated ANOVA was used to analyse the differences among repeated measurements taken over time. It was used in continuous variables normally distributed. Moreover, Mauchly's sphericity test was used when there were more than two levels in the within-subjects factor to evaluate the equality of the variances between combinations of related groups. The presence of outliers was also checked. If the analysis revealed non-sphericity, the Greenhouse-Geisser correction was used. A p-value of less than 0.05 was defined as statistically significant.

3.4.7 Mixed ANOVA

Mixed ANOVA analyses the differences between independent groups with repeated measurements. Therefore, there are two factors: the between-subjects and the within-subjects factor. It was applied for continuous variables with a normal distribution. The normality distribution of the sample and the presence of outliers were checked. The homoscedasticity and sphericity assumptions were also checked by Levene's and Mauchly's tests, respectively. The Greenhouse-Geisser correction was

applied in the case of non-sphericity. A p-value less than 0.05 was defined as statistically significant.

3.4.8 Non-parametric comparison between 3 or more groups

Friedman test was used to assess the differences between three or more related groups when variables did not follow a normal distribution. Moreover, the Kruskal-Wallis test was used to compare three or more independent groups when variables did not follow a normal distribution. Bonferroni was used to evaluate the post-hoc differences between paired moments and p-values were shown according to the Bonferroni correction. A p-value less than 0.05 was defined as statistically significant.

3.4.9 Repeatability

The repeatability of measurements was assessed by calculating the within-subject standard deviation (S_w), coefficient of variation (CoV) and the repeatability coefficient (CoR). The S_w was defined as the square root of the mean within-subject variance (Cerviño et al., 2015; McAlinden, Pesudovs and Moore, 2015; Martínez-Albert et al., 2018). The CoR was calculated as $1.96\sqrt{2}$ x S_w in accordance with the British Standard Institution (Bland and Altman, 2010). CoV was calculated as the ratio between S_w and the average value (Martínez-Albert, Esteve-Taboada and Montés-Micó, 2018).

Moreover, a Passing-Bablok graphical analysis, applied using Matlab R2018a (Passing and Bablok regression by Andrea Padoan, Jan 16, 2010) (Passing and Bablok, 1983), was also performed to compare the maximum and minimum values of the three measurements. Continuous distribution and linear relationship between both data sets were checked previous to the Passing-Bablok application. The cumulative sum linearity

test (cusum test) was used to confirm the random distribution of residuals above and below the regression line. Thus, Passing Bablok plots contain the regression line shown as y = ax + b, the identity line as y = x and the 95 % confidence intervals for the intercept and the slope of the regression line.

3.4.10 Linear regressions

Multiple linear regressions were performed to construct models that can predict a continuous variable. Variables should be statistically correlated between them. The option of stepwise regression was chosen and $p < 0.05$ was taken as the criterion for statistical significance. The following assumptions were checked: the linear relationship between the independent and dependent variables, normal distribution of residuals, homoscedasticity of residuals and predicted values and absence of multicollinearity between independent variables.

Furthermore, binomial logistic regression was performed to construct models that can predict a nominal variable. Univariate logistic regression was performed initially to identify the predictors for DED or MGD. Predictors with a p-value less than 0.15 were incorporated into the multivariate logistic regression analysis (Wang et al., 2020; Wang et al., 2021). Collinearity assumption was checked among variables. A p-value of less than 0.05 was considered statistically significant.

3.4.11 Diagnostic capability of metrics

Receiver Operating Characteristics (ROC) curves were calculated for different metrics to assess its diagnostic capability. Different parameters were obtained for each ROC curve: Sensitivity, specificity, area under the ROC curve, the cut-off value that

optimizes the diagnosis, Youden index and discriminant power (Sokolova, Japkowicz and Szpakowicz, 2006). The area under the curve was obtained using trapezoidal numerical integration. This parameter ranged from 0 to 1, with values near 1 denoting a powerful diagnostic metric (Sokolova, Japkowicz and Szpakowicz, 2006; Llorens-Quintana, Szczesna-Iskander and Iskander, 2019). The cut-off value was calculated as the point in the curve where the distance between the curve and diagonal reference line was maximum. Furthermore, the Youden index was obtained as follows: sensitivity + specificity - 1. Values near 1 denoted good metric performance. Finally, the discriminant power was calculated as: $\frac{\sqrt{3}}{\pi}$ (log ($\frac{\text{sensitivity}}{1-\text{sensitivity}}$) + log ($\frac{specificity}{1-specificity}$)). Discriminant power higher than 3 showed good discrimination, values between 2 and 3 fair discrimination, values between 1 and 2 limited discrimination, and values lower than 1 poor discrimination (Sokolova, Japkowicz and Szpakowicz, 2006; Llorens-Quintana, Szczesna-Iskander and Iskander, 2019).

Moreover, the level of agreement between objective and subjective classification scales was analysed by calculating the accuracy, Kappa index, weighted Kappa index with quadratic weights and F-measure for each metric as in previous studies (Cohen, 1968; Landis and Koch, 1977; Rosenfield and Fitzpatrick-Lins, 1986; Viera and Garrett, 2005). The three indexes denote a high level of agreement between tests when the values are near 1. Accuracy was calculated as: (true positives + true negative) / (true positives + true negatives + false positives + false negatives). Kappa index was obtained as follows: (Pr(α) – Pr(e)) / (1 – Pr(e)). Where Pr(α) is the agreement between scales and Pr(e) the hypothetic probability of a random agreement (Cohen, 1968; Landis and Koch, 1977; Rosenfield and Fitzpatrick-Lins, 1986; Viera and Garrett, 2005). The

weighted kappa was calculated using a predefined table of weights which measures the degree of disagreement between the two raters, the higher the disagreement the higher the weight. Finally, F-measure was calculated as: (2 x precision x recall) / (precision + recall); where precision was (true positives) / (true positives + false positives), and recall (true positives) / (true positives + false negatives).

CHAPTER 4: Systemic, environmental and lifestyle risk factors for dry eye disease in a Mediterranean Caucasian population

4. SYSTEMIC, ENVIRONMENTAL AND LIFESTYLE RISK FACTORS FOR DRY EYE DISEASE IN A MEDITERRANEAN CAUCASIAN POPULATION

As explained in the *Chapter 1 Introduction* and *Chapter 2 Justification*, the diagnosis of DED is challenging due to the multifactorial aetiology of DED together with the lack of a gold standard metric, the low agreement between DED signs and symptoms and the lack of an objective and quantitative method with high repeatability and sufficient diagnostic capability (Wolffsohn et al., 2017). Therefore, systemic, environmental and lifestyle risk factors for DED will be studied in this chapter; due to the influence of the multifactorial aetiology of DED in its diagnosis.

4.1 Introduction

As explained in *Chapter 1 Introduction*, the prevalence of DED is increasing substantially worldwide influenced by demographic, systemic and environmental factors (Yang et al., 2015; Stapleton et al., 2017). Moreover, the multifactorial and heterogeneous aetiology of the disease indicated the tear film and the ocular surface integrity are highly influenced by a wide range of risk factors (Stapleton et al., 2017).

The TFOS DEWS II Epidemiology Report listed several risk factors for DED (Stapleton et al., 2017). This meta-analysis showed that the prevalence of DED increases with age, female sex and Asian ethnicity. Nevertheless, very few of the studies included in the analysis incorporated young people. Also, the report highlighted that some of the listed risk factors are still inconclusive and there is not yet clear evidence that most of them induce DED (Stapleton et al., 2017). Moreover,

studies have significant differences in the methodology and in the procedure followed to diagnose DED, which makes their direct comparison and the building of global conclusions particularly challenging (Stapleton et al., 2017; Wolffsohn et al., 2017; Wang et al., 2020; Wang et al., 2021). In the report, the authors argued that there is still a considerable lack of information about risk factors for DED and that the implementation of studies to assess such factors in different geographic regions is required (Stapleton et al., 2017).

To the authors' knowledge, there are only two studies (Wang et al., 2020; Wang et al., 2021) that have evaluated DED risk factors following the TFOS DEWS II guidelines for the diagnosis and identification of potential risk factors for DED, both performed on a cohort in New Zealand. Authors found that age, ethnicity, migraine, systemic rheumatologic disease, thyroid disease, use of antidepressant medication, oral contraceptive therapy, increased digital screen exposure time and reduced caffeine consumption were independently associated with DED (Wang et al., 2020; Wang et al., 2021). Authors (Wang et al., 2020; Wang et al., 2021) also acknowledged the need to analyse non-significant potential risk factors that were not very prevalent in their population. Furthermore, these studies did not consider interactions between demographic, systemic and lifestyle risk factors, since systematic risk factors were assessed separately from lifestyle factors (Wang et al., 2020; Wang et al., 2021).

This study is the first to examine DED in a Mediterranean Caucasian population using the standardised TFOS DEWS II criteria and analyzes systemic, environmental and

lifestyle DED risk factors (Stapleton et al., 2017; Wolffsohn et al., 2017). In addition, new lifestyle and environmental risk factors have been included in the analysis.

4.2 Methodology

One hundred and twenty Caucasian volunteers ranging in age from 18 to 89 years (47.0 ± 22.8 years) participated in this cross-sectional study. In order to evaluate different health and tear film status, no exclusion based on health or tear film parameters was made. Contact lens users were instructed not to wear their contact lenses for the 48 hours prior to examination (Wang et al., 2020; Wang et al., 2021). Participants with ocular surgery within the previous three months were excluded. Only volunteers who lived in the region were enrolled to minimize environmental differences (Wang et al., 2020; Wang et al., 2021). Only the right eye of each participant was assessed to avoid data bias (except for tear osmolarity, which was measured from each eye as recommended). The study was carried out in accordance with the tenets of the Declaration of Helsinki and was approved by the Ethics Committee of the University of Valencia. Written consent from each participant was obtained after a verbal explanation of the protocol, nature and possible consequences of the study. Recruitment was carried out by advertisement within University dissemination channels, campus personnel and students, as well as in local public entities in nearby towns.

Measurements

Ocular surface was assessed using the Oculus Keratograph 5M (K5 M; Oculus GmbH, Wetzlar, Germany) and the TearLab Osmolarity device (TearLab Corporation, San Diego, CA, USA). Measurements were taken by the same experienced examiner within a single visit. Data was acquired following the guidelines of the TFOS DEWS II Diagnostic Methodology Report, to avoid the destabilization of the tear film, in the following order (Wolffsohn et al., 2017): Medical history, information regarding environmental conditions and lifestyle, OSDI, DEQ-5, NIKBUT, tear film osmolarity and ocular surface staining. The temperature and humidity of the room were maintained at 24.1 ± 1.6 °C and 44.9 ± 5.0 %, respectively. Measurements were performed between November 2018 and January 2019, minimizing seasonal variations.

Participants were asked about their lifestyle, medical history, use of oral or topical medications, history of ophthalmic surgery and environmental conditions. The risk factors included in the present study were those reported by the TFOS DEWS II Epidemiology Report (Stapleton et al., 2017; Wang et al., 2020; Wang et al., 2021). Participants with rheumatoid arthritis, gout, osteoarthritis, fibromyalgia and osteoporosis were included under the classification of systemic rheumatologic disease, while bradycardia and heart failure were included under the classification of heart disease. Participants graded the quality of their diet as good (excellent or good quality) or poor (poor or fair quality). They were instructed to consider a good diet quality if they believe as having a balanced intake of protein, carbohydrates, fruits and

vegetables; whilst a poor diet quality is an unbalanced diet, associated with the intake of ultra-processed food, ready-to-eat products and sugars.

Table 4.1 shows the risk factors evaluated in the present study. No participant reported a history of Sjögren syndrome, rosacea, acne vulgaris, psoriasis, lupus erythematosus, hepatitis C, steroids deficiency, chronic kidney disease or hematopoietic stem cell transplantation. Moreover, all participants used soft contact lenses daily; therefore, this variable was not included in the analysis since a binary logistic regression was not able to be performed.

The first NIKBUT, tear film osmometry in both eyes and ocular surface staining were assessed as explained in *Chapter 3 General Methodology*. The interocular difference in osmolarity was calculated (Wolffsohn et al., 2017; Wang et al., 2020).

The sample was classified following the indications of the TFOS DEWS II Diagnostic Methodology Report for the diagnosis of DED (Wolffsohn et al., 2017). Participants were classified into the DED group if they had dry eye symptoms (OSDI ≥ 13 or DEQ-5 ≥ 6) and at least one altered homeostasis marker (NIKBUT < 10 seconds; osmolarity ≥ 308 mOsm/L; interocular osmolarity difference > 8 mOsm/L; corneal fluorescein staining > 5 spots; conjunctival lissamine green staining > 9 spots; or lid margin staining ≥ 2 mm length and ≥ 25% width).

Table 4.1. *Risk factors evaluated in the present study.*

Characteristic
Age
Female sex
Lifestyle
Hours of sleep per day
Smoking
Number of cigarettes smoked per day
More than 5 cigarettes smoked per day
Contact lens wear
Hours per week of contact lens wear
More than 56 hours per week of contact lens wear
Computer use
Daily hours of computer use
More than 4 hours of daily computer use
Exercise
Not walking (sedentary lifestyle)
Hours walking per day
Not practising exercise
Hours practising exercise per week
Medical conditions
Menopause
Allergic rhinitis
Asthma
Hypertension
Ovarian dysfunction
Anxiety
Systemic rheumatologic disease
Diabetes
Hypercholesterolemia
Glaucoma
Migraine headaches
Depression
Heart disease
Thyroid disease
Schizophrenia
Eczema
Stress

Characteristic (continuation)
Medications
Antihistamines
Antihypertensives
Stomach protector
Oral contraceptive therapy
Anticoagulants
Anxiolytics
Blood glucose regulators
Topical anti-glaucoma medication
Antidepressants
Hypercholesterolemia medication
Anti-inflammatories
Medication for thyroids
Antipsychotics
Daily medication
Ocular surgery
Ocular Surgery
Retinal surgery
Refractive surgery
Pterygium surgery
Glaucoma surgery
Cataract surgery
Diet
Poor diet quality
Non-omnivorous diet
Non-oily fish diet
Percentage of unprocessed food in diet
Percentage of ultra-processed food in diet
Drinking alcohol
Units of alcohol per week
More than 4 units of alcohol per week
Not drinking caffeine
Units of caffeine per day
Litres of water per day
Less than 2 litres of water per day
Environment
Working
Hours working per day
Working ≥ than 8 hours per day
Urban life
Air conditioning
Hours of exposure to air conditioning per day
≥ 8 hours of exposure to air conditioning per day
Central heating
Hours of exposure to central heating per day
≥ 8 hours of exposure to central heating per day

Statistical analysis

Statistical analysis was carried out using SPSS v26.0 for Windows (IBM Corp, Armonk, New York, USA). Results are presented as the mean ± SD, as the median and interquartile range or as the number and percentage of participants, depending on the parameter.

Normality distribution for each group was assessed via the Kolmogorov-Smirnov test or the Shapiro-Wilk test. Significant differences in age between healthy and DED groups were assessed using the Mann-Whitney U test, while sex differences between groups were evaluated using the Chi-square analysis.

Univariate logistic regression was performed initially to identify the predictors of DED. Predictors with a p-value less than 0.15 were incorporated into the multivariate logistic regression analysis (Wang et al., 2020; Wang et al., 2021). Collinearity assumption was checked among variables. A p-value of less than 0.05 was considered statistically significant.

The statistical power of the sample was calculated post-hoc using the G*Power 3.1 software (Faul et al., 2007). A statistical power of 0.8 was achieved for logistic regression analysis with the sample size of 120 participants and a significance level of 0.05.

4.3 Results

One hundred and twenty right eyes from 120 participants were measured: 60 females (50 %) and 60 males (50 %). The mean ± SD age of the participants was 47.0 ±

22.8 years, ranging from 18 to 89 years. The comparison between the cohort of the sample and the Spanish population is shown in *Figure 4.1*.

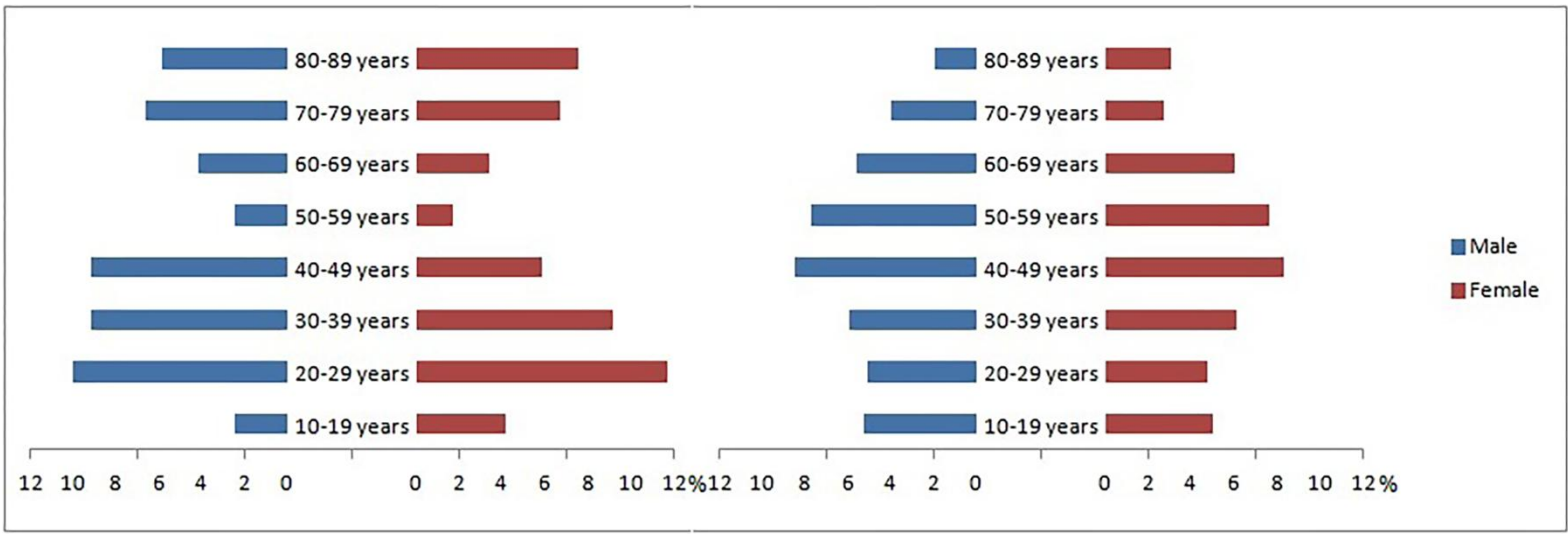

Fig. 4.1. *Tornado plots representing the sample cohort (left) and the Spanish population (right).*

No participant was previously diagnosed with DED. From the total sample, 44 participants (36.7 %) were classified into the healthy group (43.2 ± 21.2 years) and 76 (63.3 %) into the DED group (49.2 ± 23.5 years) according to the criterion described in the TFOS DEWS II Diagnostic Methodology Report. Given that the cohort does not fully represent the Spanish population (*Figure 4.1*), a corrected prevalence was calculated by multiplying the DED rate found for each age group by the age proportion in each group. Results show a corrected prevalence of DED using the TFOS DEWS II criteria for the Mediterranean Caucasian population of 57.7 % with a confidence interval of 33.3-80.9 %.

There were no statistically significant age differences between groups (Mann-Whitney U = 1886.5, p = 0.243). Sixty participants were females (50 %) and sixty males (50 %). Twenty-five per cent of females were classified into the healthy group and 75 % into the DED group, while 48 % of males were classified into the healthy group and 52 % into the DED group. The DED group had statistically higher number of females (X^2 = 7.033, p = 0.008). *Table 4.2* shows the demographic, clinical characteristics, and environmental and lifestyle factors of participants, while *Table 4.3* shows the ocular surface parameters of the participants.

Table 4.2. *Demographic, clinical, environmental and lifestyle characteristics of participants.*

Characteristic	Results
Age *(mean ± SD)*	47.0 ± 22.8 years
Female sex *(number of participants, percentage of participants)*	60, 50 %
Lifestyle	
Hours of sleep per day *(mean ± SD)*	7.1 ± 1.2
Smoking *(number of participants, percentage of participants)*	31, 26 %
Number of cigarettes smoked per day *(mean ± SD)*	2.6 ± 6.2
More than 5 cigarettes smoked per day *(number of participants, percentage of participants)*	19, 16 %
Contact lens wear *(number of participants, percentage of participants)*	37, 31 %
Hours per week of contact lens wear *(mean ± SD)*	15.6 ± 29.3
More than 56 hours per week of contact lens wear *(number of participants, percentage of participants)*	16, 13 %
Computer use *(number of participants, percentage of participants)*	71, 59 %
Daily hours of computer use *(mean ± SD)*	2.9 ± 3.1
More than 4 hours of daily computer use *(number of participants, percentage of participants)*	37, 31 %
Exercise	
Not walk (sedentary lifestyle) *(number of participants, percentage of participants)*	29, 24 %
Hours walking per day *(mean ± SD)*	1.1 ± 1.1 hours
Not practise exercise *(number of participants, percentage of participants)*	77, 64 %
Hours practising exercise per week *(mean ± SD)*	2.2 ± 4.7 hours

(continuation)	
Characteristic	**Results**
Medical conditions	
Menopause (*number of participants, percentage of participants*)	21, 18 %
Allergic rhinitis (*number of participants, percentage of participants*)	19, 16 %
Asthma *(number of participants, percentage of participants)*	7, 6 %
Hypertension *(number of participants, percentage of participants)*	21, 18 %
Ovarian dysfunction *(number of participants, percentage of participants)*	5, 4 %
Anxiety *(number of participants, percentage of participants)*	18, 15 %
Systemic rheumatologic disease *(number of participants, percentage of participants)*	16, 13 %
Diabetes *(number of participants, percentage of participants)*	12, 10 %
Hypercholesterolemia *(number of participants, percentage of participants)*	11, 9 %
Glaucoma *(number of participants, percentage of participants)*	6, 5 %
Migraine headaches *(number of participants, percentage of participants)*	8, 7 %
Depression *(number of participants, percentage of participants)*	8, 7 %
Heart disease *(number of participants, percentage of participants)*	2, 2 %
Thyroid disease *(number of participants, percentage of participants)*	5, 4 %
Schizophrenia *(number of participants, percentage of participants)*	2, 2 %
Eczema *(number of participants, percentage of participants)*	4, 3 %
Stress *(number of participants, percentage of participants)*	10, 8 %
Medications	
Antihistamines *(number of participants, percentage of participants)*	9, 8 %
Antihypertensives *(number of participants, percentage of participants)*	20, 17 %
Stomach protector *(number of participants, percentage of participants)*	4, 3 %
Oral contraceptive therapy *(number of participants, percentage of participants)*	7, 6 %
Anticoagulants *(number of participants, percentage of participants)*	7, 6 %
Anxiolytics *(number of participants, percentage of participants)*	21, 18 %
Blood glucose regulators *(number of participants, percentage of participants)*	9, 8 %
Topical anti-glaucoma medication *(number of participants, percentage of participants)*	6, 5 %
Antidepressants *(number of participants, percentage of participants)*	4, 3 %
Hypercholesterolemia medication *(number of participants, percentage of participants)*	7, 6 %
Anti-inflammatories *(number of participants, percentage of participants)*	3, 3 %
Medication for thyroids *(number of participants, percentage of participants)*	3, 3 %
Antipsychotics *(number of participants, percentage of participants)*	2, 2 %
Daily medication *(number of participants, percentage of participants)*	58, 48 %
Ocular surgery	
Ocular surgery *(number of participants, percentage of participants)*	25, 21 %
Retinal surgery *(number of participants, percentage of participants)*	2, 2 %
Refractive surgery *(number of participants, percentage of participants)*	5, 4 %
Pterygium surgery *(number of participants, percentage of participants)*	1, 1 %
Glaucoma surgery *(number of participants, percentage of participants)*	2, 2 %
Cataract surgery *(number of participants, percentage of participants)*	16, 13 %

(continuation)	
Characteristic	**Results**
Diet	
Poor diet quality *(number of participants, percentage of participants)*	19, 16 %
Non-omnivorous diet *(number of participants, percentage of participants)*	11, 9 %
Non-oily fish diet *(number of participants, percentage of participants)*	79, 66 %
Percentage of unprocessed food in diet *(mean ± SD)*	65 ± 20 %
Percentage of ultra-processed food in diet *(mean ± SD)*	8 ±11 %
Drinking alcohol *(number of participants, percentage of participants)*	83, 67 %
Units of alcohol per week *(mean ± SD)*	3.2 ± 5.0 units
More than 4 units of alcohol per week *(number of participants, percentage of participants)*	30, 25 %
Not drinking caffeine *(number of participants, percentage of participants)*	28, 23 %
Units of caffeine per day *(mean ± SD)*	1.5 ± 1.5 units
Litres of water per day *(mean ± SD)*	1.7 ± 0.8 liters
Less than 2 litres of water per day *(number of participants, percentage of participants)*	73, 61 %
Environment	
Working *(number of participants, percentage of participants)*	57, 48 %
Hours working per day *(mean ± SD)*	3.7 ± 4.1 hours
Working ≥ than 8 hours per day *(number of participants, percentage of participants)*	42, 35 %
Urban life *(number of participants, percentage of participants)*	49, 41 %
Air conditioning *(number of participants, percentage of participants)*	90, 75 %
Hours of exposure to air conditioning per day *(mean ± SD)*	4.2 ± 4.1 hours
≥ 8 hours of exposure to air conditioning per day *(number of participants, percentage of participants)*	31, 26 %
Central heating *(number of participants, percentage of participants)*	91, 76 %
Hours of exposure to central heating per day *(mean ± SD, years)*	4.7 ± 4.7 hours
≥ 8 hours of exposure to central heating per day *(number of participants, percentage of participants)*	34, 28 %

(Where SD: Standard Deviation)

Table 4.3. *Ocular surface parameters of participants.*

Characteristic	Total	Healthy group	DED group
OSDI score *(median, IQR)*	16.7, 6.3-30.3	4.2, 0-8.3	22.6, 13.9-42.7
DEQ-5 score *(median, IQR)*	7, 4-12	3, 1-5	10, 7-14
NIKBUT *(median, IQR)*	6.69, 4.40-10.66 seconds	8.54, 4.92-15.29 seconds	7.76, 4.21-8.36 seconds
Osmolarity *(median, IQR)*	318.0, 310.5-329.50 mOsmol/L	315.5, 307.75-328.50 mOsmol/L	320.0, 312.0-331.0 mOsmol/L
Difference in osmolarity between eyes *(median, IQR)*	10, 4.5-19 mOsmol/L	9, 4.5-11.5	13, 4-22
Corneal staining > 5 spots *(number of participants)*	12	2	10
Corneal staining > 9 spots *(number of participants)*	16	3	13
Lid margin staining ≥ 2 mm of length and ≥ 25 % of width *(number of participants)*	31	5	26

(Where IQR: Interquartile range, DED: Dry Eye Disease, DEQ: Dry Eye Questionnaire, mOsmol/L: Milliosmoles per liter, NIKBUT: Non-Invasive Keratograph Break-Up Time and OSDI: Ocular Surface Disease Index)

Table 4.4 shows the univariate logistic regression and multivariate-adjusted logistic regression analysis, along with the odds ratios of DED for each factor. Given that the cohort does not fully represent the Spanish population, corrected odds ratios were calculated for each risk factor by multiplying the risk factor rate found for each age group by the age proportion in each group. The ratio between the corrected prevalence of that risk factor and the corrected odds ratio was obtained and multiplied for the odds ratio to obtain the corrected odds ratio. This procedure was repeated for each risk factor. In continuous variables, the median value was used to classify participants.

Univariate logistic regression identified the following as potential risk factors for DED ($p < 0.15$): Sex, sleep hours per day, menopause, anxiety, systemic rheumatologic disease, use of anxiolytics, daily medication, ocular surgery, poor diet quality, percentage of ultra-processed food in diet, caffeine intake and hours of exposure to air conditioning per day. The interaction between DED and risk factors was statistically significant for sex, sleep hours per day, menopause, anxiety, systemic rheumatologic disease, use of anxiolytics and caffeine intake ($p < 0.05$ for all). The multivariate logistic regression revealed that sleep hours per day, menopause and use of anxiolytics were independently associated with DED ($p \leq 0.026$ for all).

Table 4.4. *Univariate and multivariate logistic regressions and odds ratios of dry eye disease for demographic and clinical characteristics.*

Characteristic	Univariate logistic regression				Multivariate logistic regression			
	Odds ratio/Corrected odds ratio	Lower CI/Corrected	Upper CI/Corrected	p-value	Odds ratio/Corrected odds ratio	Lower CI/Corrected	Upper CI/Corrected	p-value
Age	1.012/1.522	0.995/1.516	1.029/1.568	0.164	-	-	-	-
Age (per 10 years)	1.125/1.714	0.945/1.440	1.338/2.039	0.185	-	-	-	-
Female sex	**2.806/1.603**	**1.295/0.740**	**6.081/3.473**	**0.009***	-	-	-	-
Lifestyle								
Hours of sleep per day	**0.654/0.792**	**0.469/0.568**	**0.911/1.103**	**0.012***	0.588/0.712	0.388/0.470	0.891/1.079	0.012*
Smoking	1.298/2.200	0.546/0.926	3.086/5.231	0.555	-	-	-	-
Number of cigarettes smoked per day	1.030/1.746	0.961/1.629	1.104/1.872	0.406	-	-	-	-
More than 5 cigarettes smoked per day	1.307/1.861	0.458/0.652	3.726/5.304	0.617	-	-	-	-
Contact lens wear	0.788/0.770	0.355/0.348	1.747/1.712	0.557	-	-	-	-
Hours per week of contact lens wear	1.001/0.981	0.988/0.968	1.015/0.995	0.825	-	-	-	-

Characteristic	Univariate logistic regression (continuation)				Multivariate logistic regression (continuation)			
	Odds ratio/Corrected odds ratio	Lower CI/Corrected	Upper CI/Corrected	p-value	Odds ratio/Corrected odds ratio	Lower CI/Corrected	Upper CI/Corrected	p-value
Lifestyle								
More than 56 hours per week of contact lens wear	0.897/0.879	0.301/0.295	2.676/2.622	0.846	-	-	-	-
Computer use	0.745/0.874	0.347/0.418	1.598/1.927	0.449	-	-	-	-
Daily hours of computer use	0.961/1.159	0.852/1.027	1.084/1.307	0.522	-	-	-	-
More than 4 hours of daily computer use	0.567/0.766	0.257/0.347	1.254/1.694	0.161	-	-	-	-
Exercise								
Not walk (sedentary lifestyle)	0.636/0.713	0.272/0.305	1.489/1.670	0.297	-	-	-	-
Hours walking per day	1.081/1.146	0.771/0.817	1.514/1.605	0.652	-	-	-	-
Not practise exercise	1.412/1.734	0.655/0.804	3.045/3.740	0.378	-	-	-	-
Hours practising exercise per week	0.827/0.929	0.580/0.651	1.179/1.324	0.293	-	-	-	-
Medical conditions								
Menopause	**7.000/3.458**	**1.546/0.794**	**31.705/15.662**	**0.012***	8.759/4.327	1.571/0.776	48.835/2.124	0.013*
Allergic rhinitis	1.307/2.186	0.458/0.766	3.726/6.232	0.617	-	-	-	-
Asthma	1.479/1.039	0.275/0.193	7.964/5.593	0.649	-	-	-	-
Hypertension	2.080/1.502	0.705/0.509	6.138/4.432	0.185	-	-	-	-
Ovarian dysfunction	1001139339/ 624410605.7	0.000	-	0.999	-	-	-	-
Anxiety	**12.390/14.313**	**1.587/1.833**	**96.698/111.706**	**0.016***	-	-	-	-
Systemic rheumatologic disease	**4.742/2.817**	**1.024/0.608**	**21.954/13.041**	**0.047***	-	-	-	-
Diabetes	0.791/0.908	0.235/0.270	2.661/3.054	0.705	-	-	-	-
Hypercholesterolemia	1.608/1.765	0.404/0.444	6.406/1.033	0.501	-	-	-	-
Glaucoma	3.028/1.329	0.342/0.150	26.793/11.755	0.319	-	-	-	-
Migraine headaches	4.362/3.358	0.519/0.340	36.694/28.251	0.175	-	-	-	-
Depression	4.362/1.882	0.519/0.224	36.694/15.833	0.175	-	-	-	-
Heart disease	0.573/1.672	0.035/0.102	9.400/27.424	0.697	-	-	-	-
Thyroid disease	0.863/0.346	0.139/0.056	5.375/2.153	0.875	-	-	-	-
Schizophrenia	0.573/0.378	0.035/0.023	9.400/6.204	0.697	-	-	-	-
Eczema	0.566/1.373	0.057/0.138	5.612/13.610	0.627	-	-	-	-
Stress	2.471/4.308	0.501/0.874	12.194/21.261	0.267	-	-	-	-

Characteristic	Univariate logistic regression (continuation)				Multivariate logistic regression (continuation)			
	Odds ratio/ Corrected odds ratio	Lower CI/Corrected	Upper CI/Corrected	p-value	Odds ratio/Corrected odds ratio	Lower CI/Corrected	Upper CI/Corrected	p-value
Medications								
Antihistamines	1.171/2.784	0.278/0.661	4.937/11.736	0.829	-	-	-	-
Antihypertensi-ves	1.918/1.404	0.646/0.473	5.699/4.171	0.241	-	-	-	-
Stomach protector	1.767/1.150	0.178/0.116	17.526/11.404	0.627	-	-	-	-
Oral contraceptive therapy	3.686/2.027	0.429/0.236	31.666/17.410	0.235	-	-	-	-
Anticoagulants	0.759/1.275	0.162/0.272	3.560/5.979	0.727	-	-	-	-
Anxiolytics	**15.357/ 7.901**	**1.982/1.020**	**118.972/61.211**	**0.009***	11.072/5.697	1.338/0.688	91.611/47.134	0.026*
Blood glucose regulators	2.130/2.806	0.423/0.557	10.740/14.150	0.359	-	-	-	-
Topical anti-glaucoma medication	3.028/1.607	0.342/0.182	26.793/14.222	0.319	-	-	-	-
Antidepressants	1.767/1.149	0.178/0.116	17.526/11.397	0.627	-	-	-	-
Hypercholesterol emia medication	3.686/4.791	0.429/0.558	31.666/41.163	0.235	-	-	-	-
Anti-inflammatories	0.280/0.169	0.025/0.015	3.180/1.921	0.305	-	-	-	-
Medication for thyroids	0.280/0.117	0.025/0.010	3.180/1.328	0.305	-	-	-	-
Antipsychotics	0.573/0.378	0.035/0.023	9.400/6.204	0.697	-	-	-	-
Daily medication	**1.861/2.037**	**0.873/0.956**	**3.963/4.338**	**0.108**	-	-	-	-
Ocular surgery								
Ocular Surgery	**2.111/1.941**	**0.772/0.710**	**5.770/5.304**	**0.145**	-	-	-	-
Retinal surgery	960552609.3 / 2802316182	0.000	-	0.999	-	-	-	-
Refractive surgery	2.389/2.070	0.259/0.224	22.075/19.128	0.443	-	-	-	-
Pterygium surgery	0.000	0.000	-	1.000	-	-	-	-
Glaucoma surgery	960552609.3 / 421442457.3	0.000	-	0.999	-	-	-	-
Cataract surgery	1.875/1.524	0.566/0.460	6.216/5.054	0.304	-	-	-	-
Diet								
Poor diet quality	**3.644/3.430**	**0.998/0.939**	**13.312/12.532**	**0.050**	3.853/3.627	0.978/0.921	15.168/14.279	0.054
Non-omnivorous diet	1.608/1.338	0.404/0.336	6.406/5.329	0.501	-	-	-	-
Non-oily fish diet	1.166/1.558	0.535/0.715	2.539/3.393	0.700	-	-	-	-

Characteristic	Univariate logistic regression (continuation)				Multivariate logistic regression (continuation)			
	Odds ratio/Corrected odds ratio	Lower CI/Corrected	Upper CI/Corrected	p-value	Odds ratio/Corrected odds ratio	Lower CI/Corrected	Upper CI/Corrected	p-value
Diet								
Percentage of unprocessed food in diet	0.985/0.615	0.966/0.603	1.006/0.628	0.154	-	-	-	-
Percentage of ultra-processed food in diet	**1.046/1.590**	**0.994/1.511**	**1.102/1.675**	**0.084**	-	-	-	-
Drinking alcohol	1.055/1.328	0.481/0.605	2.315/2.914	0.893	-	-	-	-
Units of alcohol per week	1.026/1.210	0.948/1.118	1.111/1.310	0.529	-	-	-	-
More than 4 units of alcohol per week	1.214/1.432	0.508/0.599	2.900/3.420	0.662	-	-	-	-
Not drinking caffeine	**3.385/1.703**	**1.182/0.595**	**9.690/4.876**	**0.023***	-	-	-	-
Units of caffeine per day	0.892/0.449	0.695/0.350	1.145/0.576	0.369	-	-	-	-
Litres of water per day	0.985/1.116	0.921/1.043	1.053/1.193	0.663	-	-	-	-
Less than 2 litres of water per day	1.122/1.271	0.526/0.596	2.396/2.714	0.766	-	-	-	-
Environment								
Working	0.739/0.653	0.351/0.310	1.556/1.375	0.426	-	-	-	-
Hours working per day	0.968/0.855	0.885/0.782	1.059/0.936	0.483	-	-	-	-
Working ≥ than 8 hours per day	0.910/0.800	0.419/0.3685	1.977/1.739	0.812	-	-	-	-
Urban life	1.565/1.562	0.725/0.723	3.380/3.373	0.254	-	-	-	-
Air conditioning	1.455/1.682	0.626/0.724	3.381/3.908	0.383	-	-	-	-
Hours of exposure to air conditioning per day	**1.085/1.094**	**0.981/0.989**	**1.201/1.211**	**0.112**	-	-	-	-
≥ 8 hours of exposure to air conditioning per day	1.584/1.597	0.654/0.659	3.837/3.867	0.308	-	-	-	-
Central heating	1.074/1.189	0.453/0.502	2.547/2.820	0.871	-	-	-	-
Hours of exposure to central heating per day	0.973/1.077	0.900/0.996	1.051/1.164	0.483	-	-	-	-
≥ 8 hours of exposure to central heating per day	1.302/1.667	0.562/0.720	3.015/3.861	0.538	-	-	-	-

*(Where CI: 95 % Confidence Interval. *: Statistically significant values. Bold: Variables included in the multivariate analysis (p < 0.15))*

4.4 Discussion

The TFOS DEWS II Epidemiology Report determined that ageing, feminine sex, Asian ethnicity, computer use, contact lens wear, inadequate environment, and use of antihistamines, antidepressants and anxiolytics were DED risk factors with consistent evidence (Stapleton et al., 2017). Nevertheless, these outcomes cannot be directly compared with the ones reported in the present study, as the TFOS DEWS II Report was constructed on the basis of previous cross-sectional investigations in which the disease diagnosis criterion and methodology differed considerably between studies.

Consequently, the results of the present research can only be directly compared with the recent studies carried out by Wang et al. (2020) and Wang et al. (2021) on a New Zealand population. The present study adds the analysis of the interaction between systemic, environmental and lifestyle DED risk factors. The results of this study showed that DED was independently associated with the use of anxiolytics, menopause and sleep hours per day.

Age and sex

The association of DED with sex and ageing has been widely reported in previous studies. Several studies found an increase in DED prevalence with age (Schaumberg et al., 2003; Moss, Klein and Klein, 2008; Galor et al., 2012; Uchino et al., 2013; Ahn et al., 2014; Paulsen et al., 2014; Roh et al., 2016; Farrand et al., 2017; Millán et al., 2018;

Rico-del-Viejo et al., 2018; Shehadeh-Mashor et al., 2019; Lin et al., 2020; Wang et al., 2020; Wang et al., 2021), while some did not find a significant association (Tongg et al., 2009; Han et al., 2011; Tan et al., 2015b; Asiedu et al., 2017). Moreover, some reports indentified that feminine sex was related to DED (Schaumberg et al., 2003; Uchino et al., 2008; Galor et al., 2012; Uchina et al., 2013; Ahn et al., 2014; Paulsen et al., 2014; Tan et al., 2015b; Roh et al., 2016; Farrand et al., 2017; Rico-del-Viejo et al., 2018; Shehadeh-Mashor et al., 2019; Lin et al., 2020), while others did not find a relationship (Tongg et al., 2009; Onwubiko et al., 2014; Tan et al., 2015b; Wang et al., 2020).

In this study, no independent association was found between DED and age or sex. Even though chi-square analysis showed that the DED group had a statistically higher number of females and that the univariate analysis identified that females were 1.6 times more likely to suffer from DED ($p = 0.009$), feminine sex was not found as statistically associated with DED in the multivariate analysis, which is in agreement with a previous study (Asiedu et al., 2017). Also in consonance with the outcomes of this study, no independent association between sex and DED was found by Wang et al. (2020). Nevertheless, contrary to the Mediterranean Caucasian cohort results reported here, the authors did find an independent association between DED and age in their New Zealand cohort (Wang et al., 2020; Wang et al., 2021).

Medical conditions and medications

Wang et al. (2020) also reported an independent association with migraine headaches, systemic rheumatologic disease, thyroid disease and antidepressant medication. In the present work, participants who suffered from systemic

rheumatologic disease had 2.8 times more risk to suffer from DED in the univariate regression (p = 0.047), but it was not statistically significant in the multivariate analysis. Other studies (Paulsen et al., 2014; Na et al., 2015; Van der Vaart et al., 2015; Roh et al., 2016) have also confirmed the relationship between DED and systemic rheumatologic disease since this condition causes an increased concentration of inflammatory cytokines within the tear fluid and conjunctival epithelium, which causes an inflammatory infiltration and structural damage in the lacrimal glands (Solomon et al., 2001; Roh et al., 2016; Bron et al., 2017; Stapleton et al., 2017).

Additionally, while there is inconclusive evidence as to whether menopause is a risk factor for DED (Stapleton et al., 2017), the present study found an independent association with DED. This could be because ovaries produce very low levels of estrogens and progesterone during menopause. It is thought that estrogens are responsible for the regulation of the synthesis of lipids in the meibomian glands, and both estrogens and progesterone modulate the inflammatory response. Researchers have also reported that the decrease in androgens during menopause is also associated with DED (Sullivan et al., 2017; Vehof, Hysi and Hammond, 2017; Dang et al., 2020; García-Alfaro et al., 2020). Contrary to the outcomes of the present study, Wang et al. (2020) found that menopause was only statistically significant in the univariate analysis, but was not statistically significant when its interaction with other variables was analysed.

Several studies have found an association between DED and psychological conditions such as anxiety, depression and stress (Schaumberg et al., 2003; Karaiskos

et al., 2008; Moss, Klein and Klein, 2008; Galor et al., 2012; Malet et al., 2013; Ahn et al., 2014; Na et al., 2015; Van der Vaart et al., 2015). However, there is no evidence whether these diseases are a cause or a consequence of DED. The TFOS DEWS II Epidemiology Report acknowledged the need for clarifying the role of anxiolytics and antidepressants in DED (Galor et al., 2012; Malet et al., 2013; Stapleton et al., 2017). Different authors (Moss, Klein and Klein, 2008; Galor et al., 2012; Malet et al., 2013; Paulsen et al., 2014 ; Ferrero et al., 2018 ; Millán et al., 2018) found that anxiolytic medication was a risk factor for the development of dry eye. In support of this, the present study confirmed that anxiolytic medication was independently associated with DED. More precisely, participants who used anxiolytic medication were 5.7 times more likely to suffer from DED. Anxiety was identified as a potential predictor of DED ($p = 0.016$) in the univariate analysis, but was not independently associated with DED in the multivariate analysis. Therefore, the association between DED and anxiety could result as a consequence of the relationship between DED and anxiolytics. Besides, the use of daily medication was identified as a potential risk factor in the univariate analysis, but was not independently associated with DED in the multivariate analysis. Finally, no relationship was found with any other medical conditions.

Lifestyle, exercise and environmental conditions

Environmental factors such as air pollution, wind, low humidity, use of central heating or air conditioning have been suggested to impact the integrity of the ocular surface (Gupta et al., 2008; Novaes et al., 2010; Asiedu et al., 2017; Stapleton et al., 2017; Azzam et al., 2020). In the present study, air conditioning was identified as a

potential risk factor for DED, but it did not show a statistically significant relationship with DED in the multivariate analysis. No other variable related to the environment showed a statistically significant association with DED. In contrast to the outcomes of this study, Roh et al. (2016) found that DED was more prevalent in those residing in urban areas and with indoor occupations. Practising regular exercise showed no association with DED either, in agreement with previous studies (Moss, Klein and Klein, 2008; Na et al., 2015; Karaiskos et al., 2008; Wang et al., 2021); although Sano et al. (2018) found that physical exercise decreased dry eye symptoms in healthy office workers, which might suggest that exercise has an optimal impact on ocular surface health.

Regarding sleep hours per day, Murube (2008) hypothesized that rapid eye movement during sleep serves to increase tear secretion and to humidify and lubricate the ocular surface. The present study confirms that participants sleeping less hours are more likely to suffer from DED. Specifically, each additional sleeping hour reduced the probability of suffering DED by 0.8 times. Conversely, Wang et al. (2021) and Na et al. (2015) did not find any association between DED and hours of sleep.

It has been also reported that DED is more prevalent in contact lens wearers (Uchino et al., 2008; Uchino et al., 2011; Paulsen et al., 2014; Tan et al., 2015b; Yang et al., 2015; Stapleton et al.,2017; Wang and Craig, 2019); nevertheless, the present study did not reveal an association, in agreement with other generally more recent studies (Uchino et al., 2013; Shehadeh-Mashor et al., 2019; Wang et al., 2020). Wang et al. (2020) and Wang et al. (2021), who used the same diagnostic criterion as the present

study, did not find an independent association between contact lens wear and DED either, perhaps due to advances in contact lens materials and greater use of daily disposables (Morgan et al., 2021). Furthermore, some studies have shown that DED is more prevalent in workers using visual displays as a consequence of a reduced blink frequency and an increase in incomplete blinking during visual display visualization, which have both shown to increase tear evaporation (Uchino et al., 2008; Uchino et al., 2011; Uchino et al., 2013; Yang et al., 2015). Wang et al. (2021) found that increased hours of digital screen exposure per day was independently associated with DED. Nevertheless, in agreement with other reports (Asiedu et al., 2017; Ferrero et al., 2018; Millán et al., 2018), the present study did not reveal an association between DED and digital display use.

It has also been suggested that cigarette smoking is a risk factor for DED (Matsumoto et al., 2008; Lee, Petznick and Tong, 2012; Na et al., 2015; Stapleton et al., 2017; Makrynioti et al., 2020). Some studies state that not only is smoking a risk factor by itself, but environmental exposure to smoke can develop dry eye symptoms (Matsumoto et al., 2008; Makrynioti et al., 2020). Nevertheless, other authors did not find a significant association with DED and the TFOS DEWS II Epidemiology Report concluded that it is inconclusive whether smoking is a risk factor for DED (Moss, Klein and Klein, 2008; Uchino et al., 2008; Uchino et al., 2011; Uchino et al., 2013; Ahn et al., 2014; Tan et al., 2015b; Stapleton et al., 2017; Ferrero et al., 2018; Millán et al., 2018). In this regard, in agreement with the study of Wang et al. (2021), the results of this study did not reveal an association between DED and smoking.

Diet

Diet quality has also been reported as possibly associated with DED. Conditions such as vitamin A or D deficiency, eating disorders or a vegan diet might be related to DED (Yang et al., 2015; Stapleton et al., 2017; Liu, Dong and Wang, 2020; Machowicz et al., 2020). In the present study, poor diet quality approached the statistical significance cut-off in the multivariate analysis ($p = 0.050$). The percentage of ultra-processed food was included in the multivariate analysis since it was found to be a potential predictor of DED in the univariate analysis ($p = 0.084$). However, it did not reveal an independent association with DED. Essential fatty acids play a relevant role in the tear film and ocular surface healthiness since they enhance the tear film lipid layer and reduce the expression of some inflammatory markers (Bhargava et al., 2015; Yang et al., 2015; Wolffsohn et al., 2017). However, this role is still not fully understood (Stapleton et al., 2017). The present study did not find an association between DED and non-oily fish or non-omnivorous diet.

Regarding alcohol consumption, the TFOS DEWS II Epidemiology Report considered the evidence as inconclusive as to whether it was a risk factor for DED (Moss, Klein and Klein, 2008; Stapleton et al., 2017). In agreement with the study of Wang et al. (2021), the present study did not find an association between alcohol consumption and DED.

Some studies (Ahn et al., 2014 ; Stapleton et al., 2017 ; Millán et al., 2018) have reported that drinking caffeine increases tear production; in the present study this factor did not reveal an independent association with DED, although the univariate

analysis showed that participants who did not drink caffeine had 1.7 times more probability to suffer from DED (p = 0.023). In the study of Wang et al. (2021) reduced caffeine intake per day was identified as a risk factor for DED.

Ocular surgery

Ocular surgery, such as refractive or cataract surgery, have been identified as potential risk factors for DED (Ahn et al., 2014; Stapleton et al., 2017; Ferrero et al., 2018; Shehadeh-Mashor et al., 2019; Wang and Craig, 2019; Garg et al., 2020; Lin et al., 2020; Sambhi et al., 2020). Ocular surgery was included in the multivariate analysis since it was found to be a potential predictor of DED in the univariate analysis (p = 0.145), but it did not reveal an independent association with DED.

The present study has some limitations that must be taken into account. First, dry eye classification subtypes (aqueous deficient and evaporative) were not considered in the analysis. Thus, both types of DED were analysed altogether. Medical history, environmental and lifestyle factors were self-reported by participants, which might have induced recall bias, although this can be considered as an inherent limitation of any cross-sectional study.

The magnitude of the prevalence of DED was higher than in previous studies of similar nature. Thus, the presented prevalence was corrected for the general population and was still notably higher than that reported in New Zealand using the same diagnostic criteria (Wang et al., 2020; Wang et al., 2021). The new DED diagnostic criterion, described in the TFOS DEWS II, is less restrictive and has been

reported to increase the prevalence of the disease (Wang et al., 2020). Heat and humidity of the region could also have increased the prevalence in a Mediterranean Caucasian population. Previous research (Tesón et al., 2015) found that dry eye was more prevalent in Spain than in another country with different levels of environmental humidity. Moreover, a recent study (Darbà and Ascanio, 2020) informed that the number of patients with DED has increased steadily throughout the years in Spain, which might be partially caused by modern-day workplace in Spanish society. In addition, the high prevalence found in the present study might be in agreement with the high incidence of clinical tests, sale of dry eye products and the number of dry eye specialist visits reported in Spain (Clegg et al., 2006; Viso, Rodríguez-Ares and Gude, 2009; Viso, Gude and Rodríguez-Ares, 2011; McDonald et al., 2016; Millán et al., 2018). Although all these points might explain the high prevalence of DED in the results, the recruitment process through an open advertisement could also have induced a higher prevalence of DED than expected in the general population. Some of these limitations are also acknowledged to exist in previous studies with similar designs (Stapleton et al., 2017; Wang et al., 2020; Wang et al., 2021).

Moreover, although participants were assessed in a single visit and in the same laboratory under controlled environmental conditions, seasonal variations may have induced some variability in the results. Nevertheless, such variations can be considered minimal since measurements were performed between November 2018 and January 2019. As in a previous study (Wang et al., 2020), the wide confidence intervals found, might have decreased the study power, and the high number of variables included might have induced false-positive results. Nonetheless, this issue was partially

minimized by the fact that not all these variables were analysed together: although 76 variables were assessed as risk factors in the univariate analysis, only 12 of them were finally analysed together and included in the multivariate logistic regression.

In addition, the cohort of the present study is not completely representative of the Spanish population since there is a gap in the ’50s and ’60s. To amend this issue, a corrected prevalence for the Spanish population and a corrected risk factor odds ratio were calculated. Likewise, the chances of finding a significant value are low in the factors that are not common in the cohort. Therefore, factors that have a low percentage of people in the sample cannot be excluded as risk factor for DED. Finally, the main limitation of this work was the number of participants recruited, which could explain the lack of association with factors such as age or sex, although the sample analysis showed that such sample size was able to provide a good level of statistical power. In any case, the results of the present study allow a hypothesis to be built for testing in future studies.

Overall, the present study found that DED following the diagnostic guidelines of the TFOS DEWS II Diagnostic Methodology Report had a prevalence of 57.7 % in a Mediterranean Caucasian population. DED is independently associated with anxiolytic medication, less sleep hours per day and menopause. This work identifies the key risk factors of DED to be used in the screening of the condition. Clinicians should acknowledge the importance of triaging questions, systemic comorbidities and risk factors when managing a patient with dry eye symptoms. Moreover, the present study identifies potentially modifiable risk factors, in addition to conventional treatments for

DED. Finally, clinicians should be aware that not only ocular surface assessment, but also systemic and environmental examination are relevant for DED participants.

CHAPTER 5: Repeatability of non-invasive keratograph break-up time measurements obtained using Oculus Keratograph 5M

5. REPEATABILITY OF NON-INVASIVE KERATOGRAPH BREAK-UP TIME MEASUREMENTS OBTAINED USING OCULUS KERATOGRAPH 5M

As commented on *Chapter 1 Introduction*, the Keratograph 5M is one of the most common tools used to objectively assess the tear film (Wolffsohn et al., 2017). Moreover, the TFOS DEWS II Diagnostic Methodology Report recommended the use of NIKBUT together with other signs and symptoms to diagnose DED (Wolffsohn et al., 2017). Due to the relevance of NIKBUT in the DED diagnosis, this chapter aims to measure the repeatability of NIKBUT using the Oculus Keratograph 5M.

5.1 Introduction

As commented on *Chapter 1 Introduction*, the Keratograph 5M is one of the most used tools to analyse tear film. Nevertheless, the repeatability of this device in NIKBUT measurement is still unclear (Best, Drury and Wolffsohn, 2012; Hong et al., 2013; Koh et al., 2016; Tian et al., 2016; Wang et al., 2016; Fernández et al., 2018; Vidal-Rohr et al., 2018) and it has not yet been assessed considering different patients' classifications.

In comparison to invasive BUT using fluorescein, the Keratograph 5M tends to obtain lower NIKBUT values, probably attributed to the fact that the software evaluates more data points and might even detect non-visually-apparent small tear film changes (Goto et al., 2004a; Hong et al., 2013; Jiang et al., 2014). Another reason for the discrepancy is that the Keratograph 5M may possibly measure a change of the curvature in the tear film layer, rather than the disruption of the tear film (Goto et al.,

2004a). Nevertheless, another study found higher break-up time values with the Keratograph 5M than with fluorescein. This could be explained by the fact that BUT using fluorescein was measured with controlled volumes of fluorescein solution (Lan et al., 2014).

The aim of this study is to assess the repeatability of NIKBUT measurements obtained using the Keratograph 5M, as well as to determine the influence of age, sex and DED on repeatability. To the authors' knowledge, this is the first study to analyse the effect of different classifications on the repeatability of Keratograph 5M. Knowing the effect of age, sex and DED on repeatability might be useful to clarify the repeatability of NIKBUT in different samples. This topic is of high interest due to the relevance of NIKBUT as a biomarker for the diagnosis of DED (Wolffsohn et al., 2017).

5.2 Methodology

A total of eighty healthy volunteers aged between 30 and 89 years old (57.59 ± 19.87 years) participated in this study. Only the right eye of subjects was assessed to avoid data duplication. Subjects had no prior history of ocular complications, injury or disease in the last three months. Contact lens users were instructed not to wear their contact lenses within a week before the examination. Written consent of each subject was obtained after the explanation of the protocol. The study was approved by the Ethics Committee of the University of Valencia and was performed in accordance with the tenets of the Declaration of Helsinki.

Measurement protocol

DED evaluation was carried out according to the guidelines of the TFOS DEWS II Diagnostic Methodology Report (Wolffson et al., 2017). First, each subject was asked to complete the OSDI and DEQ-5 questionnaires. Then, an ophthalmic examination was performed in the following order: NIKBUT, osmolarity in both eyes using the TearLab Osmolarity device (TearLab Corporation, San Diego, CA, USA) and ocular surface staining. Measurements were performed as explained in *Chapter 3 General Methodology.*

NIKBUT was measured three consecutive times using the Keratograph 5M (K5 M; Oculus GmbH, Wetzlar, Germany) for each subject by the same researcher. Any subject with values above 24.73 seconds was excluded from the analysis as this value corresponds to the upper cut-off of the instrument and thus it does not reflect a true value (Markoulli et al., 2017; Dutta et al., 2019).

The sample was classified according to sex, age and DED diagnosis based on the indications of the TFOS DEWS II Diagnostic Methodology Report (Wolffsohn et al., 2017). Age classification divided the sample into young (≤ 49 years) and elderly subjects (> 49 years). Classification of age was done following the TFOS DEWS II Epidemiology Report, which stipulates a gradual increase of DED after the age of 50 (Stapleton et al., 2017). On the other hand, subjects were classified into two other groups: DED and non-DED. The TFOS DEWS II Diagnostic Methodology Report recommended the presence of symptoms and at least one positive result of homeostasis markers to diagnose DED. Therefore, subjects with symptoms (DEQ-5 ≥ 6

or OSDI ≥ 13) and at least one positive sign of dry eye (NIKBUT < 10 seconds; Osmolarity ≥ 308 mOsm/L; Interocular osmolarity difference > 8 mOsm/L; corneal fluorescein staining > 5 spots; conjunctival lissamine green staining > 9 spots; or lid margin staining ≥ 2 mm length and ≥ 25% width) were included in the DED group (Wolffsohn et al., 2017).

Statistical analysis

Statistical analysis was performed using SPSS v26.0 for Windows (IBM Corp, Armonk, New York, USA), Microsoft Excel 2010 (Microsoft, Corp, Redmind, WA) and Matlab R2018a (MathWorks, Natick, MA). Results are shown as the mean ± SD. The normality distribution of each group was checked by means of the Shapiro-Wilk test.

The repeatability of the three measurements was assessed by calculating the S_w, CoV and CoR, as explained in *Chapter 3 General Methodology*. The differences between the three consecutive measurements were evaluated by means of repeated ANOVA for the whole sample and within each gender, age and DED group (within-subjects factor). Mixed ANOVA analysis was applied to evaluate the influence of the age, gender and DED diagnosis on the changes of the NIKBUT measurements over time (interaction within-between subjects factor). The main effect of the gender, age and DED diagnosis (between-subjects factor) in the NIKBUT measurements was also assessed in this analysis. The homoscedasticity and sphericity assumptions were checked by Levene's and Mauchly's tests, respectively. The Greenhouse-Geisser correction was applied in the case of nonsphericity. A p-value less than 0.05 was defined as statistically significant.

A Passing-Bablok graphical analysis, applied using Matlab R2018a (Passing and Bablok regression by Andrea Padoan, Jan 16, 2010) (Passing and Bablok, 1983), was also performed in order to compare the maximum and minimum break-up time measurement, as explained in *Chapter 3 General Methodology*. This graphical analysis was carried out to assess the repeatability of measurements as a function of NIKBUT magnitude.

5.3 Results

In this study, eighty right eyes were assessed from 80 subjects out of which 34 were females (44.25 %) and 46 males (58.75 %). The mean age was 57.59 ± 19.87 years (ranging from 30 to 89 years). This sample size achieves an 11% of confidence in the estimates, which means that the sample size is large enough to prove the results (McAlinden, Khadka and Pesudovs, 2015). *Table 5.1* shows the main results obtained for each group and for the whole sample, while *Table 5.2* shows the comparison between groups.

Age

According to the results, there were no statistically significant differences between elderly and young subjects in the NIKBUT measurements (mixed ANOVA p = 0.084), although a tendency to longer NIKBUT values in young subjects could be seen. S_w, CoR and CoV were lower for elderly subjects than for the young (*Table 5.1*). There were no statistical differences between the three measurements in young and elderly subjects (r-ANOVA p > 0.05; *Table 5.2*). Age did not affect the change in the three repeated

NIKBUT measurements (mixed ANOVA p = 0.947; *Figure 5.1*). Passing-Bablok regression showed a slope of 0.212 and 0.244 for young and elderly subjects, respectively. The intercept was 1.949 and 1.439, respectively. The 95% confidence interval did not contain the identity line (*Figure 5.2*).

Table 5.1. *Repeatability of NIKBUT measurements in different groups.*

Group	Number of subjects	Age (years)	NIKBUT (seconds)	NIKBUT Range (seconds)	Sw	CoR	CoV (%)
Young subjects	35	37.51 ± 7.16	8.71 ± 4.15	2.51 - 17.59	5.70	15.80	65.49
Elderly subjects	45	73.20 ± 9.95	7.08 ± 4.11	3.12 - 19.37	3.91	10.82	55.21
Males	46	55.85 ± 18.56	8.21 ± 4.45	2.51 - 18.61	5.09	14.10	61.96
Females	34	59.94 ± 21.57	7.22 ± 3.77	2.63 - 19.37	4.32	11.96	59.81
Healthy subjects	28	52.25 ± 19.39	8.63 ± 4.68	2.51 - 18.61	5.36	14.85	62.10
DED subjects	52	60.46 ± 19.70	7.34 ± 3.86	2.63 - 19.37	4.43	12.27	60.38
All the sample	80	57.59 ± 19.87	7.79 ± 4.18	2.51 - 19.37	4.78	13.23	61.31

(Where DED: Dry Eye Disease; NIKBUT: Non-Invasive Keratograph Break-Up Time; Sw: Within-subject standard deviation; CoR: Repeatability Coefficient; CoV: Coefficient of Variation; SD: Standard Deviation)

Table 5.2. *Comparison between groups and association between NIKBUT measurements and groups.*

	Classification	First NIKBUT (seconds)	Second NIKBUT (seconds)	Third NIKBUT (seconds)	Within subjects effects (p-value)	Within subjects effects (p-value)	Between subjects effects (p-value)
Age	Young	7.80±5.78	9.32±6.55	9.00±6.40	0.504	0.947	0.084
	Elderly	6.17±4.40	7.44±5.19	7.62±5.87	0.161		
Gender	Males	7.57±5.70	8.59±6.12	8.49±6.47	0.579	0.776	0.295
	Females	5.95±3.99	7.82±5.53	7.87±5.66	0.111		
DED diagnosis	Healthy	7.07±5.51	9.05±6.37	9.77±7.09	0.209	0.415	0.188
	DED	6.78±4.88	7.84±5.58	7.39±5.40	0.453		

(Where DED: Dry Eye Disease; NIKBUT: Non-Invasive Keratograph Break-Up Time)

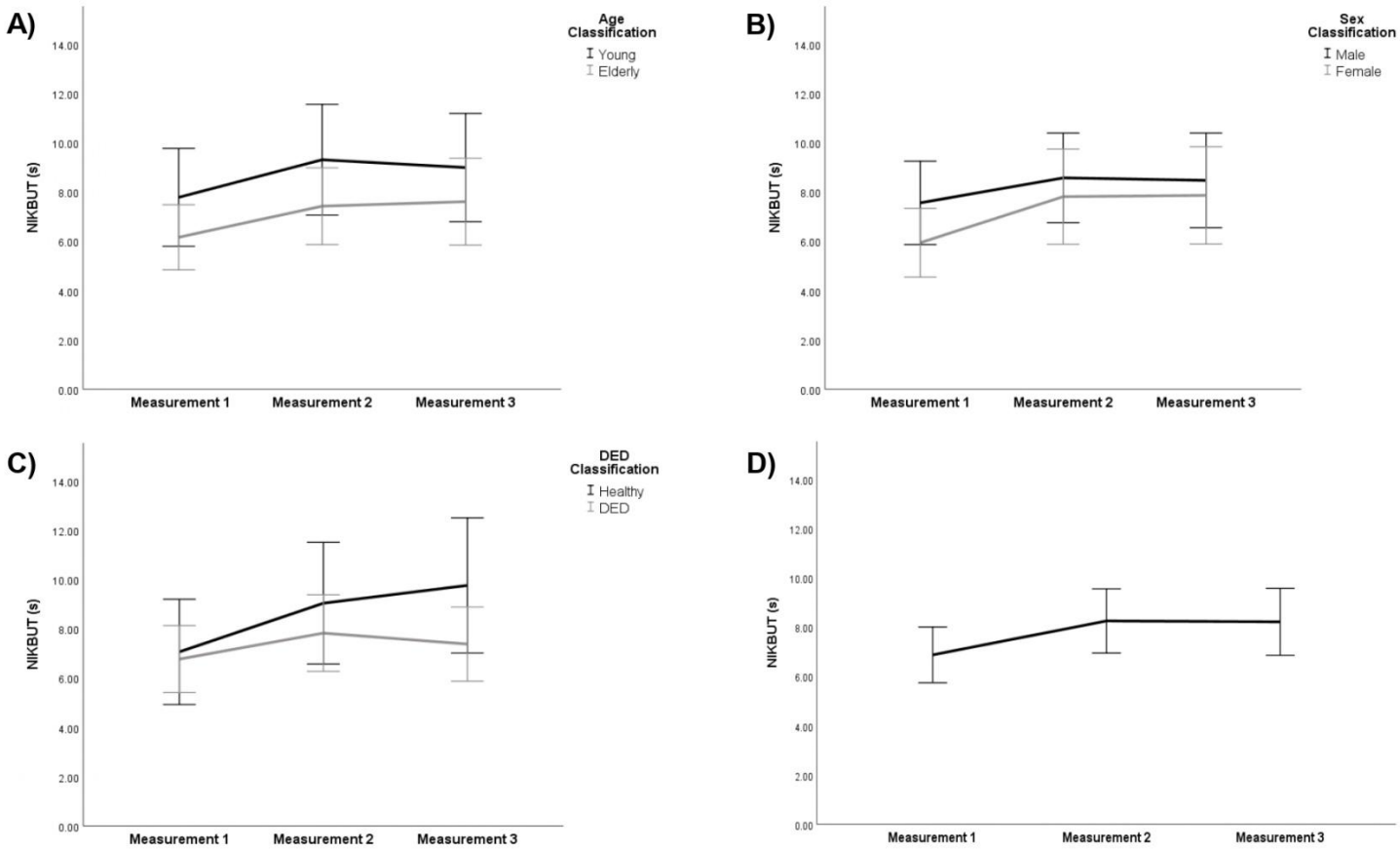

Fig. 5.1. *NIKBUT values in the three repeated measurements for each classification.*

Error bars: 95 % confidence intervals.

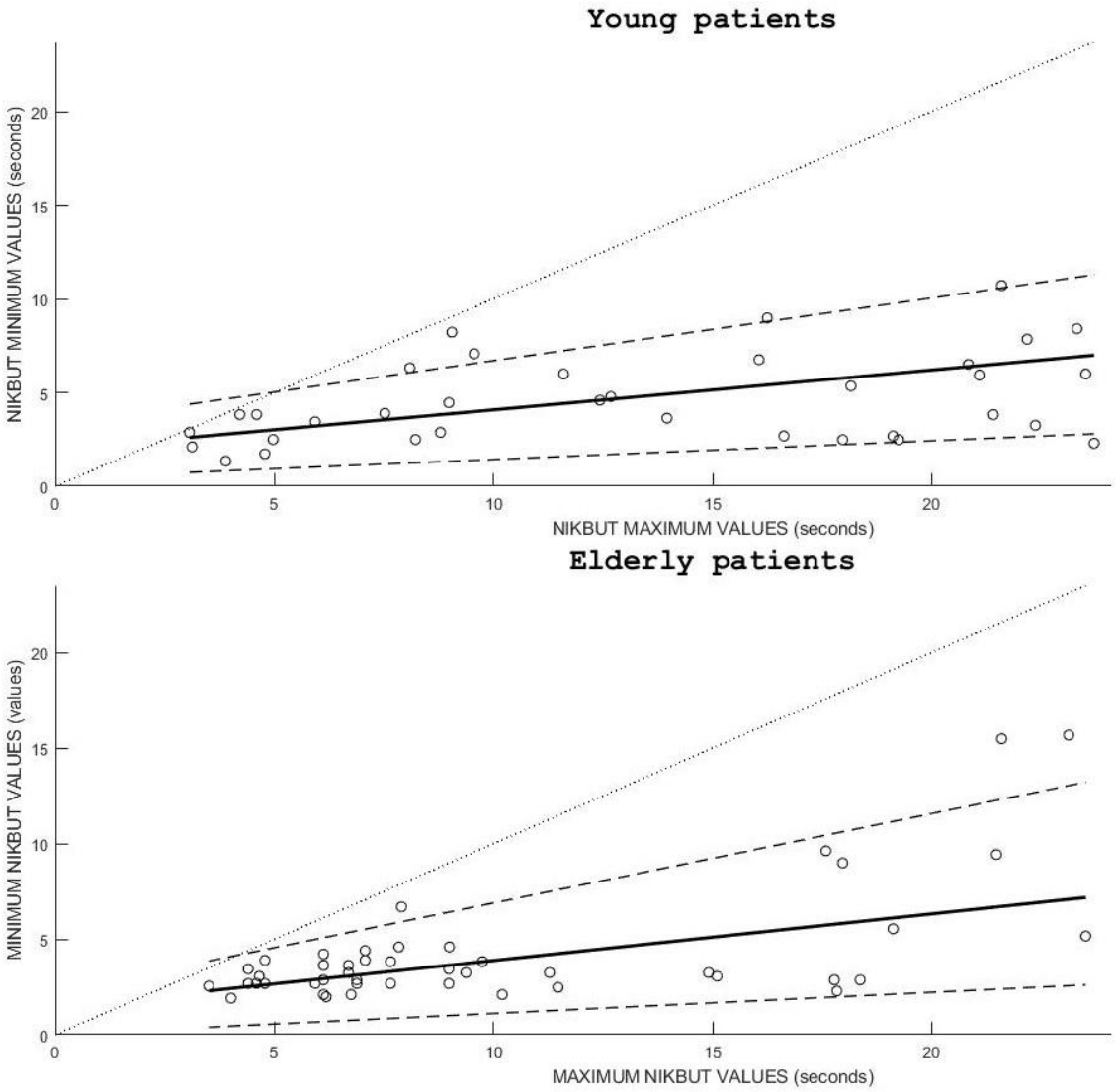

Fig. 5.2. *Passing–Bablok regression plots for age classification. Observations (white dots), identity line (dotted line), regression line (solid line) and 95% confidence intervals for regression coefficients (dashed lines).*

Gender

Results revealed no statistically significant differences between males and females in the NIKBUT measurements (mixed ANOVA p = 0.295), although males tended to manifest longer NIKBUT than females. S_w, CoR and CoV were lower for females than

for males (*Table 5.1*). Repeated ANOVA did not show statistical differences between the three measurements for males and females (r-ANOVA p > 0.05; *Table 5.2*). Gender did not influence the change in the three repeated NIKBUT measurements (mixed ANOVA p = 0.776; Figure 5.1). Passing-Bablok regression showed a slope of 0.237 and 0.247 for females and males, respectively. And the intercept was 1.809 and 0.976, respectively. The 95 % confidence interval did not contain the identity line (*Figure 5.3*).

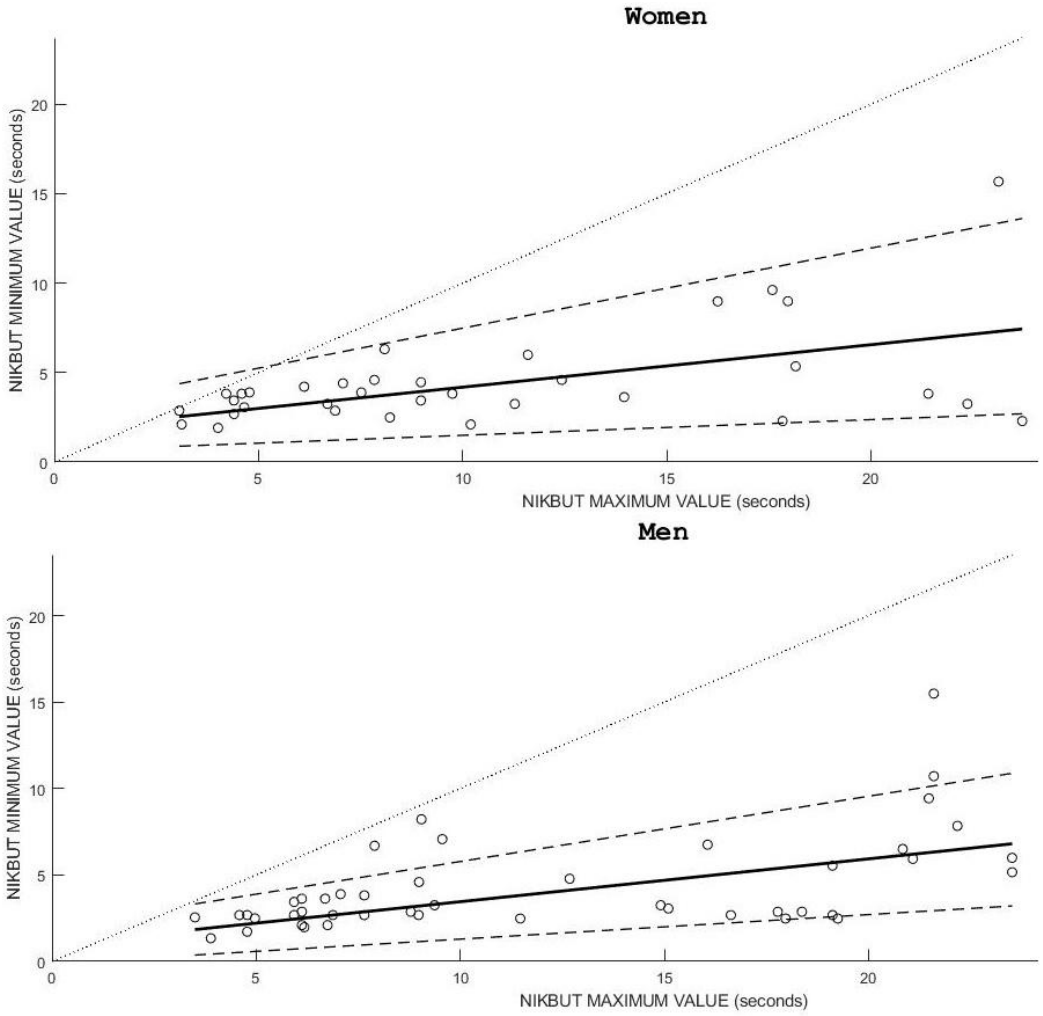

Fig. 5.3. *Passing–Bablok regression plots for sex classification. Observations (white dots), identity line (dotted line), regression line (solid line) and 95% confidence intervals for regression coefficients (dashed lines).*

Dry eye disease

Fifty-two subjects (65 % of subjects) had DED according to the TFOS DEWS II Diagnostic Methodology Report (Wolffsohn et al., 2017). Osmolarity was 319.57 ± 18.47 mOsm/L and 322.08 ± 19.88 mOsm/L; the osmolarity difference between eyes was 2.68 ± 2.03 mOsm/L and 5.38 ± 4.22 mOsm/L; total conjunctival and corneal staining score was 6.96 ± 4.35 and 9.30 ± 6.00; OSDI score was 2.98 ± 3.27 and 32.02 ± 21.52; and DEQ-5 score was 2.43 ± 2.02 and 9.84 ± 5.37, for healthy and DED subjects, respectively.

No statistically significant differences were found in NIKBUT measurements between healthy and DED subjects (mixed ANOVA p = 0.188), however a tendency to shorter NIKBUT values in DED was observed. S_w, CoR and CoV were lower for the DED group than for healthy subjects (*Table 5.1*). The three consecutive measurements did not differ significantly in healthy and DED subjects (r-ANOVA p > 0.05; *Table 5.2*). DED diagnosis did not have a significant influence on the change in the three repeated NIKBUT measurements (mixed ANOVA p = 0.776; *Figure 5.1*). Passing-Bablok regression showed a slope of 0.267 and 0.227 for healthy and DED groups, respectively. The intercept was 0.799 and 1.743, respectively. The 95 % confidence interval did not contain the identity line (*Figure 5.4*).

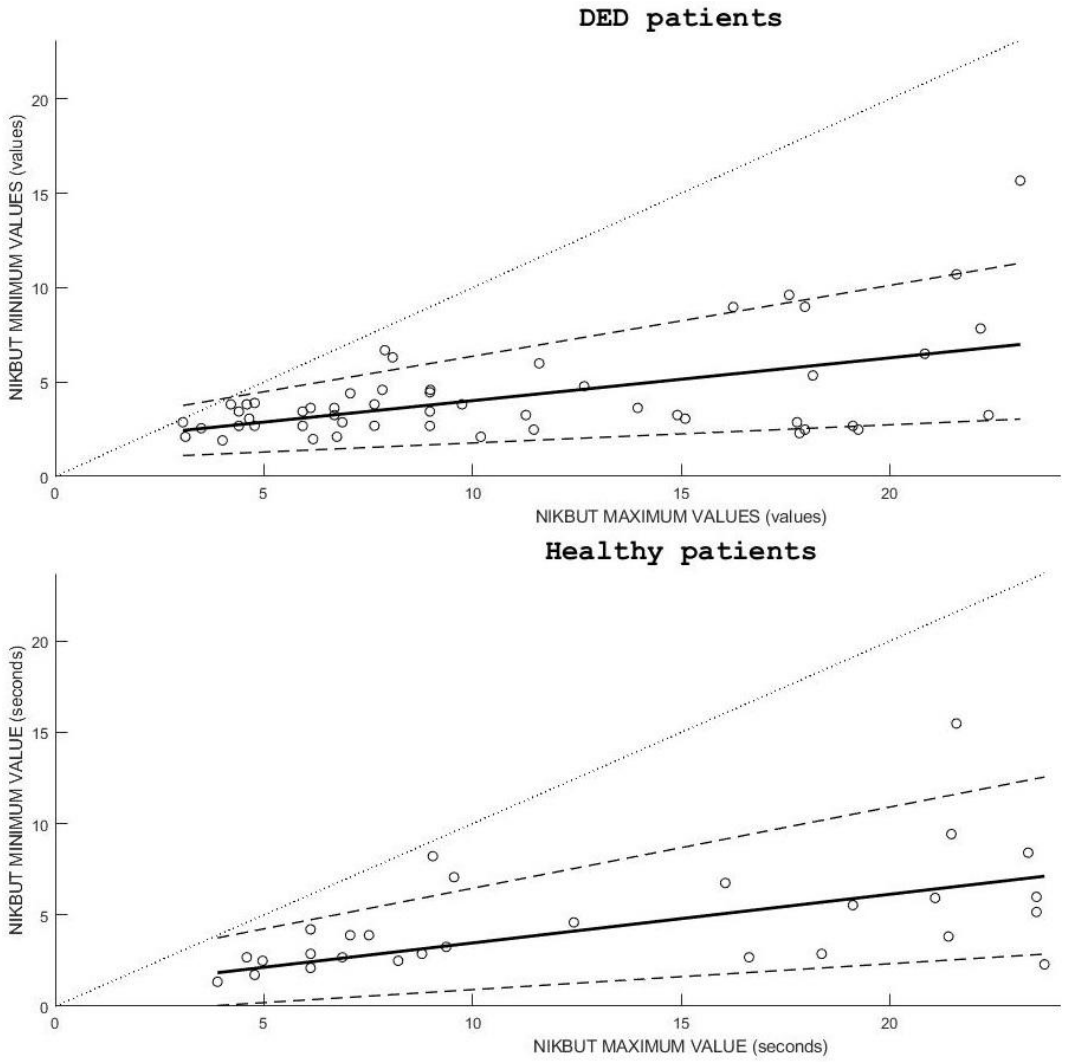

Fig. 5.4. *Passing–Bablok regression plots for dry eye classification. Observations (white dots), identity line (dotted line), regression line (solid line) and 95% confidence intervals for regression coefficients (dashed lines).*

All measurements

S_w, CoR and CoV values for the whole sample are also shown in *Table 5.1*. There were no significant differences between the repeated measurement (r-ANOVA p = 0.115, *Figure 5.1*). Passing-Bablok regression showed a slope of 0.242 and an intercept of 1.453. The 95 % confidence interval did not contain the identity line (*Figure 5.*5).

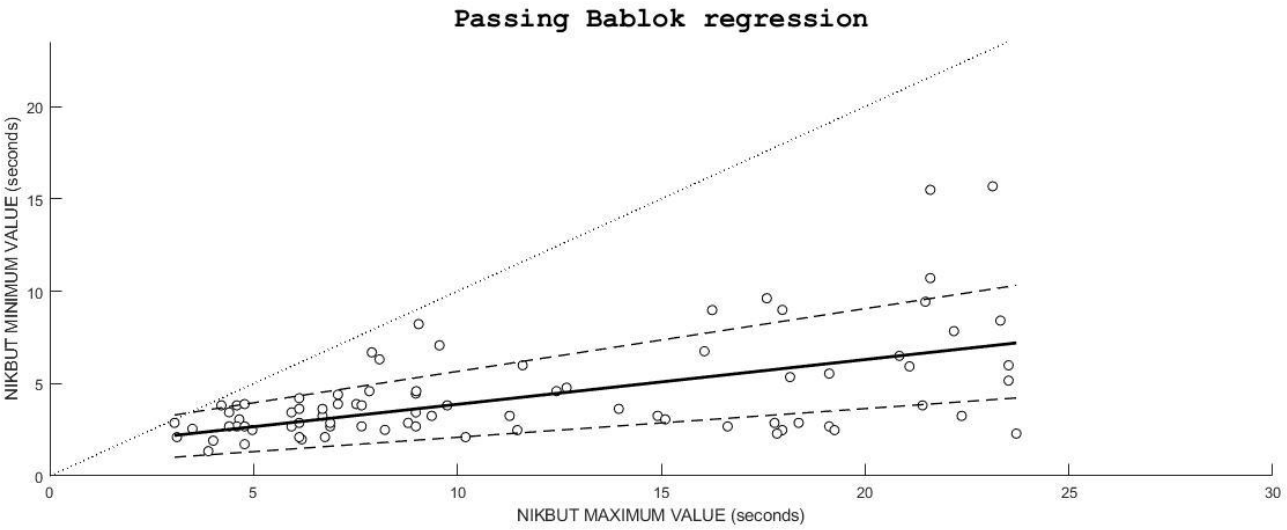

Fig. 5.5. *Passing–Bablok regression plots for the total sample. Observations (white dots), identity line (dotted line), regression line (solid line) and 95% confidence intervals for regression coefficients (dashed lines).*

Tendency of the repeated measurements

Generally, 36.25 % of subjects had a linear tendency to increase the NIKBUT value through the three repeated measurements, while 18.75% had a tendency to decrease the NIKBUT value. The NIKBUT was quite stable in 28.75 % of subjects with the three measurements within ± 2 seconds. Meantime, the other 16.25 % had random NIKBUT values without a tendency.

5.4 Discussion

Comparison of NIKBUT between groups for each classification

The present study evaluated the repeatability of NIKBUT obtained through the Keratograph 5M in a sample that was further classified into different groups. NIKBUT

measurements did not differ significantly between groups for each classification, even between healthy and DED subjects. This occurs because a subject is classified as having DED if he or she has symptoms and high osmolarity, a high osmolarity difference between eyes, a lower NIKBUT or ocular surface staining (Wolffsohn et al., 2017). Therefore, although the general tendency was that DED subjects had lower NIKBUT it ended up being not significant because not every subject classified as DED had to show low NIKBUT.

Repeatability assessment

Broadly, the three consecutive measurements did not manifest significant differences in the entire sample nor within each group. Contrary, Fernández et al. (2018) found significant differences between consecutive measurements for NIKBUT in a sample of both males and females. Despite no statistical differences between the three measurements, S_w, CoR and CoV scores were high for all groups.

Considering all classifications, S_w achieved values between 3.91 and 5.70, CoR between 10.82 and 15.80, and CoV between 55.21 % and 65.49 %. Given the fact that S_w, CoR and CoV denote good repeatability when their values are near 0 (Bland and Altman, 2010; Cerviño et al., 2015; McAlinden, Khadka and Pesudovs, 2015; Martínez-Albert, Esteve-Taboada and Montés-Micó, 2018; Martínez-Albert et al., 2018), the results obtained in this study denoted poor repeatability in all subgroups. The high variability could lead to classifying wrongly the subjects as having normal or low NIKBUT. Nonetheless, subjects with higher DED risk, such as females, elderly subjects and subjects with DED exhibited slightly better repeatability.

These results are in accordance with the outcomes found in another study (Tian et al., 2016). The authors found that NIKBUT was more reliable and repeatable in the DED group than in the healthy group (S_w = 5.24; CoV = 26.10 for the healthy group and S_w = 3.76; CoV = 23.54 for the DED group). This might be in part due to the fact that DED subjects had probably less reflex tearing than healthy subjects (Koh et al., 2014a). In accordance with these results, it is hypothesized that the small difference between measurements at lower NIKBUT scores might suggest that these subjects are more likely to suffer from DED. On the other hand, subjects with a high difference between NIKBUT measurements might be classified as having a lower chance of DED.

Markoulli et al. (2017) found similar results to those of the present study. The CoR of the first NIKBUT was 8.7 for both eyes, 12.4 for the right eye and 13.0 for the left eye. Cox, Nichols and Nichols (2015) also obtained a poor between-visit agreement, thus concluding that other dry eye measurements might be better indicators of DED. Conversely, another work (Tian et al., 2016) revealed moderate repeatability of NIKBUT measurements, where the CoV was 26.10 % and 23.54 % for healthy subjects and DED subjects, respectively. In addition, Dutta et al. (2019) reported moderate reproducibility of the device when the measurements were separated by two days (CoR = 11.9).

Passing-Bablok figures also confirmed these results. The regression lines for all groups were further away from the equality lines pointing out the high differences between the maximum and minimum NIKBUT measurements. The regression plots showed that lower repeatability was achieved in high NIKBUT values than in low

NIKBUT scores. Accordingly, the confidence interval broadened as NIKBUT increased from 10 seconds onwards not even containing all values within its range. Likewise, Cox, Nichols and Nichols (2015) and Markoulli et al. (2017) determined more variability in repeated measures at high NIKBUT values with Oculus Keratograph 4 and Keratograph 5M. Therefore, the repeatability was better at lower NIKBUT values.

NIKBUT is measured under unreal conditions since subjects are forced not to blink. Although non-invasive measurements induce less reflex tearing, the delayed blinking might induce reflex tearing and alter the following NIKBUT measurements in repeated measurements. In this regard, an increase in the meniscus curvature has been observed after the measurement of NIKBUT when using this minimally invasive method (Best, Drury and Wolffsohn, 2012; Wolffsohn et al., 2017). On top of that, it is relevant not to forget that NIKBUT has also intrinsic variability (Best, Drury and Wolffsohn, 2012; Wolffsohn et al., 2017).

In order to find out whether the low repeatability was achieved due to the device or due to the intrinsic variability of the tear film, subjects were classified into different categories depending on the tendency of the NIKBUT values. 36.25 % of the subjects had a linear tendency to increase the values, which might be related to reflex tearing because of the delayed blinking. 18.75 % had a linear tendency to decrease the scores, which could be related to the presence of debris or another artefact during the measurement. It has been reported that the presence of debris in the tear film, reflex tearing, and the tear break-up as streaks versus spots might be misinterpreted by the device as a tear film break-up and it might cause low repeatability (Arriola-Villalobos et

al., 2015; Cox, Nichols and Nichols, 2015). Meanwhile, 16.25 % had random values without a tendency. In this last case, the error could be caused by the device variability.

This study had some limitations to consider. Subjects with no previous diagnosis of DED were included. However, more of them had DED according to the TFOS DEWS II Diagnostic Methodology Report. In this work, clinical dry eye grading was not considered in the analysis. Moreover, the inherent limitations of the measurement such as the reflex tearing might have influenced the results. Future research on graded dry eye subjects is needed to assess whether the repeatability changes with the severity of the disease.

Overall, the present study has demonstrated low intraexaminer repeatability in NIKBUT measurement even when considering sex, age and DED diagnosis. Nevertheless, the low repeatability appears not to be only attributed to the device but also to the intrinsic variability of the tear film and inherent reflex tearing. The low NIKBUT repeatability can affect DED detection but it is important to note that this study did not evaluate the accuracy of the device in terms of DED diagnosis.

CHAPTER 6: Repeatability of ocular redness measurements obtained using Oculus Keratograph 5M

6. REPEATABILITY OF OCULAR REDNESS MEASUREMENTS OBTAINED USING OCULUS KERATOGRAPH 5M

Chapter 1 Introduction highlighted that Oculus Keratograph 5M is the most used tool to assess the ocular surface and nowadays it is also the most important advance in the assessment of bulbar redness (Wolffsohn et al., 2017). Ocular redness is an important sign to take into account in some inflammatory diseases (Wolffsohn et al., 2017), and therefore clinicians need reliable and repeatable metrics to diagnose, grade pathologies and evaluate the effectiveness of treatments for ocular inflammation (Wolffsohn and Purslow, 2003; Downie, Keller and Vingrys, 2015). Due to the relationship between ocular redness and DED, the present chapter aims to measure the repeatability of ocular redness measurements obtained using the Oculus Keratograph 5M.

6.1 Introduction

As explained in *Chapter 1 Introduction*, ocular surface inflammation was determined to be crucial for the inclusion of a patient in the DED definition (Craig et al., 2017). The most common clinical sign that is suggestive of ocular inflammation is conjunctival redness. This is a sign of conjunctival vascular dilatation due to a non-specific response of the ocular surface to different pathogenic stimuli (Papas, 2000; Baudouin et al., 2015; Downie, Keller and Vingrys, 2015; Wu et al., 2015; Wolffsohn et al., 2017). Therefore, bulbar redness assessment is a metric of interest in the analysis of DED and inflammation of the ocular surface (Wolffsohn et al., 2017). Conjunctival

redness is not only a sign of DED, it can also occur in some inflammatory diseases such as infective or allergic conjunctivitis, uveitis, scleritis, pterygium, chemical injury or abrasions (Cronau, Kankanala and Mauger, 2010; Wu et al., 2015; Craig et al., 2017; Wolffsohn et al., 2017; Pérez-Bartolomé et al., 2018; Portela et al., 2018). Furthermore, bulbar redness is also a common side effect described for the use of topical anti-glaucoma medications (Higginbotham et al., 2002; Jiménez et al., 2004).

Conjunctival redness can be detected through a slit-lamp or pen torch. It usually involves the image-based comparative scales for bulbar redness grading (Baudouin et al., 2015; Wu et al., 2015; Wolffsohn et al., 2017). Some standardised image-based grading scales have been developed to help clinicians quantify bulbar redness (Schulze, Hutchings and Simpson, 2011; Baudouin et al., 2015; Downie, Keller and Vingrys, 2015; Wolffsohn et al., 2017; Macchi et al., 2018). Despite these scales being quick and easy to use, subjective techniques depend on the examiner's ability, and therefore, it may increase the variability of results. For that reason, objective and quantitative image analysis methods have been developed to quantify bulbar redness (Papas, 2000; Fieguth and Simpson, 2002; Wolffsohn and Purslow, 2003; Wolffsohn, 2004; Peterson and Wolffsohn, 2007; Peterson and Wolffsohn, 2009; Amparo et al., 2013; Baudouin et al., 2015; Downie, Keller and Vingrys, 2015; Wu et al., 2015).

The Oculus Keratograph 5M is the most used tool to assess the ocular surface and nowadays it is also the most important advance in bulbar redness assessment (Wu et al., 2015; Sánchez-Brea et al., 2017; Wolffsohn et al., 2017). Nevertheless, the repeatability of this device in some measurements is still unclear (Best, Drury and

Wolffsohn, 2012; Hong et al., 2013; Tian et al., 2016; Pérez-Bartolomé et al., 2017; Fernández et al., 2018; Pérez-Bartolomé et al., 2018; Vidal-Rohr et al., 2018).

This study aims to assess whether the bulbar redness metric measured through the Oculus Keratograph 5M is a repeatable metric to analyse the redness of the ocular surface. To the authors' knowledge, this is the first study that analyses the repeatability of each metric of bulbar redness in a larger sample of healthy subjects. This topic is of high interest since ocular redness is an important sign to take into account in some inflammatory diseases (Wolffsohn et al., 2017), and therefore clinicians need reliable and repeatable metrics to diagnose, grade pathologies and evaluate the effectiveness of treatments for ocular inflammation (Wolffsohn and Purslow, 2003; Downie, Keller and Vingrys, 2015).

6.2 Methodology

A total of 78 healthy volunteers aged between 18 and 79 years were enrolled in this study. Subjects' written consent was obtained after the explanation of the protocol. The study was approved by the Ethics Committee of the University of Valencia and it was carried out following the tenets of the Declaration of Helsinki. Only the right eye was assessed due to the similar nature of both eyes. Subjects with any ocular or systemic disease were excluded from the study.

Evaluation procedure

Bulbar redness was measured three consecutive times for each subject through the Oculus Keratograph 5M (K5 M; Oculus GmbH, Wetzlar, Germany) by the same

masked observer in the same session (*Figure 6.1*). Measurements were taken as explained in *Chapter 3 General Methodology*. All images were taken in the same room and under the same conditions in terms of illumination, magnification and direction of fixation. Images without a proper detection of the eyelid and iris boundaries were not taken into account since they might alter the results.

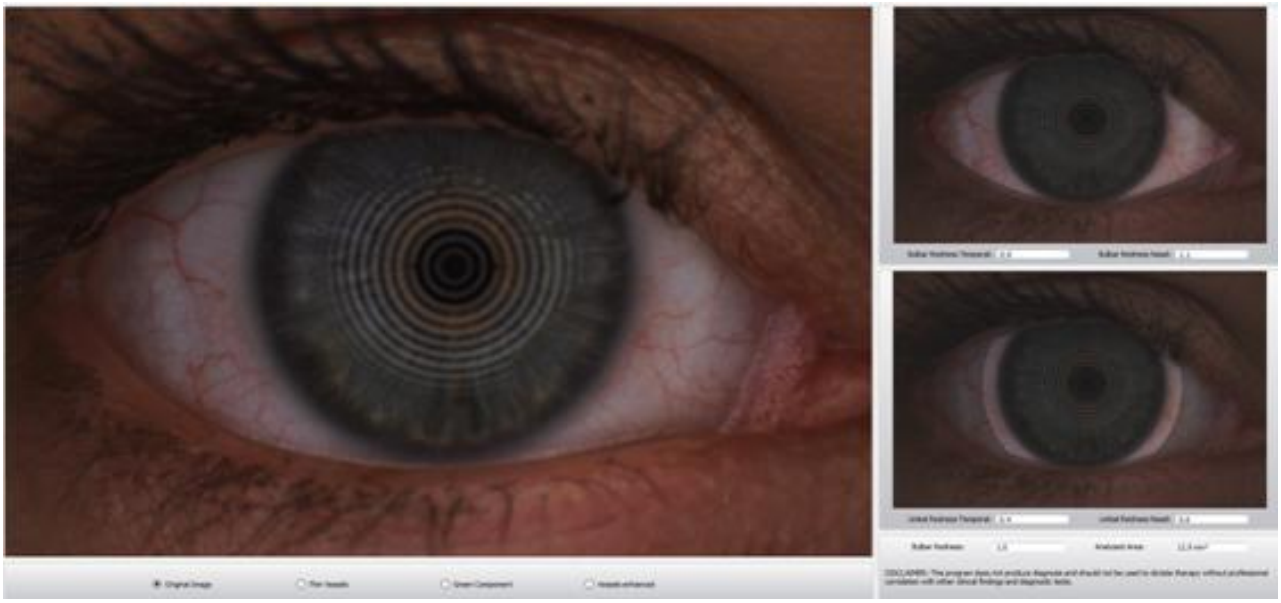

Fig. 6.1. *Screenshot of the output window of bulbar redness measurement through Keratograph 5M. The device provided five bulbar redness metrics: Temporal Bulbar Redness, Nasal Bulbar Redness, Temporal Limbal Redness, Nasal Limbal Redness and Total Bulbar Redness.*

Statistical analysis

Statistical analysis was performed using SPSS v26.0 for Windows (IBM Corp, Armonk, New York, USA), Microsoft Excel 2010 (Microsoft, Corp, Redmind, WA) and

Matlab R2019a (MathWorks, Natick, MA). Results were shown as the mean ± SD. The normality distribution of each metric was checked using the Kolmogorov-Smirnov test.

Statistically significant differences between the three consecutive measurements and between the five metrics were evaluated using the Friedman test. Moreover, a post-hoc analysis was carried out with the Bonferroni test to evaluate the differences between all pair group combinations (Martínez-Albert, Esteve-Taboada and Montés-Micó, 2018; Martínez-Albert et al., 2018). A p-value less than 0.05 was defined as statistically significant.

Repeatability was assessed by calculating the S_w, CoV and CoR, for each metric, as explained in *Chapter 3 General Methodology*. A graphic analysis was also carried out to compare the maximum and minimum redness values obtained. The Passing-Bablok regression method was applied using Matlab (Passing and Bablok regression by Andrea Padoan, Jan 16, 2010), as explained in *Chapter 3 General Methodology*.

6.3 Results

Seventy-eight eyes were included from 78 subjects of which 55 were women (70.5 %) and 23 were men (29.5 %). The mean age was 34.08 ± 21.94 years (ranging from 18 to 79 years). *Table 6.1* shows the main results obtained in each group.

Table 6.1. *Repeatability of ocular redness measurements in each metric.*

Metric	Redness score (Mean±SD)	Sw (max-min)	CoR (max-min)	CoV (%)	Comparative between the three measurements (p-value) Friedman	Post-hoc
Temporal bulbar redness	0.73±0.43	0.10	0.28	13.62	0.066[1]	
Nasal bulbar redness	0.83±0.49	0.14	0.37	16.30	0.101[1]	
Temporal limbal redness	0.41±0.36	0.07	0.18	16.20	0.005[1]*	Measurement 1-2=0.561[2] Measurement 1-3=0.013[2]* Measurement 2-3=0.07[2]
Nasal limbal redness	0.48±0.41	0.11	0.29	22.18	<0.001[1]*	Measurement 1-2=0.543[2] Measurement 1-3=0.001[2]* Measurement 2-3=0.002[2]*
Total bulbar redness	0.77±0.43	0.09	0.25	11.59	0.016[1]*	Measurement 1-2=0.623[2] Measurement 1-3=0.014[2]* Measurement 2-3=0.022[2]*

*(Where Sw: Within-subject standard deviation; CoV: Coefficient of variation; CoR: Repeatability coefficient; SD=Standard Deviation; [1] Friedman test; [2] Bonferroni test; * Statistically significant values)*

S_w, CoR and CoV manifested values near zero in all metrics. Friedman analysis did not show statistical differences between the three repeated measurements for temporal bulbar and nasal bulbar redness. However, statistical differences were found between the three measurements in the other measurements.

In temporal limbal redness, post-hoc analysis showed statistical differences between the first (0.40 ± 0.36) and the third measurement (0.43 ± 0.38), and between the second (0.40 ± 0.36) and the third. In nasal bulbar redness, statistical differences were found between the first (0.45 ± 0.40) and the third measurement (0.51 ± 0.45), as well as between the second (0.46 ± 0.41) and the third. In total bulbar redness, post-hoc analysis showed statistical differences between the first (0.75 ± 0.42) and the third measurement (0.79 ± 0.45), and between the second (0.76 ± 0.43) and the third.

Nevertheless, these differences were not clinically significant since the difference was lower than the precision of the device (0.1).

The slope and intercept of Passing-Bablok regressions are shown in *Table 6.2*. The 95% confidence interval contained the identity line in all metrics (*Figures 6.2, 6.3, 6.4, 6.5 and 6.6*).

Table 6.2. *Slope and intercept of Passing-Bablok regression for each metric.*

Metric	Slope	Intercept
Temporal Bulbar Redness	0.9310	0.0379
Nasal Bulbar Redness	0.8889	0.0333
Temporal Limbal Redness	0.9231	0.0231
Nasal Limbal Redness	0.8462	0
Total Bulbar Redness	1	-0.1

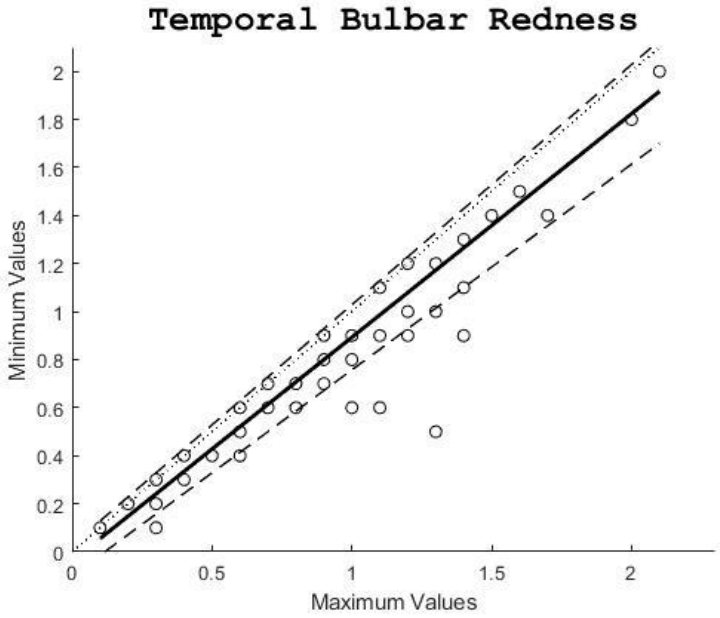

Fig. 6.2. *Passing–Bablok regression plots for temporal bulbar redness. Observations (white dots), identity line (dotted line), regression line (solid line) and 95% confidence intervals for regression coefficients (dashed lines).*

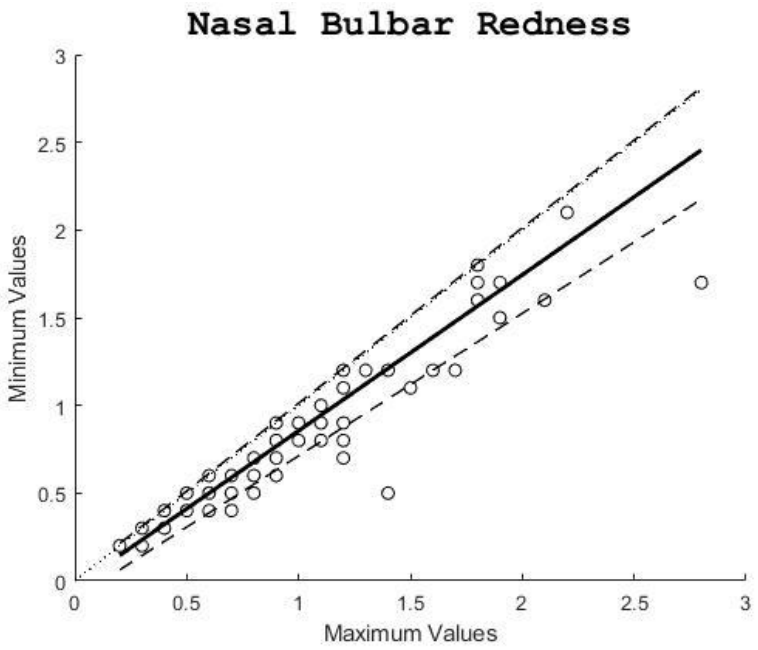

Fig. 6.3. *Passing–Bablok regression plots for nasal bulbar redness. Observations (white dots), identity line (dotted line), regression line (solid line) and 95% confidence intervals for regression coefficients (dashed lines).*

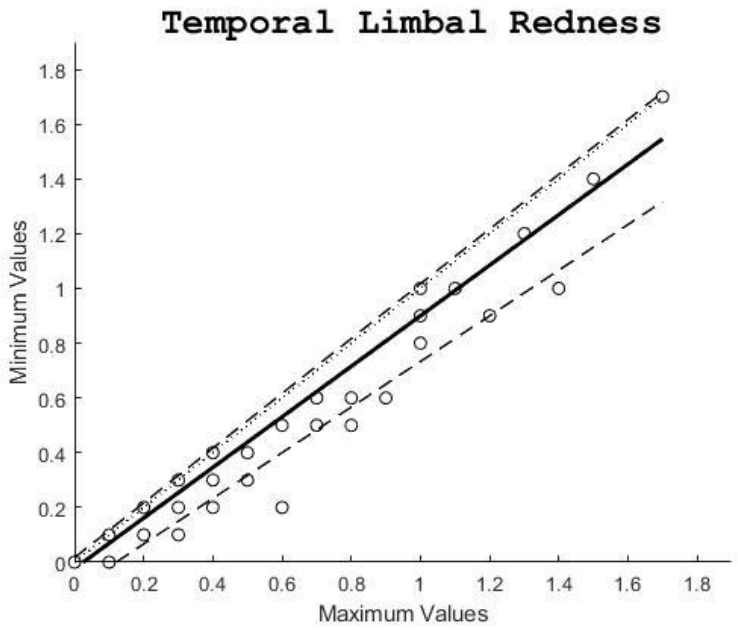

Fig. 6.4. *Passing–Bablok regression plots for temporal limbal redness. Observations (white dots), identity line (dotted line), regression line (solid line) and 95% confidence intervals for regression coefficients (dashed lines).*

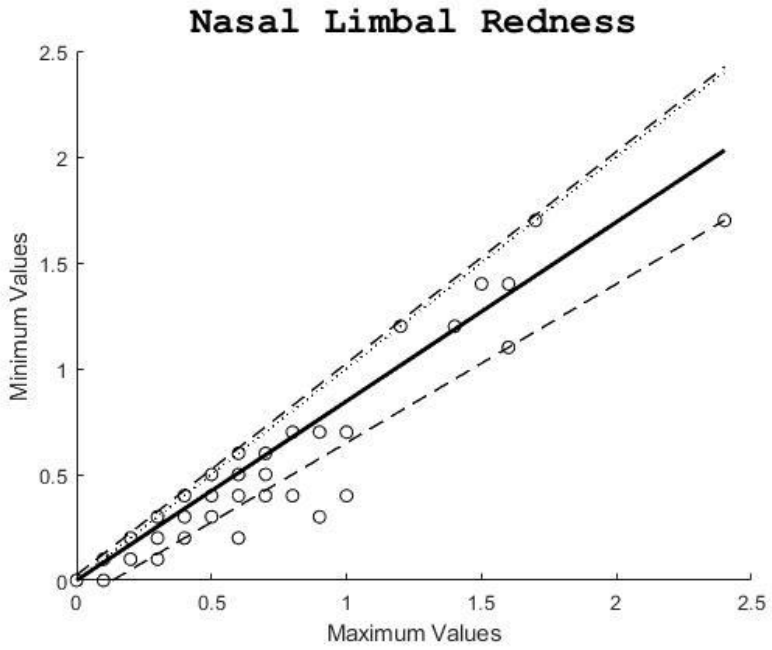

Fig. 6.5. *Passing–Bablok regression plots for nasal limbal redness. Observations (white dots), identity line (dotted line), regression line (solid line) and 95% confidence intervals for regression coefficients (dashed lines).*

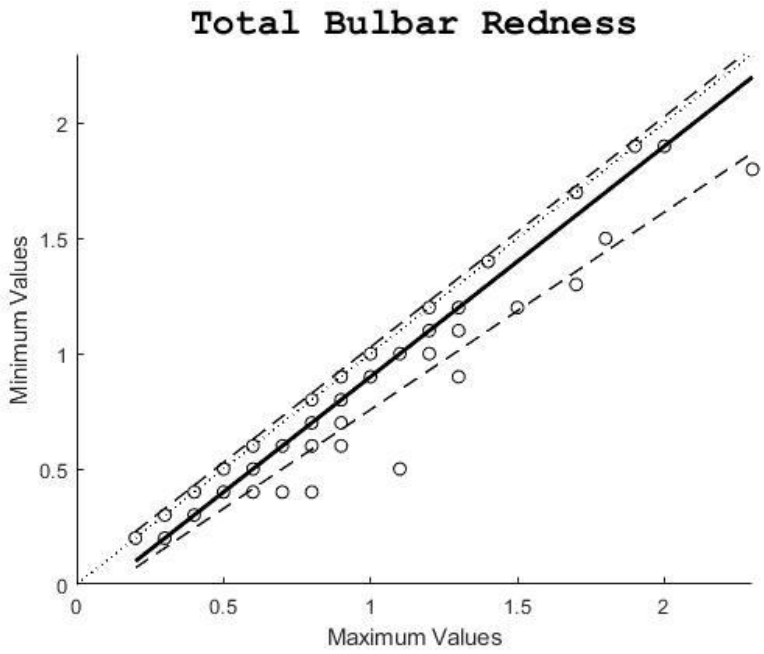

Fig. 6.6. *Passing–Bablok regression plots for total bulbar redness. Observations (white dots), identity line (dotted line), regression line (solid line) and 95% confidence intervals for regression coefficients (dashed lines).*

Differences between metrics

Table 6.3 shows the mean values of the three measurements for each metric. Friedman's test revealed statistical differences between them ($p < 0.001$). Post-hoc analysis manifested differences between all the measurements except for the comparison between total bulbar redness and temporal bulbar redness (*Table 6.4*). These differences were clinically significant between bulbar and limbal; and between nasal and temporal measurements.

Table 6.3. *Mean of the three bulbar redness measurements in each metric.*

Mean temporal bulbar redness (Mean±SD)	Mean nasal bulbar redness (Mean±SD)	Mean temporal limbal redness (Mean±SD)	Mean nasal limbal redness (Mean±SD)	Mean total bulbar redness (Mean±SD)
0.73±0.43	0.83±0.50	0.42±0.36	0.48±0.42	0.77±0.43

(Where SD: Standard Deviation)

Table 6.4. *Comparison between mean bulbar redness measurements.*

Comparison	Significance level
Nasal Limbal - Temporal Limbal	0.015[1]*
Temporal Bulbar -Temporal Limbal	<0.001[1]*
Nasal Bulbar -Temporal Limbal	<0.001[1]*
Temporal Bulbar -Nasal Limbal	<0.001[1]*
Nasal Bulbar - Nasal Limbal	<0.001[1]*
Nasal Bulbar – Temporal Bulbar	0.022[1]*
Total Redness – Temporal Limbal	<0.001[1]*
Total Redness – Nasal Limbal	<0.001[1]*
Total Redness – Temporal Bulbar	0.101[1]
Total Redness – Nasal Bulbar	0.008[1]*

*(Where [1] Bonferroni test; * Statistically significant values)*

6.4 Discussion

The present study was carried out to assess the repeatability of the different ocular redness metrics obtained using the Keratograph 5M**.** Results denoted acceptable repeatability in all metrics since S_w, CoR and CoV indicate good repeatability when their values are near zero (Bland and Altman, 2010; Cerviño et al., 2015; McAlinden, Khadka and Pesudovs, 2015; Martínez-Albert et al., 2018; Martínez-Albert, Esteve-Taboada and Montés-Micó, 2018). Therefore, the variability of ocular redness metrics is low, which might ensure the proper classification of ocular redness in an objective way.

Wu et al. (2015) also found acceptable repeatability with a CoR of 13.924, a result slightly higher than in this study. The bulbar redness score had the highest reproducibility in comparison with other grading scales (Institute for Eye Research, Efron and Validated Bulbar Redness). In comparison with the present study, the sample was smaller and the authors only assessed the total bulbar redness score. However, these results contrast sharply with the larger sample study of Pérez-Bartolomé et al. (2018), who found poor agreement in Bland-Altman analysis between objective and subjective techniques. They concluded by saying that Keratograph 5M overestimates the scores in comparison with subjective grading scales. The best agreement between objective and subjective methods was found in limbal scores. Differences between both studies might be because subjects in the second one were in treatment with anti-glaucoma drops; therefore, both populations were not comparable. Further research is needed to clarify this lack of agreement between studies.

Passing-Bablok plots also showed acceptable repeatability between the maximum and minimum values for all metrics since overall values were within the range of 95% confidence interval, which in turn contained the value 0 (Passing and Bablok, 1983; Martínez-Albert, Esteve-Taboada and Montés-Micó, 2018). Moreover, all regression lines were also near the equality lines and there were no high differences between the slope and value 1. The highest repeatability was achieved for total bulbar redness since the slope was 1; thus, only systematic errors caused by the intercept might alter the results. In the other metrics, the repeatability was poorer when the ocular redness was higher. Even in these cases, the repeatability was acceptable.

In temporal limbal, nasal limbal and total bulbar redness, Friedman's analysis revealed statistical differences between the third measurement and the first two, the third being slightly higher. This fact could be caused by the time the subject was placed on the device with the light on. Although this time was relatively short, it might have caused a slight non-clinically significant eye redness. Moreover, the difference was lower than the precision of the device. Keratograph 5M uses white light to carry out bulbar redness measurement, but if infrared light were used it may avoid the alteration of ocular surface parameters or the disturbance of tear film. Consequently, the reliability of measurements would get better.

When the different mean ocular redness values were compared, the Friedman test showed statistical differences between all the metrics except for total redness and temporal bulbar redness. Bulbar measurements had clinical higher values than limbal ones, and total redness was clinically higher than limbal measurements. Meanwhile, nasal measurements were clinically higher than temporal. The study of the different zones is relevant to certain pathologies. For instance, the analysis of the limbal zone helps in the classification of ciliary injection, which is important for follow-up in cases of uveitis (Pérez-Bartolomé et al., 2017; Wolffsohn et al., 2017). To the authors' knowledge, this is the first study that compares the different zones in Keratograph 5M. Murphy et al. (2006) analysed the redness using a grading scale. They found that temporal and nasal quadrants were redder than superior and inferior, however, in this case, the results did not reveal differences between temporal and nasal zones. Pult et al. (2008a) found similar results with the same scale. Bulbar and limbal quadrants were

significantly correlated. In accordance with the results of this study, the bulbar region had higher scores than the limbal.

Keratograph 5M provides objective and non-invasive metric that is more repeatable than previous grading scales since it does not depend on the examiner's ability. Thus, it provides information about the degree of ocular redness which might help clinicians in the diagnosis and treatment of different pathologies related to inflammation. Moreover, images provide information that might help clinicians to compare visits, or communicate better with subjects (Best, Drury and Wolffsohn, 2012). Another benefit of this device is that its scores are continuous variables. Thus, clinicians can accurately grade redness, instead of choosing between two categories of a grading scale when an intermediate score is needed (Pérez-Bartolomé et al., 2018). However, the analysis should be subject to interpretation by a clinician. Clinicians ought to judge which measurements have been taken properly since in some cases software might not detect properly the eyelid and iris boundaries. Furthermore, the major reported drawback of Keratograph 5M is that it is unable to differentiate among scleral, episcleral or conjunctival redness (Peterson and Wolffsohn, 2007; Pérez-Bartolomé et al., 2018).

The present study has some limitations that must be taken into account. Firstly, the repeatability might change depending on the level of ocular inflammation. The clinical influence of inflammation grading in the analysis was not assessed. Moreover, although subjects included in this study were healthy and did not have a previous DED diagnosis, tear film parameters were not evaluated and some subjects might be

included as DED subjects according to the criteria reported in the TFOS DEWS II Diagnostic Methodology Report (Wolffsohn et al., 2017). Furthermore, images in which eyelid boundaries were not properly detected were removed from the analysis. If it had not been carried out, the repeatability might be lower. Finally, the inherent limitations of the device such as the white light might have influenced the results, especially in the third measurement. Future research with a larger sample is needed to assess whether the repeatability changes depending on different factors such as sex, age, the severity of ocular surface inflammation or different DED grades. At the time of writing, the exact nature of the image processing software of this device has not been disclosed by the manufacturer.

Overall, the Keratograph 5M is a useful and repeatable device to assess ocular surface redness in an objective and non-invasive way. All bulbar redness metrics provided objective values with acceptable repeatability, which might help clinicians in the diagnoses and treatment of different pathologies related to ocular surface inflammation, such as DED and uveitis. However, this device should not replace a clinical examination when an accurate evaluation is needed. Finally, it is important to take into account that this is a precision study and it does not analyse the accuracy of the device in terms of diagnosis.

CHAPTER 7: Evaluation of the MGDRx EyeBag treatment in young and aged subjects with symptoms of ocular dryness

7. EVALUATION OF THE MGDRX EYEBAG TREATMENT IN YOUNG AND AGED SUBJECTS WITH SYMPTOMS OF OCULAR DRYNESS

MGDRx thermal EyeBag is one of the most used tools for the treatment of MGD-related evaporative DED (Bilkhu, Naroo and Wolffsohn, 2014a; Bilkhu, Naroo and Wolffsohn, 2014b; Wang et al., 2015; Wang et al., 2019d). In the present chapter changes in the ocular surface will be assessed using the Keratograph 5M after MGDRx thermal EyeBag application. Since the Keratograph 5M is one of the most common tools used to objectively assess the ocular surface (Wolffsohn et al., 2017), knowing its usefulness in the follow-up of treatments is relevant. Therefore, this chapter aims to evaluate the association between the application of MGDRx thermal EyeBags and ocular surface signs and symptoms in young and aged subjects.

7.1 Introduction

In *Chapter 1 Introduction*, it was explained that obstructive MGD is the most commonly observed type of MGD (Arita et al., 2009b; Geerling et al., 2017) and its treatment has the goal of increasing the flow of meibomian glands and, therefore, improving tear film stability. Warming therapy is considered to be the mainstay treatment for MGD (Knop et al., 2011; Bilkhu, Naroo and Wolffsohn, 2014a; Bilkhu, Naroo and Wolffsohn, 2014b; Murakami, Blackie and Korb, 2015; Tan et al., 2018; Ngo, Srinivasan and Jones, 2019). Some authors have reported greater tear film stability and increased tear film lipid layer after thermal treatment (Bilkhu, Naroo and Wolffsohn, 2014b; Sim et al., 2014; Wang et al., 2015; Tan et al., 2018).

Different devices have been developed in order to provide moist or dry heat to the eyelids (Friedland et al., 2011; Lane et al., 2012; Purslow, 2013; Qiao and Yan, 2013; Arita et al., 2015; Villani et al., 2015; Tan et al., 2018). However, the efficacy depends on some inherent issues such as insufficient heating, duration and frequency of use (Jones et al., 2017). MGDRx thermal EyeBag is one of the most used tools. Previous studies have found that MGDRx thermal EyeBag is a safe and effective tool for the treatment of MGD-related evaporative DED in young subjects (Bilkhu, Naroo and Wolffsohn, 2014a; Bilkhu, Naroo and Wolffsohn, 2014b; Wang et al., 2015; Wang et al., 2019d).

This study aims to evaluate the association between the application of MGDRx thermal EyeBags and ocular surface signs and symptoms in young and aged subjects, thus enabling the comparison between groups. This topic is of high interest since safe and effective treatments must be chosen by clinicians to treat pathologies related to the ocular surface, being age a possible relevant factor to take into account when treatments are chosen. Furthermore, as MGD and DED are more prevalent in aged subjects, thus knowing the effect of the device on this population is of great importance.

7.2 Methodology

A total of 60 volunteers participated in this study. Subjects between 18 and 31 years old were included in the young group while those between 61 and 90 years were included in the aged group. Written consent was obtained from each subject after the explanation of the purpose and protocol of the study. The study protocol was

approved by the Ethics Committee of the University of Valencia and it was carried out in accordance with the tenets of the Declaration of Helsinki. Only the right eye was assessed to avoid subjects' data duplication. Exclusion criteria included the presence of any systemic or ocular disease, previous DED diagnosis or medications with known eye effects. Recruitment was carried out by advertisement within University dissemination channels, campus personnel and students, as well as in local public entities in nearby towns.

Measurements

Measurements were carried out using the Oculus Keratograph 5M (Oculus Optikgeraete GmbH, Wetzlar, Germany) by the same researcher. Measurements were performed in accordance with the recommendations of the TFOS DEWS II Diagnostic Methodology Report (Wolffsohn et al., 2017). They were conducted in the following order: OSDI, DEQ-5, bulbar redness, TMH, lipid layer assessment, NIKBUT, meibomian gland secretion, meibum quality, number of obstructed glands, telangiectasia and meibography in the upper and lower eyelids. Topography was also measured in order to control for corneal shape changes after treatment with the thermal bags. Different measurements were recorded: K1, Axe1, K2 and Axe2, which are the curvature radius and axes of the principal meridians; Km, which is the mean curvature radius; and corneal astigmatism.

Bulbar redness, NIKBUT, TMH, lipid layer thickness and meibomian gland drop-out were assessed as explained in *Chapter 3 General Methodology*. Telangiectasia was graded according to the following scale (Foulks and Bron, 2003): 0=none

telangiectasia; 1=one telangiectasia; 2=between 2 and 5 telangiectasias; and 3=more than 5 telangiectasias. Meibomian gland secretion and meibum quality from the central 8 meibomian glands on the lower and upper eyelid were also graded on a point scale (Foulks and Bron, 2003) as follows. Secretion: 0=easily expressed; 1=expressed with mild pressure; 2=expressed with more than moderate pressure; 3=not expressed. Meibum quality: 0=clear meibum; 1=cloudy; 2=cloudy particulate; and 3 toothpaste-like.

Intervention

MGDRx EyeBag (The EyeBag Company Ltd, Halifax, UK) is a commercially available eyelid warming device with a simple design (Bilkhu, Naroo and Wolffsohn, 2014a; Bilkhu, Naroo and Wolffsohn, 2014b; Wang et al., 2015; Jones et al., 2017; Ngo, Srinivasan and Jones, 2019). The product consists of a cotton/silk pouch filled with flax and linseed and it is designed to retain heat aiding in meibum melting (Wang et al., 2015; Jones et al., 2017; Ngo, Srinivasan and Jones, 2019).

At the end of the baseline visit, subjects were provided with the thermal bag and detailed written instructions on how to use it at home. Despite no history of ocular pathology, only subjects with a positive score in at least one of these questionnaires (OSDI ≥ 13, DEQ-5 ≥ 6) and first NIKBUT lower than 10 seconds were finally included in the study, in accordance with the TFOS DEWS II Diagnostic Methodology Report (Wolffsohn et al., 2017). The thermal bag was self-applied every day for 2 weeks (heated previously 30 seconds in a microwave on full power) by subjects twice a day for 10 minutes in both eyes. Subjects were instructed to use the thermal bag at the

same times every day, letting 12 hours between applications. They were also instructed to conduct a manual massage immediately after the 10 minutes have elapsed, as recommended in the manufacturer's instructions (Wang et al., 2019d). After 2 weeks, the same procedure was carried out again. The second visit was performed at the same hour as the first one, being all subjects assessed when the same amount of time from the last application of thermal bag had passed.

Moreover, subjects were asked to grade the compliance of the treatment (1=no treatment; 2=rarely; 3=sometimes; 4=almost every time; and 5=every time) and the improvement after two weeks (1=worse; 2=no change; 3=slight improvement; 4=some improvement; and 5=significant improvement). Changes related to health or medication were also documented.

Statistical analysis

Statistical analysis was carried out using SPSS v26.0 for Windows (IBM Corp, Armonk, New York, USA). Results were displayed as mean ± SD. The normal distribution of the values for each group was assessed by means of the Shapiro-Wilk test.

Differences between visits for each group were assessed with the paired t-test or Wilcoxon signed-rank test, depending on the sample distribution. Moreover, the differences in the thermal bag treatment as a function of age were assessed by means of a mixed ANOVA. The association between gender and age groups was determined using the chi-square test. Finally, the Mann-Whitney U test was used to evaluate the

differences in treatment compliance and subjective improvement scores between age groups. A p-value less than 0.05 was considered statistically significant.

7.3 Results

Sixty eyes from 60 volunteers were included, who were then grouped into the young group (18 females and 12 males) and the aged group (16 females and 14 males). The Chi-square test did not show a statistical association between gender and age groups ($p = 0.602$). Mean age was 23.95 ± 3.94 (ranging from 18 to 31 years old) and 77.97 ± 8.11 (ranging from 61 to 90 years old) in young and aged subjects, respectively.

Differences between visits for each age group

Table 7.1 shows the main results obtained for each group at baseline and after MGDRx treatment. Statistical analysis showed significantly better values in meibum quality score, gland obstruction score, telangiectasia score, and both questionnaires after treatment for aged subjects. In comparison, the young group showed an improvement in first NIKBUT, mean NIKBUT, lipid layer score, upper lid drop-out percentage, OSDI and DEQ-5 scores over the two week treatment period. No adverse event was reported by any subject for the duration of the treatment. No significant differences were found in topographical measurements (curvature radius and axes of the principal meridians, the mean curvature radius, and corneal astigmatism) between visits ($p > 0.05$).

Table 7.1. *Mean values for each metric before and after the treatment.*

Measurement	Visit	Elderly subjects	Significance level	Young subjects	Significance level
First NIKBUT (Mean ± SD)	1	5.01±2.63	0.322[1]	6.39±2.06	0.003[2]*
	2	5.75±3.29		10.44±5.81	
Mean NIKBUT (Mean ± SD)	1	9.42±5.48	0.760[1]	9.44±3.70	0.001[2]*
	2	9.72±6.02		12.66±3.94	
Tear meniscus height (Mean ± SD)	1	0.35±0.18	0.672[2]	0.20±0.08	0.778[2]
	2	0.38±0.18		0.19±0.05	
Bulbar temporal redness score (Mean ± SD)	1	1.23±0.27	0.235[1]	0.61±0.32	0.657[1]
	2	1.35±0.41		0.56±0.28	
Bulbar nasal redness score (Mean ± SD)	1	1.35±0.53	0.291[2]	0.69±0.40	0.536[2]
	2	1.49±0.50		0.79±0.57	
Limbal temporal redness score (Mean ± SD)	1	0.82±0.31	0.154[2]	0.29±0.26	0.685[2]
	2	0.99±0.52		0.28±0.24	
Limbal nasal redness score (Mean ± SD)	1	0.90±0.35	0.413[1]	0.31±0.24	0.498[2]
	2	0.98±0.44		0.26±0.18	
Total bulbar redness score (Mean ± SD)	1	1.29±0.35	0.499[2]	0.66±0.32	0.383[1]
	2	1.37±0.38		0.59±0.25	
Upper eyelid gland drop-out (Mean ± SD)	1	47.21±13.56	0.096[1]	22.28±7.14	0.003[1]*
	2	46.56±11.19		19.44±7.39	
Lower eyelid gland drop-out (Mean ± SD)	1	37.85±11.13	0.470[1]	16.72±5.38	0.709[2]
	2	38.57±11.98		16.36±5.02	
Lipid layer thickness score (Median, Interquartile Range)	1	3; 2-4	0.134[2]	1.5; 1-2	0.004[2]*
	2	3; 2-4		2; 1.75-3	
Meibomian gland secretion score (Median, Interquartile Range)	1	0; 0-0	-	0; 0-1	0.157[2]
	2	0; 0-0		0; 0-0	
Meibum quality score (Median, Interquartile Range)	1	0; 0-0.75	0.008[2]*	0; 0-0	-
	2	0; 0-0		0; 0-0	
Meibomian gland obstruction score (Median, Interquartile Range)	1	0; 0-1	0.046[2]*	0; 0-0	0.317[2]
	2	0; 0-1		0; 0-0	
Telangiectasia score (Median, Interquartile Range)	1	2; 1-3	0.037[2]*	0; 0-1	0.157[2]
	2	1; 0-2		0; 0-1	
Ocular Surface Disease Index (Mean ± SD)	1	33.52±21.96	0.001[2]*	23.81±16.75	0.004[2]*
	2	17.39±16.50		12.74±8.70	
Dry Eye Questionnaire-5 (Mean ± SD)	1	10.11±5.40	0.008[2]*	11.83±3.50	<0.001[1]*
	2	7.00±4.98		7.23±4.14	
K1 (Mean ± SD)	1	7.63±0.08	0.191[2]	7.84±0.22	0.390[1]
	2	7.66±0.22		7.84±0.21	
Axe1 (Mean ± SD)	1	60.05±76.87	0.147[2]	75.36±80.32	0.398[2]
	2	67.95±73.85		75.46±82.67	
K2 (Mean ± SD)	1	7.77±0.10	0.168[a]	7.64±0.22	0.403[1]
	2	7.73±0.22		7.64±0.21	
Axe2 (Mean ± SD)	1	105.05±22.17	0.147[1]	94.92±13.91	0.173[2]
	2	100.13±20.58		93.66±12.82	
KM (Mean ± SD)	1	7.70±0.07	0.152[1]	7.74±0.21	0.396[1]
	2	7.70±0.20		7.74±0.21	
Corneal astigmatism (Mean ± SD)	1	0.95±0.47	0.317[2]	1.17±0.61	0.198[1]
	2	0.98±0.58		1.04±0.65	

*(Where D: Dioptrías; K1 and K2: curvature radius of the principal meridians; Km: mean curvature radius; mm: millimetres; NIKBUT: Non-invasive break-up time; SD: Standard deviation; [1]: paired sample t-test; [2]: Wilcoxon signed-rank test; *: Statistically significant)*

After treatment, 35.00 % of subjects had a first NIKBUT higher than 10 seconds (33.33 % of aged and 36.67 % of young subjects), and 36.67 % did not have dry eye symptoms in any questionnaire (36.67 % of the aged subjects and 36.67 % of young subjects).

At baseline, there were no statistically significant differences between young and aged subjects in NIKBUT, meibomian gland secretion score, gland obstruction score, OSDI and DEQ-5 ($p > 0.05$).

Differences in therapy outcomes depending on age group

Mixed ANOVA analysis (*Table 7.2*) was performed to evidence which parameters improved after thermal bag application, without taking into account baseline differences. It showed statistically significant differences between age groups for several parameters: first NIKBUT, TMH, redness score (bulbar and limbal), gland drop-out (upper and lower lid), lipid layer, meibum quality, gland obstruction score and telangiectasia. However, some of these parameters had baseline differences due to subjects' age. The interaction between age groups and visits had a significant effect on first NIKBUT ($p = 0.033$), mean NIKBUT ($p = 0.017$), lipid layer thickness score ($p = 0.004$) and meibum quality score ($p = 0.004$). This evidences that despite the

differences in this parameter between age groups at baseline, the treatment acted differently because of the subjects' age.

Table 7.2. *Analysis of the interaction between age and visit for each dependent variable through a mixed ANOVA.*

Measurement	Within-Subjects Effects INTERACTION BETWEEN VISIT AND AGE GROUP (Significance level)	Between-Subjects Effects AGE GROUP (Significance level)
First NIKBUT	0.033*	0.002*
Mean NIKBUT	0.017*	0.351
Tear meniscus height	0.399	<0.001*
Bulbar temporal redness score	0.145	<0.001*
Bulbar nasal redness score	0.946	<0.001*
Limbal temporal redness score	0.194	<0.001*
Limbal nasal redness score	0.262	<0.001*
Total bulbar redness score	0.346	<0.001*
Upper eyelid gland drop-out	0.819	<0.001*
Lower eyelid gland drop-out	0.476	<0.001*
Lipid layer thickness score	0.004*	0.002*
Meibomian gland secretion score	0.604	0.404
Meibum quality score	0.004*	0.004*
Meibomian gland obstruction score	0.113	0.036*
Telangiectasia score	0.068	<0.001*
Ocular Surface Disease Index	0.431	0.120
Dry Eye Questionnaire-5	0.235	0.362

*(Where NIKBUT: Non-invasive break-up time; *: Statistically significant)*

Treatment compliance and subjective improvement

70.0 % of aged subjects reported using the thermal bag "every time", 26.7 % "almost every time" and 3.3 % "sometimes". Moreover, 53.3 % of them noticed "a significant improvement" after treatment, 20.0 % "some improvement", 3.3 % "slight improvement" and 23.3 % did not notice any change. On the other hand, 30.0 % of young subjects said they used the device "every time", 56.7 % "almost every time" and 13.3 % "sometimes". Furthermore, 66.7 % of them noticed "a significant improvement" after the treatment, 23.3 % "some improvement" and 10.0 % did not

notice any change. None of them reported worse comfort after treatment. Mann-Whitney U test revealed higher treatment compliance in the aged group than in the younger one ($p = 0.002$). However, no statistical differences were found in subjective improvement ($p = 0.097$).

7.4 Discussion

The present study assessed the association between MGDRx EyeBag and tear film parameters according to age. Both aged and young subjects were assessed to find the possible differences in the treatment between groups. Different studies have already confirmed the effectiveness of thermal treatment in young subjects (Friedland et al., 2011; Lane et al., 2012; Purslow, 2013; Qiao and Yan, 2013; Bilkhu, Naroo and Wolffsohn, 2014a; Arita et al., 2015; Villani et al., 2015). Improvements in meibomian glands' area (Bilkhu, Naroo and Wolffsohn, 2014b; Arita et al., 2015), tear film stability (Bilkhu, Naroo and Wolffsohn, 2014a; Bilkhu, Naroo and Wolffsohn, 2014b; Sim et al., 2014; Arita et al., 2015; Wang et al., 2015; Tan et al., 2018; Wang et al., 2019d), ocular symptoms (Bilkhu, Naroo and Wolffsohn, 2014b; Ngo, Srinivasan and Jones, 2019) or lipid layer thickness (Bilkhu, Naroo and Wolffsohn, 2014a; Bilkhu, Naroo and Wolffsohn, 2014b; Sim et al., 2014; Wang et al., 2015; Tan et al., 2018; Wang et al., 2019d) have been reported.

Differences between visits for each age group

Several authors have confirmed that thermal devices retain heat more effectively in comparison with a face towel or warm compresses, thus leading to greater

improvement after treatment (Friedland et al., 2011; Lane et al., 2012; Purslow, 2013; Qiao and Yan, 2013; Arita et al., 2015; Villani et al., 2015; Tan et al., 2018). The meibum in MGD subjects has an altered chemical structure, increasing its melting point compared to the 32ºC physiological value (Qiao and Yan, 2013). It has been suggested that reaching temperatures over 40ºC might be required to melt meibum properly, however, meibomian lipids start to spread at 35ºC (Friedland et al., 2011). Bitton, Lacroix and Léger (2016) demonstrated the effectiveness of MGDRx EyeBag in providing stable heat retention for 12 minutes. The peak temperature was 37.6ºC at 2 minutes and 36.8ºC at minute 12. It has been reported that the MGDRx EyeBag surface temperature profile displayed higher uniformity, slower cooling, making it more effective in raising ocular temperature than other warming devices (Wang, Gokul and Craig, 2015).

The present results are consistent with previous studies, demonstrating that regular heating melts the abnormal meibum. Warming therapy liquefies the thickened viscous meibum and increases tear film stability (Knop et al., 2011; Bilkhu, Naroo and Wolffsohn, 2014a; Wang et al., 2015). Thus, positive correlations between tear film stability and lipid layer thickness, and the meibum quantity and tear film stability have been reported (Nichols et al., 2002b; Bron and Tiffany, 2004). In the present study, a statistically and clinically significant improvement in symptoms, NIKBUT, lipid layer score and upper lid drop-out percentage was found in young subjects (*Table 7.1*). These results are in accordance with a previous study published about young patients (Bilkhu, Naroo and Wolffsohn, 2014b), where subjects noticed an improvement in ocular comfort, meibomian gland drop-out, osmolarity, lipid layer thickness, tear film

stability, TMH and conjunctival hyperaemia after two weeks. Differences in TMH were not found in the present study since the thermal bag affects the lipid layer, responsible for tear film quality, and therefore does not affect tear film quantity. Longer treatment time might cause a chain reaction improving meibum, which in turn might restore the lipid layer, increase TMH and reduce bulbar redness (Bilkhu, Naroo and Wolffsohn, 2014b).

Wang et al. (2019d) also found an increase in the lipid layer and tear film stability after the application of the same thermal bag as in the present study. In this case, they did not report any change in TMH, conjunctival hyperaemia or meibomian gland drop-out. Bilkhu, Naroo and Wolffsohn (2014a) and Wang et al. (2015) also found an increase in tear film stability and lipid layer thickness in healthy subjects and in subjects with mild-to-moderate dry eye symptoms. Nevertheless, Ngo, Srinivasan and Jones (2019) only found a reduction in symptoms, while meibomian gland score and tear film stability showed no statistically significant changes after the use of the thermal bag for 4 weeks. In contrast, no changes in lipid layer or NIKBUT signs were found in aged subjects in the present study. They had clinically better values in questionnaire scores, meibum quality, gland obstruction, and telangiectasia (*Table 7.1*).

After treatment, approximately a third of the sample had a NIKBUT higher than 10 seconds and negative symptomatology in all questionnaires. This improvement might affect DED and MGD diagnosis according to TFOS DEWS II Diagnostic Methodology

Report and the International Workshop on Meibomian Gland Dysfunction Diagnosis Report (Tomlinson et al., 2011; Wolffsohn et al., 2017).

Differences in therapy outcomes depending on age group

When young and aged groups were compared, the effect of age was found in first NIKBUT, TMH, redness score (bulbar and limbal), drop-out (upper and lower lid), lipid layer, meibum quality, gland obstruction score and telangiectasia (*Table 7.2*). Nevertheless, some of these parameters had baseline differences because of the subjects' age.

Mixed ANOVA revealed that the age of subjects affected the results of the treatment regarding NIKBUT and lipid layer thickness, where greater improvement was found in young subjects. Therefore, despite the differences in the lipid layer between age groups at baseline, the treatment acted differently because of the subjects' age. This result was expected since aged subjects had higher levels of meibomian glands atrophy.

A possible explanation could be that aged subjects need a longer treatment time in order for an improvement in NIKBUT to be noticed. Moreover, DED is a pathology in which sometimes there is no correlation between signs and symptoms (Wolffsohn et al., 2017). On the other hand, meibomian glands quality, obstruction and telangiectasia might have only improved in the aged population since the young subjects had normal values at baseline.

Ngo, Srinivasan and Jones (2019) argued that it is currently unclear whether or not atrophied glands may benefit from the thermal bag treatment. The outcomes of this study suggest that not only atrophied meibomian glands with a higher drop-out are able to benefit from thermal treatment since the young population had a low degree of drop-out statistically significant from the aged group ($p < 0.001$).

Changes in topography

Warming therapy has been suggested to cause corneal deformation and visual acuity loss because of corneal temperature (McMonnies, Korb and Blackie, 2012). However, the present study confirmed dry eye signs and symptoms were improved after the application of thermal bags in a safe way since no differences were found in topographical measurements between visits in both populations. No case of corneal deformation was reported in two weeks follow-up. Bilkhu, Naroo and Wolffsohn (2014b) and Sim et al. (2014) confirmed these results since corneal topography and visual acuity were unaffected ($p > 0.05$). They suggested that corneal and visual changes may only occur during an unusually long and intense treatment therapy.

Treatment compliance and subjective improvement

Due to the importance of adherence to medical therapy, this study also attempted to quantify the level of treatment compliance. In spite of the treatment compliance being significantly higher in the aged group than in the younger one, there were no differences in the improvement score between groups. Thus, this fact also might

confirm the hypothesis that improvement in young subjects might be faster than in the aged ones.

The promising outcomes found in this study, in young and aged subjects, together with the fact that the thermal bag is a portable device, make it suitable for use in a variety of settings (Wang et al., 2015). The thermal bag is simple to heat and handle in comparison with traditional moist warm compresses which are reported to require an intensive protocol in order to optimize the treatment (Bilkhu, Naroo and Wolffsohn, 2014a). Thus, they are time-consuming and labour intensive and might lead to subject compliance problems in some cases (Geerling et al., 2017).

It is interesting to justify the choice of a two-week follow-up period. It comes as the follow-up recommended by the MGDRx EyeBag manufacturer, but also because there is supporting evidence for it. TFOS DEWS II Management and Therapy Report (Jones et al., 2017) recommended a two-week treatment period as the application of MGDRx EyeBag twice a day for two weeks improved dry eye symptoms, and these benefits lasted 6 months. Different studies used 2 weeks, or even less, as sufficient to benefit from thermal bag application (Bilkhu, Naroo and Wolffsohn, 2014a; Bilkhu, Naroo and Wolffsohn, 2014b; Wang et al., 2015; Wang et al., 2019d). In addition, Ngo, Srinivasan and Jones (2019) did not find differences in signs and symptoms in follow-ups longer than 2 weeks. More recently, Murphy et al. (2019) assessed the efficacy of MGDRx EyeBag at 2, 4 and 8 weeks, not finding significant improvement from the second week of treatment. Finally, since thermal bags were self-applied, shorter and

effective treatment times are preferable to increase adherence to the treatment protocol.

This study had some limitations that should be considered. First, the reduction of symptoms in both groups might have been affected by the placebo effect since subjects were not masked (Bilkhu, Naroo and Wolffsohn, 2014b). Second, not all the metrics were comparable between young and aged subjects since there were significant differences between groups at baseline. This issue was partially solved by using mixed ANOVA. Finally, no control group was included in the study; results were only compared with the baseline and between young and aged subjects. Future research with a larger sample, with a longer follow-up and with different MGD severity grades would be required in aged subjects in order to confirm these findings.

Overall, ocular surface integrity metrics were improved after thermal bags application in subjects with evaporative dry eye symptoms or with a lower NIKBUT. The application of thermal bags was associated with a reduction in dry eye-related symptoms in both young and aged subjects, while NIKBUT and lipid layer thickness were only improved in the young group. NIKBUT and lipid layer were affected by age, the performance being higher in young subjects after the treatment. These findings provide new insights about the effect of thermal bags on the ocular surface in young and elderly subjects, which might help in the management of MGD or DED depending on age.

CHAPTER 8: Development of new methods to assess the tear film and the ocular surface

8. DEVELOPMENT OF NEW METHODS TO ASSESS THE TEAR FILM AND THE OCULAR SURFACE

As explained in *Chapter 2 Justification*, the TFOS DEWS II Diagnostic Methodology Report recognized the need of developing new non-invasive and as objective as possible metrics to assess the tear film and the ocular surface (Wolffsohn et al., 2017). In the present chapter different metrics will be developed to assess the tear film and the ocular surface in a non-invasive and objective way. The newly developed metrics consist of image processing of pictures and videos from the ocular surface.

CHAPTER 8.1: Development of a method to assess meibomian gland visibility

8.1 DEVELOPMENT OF A METHOD TO ASSESS MEIBOMIAN GLAND VISIBILITY

In this chapter, a method to assess meibomian gland visibility will be developed from the analysis com grey pixel intensity values of meibographies obtained through non-contact infrared meibography.

CHAPTER 8.1.1: Meibomian glands' visibility assessment through a new quantitative method. Development and repeatability of new metrics

8.1.1 MEIBOMIAN GLANDS' VISIBILITY ASSESSMENT THROUGH A NEW QUANTITATIVE METHOD: DEVELOPMENT AND REPEATABILITY OF NEW METRICS

In this chapter, the development of the method will be explained and the repeatability of new gland visibility metrics will be assessed.

8.1.1.1 Introduction

Meibomian glands' assessment is based on qualitative and subjective analysis. Different grading scales have been developed (Shimazaki, Sakata and Tsubota, 1995; Bron and Tiffany, 2004; Nichols et al., 2005; Arita et al., 2008; Arita et al., 2009b; Nelson et al., 2011; Tomlinson et al., 2011; Pult and Nichols, 2012; Pult and Riede-Pult, 2013; Koprowski et al., 2016). Nevertheless, as explained in *Chapter 1 Introduction*, subjective meibomian gland grading depends on the ability of the examiner to detect alterations (Arita et al., 2009b; Tomlinson et al., 2011; McGinnigle, Eperjesi and Naroo, 2012; Sullivan et al., 2012a; Arita et al., 2013; Pult and Riede-Pult, 2013; Wolffsohn et al., 2017), which may lead to a decrease in assessment repeatability and agreement between clinicians (Nichols et al., 2005). Meanwhile, the objective grading of meibomian glands has been reported to have better intra- and interrater measurement repeatability and agreement (Nichols et al., 2005; Koh et al., 2012; Pult and Nichols, 2012; Srinivasan et al., 2012; Arita et al., 2013; Celik et al., 2013; Pult and Riede-Pult, 2013; Wolffsohn et al., 2017; Llorens-Quintana et al., 2019a; Llorens-Quintana et al., 2019b).

Up to now, only a few objective algorithms have been developed to assess meibographies and there is not a universally accepted one (Shimazaki, Sakata and Tsubota, 1995; Nichols et al., 2005; Arita et al., 2008; Koh et al., 2012; Pult and Riede-Pult, 2012b; Celik et al., 2013; Pult and Riede-Pult, 2013; Koprowski et al., 2016; Llorens-Quintana et al., 2019a). Moreover, the diagnosis of DED and MGD is still challenging; therefore, it has been reported that there is a need of developing new metrics and algorithms in order to assess the ocular surface in an objective and non-invasive way (Wolffsohn et al., 2017). This might be obtained by means of image processing (Arita et al., 2013; Celik et al., 2013; Koprowski et al., 2016; Geerling et al., 2017; Llorens-Quintana et al., 2019a).

The aim of this study is to develop and validate new quantitative metrics to assess meibomian glands' visibility objectively. To the authors' knowledge, this is the first study to analyze meibomian glands' visibility in an objective manner.

8.1.1.2 Methodology

A total of 112 healthy volunteers aged between 18 to 90 years old participated in this study. Participants had no prior history of ocular complications, injury or disease in the last three months. In order to evaluate various meibomian gland loss levels, no exclusion based on the state of the meibomian glands of subjects was made. Contact lens users were instructed not to wear their contact lenses within a week before the examination. Only the right eye was measured due to the similar nature of both eyes. Subjects having difficulties with lid eversion were excluded from the study. Written consent of each subject was obtained after the explanation of the study protocol. The

study was approved by the Ethics Committee of the University of Valencia and it was performed in accordance with the tenets of the Declaration of Helsinki.

Measurements

Non-contact infrared meibography of the upper right eyelid of each subject was obtained using Oculus Keratograph 5M (K5 M; Oculus GmbH, Wetzlar, Germany) by the same experienced researcher, as explained in *Chapter 3 General Methodology*. RGB (Red-Green-Blue) infrared meibographies were acquired with a resolution of 1360 x 1024 pixels (Koprowski et al., 2016; Llorens-Quintana et al., 2019a). Images were then exported to external software in order to analyse the grey level intensity. All meibographies were obtained in the same room and under the same controlled illumination conditions.

Percentage classification was carried out under previously published criteria (Arita et al., 2009b; Tomlinson et al., 2011). Thus, meibographies were classified into 3 groups (*Figure 8.1.1.1*), by a masked researcher, as follows: Group 1 = Patients with good subjective glands visibility and an Image J drop-out percentage of less than one-third of the total area of meibomian glands; Group 2 = Patients with low subjective glands visibility and an Image J drop-out percentage lower than one-third of the total area; and Group 3 = Patients with low subjective glands visibility and an Image J drop-out percentage higher than one-third of the total area. Once meibographies were classified into these 3 groups, images were analysed through the proposed method. In order to prove that the method was able to objectively measure gland visibility, differences between groups were analysed for each new metric. The classification into

these three groups was not based on any previous criterion, but subjects were classified into groups in order to validate the method.

Fig. 8.1.1.1. *Examples of the 3 meibography groups. From left to right: Group1, Group 2 and Group 3.*

Method development

The analysis of meibographies has several features that make it challenging. In some cases, meibography images have low contrast, non-uniform illumination, defocused areas, specular reflections or other artefacts (Celik et al., 2013; Llorens-Quintana et al., 2019a).

Matlab R2018a (MathWorks, Natick, MA) was used to develop the method. First, RGB meibographies were transformed to grey levels images. Photoshop (V S5, Adobe Systems Inc., San Jose, CA, US) was then used to eliminate specular reflexes and reduced shadows in order to provide uniform illumination in the whole eyelid (*Figure 8.1.1.2*). This reduction was carried out in the same way for all meibographies so that grey level values were comparable.

Region of Interest (ROI) was manually selected through Matlab in the same way for all meibographies by the same clinician. The upper boundary was delimited by the eyelid fold while the lower by the eyelid boundary, as in *Figure 8.1.1.2* (right).

Fig. 8.1.1.2. *Original meibography (left) and meibography after the elimination of specular reflexes and shadows reduction in the region of interest (right).*

The background illumination was subtracted from the image in order to enhance uniform illumination across the eyelid. Thus, the background was calculated through opening by using a structural element disk of 20 pixels radius. Each pixel value of the resulting image was then raised to the third power in order to enhance the contrast in the same way for all meibographies. Finally, images were smoothed by applying a 4-pixel sigma Gaussian filter to remove the remaining noise from the background (Esmaeli et al., 2016). Once the meibographies were processed, histograms were obtained from the different images and metrics were measured taking into account the grey values on the final image (*Figure 8.1.1.3*) (Haralick, 1979; Conners, Trivedi and Harlow, 1984; Clausi, 2002; Alonso-Caneiro et al., 2013). *Figure 8.1.1.4* shows a summary of the main steps in which the process of image analysis was carried out in the development of the method.

Meibomian glands show lighter than the background. Thus, glandular structures have relatively higher brightness in comparison with neighbouring non-glandular regions (Celik et al., 2013). Therefore, it was hypothesized that higher grey value scores might be related to higher meibomian glands' visibility. Grey values range from 0 (black) to 255 (white) (Haralick, 1979; Conners, Trivedi and Harlow, 1984; Clausi, 2002; Alonso-Caneiro et al., 2013; Celik et al., 2013). Different parameters were obtained in order to analyse glands' visibility: the mean, the SD, the median and the mode of the ROI pixels. Histogram shape parameters such as kurtosis and skewness were also measured (Haralick, 1979; Conners, Trivedi and Harlow, 1984; Clausi, 2002; Alonso-Caneiro et al., 2013).

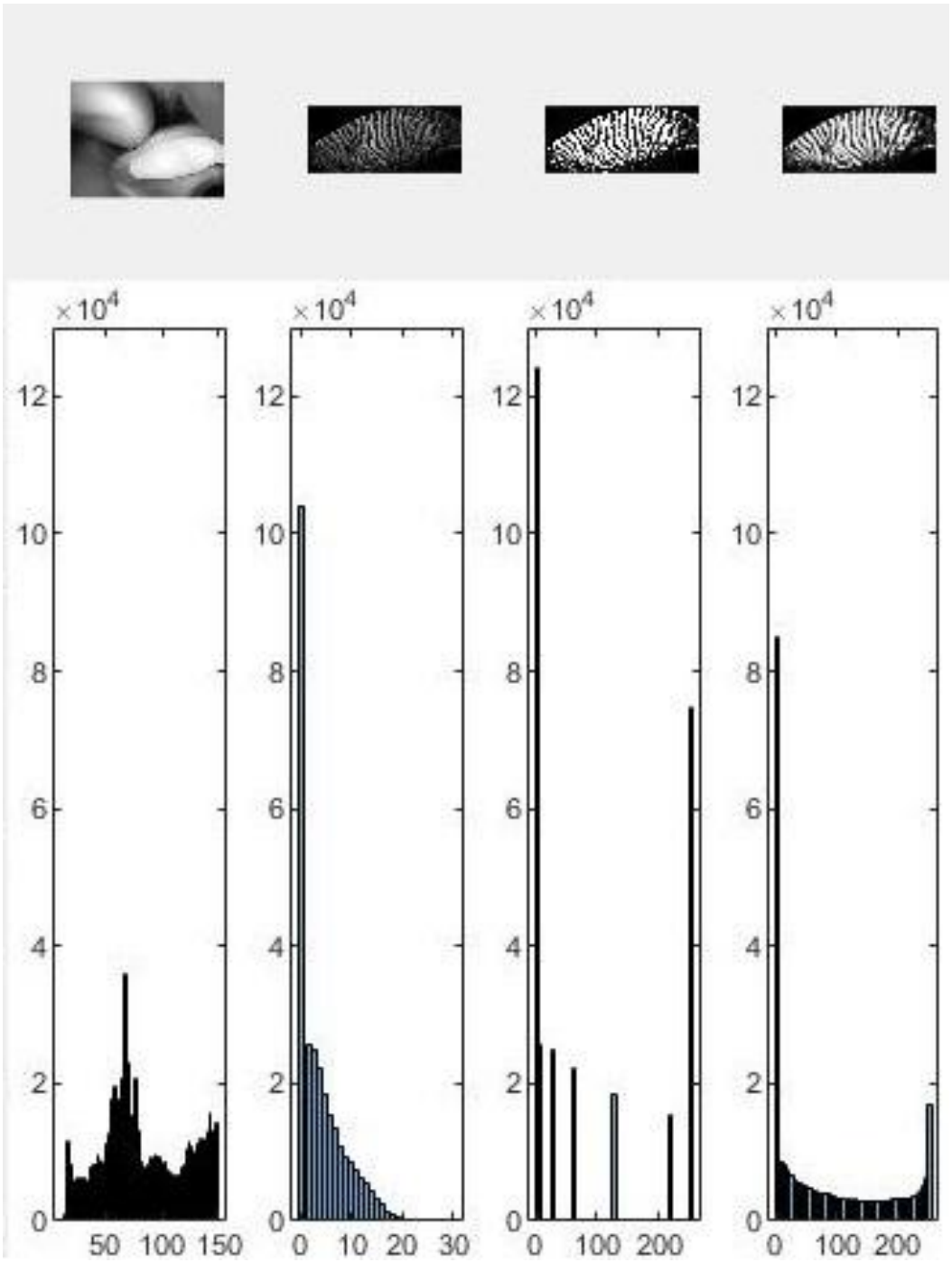

Fig. 8.1.1.3. *Images and histograms obtained through the method. From left to right: Background of the region of interest, Background subtracted from the region of interest, Contrast enhancement, and Gaussian filter (final image). In the histograms, axe "x" represents the grey level intensities (0-255), while axe "y" shows the number of pixels.*

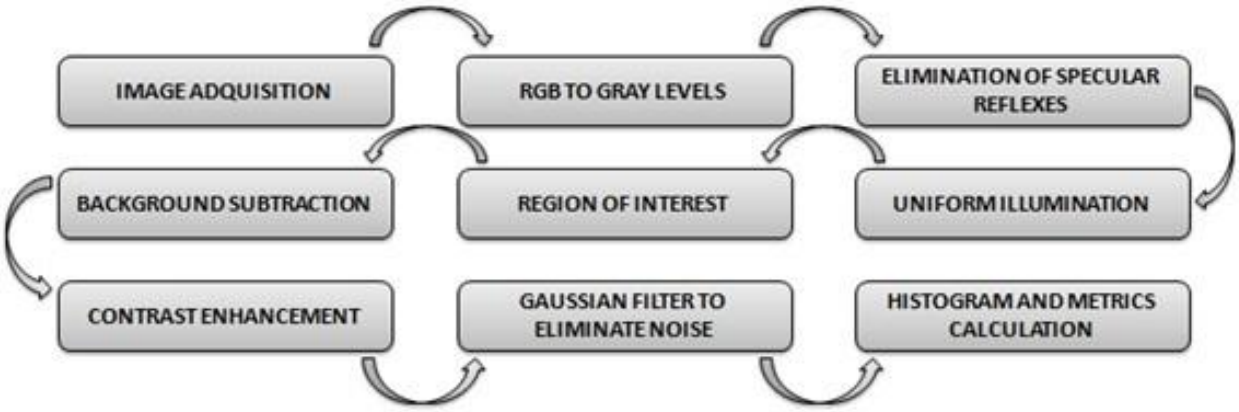

Fig. 8.1.1.4. *The main steps of image processing.*

Moreover, energy, relative energy, entropy and SD irregularity were calculated (Haralick, 1979; Conners, Trivedi and Harlow, 1984; Clausi, 2002; Alonso-Caneiro et al., 2013) as follows:

energy as: $\frac{\sum p\text{^}2}{n}$

relative energy as: $\frac{\sum(\frac{p}{pmax})\text{^}2}{n}$

entropy: $\frac{-\sum p.\log(p)}{n}$

SD irregularity as: $\frac{\sum\left(\frac{p-x}{pmax}\right)\text{^}2}{n}$

Where: p=pixels; n=number of pixels; pmax=maximum intensity of the meibography; and x=mean pixel intensity values. These parameters were divided by the number of pixels (n) to make all meibographies comparable independently of the matrix size.

The image area was divided into three horizontal cuts at 25%, 50% and 75%, as shown in *Figure 8.1.1.5*. The area under the pixel intensity curve was calculated for each cut and divided by the number of pixels. A global area under the curve was obtained by adding the three cuts. Pixel intensity changes gradually between the background and the glands (Llorens-Quintana et al., 2019a).

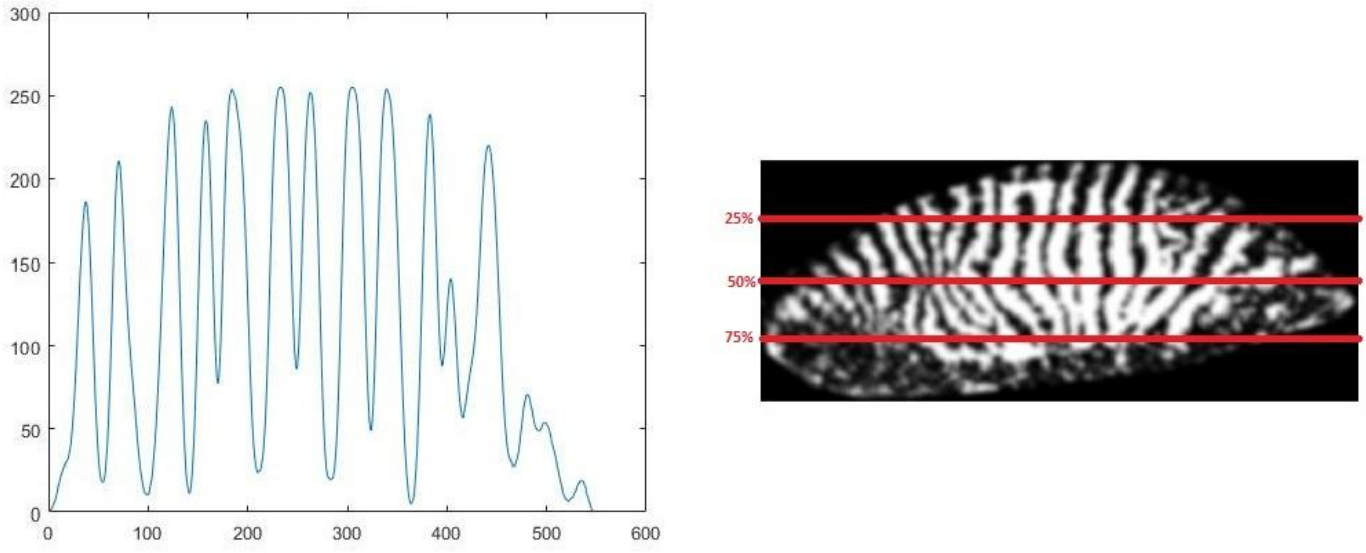

Fig. 8.1.1.5. *Three cuts at the 25%, 50% and 75 % levels in the meibography (right) and an example of the pixel intensity in one cut (left). Where: Axe "x" is the pixel position across the cut in the image and "y" shows the grey level intensity (0-255).*

Statistical analysis

Statistical analysis was carried out using SPSS v26.0 for Windows (IBM Corp, Armonk, New York, USA). Outcomes were displayed as the mean ± SD. Normality distribution for each group was checked by means of the Shapiro-Wilk or the Kolmogorov-Smirnov test, depending on the sample size.

Differences between groups for each metric were assessed with ANOVA or Kruskal-Wallis. Levene's test was used to assess if the variances between groups could be considered equal. Welch's t-test was used when the variances were not equal. Furthermore, post-hoc analysis was carried out by means of Bonferroni, Tukey or Games-Howell tests in order to evaluate the differences between all pair group combinations. A p-value less than 0.05 was defined as statistically significant.

Rho Spearman test was used to assess the correlation between each metric and Meibomian glands drop-out percentage; with the entire sample and after excluding group 2 in order to avoid the cases in which low visibility was not related to drop-out. The group 2, which had low gland drop-out and visibility, was excluded to further prove that not only was the method measuring gland drop-out, but it also measured the visibility of the glands.

Finally, the repeatability of each new metric was assessed by calculating the S_w, CoV and CoR, as explained in *Chapter 3 General Methodology*.

8.1.1.3 Results

The discussed new method was applied to one hundred and twelve right eyes from 112 subjects out of whom 70 were female (62.5%) and 42 male (37.5%). The mean age was 48.3 ± 27.5 years (ranging from 18 to 90 years). From the total sample, 56 subjects were classified in group 1 (24.5 ± 9.6 years), 19 in group 2 (69.2 ± 21.3 years) and 37 in group 3 (73.6 ± 13.7 years). Kruskal-Wallis test showed statistically significant differences in age between groups ($p < 0.001$). Age of group 1 was lower than the age of group 2 ($p < 0.001$) and 3 ($p < 0.001$), while no differences were found between group 2 and 3 ($p = 0.832$). *Table 8.1.1.1* shows the main results obtained for each metric per group and the statistical comparison between them. The method performed properly in all images when it was applied in each meibography.

No statistically significant differences were found between groups 1 and 2 in drop-out percentage. However, group 1 showed higher values than the other groups in relative energy, energy, SD irregularity, mean, SD, median, mode, kurtosis, skewness and total area.

Table 8.1.1.2 shows the correlations between the different metrics and gland drop-out percentage with the entire sample and after excluding the group 2. Rho Spearman correlations were statistically significant for all metrics except for entropy. The correlation was higher after excluding the group 2. Mode did not show a monotone relation with gland drop-out percentage.

Table 8.1.1.1. *Mean values for each group and comparison between them.*

Metric	Group	Mean±SD	Significance level (p-value)	Compatison between groups (p-value)
Gland drop-out percentage (%)	Group 1	22.71±5.38	<0.001[1]*	1-2= 0.110
	Group 2	27.42±5.30		1-3= <0.001*
	Group 3	51.04±1.68		2-3= <0.001*
Relative energy	Group 1	0.42±0.07	<0.001[2]*	1-2=<0.001*
	Group 2	0.24±0.05		1-3=<0.001*
	Group 3	0.20±0.09		2-3= 0.152
Energy	Group 1	246.56±4.59	<0.001[1]*	1-2= <0.001*
	Group 2	240.16±4.02		1-3= <0.001*
	Group 3	237.50±8.86		2-3= 0.858
Entropy	Group 1	$4.1x10^{-5}$±$1.0x10^{-5}$	0.003[1]*	1-2= 0.001*
	Group 2	$4.8x10^{-5}$±$7.2x10^{-6}$		1-3= 0.371
	Group 3	$4.3x10^{-5}$±$1.0x10^{-5}$		2-3= 0.012*
SD irregularity	Group 1	0.34±0.09	<0.001[3]*	1-2= <0.001*
	Group 2	0.16±0.04		1-3=< 0.001*
	Group 3	0.15±0.08		2-3= 0.601
Mean ROI pixels intensity	Group 1	115.86±14.69	<0.001[3]*	1-2= <0.001*
	Group 2	83.95±8.99		1-3= <0.001*
	Group 3	76.10±18.80		2-3= 0.097
SD ROI pixels intensity	Group 1	79.07±3.66	<0.001[3]*	1-2=< 0.001*
	Group 2	68.45±5.78		1-3= <0.001*
	Group 3	64.75±12.17		2-3= 0.280
Median ROI pixels intensity	Group 1	100.89±22.57	<0.001[1]*	1-2= <0.001*
	Group 2	61.00±9.79		1-3= <0.001*
	Group 3	52.65±17.16		2-3= 0.131
Mode ROI pixels intensity	Group 1	178.52±112.01	<0.001[1]*	1-2= <0.001*
	Group 2	16.89±5.26		1-3= <0.001*
	Group 3	62.19±94.54		2-3= 0.187
Kurtosis	Group 1	0.0098±0.0015	<0.001[1]*	1-2= <0.001*
	Group 2	0.0123±0.0010		1-3= <0.001*
	Group 3	0.0138±0.0022		2-3= 0.142
Skewness	Group 1	0.102±0.005	<0.001[3]*	1-2= <0.001*
	Group 2	0.113±0.005		1-3= <0.001*
	Group 3	0.120±0.010		2-3= 0.005*
Total area	Group 1	366.70±45.29	<0.001[3]*	1-2= <0.001*
	Group 2	259.13±30.87		1-3= <0.001*
	Group 3	247.89±63.30		2-3= 0.647

(Where ROI: Region of Interest; SD: Standard Deviation; Group 1: Patients with good intensity and drop-out less than one-third of the total meibomian gland area; Group 2: Patients with low intensity and drop-out less than one-third of the total meibomian gland area; Group 3: patients with low intensity and drop-out higher than one-third of

*the total meibomian gland area; [1] Kruskal-Wallis Test; [2] ANOVA test; [3] Welch Test; *Statistically significant values)*

Table 8.1.1.2. *Correlation between the different metrics and drop-out percentage with the entire sample and excluding the group 2.*

Metric	Groups	Spearman's correlation coefficient (r)	Significance level (p-value)
Relative energy	All the sample	-0.751	<0.001*
	Without group 2	-0.821	<0.001*
Energy	All the sample	-0.509	<0.001*
	Without group 2	-0.527	<0.001*
Entropy	All the sample	0.079	0.405
	Without group 2	0.145	0.166
Standard deviation irregularity	All the sample	-0.702	<0.001*
	Without group 2	-0.781	<0.001*
Mean ROI pixels intensity	All the sample	-0.745	<0.001*
	Without group 2	-0.808	<0.001*
Standard deviation ROI pixels intensity	All the sample	-0.581	<0.001*
	Without group 2	-0.649	<0.001*
Median ROI pixels intensity	All the sample	-0.767	<0.001*
	Without group 2	-0.815	<0.001*
Kurtosis	All the sample	0.769	<0.001*
	Without group 2	0.814	<0.001*
Skewness	All the sample	0.775	<0.001*
	Without group 2	0.826	<0.001*
Total area	All the sample	-0.656	<0.001*
	Without group 2	-0.747	<0.001*

(Where ROI: Region of Interest; Group 2: Patients with low intensity and drop-out less than one-third of the total meibomian gland area)

Table 8.1.1.3 shows the repeatability scores for each metric. All metrics with the exception of the mode of pixels intensity achieved acceptable repeatability since S_w and CoR values were low and the variability between the three measurements was not high, CoV achieving values between 0.04 and 4.65. The CoV shows the variability between measurements with respect to the average value as a percentage, being

useful to assess the repeatability as long as the average magnitude is not too small (Bland and Altman, 2010).

Table 8.1.1.3. *Repeatability of each metric.*

Metric	Sw (max-min)	CoR (max-min)	CoV (%)
Relative energy	0.012	0.032	3.86
Energy	3.28	9.09	1.36
Entropy	$1.8x10^{-6}$	$4.9 x10^{-6}$	0.04
Standard deviation irregularity	0.009	0.026	4.16
Mean ROI pixels intensity	2.68	7.42	2.85
Standard deviation ROI pixels intensity	0.94	2.60	1.33
Median ROI pixels intensity	3.49	9.68	4.65
Mode ROI pixels intensity	35.18	97.46	38.84
Kurtosis	0.0003	0.0007	2.16
Skewness	0.0012	0.0033	1.08
Total area	11.32	31.36	3.77

(Where CoR: Repeatability coefficient; CoV: Coefficient of variation; ROI: Region of Interest; Sw: Within-subject standard deviation)

8.1.1.4 Discussion

This study describes an objective semiautomatic method for analysing meibomian glands' visibility quantitatively. Meibography images were subjectively and objectively classified according to their visibility grade, which is different from meibomian gland loss (Llorens-Quintana et al., 2019a; Llorens-Quintana et al., 2019b).

Different objective algorithms have been developed in order to assess morphological features of meibomian glands such as length or gaps between glands (Koh et al., 2012; Llorens-Quintana et al., 2019a; Llorens-Quintana et al., 2019b), gland

drop-out (Arita et al., 2013; Celik et al., 2013; Llorens-Quintana et al., 2019a; Llorens-Quintana et al., 2019b), gland area (Celik et al., 2013; Koprowski et al., 2016; Koprowski, Tian and Olczyk, 2017), width (Llorens-Quintana et al., 2019a; Llorens-Quintana et al., 2019b) or irregularity (Llorens-Quintana et al., 2019a; Llorens-Quintana et al., 2019b). However, these studies were focused on morphological parameters related to meibomian glands while the present study analyses meibomian gland visibility.

In this study, the new proposed method was found not only able to detect gland drop-out, but could also assess objectively meibomian glands visibility. The analysis showed lower pixel intensity values for group 2, which had lower glands visibility than group 1 but similar drop-out ($p = 0.110$). This suggests that both gland drop-out and gland visibility are measured. Furthermore, this fact was also evident when correlations were stronger after excluding group 2 from the analysis. Meibomian glands drop-out and glands visibility are usually linked. Nevertheless, the group 2 had low grand drop-out and low visibility.

Relative energy, energy, SD irregularity, mean, SD, median, mode and total area under the curve displayed higher values for group 1 than for 2 and 3, suggesting higher gland intensity. Kurtosis was lower for group 1 since the histogram was wider than for the other groups. Skewness also showed lower values for group 1 due to the fact that higher intensity values were found in this group. Entropy was the only one not correlated to meibomian gland loss. This might be due to the fact that entropy measures randomness of grey level distribution (Haralick, 1979; Alonso-Caneiro et al.,

2013), being therefore useful for the analysis of other parameters related to meibography arrangement such as tortuosity of glands. This hypothesis should be checked in future studies.

Meibomian gland visibility assessment is important due to the fact that the link between gland drop-out and gland function is not clear (LLorens-Quintana et al., 2019b). Changes in meibomian gland visibility might induce alterations in lipid secretion and composition, leading to alterations in tear film properties. The new method is capable of classifying different meibography grades, since not only extreme cases were considered, but also intermediate grades were properly classified.

S_w, CoR and CoV indicate good repeatability when its values are near zero (Bland and Altman, 2010; Cerviño et al., 2015; McAlinden, Khadka and Pesudovs, 2015; Martínez-Albert, Esteve-Taboada and Montés-Micó, 2018; Martínez-Albert et al., 2018). Generally, new metrics manifested moderate-acceptable repeatability, in spite of the fact that ROI was determined manually.

It could be hypothesized that it might help clinicians to assess meibomian gland activity grade since higher gland drop-out is related to lower gland visibility. Likewise, higher gland visibility might be related to better gland activity and healthiness. These metrics might help to grade objectively the level of activity of meibomian glands and therefore facilitate clinicians the diagnosis of meibomian gland alterations such as MGD, or even monitor treatment effectiveness. Thereby, the method could add diagnostic value in MGD follow-up (Llorens-Quintana et al., 2019a).

This study had some limitations to consider. The procedure is semiautomatic and thus clinicians still have to manually eliminate reflexes and delineate the gland area. Nevertheless, the method is not instrument-specific, unlike previous ones (Llorens-Quintana et al., 2019a). In spite of the method being semiautomatic, the repeatability was unaltered. Moreover, this study was focused on images of the upper eyelids only, since it was easier to capture a uniformly focused image of the tarsal plate (Koh et al., 2012). Statistically significant differences in age were obtained between groups. Consequently, age might act as a possible confounding factor. As in previous studies, age could not be excluded from the analysis because of its strong association with MGD (Arita et al., 2018; Pult, Riede-Pult and Nichols, 2012; Rico-del-Viejo et al., 2019). And finally, lighting must be controlled to avoid changes in results (Srinivasan et al., 2012).

Overall, all metrics, with the exception of entropy, showed higher meibomian gland visibility for Group 1 than in the other two groups. The proposed method is able to assess meibomian gland visibility in an objective and repeatable way, which might help clinicians enhance MGD diagnosis and follow-up treatment. This new method might help clinicians to assess meibomian glands visibility grade since higher gland drop-out is related to lower glands visibility. Likewise, higher glands visibility might be related to better gland activity and healthiness. Further studies are needed to evaluate the diagnostic capability of the suggested parameters. Further analysis against other ocular surface parameters would be helpful to confirm whether the new metrics are helpful for meibomian gland assessment.

CHAPTER 8.1.2: Diagnostic capability of a new method to assess meibomian gland visibility

8.1.2 DIAGNOSTIC CAPABILITY OF A NEW OBJECTIVE METHOD TO ASSESS MEIBOMIAN GLAND VISIBILITY

In this chapter, the diagnostic capability of new gland visibility metrics for MGD will be assessed, as well as their correlations with other clinical signs and symptoms of DED and MGD.

8.1.2.1 Introduction

As reported in *Chapter 1 Introduction* and *Chapter 2 Justification*, the diagnosis of MGD is challenging as no single metric can solely be used to diagnose it and there is no global consensus on what criterion (a combination of metrics) to follow to diagnose it. For instance, some authors recommend the combination of dry eye symptoms, lid margin abnormalities and meiboscore to diagnose MGD (Arita et al., 2009b); others suggest symptoms, meibum expressibility and tear film stability (Ngo, Gann and Nichols, 2020); while other studies recommend symptoms, gland expressibility and ocular surface staining (Tomlinson et al., 2011). Furthermore, it has been reported that clinical features used to diagnose MGD before and after the International Workshop on MGD report are similar, implying a low impact in MGD diagnosis in clinical trials (Ngo, Gann and Nichols, 2020). Moreover, DED diagnosis is also difficult due to the low correlation between signs and symptoms, the multifactorial characteristic of the disease and the lack of a gold standard tool to diagnose it (Nichols, Mitchell and Zadnik, 2004; Arita et al., 2009b; Tomlinson et al., 2011; Barlett et al., 2015; Geerling et al., 2017; Wolffsohn et al., 2017; Ngo, Gann and Nichols, 2020; Vehof et al., 2021).

Image processing techniques can now be usefully applied to the objective assessment of images to extract valuable information from them. As meibomian glands appear lighter than the background in a meibography, the visibility of the glands might be used as a feature to aid in MGD diagnosis. Visibility is defined as the grade in which meibomian glands are seen. Thus, in a subject with high gland drop-out, the glands have lost totally their visibility. With this premise, a new method was developed, based on image analysis, to objectively assess the visibility of meibomian glands. However, not only is the visibility useful to detect gland drop-out, but it is also useful to grade the level of visibility in subjects that have similar gland drop-out. This was demonstrated in *Chapter 8.1.1* (García-Marqués et al., 2021a) by finding significantly lower pixel intensity scores in a group with low subjective gland intensity in comparison to another group with good subjective gland intensity. Both groups had a similar gland drop-out ($p = .110$).

The present study goes one step further by analyzing the diagnostic ability of meibomian gland visibility metrics. Accordingly, the purpose of this study was to apply the proposed method to healthy and MGD subjects and evaluate its ability to better discriminate between both sets of subjects. It is hypothesized that these new metrics could be used as a complementary tool for supporting the diagnosis of MGD.

8.1.2.2 Methodology

One hundred and twelve healthy, Caucasian volunteers with ages ranging from 18 to 90 years (48.3 ± 27.5 years) participated in this study. Participants had no prior history of ocular complications, injury or disease in the last three months. To evaluate

various meibomian gland loss levels, no exclusion based on the state of the meibomian glands of subjects was made. The previous diagnosis of DED or MGD was not an exclusion criterion. Contact lens users were instructed not to wear their contact lenses within a week before the examination. Only the right eye was measured due to the similar nature of both eyes. Written consent was obtained from each subject after the explanation of the study protocol. Ethics Committee approval was obtained. The study was approved by the Ethics Committee of the University of Valencia and it was performed following the tenets of the Declaration of Helsinki.

The sample was divided into two groups (healthy and MGD group) based on the criterion that follows (Arita et al., 2009b; Arita, Fukuoka and Morishige, 2017c): Participants were classified into the obstructive MGD group when any 2 of the 3 following scores were abnormal: 1) OSDI ≥ 13; 2) Lid margin abnormality score > 1; and 3) Meiboscore > 1. This criterion has been previously reported to have a sensitivity of 84.9 % and a specificity of 96.7 % (Arita et al., 2009b; Arita, Fukuoka and Morishige, 2017c).

Measurements

All measurements were obtained using the Oculus Keratograph 5M (K5 M; Oculus GmbH, Wetzlar, Germany) by the same experienced and masked researcher. The ocular surface assessment was performed in the same laboratory, under constant conditions of illumination (200 lux), temperature (24.1 ± 1.6 °C) and humidity (44.9 ± 5.0 %). Measurements were carried out following the guidelines reported by the TFOS DEWS II, to avoid the destabilization of the tear film. They were performed in the

following order (Wolffsohn et al., 2017): OSDI, bulbar redness, TMH, NIKBUT, lid margin abnormalities, obstruction score, gland expressibility and upper eyelid meibography. Measurements were taken as explained in *Chapter 3 General Methodology*.

Lid margin abnormalities were evaluated in the upper and lower eyelids using scores between 0 and 4, according to the number of these findings in the eye, encompassing irregular lid margin, vascular engorgement, plugged meibomian gland orifices, and anterior or posterior replacement of the mucocutaneous junction (Arita et al., 2009b). Obstruction score was obtained from the number of obstructed glands in both eyelids. Expressibility of the central 8 meibomian glands of the upper and lower eyelids was graded according to a point scale proposed by Arita et al. (2009a) as follows 0 = clear meibum and easily expressed; 1 = cloudy meibum and expressed with mild pressure; 2 = cloudy meibum and expressed with more than moderate pressure; 3 = meibum not expressed. Meiboscore and gland drop-out percentage were assessed as explained in *Chapter 3 General Methodology*.

Development of the method to measure meibomian gland visibility

Meibomian glands have higher brightness in comparison with surrounding non-glandular regions. Thus, higher gray values might be related to higher meibomian gland visibility. For instance, *Figure 8.1.2.1* shows three meibography types. *Figure 8.1.2.1 A* shows a meibography without gland drop-out and good visibility; *Figure 8.1.2.1 B* shows a meibography without gland drop-out but with low gland visibility;

finally, *Figure 8.1.2.1 C* shows a meibography with both high gland drop-out and low visibility.

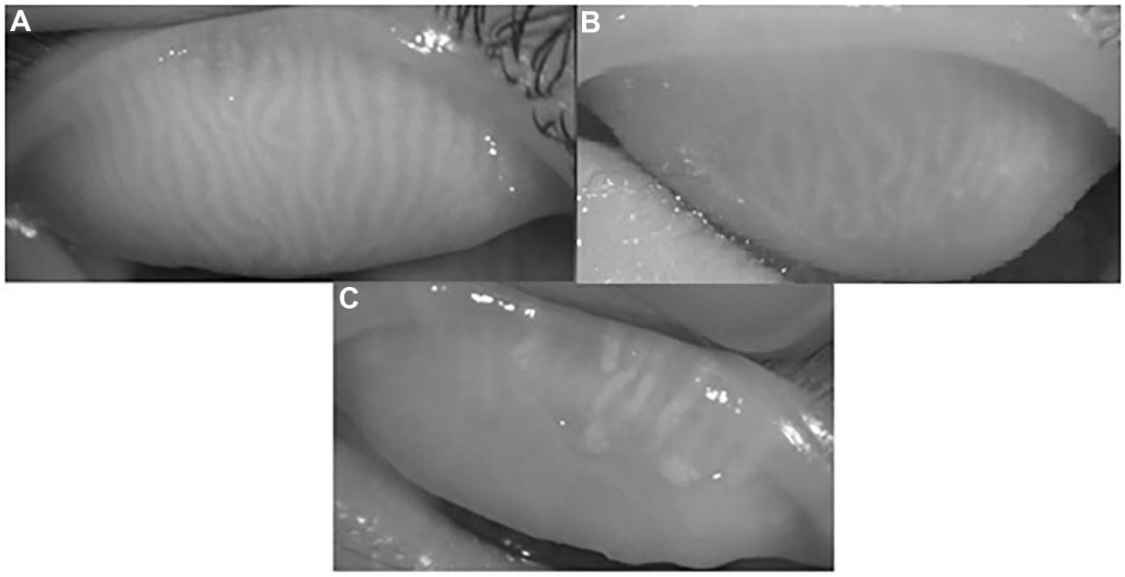

Fig. 8.1.2.1. *Different meibography types. A: low gland drop-out and high gland visibility; B: low gland drop-out and low gland visibility; and C: high gland drop-out and low gland visibility.*

The present method was developed using Matlab© R2018a software (MathWorks, Natick, MA) as follows. Meibographies without contrast enhancement provided by the Keratograph 5M were used in the present study. First, RGB meibographies were transformed to grayscale levels and specular reflexes and shadows were removed using Photoshop (V S5, Adobe Systems Inc., San Jose, CA, US). The region of interest was then manually selected and extracted with Matlab©. The upper boundary was delimited by the eyelid fold while the lower by the eyelid boundary. Furthermore, the background illumination was subtracted from the image to enhance uniform illumination across the eyelid. Thus, the background was calculated through opening

by using a structural element disk of 20 pixels radius. The intensity level of each pixel was then raised to the third power to increase image contrast. Finally, the noise was removed by applying a 4-pixel sigma Gaussian filter (Esmaeli et al., 2016).

Histogram and visibility metrics were calculated from the gray level values (0-black to 255-white) of the modified meibography image (Alonso-Caneiro et al., 2013). As meibomian glands show lighter than the background; the lower their grey intensity value, the lower their visibility. Mean, SD, median, mode, kurtosis and skewness of the histogram were calculated. Besides, energy, relative energy and SD irregularity were calculated as follows (Alonso-Caneiro et al., 2013):

Energy as: $\frac{\sum p\text{^}2}{n}$

Relative energy as: $\frac{\sum(\frac{p}{pmax})\text{^}2}{n}$

SD irregularity as: $\frac{\sum\left(\frac{p-x}{pmax}\right)\text{^}2}{n}$.

Where: p = pixel intensity value; n = number of pixels; pmax = maximum pixel intensity; and x = mean pixel intensity values.

Parameters were divided by the number of pixels (n) so that all meibographies were comparable independently of the size of the region of interest. A more detailed description of all this process can be found in *Chapter 8.1.1* (García-Marqués et al. (2021a). In that study, it was found that gland visibility metrics had acceptable repeatability.

Examiner was masked to the study group allocation of meibographies during image processing analysis.

Statistical analysis

A priori, sample size calculation was performed using MedCalc for Windows version 19.5.1 (MedCalc Software, Ostend, Belgium). The area under the curve to detect (alternative hypothesis) was chosen to be 0.85 since it denotes high diagnostic power. The area value for the null hypothesis was 0.5 while α and β at 0.05 and 0.2, respectively. The sample required consisted of 68 negative subjects (healthy group) and 34 positive subjects (MGD group). This means that the sample size is large enough.

Statistical analysis was performed using SPSS v26.0 for Windows (IBM Corp, Armonk, New York, USA). Normality distribution for each group was checked through the Shapiro-Wilk or Kolmogorov-Smirnov test, depending on the sample size. Differences between healthy and MGD groups were evaluated for each metric using unpaired Student t-test or Mann-Whitney U test. Moreover, correlations between gland visibility metrics, age and ocular signs and symptoms were assessed using Rho Spearman correlation for the whole sample. A *P*-value of less than 0.05 was defined as statistically significant.

The sensitivity, specificity area under the ROC curve, the cut-off value that optimizes the diagnosis, Youden index and discriminant power were calculated as explained in *Chapter 3 General Methodology* (Sokolova, Japkowicz and Szpakowicz, 2006; Llorens-Quintana, Szczesna-Iskander and Iskander, 2019).

Moreover, logistic regression was applied to obtain different combinations of the current metrics. From these models, the best combination of the current metrics was selected based on the Akaike Information Criteria, the highest area under the ROC curve and the Younden index (Hosmer and Lemesbow, 1980; Friedman, Hastie and Tibshirani, 2000). Then, each new metric based on gland visibility was combined with the best model of the current techniques. The aforementioned calculations were also performed in these combined models.

8.1.2.3 Results

The described new method based on gland visibility was applied to one hundred and twelve right eyes from 112 subjects, 70 female (62.5 %) and 42 male (37.5 %). From the total sample, 76 subjects were classified into the healthy group (35.4 ± 23.0 years) and 36 into the MGD group (75.5 ± 11.6 years). Mann-Whitney U test showed statistically significant differences in age between groups ($U = 367.5$, $p < 0.001$).

Differences between groups

The method was able to calculate objective gland visibility metrics in all meibographies. The main results obtained for each current and new gland visibility metric, and the statistical comparison between healthy and MGD groups are shown in *Table 8.1.2.1*. The MGD group had statistically lower values in relative energy, energy, SD irregularity, mean pixels intensity, SD, median pixels intensity and mode pixels intensity. Higher values were found in the MGD group for kurtosis, skewness, gland drop-out percentage, bulbar redness, TMH, OSDI, obstruction score, lid margin

abnormality score and meiboscore. However, no statistically significant differences were found between groups in median first NIKBUT and gland expressibility score.

Table 8.1.2.1. *Results for each metric and statistical comparison between groups.*

Metric	Group		Significance level
	Healthy (Mean ± SD; CI)	MGD (Mean ± SD; CI)	
Relative Energy	0.4 ± 0.1; 0.4-0.4	0.2 ± 0.1; 0.2-0.2	U = 365; p < .001[2]*
Energy	245.2 ± 6.3; 245.0-247.2	236.8 ± 6.5; 235.9-241.2	t = 6.513; p < .001[1]*
SD Irregularity	0.3 ± 0.1; 0.3-0.3	0.1 ± 0.1; 0.1-0.2	t = 6.546; p < .001[1]*
Mean ROI Pixels Intensity	106.9 ± 22.1; 105.5-114.7	77.0 ± 14.0; 73.7-83.9	U = 339; p < .001[2]*
SD ROI Pixels Intensity	75.2 ± 9.1; 75.2-78.4	66.8 ± 10.3; 63.6-71.2	U = 606; p < .001[2]*
Median ROI Pixels Intensity	90.6 ± 27.7; 87.7-100.1	51.9 ± 11.6; 49.1-58.3	t = 8.025; p < .001[1]*
Mode ROI Pixels Intensity	148.7 ± 118.9; 128.8-184.9	36.6 ± 66.9; 4.2-54.2	U = 680; p < .001[2]*
Kurtosis	0.010 ± 0.002; 0.010-0.011	0.013 ± 0.001; 0.012-0.014	U = 354; p < .001[2]*
Skewness	0.10 ± 0.01; 0.10-0.11	0.11 ± 0.01; 0.11-0.12	U = 362; p < .001[2]*
Meibomian gland drop-out percentage (%)	23.2 ± 5.8; 23.6-29.1	41.2 ± 11.9;33.7-44.9	t = -4.282; p < .001[1]*
Bulbar Redness	0.8 ± 0.5; 0.6-0.8	1.3 ± 0.5; 1.0-1.5	U = 543; p < .001[2]*
TMH (mm)	0.2 ± 0.1; 0.2-0.2	0.4 ± 0.2; 0.3-0.5	U = 554.5; p < .001[2]*
Median First NIKBUT (seconds)	10.2 ± 5.8; 9.1-12.1	9.1 ± 4.5; 7.4-11.0	U = 1060; p = .083[2]
Meibomian Gland Expressibility Score	0.0 (0.0 to 0.0)±	1.0 (0.0 to 1.0)±	U = 657.5; p = .055[2]
Obstruction Score	0.0 (0.0 to 0.0)±	0.0 (0.0 to 1.0)±	U = 978; p < .001[2]*
Lid Margin Abnormality Score	0.0 (0.0 to 1.0)±	1.0 (0.0 to 1.0)±	U = 678; p < .001[2]*
OSDI	15.4 ± 14.1; 4.9-19.7	33.0 ± 24.9; 21.0-41.8	U = 754.5; p < .001[2]*
Meiboscore	1.0 (1.0 to 1.0)±	2.0 (2.0 to 2.0)±	U = 788; p < .001[2]*

*(Where CI: 95% Confidence Interval; MGD: Meibomian Gland Dysfunction; mm: Milimeters; NIKBUT: Non-Invasive Keratograph Break-Up Time; OSDI: Ocular Surface Disease Index; ROI: Region Of Interest; SD: Standard Deviation; TMH: Tear Meniscus Height; [1]T-test (t); [2]Mann-Whitney U test (U); *Statistically significant values; [±]Median (Interquartile range))*

Correlations between gland visibility metrics, age and ocular surface parameters

Statistically significant correlations between objective meibomian gland visibility metrics, age and ocular DED signs are shown in *Table 8.1.2.2*. Statistically significant correlations were found between meibomian gland visibility metrics and bulbar redness, TMH, meibomian glands expressibility and median first NIKBUT.

Table 8.1.2.2. *Statistically significant Rho Spearman correlations between objective meibomian glands visibility metrics, age and ocular signs and symptoms.*

Meibomian gland visibility metrics	Metric 2	Correlation coefficient	Significance level
Relative energy	Age	-0.66	<0.001
	Bulbar redness	-0.56	<0.001
	Meibomian gland expressibility score	-0.25	0.005
	Median First NIKBUT	0.38	0.003
	TMH	-0.40	<0.001
Energy	Age	-0.52	<0.001
	Bulbar redness	-0.47	<0.001
	Meibomian gland expressibility score	-0.24	0.004
	Median First NIKBUT	0.37	0.004
	TMH	-0.37	<0.001
Standard Deviation Irregularity	Age	-0.66	<0.001
	Bulbar redness	-0.55	<0.001
	Meibomian gland expressibility score	-0.23	0.012
	Median First NIKBUT	0.35	0.010
	TMH	-0.37	<0.001
Mean ROI Pixels Intensity	Age	-0.66	<0.001
	Bulbar redness	-0.56	<0.001
	Meibomian gland expressibility score	-0.24	0.004
	Median First NIKBUT	0.38	0.003
	TMH	-0.40	<0.001
Standard Deviation ROI Pixels Intensity	Age	-0.60	<0.001
	Bulbar redness	-0.50	<0.001
	TMH	-0.31	0.001

(continuation)			
Meibomian gland visibility metrics	Metric 2	Correlation coefficient	Significance level
Median ROI Pixels Intensity	Age	-0.65	<0.001
	Bulbar redness	-0.58	<0.001
	Meibomian gland expressibility score	-0.24	0.004
	Median First NIKBUT	0.39	0.002
	TMH	-0.44	<0.001
Mode ROI Pixels Intensity	Age	-0.45	<0.001
	Bulbar redness	-0.43	<0.001
	Meibomian gland expressibility score	-0.22	0.043
	Median First NIKBUT	0.31	0.029
	TMH	-0.23	0.017
Kurtosis	Age	0.62	<0.001
	Bulbar redness	0.56	<0.001
	Meibomian gland expressibility score	0.26	0.003
	Median First NIKBUT	-0.38	0.003
	TMH	0.41	<0.001
Skewness	Age	0.66	<0.001
	Bulbar redness	0.57	<0.001
	Meibomian gland expressibility score	0.25	0.004
	Median First NIKBUT	-0.27	0.004
	TMH	0.42	<0.001

(Where NIKBUT: Non-Invasive Break-Up Time; ROI: Region Of Interest; TMH: Tear Meniscus Height)

Diagnostic capability of ocular surface parameters and gland visibility metrics

Table 8.1.2.3 summarizes the diagnostic power and the cut-off values for each metric. New gland visibility metrics were powerful indicators for differentiating between MGD and healthy subjects since the area under the curve, sensitivity and specificity obtained were high. Median pixel intensity was the metric with the highest sensitivity, area under the curve, Youden index and discriminant power. On the other hand, the mode of pixel intensity values was the metric with the lowest diagnostic power, with a specificity of 0.61.

Table 8.1.2.3. *ROC curve parameters of gland visibility metrics and ocular surface parameters.*

Metric	Sensitivity	Specificity	Area under the curve (CI)	Cut-off value	Youden index	Discriminant power
Relative Energy	0.97	0.71	0.87 (0.80–0.93)	0.3	0.68	2.46
Energy	0.89	0.79	0.86 (0.79-0.93)	242.4	0.68	1.88
Standard Deviation Irregularity	0.92	0.72	0.84 (0.77-0.91)	0.2	0.64	1.85
Mean ROI Pixels Intensity	0.83	0.84	0.88 (0.82-0.94)	86.3	0.68	1.81
Standard Deviation ROI Pixels Intensity	0.81	0.72	0.78 (0.69-0.87)	74.3	0.53	1.31
Median ROI Pixels Intensity	1.00	0.74	0.89 (0.83-0.95)	75.5	0.74	4.37
Mode ROI Pixels Intensity	0.89	0.61	0.75 (0.66-0.84)	24.5	0.49	1.38
Kurtosis	0.97	0.75	0.87 (0.80-0.94)	0.011	0.72	2.57
Skewness	0.97	0.74	0.87 (0.80-0.94)	0.107	0.71	2.53
Meibomian Gland Drop-Out Percentage	0.92	0.65	0.80 (0.75-0.90)	27.5	0.56	1.65
Bulbar Redness	0.81	0.74	0.80 (0.68-0.91)	1.0	0.54	1.35
TMH	0.78	0.72	0.80 (0.70-0.91)	0.2	0.50	1.22
First Median NIKBUT	0.69	0.50	0.60 (0.49-0.71)	8.9	0.19	0.45
Obstruction Score	0.33	0.95	0.64 (0.50-0.80)	0.5	0.28	1.21
Meibomian Gland Expressibility Score	0.1	0.99	0.54 (0.40-0.70)	0.5	0.08	1.14
Lid Margin Abnormality Score	0.72	0.75	0.75 (0.60-0.86)	0.5	0.47	1.13
OSDI	0.78	0.66	0.72 (0.52-0.82)	14.8	0.44	1.05
Meiboscore	0.67	0.79	0.71 (0.60-0.82)	1.5	0.456	1.11

(Where CI: 95 % Confidence Interval; NIKBUT: Non-Invasive Keratograph Break-Up Time; OSDI: Ocular Surface Disease Index; ROC: Receiver Operating Characteristics; ROI: Region Of Interest; and TMH: Tear Meniscus Height)

The ROC curves for each metric are shown in *Figure 8.1.2.2* (metrics inversely proportional to MGD) and *Figure 8.1.2.3* (metrics directly proportional to MGD). Generally, both tables showed that new gland visibility metrics performed better than current single metrics.

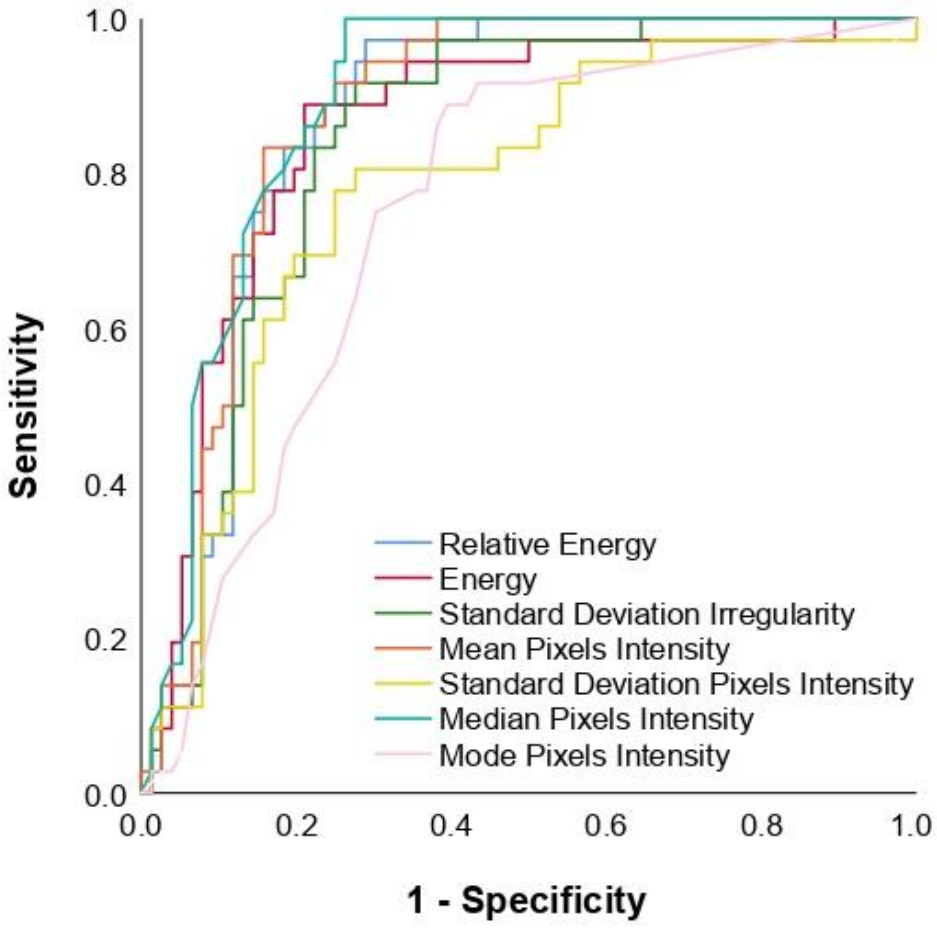

Fig. 8.1.2.2. *ROC curves for metrics inversely proportional to meibomian gland dysfunction. (Where: ROC=Receiver Operating Characteristics)*

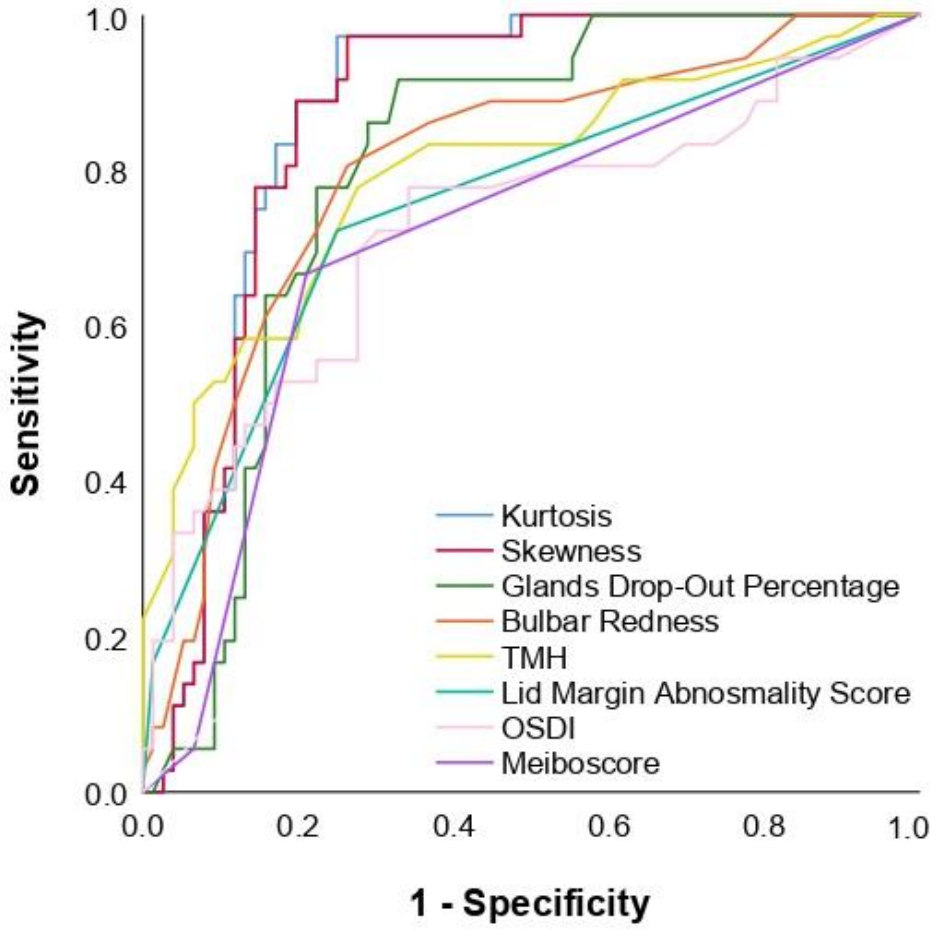

Fig. 8.1.2.3. *ROC curves for metrics directly proportional to meibomian gland dysfunction. (Where OSDI=Ocular Surface Disease Index; ROC=Receiver Operating Characteristics; TMH=Tear Meniscus Height)*

The cut-off value that optimizes the diagnosis determines the best score to diagnose the disease. Thus, a subject with a higher score than the cut-off value in kurtosis and skewness is classified as having MGD, since these metrics are directly proportional to MGD, while a user with a lower score than the cut-off value in the rest of the new gland visibility metrics is classified as having MGD.

Bulbar redness and TMH were the current metrics with the highest area under the curve and the best relationship between sensitivity and specificity. Meibomian gland drop-out percentage had good sensitivity (0.92), but a limited specificity (0.65); while meiboscore had good specificity (0.79) and limited sensitivity (0.67). Lid margin abnormality score and OSDI had moderate sensitivity (0.72 and 0.78, respectively) and specificity (0.75 and 0.66, respectively). Nevertheless, the first median NIKBUT, obstruction score and gland expressibility score showed low diagnostic ability, as revealed by a low area under the curve, sensitivity, specificity, Youden index and discriminant power.

Diagnostic capability of combined metrics

The diagnostic ability of the combination of gland visibility metrics with current ones was assessed using logistic regression analysis. Each one of the gland visibility metrics was included in a model with the current metrics (gland drop-out, TMH, lid margin abnormality and OSDI). The model with the highest area under the curve and the highest Youden index was chosen to perform the analysis. *Table 8.1.2.4* shows the ROC curve parameters and the cut-off values for each combination.

The area under the curve, sensitivity, specificity and Youden index improved notably when gland visibility metrics were added to the combination, achieving values near 1.0 for all combinations. The discriminant power also increased. Furthermore, the diagnostic power was higher when gland visibility metrics were included than when only current metrics were combined. The combination of current metrics with median pixel intensity was the criterion with the best sensitivity, area under the curve and

Youden index. The coefficients of this model (R^2 = 0.893) were -0.95 for gland drop-out percentage, 8.01 for TMH, 4.33 for lid margin abnormality, 0.98 for OSDI and -2.02 for median pixel intensity. All variables were statistically significant to be included in the model ($p < 0.005$). *Figure 8.1.2.4* shows the ROC curves for each combination.

Table 8.1.2.4. *ROC curve parameters and cut-off values for each combination of metrics.*

Ocular surface parameters	New metrics	Sensitivity	Specificity	Area under the curve (CI)	Cut-off value	Youden index	Discriminant power
Meibomian Gland Drop-Out Percentage + TMH + Lid Margin Abnormality Score + OSDI	-	0.93	0.83	0.94 (0.89-0.96)	0.22	0.76	2.30
	+ Relative Energy	0.97	0.93	0.99 (0.97-1.00)	0.25	0.91	3.42
	+ Energy	1.00	0.84	0.97 (0.94-1.00)	0.16	0.84	-
	+ Standard Deviation Irregularity	0.94	0.96	0.99 (0.97-1.00)	0.46	0.91	3.32
	+ Mean ROI Pixels Intensity	0.94	0.92	0.97 (0.94-1.00)	0.39	0.87	2.91
	+ Standard Deviation ROI Pixels Intensity	0.97	0.95	0.99 (0.97-1.00)	0.35	0.92	3.54
	+ Median ROI Pixels Intensity	1.00	0.93	0.99 (0.97-1.00)	0.25	0.93	-
	+ Mode ROI Pixels Intensity	0.94	0.91	0.97 (0.94-1.00)	0.31	0.85	2.82
	+ Kurtosis	0.97	0.88	0.97 (0.95-1.00)	0.17	0.85	3.06
	+ Skewness	0.97	0.88	0.97 (0.95-1.00)	0.18	0.85	3.06

(Where CI: 95 % Confidence Interval; OSDI: Ocular Surface Disease Index; ROC: Receiver Operating Characteristics; ROI: Region Of Interest; and TMH: Tear Meniscus Height)

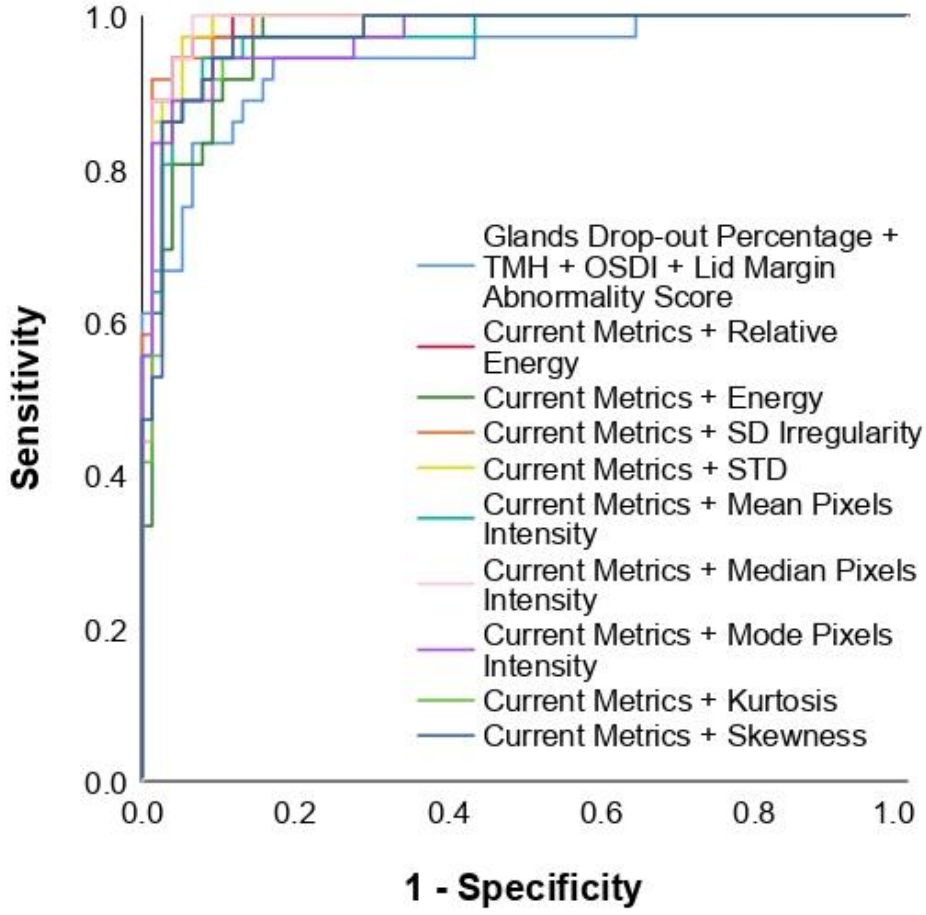

Fig. 8.1.2.4. *ROC curves for each combination between metrics. (Where: OSDI=Ocular Surface Disease Index; ROC=Receiver Operating Characteristics; SD: Standard Deviation; STD: Standard Deviation of the Mean Pixels Intensity Value; TMH=Tear Meniscus Height)*

8.1.2.4 Discussion

In the present study, the diagnostic ability of new metrics based on the gray level values of meibographies was assessed. The visibility of the glands has been assessed, which is different from gland drop-out because a subject can have low gland drop-out

and low gland visibility, as demonstrated in *Chapter 8.1.1* (García-Marqués et al., 2021a).

Differences between groups

Differences between MGD and control subjects were evaluated. Gland drop-out, bulbar redness, TMH, obstruction score, lid margin abnormality score, OSDI and meiboscore were statistically different between both groups. Nonetheless, median first-NIKTBUT and gland expressibility were not. MGD causes atrophy in meibomian glands and, subsequently, gland loss due to the keratinisation increase of the epidermal epithelium (Bron et al., 2017). This fact induces alterations in lipid composition, causing an increase in meibum viscosity, potentially leading to a decrease in NIKBUT (Bron et al., 2017). MGD is related to ocular surface inflammation and damage; therefore, explaining the higher scores of bulbar redness found in MGD subjects (Bron et al., 2017). Besides, in agreement with the outcomes of the present study, previous studies reported an increase in TMH in MGD subjects as a result of a compensatory reflex tearing due to a higher tear film evaporation (Chhadva, Goldhardt and Galor, 2017; Llorens-Quintana et al., 2019b).

Different studies have also found lower tear film stability (Arita et al., 2009b; Qi et al., 2017; Giannaccare et al., 2018; Adil et al., 2019; Yin and Gong, 2019), and higher meibomian gland drop-out (Giannaccare et al., 2018; Xiao et al., 2020), bulbar redness (Llorens-Quintana et al., 2019b; Rico-del-Viejo et al., 2019), TMH (Chhadva, Goldhardt and Galor, 2017; Llorens-Quintana et al., 2019b), meiboscore (Arita et al., 2009b; Yin and Gong, 2019; Xiao et al., 2020), OSDI (Arita et al., 2009b; Qi et al., 2017;

Giannaccare et al., 2018 ; Yin and Gong, 2019), and lid abnormality score (Arita et al., 2009b; Yin and Gong, 2019) in MGD subjects. Aligned with the outcomes reported in the present study, Xiao et al. (2020) did not find differences in meibum expressibility. However, Adil et al. (2019), Yin and Gong (2019) and Arita et al. (2009b) reported lower meibum expression in MGD subjects than in normal. These differences between studies might be due to the low objectivity and reproducibility of the meibum score assessment since the pressure applied on the eyelid is likely to vary between examiners (Arita et al., 2009b). Furthermore, differences might also be due to the different criteria used to define MGD.

Correlations between gland visibility metrics and ocular surface parameters

Low but significant correlations were found between meibomian gland visibility metrics and bulbar redness, TMH, gland expressibility score and first NIKBUT, respectively. In general, the more visible the meibomian glands, the better the first NIKBUT, gland expressibility and bulbar redness values. Although the correlations obtained were low, this is considered an acceptable correlation in dry eye studies, since the multifactorial character of the disease makes strong correlations very rare to achieve (Craig et al., 2017; Wolffsohn et al., 2017). Moreover, in *Chapter 8.1.1* (García-Marqués et al., 2021a), it was also found that gland visibility was correlated with meibomian gland drop-out.

MGD and abnormal gland expressibility are associated with ocular surface inflammation and damage. This might explain the higher bulbar redness scores found in subjects with low visibility of meibomian glands (Shimazaki, Sakata and Tsubota,

1995; Bron et al., 2017). In accordance with the results of the present study, Llorens-Quintana et al. (2019b) reported a positive significant correlation between gland drop-out and bulbar hyperemia, and Rico-del-Viejo et al. (2019) found differences in bulbar redness amongst groups with different levels of meibomian gland loss.

Regarding TMH, previous studies have reported a positive correlation between gland drop-out and tear volume (Chhadva, Goldhardt and Galor, 2017; Llorens-Quintana et al., 2019b). Similarly, TMH has been found to be lower in healthy than in subjects with MGD (Robin et al., 2019). These findings can be as a result of a compensatory reflex tearing due to the higher tear film evaporation and consequently ocular surface stimulation present in these subjects (Chhadva, Goldhardt and Galor, 2017).

Diagnostic capability of ocular surface parameters and gland visibility metrics

Furthermore, the diagnostic capability of a new method developed to measure meibomian gland visibility was assessed. All new gland visibility metrics showed statistical differences between healthy and MGD groups. This fact might suggest that gland visibility metrics could have higher discrimination between healthy and MGD subjects than some current measurements, for which no statistical differences were found.

To test this hypothesis, ROC curves analysis was applied. It has been previously reported that a 70 % level of sensitivity and specificity is accepted as appropriate for the diagnosis of a disease (Tomlinson et al., 2011). Sensitivity and specificity were higher than 0.7 for all metrics except for mode pixel gray values, where the specificity

was 0.61. This implies that mode pixel intensity was found as powerful enough to detect pathological subjects (sensitivity = 0.89), but there is a 39 % probability that a healthy subject is misclassified as having MGD.

Based on a previous report (Hosmer, Lemeshow and Sturdivant, 2013), an area under the curve of 0.5 or lower indicates no discrimination, between 0.7 and 0.8 acceptable discrimination, between 0.8 and 0.9 excellent discrimination and higher than 0.9 indicates outstanding discrimination. According to this classification, the new gland visibility metrics showed areas under the curve between acceptable (0.75; mode pixels intensity) and outstanding (0.89; median pixels intensity) discrimination. Thus, gland visibility metrics can be considered powerful aides to discriminate between MGD and healthy subjects.

Furthermore, the new metrics based on gland visibility showed higher sensitivity, specificity, area under the curve and Youden index than other current metrics. As reported in previous studies (Arita et al., 2009b; Pult and Riede-Pult, 2012b; Finis et al., 2014; Wolffsohn et al., 2017), meibomian gland loss alone does not appear to be sufficient for MGD diagnosis and it should be interpreted together with other clinical parameters. Meibomian gland drop-out percentage, bulbar redness and TMH were the current metrics with the highest diagnostic ability. In comparison with previous studies (*Table 8.1.2.5*), the gland visibility metrics showed similar or higher diagnostic ability than current metrics (Tomlinson et al., 2006; Arita et al., 2009b; Pult, Riede-Pult and Nichols, 2012; Finis et al., 2013; Finis et al., 2014; Koprowski et al., 2016; Su et al., 2017; Giannaccare et al., 2018; Adil et al., 2019; Yin and Gong, 2019; Xiao et al., 2020).

Table 8.1.2.5. *Diagnostic ability of current metrics to diagnose MGD.*

Study	Metric	Sensitivity	Specificity	Area under the curve	Cut-off value	Youden index
Arita et al. (2009b)	Dry eye symptoms			0.95		
	Lid abnormality	0.81	0.83	0.93	2	0.64
	Meiboscore			0.92		
	Meibum			0.80		
	BUT			0.86		
Yin and Gong (2019)	Meiboscore	0.94	0.96	0.95	1	0.89
	Gland vagueness	0.64	0.83	0.77	21	0.47
	BUT	0.89	0.81	0.93	5 seconds	0.70
Adil et al. (2019)	Meiboscore	0.97	0.85		0.5	0.82
Tomlinson et al. (2006)	Osmolarity	0.59	0.94		316 mOsm/L	0.53
Finis et al. (2014)	Meiboscore	0.28	0.80		4	0.08
Finis et al. (2013)	Lipid layer thickness	0.66	0.63		75 nm	0.29
Giannaccare et al. (2018)	Non-invasive break-up time using Tearscope	0.66	0.63	0.69	9.6 seconds	0.29
	Gland loss	0.60	0.61	0.60	20 %	0.21
	Lipid layer thickness	0.58	0.33	0.54	2	-0.09
	Osmolarity	0.49	0.54	0.55	303 mOsm/L	0.03
Su et al. (2017)	Eyelid margin temperature	0.90	0.88	0.92		0.78
Koprowski et al. (2016)	Area occupied by the glandS in a automatic algorithm	0.99	0.97			0.97
Xiao et al. (2020)	Meiboscore	0.93	0.97	0.98	1.5	0.90
	Number of distorted glands	0.93	0.90	0.96	6	0.83
	Meibum expressibility			0.62		
	Gland loss			0.98		

(Where BUT: fluorescein Break-Up Time; mOsm/L: miliosmoles per liter; and nm: nanometers)

Diagnostic capability of combined metrics

Sensitivity and specificity were increased by performing a sequential analysis combining other parameters. When each gland visibility metric was combined with currently available metrics the area under the curve, sensitivity, specificity, Youden index and discriminant power increased. The inclusion of gland visibility metrics in the combination provided higher diagnostic ability. The combination with median pixel intensity was the best to distinguish between MGD and healthy subjects since it achieved the highest area under the curve (0.99) and excellent sensitivity (1.00) and specificity (0.93).

This study had some limitations to consider. As previously reported, no clear diagnostic criterion has been established to define MGD and thus, it significantly varies between studies (Tomlinson et al., 2011; Wolffsohn et al., 2017; Chan et al., 2019; Ngo, Gann and Nichols, 2020). Therefore, it is difficult to assess the diagnostic ability of metrics and to establish cut-off values since it is not completely clear when a subject is pathological or not. Moreover, statistically significant age differences were obtained between groups and gland visibility was correlated with age. Consequently, age might act as a possible confounding factor. As in previous studies, age could not be excluded from the analysis because of its strong association with MGD (Arita et al., 2008; Pult, Riede-Pult and Nichols, 2012; Rico-del-Viejo et al., 2019). In addition, the procedure is semiautomatic as the clinician still has to delineate manually the region of interest and eliminate reflexes, which can increase diagnostic time and variability. The surrounding illumination and the focusing of the eyelid are relevant factors to take into account so

that the results are not altered. Finally, only the upper eyelid was evaluated because it was easier to capture a uniformly focused area (Koh et al., 2012). Finally, the sample appeared to represent mild MGD subjects since relatively small differences were found in clinical signs between groups. The diagnostic ability of the gland visibility metrics on moderate and severe cases might be assessed in future studies. Nevertheless, the present study demonstrated that the new gland visibility metrics had good diagnostic power even in mild MGD cases, which have been reported to be more challenging to diagnose (Arita, Fukuoka and Morishige, 2017c; Craig et al., 2017; Wolffsohn et al., 2017). Further research is also needed to include both eyelids in the analysis and to establish cut-off values depending on the age of the subjects.

Overall, the present study proves the utility and validity of new self-developed metrics based on meibomian gland visibility to better diagnose MGD. Meibomian gland visibility can be objectively measured and it can provide new insights about meibomian gland features. Meibomian gland visibility metrics have higher diagnostic power than current single metrics and can serve as a complementary objective tool for the diagnosis of MGD. These results suggest that gland visibility metrics are suitable to be incorporated into MGD diagnosis assessment, particularly the combination of median pixels intensity with gland drop-out percentage, TMH, OSDI and lid margin abnormality score.

CHAPTER 8.2: An emerging method to assess tear film spread and dynamics as possible tear film homeostasis markers

8.2 AN EMERGING METHOD TO ASSESS TEAR FILM SPREAD AND DYNAMICS AS POSSIBLE TEAR FILM HOMEOSTASIS MARKERS

In this chapter, a method to assess tear film spread and dynamics will be developed by tracking the tear film particles post-blink. Moreover, the repeatability of these new metrics and their relationship with DED signs and symptoms will be assessed.

8.2.1. Introduction

Currently, the dynamic stability of the tear film is measured through NIKBUT or Interferometry, as explained in *Chapter 1 Introduction*; nonetheless, NIKBUT procedure does not allow the assessment of the tear film under completely natural conditions, since subjects must keep the eyes opened forcefully and this might produce reflex tearing (King-Smith, Begley and Braun, 2018; Lai et al., 2019). Furthermore, some patients, such as elderly subjects or children, are not able to complete the procedure. For these reasons, a method to measure tear film-dynamic in natural conditions has been proposed in this work. This metric might be used as an alternative parameter to assess the quality of the tear film. Indeed, as discussed in *Chapter 2 Justification*, the TFOS DEWS II Diagnostic Methodology Report recognized the need of developing new non-invasive and as automatic as possible metrics to assess the tear film. They also acknowledged the potential of using the tear film particle dynamics as an emerging measure of tear film quality (Wolffsohn et al., 2017).

Tear film-dynamic has been previously measured (Owens and Phillips, 2001; Varikooty, Keir and Simpson, 2012; Lai et al., 2019). Studies have reported that tear film-dynamic is related to the viscosity and homeostasis of the tear film (Owens and Phillips, 2001; Varikooty, Keir and Simpson, 2012; Li et al., 2015a; Pult et al., 2015; Lai et al., 2019). The method was proposed by Owens and Phillips (2001), who assessed tear film homeostasis by observing the movement of reflective light particles after blink. Light particles are a combination of eroded epithelial corneal cells, tarsal conjunctival cells, mucin-contaminated lipid particles and small air bubbles (Owens and Phillips, 2001; Khanal and Millar, 2010; Varikooty, Keir and Simpson, 2012; Lai et al., 2019). They are visible because they protrude outward from the superficial surface of the tear film (Owens and Phillips, 2001; López-García, García-Lozano and Martínez-Garchitorena, 2003).

Owens and Philips (2001) found that the initial particle speed and the time for tear film stabilization are independent descriptors of tear spreading, which could provide new insights into the non-invasive assessment of the tear film. Nevertheless, this method was rudimentary since particle position was calculated manually by measuring the particle position across the screen. Varikooty, Keir and Simpson (2012) also implemented a manual approach. In this case, they used a slit-lamp and the Image J tool to track particles' position in subjects fitted with contact lenses. Recently, Lai et al. (2019) measured the momentary moving speed of particles using the Image J tool and standardized a tear film particle-tracking procedure, which minimizes the effect of involuntary eye movements.

All of these studies stated that this was a promising method for analyzing the homeostasis of the tear film. Nevertheless, tear film metrics from these studies have been manually calculated so that, up to now, there is not any algorithm especially developed to assess tear film-dynamic. They only argued that new metrics could be used to assess the spreading of the tear film, but they did not evaluate which ocular surface parameters they were analyzing. The primary aim of this study is to develop and assess the performance of an analysis method to measure in vivo the spreading speed of tear film particles post-blink. The hypothesis is that a high particle speed might be related to adequate homeostasis in tear film, while a low speed could be related to an irregular or viscous tear film. Thus, the second objective is to assess the repeatability of new metrics and evaluate the relationship of this new metric with ocular surface signs and DED symptoms in order to extract new insights about the assessment of tear film-dynamic and its homeostasis.

8.2.2. Methodology

Eighty-one healthy volunteers ranging in age from 18 to 90 years (43.7 ± 27.0 years) participated in this study. Participants had no prior history of ocular disease or injury in the last three months. In order to evaluate the different status of the tear film, no exclusion based on tear film or meibomian gland parameters was made. Contact lens users were instructed not to wear their contact lenses within a week before the examination. Only the right eye of subjects was assessed to avoid volunteers' data duplication. The study was carried out in accordance with the tenets of the Declaration of Helsinki and was approved by the Ethics Committee of the

University of Valencia. Written consent of each participant was obtained after a verbal explanation of the study protocol.

Measurements

Subjects' ocular surface was assessed using Oculus Keratograph 5M (K5 M; Oculus GmbH, Wetzlar, Germany). The illuminance, temperature and humidity of the room were maintained at 200 lux, 24.1 ± 1.6 °C and 44.9 ± 5.0 %, respectively. Measurements were taken by the same masked and experienced researcher following the guidelines of the TFOS DEWS II Diagnostic Methodology Report (Wolffsohn et al., 2017). Measurements were taken in the following order to avoid tear film destabilization: OSDI, DEQ-5, total bulbar redness, TMH, tear film-dynamic, lipid layer thickness, NIKBUT, meibomian glands expressibility and upper eyelid meibography.

Bulbar redness, TMH, lipid layer thickness, NIKBUT and meibomian gland drop-out percentage were assessed as explained in *Chapter 3 General Methodology*. Meibomian glands expressibility was evaluated in the central 8 meibomian glands of the upper eyelid using the following grading scale (Bron, Benjamin and Snibson, 1991; Shimazaki, Sakata and Tsubota, 1995; Shimazaki et al., 1998; Foulks and Bron, 2003; Nelson et al., 2011; Tomlinson et al., 2011): 0 = easily expressed; 1 = expressed with mild pressure; 2 = expressed with more than moderate pressure; 3 = not expressed.

Tear film-dynamic and data analysis using the proposed method

Keratograph 5M provides a tool called tear film-dynamic to record the movement of tear film particles after blinking. The device was used to record a video at 32 frames

per second with a resolution of 1360 x 1024 pixels, while two white LED spots illuminated the eye. The examiner focused on the white spots, reflected on the anterior corneal surface, to ensure that the tear film remained in focus. Three different natural and spontaneous blinks were recorded. The post-blink distribution of light particles spreading over the cornea was observed using high magnifications. *Figure 8.2.1* shows one video frame with the light particles spreading after blink.

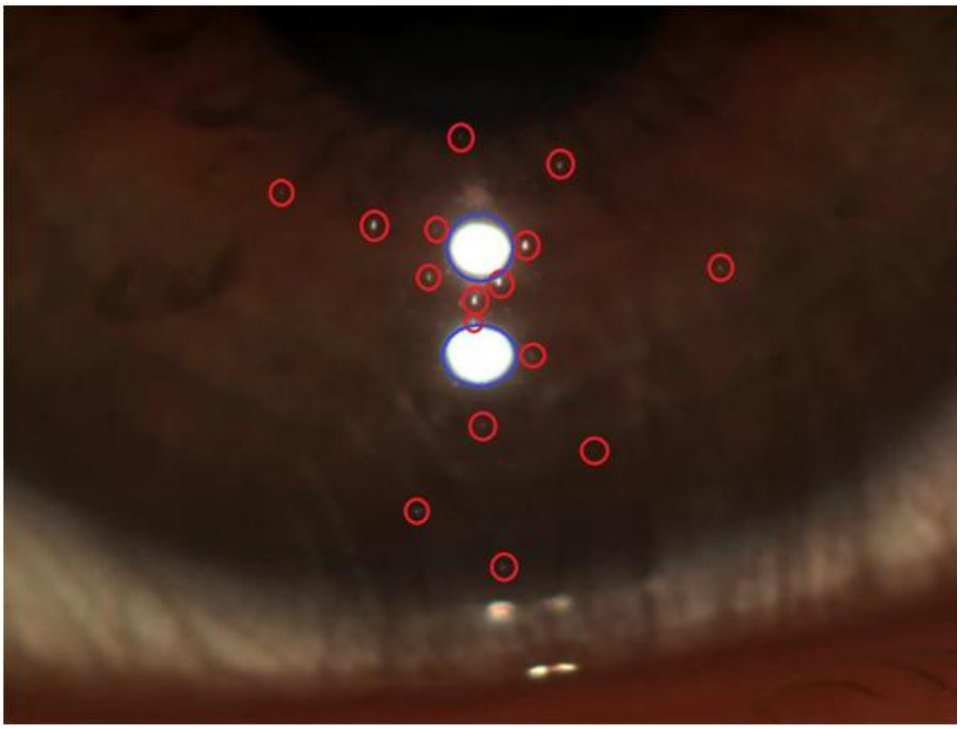

Fig. 8.2.1. *Measurement of tear film-dynamic. Light particles spreading over the cornea (red circles) and the reflection of the two white LEDs (blue circles).*

Once the video was recorded, it was analyzed through the proposed method. The method was developed using Matlab R2018a® (MathWorks, Natick, MA). The software automatically decomposed the video into image frames with a time interval of 0.031 seconds between frames. Thus, the rate in which particle position was sampled was

32.3 hertz. The frames after a spontaneous, complete and natural blink were selected by the examiner as the frames of interest.

The sequence of frames selected showed the particles clearly in focus. Furthermore, the reflection of the two white LEDs on the cornea was used to control the quality and stabilization of the image. In order to control involuntary eye movements the reflection should not be distorted. If reflections were distorted in any frame, that frame was excluded from the analysis. Moreover, the reflection of the two white LEDs was used as a reference for particle position. Thus, the examiner selected the position of the two LED references and if they moved in any direction, the software added or subtracted the amount of this movement to the particle position.

A time period of 1.75 seconds after blink was measured since this period is enough for the tear film to stabilize after blink (Owens and Phillips, 2001; Varikooty, Keir and Simpson, 2012; Willcox et al., 2017; Lai et al., 2019). Each measure consisted of 53 frames. The program showed each frame in chronological order and the examiner had to manually select the particle position in each frame. The software automatically recorded the values and calculated the speed of the particle between two successive video frames using the following equation:

Momentary speed: $\frac{\sqrt{(Xpost-Xprev)^2+(Ypost-Yprev)^2}}{t}$

Where: Xpost and Ypost are the X and Y position of the particle at the frame of the calculation of momentary speed; Xprev and Yprev are the X and Y position of the particle at the previous frame; and t is the time period between both frames.

The examiner measured at least 8 particles and the momentary speed presented at the same moment was then averaged. Thus, a global measure of the particles' speed at each frame was calculated and different metrics were obtained from that measure. For each subject, twelve different metrics were obtained: Mean, median, maximum and minimum particle speed, particle speed at 0.25 seconds, 0.50, 0.75, 1.00, 1.25, 1.50 and 1.75 seconds after blink and the number of seconds for particle speed to decrease to < 1.20 mm/second. 1.20 mm/second was chosen as the cut-off value since the particle' speed had a transition between more and less than 1.20 mm/second in all participants. The speed was interpolated considering the previous and posterior frames when the particle' speed was not available for a specific moment. Mean and median speed was calculated as the average and median, respectively, of particle speed of each moment from 0 to 1.75 seconds.

A calibration scale of known distances was captured in order to find the correspondence between pixels and millimeters. Thus, metrics were converted from pixels/second to mm/second.

It is important to note that the particles' speed represents the speed of the particles after blinking, but not that of the tear fluid. The tear film-dynamic analysis process is summarized in *Figure 8.2.2*. Three videos were acquired and were analyzed so as to calculate the repeatability of the software to obtain tear film-dynamic metrics.

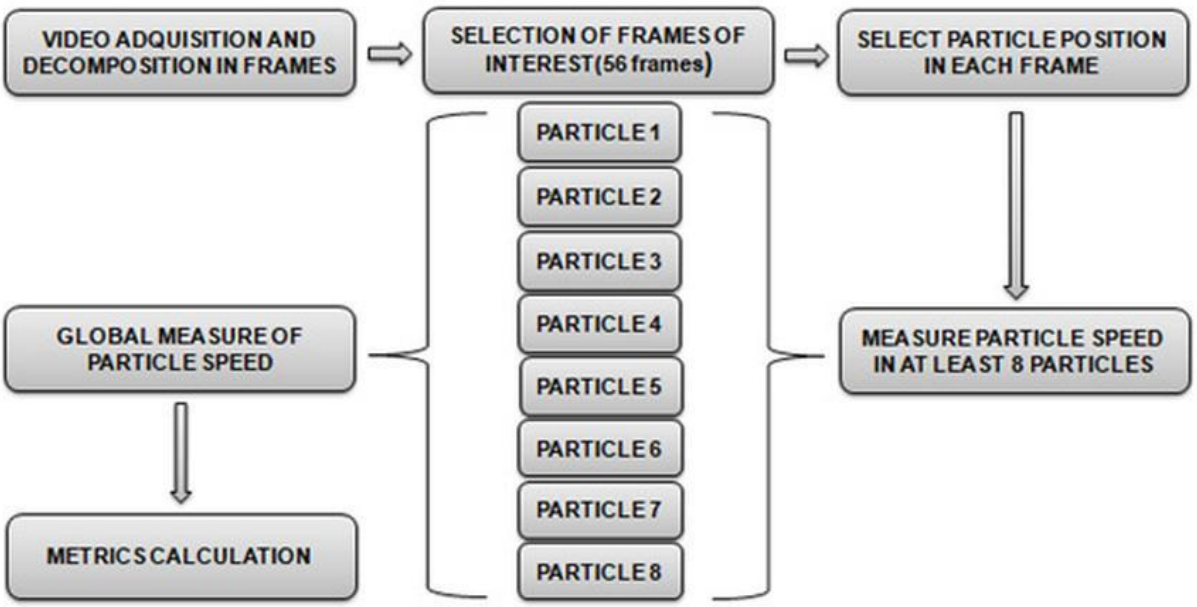

Fig. 8.2.2. *The main steps of tear film-dynamic analysis.*

Statistical analysis

Statistical analysis was carried out using SPSS v26.0 for Windows (IBM Corp, Armonk, New York, USA). Results were shown as the mean ± SD. Particle speed was expressed as mm/second.

Repeatability of each tear film-dynamic metric was assessed by analyzing three different blinks from three different videos of the same subject and by calculating the S_w, CoV and CoR, as explained in *Chapter 3 General Methodology*. Friedman test was used to assess the differences between the particle speeds at each moment. Bonferroni was used to evaluate the post-hoc differences between paired moments and p-values were shown according to the Bonferroni correction.

The sample was divided into different groups according to the cut-off values reported by the Diagnostic Methodology Report of TFOS DEWS II (Wolffsohn et al.,

2017): OSDI < 13 or OSDI ≥ 13; DEQ-5 < 6 or DEQ-5 ≥ 6; total bulbar redness ≤ 1 or total bulbar redness > 1; TMH < 0.20mm or TMH ≥ 0.20mm; lipid layer pattern ≤ grade 2 or > grade 2; NIKBUT < 10 seconds or NIKBUT ≥ 10 seconds; glands expressibility score ≤ 1 or glands expressibility score > 1; and meibomian glands drop-out percentage ≤ 1/3 or > 1/3.

Normality distribution for each group and the total sample was assessed through Shapiro-Wilk or Kolmogorov-Smirnov test, depending on the sample size. Differences in tear film-dynamic results between groups were evaluated by means of unpaired T-Student or Mann-Whitney U test. Levene's test was used to assess the assumption of homogeneity of variances. Correlations between ocular surface signs and symptoms and tear film-dynamic metrics were analyzed using Rho Spearman correlation for the whole sample. Finally, binomial logistic regression was performed to assess the predictability of tear film-dynamic metrics to ocular signs that had statistically significant correlations. A p-value less than 0.05 was defined as statistically significant.

8.2.3. Results

The described method was applied to eighty one right eyes from 81 volunteers, 46 female (56.79 %) and 35 male (43.21 %). The mean age was 43.7 ± 27.0 years, ranging from 18 to 90 years. No subject used dry eye drops. The program performed properly in all subjects, except in four of them for which particles were not visible enough.

Tear film-dynamic metrics and movement

Mean particle speed was 1.48 ± 0.49 mm/second, median particle speed was 1.17 ± 0.47 mm/second, maximum particle speed was 3.37 ± 1.26 mm/second, minimum particle speed was 0.66 ± 0.34 mm/second and time for particle speed to decrease to < 1.20 mm/second was 0.97 ± 0.48 seconds. *Figure 8.2.3* shows the mean values and SD for the mean speed of particles as a function of time. The particles moved faster immediately after blink and slowed down thereafter. In all subjects, particles moved upwards and, in some cases, they were slightly nasal or temporally deviated. This can be seen in *Figure 8.2.3*, where the particle speed decreased from 0.25 to 1.75 seconds after blinking. Friedman test revealed statistically significant differences between the speed at each moment ($p < 0.001$). *Figure 8.2.3* also shows the post-hoc comparison of speed depending on the moment after blinking. From 1.00 second onwards the speed did not show statistical differences between groups. Therefore, particle speed started to stabilize 1.00 second after blinking.

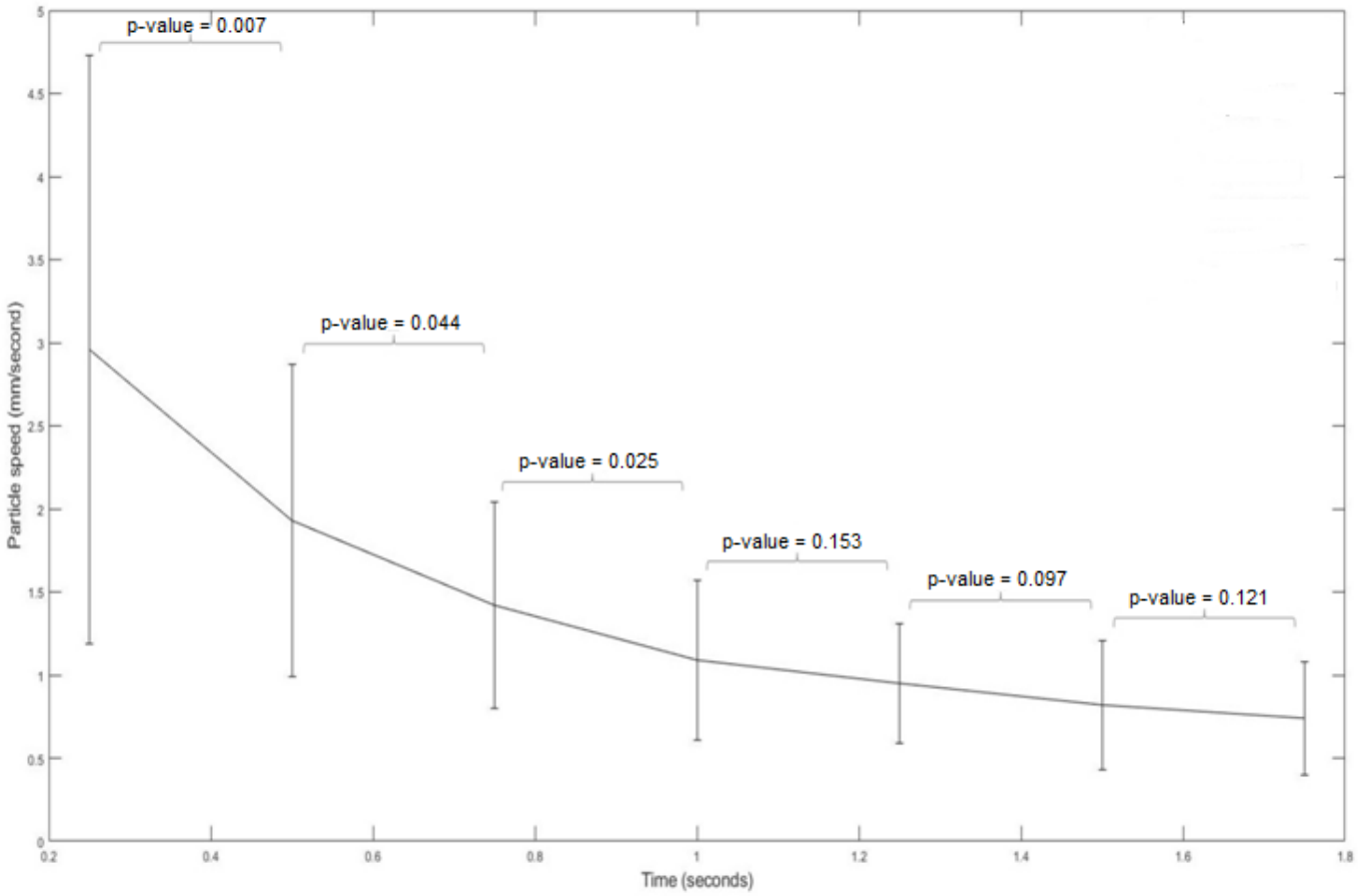

Fig. 8.2.3. *Comparison of mean particle' speed and error bars depending on the moment after blinking.*

Repeatability of each tear film-dynamic metric

Table 8.2.1 shows the repeatability scores for each metric. Particle speed at 0.25 seconds after blinking and the maximum particle speed showed moderate repeatability since CoV was of 12.24 % and 14.37 %, respectively. The CoV shows the variability between measurements with respect to the average value as a percentage, being useful to assess the repeatability as long as the average magnitude is not too small (Bland and Altman, 2010; Martínez-Albert et al., 2018).

Table 8.2.1. *Repeatability of each tear film-dynamic metric.*

Metric	S_w	CoR	CoV (%)
Particle speed at 0.25 seconds	0.35	0.97	12.24
Particle speed at 0.50 seconds	0.19	0.54	9.88
Particle speed at 0.75 seconds	0.13	0.37	10.19
Particle speed at 1.00 second	0.08	0.23	7.39
Particle speed at 1.25 seconds	0.06	0.17	6.70
Particle speed at 1.50 seconds	0.05	0.15	6.05
Particle speed at 1.75 seconds	0.04	0.12	5.64
Mean particle speed	0.08	0.22	5.32
Median particle speed	0.07	0.20	6.24
Maximum particle speed	0.52	1.43	14.37
Minimum particle speed	0.07	0.20	6.73
Time for particle speed to decrease to < 1.20 mm/second	0.06	0.16	5.49

(Where S_w: Within-subject standard deviation; CoV: Coefficient of variation; CoR: Repeatability coefficient)

Repeatability in the rest of metrics was acceptable since Sw and CoR values were low and the variability between the three measurements was not high, CoV achieving values between 5.32 and 10.19 %.

As seen, metrics that were measured just after blinking tended to have lower repeatability than those measured 1.00 second after blink since more positional variation of particles causes less repeatability. This might also be due to the fact that particles move faster just after blink, and in some cases, this causes particles to look like a stain instead of a point. Therefore, determining accurately the centre of particles' position by the examiner was more challenging.

Correlations between tear film-dynamic metrics and DED signs and symptoms

Spearman's significant correlations between tear film-dynamic metrics and ocular DED parameters are shown in *Table 8.2.2*. There were moderate positive correlations between tear film-dynamic metrics and NIKBUT, while tear film-dynamic was negatively correlated with meibomian gland drop-out percentage in some cases. No statistically significant correlation was obtained with other DED signs and symptoms.

Table 8.2.2. *Statistically significant Rho Spearman correlations between tear film-dynamic metrics and ocular signs.*

Tear film-dynamic metrics	Metric 2	Correlation coefficient	Significance level
Particle speed at 0.25 seconds	Mean mean NIKBUT	0.23	0.044
Particle speed at 0.50 seconds	First mean NIKBUT	0.38	0.015
	Mean mean NIKBUT	0.35	0.031
Particle speed at 1.00 second	First mean NIKBUT	0.36	0.020
	Meibomian glands drop-out percentage	-0.22	0.048
Particle speed at 1.25 seconds	Meibomian glands drop-out percentage	-0.22	0.049
Particle speed at 1.50 seconds	First mean NIKBUT	0.38	0.026
Particle speed at 1.75 seconds	First mean NIKBUT	0.30	0.030
Median particle speed	First mean NIKBUT	0.27	0.018
Minimum particle speed	First mean NIKBUT	0.37	0.015
	Meibomian glands drop-out percentage	-0.37	0.014
Time for particle speed to decrease to < 1.20 mm/second	First mean NIKBUT	0.42	0.004
	Mean mean NIKBUT	0.34	0.034
	Meibomian glands drop-out percentage	-0.35	0.024

(Where NIKBUT: Non-Invasive Break-Up Time)

Differences between groups

Participants were divided into two groups depending on each ocular surface parameter. Mann-Whitney U test did not show statistically significant differences in age between groups, with the exception of meibomian gland drop-out percentage where the group with higher gland drop-out percentage was more elderly ($p < 0.001$).

Table 8.2.3 shows the statistically significant differences in tear film-dynamic metrics for each ocular surface parameter. There were significant differences between high and low NIKBUT groups, and high and low meibomian gland drop-out percentage ($p < 0.05$). No significant differences were obtained for the other ocular surface parameters measured in the study ($p > 0.05$).

Table 8.2.3. *Statistically significant differences in tear film-dynamic metric for each ocular surface parameter.*

Tear film-dynamic metrics	Group (Mean ± SD)		Significance level
	First mean NIKBUT < 10s	First mean NIKBUT > 10s	
Mean particle speed (mm/second)	1.40 ± 0.51	1.60 ± 0.42	0.040[1]
Median particle speed (mm/second)	1.08 ± 0.48	1.32 ± 0.41	0.006[2]
Minimum particle speed (mm/second)	0.57 ± 0.31	0.80 ± 0.32	0.004[2]
Particle speed at 0.50 seconds (mm/second)	1.75 ± 0.94	2.19 ± 0.88	0.011[2]
Particle speed at 1.00 second (mm/second)	0.98 ± 0.50	1.24 ± 0.42	0.005[2]
Particle speed at 1.25 seconds (mm/second)	0.77 ± 0.29	1.10 ± 0.28	0.047[2]
Particle speed at 1.50 seconds (mm/second)	0.69 ± 0.30	1.00 ± 0.34	0.045[2]
Particle speed at 1.75 seconds (mm/second)	0.67 ± 0.31	0.86 ± 0.33	0.030[2]
Time for particle speed to decrease to < 1.20 mm/second (seconds)	0.84 ± 0.47	1.16 ± 0.44	0.002[2]
	Mean mean NIKBUT < 10s	Mean mean NIKBUT > 10s	
Mean particle speed (mm/second)	1.34 ± 0.51	1.58 ± 0.45	0.042[1]
Maximum particle speed (mm/second)	2.99 ± 1.34	3.68 ± 1.11	0.019[1]
Particle speed at 0.25 seconds (mm/second)	2.59 ± 2.30	3.24 ± 1.41	0.009[2]
Particle speed at 0.50 seconds (mm/second)	1.52 ± 0.77	2.18 ± 0.96	0.003[1]
Time for particle speed to decrease to < 1.20 mm/second (seconds)	0.82 ± 0.48	1.08 ± 0.44	0.040[2]
	Meibomian gland drop-out ≤ 1/3	Meibomian gland drop-out > 1/3	
Minimum particle speed (mm/second)	0.72 ± 0.34	0.54 ± 0.30	0.039[2]
Particle speed at 1.00 second (mm/second)	1.16 ± 0.50	0.87 ± 0.34	0.024[2]
Particle speed at 1.25 seconds (mm/second)	1.00 ± 0.36	0.80 ± 0.33	0.037[2]
Time for particle speed to decrease to < 1.20 mm/second (seconds)	1.09 ± 0.44	0.82 ± 0.42	0.042[1]

(Where SD: Standard Deviation; NIKBUT: Non-Invasive Break-Up Time; [1]T-Student; [2]Mann-Whitney U test)

Binomial logistic regression

Binomial logistic regression analysis (*Table 8.2.4*) revealed that tear film-dynamic metrics were able to predict NIKBUT. Nevertheless, no statistically significant association was found between new metrics and gland drop-out.

Table 8.2.4. *Binomial logistic regression' odds ratio of NIKBUT and meibomian gland drop-out by tear film-dynamic metrics.*

	First mean NIKBUT				Mean mean NIKBUT				Meibomian gland drop-out			
Tear film-dynamic metrics	Odd ratio	Lower CI	Upper CI	p-valor	Odd ratio	Lower CI	Upper CI	p-valor	Odd ratio	Lower CI	Upper CI	p-valor
Particle speed at 0.25 seconds	1.08	0.83	1.40	0.572	1.30	0.91	1.87	0.148	0.96	0.72	1.28	0.797
Particle speed at 0.50 seconds	1.77	1.02	4.00	0.034*	2.84	1.37	5.88	0.005*	0.75	0.42	1.32	0.313
Particle speed at 0.75 seconds	1.54	0.73	3.23	0.255	1.56	0.68	3.57	0.297	0.93	0.42	2.06	0.866
Particle speed at 1.00 second	3.24	1.16	9.07	0.015*	1.37	0.49	3.82	0.548	0.41	0.13	1.25	0.118
Particle speed at 1.25 seconds	3.42	0.91	12.40	0.045*	1.25	0.32	4.92	0.750	0.25	0.06	1.13	0.072
Particle speed at 1.50 seconds	3.84	0.99	14.94	0.042*	2.08	0.50	8.58	0.311	0.34	0.08	1.62	0.186
Particle speed at 1.75 seconds	7.02	1.059	46.568	0.033*	3.00	0.45	19.99	0.255	0.49	0.07	3.34	0.465
Mean particle speed	2.79	1.025	7.593	0.035*	3.01	1.02	8.93	0.027*	0.58	0.21	1.59	0.288
Median particle speed	3.31	1.15	9.54	0.017*	1.33	0.47	3.77	0.595	0.63	0.21	1.86	0.402
Maximum particle speed	1.27	0.88	1.83	0.208	1.62	1.07	2.44	0.012*	0.99	0.67	1.45	0.937
Minimum particle speed	7.75	1.67	35.92	0.004*	1.76	0.40	7.67	0.451	0.24	0.05	1.22	0.085
Time for particle speed < 1.20 mm/second	4.64	1.62	13.34	0.001*	2.23	0.98	6.35	0.033*	0.48	0.17	1.36	0.167

*(Where CI: Confidence Interval; NIKBUT: Non-Invasive Break-Up Time; *Statistically significant values)*

8.2.4. Discussion

In the present study, the movement of tear film particles was used to indirectly measure the quality of the tear film after blinking. Conversely to NIKBUT, tear film-dynamic has the advantage of being measured under more natural conditions. The present study developed and assessed the outcomes of a method that could be used by clinicians to assess tear film stability objectively and in a more non-invasively way than NIKBUT since it only requires to analyze particle' speed in a blink. It could be easier to apply in children in comparison with NIKBUT since it does not require subjects to keep their eyes opened forcefully. Moreover, the need of developing new objective and non-invasive methods to assess the tear film stability has been recognized by the TFOS DEWS II Diagnostic Methodology Report (Wolffsohn et al., 2017), acknowledging particles' movement assessment as a potential tool to describe the spread of the tear film.

The spreading of the tear film is influenced by its quality, stability and viscosity as well as by gravity, and airflow (McDonald, 1969; Nikolov et al., 2002). Additionally, tear film viscosity is approximately three times higher in dry eye patients (Li et al., 2015a; Pult et al., 2015). The spreading speed of the tear film over the ocular surface depends on the velocity of the upper eyelid during blinking. It has been reported that the speed of a spontaneous blink is 120 mm/second (Nakamura et al., 2008; Kwon et al., 2013)[37,38]. Berger and Corrsin (1974) reported that the peak velocity of tear spreading after blink was approximately 10 mm/second.

Tear film-dynamic metrics and movement

As in previous studies (Owens and Phillips, 2001; Varikooty, Keir and Simpson, 2012; Lai et al., 2019), tear spreading can be observed as a rapid upward movement of particles after blink, followed by a slowdown. Owens and Phillips (2001) also found that particle speed decreased with time, and the least-squares fitted line regressed from 20 normal subjects was: Particle Speed (time) = -2.21 X Ln (time) + 0.025. They reported that mean velocity was 7.34 ± 2.73 mm/second, 40 milliseconds after blink.

Moreover, as found by other authors (Owens and Phillips, 2001; Varikooty, Keir and Simpson, 2012; Lai et al., 2019), particle speed started to stabilize 1.00 second after blinking since no statistically significant differences were found in particle speed from 1 second. Nevertheless, particle speed was not fully stabilized since it still tends toward zero. Nonetheless, studies are not directly comparable due to differences in methodology.

The particle movement can be explained by the spreading of the tear film post-blinking. When the eyelid stops moving, the tear film diminishes its speed and starts to stabilize. After blink, tear film spreading occurs because of the negative hydrostatic pressure within the nascent menisci (Johnson and Murphy, 2006). Between blinks, tear film thins and breaks-up, which causes the beginning of another blink cycle (Braun et al., 2015; Willcox et al., 2017).

Repeatability of each tear film-dynamic metric

Two causes could cause low repeatability. The first one is that the method is not accurate in the measurements and its repeatability in the measurement is poor, while the second cause could be attributable to the behaviour of the tear film or the blinking pattern. Only complete and spontaneous blinks were assessed in this study, which minimizes the effect of blinking pattern on particles speed. Metrics achieve good repeatability when the repeatability scores (Sw, CoR and CoV) are near zero (Bland and Altman, 2010; Cerviño et al., 2015; McAlinden, Khadka and Pesudovs, 2015; Martínez-Albert et al., 2018). Generally, new metrics manifested moderate-acceptable repeatability, even though the particle position was determined manually. This suggests that the repeatability of the method was acceptable and the tear film did not change between the analyzed blinks. Repeatability tended to be lower just after blinking since particles moved quicker and hence tracking particle position in each moment was more challenging for the examiner.

Correlations between tear film-dynamic metrics and DED signs and symptoms

Moderate positive significant correlations were found between tear film-dynamic metrics and NIKBUT, while some tear film-dynamic metrics were negatively correlated with meibomian gland drop-out percentage. This means that for longer NIKBUT or lower meibomian gland drop-out, particles will move faster. These correlations could be explained by the fact that NIKBUT is directly related to the spreading and stabilization of the tear film. Additionally, meibomian glands secrete meibum, which contributes to the tear film lipid layer, reducing the evaporation and enhancing their

stability and spread (Willcox et al., 2017; Wolffsohn et al., 2017). Despite correlations being low, this is not unusual in studies related to tear film, due to the multifactorial nature of DED which precludes strong associations between variables (Willcox et al., 2017; Wolffsohn et al., 2017). Strikingly, no statistically significant correlation was found between the tear film-dynamic metrics and the lipid layer pattern. It has been previously reported (Owens and Phillips, 2001) that the particles are much larger than the thickness of the lipid layer, and therefore, they might protrude into the aqueous-lipid interface. This fact could suggest that that particle speed might reflect the movement of the lipid and aqueous layer (Owens and Phillips, 2001). Thus, the stabilization of tear film might depend on the spreading of both layers, and not on the spreading of the lipid layer alone (Yokoi et al., 2008).

Differences between groups

When participants were classified into different groups according to the cut-off values reported by the TFOS DEWS II Diagnostic Methodology Report (Wolffsohn et al., 2017), statistical differences in tear film-dynamic metrics were found between high and low NIKBUT groups, and high and low meibomian gland drop-out percentage groups. These results are aligned with the correlations.

Binomial logistic regression

Binomial logistic regression was performed in order to assess whether new metrics were predictable of NIKBUT and meibomian gland drop-out. Results confirmed new metrics are able to predict NIKBUT. Nevertheless, new metrics were not

predictive of meibomian gland drop-out, which could suggest that the association with gland drop-out in *Tables 8.2.2* and *8.2.3* is a consequence of the association with NIKBUT.

The present study had some limitations to consider. There was a significant difference in age distribution between high and low meibomian glands drop-out groups and this might have acted as a possible confounding factor. Regarding the developed method, the examiner still has to manually select the particle position. Although the tracking of particles was the only manual part of the analysis, it can increase variability and diagnostic time. However, the present study showed that repeatability of metrics was acceptable. Furthermore, only the gland drop-out of the upper eyelid was evaluated because it was easier to capture a uniformly focused area. Finally, if there are particles with a thickness higher than the whole tear film thickness, their motion could be influenced by the interaction with the epithelial surface.

Overall, new tear film-dynamic metrics are emerging homeostasis parameters for indirectly assessing the quality of the tear film after blinking. These metrics provide non-invasive and quantitative insights about the in-vivo dynamics of the tear film with an acceptable repeatability. They present the additional advantage of being less invasive and measuring the stability of the tear film in more natural conditions than NIKBUT

The metric called "time for particle speed to decrease to < 1.20 mm/second" can be considered the best metric to describe the spreading of tear film since it was more strongly correlated with NIKBUT, it was more strongly associated in the binomial

logistic regression analysis with NIKBUT and showed acceptable repeatability. Thus, the higher the time for particle speed to decrease to < 1.20 mm/second, the larger NIKBUT and the better stability of the tear film. The combination of tear film-dynamic metrics with commonly used clinical tests for ocular surface assessment could aid in the diagnosis of DED and in the follow-up of treatments. Further investigation is required in order to evaluate the potential utility of these new metrics in DED assessment and their diagnostic capability.

CHAPTER 8.3: Validation of a new objective method to assess lipid layer thickness without the need of an interferometer

8.3 VALIDATION OF A NEW OBJECTIVE METHOD TO ASSESS LIPID LAYER THICKNESS WITHOUT THE NEED OF AN INTERFEROMETER

In this chapter, a method to objectively assess the lipid layer thickness will be developed through the analysis of grey intensity values obtained from the Placido disk pattern reflected onto the tear film. The repeatability of these new metrics and their relationship with DED signs and symptoms will be assessed. Moreover, the diagnostic capability and the accuracy of these new metrics to objectively grade the lipid layer will be evaluated.

8.3.1. Introduction

Given the key role of the lipid layer in maintaining the properties of the tear film (as explained in *Chapter 1 Introduction*), the assessment of the lipid layer thickness is essential in DED and MGD (Guillon, 1998a; Wolffsohn et al., 2017). One of the most common methods for assessing the lipid layer is the evaluation of the colour and brightness of its interference patterns using an interferometer.

It has been reported that subjective diagnostic tests, such as grading scales, rely on the examiner's ability, which might decrease inter and intra-observer repeatability (Nichols et al., 2005; Arita et al., 2009b; Tomlinson et al., 2011; Wolffsohn et al., 2017). Likewise, in some cases, the grading of the interference patterns is difficult to perform, especially when dealing with thinner lipid layers (Remeseiro et al., 2013; Wolffsohn et al., 2017). Currently, only the LipiView® system can provide quantitative values of the lipid layer thickness. However, it has a small area of measurement and it only

measures the lipid layer thickness in blinking conditions (Remeseiro et al., 2014b; Markoulli et al., 2017).

Lately, several studies have tried to solve the aforementioned problems by developing algorithms, based on the analysis of the texture, structure or colour of the interference patterns, which objectively assess the lipid layer thickness (Wu et al., 2008; García-Resúa et al., 2013; Remeseiro et al., 2013; Lu et al., 2014; Remeseiro et al., 2014c; Peteiro-Barral et al., 2016; Hwang et al., 2017; Bai and Nichols, 2019; da Cruz et al., 2020). Likewise, other authors have used high-resolution microscopy systems to characterize the lipid layer thickness (Bai, Ngo and Nichols, 2019) or have combined optical coherence tomography with interferometry to develop novel imaging systems (Lu et al., 2014; Bai and Nichols, 2017). Nonetheless, none of these methods has been globally accepted and most of them are considerably time-consuming. Moreover, they require interferometers to be performed, which are too costly and sophisticated to be implemented in the clinic, being more suitable for research purposes.

During corneal topography measurement, the tear film acts as a mirror and reflects the projected Placido disk ring pattern. Placido disk rings show lighter than the background. The healthy tear film surface forms a well-structured and reflected pattern with good intensity of reflection, while an altered tear film produces an irregular pattern with low reflectivity (Alonso-Caneiro et al., 2013). Accordingly, the primary aim of the present study was to develop and validate a novel method to objectively assess the lipid layer through the analysis of grey intensity values obtained

from the Placido disk pattern reflected onto the tear film, without the need of an interferometer, thus making the method widely accessible.

The base of the method is that a thicker lipid layer has more lipids (Willcox et al., 2017), which will reflect the light of the Placido disk ring pattern with higher intensity. It could be hypothesized that high grey intensity values might be related to a thicker lipid layer, while low grey intensity values might be related to a thinner lipid layer. This method was developed following previous research (Alonso-Caneiro et al., 2013), which shows that the analysis of grey level intensity values of videokeratoscopy images may significantly improve the diagnosis of DED in comparison to other image analysis approaches.

8.3.2. Methodology

Ninety-four healthy volunteers ranging in age from 18 to 90 years (43.8 ± 26.8 years) were enrolled in this study. Only the right eye of participants was assessed to avoid subjects' data duplication. Subjects had no prior history of ocular disease or injury in the last three months. No exclusion based on ocular surface parameters was made to evaluate different tear film status. Contact lens users were instructed not to wear their contact lenses within a week before the examination. The work was performed in accordance with the tenets of the Declaration of Helsinki and was approved by the Ethics Committee of the University of Valencia. Written consent of each subject was obtained after a verbal explanation of the study protocol.

Measurements

Participants' ocular surface was evaluated using Oculus Keratograph 5M (K5 M; Oculus GmbH, Wetzlar, Germany). Measurements were taken by the same experienced researcher following the guidelines of the TFOS DEWS II Diagnostic Methodology Report (Wolffsohn et al., 2017), and were performed in the following order to avoid tear film destabilization: OSDI, DEQ-5, total bulbar redness, TMH, lipid layer thickness, NIKBUT, meibomian glands expressibility and upper eyelid meibography. The illuminance, temperature and humidity of the room were maintained constant at 200 lux, 24.1 ± 1.6 °C and 44.9 ± 5.0 %, respectively.

OSDI, DEQ-5, bulbar redness, TMH, lipid layer thickness, NIKBUT and meibomian gland drop-out were assessed as explained in *Chapter 3 General Methodology*. The expressibility of the central 8 meibomian glands of the upper eyelid was assessed using a subjective grading scale (Bron, Benjamin and Snibson, 1991; Shimazaki, Sakata and Tsubota, 1995; Tomlinson et al., 2011).

Data analysis using the proposed method

Oculus Keratograph 5M was used to record a video of the NIKBUT measurement at 32 frames per second with a spatial resolution of 680 x 512 pixels. This video was recorded and saved to be later analysed. The proposed software was developed using Matlab R2019a® (MathWorks, Natick, MA). The software automatically decomposed the video into frames with a time interval of 0.031 seconds between them. The examiner manually selected the frames at 0.33, 5.33, 10.33, 15.33 and 20.33 seconds

after blinking. The frame of 0.33 was selected since the eye was completely open after this time in all videos. Likewise, intervals of 5.00 seconds from this moment on were chosen to analyse whether the grey intensity values changed over time.

Once the frames of interest were selected, the software automatically processed the images. First, RGB images were transformed into grey-level images. Given that input images contained irrelevant information of external areas, the centre of the Placido disk ring pattern was isolated by the examiner through Matlab. After clicking the centre of the image, the software automatically selected a square of 241 x 241 pixels surrounding the centre of the rings, as the area to perform the image processing.

Next, a band-pass filter was used to eliminate the background illumination and highlight the rings. Furthermore, the images were then smoothed by applying a 4-pixel sigma Gaussian filter to remove the remaining noise from the background (Esmaeili et al., 2016). After that, the final ROI was selected by the examiner, who manually selected the region of the image comprising solely the pupil, to avoid the influence of the iris on the results.

Finally, to increase the differences between normal and altered tear films, each pixel value of the resulting image was multiplied by 255 and divided by 85, thus enhancing the contrast between rings and non-ring spaces. These values were selected since they produced the highest possible contrast enhancement.

Once the images were processed, histograms were obtained from their pixel intensity values and metrics were calculated (*Figure 8.3.1*). *Figure 8.3.2* shows a summary of the main steps of image processing.

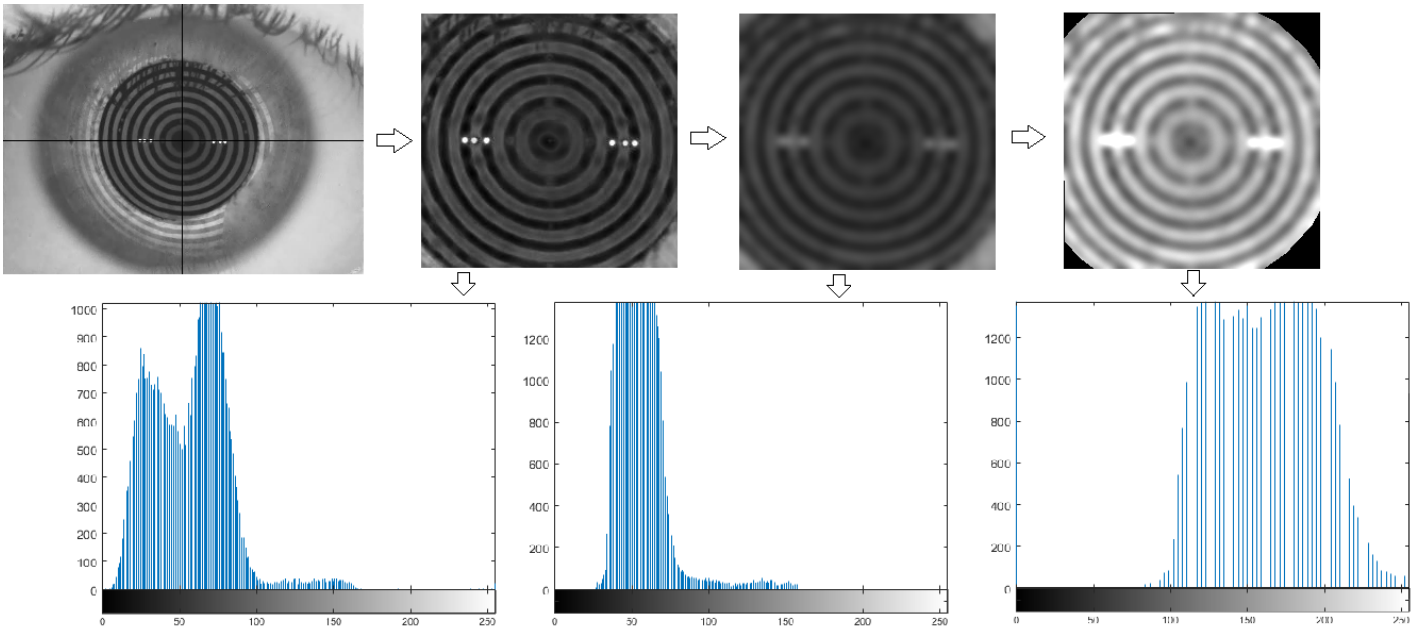

Fig. 8.3.1. *Images and histograms of the main steps of the image processing in a random frame. From left to right: Selection of the centre of the image; Pass-band filter implementation; Gaussian filter implementation; Selection of the final ROI and contrast enhancement (final image). In the histograms, axe "x" represents the grey level intensities (0-255), while axe "y" shows the number of pixels.*

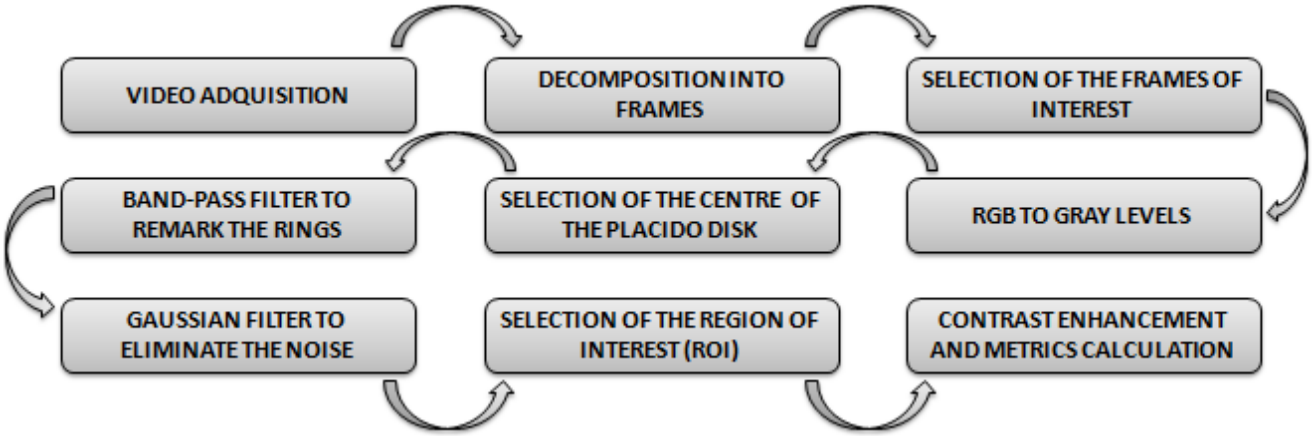

Fig. 8.3.2. *The main steps of the image processing.*

The base of this method is that a thicker lipid layer has more lipids (Willcox et al., 2017), which will reflect the Placido disk rings with higher intensity. Thus, higher grey intensity values might be related to a thicker lipid layer thickness, while lower grey intensity values could be related to a thinner lipid layer thickness.

Mean, SD, median, mode, kurtosis and skewness of the histogram of the grey level intensity values were calculated. The minimum grey level in the image was also calculated. Besides, energy, relative energy, entropy and SD irregularity were calculated as follows (Alonso-Caneiro et al., 2013):

Energy as: $\frac{\sum p\text{^}2}{n}$

Relative energy as: $\frac{\sum(\frac{p}{pmax})\text{^}2}{n}$

Entropy: $\frac{-\sum p.\log r(p)}{n}$

SD irregularity as: $\frac{\sum\left(\frac{p-x}{pmax}\right)\text{^}2}{n}$.

Where: p = pixel grey value; n = number of pixels of the ROI; pmax = maximum pixel intensity; and x = mean pixel intensity values.

Metrics were divided by the number of pixels of the ROI (n) so that all images were comparable independently of the size of the ROI. Finally, the total area under the pixel intensity three-dimensional curve of the image was calculated and divided by the number of pixels in the ROI (*Figure 8.3.3*).

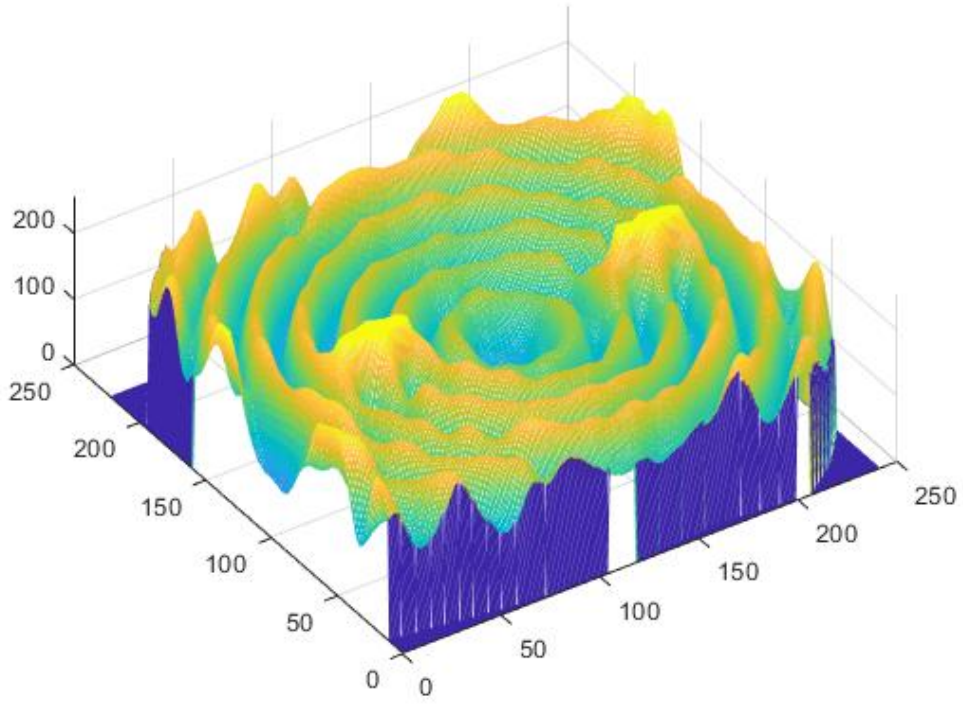

Fig. 8.3.3. *Three-dimensional graphic of the grey intensity values in the image. The "x" and "y" axis represent the size of the image, and "z" the grey intensity value for each pixel.*

Statistical analysis

Statistical analysis was carried out using SPSS v26.0 for Windows (IBM Corp, Armonk, New York, USA). Outcomes were shown as the mean ± SD.

Repeated mixed model ANOVA was used to evaluate the differences in pixel intensity values depending on the moment after blinking. Bonferroni was used to assess the post-hoc differences between paired moments.

As three NIKBUT videos were recorded, the three videos were analyzed so as to calculate the repeatability of the software in the calculation Placido disk' reflectivity metrics. Repeatability of each Placido disk' reflectivity metric was assessed by calculating the S_w, CoV and CoR, as explained in *Chapter 3 General Methodology* (Bland and Altman, 2010; McAlinden, Khadka and Pesudovs, 2015; Martínez-Albert et al., 2018).

Rho Spearman correlations were used to analyse the correlations between ocular surface signs and symptoms and new metrics, for the whole sample. Moreover, the sample was divided into different groups according to the cut-off values reported by the Diagnostic Methodology Report of TFOS DEWS II (Wolffsohn et al., 2017).

Differences in Placido disk' reflectivity metrics between groups was assessed by means of Mann-Whitney U test or Kuskal-Wallis test. A p-value less than 0.05 was defined as statistically significant.

Multiple linear regressions were performed to assess the predictability of tear film-dynamic metrics to ocular signs that had statistically significant correlations.

Multiple linear models were constructed with new metrics as dependent variables and current metrics as independent variables to assess the relative importance of each independent variable and their contribution to the change of dependent variables. The following assumptions were checked: the linear relationship between the independent and dependent variables, normal distribution of residuals, homoscedasticity of residuals and predicted values and absence of multicollinearity between independent variables.

Each new metric was validated by means ROC curves. The probability density functions for an altered (lipid layer thickness = 1) or normal (lipid layer thickness ≥ 2) lipid layer thickness were calculated (Wolffsohn et al., 2017) and different parameters were obtained for each ROC curve, as explained in *Chapter 3 General Methodology*: Sensitivity, specificity, area under the ROC curve, the cut-off value that optimizes the diagnosis, Youden index and discriminant power (Sokolova, Japkowicz and Szpakowicz, 2006).

Finally, each Placido disk image was objectively classified into lipid layer thickness groups depending on the cut-off values obtained in the ROC curves. The level of agreement between this objective classification and the subjective ones was analysed by calculating the accuracy, Kappa index, weighted Kappa index with quadratic weights and F-measure for each metric, as explained in *Chapter 3 General Methodology* (Cohen, 1968; Landis and Koch, 1977; Rosenfield and Fitzpatrick-Lins, 1986; Viera and Garret, 2005).

8.3.3. Results

The described method was applied to ninety-four eyes from 94 volunteers, 54 females (57.4 %) and 40 males (42.6 %). The mean age was 43.8 ± 26.8 years, ranging from 18 to 90 years. The method was able to obtain objective metrics in all subjects.

Placido disk reflectivity metrics over time

Table 8.3.1 shows the mean values and SD for each Placido disk reflectivity metric at 0.33, 5.33, 10.33, 15.33 and 20.33 seconds after blinking. Repeated mixed model ANOVA showed statistical higher pixel intensity values at 10.33, 15.33 and 20.33 seconds than at 0.33 seconds. Nevertheless, CoV revealed a low variability of metrics over time. Thus, pixel intensity of the Placido disk was stable in the same subject throughout the measuring period. CoV between seconds after blinking achieved values between 4.42 % and 16.92 %. Total area under pixel intensity curve, mean pixels intensity, SD of pixels intensity, median pixels intensity and skewness had a CoV < 10 %, which evidenced that metrics did not change after blinking.

Table 8.3.1. *Mean values for each Placido disk reflectivity metric.*

Metric		Number of subjects	Mean ± SD	Significance level	Statistically significant post-hoc differences (p-value)	CoV between seconds after blinking (%)
Total area	0.33 s	94	113.63 ± 9.57	< 0.001[1]*	1-4 < 0.001 1-5 < 0.001	4.42
	5.33 s	90	116.79 ± 8.48			
	10.33 s	66	117.15 ± 9.18			
	15.33 s	49	119.22 ± 8.30			
	20.33 s	37	120.30 ± 7.87			
Minimum pixel intensity	0.33 s	94	67.12 ± 17.37	0.082[1]		13.58
	5.33 s	90	69.10 ± 16.20			
	10.33 s	66	70.00 ± 18.84			
	15.33 s	49	75.12 ± 18.98			
	20.33 s	37	70.58 ± 18.16			
Energy	0.33 s	94	240.78 ± 8.89	<0.001[1]*	1-3 < 0.001 1-4 < 0.001 1-5 < 0.001	14.84
	5.33 s	90	244.72 ± 7.06			
	10.33 s	66	249.45 ± 5.02			
	15.33 s	49	251.82 ± 3.32			
	20.33 s	37	253.82 ± 2.02			
Relative energy	0.33 s	94	0.46 ± 0.26	<0.001[1]*	1-3 < 0.001 1-4 < 0.001 1-5 < 0.001	15.78
	5.33 s	90	0.54 ± 0.26			
	10.33 s	66	0.57 ± 0.28			
	15.33 s	49	0.63 ± 0.27			
	20.33 s	37	0.68 ± 0.27			
Entropy	0.33 s	94	$2.0x10^{-4} \pm 1.2 x10^{-4}$	0.906[1]		16.92
	5.33 s	90	$2.0x10^{-4} \pm 1.2 x10^{-4}$			
	10.33 s	66	$2.0x10^{-4} \pm 1.2 x10^{-4}$			
	15.33 s	49	$2.0x10^{-4} \pm 1.2 x10^{-4}$			
	20.33 s	37	$2.0x10^{-4} \pm 1.2 x10^{-4}$			
SD irregularity	0.33 s	94	0.08 ± 0.12	0.002[1]*	1-4 = 0.005 1-5 = 0.001	15.26
	5.33 s	90	0.10 ± 0.12			
	10.33 s	66	0.12 ± 0.14			
	15.33 s	49	0.13 ± 0.12			
	20.33 s	37	0.17 ± 0.17			
Mean pixels intensity	0.33 s	94	130.38 ± 26.74	<0.001[1]*	1-3 < 0.001 1-4 < 0.001 1-5 < 0.001	9.31
	5.33 s	90	137.24 ± 26.96			
	10.33 s	66	140.58 ± 29.76			
	15.33 s	49	146.55 ± 29.27			
	20.33 s	37	153.06 ± 31.80			
SD of pixels intensity	0.33 s	94	26.89 ± 4.63	<0.001[1]*	1-3 < 0.001 1-4 < 0.001 1-5 < 0.001	8.73
	5.33 s	90	29.62 ± 4.84			
	10.33 s	66	30.43 ± 4.50			
	15.33 s	49	31.19 ± 4.92			
	20.33 s	37	32.62 ± 4.83			

(continuation)						
Metric		Number of subjects	Mean ± SD	Significance level	Statistically significant post-hoc differences (p-value)	CoV between seconds after blinking (%)
Median pixels intensity	0.33 s	94	127.12 ± 27.47	<0.001[1]*	1-4 < 0.001	9.73
	5.33 s	90	136.27 ± 27.97		1-5 < 0.001	
	10.33 s	66	139.68 ± 31.12			
	15.33 s	49	145.59 ± 30.56			
	20.33 s	37	152.52 ± 33.03			
Mode pixels intensity	0.33 s	94	142.40 ± 40.12	<0.001[1]*	1-3 = 0.004	16.79
	5.33 s	90	150.03 ± 47.08		1-4 = 0.001	
	10.33 s	66	152.90 ± 50.89		1-5 < 0.001	
	15.33 s	49	164.27 ± 55.38			
	20.33 s	37	175.22 ± 60.98			
Kurtosis	0.33 s	94	0.017 ± 0.001	<0.001[1]*	1-4 < 0.001	11.37
	5.33 s	90	0.015 ± 0.003		1-5 < 0.001	
	10.33 s	66	0.015 ± 0.003			
	15.33 s	49	0.014 ± 0.003			
	20.33 s	37	0.014 ± 0.003			
Skewness	0.33 s	94	0.14 ± 0.02	<0.001[1]*	1-4 < 0.001	6.90
	5.33 s	90	0.13 ± 0.01		1-5 < 0.001	
	10.33 s	66	0.13 ± 0.02			
	15.33 s	49	0.13 ± 0.02			
	20.33 s	37	0.12 ± 0.02			

*(Where CoV: Coefficient of Variation; s: Seconds; SD: Standard Deviation; [1]Repeated mixed model ANOVA; *Statistically significant values)*

Repeatability of Placido disk reflectivity metrics

Table 8.3.2 shows the repeatability scores for each metric. All metrics showed acceptable repeatability since Sw, CoR and CoV values were low and the variability between the three measurements was not high. Sw achieved values between $2x10^{-6}$ and 7.07, CoR between $6x10^{-6}$ and 19.59, and CoV between 0.09 and 5.15.

Table 8.3.2. *Repeatability of each Placido disk reflectivity metric.*

Metric	S_w	CoR	CoV (%)
At 0.33 s			
Total area	0.63	1.74	0.54
Minimum pixel intensity	2.95	8.16	4.42
Energy	0.23	0.64	0.09
Relative energy	0.01	0.04	2.85
Entropy	$2x10^{-6}$	$6x10^{-6}$	1.95
SD irregularity	0.003	0.01	3.66
Mean pixels intensity	1.28	3.55	0.97
SD pixels intensity	0.34	0.96	1.25
Median pixels intensity	1.30	3.59	0.99
Mode pixels intensity	7.02	19.44	5.11
Kurtosis	$3x10^{-4}$	$9x10^{-4}$	2.39
Skewness	0.002	0.006	1.56
At 5.33 s			
Total area	0.54	1.49	0.47
Minimum pixel intensity	2.82	7.82	4.23
Energy	0.23	0.64	0.09
Relative energy	0.01	0.04	2.84
Entropy	$2x10^{-6}$	$6x10^{-6}$	1.94
SD irregularity	0.003	0.01	3.64
Mean pixels intensity	1.06	2.93	0.80
SD pixels intensity	0.34	0.93	1.21
Median pixels intensity	1.29	3.56	0.98
Mode pixels intensity	7.01	19.40	5.10
Kurtosis	$3x10^{-4}$	$8x10^{-4}$	2.01
Skewness	0.001	0.004	1.11
At 10.33 s			
Total area	0.59	1.64	0.51
Minimum pixel intensity	2.76	7.64	4.15
Energy	0.23	0.64	0.09
Relative energy	0.01	0.04	2.89
Entropy	$2x10^{-6}$	$8x10^{-6}$	2.49
SD irregularity	0.003	0.01	3.97
Mean pixels intensity	1.33	3.67	1.00
SD pixels intensity	0.35	0.97	1.26
Median pixels intensity	1.30	3.61	0.99
Mode pixels intensity	7.03	19.48	5.12
Kurtosis	$3x10^{-4}$	$9x10^{-4}$	2.09
Skewness	0.002	0.004	1.21

(continuation)			
Metric	S_w	CoR	CoV (%)
At 15.33 s			
Total area	0.60	1.67	0.52
Minimum pixel intensity	2.81	7.78	4.19
Energy	0.23	0.64	0.09
Relative energy	0.01	0.04	2.90
Entropy	$3x10^{-6}$	$8x10^{-6}$	2.56
SD irregularity	0.003	0.01	4.05
Mean pixels intensity	1.35	3.75	1.02
SD pixels intensity	0.42	1.16	1.50
Median pixels intensity	1.32	3.66	1.01
Mode pixels intensity	7.06	19.57	5.14
Kurtosis	$3x10^{-4}$	$9x10^{-4}$	2.07
Skewness	0.002	0.005	1.42
At 20.33 s			
Total area	0.68	1.87	0.58
Minimum pixel intensity	3.14	8.69	4.69
Energy	0.23	0.64	0.09
Relative energy	0.01	0.04	2.93
Entropy	$3x10^{-6}$	$8x10^{-6}$	2.62
SD irregularity	0.003	0.01	4.21
Mean pixels intensity	1.44	4.00	1.09
SD pixels intensity	0.42	1.16	1.51
Median pixels intensity	1.34	3.71	1.02
Mode pixels intensity	7.07	19.59	5.15
Kurtosis	$3x10^{-4}$	$9x10^{-4}$	2.37
Skewness	0.004	0.01	2.73

(Where CoR: Repeatability coefficient; CoV: Coefficient of variation; s: Seconds; SD: Standard Deviation; S_w: Within-subject standard deviation)

Correlations between new metrics and DED signs and symptoms

Following the results of the previous sections, showing no variation of the metrics over time, only the metrics at 0.33, 5.33 and 10.33 seconds after blinking were further assessed. Metrics at 15.33 and 20.33 seconds were excluded from further analysis as most patients need to suppress blinking forcefully and thus they don't represent in most cases a real scenario.

Spearman's significant correlations between each Placido disk reflectivity metric and DED signs and symptoms are shown in *Table 8.3.3*. Generally, there were moderate negative correlations between new metrics based on the grey intensity of pixels of Placido disk images and age, meibomian glands drop-out percentage, bulbar redness, TMH and OSDI. Meanwhile, Placido disk reflectivity metrics were positively correlated with lipid layer thickness and NIKBUT. The correlation with lipid layer thickness was the strongest. Given that lipid layer thickness was statistically correlated with age ($r = -0.298$, $p = 0.002$), gland drop-out ($r = -0.271$, $p = 0.004$), mean first NIKBUT ($r = -0.209$, $p = 0.008$), median first NIKBUT, mean mean NIKBUT and median mean NIKBUT, it might be possible that the correlation of new metrics with the other ocular surface metrics was as consequence of the correlation with lipid layer thickness. Nevertheless, lipid layer thickness was not statistically correlated with bulbar redness, TMH and OSDI.

Entropy was the only metric which was not correlated with lipid layer thickness. Likewise, new metrics were not correlated with meibomian gland expressibility or DEQ-5 score. The metrics measured at 5.33 and 10.33 can be considered the best to describe the lipid layer thickness since they revealed the strongest correlations.

Table 8.3.3. *Statistically significant Rho Spearman correlations between Placido disk reflectivity metrics and DED signs and symptoms.*

New metrics	Current metrics	Correlation coefficient (r)	Significance level
At 0.33 s			
Total area	Age	-0.372	< 0.001
	Drop-out percentage	-0.277	0.007
	Lipid layer thickness	0.413	< 0.001
	Mean mean NIKBUT	0.209	0.048
Minimum pixel intensity	Age	-0.387	< 0.001
	Drop-out percentage	-0.236	0.022
	Lipid layer thickness	0.345	0.001
Energy	Age	-0.346	< 0.001
	Drop-out percentage	-0.236	< 0.001
	Lipid layer thickness	0.408	< 0.001
Relative energy	Age	-0.356	< 0.001
	Drop-out percentage	-0.266	0.010
	Lipid layer thickness	0.407	< 0.001
	TMH	-0.205	0.048
Entropy	Age	-0.670	< 0.001
	Drop-out percentage	-0.517	< 0.001
	Bulbar redness	-0.615	< 0.001
	TMH	-0.395	< 0.001
	Mean first NIKBUT	0.223	0.033
	Median first NIKBUT	0.226	0.030
	OSDI	-0.316	0.002
SD irregularity	Age	-0.448	< 0.001
	Drop-out percentage	-0.322	0.002
	Bulbar redness	-0.306	0.003
	Lipid layer thickness	0.454	< 0.001
Mean pixels intensity	Age	-0.388	< 0.001
	Drop-out percentage	-0.285	0.005
	Bulbar redness	-0.210	0.043
	Lipid layer thickness	0.426	< 0.001
	Mean mean NIKBUT	0.210	0.046
SD pixels intensity	Age	-0.507	< 0.001
	Drop-out percentage	-0.331	0.001
	Bulbar redness	-0.400	< 0.001
	Lipid layer thickness	0.446	< 0.001
Median pixels intensity	Age	-0.383	< 0.001
	Drop-out percentage	-0.294	0.004
	Lipid layer thickness	0.426	< 0.001
Mode pixels intensity	Age	-0.305	0.003
	Drop-out percentage	-0.234	0.023
	Lipid layer thickness	0.418	< 0.001
Kurtosis	Lipid layer thickness	-0.515	< 0.001
	Mean mean NIKBUT	-0.252	0.016
	Median mean NIKBUT	-0.251	0.017
Skewness	Lipid layer thickness	-0.510	< 0.001
	Mean mean NIKBUT	-0.237	0.024
	Median mean NIKBUT	-0.230	0.029

(continuation)			
New metrics	Current metrics	Correlation coefficient (r)	Significance level
At 5.33 s			
Total area	Lipid layer thickness	0.647	< 0.001
	Mean first NIKBUT	0.265	0.011
	Mean mean NIKBUT	0.233	0.029
Minimum pixel intensity	Lipid layer thickness	0.589	< 0.001
	Mean first NIKBUT	0.229	0.030
Energy	Lipid layer thickness	0.548	< 0.001
	Mean first NIKBUT	0.223	0.019
Relative energy	Lipid layer thickness	0.655	< 0.001
	Mean first NIKBUT	0.237	0.024
Entropy	Age	-0.642	< 0.001
	Drop-out percentage	-0.572	< 0.001
	Bulbar redness	-0.564	< 0.001
	TMH	-0.403	< 0.001
	Mean first NIKBUT	0.221	0.036
	Median first NIKBUT	0.219	0.038
	OSDI	-0.260	0.013
SD irregularity	Age	-0.327	0.002
	Drop-out percentage	-0.249	0.018
	Lipid layer thickness	0.662	< 0.001
Mean pixels intensity	Lipid layer thickness	0.665	< 0.001
	Mean first NIKBUT	0.235	0.026
SD of pixels intensity	Age	-0.408	< 0.001
	Drop-out percentage	-0.272	0.009
	Bulbar redness	-0.247	0.019
	Lipid layer thickness	0.572	< 0.001
Median pixels intensity	Lipid layer thickness	0.674	< 0.001
	Mean first NIKBUT	0.246	0.020
	Mean mean NIKBUT	0.220	0.040
Mode pixels intensity	Lipid layer thickness	0.657	< 0.001
	Mean first NIKBUT	0.233	0.027
Kurtosis	Lipid layer thickness	-0.672	< 0.001
Skewness	Lipid layer thickness	-0.673	< 0.001
At 10.33 s			
Total area	Lipid layer thickness	0.645	< 0.001
Minimum pixel intensity	Lipid layer thickness	0.523	< 0.001
Energy	Lipid layer thickness	0.660	<0.001
Relative energy	Lipid layer thickness	0.654	< 0.001
Entropy	Age	-0.668	< 0.001
	Drop-out percentage	-0.596	< 0.001
	Bulbar redness	-0.542	< 0.001
	TMH	-0.536	< 0.001
	Mean first NIKBUT	0.260	0.034
	Median first NIKBUT	0.282	0.021
	OSDI	-0.300	0.014
SD irregularity	Age	-0.282	0.021
	Lipid layer thickness	0.689	< 0.001
Mean pixels intensity	Lipid layer thickness	0.684	< 0.001
SD of pixels intensity	Age	-0.371	0.002
	Lipid layer thickness	0.644	< 0.001
Median pixels intensity	Lipid layer thickness	0.687	< 0.001
Mode pixels intensity	Lipid layer thickness	0.654	< 0.001

(continuation)			
New metrics	Current metrics	Correlation coefficient (r)	Significance level
At 10.33 s			
Kurtosis	Lipid layer thickness	-0.659	< 0.001
Skewness	Lipid layer thickness	-0.665	< 0.001

(Where NIKBUT: Non-Invasive Keratograph Break-Up Time; OSDI: Ocular Surface Disease Index; s: Seconds; TMH: Tear Meniscus Height)

Differences between groups

The new metrics were analysed according to age and the different ocular surface parameters. *Table 8.3.4* shows the statistically significant differences in Placido disk reflectivity metrics between classification groups. These outcomes were in accordance with correlations. Statistically higher pixel intensity values were found in young subjects, lower gland drop-out, high NIKBUT, low TMH and thick lipid layer thickness. However, no statistical differences were found between grade 3 (wave) and 4 (colour fringe) interference patterns in the assessment of the lipid layer thickness ($p > 0.005$).

Table 8.3.4. *Statistically significant differences in Placido disk reflectivity metrics for each ocular surface parameter.*

New metrics	n	Groups	Mean ± SD	Significance level	Statistically significant post-hoc differences (p-value)
Age					
At 0.33 s					
Total area	60	< 49 years	117.43 ± 11.62	< 0.001[1]	
	34	> 49 years	111.47 ± 7.46		
Minimum pixel intensity	60	< 49 years	75.44 ± 20.64	< 0.001[1]	
	34	> 49 years	62.40 ± 13.20		
Energy	60	< 49 years	254.18 ± 4.38	< 0.001[1]	
	34	> 49 years	245.28 ± 4.38		
Relative energy	60	< 49 years	0.59 ± 0.30	< 0.001[1]	
	34	> 49 years	0.38 ± 0.19		
Entropy	60	< 49 years	$3.0x^{-4} \pm 1.5x10^{-4}$	< 0.001[1]	
	34	> 49 years	$1.0x^{-4} \pm 4x10^{-5}$		
SD irregularity	60	< 49 years	0.13 ± 0.16	< 0.001[1]	
	34	> 49 years	0.04 ± 0.03		
Mean pixels intensity	60	< 49 years	143.32 ± 33.52	< 0.001[1]	
	34	> 49 years	119.92 ± 17.24		
SD of pixels intensity	60	< 49 years	30.05 ± 5.21	< 0.001[1]	
	34	> 49 years	25.10 ± 3.09		
Median pixels intensity	60	< 49 years	142.32 ± 34.97	< 0.001[1]	
	34	> 49 years	118.50 ± 17.22		
Mode pixels intensity	60	< 49 years	155.03 ± 53.85	0.006[1]	
	34	> 49 years	125.85 ± 24.52		
At 5.33 s					
Entropy	59	< 49 years	$3.0x^{-4} \pm 2.1x10^{-4}$	< 0.001[1]	
	31	> 49 years	$1.0x^{-4} \pm 5x10^{-5}$		
SD irregularity	59	< 49 years	0.15 ± 0.15	0.002[1]	
	31	> 49 years	0.07 ± 0.08		
Mean pixels intensity	59	< 49 years	147.34 ± 32.78	0.044[1]	
	31	> 49 years	131.92 ± 21.83		
SD of pixels intensity	59	< 49 years	32.53 ± 5.47	< 0.001[1]	
	31	> 49 years	28.09 ± 3.68		
Mode	59	< 49 years	169.26 ± 58.13	0.043[1]	
	31	> 49 years	139.93 ± 36.77		
At 10.33 s					
Entropy	43	< 49 years	$3.0x^{-4} \pm 1.7x10^{-4}$	< 0.001[1]	
	23	> 49 years	$1.0x^{-4} \pm 4x10^{-5}$		
SD irregularity	43	< 49 years	0.17 ± 0.19	0.011[1]	
	23	> 49 years	0.08 ± 0.09		
SD of pixels intensity	43	< 49 years	32.62 ± 4.10	0.002[1]	
	23	> 49 years	29.10 ± 4.37		

(continuation)

New metrics	n	Groups	Mean ± SD	Significance level	Statistically significant post-hoc differences (p-value)
Bulbar redness					
At 0.33 s					
Total area	60	< 1	116.59 ± 11.70	0.008[1]	
	34	> 1	111.18 ± 7.73		
Minimum pixel intensity	60	< 1	73.32 ± 20.77	0.004[1]	
	34	> 1	63.60 ± 14.12		
Energy	60	< 1	254.08 ± 4.40	< 0.001[1]	
	34	> 1	245.44 ± 21.94		
Relative energy	60	< 1	0.57 ± 0.29	0.002[1]	
	34	> 1	0.39 ± 0.21		
Entropy	60	< 1	$3.0x10^{-4} \pm 1.5x10^{-4}$	< 0.001[1]	
	34	> 1	$1.0x10^{-4} \pm 4x10^{-5}$		
SD irregularity	60	< 1	0.13 ± 0.16	< 0.001[1]	
	34	> 1	0.05 ± 0.04		
Mean pixels intensity	60	< 1	140.99 ± 33.54	0.001[1]	
	34	> 1	121.23 ± 18.82		
SD of pixels intensity	60	< 1	29.98 ± 5.08	< 0.001[1]	
	34	> 1	25.14 ± 3.27		
Median pixels intensity	60	< 1	139.94 ± 34.98	0.001[1]	
	34	> 1	119.85 ± 18.87		
Mode pixels intensity	60	< 1	152.92 ± 54.38	0.011[1]	
	34	> 1	127.05 ± 25.23		
Skewness	60	< 1	0.14 ± 0.03	0.044[1]	
	34	> 1	0.15 ± 0.01		
At 5.33 s					
Entropy	58	< 1	$3.0x^{-4} \pm 2.1x10^{-4}$	< 0.001[1]	
	32	> 1	$1.0x^{-4} \pm 5x10^{-5}$		
SD irregularity	58	< 1	0.14 ± 0.15	0.028[1]	
	32	> 1	0.07 ± 0.08		
SD of pixels intensity	58	< 1	31.99 ± 5.58	0.002[1]	
	32	> 1	28.30 ± 3.84		
Entropy	40	< 1	$3.0x^{-4} \pm 1.7x10^{-4}$	< 0.001[1]	
	25	> 1	$1.0x^{-4} \pm 4x10^{-5}$		
SD of pixels intensity	40	< 1	131.72 ± 4.24	0.024[1]	
	25	> 1	129.42 ± 5.59		
Meibomian gland drop-out					
At 0.33 s					
Total area	50	< 1/3	115.94 ± 10.62	0.008[1]	
	44	> 1/3	111.59 ± 8.12		
Minimum pixel intensity	50	< 1/3	71.80 ± 19.69	0.008[1]	
	44	> 1/3	63.00 ± 13.97		
Energy	50	< 1/3	254.12 ± 4.20	0.002[1]	
	44	> 1/3	245.94 ± 4.18		
Relative energy	50	< 1/3	0.54 ± 0.28	0.007[1]	
	44	> 1/3	0.39 ± 0.22		
Entropy	50	< 1/3	$2.0x10^{-4} \pm 1.4x10^{-4}$	<0.001[1]	
	44	> 1/3	$2.0x10^{-4} \pm 7.0x10^{-5}$		

(continuation)

New metrics	n	Groups	Mean ± SD	Significance level	Statistically significant post-hoc differences (p-value)
Meibomian gland drop-out					
At 0.33 s					
SD irregularity	50	< 1/3	0.12 ± 0.15	0.001[1]	
	44	> 1/3	0.05 ± 0.04		
Mean pixels intensity	50	< 1/3	136.92 ± 31.60	0.005[1]	
	44	> 1/3	120.87 ± 18.90		
SD of pixels intensity	50	< 1/3	28.65 ± 5.29	0.002[1]	
	44	> 1/3	25.35 ± 3.30		
Median pixels intensity	50	< 1/3	135.95 ± 32.77	0.005[1]	
	44	> 1/3	119.34 ± 18.90		
Mode pixels intensity	50	< 1/3	148.50 ± 48.31	0.020[1]	
	44	> 1/3	125.76 ± 27.54		
At 5.33 s					
Entropy	48	< 1/3	$3.0x10^{-4} \pm 2.0x10^{-4}$	< 0.001[1]	
	42	> 1/3	$1.0x10^{-4} \pm 8.0x10^{-5}$		
SD irregularity	48	< 1/3	0.13 ± 0.14	0.031[1]	
	42	> 1/3	0.07 ± 0.09		
SD of pixels intensity	48	< 1/3	31.08 ± 5.39	0.013[1]	
	42	> 1/3	28.34 ± 3.93		
At 10.33 s					
Entropy	33	< 1/3	$3.0x10^{-4} \pm 1.6x10^{-4}$	< 0.001[1]	
	33	> 1/3	$1.0x10^{-4} \pm 4.0x10^{-5}$		
SD irregularity	33	< 1/3	0.14 ± 0.16	0.046[1]	
	33	> 1/3	0.09 ± 0.10		
SD of pixels intensity	33	< 1/3	31.48 ± 4.06	0.021[1]	
	33	> 1/3	29.17 ± 4.80		
TMH					
At 0.33 s					
Entropy	60	> 0.20 mm	$3.0x10^{-4} \pm 1.6x10^{-4}$	< 0.001[1]	
	34	< 0.20 mm	$2.0x10^{-4} \pm 5.0x10^{-5}$		
At 5.33 s					
Entropy	55	> 0.20 mm	$3.0x10^{-4} \pm 2.2x10^{-4}$	< 0.001[1]	
	35	< 0.20 mm	$1.0x10^{-4} \pm 5.0x10^{-5}$		
At 10.33 s					
Entropy	38	> 0.20 mm	$3.0x10^{-4} \pm 1.7x10^{-4}$	< 0.001[1]	
	28	< 0.20 mm	$1.0x10^{-4} \pm 4.0x10^{-5}$		
Mean first NIKBUT					
At 0.33 s					
Entropy	41	> 10 s	$2.0x10^{-4} \pm 1.3x10^{-4}$	0.034[1]	
	53	< 10 s	$2.0x10^{-4} \pm 9.0x10^{-5}$		
At 5.33 s					
Entropy	41	> 10 s	$2.0x10^{-4} \pm 1.8x10^{-4}$	0.042[1]	
	49	< 10 s	$2.0x10^{-4} \pm 1.2x10^{-4}$		

(continuation)

New metrics	n	Groups	Mean ± SD	Significance level	Statistically significant post-hoc differences (p-value)
Mean first NIKBUT					
At 10.33 s					
Entropy	36	> 10 s	$2.0x10^{-4} \pm 1.6x10^{-4}$	0.026[1]	
	30	< 10 s	$2.0x10^{-4} \pm 1.0x10^{-4}$		
Lipid layer thickness					
At 0.33 s					
Total area	28	Grade 1	109.67 ± 8.76	< 0.001[2]	1-3 < 0.001
	38	Grade 2	111.96 ± 8.70		1-4 = 0.002
	15	Grade 3	120.70 ± 10.16		2-3 = 0.001
	13	Grade 4	119.26 ± 7.30		2-4 = 0.008
Minimum pixel intensity	28	Grade 1	60.75 ± 11.06	0.001[2]	1-3 = 0.001
	38	Grade 2	62.60 ± 12.72		1-4 = 0.041
	15	Grade 3	83.79 ± 22.62		2-3 = 0.001
	13	Grade 4	75.92 ± 21.02		2-4 = 0.046
Energy	28	Grade 1	239.86 ± 26.07	< 0.001[2]	1-2 = 0.032
	38	Grade 2	243.52 ± 22.66		1-3 < 0.001
	15	Grade 3	254.55 ± 2.08		1-4 ≤ 0.001
	13	Grade 4	254.99 ± 0.01		2-3 = 0.002
					2-4 = 0.001
Relative energy	28	Grade 1	0.33 ± 0.13	< 0.001[2]	1-3 < 0.001
	38	Grade 2	0.40 ± 0.20		1-4 = 0.002
	15	Grade 3	0.73 ± 0.29		2-3 = 0.001
	13	Grade 4	0.72 ± 0.29		2-4 = 0.016
SD irregularity	28	Grade 1	0.03 ± 0.01	< 0.001[2]	1-3 < 0.001
	38	Grade 2	0.05 ± 0.03		1-4 < 0.001
	15	Grade 3	0.18 ± 0.18		2-3 = 0.008
	13	Grade 4	0.15 ± 0.17		2-4 = 0.014
Mean pixels intensity	28	Grade 1	115.09 ± 11.56	< 0.001[2]	1-3 < 0.001
	38	Grade 2	121.47 ± 17.40		1-4 = 0.001
	15	Grade 3	156.54 ± 35.25		2-3 = 0.002
	13	Grade 4	155.23 ± 32.90		2-4 = 0.008
SD of pixels intensity	28	Grade 1	24.50 ± 2.25	< 0.001[2]	1-3 = 0.001
	38	Grade 2	26.06 ± 3.35		1-4 < 0.001
	15	Grade 3	30.37 ± 6.17		2-3 = 0.027
	13	Grade 4	30.84 ± 5.66		2-4 = 0.008
Median pixels intensity	28	Grade 1	113.68 ± 11.76	< 0.001[2]	1-3 < 0.001
	38	Grade 2	119.92 ± 17.47		1-4 = 0.001
	15	Grade 3	156.21 ± 36.16		2-3 = 0.002
	13	Grade 4	157.08 ± 34.84		2-4 = 0.009
Mode pixels intensity	28	Grade 1	120.22 ± 15.53	< 0.001[2]	1-3 < 0.001
	38	Grade 2	122.68 ± 19.12		1-4 = 0.002
	15	Grade 3	178.72 ± 57.03		2-3 < 0.001
	13	Grade 4	178.92 ± 55.12		2-4 = 0.002
Kurtosis	28	Grade 1	0.019 ± 0.003	< 0.001[2]	1-3 < 0.001
	38	Grade 2	0.018 ± 0.003		1-4 < 0.001
	15	Grade 3	0.014 ± 0.003		2-3 = 0.001
	13	Grade 4	0.015 ± 0.003		2-4 = 0.030

(continuation)					
New metrics	n	Groups	Mean ± SD	Significance level	Statistically significant post-hoc differences (p-value)
Lipid layer thickness					
At 0.33 s					
Skewness	28	Grade 1	0.15 ± 0.01	< 0.001[2]	1-3 < 0.001
	38	Grade 2	0.15 ± 0.01		1-4 = 0.001
	15	Grade 3	0.13 ± 0.02		2-3 = 0.001
	13	Grade 4	0.13 ± 0.02		2-4 = 0.023
At 5.33 s					
Total area	27	Grade 1	110.03 ± 6.85	< 0.001[2]	1-2 = 0.004
	37	Grade 2	116.70 ± 7.62		1-3 < 0.001
	15	Grade 3	123.84 ± 5.40		1-4 < 0.001
	11	Grade 4	124.25 ± 3.88		2-3 = 0.002
					2-4 = 0.005
Minimum pixel intensity	27	Grade 1	57.44 ± 8.43	< 0.001[2]	1-2 = 0.001
	37	Grade 2	69.08 ± 14.20		1-3 < 0.001
	15	Grade 3	82.93 ± 19.00		1-4 < 0.001
	11	Grade 4	79.64 ± 14.03		2-3 = 0.023
Energy	27	Grade 1	238.28 ± 23.74	< 0.001[2]	1-2 = 0.007
	37	Grade 2	242.24 ± 20.14		1-3 < 0.001
	15	Grade 3	254.14 ± 2.28		1-4 < 0.001
	11	Grade 4	254.45 ± 0.39		2-3 < 0.001
					2-4 < 0.001
Relative energy	27	Grade 1	0.33 ± 0.13	< 0.001[2]	1-2 = 0.005
	37	Grade 2	0.52 ± 0.23		1-3 < 0.001
	15	Grade 3	0.79 ± 0.20		1-4 < 0.001
	11	Grade 4	0.80 ± 0.17		2-3 = 0.002
					2-4 = 0.003
SD irregularity	27	Grade 1	0.04 ± 0.01	0.001[2]	1-2 = 0.023
	37	Grade 2	0.06 ± 0.04		1-3 < 0.001
	15	Grade 3	0.23 ± 0.18		1-4 < 0.001
	11	Grade 4	0.20 ± 0.15		2-3 = 0.001
					2-4= 0.001
Mean pixels intensity	27	Grade 1	116.87 ± 9.94	< 0.001[2]	1-2 = 0.005
	37	Grade 2	132.69 ± 19.70		1-3 < 0.001
	15	Grade 3	166.37 ± 27.89		1-4 < 0.001
	11	Grade 4	166.26 ± 23.58		2-3 = 0.002
					2-4 = 0.002
SD of pixels intensity	27	Grade 1	27.05 ± 2.86	< 0.001[2]	1-3 < 0.001
	37	Grade 2	28.25 ± 3.58		1-4 < 0.001
	15	Grade 3	34.20 ± 5.77		2-3 = 0.001
	11	Grade 4	34.85 ± 3.59		2-4 < 0.001
Median pixels intensity	27	Grade 1	115.00 ± 10.78	< 0.001[2]	1-2 = 0.004
	37	Grade 2	131.68 ± 10.78		1-3 < 0.001
	15	Grade 3	166.93 ± 29.20		1-4 < 0.001
	11	Grade 4	166.73 ± 24.05		2-3 = 0.001
					2-4 = 0.002

(continuation)					
New metrics	n	Groups	Mean ± SD	Significance level	Statistically significant post-hoc differences (p-value)
Lipid layer thickness					
At 5.33 s					
Mode pixels intensity	27	Grade 1	116.33 ± 21.15	<0.001[2]	1-2 = 0.003
	37	Grade 2	140.35 ± 23.95		1-3 < 0.001
	15	Grade 3	198.64 ± 55.22		1-4 < 0.001
	11	Grade 4	202.90 ± 52.29		2-3 = 0.006 2-4 = 0.003
Kurtosis	27	Grade 1	0.017 ± 0.001	<0.001[2]	1-3 < 0.001
	37	Grade 2	0.016 ± 0.002		1-4 < 0.001
	15	Grade 3	0.012 ± 0.002		2-3 < 0.001
	11	Grade 4	0.012 ± 0.002		2-4 = 0.001
Skewness	27	Grade 1	0.14 ± 0.01	<0.001[2]	1-3 < 0.001
	37	Grade 2	0.14 ± 0.01		1-4 < 0.001
	15	Grade 3	0.12 ± 0.01		2-3 < 0.001
	11	Grade 4	0.12 ± 0.01		2-4 = 0.001
At 10.33 s					
Total area	18	Grade 1	110.14 ± 8.54	< 0.001[2]	1-3 < 0.001
	28	Grade 2	115.47 ± 8.34		1-4 < 0.001
	11	Grade 3	125.88 ± 3.45		2-3 < 0.001
	9	Grade 4	124.59 ± 2.56		2-4 = 0.012
Minimum pixel intensity	18	Grade 1	58.00 ± 11.69	< 0.001[2]	1-3 < 0.001 1-4 = 0.004 2-3 = 0.001
	28	Grade 2	66.43 ± 15.16		
	11	Grade 3	91.64 ± 19.27		
	9	Grade 4	88.33 ± 14.93		
Energy	18	Grade 1	238.22 ± 20.54	< 0.001[2]	1-3 < 0.001
	28	Grade 2	242.01 ± 19.16		1-4 < 0.001
	11	Grade 3	254.01 ± 2.09		2-3 = 0.001
	9	Grade 4	254.04 ± 0.42		2-4 = 0.004
Relative energy	18	Grade 1	0.36 ± 0.18	< 0.001[2]	1-3 < 0.001
	28	Grade 2	0.50 ± 0.25		1-4 < 0.001
	11	Grade 3	0.89 ± 0.16		2-3 < 0.001
	9	Grade 4	0.80 ± 0.13		2-4 = 0.010
SD irregularity	18	Grade 1	0.04 ± 0.01	< 0.001[2]	1-3 < 0.001
	28	Grade 2	0.07 ± 0.05		1-4 < 0.001
	11	Grade 3	0.29 ± 0.21		2-3 <0.001
	9	Grade 4	0.21 ± 0.13		2-4 = 0.004
Mean pixels intensity	18	Grade 1	117.99 ± 13.74	< 0.001[2]	1-3 < 0.001
	28	Grade 2	132.00 ± 22.31		1-4 < 0.001
	11	Grade 3	178.50 ± 25.59		2-3 < 0.001
	9	Grade 4	170.99 ± 19.92		2-4 = 0.003
SD of pixels intensity	18	Grade 1	27.04 ± 2.96	< 0.001[2]	1-3 < 0.001
	28	Grade 2	29.48 ± 3.57		1-4 < 0.001
	11	Grade 3	33.99 ± 4.04		2-3 = 0.006
	9	Grade 4	35.10 ± 4.34		2-4 = 0.004

(continuation)					
New metrics	n	Groups	Mean ± SD	Significance level	Statistically significant post-hoc differences (p-value)
Lipid layer thickness					
At 10.33 s					
Median pixels intensity	18	Grade 1	116.17 ± 14.40	< 0.001[2]	1-3 < 0.001
	28	Grade 2	130.82 ± 23.06		1-4 < 0.001
	11	Grade 3	179.45 ± 27.88		2-3 < 0.001
	9	Grade 4	170.67 ± 20.63		2-4 = 0.004
Mode pixels intensity	18	Grade 1	117.67 ± 23.25	< 0.001[2]	1-3 < 0.001
	28	Grade 2	137.79 ± 31.60		1-4 < 0.001
	11	Grade 3	214.36 ± 49.28		2-3 < 0.001
	9	Grade 4	192.67 ± 49.86		2-4 = 0.002
Kurtosis	18	Grade 1	0.017 ± 0.002	< 0.001[2]	1-3 < 0.001
	28	Grade 2	0.015 ± 0.003		1-4 = 0.001
	11	Grade 3	0.012 ± 0.002		2-3 = 0.001
	9	Grade 4	0.013 ± 0.003		2-4 = 0.015
Skewness	18	Grade 1	0.14 ± 0.01	< 0.001[2]	1-3 < 0.001
	28	Grade 2	0.13 ± 0.01		1-4 = 0.001
	11	Grade 3	0.11 ± 0.01		2-3 = 0.001
	9	Grade 4	0.11 ± 0.01		2-4 = 0.011

(Where mm: millimetres; n: number of patients; NIKBUT: Non-Invasive Keratograph Break-Up Time; s: Seconds; SD: Standard Deviation; TMH: Tear Meniscus Height; [1]Mann-Whitney U test; [2]Kuskal-Wallis test)

Multiple linear regressions

Since the metrics at 5.33 seconds after blinking have proved to differentiate between grades 1 (open meshwork), 2 (closed meshwork) and 3 (wave) of the lipid layer thickness, only the metrics at 5.33 seconds after blinking will be assessed in this section of the manuscript.

Multiple linear regressions (*Table 8.3.5*) were performed to show the current metrics that were associated with new metrics, avoiding that the interaction between current metrics mislead results. Multiple linear regressions showed that new metrics

were statistically significant associated with lipid layer thickness, explaining the variability between 7.1 % and 47.0 % depending on the metric. Kurtosis and skewness showed a weak association with gland drop-out percentage instead of with lipid layer thickness. Energy also appeared to be associated with the first median NIKBUT together with lipid layer thickness. No association was found with the remaining variables. Generally, these results suggest that the main predictor factor of new metrics was the lipid layer thickness.

*Diagnostic capability and validation of the new metric*s

Table 8.3.6 summarizes the diagnostic power and the cut-off values for each new metric when grade 1 of lipid layer thickness was compared with other grades. New developed metrics were powerful indicators to detect subjects with an altered lipid layer (grade 1 – open meshwork) since the area under the curve, sensitivity and specificity obtained were high. Mean pixel intensity, median pixel intensity and relative energy were the metrics with the highest sensitivity, specificity, area under the curve, Youden index, discriminant power, accuracy, Kappa index and F-measure.

Table 8.3.5. *Multiple linear regressions for new metrics at 5.33 seconds where the independent variables included were gland drop-out percentage, bulbar redness, lipid layer thickness, tear meniscus height, first and mean NIKBUT, gland expressibility, OSDI and DEQ-5.*

New metrics	Current metrics	β	SE	Sβ	Significance level	Adjusted R square
Total area	Constant	129.99	140.09		<0.001	0.470
	Lipid layer thickness	18.64	2.62	0.71	<0.001	
Minimum pixel intensity	Constant	40.34	9.86		<0.001	0.325
	Lipid layer thickness	9.72	1.83	0.60	<0.001	
Energy	Constant	261.47	8.09		<0.001	0.214
	Lipid layer thickness	5.27	1.50	0.42	0.001	
	First median NIKBUT	1.24	0.61	0.64	0.045	
Relative energy	Constant	0.87	0.14		<0.001	0.404
	Lipid layer thickness	0.17	0.03	0.69	<0.001	
Entropy	Constant	0.000	0.000		<0.001	0.050
	First median NIKBUT	0.00000063	0.00	0.73	0.037	
SD irregularity	Constant	0.13	0.03		<0.001	0.071
	Lipid layer thickness	0.014	0.005	0.39	0.005	
Mean pixels intensity	Constant	137.78	15.63		<0.001	0.457
	Lipid layer thickness	20.26	2.91	0.70	<0.001	
SD of pixels intensity	Constant	25.15	1.81		<0.001	0.193
	Lipid layer thickness	1.22	0.34	0.45	0.001	
Median pixels intensity	Constant	140.60	16.64		<0.001	0.468
	Lipid layer thickness	21.89	3.09	0.70	<0.001	
Mode pixels intensity	Constant	130.92	22.42		<0.001	0.432
	Lipid layer thickness	28.37	4.17	0.70	<0.001	
Kurtosis	Constant	0.012	0.001		<0.001	0.114
	Gland drop-out percentage	0.000031	0.000	0.33	0.042	
Skewness	Constant	0.119	0.005		<0.001	0.099
	Gland drop-out percentage	0.000	0.000	0.36	0.029	

(Where β: Unstandardized coefficient; NIKBUT: Non-Invasive Keratograph Break-Up Time; Sβ: Standardized coefficient; SD: Standard Deviation; SE: Standard Error)

Table 8.3.6. *ROC curve parameters of newly developed metrics to differentiate grade 1 of lipid layer thickness from other grades at 5.33 seconds.*

Metric	Sensitivity	Specificity	Area under the curve (CI)	Cut-off value	Youden index	Discriminant power	Accuracy	Kappa index	F-measure
Total area	0.94	0.76	0.89 (0.83 – 0.96)	117.74	0.70	2.18	0.83	0.72	0.81
Minimum pixel intensity	0.92	0.74	0.88 (0.82 – 0.95)	67.50	0.65	1.89	0.82	0.70	0.80
Energy	0.87	0.77	0.82 (0.71 – 0.88)	239.15	0.65	1.77	0.82	0.70	0.80
Relative energy	0.92	0.81	0.91 (0.83 – 0.96)	0.48	0.73	2.13	0.86	0.76	0.84
SD irregularity	0.89	0.77	0.86 (0.79 – 0.94)	0.05	0.66	1.83	0.82	0.70	0.79
Mean pixels intensity	0.94	0.79	0.89 (0.83 – 0.96)	128.62	0.74	2.29	0.86	0.76	0.84
SD of pixels intensity	0.83	0.70	0.78 (0.68 – 0.88)	28.08	0.53	1.35	0.74	0.57	0.73
Median pixels intensity	0.92	0.81	0.91 (0.84 – 0.97)	124.50	0.73	2.13	0.86	0.76	0.84
Mode pixels intensity	0.83	0.77	0.87 (0.80 – 0.94)	133.50	0.61	1.56	0.80	0.66	0.78
Kurtosis	0.89	0.76	0.83 (0.74 – 0.92)	0.015	0.64	1.77	0.78	0.63	0.76
Skewness	0.92	0.72	0.84 (0.75 – 0.92)	0.13	0.63	1.84	0.80	0.66	0.78

(Where CI: 95 % Confidence Interval; SD: Standard Deviation)

Tables 8.3.7 and *8.3.8* show the diagnostic power of each new metric to differentiate between grades 1 and 2, and between grades 2 and 3, respectively. This step allowed finding the cut-off values for each new metric to objectively classify the lipid layer into different grades. The cut-off value that optimizes the diagnosis determines the best score to diagnose the disease. Thus, a subject with a higher score than the cut-off value in kurtosis and skewness was classified into the thinner lipid layer thickness group, while a subject with a higher score than the cut-off value in the rest of the newly developed metrics was classified into the thicker lipid layer thickness

group. The SD of pixels intensity had a low specificity to distinguish between grades 1 and 2, which could lead to the lipid layer being misclassified.

Table 8.3.7. *ROC curve parameters of new developed metrics to differentiate between grades 1 and 2 of lipid layer thickness at 5.33 seconds.*

Metric	Sensitivity	Specificity	Area under the curve (CI)	Cut-off value	Youden index	Discriminant power
Total area	0.89	0.70	0.83 (0.73-0.94)	116.20	0.59	1.62
Minimum pixel intensity	0.86	0.74	0.86 (0.77-0.95)	64.50	0.60	1.58
Energy	0.86	0.73	0.81 (0.71-0.91)	238.59	0.59	1.55
Relative energy	0.92	0.74	0.83 (0.72-0.94)	0.48	0.66	1.90
SD irregularity	0.83	0.70	0.78 (0.66-0.90)	0.05	0.54	1.36
Mean pixels intensity	0.92	0.74	0.84 (0.73-0.95)	126.93	0.66	1.90
SD of pixels intensity	0.83	0.48	0.66 (0.53-0.80)	28.22	0.31	0.84
Median pixels intensity	0.92	0.74	0.85 (0.74-0.95)	124.50	0.66	1.90
Mode pixels intensity	0.83	0.70	0.82 (0.71-0.93)	133.50	0.54	1.36
Kurtosis	0.89	0.63	0.74 (0.60-0.87)	0.015	0.52	1.44
Skewness	0.83	0.67	0.74 (0.60-0.87)	0.14	0.5	1.27

(Where CI: 95 % Confidence Interval; SD: Standard Deviation)

Table 8.3.8. *ROC curve parameters of new developed metrics to differentiate between grade 2 and 3 of lipid layer thickness at 5.33 seconds.*

Metric	Sensitivity	Specificity	Area under the curve (CI)	Cut-off value	Youden index	Discriminant power
Total area	0.78	0.81	0.80 (0.65-0.95)	123.97	0.59	1.50
Minimum pixel intensity	0.71	0.69	0.74 (0.57-0.91)	79.50	0.40	0.94
Energy	0.71	0.84	0.78 (0.62-0.93)	248.19	0.55	1.41
Relative energy	0.74	0.88	0.81 (0.67-0.96)	0.72	0.62	1.65
SD irregularity	0.89	0.69	0.82 (0.68-0.97)	0.12	0.58	1.58
Mean pixels intensity	0.78	0.88	0.83 (0.68-0.97)	150.69	0.65	1.76
SD of pixels intensity	0.82	0.69	0.80 (0.65-0.95)	32.36	0.50	1.25
Median pixels intensity	0.70	0.88	0.83 (0.69-0.97)	160.50	0.58	1.55
Mode pixels	0.96	0.63	0.80 (0.63-0.96)	183.00	0.59	2.08
Kurtosis	0.82	0.75	0.82 (0.68-0.96)	0.013	0.57	1.42
Skewness	0.93	0.69	0.84 (0.70-0.97)	0.12	0.61	1.83

(Where CI: 95 % Confidence Interval; SD: Standard Deviation)

Once the cut-off values were calculated, the lipid layer was objectively classified. The level of agreement between the newly developed objective and existing subjective classifications was evaluated (*Table 8.3.9*). Since different lipid layer thickness grades were evaluated, the weighted Kappa index was calculated (Cohen, 1968). Mean pixels intensity, median pixels intensity and relative energy were the metrics with the highest area under the curve, best relationship between sensitivity and specificity and higher agreement between objective and subjective methods for the classification of the lipid layer thickness.

Table 8.3.9. *Agreement between the subjective and objective classification of the lipid layer thickness for each parameter at 5.33 seconds.*

Metric	Accuracy	Kappa index	F-measure
Total area	0.72	0.73	0.84
Minimum pixel intensity	0.68	0.66	0.81
Energy	0.72	0.73	0.84
Relative energy	0.76	0.76	0.86
SD irregularity	0.71	0.73	0.83
Mean pixels intensity	0.77	0.77	0.87
SD of pixels intensity	0.63	0.61	0.78
Median pixels intensity	0.76	0.77	0.86
Mode pixels intensity	0.71	0.67	0.83
Kurtosis	0.69	0.69	0.82
Skewness	0.70	0.69	0.82

(Where SD: Standard Deviation)

8.3.4. Discussion

The present study introduces a new self-developed technique for the non-invasive objective evaluation of the lipid layer thickness, which might be implemented in any Placido disk topograph. The validity and applicability of new metrics calculated from the grey level intensity values of the Placido disk pattern reflected onto the tear film have been tested. Alonso-Caneiro et al. (2013) performed a similar study, in which they used texture analysis of videokeratoscopy images and denoted that the proposed technique offered clinical utility in the diagnosis of DED (Area under the curve from 0.77 to 0.82, sensitivity of 0.9 and specificity of 0.6). However, the authors did not explain why this could be a predictor of DED since they did not study the correlations of the metric with ocular surface parameters. Therefore, they did not evidence which parameter of the tear film they were measuring.

The present work makes three important contributions: 1) the development of a new method to assess the lipid layer thickness in an unbiased, objective, quick and non-invasive way; 2) the possibility of assessing the lipid layer without the need of an interferometer, making the method widely accessible; 3) the validation of the new technique through the study of its repeatability, diagnostic capability and correlations with ocular surface parameters.

Correlations between Placido disk reflectivity metrics and ocular surface parameters

Moderate positive significant correlations were found between grey level intensities of the Placido disk pattern and lipid layer thickness and NIKBUT. The correlations between new developed metrics and age, meibomian glands drop-out, bulbar redness, TMH and OSDI (*Table 8.3.3*) might be a consequence of their correlation with lipid layer thickness since lipid layer thickness is also correlated with age, meibomian glands drop-out and NIKBUT (Bron and Tiffany, 2004; Hosaka et al., 2011; Pult, Riede-Pult and Nichols, 2012; Eom et al., 2013; Finis et al., 2013).

Despite the above, in the present study, lipid layer thickness revealed no correlation with bulbar redness, TMH and OSDI. Finis et al. (2013) neither found a significant correlation between DED symptoms and lipid layer thickness, although this was not in accordance with others (Foulks, 2007; Hosaka et al., 2011; Best, Drury and Wolffsohn, 2012; Pult, Riede-Pult and Nichols, 2012). New metrics, though less strongly correlated with bulbar redness, TMH and OSDI than with lipid layer thickness, could still be used to assess these ocular surface parameters.

Entropy measures the randomness of a grey level distribution (Alonso-Caneiro et al., 2013), and as a result might change as the tear film becomes thinner and the Placido disk pattern becomes more unstructured (Alonso-Caneiro et al., 2013). This metric was not correlated with the lipid layer thickness, although it revealed a significant correlation with gland drop-out, bulbar redness, TMH, NIKBUT and OSDI, and thus it might be used to predict these parameters.

Moreover, despite that new metrics were correlated with the lipid layer thickness, no statistically significant correlations were found with meibomian gland expressibility, although previous research did find a correlation between these parameters (Finis et al., 2013).

Differences between groups

When the sample was subjectively divided into 4 different lipid layer thickness groups, using grade scales of interference patterns, statistically significant differences in the new metrics were found between them (*Table 8.3.4*). The measurements at 5.33 seconds after blinking were the best to differentiate among the different lipid layer thickness grades since metrics were able to distinguish between grades 1 and 2, and grades 2 and 3. Nonetheless, the method could not differentiate between grades 3 (wave) and 4 (colour fringe pattern). This could be due to the fact that grade 4 differs from grade 3 in that 4 is the only grade, in the interference scale, to imply a coloured pattern, which cannot be detected using grey level values. Hence, as already reported by other authors (Remeseiro et al., 2013), it would be necessary to incorporate a colour analysis to differentiate between grades 3 and 4.

Nevertheless, since the TFOS DEWS II Diagnostic Methodology Report reported that a subject is classified as having DED when the lipid layer thickness has a grade of 1, differentiating between grade 3 and 4 has a low clinical utility. Additionally, thinner patterns are more difficult to characterize by an examiner (García-Resúa et al., 2013; Wolffsohn et al., 2017).

In addition to being capable of differentiating between lipid layer thickness grades, the metrics at 5.33 seconds after blinking are performed under more realistic conditions than at later times, as subjects are not required to forcefully suppress blinking. Moreover, metrics at 0.33 seconds might not have achieved a similar performance than at 5.33 seconds in assessing the lipid layer thickness since at 0.33 seconds after blinking the lipid layer might not have stabilized yet.

Placido disk reflectivity metrics over time

Repeated mixed model ANOVA showed statistical higher pixel intensity values at 10.33, 15.33 and 20.33 seconds than at 0.33 seconds (*Table 8.3.1*). This might be due to the fact that the sample size decreased as the seconds after blink increased. Thus, only subjects with larger NIKBUT values were able to maintain the eye opened for 20.33 seconds. This may be behind the observed differences as the lipid layer thickness and NIKBUT were positively correlated with pixel intensity.

Nevertheless, despite that ANOVA revealed differences in the metrics between periods, when all subjects were analyzed together, CoV, which evaluated the variability in each subject individually, revealed a low variability of metrics over time.

Repeatability of each Placido disk reflectivity metric

The present method has the limitation that is semiautomatic since the centre of the Placido disk pattern and the ROI must be selected manually by the examiner. In spite of this, the repeatability was acceptable in all metrics (*Table 8.3.2*) and the analysis can be carried out in less than 10 seconds. It has been previously reported that this time is considered appropriate for a clinical test (Remeseiro et al., 2014a).

Multiple linear regressions

As correlations showed, the lipid layer thickness was the clinical parameter that was more strongly correlated with new metrics. Nevertheless, other parameters were also correlated. This could be a bias since different metrics can confound results, affecting the classification of the lipid layer thickness. Therefore, multiple linear regression analysis has been performed to show which current metrics are independently associated with new metrics. Results showed that for most metrics, the lipid layer thickness was the only parameter associated. This suggests that new metrics are predictors of the lipid layer thickness and can be used to objectively assess it. Nevertheless, kurtosis and skewness were associated with gland drop-out and energy with the lipid layer thickness together with NIKBUT.

Diagnostic capability and validation of the new metrics

ROC curves were calculated to analyse the diagnostic ability of the new metrics. It has been previously reported that a 70 % level of sensitivity and specificity is

acceptable for the diagnosis of a disease (Tomlinson et al., 2011). Sensitivity and specificity were higher than 0.7 for most of the developed new metrics.

According to the classification on a previous report (Hosmer, Lemeshow and Sturdivant, 2013), the newly developed metrics showed areas under the curve between acceptable (0.74) and outstanding (0.91) discrimination. Thus, new metrics can be considered powerful aides to objectively assess the lipid layer.

It has been reported that accuracy, F-measure and kappa index denote good agreement between tests when they are close to 1 (Cohen, 1968; Landis and Koch, 1977; Rosenfield and Fitzpatrick-Lins, 1986; Viera and Garret, 2005; Sokolova, Japkowicz and Szpakowicz, 2006). Generally, the agreement between new metrics and subjective classification methods of the lipid layer thickness showed an accuracy between 0.63 and 0.77, an F-measure between 0.78 and 0.87 and a Kappa index between 0.61 and 0.77 (very good agreement) (*Table 8.3.8*).

Mean pixel intensity, median pixel intensity and relative energy at 5.33 seconds after blinking were the metrics with the highest diagnostic capability in terms of sensitivity, specificity, area under the curve, Youden index and discriminant power (*Table 8.3.5*) and the metrics with the highest agreement with the subjective grading in terms of accuracy, Kappa index and F-measure (*Table 8.3.8*).

In comparison with previous studies on the analysis of interference patterns (Wu et al., 2008; García-Resúa et al., 2013; Remeseiro et al., 2013; Remeseiro et al., 2014b; Remeseiro et al., 2014c; Peteiro-Barral et al., 2016; Hwang et al., 2017; Bai and

Nichols, 2019; da Cruz et al., 2020), the new metrics showed slightly lower diagnostic ability and agreement with the subjective classification of the lipid layer thickness. Nevertheless, this method adds the possibility of objectively assessing the lipid layer thickness without the need of having an interferometer, which might broad the assessment of the lipid layer in clinical practice.

This study had some limitations to consider. First, statistically significant correlations between new metrics and age were found. Consequently, age might act as a possible confounding factor. As in previous studies, age could not be excluded from the analysis because of its strong association with DED and MGD (Pult, Riede-Pult and Nichols, 2012; Rico-del-Viejo et al., 2019). Furthermore, the surrounding illumination and the focussing of the Placido disk pattern should be carefully controlled. In addition, the lipid layer thickness has not been measured objectively. However, it has been measured subjectively with a validated grading scale, which suggests that the present method is able to objectify the subjective measurement of this grading scale. It has been reported that this subjective grading scale is correlated with the lipid layer thickness (Guillon, 1998a; Nichols et al., 2005; Tomlinson et al., 2011; Wolffsohn et al., 2017). Therefore, these issues are not expected to affect results significantly. Future studies could assess the predictability of the lipid layer thickness measured objectively with the new metrics. Finally, the method only measures the grey intensity values of the Placido disk pattern within the pupil. Nevertheless, this issue is not expected to influence the outcomes since all the metrics have been designed to be pupil-independent. Moreover, the present study has demonstrated that the analysis of the pixels within the pupil area is enough to assess the lipid layer thickness.

Overall, the analysis of grey level intensity values in videokeratography is able to assess the tear film behaviour. Grey level intensity can be used as an alternative biomarker to objectively grade the lipid layer thickness. It has been demonstrated that the method is quick, objective, non-invasive, repeatable and with acceptable sensitivity and specificity. Therefore, it could be easily included in a battery of tests to improve the detection and monitoring of DED and MGD in clinical practice.

Further research is needed to assess the performance of these metrics in subjects diagnosed with DED or MGD. Likewise, the software could be further developed to be fully automatic and to distinguish between grades 3 and 4 of lipid layer thickness Nonetheless, although these outcomes are preliminary, they are highly encouraging. This study could be the base for future works which attempt to assess the lipid layer objectively without the need of an interferometer.

CHAPTER 9: Effect of contact lenses on the tear film and the ocular surface

9. EFFECT OF CONTACT LENSES ON THE TEAR FILM AND THE OCULAR SURFACE

As explained in *Chapter 1 Introduction*, contact lens wear has been reported to impact the ocular surface homeostasis (Stapleton et al., 2006; Stapleton et al., 2017). Thus, contact lens wear is associated with DED (Gomes et al., 2017; Stapleton et al., 2017). Moreover, the increasing number of contact lens wearers has highlighted the need of studying iatrogenic dry eye (Gomes et al., 2017). Therefore, due to the relevance of contact lens wear on the ocular surface, in the present chapter, the effect of different contact lenses on the tear film and the ocular surface will be assessed using current metrics and the newly developed metrics in this dissertation.

CHAPTER 9.1: Effect of a dual-focus and a single-vision contact lens on light disturbance, optical quality, visual performance and the tear film

9.1 EFFECT OF A DUAL-FOCUS AND A SINGLE-VISION CONTACT LENS ON LIGHT DISTURBANCE, OPTICAL QUALITY, VISUAL PERFORMANCE AND THE TEAR FILM

In this chapter, the short-term effect of a dual-focus contact lens design on the tear film, visual performance and optical quality will be assessed and compared to a single-vision contact lens design built with the same material.

CHAPTER 9.1.1: Comparison of short-term light disturbance, optical and visual performance outcomes between a myopia control contact lens and a single-vision contact lens

9.1.1 COMPARISON OF SHORT-TERM LIGHT DISTURBANCE, OPTICAL AND VISUAL PERFORMANCE OUTCOMES BETWEEN A MYOPIA CONTROL CONTACT LENS AND A SINGLE-VISION CONTACT LENS

In this first part of the chapter, the short-term light disturbance, optical quality and visual performance of a dual-focus and a single-vision contact lens will be compared.

9.1.1.1 Introduction

It has been reported that a reduction in myopia progression might be achieved by using central-distance dual-focus contact lenses designs through the reduction of the off-axis hyperopia (Ruiz-Pomeda et al., 2018b; Hughes et al., 2020; Przekoracka et al., 2020). Thus, these new designs are also being applied to control myopia progression (González-Méijome et al., 2016; Ruiz-Pomeda et al., 2019). However, even though visual acuity is acceptable in the vast majority of patients, many still complain about insufficient quality of vision and dysphotopsia (González-Méijome et al., 2016). Therefore, the evaluation of photic phenomena and ocular aberrations would add valuable information to the simple visual acuity assessment (Brito et al., 2015).

Ruiz-Pomeda et al. (2019) reported that dual-focus design contact lenses increase light disturbance in comparison with a monofocal spectacle correction. However, light disturbance scores were low and decreased over the follow-up. Generally, dual-focus multifocal designs produce a reduction in contrast sensitivity, an increase in photic phenomena and changes in aberrations, particularly for primary spherical aberration

(Fedtke et al., 2017). Poor visual satisfaction due to photic phenomena, visual fluctuations and inadequate visual quality is the most common reason for multifocal contact lens wear discontinuation in presbyopes. However, it is not expected that children, doing most of their activities under good lighting conditions would complain of those photic phenomena and the high rates of retention in clinical trials involving dual-focus lenses indirectly confirm that (Chamberlain et al., 2019; Remón et al., 2020).

Little is known about the visual performance of concentric design contact lenses for myopia control in children. This topic is of high interest since myopia control depends on an acceptable visual performance through the lens. Nevertheless, the present study is not intended to assess the effect of the lenses on myopia control. Instead, it aims to determine the short-term effect of a dual-focus contact lens design on visual and optical performance and compare it to a single-vision contact lens design built with the same material. This work adds new insights about the performance of dual-focus contact lenses since differences resulting from this study would be only due to the differences in design of the contact lenses and not masked by differences in the lens material. It is hypothesized that the different optic zone of the dual-focus lens will decrease the optical quality when compared to a single-vision lens of the same material. The present study was not carried out on children since some parts of the protocol might be difficult to follow by patients of that age. Instead, study sample were young adults who represent a population with high visual and comfort demands similar to those in children (Kollbaum et al., 2013).

9.1.1.2 Methodology

This was a randomized, double-masked, crossover study. A total of 28 healthy myopic volunteers between 18 and 32 years with an astigmatism of ≤0.75D participated in this study (Kollbaum et al., 2013). Prior contact lens wear was not considered. Inclusion criteria involved best-corrected visual acuity of 0.00 logMAR or better in each eye. Subjects with any ocular disease or binocular anomaly, as well as, subjects taking any medication that contraindicates or interferes with the use of contact lenses, were excluded from the study. Written consent was obtained from each subject after explanation of the purpose and study protocol. The study procedures were approved by the Ethics Committee of University of Minho and were carried out in accordance with the tenets of Declaration of Helsinki.

Although both eyes were randomly fitted with contact lenses, the sensorial dominant eye for distance vision was measured in order to avoid duplication of data. Eye dominance was evaluated by means of sensory dominance with the "+1.50 D blur" method (Lopes-Ferreira et al., 2013; Fernandes et al., 2018). Luminance and illuminance were measured at all times using a luminance meter (Konica Minolta LS-100 Sensing Americas Inc, Ramsey, NJ, USA) and an illuminance meter (*T-10*, *Minolta* Sensing Inc, Tokyo, Japan), respectively. The varying daylight was removed using black-out curtains. The illuminance was 255.55 ± 8.14 lux and 3.45 ± 0.13 lux for photopic and mesopic conditions, respectively. The mean luminance was 203.07 ± 3.75 cd/m^2, 48.05 ± 1.18 cd/m^2 and 0.62 ± 0.01 cd/m^2 for the measurement of visual acuity, photopic contrast sensitivity and mesopic contrast sensitivity, respectively.

The study can be divided in 3 parts: 1) baseline measurements, and visual and optical performance assessments 2) with the dual-focus lens and 3) with the single-vision lens.

The procedures performed in each part of the protocol and the order in which they were performed, were the following: Case history, refraction with trial lenses, visual acuity and aberrations assessed for a pupil diameter of 3 mm and 5 mm were determined at baseline. Refraction was used to determine the power of the contact lenses. For both contact lenses, over-refraction with trial lenses, symptoms questionnaire, visual acuity, stereopsis, photopic and mesopic contrast sensitivity, light disturbance assessment and aberrations for a pupil diameter of 3 mm and 5 mm were assessed. Measurements were performed as explained in *Chapter 3 General Methodology*.

Photopic and mesopic pupil diameters were evaluated in each lens using Grand Seiko Autorefractometer WAM-5500. Pupil diameter was evaluated in the contralateral eye while subjects were carrying out the LDA test using the NeurOptics® VIP™-200 Pupillometer (Irvine, California, USA) under the same illumination conditions as those for light disturbance measurements.

After measurements were carried out with the first contact lens design *in situ*, the lens was removed and a 15 minute washout period was allowed before fitting the second lens design. After measurements in both contact lenses, subjects were asked to choose a preferred contact lens, first or second design, right after protocol completion.

Contact lenses

Subjects were binocularly fitted with the two lenses, in a random way – one lens with a dual-focus design for myopia control (MiSight, CooperVision Inc., Pleasanton, CA) and the other lens with a single-vision design (Proclear 1-day, CooperVision Inc., Pleasanton, CA). Both contact lenses were fitted according to the manufacturer's guidelines for the initial lens selection.

Both contact lenses used in this study were made of the same material (Omafilcon A) with the same water content (60% water content, non-ionic), same base curve (8.70mm) and same lens diameter (14.2 mm). The dual-focus design has an 11.66 mm optic zone with four alternating zones for distance and near vision surrounding a central diameter of 3.36 mm for distance vision (Ruiz-Pomeda et al., 2018b; Chamberlain et al., 2019). This lens provides a 2 D add power, which produces a second focus. The distance focus lies on the retina and the near focus is in front of the retina at the distance of 0.6 mm, approximately. The near zone is known as the "treatment zone" (Ruiz-Pomeda et al., 2018b; Chamberlain et al., 2019).

Lens fitting

Contact lens correct movement and centration were checked using a slit-lamp. Measurements were carried out 25 minutes after contact lens insertion to allow contact lens settling, being this time strictly the same for both contact lenses for comparison purposes (Kollbaum et al., 2013). A washout period of 15 minutes between contact lenses was allowed (Sánchez et al., 2018; Martins et al., 2019).

Statistical analysis

Statistical analysis was carried out using SPSS v26.0 for Windows (IBM Corp, Armonk, New York, USA). Outcomes were reported as median and interquartile ranges. Normality distribution was checked by means of the Shapiro-Wilk test.

Differences between contact lens designs for each variable were assessed with the paired t-test or Wilcoxon signed rank test, depending on sample distribution. Moreover, differences between baseline and both designs in visual acuity and aberrations were assessed using the Friedman test. Post-hoc analysis was carried out by means of the Bonferroni test in order to evaluate differences between all pair group combinations. A p-value less than 0.05 was defined as statistically significant.

9.1.1.3 Results

Twenty-eight eyes from 28 subjects were included, out of which 17 were females (61 %) and 11 males (39 %). The mean age was 23.5 ± 4.1 years, ranging from 18 to 32 years. Median sphere and cylinder were -1.00 D (interquartile range: -2.31 to -0.27 D) and 0.00 D (interquartile range: -0.50 to 0.00 D), respectively.

After lens fitting, median sphere over-refraction was 0.25 D (interquartile range: 0.00 to +0.50 D) and 0.25 D (interquartile range: 0.00 to +0.52 D), for dual-focus and single-vision designs, respectively.

Visual Acuity, Stereopsis and Contrast Sensitivity

Table 9.1.1.1 summarizes the main outcomes obtained at baseline and after each contact lens design fit for best-corrected distance visual acuity, stereopsis and best-corrected contrast sensitivity under photopic and mesopic conditions. 60 % from single-vision group achieved a stereopsis of 20 seconds of arc and 40 % of 30 seconds of arc. In the dual-focus group, 57 % achieved a stereopsis of 20 seconds of arc and 43 % of 30 seconds of arc.

Although there were no statistically significant differences in visual acuity and stereopsis between both lenses, dual-focus lens designs led to a statistically significant decrease in both photopic and mesopic contrast sensitivity when compared to single-vision lens ($p < 0.05$), except for mesopic contrast sensitivity at the frequency of 18 cycles per degree ($p = 0.23$). Contrast sensitivity function pattern followed a typical physiological shape with the highest peak of sensitivity at 3 cycles per degree (*Figure 9.1.1.1*). Despite the differences found between dual-focus and single-vision lenses, both photopic contrast sensitivity curves of the lenses were inside the normality zone (Ginsburg et al., 1984) in all frequencies.

Table 9.1.1.1. *Best-corrected distance visual acuity, stereopsis and best-corrected photopic and mesopic contrast sensitivity for each contact lens.*

Measurement	Contact lens	Median (Interquartile range)	Significance level (Statistic, p-value)
Best-corrected Distance Visual Acuity (logMAR)	Baseline	-0.10 (-0.20 to -0.10)	$p=0.18^{1}$
	Single-vision	-0.12 (-0.18 to -0.10)	
	Dual-focus	-0.10 (-0.15 to -0.10)	
Stereopsis (seconds of arc)	Single-vision	20 (20 to 25)	$(Z_{27}=0.00, p=1.0)^{2}$
	Dual-focus	20 (20 to 25)	
Photopic Contrast Sensitivity 1.5 cpd (dB)	Single-vision	70 (65 to 70)	$(Z_{27}=-3.21, p=0.001)^{2}$*
	Dual-focus	35 (35 to 70)	
Photopic Contrast Sensitivity 3 cpd (dB)	Single-vision	170 (100 to 170)	$(Z_{27}=-3.35, p=0.001)^{2}$*
	Dual-focus	85 (85 to 153)	
Photopic Contrast Sensitivity 6 cpd (dB)	Single-vision	125 (125 to 185)	$(Z_{27}=-2.81, p=0.005)^{2}$*
	Dual-focus	70 (70 to 170)	
Photopic Contrast Sensitivity 12 cpd (dB)	Single-vision	65 (55 to 116)	$(Z_{27}=-3.24, p=0.001)^{2}$*
	Dual-focus	46 (32 to 88)	
Photopic Contrast Sensitivity 18 cpd (dB)	Single-vision	20 (15 to 40)	$(Z_{27}=-3.04, p=0.002)^{2}$*
	Dual-focus	15 (10 to 24)	
Mesopic Contrast Sensitivity 1.5 cpd (dB)	Single-vision	35 (35 to 37)	$(Z_{27}=-3.54, p<0.001)^{2}$*
	Dual-focus	20 (20 to 35)	
Mesopic Contrast Sensitivity 3 cpd (dB)	Single-vision	55 (44 to 85)	$(Z_{27}=-4.04, p<0.001)^{2}$*
	Dual-focus	28 (24 to 44)	
Mesopic Contrast Sensitivity 6 cpd (dB)	Single-vision	44 (21 to 45)	$(Z_{27}=-3.94, p<0.001)^{2}$*
	Dual-focus	21 (13 to 21)	
Mesopic Contrast Sensitivity 12 cpd (dB)	Single-vision	8 (6 to 15)	$(Z_{27}=-3.85, p<0.001)^{2}$*
	Dual-focus	5 (5 to 6)	
Mesopic Contrast Sensitivity 18 cpd (dB)	Single-vision	4 (0 to 7)	$(Z_{27}=-1.20, p=0.23)^{2}$
	Dual-focus	4 (0 to 4)	

*(Where cpd: cycles per degree; dB: decibel; [1]Friedman; [2]Wilcoxon; *Statistically significant differences)*

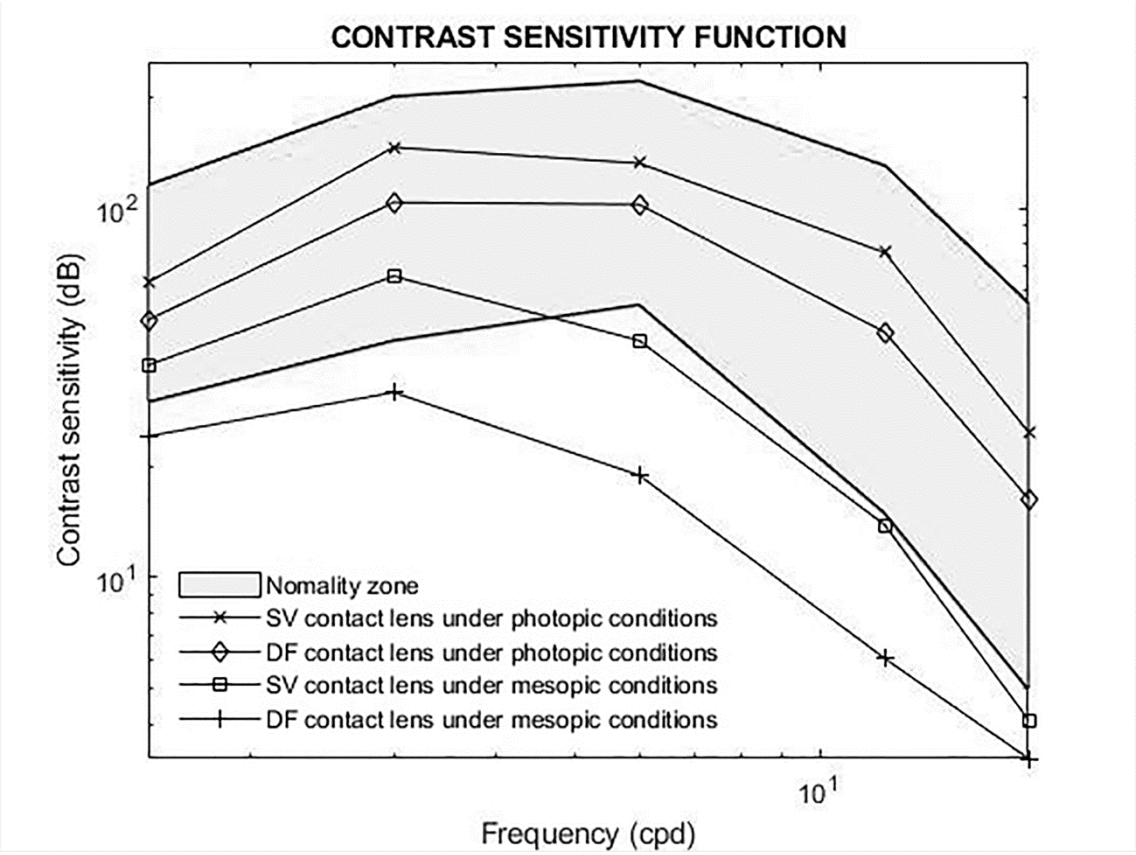

Fig. 9.1.1.1. *Best-corrected contrast sensitivity function for each contact lens under photopic and mesopic conditions. Where cpd: cycles per degree; dB: decibel; DF: Dual-Focus and SV: Single-Vision.*

During the aforementioned measurements, the mean pupil diameter under photopic conditions was 4.40 ± 0.42 mm and 4.42 ± 0.42 for dual-focus and single-vision contact lenses, respectively (t_{27} = -0.94, p = 0.35; T test). Mean pupil diameter under mesopic conditions was 6.37 ± 0.37 mm and 6.38 ± 0.34 for dual-focus and single-vision contact lenses, respectively (t_{27} = -1.14, p = 0.26; T test). Statistically significant differences were found between photopic and mesopic conditions for dual-focus (t_{27} = -13.50, p < 0.001; T test) and single-vision contact lenses (t_{27} = -16.83, p < 0.001; T test).

Light disturbance

Table 9.1.1.2 shows the main outcomes obtained for each contact lens design with the LDA. Mean pupil diameter while subjects were being assessed with LDA was 5.13 ± 0.66 and 5.10 ± 0.80 mm, for dual-focus and single-vision contact lenses, respectively (t_{27} = 0.34, p = 0.74; T test). Disturbance area, LDI, BFC radius, BFC irregularity and BFC irregularity SD were higher for the dual-focus than for the single-vision design (p < 0.001).

Table 9.1.1.2. *Light disturbance measurements for each contact lens.*

Measurement	Contact lens	Median (Interquartile range)	Significance level (Statistic, p-value)
Disturbance Area (mm^2)	Single-vision	1160 (784 to 1921)	(Z_{27}=3.96, p<0.001)[1]*
	Dual-focus	2608 (1716 to 3348)	
Light Distortion Index (%)	Single-vision	5.77 (3.90 to 9.56)	(Z_{27}=3.96, p<0.001)[1]*
	Dual-focus	12.97 (8.54 to 16.65)	
Best Fit Circle Radius (mm)	Single-vision	19.65 (16.17 to 25.15)	(Z_{27}=3.93, <0.001)[1]*
	Dual-focus	29.19 (23.65 to 33.15)	
Best Fit Circle Irregularity (mm)	Single-vision	0.30 (0.02 to 0.44)	(Z_{27}=3.95, p<0.001)[2]*
	Dual-focus	0.74 (0.34 to 1.17)	
Best Fit Circle Irregularity SD (mm)	Single-vision	3.30 (2.14 to 4.02)	(Z_{27}=3.12, p=0.002)[1]*
	Dual-focus	4.00 (3.36 to 4.59)	

*(Where mm: millimetres; SD: Standard Deviation; [1]T-test; [2]Wilcoxon; *Statistically significant differences)*

Aberrations

Table 9.1.1.3 shows lower-order, higher-order and total aberrations for each contact lens design for 3 and 5 mm of pupil diameter. The Friedman test revealed statistically significant differences between conditions (baseline, single-vision and dual-focus) in all variables. Post-hoc analysis showed statistically significant differences

between baseline and single-vision lens for lower-order and total aberrations for 3 and 5mm pupils; and between baseline and dual-focus lens for higher-order aberrations only for both 3 and 5mm pupils analysis. However, it is important to consider that baseline measurements were taken with naked eye (without any kind of correction) and that in the measurements with dual-focus and single-vision lenses the subjects were partially or fully corrected with the lenses. Thus, the higher amount of lower-order and total aberrations at baseline (when in comparison with measurements with the lenses) is related to the residual refractive error of the subjects.

When comparing both lenses, it is seen that the RMS of the higher-order aberrations and RMS of total aberrations were significantly higher for the dual-focus contact lens design than for the single-vision contact lens, for both pupil diameters analysed. There were also a statistically significant differences between both lenses for RMS of lower- order aberrations for 5mm pupil diameter ($p = 0.02$) but not for 3mm pupil diameter ($p = 0.08$), with the dual-focus lens depicting higher values in both conditions.

Table 9.1.1.3. *Lower-order, higher-order and total aberrations for a pupil diameter of 3 mm and 5 mm in each contact lens.*

Measurement	Contact lens	Median (Interquartile range)	Significance level	Post-hoc
Lower-Order 3 mm RMS (μm)	Baseline	0.42 (0.16 to 0.84)	0.012[1]*	Baseline-SV: 0.02[2]*
	Single-vision	0.19 (0.10 to 0.30)		Baseline-DF: 0.58[2]
	Dual-focus	0.27 (0.16 to 0.38)		SV-DF: 0.08[2]*
Higher-Order 3 mm RMS (μm)	Baseline	0.08 (0.07 to 0.09)	<0.001[1]*	Baseline-SV: 0.58[2]
	Single-vision	0.08 (0.06 to 0.10)		Baseline-DF: <0.001[2]*
	Dual-focus	0.15 (0.12 to 0.20)		SV-DF: <0.001[2]*
Total 3mm RMS (μm)	Baseline	0.59 (0.43 to 0.19)	0.004[1]*	Baseline-SV: 0.011[2]*
	Single-vision	0.21 (0.14 to 0.32)		Baseline-DF: 0.72[2]
	Dual-focus	0.32 (0.22 to 0.42)		SV-DF: 0.011[2]*
Lower-Order 5 mm RMS (μm)	Baseline	1.34 (0.54 to 2.59)	0.008[1]*	Baseline-SV: 0.010[2]*
	Single-vision	0.42 (0.30 to 0.73)		Baseline-DF: 0.55[2]
	Dual-focus	0.94 (0.68 to 1.12)		SV-DF: 0.018[2]*
Higher-Order 5 mm RMS (μm)	Baseline	0.19 (0.15 to 0.21)	<0.001[1]*	Baseline-SV: 0.66[2]
	Single-vision	0.19 (0.16 to 0.22)		Baseline-DF: <0.001[2]*
	Dual-focus	0.46 (0.42 to 0.52)		SV-DF: <0.001[2]*
Total 5 mm RMS (μm)	Baseline	1.36 (0.57 to 2.60)	0.004[1]*	Baseline-SV: 0.02[2]*
	Single-vision	0.46 (0.38 to 0.74)		Baseline-DF: 0.66[2]
	Dual-focus	1.07 (0.83 to 1.20)		SV-DF: 0.006[2]*

*(Where DF: Dual-Focus; RMS: Root Mean Square; μm: micrometers; SV: Single-Vision; [1]Friedman; [2]Bonferroni; *Statistically significant differences)*

Questionnaires

Table 9.1.1.4 shows QoV questionnaire values for each contact lens. Statistically significant differences were revealed between contact lens designs, with scores being lower for the single-vision contact lens across the frequency, severity and bothersome subscales of the instrument. Twenty-seven subjects (96 %) preferred the single-vision contact lens design, whilst 1 subject (4 %) preferred the dual-focus contact lens.

Table 9.1.1.4. *Quality of Vision questionnaire scores and comfort visual analogue scales for each contact lens.*

Measurement	Contact lens	Median (Interquartile range)	Significance level (Statistic, p-value)
QoV Frequency Score	Single-vision	15 (0 to 36)	(Z_{27}=4.32, p<0.001)[1]*
	Dual-focus	48 (37 to 59)	
QoV Severity Score	Single-vision	13 (0 to 31)	(Z_{27}=4.33, p<0.001)[1]*
	Dual-focus	39 (32 to 49)	
QoV Bothersome Score	Single-vision	0 (0 to 23)	(Z_{27}=4.11, p<0.001)[1]*
	Dual-focus	37 (29 to 56)	

*(Where QoV: Quality of Vision; [1]T-test; *Statistically significant differences)*

9.1.1.4 Discussion

In the present study, dual-focus and single-vision contact lenses provided excellent visual acuity and stereopsis despite differences in contrast sensitivity, light disturbance, higher-order aberrations and visual comfort scores. To the authors' knowledge, there is no prior study assessing visual performance of a dual-focus contact lens design compared to a single-vision contact lens design of the same material, eliminating the effect of material differences on the differences in the outcomes. A direct comparison with another study is not possible, although previous studies compared other multifocal and monofocal contact lenses (Madrid-Costa et al., 2012; García-Lázaro et al., 2015; Martins et al., 2019).

Visual acuity and stereopsis

High contrast visual acuity is not a sensitive measure of visual quality (Kang, McAlinden and Wildsoet, 2016). Different studies have not reported significant differences in distance visual acuity and stereopsis under light conditions between

myopia control dual-focus and single-vision contact lenses or spectacles (Anstice and Phillips, 2011; Kollbaum et al., 2013; Fernandes et al., 2018; Chamberlain et al., 2019). Sha et al. (2018) found that the the dual-focus design used in the present study and a center-distance multifocal contact lens (Proclear Multifocal Dominant, CooperVision Inc., Pleasanton, CA) provided excellent high and low contrast visual acuity at all distances. Similar results were reported in the multicentric clinical trial by Chamberlain et al. (2019).

The present study confirms these findings. However, controversy exists in the literature since other studies found statistically significant differences between a dual-focus design and best spectacle correction (Kollbaum et al., 2013) or a monofocal contact lens (Fedtke et al., 2016a).

Similar to the results of the present study, Ruiz-Pomeda et al. (2018c) did not find differences in stereopsis between subjects fitted with dual-focus design contact lenses and single-vision spectacle-corrected subjects. They found worse stereopsis values than those obtained in the present study (30.24 ± 12.09 and 38.18 ± 31.77 seconds of arc, for dual-focus contact lenses and single-vision spectacles, respectively).

Contrast sensitivity

Contrast sensitivity function characterizes visual performance better than high contrast visual acuity alone (Przekoracka et al., 2020). Multifocal contact lenses based on simultaneous vision designs alter the proportion of light focused at different distances depending on the pupil size, being the out-of-focus images and light

distribution between distance and near focus the main cause of this decrease (García-Lázaro et al., 2015). The abrupt change of power and discontinuity between zones may produce and increase light scatter and disturbance. This fact is even more evident under low-light conditions due to an increase of pupil size (Fernandes et al., 2018; Ruiz-Pomeda et al., 2019).

Several studies confirmed that contrast sensitivity in eyes fitted with multifocal contact lenses provide a lower slope for high spatial frequencies than with monofocal lens or spectacles (Madrid-Costa et al., 2012; García-Lázaro et al., 2015; Sha et al., 2015; Sánchez et al., 2018; Martins et al., 2019; Przekoracka et al., 2020). Nevertheless, Anstice and Phillips (2011) did not find contrast sensitivity differences between a dual-focus design contact lens and a single-vision one. This fact might be explained to the use of Pelli-Robson chart in their study, which only measures threshold for medium frequencies (Leat and Wegmann, 2004). In the present study the Vision Contrast Test System VCTS 6500 was used, which its poor reliability was also acknowledged (Pesudovs, 2004).

In accordance with a previous work (Kollbaum et al., 2013), the present study confirms a reduction in contrast sensitivity under photopic and mesopic conditions with dual-focus design contact lenses, generalized for every spatial frequency with the exception of 18 cycles per degree under mesopic conditions. In spite of this decrease in contrast sensitivity, the results of the present work revealed that under photopic conditions both lenses provide contrast sensitivity within normality zone limits.

Nevertheless, young subjects would be expected to be in the top of the normality zone since the normative values are from subjects of all ages.

Aberrations

It has been reported that higher-order aberrations are in part responsible for the lower contrast sensitivity in multifocal contact lenses (Wahl et al., 2018). Wavefront aberrations while wearing contact lenses can be considered the sum of eye aberrations and contact lens aberrations (López-Gil et al., 2002). Different authors have reported an increase in higher-order aberrations with dual-focus design contact lenses and other multifocal contact lenses due to the radial refractive gradient (Ji et al., 2018; Martins et al., 2019; Wolffsohn and Davies, 2019; Hughes et al., 2020).

The present study also found higher values of higher-order aberrations with dual-focus than single-vision contact lenses. This increase is dependent on multifocal design and affects visual performance differently. Distance-center dual-focus design contact lenses produce an increase in positive spherical aberration ranging from 0.125 µm in low addition to 0.245 µm in high addition in a pupil of 5 mm, while center-near contact lenses induce negative spherical aberration (Kollbaum et al., 2013; Fernandes et al., 2018; Lopes-Ferreira et al., 2018; Fedtke, Ehrmann and Bakaraju, 2020; Hughes et al., 2020). However, in the present study spherical aberration was not assessed alone, only global higher-order aberrations RMS value.

Therefore, the concentric power profile in multifocal contact lenses produces changes in higher-order aberrations which are pupil-dependent. Martins et al. (2019)

reported that contact lenses with larger stabilized areas for distance vision reduce higher-order aberrations since a higher light percentage is focused into the distance focus.

The Hartmann-Shack aberrometer data is extracted from the wavefront slope using Zernike polynomial fitting. This can fail when aberrations are measured in a dual-focus contact lens because the discontinuous lens power changes across the optic zone.

Light disturbance

Light disturbance can be caused by defocus, degradation of an optical system, scattering, opacities in optical media, diffraction or aberrations (Amorim-de-Sousa et al., 2019; Ruiz-Pomeda et al., 2019; Wolffsohn and Davies, 2019). An increase in positive spherical aberration is related to an increase in light disturbance, while negative spherical aberrations is associated with lower levels of light disturbance (Macedo-de-Araújo et al., 2016; Martins et al., 2019). Macedo-de-Araújo et al. (2016) reported that an increase of +0.15 μm in spherical aberration leads to an increase between 10 and 20 % in LDI. However, they did not find any impact of negative spherical aberrations in light disturbance. Amorim-de-Sousa et al. (2019) reported an increase in light disturbance size in uncorrected positive and negative refractive errors, and spherical-like aberrations; and an increase in light disturbance irregularities in coma-like and total higher-order aberrations. In the case of the present study, both size and shape of the light disturbance were higher with dual-focus design contact

lenses, as expected. LDI and the disturbance area were 1.5 times higher in the dual-focus than in the single-vision contact lens.

Similar to the outcomes of the present study, different authors (Brito et al., 2015; Fernandes et al., 2018; Martins et al., 2019) found higher light disturbance with multifocal contact lenses than with monofocal lenses, being worse with lenses with smaller areas for distance. Nevertheless, in spite of the photic phenomena, it has been reported that dual-focus design contact lenses are well accepted by children (Chamberlain et al., 2019).

Halo size was measured by Ruiz-Pomeda et al. (2019) and found that dual-focus design contact lenses increase light disturbance slightly in comparison with single-vision correction. Nevertheless, light disturbance decreased over the follow-up time, probably due to neuroadaptation. In comparison with the present results, they found slightly lower light disturbance parameters after 24 months of dual-focus contact lens use (LDI was 12.02 ± 6.15 %, BFC Radius 27.29 ± 7.21 mm, BFC Irregularity 0.84 ± 1.29 mm and 4.53 ± 1.45 mm). Therefore, light disturbance found in the present study might decrease in a longer follow-up. On the other hand, the present study found higher light disturbance values for the single-vision design contact lenses compared to those for single-vision lenses reported by Ruiz-Pomeda et al. (2019) except for BFC irregularity. This difference might be due to differences in contact lens material or, as in the previous case, to the different follow-up period.

Ferrreira-Neves et al. (2015) and Pomeda-Ruiz A et al. (2019) validated light distortion measurements with the LDA system and demonstrated that changing the

pupil size from 3 to 6 mm does not have a significant impact on light disturbance. Thus, the role of the pupil in aberrations is clear but not in light disturbance. However, Villa et al. (2007) found a moderate but significant positive correlation between pupil size and light disturbance. In the present study pupil diameter did not differ between lenses.

Questionnaires

Light disturbance might produce an increase of vision-related symptoms in dual-focus contact lens wearers. In accordance with the present study, different authors found an increase in subjective symptoms with different multifocal contact lenses (Fedtke et al., 2016a; Kang, McAlinden and Wildsoet, 2016; Wahl et al., 2018). Fedtke et al. (2016b) reported that decentred multifocal contact lenses and with higher power variations produce lower subjective ratings. Sha et al. (2018) found that two prototype lenses were better tolerated by non-presbyopic myopes than the dual-focus design lens used in the present study and another commercially available center-distance multifocal contact lens. Wahl et al. (2018) found that disability glare was higher with a center-distance contact lens than with a center-near one. However, Fernandes et al. (2018) did not find significant changes in QoV score among baseline, an aspheric multifocal contact lens and monovision.

Neuroadaptation plays a key role in multifocality adaptation (Fernandes et al., 2018; Ruiz-Pomeda et al., 2019), improving vision-related quality of life scores with dual-focus design contact lens in comparison with spectacle wear in children after 24 months.[40] However, the process of neural adaptation is not well understood. Authors

have hypothesized that the brain suppresses the blurred component of the simultaneous image (Ruiz-Pomeda et al., 2018d).

This study had limitations to be considered. It reports the short-term monocular outcomes after fitting these contact lens designs. Binocular summation effect as well as neural adaptation process might improve light disturbance scores and visual performance in long term follow-up, as found in different studies (Kang, McAlinden and Wildsoet, 2016; Lopes-Fereira et al., 2018; Ruiz-Pomeda et al., 2019). Second, several tests used in this study challenge the visual system by evaluating visual function under dim-lighting conditions or in the presence of glare which is not typical for children, as it might be for adults who drive at night, for example. Therefore, the present results might underestimate visual performance with dual-focus design contact lenses under binocular and children real-life conditions. Furthermore, prior history of contact lens wear was not considered in the inclusion criteria, and this might have an impact in the visual scores analyzed since some of the subjects enrolled were new contact lens wearers. Finally, the study was carried out in a young adult sample. Results in adults might not be representative of those in children. As the task and protocol were long, young adults were chosen as sample so that they could respond accurately (Sha et al., 2018). These facts are not expected to affect the observed outcomes significantly. Further investigation is needed in order to evaluate visual performance with other multifocal or dual-focus design contact lenses with different geometries and assess the tear film role with multifocal designs. Finally, the role of neuroadaptation should be specifically addressed in future studies.

Overall, dual-focus contact lens design decreases the psychophysical and psychometric visual quality scores in the short-term under dim-light conditions when compared to a single-vision contact lens design with the same material. Visual acuity and stereopsis were not affected by lens design. However, a relatively small clinical impact might be expected under photopic lighting conditions, in which children using dual-focus lenses perform most of their activities.

CHAPTER 9.1.2: Tear film stability over a myopia control contact lens compared to a monofocal design

9.1.2 TEAR FILM STABILITY OVER A MYOPIA CONTROL CONTACT LENS COMPARED TO A MONOFOCAL DESIGN

In this second part of the chapter, the short-term pre-lens tear film stability and comfort of a dual-focus and a single-vision contact lens will be compared.

9.1.2.1 Introduction

It has been reported that dual-focus contact lenses based on a center-distance design cause a reduction in myopia progression by reducing the off-axis hyperopia (Anstice and Phillips, 2011; Ruiz-Pomeda et al., 2018b). However, despite acceptable visual acuity, subjects might complain about quality of vision symptoms (Ruiz-Pomeda et al., 2019; Wolffsohn and Davies, 2019). Different studies have found an increase in spherical and higher-order aberrations, a reduction in contrast sensitivity, higher light disturbance and a decrease in the subjective quality of vision (as found in *Chapter 9.1.1*) (Fernandes et al., 2018; Amorim-de-Sousa et al., 2019; Ruiz-Pomeda et al., 2019; Wolffsohn and Davies, 2019).

Tear film assessment is essential in contact lens wearers (Foulks et al., 2013). Since a contact lens is inserted on the eye, tear film destabilizes (Korb, Greiner and Glonek, 1996) as the contact lens divides the tear film into two layers: pre-lens tear film and post-lens tear film. The pre-lens tear film portion plays a key role in visual quality and comfort (Wolffsohn et al., 2017), therefore assessing pre-lens tear film stability is a topic of high interest in the contact lens field.

To the knowledge of the authors, this is the first study which intends to analyse the effect of a front-surface dual-focus design with abrupt changes in power on pre-lens tear film stability in comparison with a single-vision contact lens of the same material in order to minimize material effect on tear film stability, such as wettability, water content or dehydration. Thus, the only difference between lenses was the optical design. It has been hypothesized that pre-lens tear film stability might be altered by the anterior design of the dual-focus contact lens, which could be another factor degrading visual quality in addition to the effects of bifocality. The aim of this study was to assess the short-term effect of a dual-focus design on pre-lens tear film stability in comparison with a single-vision contact lens of the same material.

9.1.2.2 Methodology

This is a randomized, double-masked, crossover study. Twenty-eight healthy volunteers between 18 and 32 years old participated in this study. The inclusion criteria were subjects with an astigmatism ≤ 0.75D and best-corrected visual acuity ≥ 0.00 logMAR in each eye. Subjects were not required to be contact lens wearers. Contact lens wearers were instructed not to wear their contact lenses within a week before the examination. Written consent of each subject was obtained after the explanation of the purpose and the protocol of the study. The study procedures were approved by the Ethics Committee of University of Minho and in accordance with the tenets of Declaration of Helsinki. Subjects with any ocular disease or binocular anomaly, and subjects taking any medication with ocular affection or with potential to interfere with contact lens wear, were excluded from the study.

A random eye was assessed in order to avoid duplication of data. Nevertheless, both eyes were fitted with contact lenses to guarantee the normal and binocular visual conditions.

Subjects completed 2 visits: first visit (baseline) and second visit (assessment of single-vision and dual-focus contact lenses). During the first session, the inclusion and exclusion criteria were evaluated and baseline data (naked eye) was obtained. Refraction, best-corrected distance visual acuity and pre-corneal tear film stability assessment (without contact lens) were recorded. Refraction was objectively measured with Grand Seiko Autorefractometer WAM-5500 (Grand Seiko Co., Ltd., Hiroshima, Japan) and subjectively adjusted using the end-point criterion of maximum plus for the best visual acuity. Tear film stability was evaluated using Medmont E 300 6.1 version (Medmont Pty., Ltd, Melbourne, Australia) with the built-in software for tear film analysis.

The second visit was performed 1 week after the first one. During the second session, measurements with both contact lenses were done. Although only one eye was considered for evaluation, contact lenses were fitted binocularly in a random order. Over-refraction, best-corrected distance visual acuity, pre-lens tear film stability (with Medmont) and comfort (with visual analogue scales) were assessed. Over-refraction was also assessed with the autorefractor and then adjusted subjectively. Best-corrected distance visual acuity at distance was assessed using the chart 1 of Logarithmic Visual Acuity Chart 2000 (www.precision-vision.com). Temperature and humidity of the room were controlled to ensure that they were constant in all visits.

Contact lenses

During the second visit, subjects were fitted in a random order with the single-vision Proclear 1-day® contact lens (CooperVision, Inc., Pleasanton, CA) and the dual-focus contact lens MiSight® (CooperVision, Inc., Pleasanton, CA) according to the manufacturer's fitting guidelines for the initial lens selection. The contact lenses had different design, but both were made of Omafilcon A (60% water content, non-ionic), in order to minimize material influence on tear film stability such as wettability, water content or dehydration. Moreover, according to the manufacturer, both lenses were supplied sterile in blisters containing buffered saline solution and had the same edge profile. Thus, the only difference between lenses was the optical design. Base curve and lens diameter was also equal between lens types: 8.70mm and 14.2 mm, respectively. The dual-focus contact lens is comprised of an 11.66 mm optic zone with four alternating zones for distance and near vision surrounding a central diameter of 3.36 mm for distance vision (Kollbaum et al., 2013; Ruiz-Pomeda et al., 2018b; Chamberlain et al., 2019; Ruiz-Pomeda et al., 2019). This dual-focus contact lens has a 2 D maximum add power, which provides a second focus in front of the retina (Ruiz-Pomeda et al., 2018b; Chamberlain et al., 2019).

Given that the rationale for the study is that tear film stability may be affected by lens front surface design, *Figure 9.1.2.1* shows the tangential curvature maps of pre-lens topographies while the same subject is wearing the contact lenses in order to show how varies the curvature radius of the front surface of the lens between both contact lenses. Topography measurement when the lens is worn does not reflect the

true curvature radius of the front surface the lens. Nevertheless, the aim was not to show the exact curvature radius, the aim was to evidence that both lenses have a different front surface shape. Moreover, different studies have reported that the dual-focus contact lens has a dual-focus surface on the front surface of the lens. This multifocal surface is created by changing the curvature radius of the front surface of the lens in each concentric ring (Fernandes et al., 2018; Ruiz-Pomeda et al., 2018b; Amorim-de-Sousa et al., 2019; Ruiz-Pomeda et al., 2019).

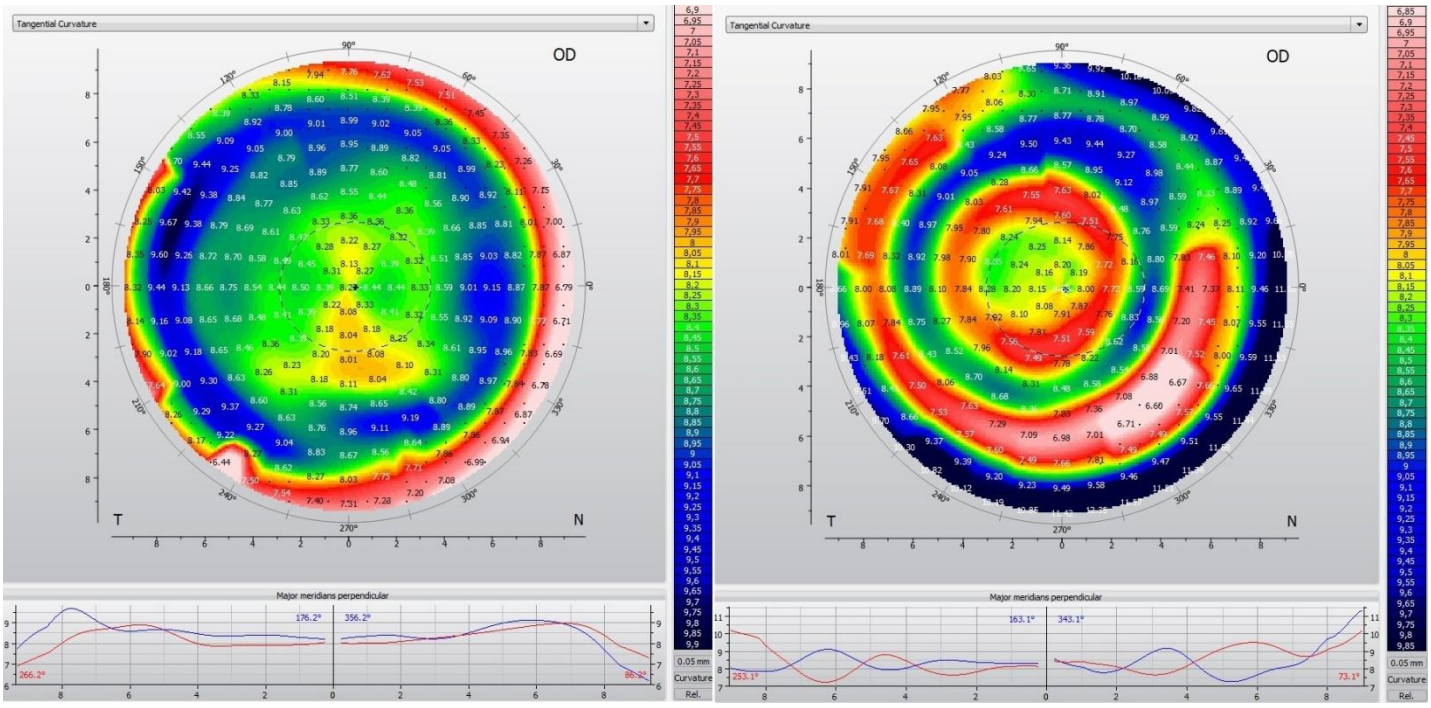

Fig. 9.1.2.1. *Tangential maps of pre-lens topographies for the single-vision contact lens (left) and the dual-focus contact lens (right).*

Lens fitting

Movement, centration and coverage of both contact lenses were checked using a slit-lamp. Tear film was assessed 25 minutes after contact lens insertion in order to

provide the adequate contact lens stabilization. It has been reported that this period of time is adequate to assess the short-term performance and comfort of contact lenses (Efron et al., 1987; Brennan et al., 1990; Paugh et al., 2001; Nichols and King-Smith, 2003; Foulks et al., 2013). This period of time was maintained for all contact lens fittings so that the results were comparable between conditions (Kollbaum et al., 2013; Sánchez et al., 2018). A period of 15 minutes was established as the washout period between different contact lens fittings (Sánchez et al., 2018; Martins et al., 2019).

Tear film assessment

TFSQ was evaluated using Medmont E 300, as explained in *Chapter 3 General Methodology*. Thus, TFSQ, TFSQ area and auto Tear Break-Up Time were measured automatically with Medmont Tear Film analysis software. More information about the validation of the algorithm can be found in previously published works (Alonso-Caneiro, Iskander and Collins, 2009; Downie, 2015). Contact lens was then removed and the next contact lens was fitted after the washout period. After measurements for both sets of contact lenses were completed, subjects were asked to choose a preferred contact lens design.

Visual analogue scales

Visual analogue scales (continuous scale between 0 and 10) were used to assess general comfort, physical comfort and visual comfort. Lower scores suggested good comfort, and values close to 10 a poorer comfort. Subjects were first asked for the general comfort with the following question: “How do you rate your overall comfort

with the lens?" After that, they were asked for the physic comfort: "How do you rate your physical comfort (pain, foreign body sensation, gritty sensation, dryness, itching…) with the lens?" Finally, they were asked for the visual comfort: "How do you rate your visual comfort (blurred vision, distortion or halos, glare and flare around lights) with the lens?"

Statistical analysis

Statistical analysis was performed using SPSS v26.0 for Windows (IBM Corp, Armonk, New York, USA). Obtained results were shown as the mean ± SD. Normality distribution of each contact lens sample was checked by means of the Shapiro-Wilk test.

The interaction between contact lens type and the order in which they were fitted was assessed by means mixed ANOVA. Differences between comfort scores in contact lenses were evaluated using the Wilcoxon signed rank test. The Friedman test was used to assess differences between baseline and both contact lens types in visual acuity and in tear film stability metrics. Post-hoc analysis was carried out using the Bonferroni test with the correction for multiple testing in order to evaluate the differences between all pair group combinations. A p-value less than 0.05 was defined as statistically significant.

9.1.2.3 Results

Twenty-eight eyes of 28 participants with a mean age of 23.5 ± 4.1 years, ranging from 18 to 32 years old, were assessed. Seventeen were females (60.7 %) and eleven

males (39.3 %). Moreover, 20 (71.4 %) were contact lens users and 8 (28.6 %) were not. Mean refractive sphere and cylinder were -1.36 ± 1.04 D (ranging from -6 to -0.25 D) and -0.23 ± 0.30 D (ranging from -0.75 to 0.00 D), respectively. All contact lenses had a correct movement, centration and coverage in all subjects.

Sample size was calculated post-hoc using G-Power. The statistical power obtained with a sample size of 28 subjects, an effect size of 0.74 in TFSQ and a significance level of 0.05 was 0.96.

No statistical significant interaction was found between contact lens type and the order in which they were fitted in any outcome reported in this study (Mean TFSQ: p = 0.508; Median TFSQ: p = 0.520; Mean TFSQ area: p = 0.782; Median TFSQ area: p = 0.561; Mean auto Tear Break-Up Time: p = 0.534; Median auto Tear Break-Up Time: p = 0.412; general comfort score: p = 0.305; physical comfort score: p = 0.861; visual comfort score: p = 0.864). This evidences that the order in which lenses were fitter did not act as a confounding factor in results.

Over-refraction and visual acuity

The median and interquartile range of over-refraction were +0.25 D (0.00 to +0.52 D) and +0.25 D (0.00 to +0.50 D), for single-vision and dual-focus designs, respectively. The median and interquartile range of best-corrected distance visual acuity were -0.10 (-0.20 to -0.10), -0.12 (-0.18 to -0.10) and -0.10 (-0.15 to -0.10), for baseline, single-vision and dual-focus contact lenses, respectively. Friedman test did not reveal statistically significant differences between conditions (p = 0.18).

Tear film stability

Table 9.1.2.1 shows the results of tear film analysis at baseline (pre-corneal tear film stability) and with each contact lens (pre-lens tear film stability). Contact lens wear increased the mean value of TFSQ metric (meaning a more unstable tear film) when compared to baseline assessment, with dual-focus contact lens providing a greater tear film instability than the single-vision contact lens (0.39 ± 0.14 vs 0.27 ± 0.13, p = 0.017, Bonferroni). Mean TFSQ area also underwent a statistically significant increase with both contact lenses when compared to baseline. TFSQ area was greater when measured with the dual-focus contact lens (34.84 ± 14.31) than with the single-vision contact lens (22.38 ± 12.91), with a statistically significant difference between them (p = 0.007, Bonferroni). Auto Tear Break-Up Time was statistically lower in both contact lenses than at baseline, this decrease being higher with the dual-focus contact lens than with the single-vision contact lens (3.09 ± 1.72 sec vs 5.58 ± 4.80 sec). However, in this case, no statistically significant differences were found between the two contact lenses.

Table 9.1.2.1. *Tear Film Surface Quality metrics obtained in each experimental condition.*

Measurement	Condition	Median (Interquartile range)	95% Confidence interval	p-value	Post-hoc (Adjusted p-value)
Mean TFSQ	Baseline	0.13 (0.08-0.20)	0.11-0.19	<0.001[1]*	Baseline-Single-vision: 0.017[2]* Baseline-Dual-focus: <0.001[2]* Single-vision-Dual-focus: 0.017[2]*
	Single-vision	0.24 (0.19-0.36)	0.22-0.32		
	Dual-focus	0.44 (0.26-0.49)	0.33-0.44		
Median TFSQ	Baseline	0.10 (0.07-0.17)	0.09-0.17	<0.001[1]*	Baseline-Single-vision: 0.025[2]* Baseline-Dual-focus: <0.001[2]* Single-vision-Dual-focus: 0.025[2]*
	Single-vision	0.23 (0.16-0.36)	0.21-0.32		
	Dual-focus	0.44 (0.23-0.52)	0.32-0.45		
Mean TFSQ Area (%)	Baseline	7.17 (1.44-14.37)	5.70-12.67	<0.001[1]*	Baseline-Single-vision: 0.025[2]* Baseline-Dual-focus: <0.001[2]* Single-vision-Dual-focus: 0.007[2]*
	Single-vision	20.58 (13.68-33.03)	17.17-27.60		
	Dual-focus	38.83 (22.57-45.70)	29.06-40.62		
Median TFSQ Area (%)	Baseline	4.10 (0.87-12.85)	3.93-12.07	<0.001[1]*	Baseline-Single-vision: 0.025[2]* Baseline-Dual-focus: <0.001[2]* Single-vision-Dual-focus: 0.007[2]*
	Single-vision	16.25 (8.28-31.63)	14.63-26.09		
	Dual-focus	37.40 (21.38-49.23)	27.67-41.24		
Mean Auto Tear Break-Up Time (seconds)	Baseline	7.12 (4.73-11.46)	5.89-12.18	<0.001[1]*	Baseline-Single-vision: 0.029[2]* Baseline-Dual-focus: <0.001[2]* Single-vision-Dual-focus: 0.112[2]
	Single-vision	3.77 (2.77-6.95)	3.64-7.52		
	Dual-focus	2.47 (2.40-2.54)	2.39-3.78		
Median Auto Tear Break-Up Time (seconds)	Baseline	6.89 (4.73-10.74)	5.53-11.98	<0.001[1]*	Baseline-Single-vision: 0.023[2]* Baseline-Dual-focus: <0.001[2]* Single-vision-Dual-focus: 0.166[2]
	Single-vision	3.45 (2.58-6.13)	3.21-6.90		
	Dual-focus	2.45 (2.40-2.52)	2.26-3.49		

*(Where TFSQ: Tear Film Surface Quality; [1]Friedman; [2]Bonferroni; *Statistically significant values)*

Comfort

No subject had any problem to understand and respond to the questionnaire. The results of the visual analogue scale questionnaire (*Table 9.1.2.2*) revealed that the single-vision contact lens provided better comfort scores than the dual-focus contact lens (0.77 ± 1.14 vs 3.12 ± 2.79, $p < 0.001$, Wilcoxon). Additionally, comfort was divided into physical and visual comfort. Compared to the dual-focus contact lens, the single-vision contact lens also provided better physical (0.96 ± 1.46 vs 2.19 ± 2.45, $p = 0.015$, Wilcoxon) and visual (1.27 ± 1.66 vs 3.92 ± 2.04, $p < 0.001$, Wilcoxon) comfort ratings. Also, physical comfort was slightly better than visual comfort for both of the analysed lenses. Moreover, twenty-seven subjects (96 %) preferred the single-vision contact lens, whilst one subject (4 %) preferred the dual-focus contact lens.

Table 9.1.2.2. *Visual comfort analogue scales results for each tested contact lens.*

Measurement	Contact lens	Median (Interquartile range)	95% confidence interval	p-value
Overall Comfort Score	Single-vision	0.00 (0.00-1.00)	0.31-1.23	<0.001[1]*
	Dual-focus	2.00 (0.00-6.00)	1.99-4.24	
Physical Comfort Score	Single-vision	0.00 (0.00-1.25)	0.37-1.55	0.015[1]*
	Dual-focus	1.00 (0.00-4.25)	1.20-3.18	
Visual Comfort Score	Single-vision	0.50 (0.00-3.00)	0.60-1.94	<0.001[1]*
	Dual-focus	4.00 (2.00-5.25)	3.10-4.75	

*(Where [1]Wilcoxon; *Statistically significant values)*

9.1.2.4 Discussion

In the present study, pre-lens tear film stability has been measured using the previously validated TFSQ algorithm (Alonso-Caneiro, Iskander and Collins, 2009; Downie, 2015). To the knowledge of the authors, there is no other study which has

assessed the effect of the dual-focus design on pre-lens tear film stability in comparison with a single-vision contact lens. For that reason, a direct comparison with another study is not possible. Contact lens material and care regimen were the same for dual-focus and single-vision contact lenses in order to minimize material effect on tear film stability, such as wettability, water content or dehydration. Thus, contact lens optic design was the main difference between lenses. The present study adds that TFSQ is also able to distinguish between contact lens optic designs.

Tear film stability

As expected, with both contact lens types pre-lens tear film stability was reduced in comparison to pre-corneal tear film stability. Several studies reported that contact lenses lead to a decrease in pre-lens tear film quality, an increase in tear osmolarity and lower tear meniscus height values, especially in high water content contact lenses (Nichols and Sinnott, 2006; Szczesna-Iskander, 2018; García-Montero et al., 2019c; Lafosse et al., 2019; Lorente-Velázquez et al., 2019). These biophysical changes increase dryness symptoms (Nichols and Sinnott, 2006; Szczesna-Iskander, 2018; García-Montero et al., 2019c; Lafosse et al., 2019; Lorente-Velázquez et al., 2019). In contrast to these studies, García-Montero et al. (2019a) reported that a monthly silicone hydrogel contact lens did not lead to significant changes in the ocular surface over 15 days of use.

Contact lenses divide the tear film into two layers, pre-lens and post-lens tear film. This fact results in a thinning in the pre-lens lipid layer. Therefore, a lower pre-lens stability is expected, which could decrease comfort and quality of vision (Ferrer-Blasco

et al., 2009). Pre-lens tear film plays a relevant role in comfort, visual quality, lubrication and hydration of the contact lens front surface. It also facilitates palpebral interaction with the contact lens surface and provides a smooth optical surface (Dumbleton et al., 2013b).

Post-hoc analysis revealed that the dual-focus contact lens altered TFSQ and TFSQ area to a greater extent than the single-vision contact lens. Due to the fact that both lenses were made of the same material, the only difference between them was the optical design. Therefore, differences in tear film stability between them could be explained by the fact that the dual-focus contact lens has a front-surface bifocal design with abrupt changes in power, which can alter the proper distribution and stabilization of the tear film across the contact lens surface.

Generally, as found in *Chapter 9.1.1*, multifocal contact lenses and dual-focus contact lenses cause worse contrast sensitivity, an increase in photic phenomena and higher aberrations, especially primary spherical aberration (Dumbleton et al., 2013b; Fedtke, Ehrmann and Bakaraju, 2020; García-Marqués et al., 2020). This fact, together with worse pre-lens tear film stability, might lead to a deterioration of the visual quality even more, since it has been reported that a decrease in auto Tear Break-Up Time might induce changes in optical quality (Rae and Price, 2009).

In spite of the fact that results did not show statistical differences between contact lenses in auto Tear Break-Up Time, the dual-focus contact lens had lower auto Tear Break-Up Time than the single-vision contact lens. A previous study measured auto Tear Break-Up Time in a center-near multifocal contact lens (Lorente-Velázquez et al., 2019). In comparison with the present study, auto Tear Break-Up Time was

higher (9.29 ± 3.67 seconds) after 20 minutes of contact lens wear. In the same study, Auto Tear Break-Up Time worsened 8 hours after contact lens wear. Therefore, it is possible that auto Tear Break-Up Time results in this work might have been lower if a greater wearing time had been tested, since auto Tear Break-Up Time decreases progressively along the contact lens time wear (Lorente-Velázquez et al., 2019). Also, Lafosse et al. (2019) found that fluorescein Tear Break-Up Time (after lens removal) and osmolarity worsened over the first day of wearing an aspheric center-near multifocal contact lens.

Only one previous study has evaluated some tear film parameter in subjects fitted with the same dual-focus contact lens as in this study. Ruiz-Pomeda et al. (2018a) did not report significant changes in osmolarity over 24-months in the dual-focus lens and single-vision spectacles (naked eyes). However, in this case, the osmolarity measurement was performed after 30 minutes of contact lens removal**.**

Comfort

Regarding comfort, the results suggest that not only were visual comfort and general comfort affected by the dual-focus design, but physical comfort was also altered. This fact suggests that the dual-focus design might alter visual and physical comfort. Nevertheless, from the results of this study, it cannot be concluded that the tear film instability justifies higher discomfort. In previous studies (Chamberlain et al., 2019; Ruiz-Pomeda et al., 2019), children wearing dual-focus contact lenses did not have worse comfort outcomes compared to a single-vision contact lens made of the same material or spectacle lenses, respectively. However, the present study highlights

the potential interplay between physical and visual discomfort, such as the fact that the visual instability might indirectly affect the outcomes of the survey on physical discomfort.

Ocular dryness and discomfort are the main complaints made by contact lens wears (Dumbleton et al., 2013b). Rico-del-Viejo et al. (2018) reported that contact lens thickness differences between monofocal and multifocal contact lenses might be the most important factor which reduces comfort in multifocal contact lenses. Contact lens power might also induce changes in tear film stability due to inherent differences of contact lens thicknesses. However, in the present study, parameters were maintained for both contact lens types, including thickness with optical design as the difference factor.

Tear film and comfort outcomes where in accordance with the preferred contact lens chosen by subjects since 27 of them (96 %) chose the single-vision contact lens. This fact suggests that the outcomes are clinically significant.

Visual acuity

In spite of the fact that visual comfort was diminished in the dual-focus contact lens, no statistically significant differences were found between contact lenses in visual acuity. This could be to the fact that high contrast visual acuity is not a sensitive measure of visual quality (Kang, McAlinden and Wildsoet, 2016). Thus, the lower visual comfort reported by subjects could be related to more precise measurements of visual quality such as contrast sensitivity (García-Marqués et al., 2020).

This study has some limitations to consider. First, results were obtained in young adults while the target population for the dual-focus contact lenses is young children and adolescents, or presbyopic subjects wearing contact lenses with similar designs (bifocal lenses). Therefore, the present results cannot be directly extrapolated to those populations. Although visual analogue scales have been extensively used, using a standardized questionnaire would have also been interesting. Nevertheless, a visual analogue scale was used to differentiate between general, physic and visual comfort.

The present study shows short-term tear film stability results; however, tear film might be worse after more hours of wear and both lenses could result in similar tear film stability. Tear film was assessed 25 minutes after contact lens insertion. Even though some studies (Efron et al., 1987; Brennan et al 1990; Paugh et al., 2001; Nichols and King-Smith, 2003) reported that this period of time is adequate to assess the short-term performance and comfort of contact lenses since tear film varies in the first 20 minutes of contact lens wear, others (Little and Bruce, 1994; Nichols and King-Smith, 2004) argued that the pre-lens tear film thinned significantly over the first 30 minutes of contact lens wear. Therefore, there is still controversy in this topic. Anyway, this issue is not expected to influence the comparison between these two contact lenses since tear film was assessed after the same time and after the same washout period for both contact lenses so that outcomes were comparable between them. Besides, Efron et al. (1987) confirmed that the majority of dehydration occurs within the first 5 minutes of wear. Moreover, the randomness in the fitting of the lenses avoids the bias. Still the results allow building a hypothesis to be tested in future studies in those specific populations. The results could probably be extrapolated to

other dual-focus or differently designed multifocal contact lenses for presbyopic subjects; nevertheless, this should be tested in future studies. Present results might be relevant for the presbyopic population as the assessment of pre-lens tear film stability might help to understand the visual complaints regarding contact lens designs with abrupt changes of curvature within the optic zone. In these subjects, the tear film quality is already reduced showing higher levels of dehydration and this might even worsen the outcomes (Craig et al., 2017).

Furthermore, the fact that subjects with and without previous contact lens experience were included might affect comfort scores since it was the first time that some of them wore contact lenses. Finally, it is also important to highlight that not only pre-lens tear film may be altered by the dual-focus design of the contact lens, but Medmont system might be very sensitive and detect non-tear film related changes on the dual-focus contact lens surface. However, the differences in the comfort rating between lenses were in agreement with the TFSQ results (better performance with the single-vision contact lens). Tear film stability assessment with other devices such as interferometers (Tearscope or LipiView, for instance) in dual-focus contact lens should also be considered in future studies to compare it with the outcomes of Medmont software. Further research is needed in order to assess tear film stability in other dual-focus or multifocal contact lens designs and materials after a longer wearing time in children and presbyopic subjects.

Overall, the present study compares the short-term effect of the dual-focus design on pre-lens tear film stability in comparison with a single-vision contact lens made of

the same material. A slight reduction in short-term pre-lens tear film instability and higher discomfort ratings was found in the dual-focus design than in the single-vision contact lens with the same material. The increased pre-lens tear film instability might also deteriorate the visual performance further with dual-focus contact lenses. Therefore, tear film should be carefully assessed before selecting dual-focus contact lens wearers since subjects with an altered tear film stability before lens insertion might not be an adequate target population because dual-focus contact lens will deteriorate the tear film stability in a higher magnitude than a single-vision contact lens.

CHAPTER 9.2: Short-term tear film stability, optical quality and visual performance in two dual-focus contact lenses for myopia control with different optical designs

9.2 SHORT-TERM TEAR FILM STABILITY, OPTICAL QUALITY AND VISUAL PERFORMANCE IN TWO DUAL-FOCUS CONTACT LENSES FOR MYOPIA CONTROL WITH DIFFERENT OPTICAL DESIGNS

In the previous chapter (*Chapter 9.1*), it was found that a dual-focus contact lens affected visual performance, optical quality, light disturbance, tear film stability and comfort in comparison to a single-vision contact lens. Both lenses were made of the same material; therefore, differences were due to the optical design of the lenses. The present chapter goes one step further by comparing short-term visual quality, optical quality, light disturbance, comfort and tear film stability between two dual-focus prototype contact lenses for myopia control made from the same material. The aim is to assess whether parameters are influenced by the different optical designs of two dual-focus contact lenses. One of them has a short central diameter and the other one has a medium central diameter.

9.2.1. Introduction

Dual-focus contact lenses induce peripheral defocus to reduce the off-axis hyperopia, which is thought to act as a stimuli to reduce the axial elongation of the eye (Kollbaum et al., 2013; González-Méijome et al., 2016; Li et al., 2016; Faria-Ribeiro, Amorim-de-Sousa and González-Méijome, 2018; Ruiz-Pomeda et al., 2018b; Chamberlain et al., 2019; Martins et al., 2019; Hughes et al., 2020; Przekoracka et al., 2020; Chamberlain et al., 2021).

In spite of the positive effect on controlling eye growth, dual-focus contact lenses have the drawback of limiting the retinal image quality since the light that enters through the pupil is redistributed into different focuses (as found in *Chapter 9.1.1*) (González-Méijome et al., 2016; Fedtke et al., 2017; Ruiz-Pomeda et al., 2019; García-Marqués et al., 2020). Generally, as found in *Chapter 9.1.1*, dual-focus contact lenses cause a reduction in mesopic visual acuity and contrast sensitivity; and induce higher light disturbance and higher spherical and higher-order aberrations (Kollbaum et al., 2013; González-Méijome et al., 2016; Fedtke et al., 2017; Martins et al., 2019; García-Marqués et al., 2020; Monsálvez-Romín et al., 2020). These effects might be pupil-dependent because the percentage of light distributed in the far and near focus depends on the pupil diameter. Thus, the performance of dual-focus contact lenses is influenced by the zones of the lenses destined to far and near vision and the pupil diameter exposed to these zones (Montés-Micó et al., 2014; Madrid-Costa et al., 2015; Cardona and López, 2016; Papadatou et al., 2017; Faria-Ribeiro and González-Méijome, 2019; Monsálvez-Romín et al., 2020; Talens-Estarelles, García-Del Valle and García-Lázaro, 2022).

It has also been reported that visual quality and subjects' satisfaction might be improved by adjusting the zones of the lens with distance and near powers (Lopes-Ferreira et al., 2011; Faria-Ribeiro, Amorim-de-Sousa and González-Méijome, 2018; Martins et al., 2019; Talens-Estarelles, García-Del Valle and García-Lázaro, 2022). For instance, Martins et al. (2019) and Talens-Estarelles, García-Del Valle and García-Lázaro (2022) found that the quality of vision was less affected by lenses with higher areas for

distance vision. Nevertheless, these studies are not directly comparable with the present one since different contact lenses were used.

Another major contribution to the image quality perceived when fitted with any contact lens, dual-focus or not, is the assessment of quality of the tear film. The tear film plays a vital role in the fitting and comfort of contact lenses and the visual quality of the eye (Foulks et al., 2013; García-Marqués et al., 2021b). As found in *Chapter 9.1.2* (García-Marqués et al., 2021b), the concentric ring pattern of a dual-focus contact lens for myopia control induced a reduction in the tear film stability and comfort when compared to a single-vision contact lens of the same material. This might be caused by a worse spreading of the pre-lens tear film across the surface of the contact lens as a consequence of the abrupt change in curvature over the anterior surface of the contact lens.

Only a few studies have attempted to assess the influence of myopia control contact lenses on visual quality and tear film stability (Faria-Ribeiro, Amorim-de-Sousa and González-Méijome, 2018; Martins et al., 2019; García-Marqués et al., 2020; García-Marqués et al., 2021b). Due to the relevant role of visual quality, comfort and tear film in contact lens fitting and treatment adherence it is of clinical relevance to expand the knowledge on how different designs and materials affect these clinical parameters.

In this study, short-term visual quality, optical quality, light disturbance, comfort and tear film stability was compared between two dual-focus prototype contact lenses for myopia control made from the same material (Faria-Ribeiro, Amorim-de-Sousa and

González-Méijome, 2018). It is hypothesized that these parameters might be influenced by the different optical design of the two contact lenses. The present study might help clinicians to adjust the design of the lens depending on patients' necessities to improve their adherence and satisfaction with dual-focus contact lenses.

9.2.2. Methodology

Twenty-eight healthy myopic volunteers aged between 18 and 32 years old were enrolled in this non-dispensing, comparative, randomized, double-masked, crossover study. Written consent of each subject was obtained after the explanation of the purpose and the protocol of the study. The study followed the tenets of the Declaration of Helsinki and was approved by the Ethics Subcommittee for life and health sciences of the University of Minho. Inclusion criteria involved best-corrected visual acuity ≤ 0.00 logMAR in each eye. Subjects with any ocular disease, binocular anomaly, astigmatism > 0.75D (Kollbaum et al., 2013) or who had any medication that contraindicates the use of contact lenses were excluded from the study. Regular contact lens wearers were instructed not to wear their contact lenses within a week before the examination.

Luminance and illuminance were evaluated using a luminance meter (Konica Minolta LS-100 Sensing Americas Inc, Ramsey, NJ, USA) and an illuminance meter (*T-10*, *Minolta* Sensing Inc, Tokyo, Japan), respectively. The varying daylight was removed by using black-out curtains in the examination room. Room illuminance was 255.58 ± 8.22 lux and 3.52 ± 0.12 lux under photopic and mesopic conditions, respectively. The mean luminance was 203.10 ± 3.68 cd/m^2, 48.09 ± 1.15 cd/m^2 and 0.63 ± 0.01 cd/m^2

for the measurement of visual acuity, photopic contrast sensitivity at 3 meters and mesopic contrast sensitivity at 3 meters, respectively.

Experimental procedure

The protocol consisted of two visits. In the first visit (Baseline visit), the case history, subjective refraction with trial lenses, visual acuity, wavefront aberrations and pre-corneal tear film stability were assessed. The nominal power of the contact lenses (-2.00 D, -3.50 D or -5.00 D) was chosen based on the subjective refraction results. Since only three powers were available, the power that was more similar to the refraction of subjects was chosen. In the second visit, both dual-focus contact lenses were fitted binocularly in a random order and the listed parameters were assessed in the following order: Over-refraction with trial lenses, QoV questionnaire, comfort assessment, visual acuity, stereopsis, photopic and mesopic contrast sensitivity, light disturbance assessment, aberrations and pre-lens tear film stability. Only the results of the sensorial dominant eye were included in the present study. Sensorial dominance was obtained by means of the "+1.50 D blur" method (Lopes-Ferreira et al., 2013; Fernandes et al., 2018).

Dual-Focus Contact Lenses

Both contact lens prototypes have a centre-distance inner zone with either 2.1 mm or 4.0 mm of diameter, surrounded by alternating zones with +2.0 D of add power (*Figures 9.2.1* and *9.2.2*) (Pauné et al., 2014; Pauné et al., 2015; Faria-Ribeiro, Amorim-de-Sousa and González-Méijome, 2018; Martins et al., 2019). Contact lens parameters

are summarized in *Table 9.2.1*. The lenses were manufactured by Precilens (Precilens, Creteil, France). The optical design was the only difference between contact lenses. The short central diameter (S design) had an inner central zone of 2.1 mm and the medium central diameter (M design) had an inner zone of 4.0 mm.

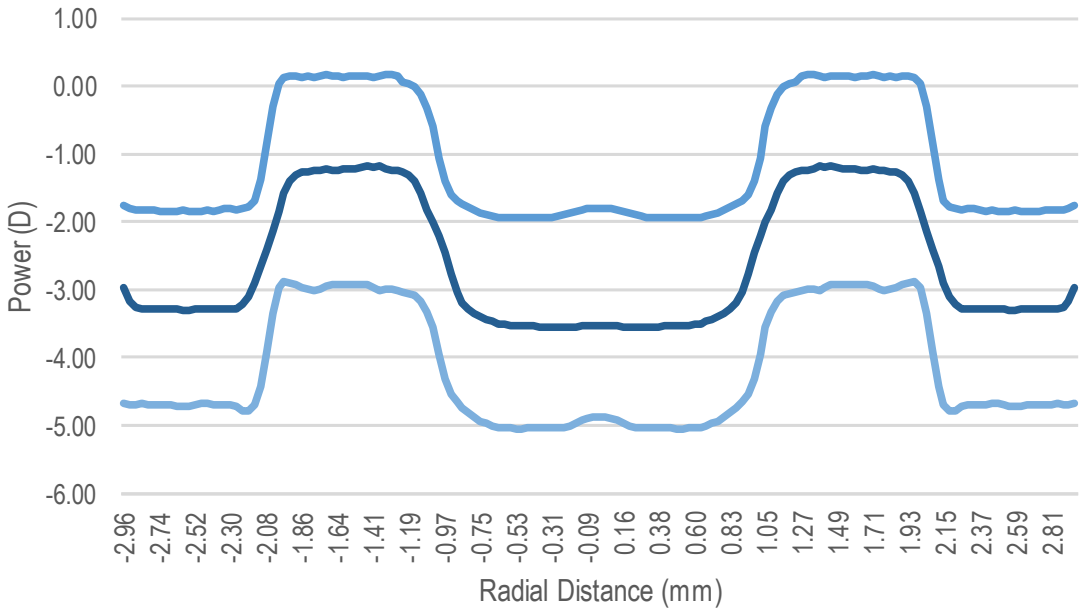

Fig. 9.2.1. *Power profile of the contact lens with the short diameter for a central distance nominal power of -2.00 D, -3.50 D and -5.00 D.*

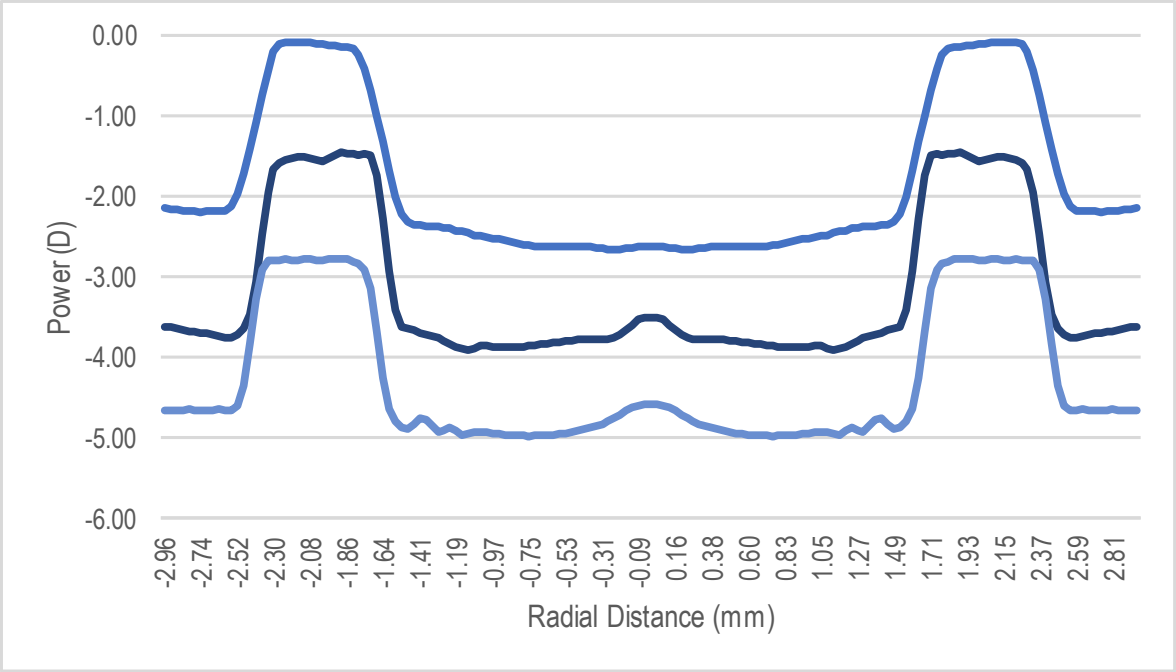

Fig. 9.2.2. *Power profile of the contact lens with the medium diameter for a central distance nominal power of -2.00 D, -3.50 D and -5.00 D.*

Table 9.2.1. *Parameters of each contact lens.*

	Design S	Design M
Inner zone	2.1 mm	4.0 mm
Add power	+2.0 D	+2.0 D
Material	Filcon V3	Filcon V3
Dk	60 units	60 units
Base curve	8.6	8.6
Lens diameter	14.0	14.0

(Where Dk: Permeability; S: Contact lens with the short diameter for central distance ring; M: Contact lens with the medium diameter for central distance ring)

Movement and centration of each fitted contact lens was assessed using a slit-lamp. All measurements were performed 25 minutes after contact lens insertion to allow for contact lens settling. This time was the same for both contact lenses to be

comparable (Kollbaum et al., 2013). A wash-out period of fifteen minutes was established between contact lenses (Sánchez et al., 2018; Martins et al., 2019). At the end of the visit, subjects were asked to choose a preferred contact lens.

Measurements

Over-refraction was assessed as explained in *Chapter 3 General Methodology*. A plano lens was inserted in the case that no over-refraction was needed so that all subjects were measured under the same conditions. After assessing the over-refraction, subjects were asked to wait 25 minutes wearing the over-refraction until the protocol started. This was performed because there were only three powers available.

Subjective quality of vision was assessed using the QoV questionnaire, as explained in *Chapter 3 General Methodology*. General comfort, physical comfort and visual comfort were assessed using continuous visual analogue scales between 0 and 10. Lower scores suggested better comfort. Subjects were first asked for the general comfort, after that they were asked for the physical comfort and finally for the visual comfort: “How do you rate your overall comfort with the lens?” “How do you rate your physical comfort (pain, foreign body sensation, gritty sensation, dryness, itching…) with the lens?” “How do you rate your visual comfort (blurred vision, distortion or halos, glare and flare around lights) with the lens?”

Photopic visual acuity, stereopsis at 40 cm, best-corrected photopic and mesopic contrast sensitivities, light disturbance, aberrations and TFSQ were assessed as

explained in *Chapter 3 General Methodology*. The photopic condition is considered from 3 cd/m^2 and the mesopic one is from 0.01 cd/m^2 until 3 cd/m^2. A dim light was used to manually adjust the light of the room. Photopic and mesopic pupil diameters were measured using the Grand Seiko autorefractometer WAM-5500. Pupil diameter was measured in the contralateral eye while subjects were performing the task using NeurOptics® VIP™-200 Pupillometer (Irvine, California, USA). Room temperature and humidity were remained stable in all visits.

Statistical analysis

SPSS v26.0 for Windows (IBM Corp, Armonk, New York, USA) was used to perform the statistical analysis. Shapiro-Wilk test was used to check the normality distribution of the data. Results were reported as median and interquartile ranges.

Differences between contact lenses in each parameter were evaluated with the paired t-test or Wilcoxon signed-rank test, depending on sample distribution. Differences between baseline and both contact lenses in visual acuity, aberrations and tear film analysis were evaluated using the ANOVA or Friedman test. Post-hoc pairwise comparisons were carried out using Bonferroni correction. P-values < 0.05 were considered statistically significant.

9.2.3. Results

Twenty-eight eyes from 28 subjects (17 females and 11 males) were included in the study, out of which 20 were contact lens wearers. The mean age was 23.5 ± 4.1 years, ranging from 18 to 32 years. Median spherical refraction was -1.00 D

(interquartile range: -2.31 to -0.27 D), while median cylinder was 0.00 D (interquartile range: -0.50 to 0.00 D), respectively.

Eighteen subjects were fitted with a contact lens having distance nominal power of -2.00 D, six with -3.50 D and four with -5.00 D. After lens fitting, the median spherical over-refraction was +1.00 D (interquartile range: +0.50 to +1.25 D) and +1.00 D (interquartile range: +0.56 to +1.25 D) for the small and medium diameter inner optic zones, respectively. Contact lenses had a correct movement, centration and coverage in all subjects.

Visual Acuity, Stereopsis and Contrast Sensitivity

Results obtained at baseline and with each contact lens design, for distance best-corrected visual acuity, stereopsis and best-corrected contrast sensitivity under photopic and mesopic conditions are shown in *Table 9.2.2*. The great majority of subjects (60.7 %) wearing S design achieved a stereopsis of 20 seconds of arc and 39.3 % a stereopsis of 25 seconds of arc. Regarding M design, 50 % of the eyes evaluated achieved stereopsis of 20 seconds of arc, 46.4 % a stereopsis of 25 seconds of arc and 3.6 % a stereopsis of 40 seconds of arc.

Visual acuity slightly decreased with both contact lenses compared to baseline; however, no clinically significant differences were found. No statistically significant differences were found between both dual-focus contact lenses for visual acuity, stereopsis, photopic and mesopic contrast sensitivity, except for photopic contrast

sensitivity at the spatial frequency of 18 cycles per degree ($p < 0.001$), in which contrast sensitivity was higher in the M design.

Contrast sensitivity function pattern followed a normal physiological shape with the highest sensitivity at 3 cycles per degree (*Figure 9.2.3*). Both contact lenses showed similar performance under both photopic and mesopic conditions. Photopic contrast sensitivity curves were inside the normality zone (Ginsburg, 1984) in all spatial frequencies, except for the S design at 6 cycles per degree. However, mesopic contrast sensitivity was below the normality zone for all spatial frequencies with both contact lenses.

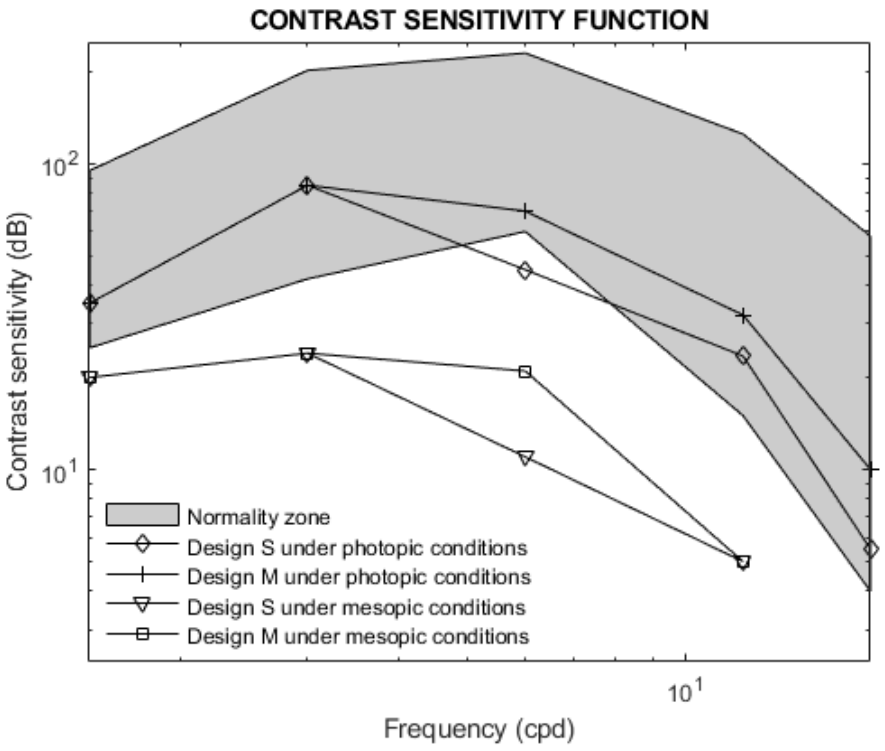

Fig. 9.2.3. *Best-corrected contrast sensitivity function for each contact lens design under photopic and mesopic conditions. Where S: Short central diameter; M: Medium central diameter.*

Table 9.2.2. *Best-corrected distance visual acuity, stereopsis and best-corrected photopic and mesopic contrast sensitivity for each contact lens design.*

Measurement	Condition	Median (Interquartile range)	Significance level (Statistic, p-value)	Post-hoc (p-value)
Best-corrected Distance Visual Acuity (logMAR)	Baseline	-0.10 (-0.20 to -0.10)	$p < 0.001$[1]*	Baseline-S: <0.001[2]*
	S	-0.05 (0.00 to -0.10)		Baseline-M: 0.048[2]*
	M	-0.10 (-0.02 to -0.10)		A-B: 0.326[2]
Stereopsis (seconds of arc)	S	22.0 (20 to 25)	(Z_{27}=1.51, p=0.132)[3]	
	M	22.5 (20 to 25)		
Photopic Contrast Sensitivity 1.5 cpd (dB)	S	35 (35 to 70)	(Z_{27}=-1.14, p=0.252)[3]	
	M	35 (23.75 to 35)		
Photopic Contrast Sensitivity 3 cpd (dB)	S	85 (85 to 170)	(Z_{27}=-1.04, p=0.299)[3]	
	M	85 (54.25 to 170)		
Photopic Contrast Sensitivity 6 cpd (dB)	S	45 (45 to 111.25)	(Z_{27}=1.14, p=0.256)[3]	
	M	70 (45 to 70)		
Photopic Contrast Sensitivity 12 cpd (dB)	S	23.50 (15 to 32)	(Z_{27}=0.79, p=0.433)[3]	
	M	32 (15 to 55)		
Photopic Contrast Sensitivity 18 cpd (dB)	S	5.50 (4 to 10)	(Z_{27}=3.88, p<0.001)[3]*	
	M	10 (10 to 15)		
Mesopic Contrast Sensitivity 1.5 cpd (dB)	S	20 (20 to 20)	(Z_{27}=0.12, p=0.902)[3]	
	M	20 (20 to 20)		
Mesopic Contrast Sensitivity 3 cpd (dB)	S	24 (24 to 44)	(Z_{27}=-0.97, p=0.330)[3]	
	M	24 (24 to 44)		
Mesopic Contrast Sensitivity 6 cpd (dB)	S	11 (6.5 to 21)	(Z_{27}=-1.63, p=0.104)[3]	
	M	21 (11 to 21)		
Mesopic Contrast Sensitivity 12 cpd (dB)	S	5 (0 to 5)	(Z_{27}=0.29, p=0.774)[3]	
	M	5 (5 to 7.25)		
Mesopic Contrast Sensitivity 18 cpd (dB)	S	0 (0 to 4)	(Z_{27}=1.64, p=0.101)[3]	
	M	0 (0 to 4)		

*(Where cpd: cycles per degree; dB: decibel; S: Contact lens with the short diameter for central distance ring; M: Contact lens with the medium diameter for central distance ring; [1]Friedman; [2]Bonferroni; [3]Wilcoxon; *Statistically significant differences)*

The mean pupil diameter under photopic conditions was 4.44 ± 0.43 mm and 4.45 ± 0.42 mm for S and M designs, respectively (t_{27} = -0.96, p = 0.39; T-test); while the mean pupil diameter under mesopic conditions was 6.39 ± 0.38 mm and 6.36 ± 0.35 for S and M designs, respectively (t_{27} = -1.16, p = 0.24; T-test). Pupil diameter was

statistically higher under mesopic than under photopic conditions for the S design (t_{27} = -13.73, p < 0.001; T-test) and M design (t_{27} = -16.92, p < 0.001; T-test).

Light disturbance

Table 9.2.3 shows light distortion results for both contact lens designs. Disturbance area, light distortion index and BFC radius were higher for the S design than for the M design (p ≤ 0.017). Nevertheless, no statistically significant differences between contact lenses were found in the irregularity of the light distortion (BFC irregularity and Standard deviation of BFC irregularity). Mean pupil diameter while subjects were being assessed with LDA was 5.20 ± 0.76 and 5.15 ± 0.79 mm, for S and M designs, respectively (t_{27} = 0.29, p = 0.82; T-test).

Table 9.2.3. *Light disturbance for each contact lens.*

Measurement	Lens	Median (Interquartile range)	Significance level (Statistic, p-value)
Disturbance Area (mm^2)	S	3384 (2396 to 5504)	(Z_{27}=-2.46, p=0.014)[1]*
	M	2744 (1852 to 4148)	
Light Distortion Index (%)	S	16.83 (11.92 to 27.38)	(Z_{27}=-2.44, p=0.015)[1]*
	M	13.65 (9.21 to 20.63)	
Best Fit Circle Radius (mm)	S	33.30 (28.18 to 42.65)	(Z_{27}=-2.39, p=0.017)[1]*
	M	30.00 (24.85 to 36.98)	
Best Fit Circle Irregularity (mm)	S	0.71 (0.37 to 0.98)	(Z_{27}=-0.08, p=0.936)[1]
	M	0.79 (0.34 to 1.03)	
Best Fit Circle Irregularity SD (mm)	S	4.86 (4.06 to 7.65)	(Z_{27}=-1.48, p=0.139)[1]
	M	4.78 (3.15 to 5.95)	

(Where M: Contact lens with the medium diameter for central distance ring; mm: millimetres; S: Contact lens with the short diameter for central distance ring;

*[1]Wilcoxon; *Statistically significant differences)*

Wavefront Aberrations

Table 9.2.4 describes the values for lower-order, higher-order and total aberrations fitted for 3 mm and 5 mm of pupil diameter for all subjects while wearing both contact lenses. Statistically significant differences between conditions (baseline, S design and M design) were found in lower-order and higher-order aberrations. No differences between conditions were found in total aberrations. Post-hoc analysis revealed statistically significant differences between baseline and both designs in lower-order and higher-order aberrations for 3 and 5 mm pupil diameters. Nevertheless, baseline measurements were taken with the naked eye. Moreover, in the measurements with the contact lenses subjects were corrected with a lens with similar power to the refraction of the subject (-2.00 D, -3.50 D or -5.00 D). Thus, lower-order aberrations and total aberrations comparisons were related to the residual refractive error of subjects.

Regarding the comparison of both contact lenses, the M design showed statistically higher levels of higher-order aberrations for 5 mm of pupil diameter compared to the S design. No other statistically significant difference between lenses was found.

Table 9.2.4. *Lower-order, higher-order and total aberrations for a pupil diameter of 3 mm and 5 mm, in each condition.*

Measurement	Condition	Median (Interquartile range)	Significance level (p-value)	Post-hoc (p-value)
Lower-Order 3 mm RMS (µm)	Baseline	0.37 (0.16 to 0.84)	0.045[2]*	Baseline-S: 0.023[3]*
	S	0.30 (0.19 to 0.39)		Baseline-M: 0.738[3]
	M	0.37 (0.27 to 0.50)		S-M: 0.158[3]
Higher-Order 3 mm RMS (µm)	Baseline	0.08 (0.07 to 0.09)	<0.001[1]*	Baseline-S: <0.001[3]*
	S	0.23 (0.19 to 0.25)		Baseline-M: <0.001[3]*
	M	0.22 (0.17 to 0.27)		S-M: 1.00[3]
Total 3mm RMS (µm)	Baseline	0.59 (0.43 to 0.19)	0.482[2]	
	S	0.38 (0.31 to 0.45)		
	M	0.44 (0.32 to 0.52)		
Lower-Order 5 mm RMS (µm)	Baseline	1.34 (0.54 to 2.59)	0.002[2]*	Baseline-S: 0.015[3]*
	S	0.55 (0.36 to 0.81)		Baseline-M: 0.005[3]*
	M	0.42 (0.30 to 0.93)		S-M: 1.00[3]
Higher-Order 5 mm RMS (µm)	Baseline	0.19 (0.15to 0.21)	<0.001[2]*	Baseline-S: 0.001[3]*
	S	0.37 (0.33 to 0.42)		Baseline-M: <0.001[3]*
	M	0.51 (0.44 to 0.54)		S-M: 0.015[3]*
Total 5 mm RMS (µm)	Baseline	1.36 (0.57 to 2.60)	0.065[2]	
	S	0.63 (0.55 to 0.89)		
	M	0.69 (0.60 to 1.05)		

*(Where M: Contact lens with the medium diameter for central distance ring; RMS: Root Mean Square; S: Contact lens with the short diameter for central distance ring; µm: micrometers; [1]ANOVA; [2]Friedman; [3]Bonferroni; *Statistically significant differences)*

Tear film stability

Results of the tear film stability at baseline (pre-corneal tear film stability) and with each contact lens (pre-lens tear film stability) are shown in *Table 9.2.5*. Tear film stability was worse when subjects were wearing both contact lenses (higher TFSQ and TFSQ area, and lower auto Tear Break-Up Time) in comparison with baseline. However, no statistically significant differences were found between contact lenses in the tear

film stability, which suggests that differences in the diameter of the inner zone of the lens do not cause changes in tear film stability.

Table 9.2.5. *Tear Film Surface Quality metrics for each experimental condition.*

Measurement	Condition	Median (Interquartile range)	Significance level (p-value)	Post-hoc (p-value)
Mean TFSQ	Baseline	0.13 (0.08-0.20)	<0.001[1]*	Baseline-S: <0.001[2]*
	S	0.37 (0.26-0.45)		Baseline-M: <0.001[2]*
	M	0.38 (0.31-0.51)		S-M: 0.544[2]
Median TFSQ	Baseline	0.10 (0.07-0.17)	<0.001[1]*	Baseline-S: <0.001[2]*
	S	0.36 (0.23-0.43)		Baseline-M: <0.001[2]*
	M	0.38 (0.32-0.53)		S-M: 0.544[2]
Mean TFSQ Area (%)	Baseline	7.17 (1.44-14.37)	<0.001[1]*	Baseline-S: <0.001[2]*
	S	32.20 (23.84-46.18)		Baseline-M: <0.001[2]*
	M	37.10 (27.20-52.36)		S-M: 1.00[2]
Median TFSQ Area (%)	Baseline	4.10 (0.87-12.85)	<0.001[1]*	Baseline-S: <0.001[2]*
	S	32.90 (21.78-44.75)		Baseline-M: <0.001[2]*
	M	38.45 (25.60-54.08)		S-M: 0.425[2]
Mean Auto Tear Break-Up Time (seconds)	Baseline	7.12 (4.73-11.46)	<0.001[1]*	Baseline-S: <0.001[2]*
	S	2.54 (2.40-2.60)		Baseline-M: <0.001[2]*
	M	2.47 (2.40-2.56)		S-M: 1.00[2]
Median Auto Tear Break-Up Time (seconds)	Baseline	6.89 (4.73-10.74)	<0.001[1]*	Baseline-S: <0.001[2]*
	S	2.50 (2.40-2.60)		Baseline-M: <0.001[2]*
	M	2.50 (2.40-2.60)		S-M: 1.00[2]

*(Where M: Contact lens with an inner zone diameter of 4.0 mm; S: Contact lens with an inner zone diameter of 2.1 mm; TFSQ: Tear Film Surface Quality; [1]Friedman; [2]Bonferroni; *Statistically significant differences)*

Questionnaires

Table 9.2.6 shows the results of the QoV questionnaire. No statistically significant differences were found between contact lenses in QoV values in the frequency, severity and bothersome subscales. *Table 9.2.7* shows the results of the visual

analogue scale questionnaire. Scores did not differ significantly between contact lens designs for overall, physical and visual comfort. Finally, thirteen subjects (46.4 %) preferred the S design, whilst fifteen subjects (53.6 %) preferred the M design.

Table 9.2.6. *Quality of Vision questionnaire scores for each contact lens.*

Measurement	Lens	Median (Interquartile range)	Significance level (Statistic, p-value)
QoV Frequency Score	S	49 (42 to 59)	(Z_{27}=-0.99, p=0.324)[2]
	M	49 (37 to 52)	
QoV Severity Score	S	42 (35 to 48.5)	(Z_{27}=-1.16, p=0.246)[1]
	M	39 (32 to 47)	
QoV Bothersome Score	S	42 (29 to 53)	(t_{27}=0.38, p=0.704)[2]
	M	38 (29 to 49)	

(Where M: Contact lens with an inner zone diameter of 4.0 mm; QoV: Quality of Vision; S: Contact lens with an inner zone diameter of 2.1 mm; [1]T-test; [2]Wilcoxon)

Table 9.2.7. *Visual analogue scale results for each contact lens.*

Measurement	Lens	Median (Interquartile range)	Significance level (Statistic, p-value)	p-value
Overall Comfort Score	S	3.00 (2.00-4.00)	0.31-1.23	0.329[1]
	M	3.50 (2.00-5.00)	1.99-4.24	
Physical Comfort Score	S	3.00 (2.00-4.00)	0.37-1.55	0.887[1]
	M	3.00 (2.00-4.00)	1.20-3.18	
Visual Comfort Score	S	4.00 (3.00-5.75)	0.60-1.94	0.258[1]
	M	4.00 (3.00-4.75)	3.10-4.75	

(Where M: Contact lens with an inner zone diameter of 4.0 mm; S: Contact lens with a inner zone diameter of 2.1 mm; [1]Wilcoxon)

9.2.4. Discussion

To investigate the influence of the inner zone diameter on visual performance, two prototype dual-focus contact lenses designed to reduce myopia progression were

assessed in this study. Dual-focus contact lenses are pupillary-dependent and their performance is influenced by the ratio between distance and add power zones and the area of the pupil exposed to these zones (Martin and Roorda, 2003; De Gracia, Dorronsoro and Marcos, 2013; Montés-Micó et al., 2014; Madrid-Costa et al., 2015; Cardona and López, 2016; Papadatou et al., 2017; Faria-Ribeiro, Amorim-de-Sousa and González-Méijome, 2018; Faria-Ribeiro and González-Méijome, 2019; Monsálvez-Romín et al., 2020; Talens-Estarelles, García-del-Valle and García-Lázaro, 2022). Thus, it has been reported that larger areas made for distance vision tended to affect less the visual and optical quality (Faria-Ribeiro, Amorim-de-Sousa and González-Méijome, 2018; Martins et al., 2019; Monsálvez-Romín et al., 2020; Talens-Estarelles, García-del-Valle and García-Lázaro, 2022). This might be expected since wider central diameters have the add power located further away from the centre of the visual field, which causes less impairment of central vision (Przekoracka et al., 2020). For instance, Faria-Ribeiro, Amorim-de-Sousa and González-Méijome (2018) on a computational study involving 3 different dual-focus lens designs combined with different pupil sizes found that image quality depends on the diameter of the most inner zone of the contact lens.

In the next subsections, the main findings of this work will be discussed and how they relate to current existing knowledge.

Visual Acuity, Stereopsis and Contrast Sensitivity

Although visual acuity was statistically higher in baseline than with both contact lenses, this difference was not clinically significant. Results showed that both contact lenses provided excellent visual acuity and stereopsis. Visual acuity, stereopsis and

contrast sensitivity were similar to the results found in *Chapter 9.1.1* with another dual-focus contact lens (García-Marqués et al., 2020). When fitted with the S design, subjects showed a larger decrease from baseline in visual acuity compared to the M design. However, no statistically significant differences were found between contact lenses in visual acuity and stereopsis. Talens-Estarelles, García-del-Valle and García-Lázaro (2022) and Martins et al. (2019) found better distance visual acuity in contact lenses with larger stabilized areas for distance vision. Moreover, Przekoracka et al. (2020) found that a myopia control contact lens with a central zone of 3 mm, 4.0 D of addition and a polynomial progression zone decreased distance visual acuity in comparison to a contact lens with a central zone of 4.5 mm. However, they did not find this reduction with an addition of 2.0 D. The authors also found that both diameters affected contrast sensitivity in the same amount, which suggests that even medium distance central diameters might impair contrast sensitivity. These results are aligned with the ones found in this study since the lenses of this study had an add power of 2.0 D. Therefore, visual acuity might have been altered if a higher add power had been used, which could be assessed in future studies. However, all of these studies are not directly comparable due to differences in methodology and lenses used.

Photopic contrast sensitivity curves were inside the normality zone (Ginsburg, 1984) in all spatial frequencies except for the S design at 6 cycles per degree. Nevertheless, young subjects were expected to lie at the top of the normality zone. Mesopic contrast sensitivity was outside of the normality zone for all spatial frequencies. Photopic and mesopic contrast sensitivity were not different between designs, except for photopic contrast sensitivity at the spatial frequency of 18 cycles

per degree ($p < 0.001$), in which contrast sensitivity was higher in the M design. This is in accordance with the results found by Martins et al. (2019) and Talens-Estarelles, García-del-Valle and García-Lázaro (2022), who found that subjects fitted with designs having larger inner zone diameters showed better contrast sensitivity at medium and high spatial frequencies.

Different authors have also found lower contrast sensitivity at high spatial frequencies in eyes fitted with multifocal contact lenses (Madrid-Costa et al., 2012; García-Lázaro et al., 2015; Sánchez et al., 2018; Martins et al., 2019; García-Marqués et al., 2020; Przekoracka et al., 2020). Considering that both dual-focus and multifocal contact lenses have zones of power that overcorrects the distant focus, these superimposed out-of-focus images will act as a veiling on the retina and decreasing contrast modulation (Bradley et al., 2014; García-Lázaro et al., 2015; Faria-Ribeiro and González-Méijome, 2019). Therefore, it is expected to find better quality of vision at distance with designs that have higher contribution to the distance focus, offering a lower reduction of distance contrast sensitivity.

Light disturbance

Generally, dual-focus and multifocal contact lenses induce higher levels of light disturbance due to out-of-focus light refracted by the add power zones (Fernandes et al., 2018; Martins et al., 2019; Ruiz-Pomeda et al., 2019; García-Marqués et al., 2020; Monsálvez-Romín et al., 2020). Nonetheless, despite inducing photic phenomena, dual-focus contact lenses are well accepted by children (Chamberlain et al., 2019). Previous studies (Brito et al., 2015; Fernandes et al., 2018; Martins et al., 2019) found

higher light disturbance rates with multifocal contact lenses compared to single-vision contact lenses, which tended to increase with contact lenses having smaller zones for distance vision. Nevertheless, not only is this effect attributable to the inner zone diameter of the lens, but it also depends on several factors such as the ratio of the area for distance and add power zones covered by the pupil, and the add power magnitude itself.

In this study, the size of the light disturbance (disturbance area, light distortion index and BFC radius) was also affected by the design of the lens, being higher for the S design. Nevertheless, the shape of the light disturbance was not affected (BFC irregularity and standard deviation BFC irregularity). These findings are aligned with a previous study (Martins et al., 2019) that found smaller light disturbance in myopia control lenses with larger stabilized areas for distance vision, without differences in the shape of the halo. This might be explained by the fact that lenses with larger stabilized areas for distance vision send a higher percentage of light to the distance focus, reducing the amount of out-of-focus light which is translated in smaller light disturbance and increased contrast modulation. However, the shape of the light disturbance could have remained unaltered between lenses because both lenses have circular rings with the same shape.

Although not directly comparable, the contact lens with the medium inner zone diameter had similar light disturbance to a dual-focus contact lens for myopia control assessed in *Chapter 9.1.1* (García-Marqués et al., 2020). Nevertheless, the design with

the small inner zone diameter had a higher light disturbance in comparison with the results found in that study.

Wavefront Aberrations

In the present study, both contact lenses also induced more higher-order aberrations in comparison with the naked eye condition. This is in agreement with previous studies (Fedtke et al., 2016a; Ji et al., 2018; Martins et al., 2019; Hughes et al., 2020; García-Marqués et al., 2020), which found that dual-focus and multifocal contact lenses induce higher levels of higher-order aberrations (*Chapter 9.1.1)*. This is expected due to the concentric zones of increased power.

The design with the medium inner zone diameter showed higher levels of higher-order aberrations for a 5 mm pupil diameter compared to the design with a small inner zone diameter. This does not seem to correlate with light disturbance findings found in this study, were subjects fitted with the M design reported smaller light disturbances compared to the S design.

The highest aberrations obtained in the contact lens with the medium central zone diameter might be explained by the fact that in this design the variation of the power is more progressive than in the S design, in which is more abrupt. In opposition to these findings, Martins et al. (2019) found lower high-order aberrations in lenses with larger stabilized areas for distance vision. Moreover, it has also been reported that the image quality of contact lenses with a large central diameters is less affected by spherical aberration (Faria-Ribeiro, Amorim-de-Sousa and González-Méijome, 2018).

However, all of these studies used other methodological procedures and other contact lenses, which make them not directly comparable.

Higher-order aberrations in the present study were also similar to those found in *Chapter 9.1.1* (García-Marqués et al., 2020) with another myopia control contact lens. Besides, higher-order aberrations in the contact lens with the S design of this study (2.1 mm) are also lower than those found in this previous study with a contact lens with a larger central diameter (3.36 mm), which might be aligned with the results found in the present work.

It is worth noting that due to the abrupt changes in the power profiles of both designs, these wavefronts might not be well represented with a Zernike expansion (McAlinden, McCartney and Moore, 2011). This might limit some of the conclusions stated above based on the magnitude of the Zernike coefficients obtained from wavefront reconstruction.

Tear film stability

When a contact lens is fitted in the eye, it splits the tear film into two layers, which destabilizes the tear film (Korb, Greiner and Glonek, 1996; Wolffsohn et al., 2017; García-Marqués et al., 2021b). Different studies (Nichols and Sinnott, 2006; Szczesna-Iskander, 2018; García-Montero et al., 2019c; Lafosse et al., 2019; Lorente-Velázquez et al., 2019; García-Marqués et al., 2021b) found a decrease in pre-lens tear film stability, lower tear meniscus height, and higher osmolarity during contact lens wear, especially for high water content contact lenses. As expected, in the present study, both contact lenses decreased the stability of the tear film in comparison to the naked

eye. However, tear film stability did not show differences between contact lenses, suggesting that changes in the diameter of the zones of dual-focus contact lenses do not affect pre-lens tear film spreading and stability across the contact lens surface.

To my knowledge, only a previous study measured the pre-lens tear film stability in a dual-focus contact lens (*Chapter 9.1.1*) (García-Marqués et al., 2021b). Authors found worse tear film stability in a dual-focus contact lens in comparison to a single-vision contact lens made of the same material. This might be caused due to a worse spreading of pre-lens tear film across the concentric ring pattern. Thus, the increased tear film stability together with the worse optical and visual quality might deteriorate even more the visual performance in dual-focus contact lenses. In comparison with this previous study, tear film stability was similar or slightly better in the contact lenses assessed in this work, but again results are not directly comparable due to differences in methodology and lenses used.

The present study assessed the short-term tear film stability 25 minutes after lens insertion. Thus, tear film stability might change after longer periods of contact lens wear. Nevertheless, different studies found that this period is adequate to evaluate the short-term performance of contact lenses (Efron et al., 1987; Brennan et al., 1990; Nichols and King-Smith, 2003; Paugh et al., 2021). They found that the tear film changes in the first twenty minutes after insertion. Efron et al. (1987) reported that the majority of lens dehydration takes place in the first 5 minutes. However, other authors claimed that tear film changes over the first 30 minutes (Little and Bruce, 1994; Nichols and King-Smith, 2004). Therefore, there is still controversy on this topic.

This fact is not expected to alter the comparison between contact lenses since both were assessed after the same time and wash-out period. Furthermore, randomness in lens fitting avoids bias. It is also important to comment that Medmont might be too sensitive in assessing tear film changes over a dual-focus contact lens and it could have detected changes non-related with the tear film.

Questionnaires

Pre-lens tear film plays a key role in physical and visual comfort since it lubricates the ocular surface and the front surface of the contact lens. Moreover, it provides a smooth optical surface and avoids friction between lids and the contact lens (Dumbleton et al., 2013b). Different studies have found increased symptoms during multifocal and dual-focus contact lens wear (for instance, it was found in *Chapter 9.1*) (Fedtke et al., 2016a; Kang, McAlinden and Wildsoet, 2016; Wahl et al., 2018; García-Marqués et al., 2020; García-Marqués et al., 2021b). In the present study, no statistically significant differences were found in the QoV scores between contact lenses. This suggests that despite the contact with the short central diameter inducing more light disturbance and lower contrast sensitivity at higher frequencies, subjective visual comfort is not affected. In comparison with two previous studies (*Chapter 9.1.1* and *Chapter 9.1.2*) (García-Marqués et al., 2020; García-Marqués et al., 2021b) with another dual-focus contact lens for myopia control called MiSight, QoV scores, overall and physical comfort scores were similar, but visual comfort was worse in the present study.

Moreover, the present study assessed the short-term effect of the contact lenses on visual quality, optical quality, light distortion and comfort. Therefore, binocular summation and the process of neuroadaptation might improve these values in a longer follow-up (Kang, McAlinden and Wildsoet, 2016; Fernandes et al., 2018; Lopes-Ferreira et al., 2018; Ruiz-Pomeda et al., 2019). Thus, this study represents the less optimistic view of the performance of these dual-focus contact lenses. Nevertheless, the reported results are still relevant for comparison purposes. These results might also be applied to presbyopic subjects, due to the similarities between dual-focus contact lenses and multifocal contact lenses.

Apart from the limitations above commented, the present study has also other limitations to be considered. Tests used in this study challenges the visual system since they are performed in dim light or glare conditions, which is not a typical condition in children. This might underestimate the visual performance of dual-focus contact lenses under normal conditions in children. Besides, prior history of contact lens wear was not taken into account and some of them were new contact lens wearers, which could have underestimated the visual and physical comfort of the contact lenses. Moreover, only the quality of vision in distance was assessed. Future research should include the analysis of visual performance in near distances. Finally, the study was performed in a young adult sample with high visual and comfort demands, who might not be representative of children. Young adults were assessed because some tasks were challenging and the protocol was long so that they could respond accurately (Sha et al., 2018). These aspects are not expected to alter the findings significantly.

Overall, this comprehensive evaluation of the optical and visual performance contributes to further improve the dual-focus lens design to provide the best visual performance. The present study might help clinicians to adjust the design of the lens depending on patients' necessities to improve their adherence and satisfaction with the dual-focus contact lenses. Both contact lenses provided acceptable visual performance under photopic conditions. Nevertheless, both contact lenses decreased tear film stability, and induced higher levels of higher-order aberrations in the short-term in comparison with the naked eye. The lens with a medium central inner zone provided better photopic contrast sensitivity in high spatial frequencies and induced less size of light disturbance. However, the lens with the short central zone diameter induced less higher-order aberrations with a pupil diameter of 5 mm. Despite differences between lenses in visual quality, no differences in visual comfort were found between lens designs, which suggest that both diameters caused the same subjective quality of vision in subjects. No differences were found between designs in visual acuity, stereopsis, mesopic contrast sensitivity, light disturbance shape, higher-order aberrations at 3 mm of pupil diameter and tear film stability. Further studies are needed to assess the effect on the visual performance of dual-focus contact lenses with bilaterally visual performance evaluation in a dispensing study with longer follow-up time. Other paths to deepen the knowledge in this field will eventually require the use of other lens designs, different materials different pupil size conditions or investigating the effects under different lighting and viewing distance conditions.

CHAPTER 9.3: The influence of blinking, artificial tears and contact lenses on light disturbance, tear film stability and corneal aberrations

9.3 THE INFLUENCE OF BLINKING, ARTIFICIAL TEARS AND CONTACT LENSES ON LIGHT DISTURBANCE, TEAR FILM STABILITY AND CORNEAL ABERRATIONS

In previous chapters (*Chapters 9.1.1 and 9.1.2*), it has been found that dual-focus contact lenses cause lower visual quality, lower tear film stability and higher light disturbance in comparison with a single-vision contact lens. It was reported that the lower tear film stability could increase even more the light disturbance in dual-focus contact lenses but it was not demonstrated. The present chapter goes one step further by assessing the light disturbance related to changes in the tear film stability parameters to validate the LDA device as a reliable and useful tool to assess the optical quality-related changes induced by the tear film. Thus, light disturbance, tear film stability and corneal aberrations were evaluated under different conditions: Different blinking patterns, with and without artificial tears, and with a single-vision and a dual-focus contact lens.

9.3.1. Introduction

As explained in *Chapter 1 Introduction*, the tear film plays a vital role in maintaining a regular optical surface and clear vision because it is the outermost refractive surface of the eye due to the high difference in the refractive index between the tear film and air (Montés-Micó et al., 2010a; Denoyer, Rabut and Baudouin, 2012; Kottaiyan et al., 2012; Ring et al., 2015; Willcox et al., 2017). In this way, variations in tear film regularity or thickness will induce ocular aberrations that could degrade the optical quality of the eye (Tutt et al., 2000). It has been reported that this optical

deterioration impacts negatively the visual symptoms and may induce a reduction in quality of life because of driving difficulties, visual fluctuations, difficulties using computers, psychological problems and loss of productivity (Benítez-del-Castillo et al., 2017). Therefore, assessing the optical quality might help to understand better the symptoms that subjects with dry eye symptoms experience.

It has been previously reported that some conditions such as low blinking frequency or contact lens wear can alter the tear film stability and consequently affect the optical quality of the eye (Ferrer-Blasco et al., 2009; Denoyer, Rabut and Baudouin, 2012; Willcox et al., 2017; Talens-Estarelles et al., 2020; Talens-Estarelles et al., 2021a). Thus, tear film instability is reported to increase the corneal higher-order aberrations after a blink (Ferrer-Blasco et al., 2009). Moreover, it has also been claimed that the instillation of artificial tears can decrease corneal higher-order aberrations, improving the optical quality of the eye (Montés-Micó et al., 2010b).

Several authors have reported that DED patients have higher levels of aberrations, light scatter and low optical quality than healthy patients (Montés-Micó et al., 2010b; Denoyer, Rabut and Baudouin, 2012; Kottaiyan et al., 2012; Lin and Yiu, 2014; Ring et al., 2015; Koh, Higashiura and Maeda, 2016; Chan et al., 2017). Thus, optical quality assessment has become a tool to indirectly detect and monitor DED in an objective and non-invasive way, which has the advantage of assessing the tear film stability in real time (McGinnigle, Eperjesi and Naroo, 2014; Tan et al., 2015a; Wolffsohn et al., 2017). Although ocular scatter index is a measurement done regularly in subjects with dry eye, no data is currently available regarding light disturbance for these subjects.

The LDA, which was explained in *Chapter 3 General Methodology*, might be used as an alternative to assess the optical quality-related changes induced by the tear film. Indeed, the TFOS DEWS II Diagnostic Methodology Report recognized the need of developing new non-invasive metrics to assess the tear film (Wolffsohn et al., 2017). Several questionnaires are currently used to assess visual discomfort (Wolffsohn et al., 2017). Thus, the development of new metrics to assess the optical quality in a standardized way might help in the diagnosis and management of DED, understanding in a better way optical quality symptoms reported by patients.

The primary aim of this study was to assess the light disturbance related to changes in the tear film stability parameters to validate the LDA device as a reliable and useful tool to assess the optical quality-related changes induced by the tear film. To evaluate this, light disturbance, tear film stability and corneal aberrations were assessed under different conditions: Different blinking patterns (natural, optimal blinking and delayed blinking), with and without artificial tears, and with two contact lenses (a single-vision and a dual-focus contact lens).

9.3.2. Methodology

A total of 40 healthy myopic volunteers between 19 and 38 years with astigmatism of ≤ 0.75 D (Kollbaum et al., 2013) were included in this randomized, double-masked, crossover study. The inclusion criteria were subjects with a best-corrected visual acuity ≤ 0.00 logMAR in each eye. Prior contact lens wear was not considered. Contact lens wearers were instructed not to wear their contact lenses within a week before the examination. Subjects with any ocular disease or taking any

medication that contraindicates or interferes with the use of contact lenses were excluded from the study. Written consent was obtained from each subject after an explanation of the purpose and study protocol. The study procedures were approved by the Ethics Committee of the University of Minho and were carried following the tenets of the Declaration of Helsinki.

Both eyes were fitted with contact lenses to guarantee the normal and binocular visual conditions, but only the sensorial dominant eye for distance vision was measured to avoid duplication of data. Sensorial dominance was assessed using the "+1.50 blur" method (Lopes-Ferreira et al., 2013; Fernandes et al., 2018). The daylight was removed using black-out curtains. Luminance and illuminance were controlled using a luminance meter (Konica Minolta LS-100 Sensing Americas Inc, Ramsey, NJ, USA) and an illuminance meter (*T10, Minolta* Sensing Inc, Tokyo, Japan), respectively. The illuminance was 255.58 ± 8.19 lux and 3.48 ± 0.12 lux for photopic and mesopic conditions, respectively. The mean luminance was 203.17 ± 3.85 cd/m^2 for the measurement of best-corrected visual acuity.

Subjects completed two visits. Visit 1: Baseline measurements and measurements with the naked eye; Visit 2: Measurements with single-vision and dual-focus contact lenses. During the first visit, inclusion and exclusion criteria were checked and baseline measurements with the naked eye were obtained without and with artificial tears instillation and with different blinking rates. Temperature and humidity of the room were also controlled to ensure that they were constant in all visits.

Contact lenses

In the second visit, subjects were fitted with contact lenses according to the manufacturer's fitting guidelines for the initial lens selection. The single-vision was the Proclear 1-day® contact lens (CooperVision, Inc., Pleasanton, CA) and the dual-focus was the MiSight® (CooperVision, Inc., Pleasanton, CA). Lenses were fitted in a random order. Both contact lenses were made of Omafilcon A (60% water content, non-ionic). Thus, material influence on tear film stability such as wettability, water content or dehydration was minimized. Base curve (8.7 mm) and lens diameter (14.2 mm) were also the same in both contact lenses. In this way, the only difference between contact lenses was the optical design. The dual-focus contact lens consisted of an 11.66 mm optic zone with four alternating zones for distance and near vision surrounding a central diameter of 3.36 mm for distance vision (Chamberlain et al., 2019; Ruiz-Pomeda et al., 2019). It has a 2 D maximum add power, which provides a second focus in front of the retina (Ruiz-Pomeda et al., 2018b).

Lens fitting

After the insertion of the lens, the movement, centration and coverage of both contact lenses were assessed with a slit-lamp. Measurements were performed twenty-five minutes after lens insertion to provide proper contact lens stabilization. Previous studies have confirmed that this period is adequate to assess the short-term performance of contact lenses (Paugh et al., 2001; Foulks et al., 2013). This time was maintained constant for both contact lenses in both subjects so that results were

comparable. A wash-out period of 15 minutes was established between contact lens fittings (Sánchez et al., 2018; Martins et al., 2019).

Measurement conditions

Light disturbance, tear film stability and corneal aberrations were assessed under different conditions to evaluate the effect of different blinking patterns (natural blinking, optimal blinking and delayed blinking), artificial tears and contact lenses on these metrics. *Table 9.3.1* shows a summary of the measurements performed. In visit 1, light disturbance, tear film stability and corneal aberrations were assessed with and without artificial tears for each blinking pattern (natural blinking, blinking every 6 seconds and blinking every 12 seconds) while light disturbance was being measured. These values were chosen as previous studies used these blinking frequencies (Montés-Micó et al., 2004; Montés-Micó, Alió and Charman, 2005b; Ferrer-Blasco et al., 2009; Koh et al., 2010; Willcox et al., 2017; García-Montero et al., 2019c; Xi, Qin and Bao, 2019). Moreover, the frequency of 6 seconds per blink was chosen as it was previously reported that this was the optimal blinking frequency in which the best optical quality was achieved after blinking (Zaman, Doughty and Button, 1998; Doughty, 2001; Montés-Micó, Alió and Charman, 2005b; Ferrer-Blasco et al., 2009; Wolffsohn et al., 2017). Moreover, for the delayed blinking (12 seconds) a time higher than 10 seconds was chosen since this is the cut-off value for DED reported by the TFOS DEWS II Diagnostic Methodology Report (Wolffsohn et al., 2017). Thus, the double of the optimal blinking frequency was chosen as the delayed blinking frequency.

In the natural blinking pattern, subjects were instructed to blink whenever they want while they were performing the LDA task. In the monitored blinking patterns (every 6 and 12 seconds), the examiner listened to a periodic beep through earphones and instructed subjects to blink while they were performing the LDA task. Subjects were instructed to only blink when the examiner tells them. After LDA measurement, tear film stability and corneal aberrations were measured using Medmont and a wash-out period of 3 minutes was established between measurements. Blinking patterns were measured in a random order to avoid bias. During the natural blinking, the number of blinks performed in 30 seconds was recorded by the examiner.

After assessing the ocular surface parameters in each blinking condition without artificial tears, measurements were repeated with artificial tears. One drop of Systane® Ultra (Alcon SL, Geneva, Switzerland) single-dose artificial tears was instilled on each eye, 2 minutes before the assessment of LDA in each condition. Two minutes were allowed to artificial tears stabilizing across the ocular surface, avoiding optical quality interferences (Jones et al., 2017; Talens-Estarelles et al., 2020).

In the second visit, the protocol was repeated with each contact lens fitted in random order. However, to shorten the protocol time, only the natural blinking pattern was assessed with artificial tears. The ocular protection index was calculated for each condition as:

$$\text{Ocular protection index} = \frac{Tear\ Film\ Break{-}Up\ Time}{Interblink\ Interval}$$

Thus, an ocular protection index > 1 indicates that the ocular surface is protected, and an ocular protection index < 1 means that the ocular surface is unprotected because the interblink interval is higher than the break-up time (Ousler et al., 2008).

Table 9.3.1. *Summary of the protocol of the study.*

Visit 1		Visit 2 (random order)			
Naked eye		Single-vision contact lens		Dual-focus contact lens	
Without artificial tears	With artificial tears	Without artificial tears	With artificial tears	Without artificial tears	With artificial tears
• Case history • Refraction • Photopic and mesopic pupil diameter • Best-corrected visual acuity • Sensorial dominance		• Overrefraction • Photopic and mesopic pupil diameter • Best-corrected visual acuity		• Overrefraction • Photopic and mesopic pupil diameter • Best-corrected visual acuity	
• Light disturbance • TFSQ • Corneal aberrations (Natural blinking, optimal blinking and delayed blinking, random order)	• Light disturbance • TFSQ • Corneal aberrations (Natural blinking, optimal blinking and delayed blinking, random order)	• Light disturbance • TFSQ • Corneal aberrations (Natural blinking, optimal blinking and delayed blinking, random order)	• Light disturbance • TFSQ • Corneal aberrations (Natural blinking)	• Light disturbance • TFSQ • Corneal aberrations (Natural blinking, optimal blinking and delayed blinking, random order)	• Light disturbance • TFSQ • Corneal aberrations (Natural blinking)

(Where TFSQ: Tear Film Surface Quality)

Protocol

In the first visit, measurements were performed in the following order: Case history, refraction with trial lenses, best-corrected distance visual acuity, sensorial dominance, LDA with each condition and using trial lenses, and pre-corneal tear film

stability assessment (without contact lens) and corneal aberrations with each condition were recorded.

Refraction was objectively measured with the open-field autorefractor Grand Seiko Autorefractometer WAM-5500 (Grand Seiko Co., Ltd., Hiroshima, Japan). It was subjectively adjusted using the end-point criterion of maximum plus for the best visual acuity (Ferreira-Neves et al., 2015). Refraction was used to choose the power of the contact lenses. Distance best-corrected photopic visual acuity, light disturbance, TFSQ and corneal aberrations were assessed as explained in *Chapter 3 General Methodology*. Pupil diameter was measured under photopic and mesopic conditions using the Grand Seiko Autorefractometer WAM-5500.

The second visit was performed 1 week after the first one, the same day of the week and at the same hour. Contact lenses were fitted binocularly in random order. For both contact lenses, over-refraction with trial lenses, best-corrected visual acuity, light disturbance assessment for each condition (LDA) and pre-lens tear film stability assessment (Medmont) and pre-lens aberrations for each condition (Medmont) were assessed. Over-refraction was also assessed with the open-field autorefractor and subjectively adjusted with spheres. In the case that no over-refraction was needed, a plano lens was inserted to perform LDA so that all subjects were assessed under the same conditions. Once the protocol was completed for the first contact lens in situ, contact lens was then removed and a 15 minute washout period was allowed before fitting the second lens design (Sánchez et al., 2018; Martins et al., 2019).

Statistical analysis

Statistical analysis was performed using SPSS v26.0 for Windows (IBM Corp, Armonk, New York, USA). Results were reported as median and interquartile ranges. Normality distribution was checked using the Shapiro-Wilk test. Differences between blinking patterns (natural blinking, optimal blinking and delayed blinking) and differences between the naked eye and both contact lenses were assessed with repeated ANOVA or Friedman test, depending on sample distribution. Bonferroni test with the correction for multiple testing was used to evaluate differences between all pair group combinations. Moreover, differences between pre and post artificial tears instillation were assessed by means of the paired t-test or Wilcoxon signed-rank test, depending on sample distribution. A p-value less than 0.05 was defined as statistically significant.

9.3.3. Results

Forty eyes from 40 subjects were included in this study, out of which 23 were females (57.5 %) and 17 males (42.5 %). The mean age was 26.6 ± 5.1 years, ranging from 19 to 38 years. Median sphere and cylinder were -1.00 D (interquartile range: -2.06 to -0.36 D) and 0.00 D (interquartile range: -0.50 to 0.00 D), respectively.

After lens fitting, median sphere over-refraction was 0.25 D (interquartile range: 0.00 to 0.50 D) and 0.25 D (interquartile range: 0.00 to 0.50 D) for single-vision and dual-focus contact lenses, respectively. LogMAR best-corrected visual acuity with the naked eye was -0.10 (-0.12 to -0.10) and visual acuity with the contact lenses and over-

refraction was -0.10 (-0.14 to -0.09) and -0.10 (-0.12 to -0.04) for single-vision and dual-focus lenses, respectively. Wilcoxon signed-rank test did not reveal statistically significant differences in best-corrected visual acuity between conditions ($p = 0.101$). *Table 9.3.2* summarizes the main results obtained for each condition.

Differences between blinking patterns

Table 9.3.3 shows the statistical comparison between blinking patterns (natural blinking, optimal blinking and delayed blinking) for tear film stability metrics, light disturbance and corneal aberrations, without and with artificial tears, respectively.

Regarding the naked eye condition, no differences were found in blinking frequency between natural blinking (median 4.5 blinks per 30 seconds) and blinking every 6 seconds (5 blinks per 30 seconds). Blinking every 12 seconds showed statistically less blinking frequency than the other conditions (2.5 blinks per 30 seconds). Despite this, it did not cause differences in tear film stability, light disturbance and corneal aberrations when measured without contact lenses.

There were no statistically significant changes for tear film and corneal aberrations outcomes between single-vision and dual-focus contact lenses for the different blinking frequencies. Nevertheless, when subjects blinked with less frequency (every 12 seconds) the size and shape of the light disturbance increased in both contact lenses.

Table 9.3.2. *Metrics obtained for each condition.*

Parameters	Condition	WITHOUT ARTIFICIAL TEARS Median (Interquartile range)			WITH ARTIFICIAL TEARS Median (Interquartile range)		
		Natural blinking	6 seconds	12 seconds	Natural blinking	6 seconds	12 seconds
TFSQ	Naked	0.10 (0.08 to 0.21)	0.10 (0.08 to 0.19)	0.10 (0.07 to 0.16)	0.09 (0.06 to 0.14)	0.09 (0.07 to 0.16)	0.09 (0.06 to 0.14)
	Single-vision	0.24 (0.17 to 0.30)	0.19 (0.13 to 0.0.29)	0.22 (0.14 to 0.30)	0.13 (0.09 to 0.0.17)		
	Dual-focus	0.33 (0.26 to 0.44)	0.35 (0.25 to 0.43)	0.33 (0.21 to 0.42)	0.18 (0.15 to 0.23)		
TFSQ area (%)	Naked	2.25 (0.85 to 15.72)	3.15 (1.22 to 12.05)	3.75 (0.50 to 9.78)	2.65 (0.45 to 8.20)	2.40 (0.80 to 8.95)	1.60 (0.63 to 7.53)
	Single-vision	18.60 (10.00 to 26.82)	13.80 (6.47 to 27.27)	17.60 (9.13 to 28.63)	8.00 (1.72 to 14.05)		
	Dual-focus	34.10 (23.22 to 42.57)	31.40 (22.57 to 42.45)	3080 (16.70 to 41.90)	12.50 (8.00 to 21.15)		
Auto Tear Break-Up Time (seconds)	Naked	16.54 (5.9 to 30.0)	13.05 (5.23 to 30.0)	12.70 (4.62 to 30.0)	20.90 (6.78 to 30.00)	20.80 (5.85 to 30.00)	24.00 (12.10 to 30.00)
	Single-vision	5.55 (2.88 to 9.75)	5.10 (2.65 to 10.00)	5.20 (2.40 to 11.45)	14.35 (4.70 to 29.80)		
	Dual-focus	2.50 (2.30 to 2.60)	2.40 (2.30 to 2.57)	2.40 (2.30 to 2.60)	2.50 (2.40 to 5.40)		
Light Distortion Index (%)	Naked	6.25 (3.90 to 9.43)	3.72 (4.46 to 9.39)	6.45 (4.54 to 9.13)	5.49 (3.82 to 8.83)	5.77 (4.46 to 9.03)	5.33 (4.14 to 8.47)
	Single-vision	6.21 (4.14 to 8.57)	6.80 (4.46 to 8.30)	10.35 (6.27 to 15.10)	5.05 (3.90 to 8.47)		
	Dual-focus	15.16 (10.35 to 18.52)	15.40 (10.07 to 18.14)	19.10 (12.54 to 24.79)	12.65 (8.71 to 16.19)		
Best Fit Circle Irregularity (mm)	Naked	0.26 (0.01 to 0.50)	0.30 (0.06 to 0.54)	0.32 (0.14 to 0.48)	0.25 (0.01 to 0.46)	0.26 (0.02 to 0.46)	0.32 (0.10 to 0.45)
	Single-vision	0.32 (0.09 to 0.70)	0.42 (0.14 to 0.52)	0.45 (0.31 to 0.66)	0.30 (0.06 to 0.56)		
	Dual-focus	0.45 (0.16 to 1.10)	0.45 (0.16 to 0.91)	0.58 (0.28 to 1.38)	0.53 (0.26 to 1.24)		
Best Fit Circle Irregularity SD (mm)	Naked	3.09 (0.53 to 3.77)	3.38 (2.75 to 4.02)	3.57 (2.14 to 4.00)	3.09 (0.54 to 3.99)	2.99 (2.14 to 4.01)	3.01 (2.14 to 3.91)
	Single-vision	3.51 (2.14 to 3.93)	3.32 (2.25 to 3.84)	4.11 (3.36 to 5.64)	2.96 (2.14 to 3.72)		
	Dual-focus	3.97 (3.48 to 5.79)	3.77 (3.30 to 4.82)	5.60 (3.90 to 6.64)	3.72 (3.21 to 4.87)		
Blinks in 30 seconds	Naked	4.5 (2.0 to 7.0)	5.0 (5.0 to 5.0)	2.5 (2.5 to 2.5)	4.5 (2.0 to 8.0)	5.0 (5.0 to 5.0)	2.5 (2.5 to 2.5)
	Single-vision	4.0 (2.0 to 9.0)	5.0 (5.0 to 5.0)	2.5 (2.5 to 2.5)	6.0 (3.0 to 9.7)		
	Dual-focus	6.0 (3.0 to 11.0)	5.0 (5.0 to 5.0)	2.5 (2.5 to 2.5)	4.0 (3.0 to 10.75)		

(continuation)							
Parameters	Condition	WITHOUT ARTIFICIAL TEARS Median (Interquartile range)			WITH ARTIFICIAL TEARS Median (Interquartile range)		
		Natural blinking	6 seconds	12 seconds	Natural blinking	6 seconds	12 seconds
Ocular Protection Index	Naked	1.80 (1.00 to 4.00)	2.17 (0.93 to 5.00)	1.10 (0.83 to 2.00)	2.00 (1.00 to 5.00)	3.47 (0.98 to 5.00)	2.00 (1.01 to 2.50)
	Single-vision	1.14 (0.69 to 2.13)	0.93 (0.47 to 1.47)	0.45 (0.19 to 0.85)			
	Dual-focus	0.69 (0.38 to 1.04)	0.40 (0.38 to 0.43)	0.20 (0.19 to 0.22)			
Higher-order aberrations (µm)	Naked	-0.01 (-0.03 to 0.03)	-0.02 (-0.04 to 0.01)	-0.01 (-0.03 to 0.01)	-0.01 (-0.05 to 0.01)	-0.01 (-0.03 to 0.01)	-0.01 (-0.04 to 0.01)
	Single-vision	-0.01 (-0.03 to 0.01)	-0.01 (-0.04 to 0.02)	0.01 (-0.02 to 0.02)	-0.01 (-0.04 to 0.01)		
	Dual-focus	-0.01 (-0.06 to 0.08)	0.01 (-0.03 to 0.05)	0.01 (-0.05 to 0.05)	-0.01 (-0.07 to 0.09)		
Spherical aberration (0,4) (µm)	Naked	-0.021 (-0.036 to -0.007)	-0.017 (-0.033 to -0.001)	-0.020 (-0.041 to -0.006)	-0.022 (-0.035 to -0.005)	-0.014 (-0.031 to -0.007)	-0.018 (-0.031 to -0.007)
	Single-vision	-0.018 (-0.032 to -0.004)	-0.016 (-0.040 to -0.004)	-0.022 (-0.034 to -0.001)	-0.017 (-0.036 to -0.003)		
	Dual-focus	-0.008 (-0.051 to 0.032)	0.001 (-0.020 to 0.033)	-0.016 (-0.060 to 0.031)	-0.007 (-0.047 to 0.025)		
Horizontal coma (1,3) (µm)	Naked	0.005 (-0.021 to 0.017)	0.003 (-0.017 to 0.021)	-0.004 (-0.016 to 0.015)	0.001 (-0.022 to 0.016)	-0.003 (-0.017 to 0.016)	-0.001 (-0.015 to 0.020)
	Single-vision	-0.002 (-0.011 to 0.011)	-0.003 (-0.020 to 0.015)	0.004 (-0.017 to 0.016)	0.006 (-0.014 to 0.015)		
	Dual-focus	-0.006 (-0.048 to 0.034)	-0.017 (-0.045 to 0.026)	0.004 (-0.043 to 0.050)	0.012 (-0.035 to 0.064)		
Vertical coma (-1,3) (µm)	Naked	-0.003 (-0.026 to 0.015)	-0.008 (-0.047 to 0.015)	-0.005 (-0.038 to 0.016)	-0.005 (-0.042 to 0.012)	0.003 (-0.011 to 0.011)	0.001 (-0.026 to 0.029)
	Single-vision	-0.009 (-0.019 to 0.017)	0.001 (-0.031 to 0.018)	-0.009 (-0.029 to 0.009)	0.002 (-0.022 to 0.016)		
	Dual-focus	0.024 (-0.046 to 0.086)	0.014 (-0.007 to 0.098)	-0.004 (-0.068 to 0.041)	0.007 (-0.048 to 0.031)		

(Where SD: Standard Deviation; TFSQ: Tear Film Surface Quality)

Changes after the instillation of artificial tears

Table 9.3.4 shows the differences in results after artificial tears instillation for all conditions. Regarding naked eye (no lens) outcomes, no statistically significant differences were found in any parameter for natural blinking and 6 seconds interval blinking. However, there was an increase in the mean auto Tear Break-Up Time and a

decrease in the size of the light disturbance after the instillation of artificial tears for the 12 seconds interval blinking condition. No statistically significant differences were found in the irregularity of the light disturbance, the number of blinks per 30 seconds and corneal aberrations.

Regarding single-vision and dual-focus contact lenses with natural blinking, after artificial tears instillation tear film stability increased (lower TFSQ and TFSQ area and higher auto Tear Break-Up Time) and the size of the light disturbance decreased in both contact lenses evaluated. Moreover, BFC Irregularity of the light disturbance also decreased in the dual-focus contact lens after the instillation of artificial tears. No differences were found for the other parameters.

Table 9.3.3. *Comparison between blinking patterns for each metric.*

Parameters	Condition	WITHOUT ARTIFICIAL TEARS		WITH ARTIFICIAL TEARS	
		p-value between blinking patterns	Post-hoc (Adjusted p-value)	p-value between blinking patterns	Post-hoc (Adjusted p-value)
TFSQ	Naked	0.608[2]		0.694[2]	
	Single-vision	0.249[1]			
	Dual-focus	0.118[1]			
TFSQ area (%)	Naked	0.490[2]		0.313[2]	
	Single-vision	0.426[2]			
	Dual-focus	0.362[1]			
Auto Tear Break-Up Time (seconds)	Naked	0.785[2]		0.659[2]	
	Single-vision	0.953[2]			
	Dual-focus	0.258[2]			
Light Distortion Index (%)	Naked	0.156[2]		0.167[2]	
	Single-vision	<0.001[2]*	Natural-6 seconds: 0.502[3] Natural-12 seconds: <0.001[3]* 6 seconds-12 seconds: <0.001[3]*		
	Dual-focus	<0.001[2]*	Natural-6 seconds: 0.911[3] Natural-12 seconds: 0.001[3]* 6 seconds-12 seconds: 0.001[3]*		
Best Fit Circle Irregularity (mm)	Naked	0.582[2]		0.639[2]	
	Single-vision	0.547[2]			
	Dual-focus	0.040[2]*	Natural-6 seconds: 0.911[3] Natural-12 seconds: 0.034[3]* 6 seconds-12 seconds: 0.025[3]*		
Best Fit Circle Irregularity SD (mm)	Naked	0.075[2]		0.950[2]	
	Single-vision	0.010[2]*	Natural-6 seconds: 0.696[3] Natural-12 seconds: 0.003[3]* 6 seconds-12 seconds: 0.011[3]*		
	Dual-focus	<0.001[2]*	Natural-6 seconds: 0.281[3] Natural-12 seconds: 0.029[3]* 6 seconds-12 seconds: <0.011[3]*		
Blinks in 30 seconds	Naked	<0.001[2]*	Natural-6 seconds: 0.172[3] Natural-12 seconds: 0.002[3]* 6 seconds-12 seconds: <0.001[3]*	<0.001[2]*	Natural-6 seconds: 0.057[3] Natural-12 seconds: 0.008[3]* 6 seconds-12 seconds: <0.001[3]*
	Single-vision	<0.001[2]*	Natural-6 seconds: 0.281[3] Natural-12 seconds: 0.001[3]* 6 seconds-12 seconds: <0.001[3]*		
	Dual-focus	<0.001[2]*	Natural-6 seconds: 0.911[3] Natural-12 seconds: <0.001[3]* 6 seconds-12 seconds: <0.001[3]*		

(continuation)					
Parameters	Condition	WITHOUT ARTIFICIAL TEARS		WITH ARTIFICIAL TEARS	
		p-value between blinking patterns	Post-hoc (Adjusted p-value)	p-value between blinking patterns	Post-hoc (Adjusted p-value)
Ocular Protection Index	Naked	0.101[2]		0.103[2]	
	Single-vision	<0.001[2]*	Natural-6 seconds: 0.821[3] Natural-12 seconds: <0.001[3]* 6 seconds-12 seconds: <0.001[3]*		
	Dual-focus	<0.001[2]*	Natural-6 seconds: 0.450[3] Natural-12 seconds: <0.001[3]* 6 seconds-12 seconds: <0.001[3]*		
Higher-order aberrations (µm)	Naked	0.150[2]		0.461[2]	
	Single-vision	0.397[2]			
	Dual-focus	0.926[2]			
Spherical aberration (0,4) (µm)	Naked	0.921[2]		0.741[2]	
	Single-vision	0.723[2]			
	Dual-focus	0.116[2]			
Horizontal coma (1,3) (µm)	Naked	0.799[2]		0.975[2]	
	Single-vision	0.839[2]			
	Dual-focus	0.614[2]			
Vertical coma (-1,3) (µm)	Naked	0.723[2]		0.905[2]	
	Single-vision	0.407[2]			
	Dual-focus	0.132[2]			

*(Where SD: Standard Deviation; TFSQ: Tear Film Surface Quality; [1]ANOVA; [2]Friedman; [3]Bonferroni; *Statistically significant values)*

Table 9.3.4. *Differences in results after artificial tears instillation for all conditions.*

Parameters	Condition	p-value between without and with artificial tears		
		Natural blinking	6 seconds	12 seconds
TFSQ	Naked	0.199[1]	0.117[1]	0.058[1]
	Single-vision	<0.001[1]*		
	Dual-focus	<0.001[1]*		
TFSQ area	Naked	0.365[1]	0.464[1]	0.187[1]
	Single-vision	<0.001[1]*		
	Dual-focus	<0.001[1]*		
Auto Tear Break-Up Time	Naked	0.614[1]	0.108[1]	0.019[1]*
	Single-vision	<0.001[1]*		
	Dual-focus	0.003[1]*		
Light Distortion Index	Naked	0.155[1]	0.411[1]	0.025[1]*
	Single-vision	0.001[1]*		
	Dual-focus	0.001[1]*		
Best Fit Circle Irregularity	Naked	0.775[1]	0.586[1]	0.993[1]
	Single-vision	0.154[1]		
	Dual-focus	0.835[1]		
Best Fit Circle Irregularity SD	Naked	0.865[1]	0.056[1]	0.442[1]
	Single-vision	0.060[1]		
	Dual-focus	0.030[1]*		
Blinks in 30 seconds	Naked	0.890[1]	1.00[1]	1.00[1]
	Single-vision	0.239[1]		
	Dual-focus	0.179[1]		
Higher-order aberrations	Naked	0.767[1]	0.139[1]	0.226[1]
	Single-vision	0.628[1]		
	Dual-focus	0.747[1]		
Spherical aberration (0,4)	Naked	0.778[1]	0.968[1]	0.851[1]
	Single-vision	0.778[1]		
	Dual-focus	0.952[1]		
Horizontal coma (1,3)	Naked	0.936[1]	0.519[1]	0.507[1]
	Single-vision	0.819[1]		
	Dual-focus	0.150[1]		
Vertical coma (-1,3)	Naked	0.428[1]	0.382[1]	0.170[1]
	Single-vision	0.819[1]		
	Dual-focus	0.310[1]		

*(Where SD: Standard Deviation; TFSQ: Tear Film Surface Quality; [1]Wilcoxon signed-rank test; *Statistically significant values)*

Differences between the naked eye and both contact lenses

Table 9.3.5 shows the results for the different conditions (naked eye and both contact lenses). For natural blinking without artificial tears and for delayed blinking, both contact lenses increased TFSQ and TFSQ area (meaning a more unstable tear film) when compared to naked eye assessment. Likewise, the dual-focus contact lens provided greater tear film instability than the single-vision contact lens in all blinking patterns. Auto Tear Break-Up Time also underwent a statistically significant decrease in dual-focus contact lens in comparison with the naked eye and single-vision contact lens.

Nevertheless, when subjects blinked every 6 seconds, no significant differences were found between the naked eye and single-vision for TFSQ and TFSQ area. Statistically significant differences were found in auto Tear Break-Up Time for all conditions (naked eye, single-vision and dual-focus) when subjects blinked every 6 seconds.

Statistically significant increases were found in light disturbance size between all paired groups (naked eye, single-vision and dual-focus) when subjects were instructed to blink every 12 seconds. Light disturbance size was higher in the dual-focus contact lens than in the naked eye and single-vision contact lens when subjects blink naturally and every 6 seconds. The dual-focus contact lens also caused higher light disturbance irregularity than the naked eye for all blinking patterns, and the single-vision contact lens had lower BFC irregularity SD than the dual-focus contact lens in the natural

blinking and blinking every 6 seconds. No differences were found in corneal aberrations between conditions (naked eye, single-vision and dual-focus).

When artificial tears were instilled, lower TFSQ, TFSQ area, light disturbance size and irregularity, and higher auto Tear Break-Up Time were found in the naked eye and single-vision contact lens in comparison with the dual-focus contact lens after the instillation of artificial tears.

During the aforementioned measurements, the mean pupil diameter under photopic conditions was 5.42 ± 0.83 mm, 4.88 ± 0.72 mm and 4.99 ± 0.78 for naked eye, single-vision and dual-focus contact lenses, respectively ($p = 0.258$). Mean pupil diameter under mesopic conditions was 6.36 ± 0.78 mm, 6.04 ± 0.88 mm and 6.38 ± 0.34 for naked eye, single-vision and dual-focus contact lenses, respectively ($p = 0.256$). Statistically significant differences were found between photopic and mesopic conditions for naked eye ($p < 0.001$; T test), single-vision ($p < 0.001$; T test) and dual-focus contact lenses ($p < 0.001$; Wilcoxon test).

Table 9.3.5. *Comparison between the naked eye and both contact lenses for each metric.*

Parameters	Without artificial tears						With artificial tears	
	Natural blinking		6 seconds		12 seconds		Natural blinking	
	p-value between conditions (naked eye – contact lenses)	Post-hoc (Adjusted p-value)	p-value between conditions (naked eye – contact lenses)	Post-hoc (Adjusted p-value)	p-value between conditions (naked eye – contact lenses)	Post-hoc (Adjusted p-value)	p-value between conditions (naked eye – contact lenses)	Post-hoc (Adjusted p-value)
TFSQ	<0.001[1]*	Naked eye-SV: 0.002[2]* Naked eye-DF: <0.001[2]* SV-DF: 0.001[2]*	<0.001[1]*	Naked eye-SV: 0.076[2] Naked eye-DF: <0.001[2]* SV-DF: <0.001[2]*	<0.001[1]*	Naked eye-SV: 0.014[2]* Naked eye-DF: <0.001[2]* SV-DF: 0.001[2]*	<0.001[1]*	Naked eye-SV: 0.221[2] Naked eye-DF: <0.001[2]* SV-DF: <0.001[2]*
TFSQ area	<0.001[1]* <0.001[1]*	Naked eye-SV: 0.004[2]* Naked eye-DF: <0.001[2]* SV-DF: 0.001[2]*	<0.001[1]*	Naked eye-SV: 0.180[2] Naked eye-DF: <0.001[2]* SV-DF: <0.001[2]*	<0.001[1]*	Naked eye-SV: 0.005[2]* Naked eye-DF: <0.001[2]* SV-DF: 0.008[2]*	<0.001[1]*	Naked eye-SV: 0.791[2] Naked eye-DF: <0.001[2]* SV-DF: <0.001[2]*
Auto Tear Break-Up Time		Naked eye-SV: 0.088[2] Naked eye-DF: <0.001[2]* SV-DF: <0.001[2]*	<0.001[1]*	Naked eye-SV: 0.036[2]* Naked eye-DF: <0.001[2]* SV-DF: <0.001[2]*	<0.001[1]*	Naked eye-SV: 0.071[2] Naked eye-DF: <0.001[2]* SV-DF: 0.006[2]*	<0.001[1]*	Naked eye-SV: 0.867[2] Naked eye-DF: <0.001[2]* SV-DF: <0.001[2]*
Light Distortion Index	<0.001[1]	Naked eye-SV: 0.371[2] Naked eye-DF: <0.001[2]* SV-DF: <0.001[2]*	<0.001[1]*	Naked eye-SV: 0.576[2] Naked eye-DF: <0.001[2]* SV-DF: <0.001[2]*	<0.001[1]*	Naked eye-SV: 0.006[2]* Naked eye-DF: <0.001[2]* SV-DF: <0.001[2]*	<0.001[1]*	Naked eye-SV: 0.943[2] Naked eye-DF: <0.001[2]* SV-DF: <0.001[2]*
Best Fit Circle Irregularity	0.006[1]*	Naked eye-SV: 0.656[2] Naked eye-DF: 0.005[2]* SV-DF: 0.172[2]	0.026[1]*	Naked eye-SV: 0.394[2] Naked eye-DF: 0.022[2]* SV-DF: 0.721[2]	0.012[1]*	Naked eye-SV: 0.656[2] Naked eye-DF: 0.009[2]* SV-DF: 0.249[2]	0.001[1]*	Naked eye-SV: 0.696[2] Naked eye-DF: 0.002[2]* SV-DF: 0.006[2]*
Best Fit Circle Irregularity SD	<0.001[1]*	Naked eye-SV: 0.696[2] Naked eye-DF: <0.001[2]* SV-DF: 0.001[2]*	0.007[1]*	Naked eye-SV: 0.791[2] Naked eye-DF: 0.006[2]* SV-DF: 0.006[2]*	<0.001[1]*	Naked eye-SV: 0.088[2] Naked eye-DF: <0.001[2]* SV-DF: 0.057[2]	<0.001[1]*	Naked eye-SV: 0.502[2] Naked eye-DF: 0.008[2]* SV-DF: 0.057[2]

(continuation)								
Parameters	Without artificial tears						With artificial tears	
	Natural blinking		6 seconds		12 seconds		Natural blinking	
	p-value between conditions (naked eye – contact lenses)	Post-hoc (Adjusted p-value)	p-value between conditions (naked eye – contact lenses)	Post-hoc (Adjusted p-value)	p-value between conditions (naked eye – contact lenses)	Post-hoc (Adjusted p-value)	p-value between conditions (naked eye – contact lenses)	Post-hoc (Adjusted p-value)
Blinks in 30 seconds	0.130[1]	Naked eye-SV: 0.791[2] Naked eye-DF: 0.130[2] SV-DF: 0.438[2]	1.00[1]		1.00[1]		0.146[1]	
Higher-order aberrations	0.905[1]		0.368[1]		0.614[1]		0.723[1]	
Spherical aberration (0,4)	0.241[1]		0.061[1]		0.928[1]		0.153[1]	
Horizontal coma (1,3)	0.699[1]		0.926[1]		0.735[1]		0.294[1]	
Vertical coma (-1,3)	0.294[1]		0.273[1]		0.839[1]		0.622[1]	

*(Where DF: Dual-Focus Contact Lens; SD: Standard Deviation; SV: Single-Vision Contact Lens; TFSQ: Tear Film Surface Quality; [1]Friedman; [2]Bonferroni; *Statistically significant values)*

9.3.4. Discussion

In the present study, a higher light disturbance was found in conditions in which the tear film was destabilized such as in low blinking frequency and wearing contact lenses. Moreover, in general, light disturbance decreased after the instillation of

artificial tears. In this way, the present study supports the work of previous authors, who demonstrated that the irregular thinning of the tear film after blinking in subjects with dry eye can affect the light pathway, reducing visual acuity and contrast sensitivity and increasing higher-order aberrations, light scattering and fluctuations in vision (Thibos and Hong, 1999; Tutt et al., 2000; Németh, Erdélyi and Csákány, 2001; Himebaugh et al., 2003; Montés-Micó, Alió and Charman, 2005a; Montés-Micó, Alió and Charman, 2005b; Ferrer-Blasco et al., 2009; Denoyer, Rabut and Baudouin, 2012; Kobashi et al., 2015; Gouvea et al., 2019).

Assessing the optical quality of DED subjects is vital due to the relevant role that the tear film plays in optical quality and the relevance of these visual symptoms in the quality of life of subjects with dry eye. The measurement of light disturbance might help to assess and manage DED subjects since it reflects the completeness of visual symptoms experienced by subjects. Likewise, it might increase clinicians' knowledge on the impact of DED on visual quality (Díaz-Doutón et al., 2006). Indeed, the TFOS DEWS II Diagnostic Methodology Report recognized the need of developing new metrics to assess the tear film and its influence on the optical quality (Wolffsohn et al., 2017).

Differences between blinking patterns

During the inter-blink time, the tear film becomes thinner due to evaporation and breaks-up until the next blink occurs (Koh et al., 2008a; Lemp, 2008; Kobashi et al., 2013; Kobashi et al., 2015; Yu et al., 2016; Willcox et al., 2017; García-Montero et al., 2019c; Xi, Qin and Bao, 2019; D'Souza et al., 2020). This break-up is called BUT and it

has been reported to cause a loss in the optical quality, increasing higher-order aberrations and light scattering after blinking (Tutt et al., 2000; Koh and Maeda, 2007; Koh et al., 2008b; Koh et al., 2008c; Ferrer-Blasco et al., 2009; Liu et al., 2010; Montés-Micó et al., 2010b; Kobashi et al., 2013; Tan et al., 2015a; Gouvea et al., 2019). Thus, the tear film must be frequently replenished by blinking to maintain good optical quality (Bron et al., 2017). In the present study, natural blinking occurs approximately every 6.5 seconds, which is in agreement with the spontaneous blinking frequency found in previous studies (Tsubota, 1996; Zaman, Doughty and Button, 1998; Doughty, 2001; Montés-Micó et al., 2004; Montés-Micó, Alió and Charman, 2005b; Wolffsohn et al., 2017).

It has been reported that the eye has the highest optical quality 5-7 seconds after blinking (Montés-Micó, Alió and Charman, 2005b; Ferrer-Blasco et al., 2009). In the present study, blinking patterns did not cause differences in light disturbance, higher-order aberrations and tear film stability when measured without contact lenses. In this condition, the mean auto Tear Break-Up Time was higher than 12 seconds for all blinking patterns (higher than the interblink intervals tested), thus the tear film was not destabilized between blinks and did not interfere with the outcomes evaluated. This leads to an ocular protection index > 1, protecting the ocular surface against desiccation even in the low blinking frequency. In agreement with these results, other authors (Montés-Micó, Alió and Charman, 2005b; Koh et al., 2008b) found that higher-order aberrations did not change over 10 seconds after bliking (Koh et al., 2002) and light disturbance over a 20 seconds period in healthy subjects (Díaz-Valle et al., 2012) but subjects with short BUT showed higher loss of the optical quality (Kobashi et al.,

2013). It might be possible that with a higher interblink interval, optical quality might have decreased in the present study.

Nevertheless, an augmented size and shape of light disturbance during both contact lens wear was shown with the lowest blinking rate. Both contact lenses (dual-focus and single-vision) affected tear film stability, by means of a decreased auto Tear Break-Up Time and decreased TFSQ. Consequently, this affected the ocular protection index, which showed that in the condition with low blinking frequency the ocular surface was unprotected (Ocular protection index < 1), increasing the light disturbance. Thus, when subjects blink with less frequency, the tear film is worse spread across the lens surface, affecting light disturbance. This is in accordance with a previous study (Koh et al., 2008c) that found that higher-order aberrations deteriorated in subjects with short BUT by suppressed blinking due to increased evaporation and thinning of the tear film at the centre of the cornea. Nevertheless, in the present study, no differences were found in corneal aberrations and tear film stability between blinking patterns. As blinking patterns only were performed during LDA measurement (2 minutes approximately) it did not affect tear film stability and optical aberrations, which were measured after LDA. Moreover, higher-order aberrations have been reported to contribute only a 7 % to the optical quality (Kobashi et al., 2013).

These results suggest that subjects who have higher interblink intervals, i.e. 12 seconds (for instance, computer users (García-Montero et al., 2019c; Talens Estarelles et al., 2020; Talens Estarelles et al., 2021)) are more likely to experience higher light

disturbance while wearing contact lenses than subjects who have higher blinking frequency. This long eye open is not unrealistic and is known to occur during tasks that require concentration (Doughty, 2001; Liu et al., 2010; Talens-Estarelles et al., 2021a). Moreover, in *Chapter 9.1.1* and *Chapter 9.1.2* (García-Marqués et al., 2020; García-Marqués et al., 2021b), it was found that the same dual-focus contact lens of this study promoted higher light disturbance and lower tear film stability than a single-vision contact lens due to optical design differences. This study adds that a low blinking frequency deteriorates light disturbance even more with a dual-focus contact lens, suggesting that not only is the optical design affecting light disturbance in these lenses, but also tear film spreading across the surface of the contact lens. Monitoring blinking to blink with more frequency might decrease the light disturbance and could be an option to manage contact lens users with short BUT to minimize tear and optical alterations.

Changes after the instillation of artificial tears

In agreement with the results found in the present study, artificial tears improve tear film stability and decrease higher-order aberrations and light scattering after instillation due to they provide a more stable and regular tear film (Montés-Micó, 2007; Montés-Micó et al., 2010b; Díaz-Valle et al., 2012; Igarashi et al., 2015; Kobashi et al., 2015; Schafer et al., 2018; Vandermeer, Chamy and Pisella, 2018). Nevertheless, some studies (Ridder et al., 2005; Berger, Head and Salmon, 2009; Hiraoka et al., 2010; Koh et al., 2013a; Koh et al., 2013b) found an initial decrease in optical quality in artificial tears with high viscosity. Previous studies with the same artificial tears as in

the present study found that they were effective for alleviating symptoms of dryness and increased tear film stability, being also safe and compatible with contact lenses (Kading, 2010; Benelli, 2011; McDonald et al., 2014; Gokul, Wang and Craig, 2018; Belalcázar-Rey et al., 2021). To the authors' knowledge, there are no previous studies assessing the optical quality with the artificial tears assessed in this study.

In some cases, the inter-blink interval can be increased after artificial tear instillation (Willcox et al., 2017; Wolffsohn et al., 2017). Nevertheless, in the present study no statistically significant differences were found in blinking frequency after instillation of artificial tears. In the delayed blinking with the naked eye, mean auto Tear Break-Up Time increased and the size of the light disturbance decreased after the instillation of artificial tears. This suggests that tear film instillation can increase tear film stability and optical quality under dim light conditions in subjects with a delayed blinking pattern.

When both contact lenses were fitted, artificial tears increased tear film stability with natural blinking (lower TFSQ and TFSQ area and higher auto Tear Break-Up Time) and decreased the size of the light disturbance in both contact lenses. Likewise, artificial tears also improved BFC Irregularity of the light disturbance in the dual-focus contact lens. These results suggest that the higher light disturbance phenomena (size and irregularity) found with the dual-focus contact lenses in the present study and in a previous one (*Chapter 9.1.1*) (García-Marqués et al., 2020) are not only due to differences in the optical design of the lens, but also due to the spreading of the tear film across the anterior surface of the contact lens.

Differences between the naked eye and both contact lenses

Contact lens wear destabilizes the tear film (Korb, Greiner and Glonek, 1996). Contact lens divides the tear film into two layers: pre-lens tear film and post-lens tear film. Thus, contact lens wearers that experience blurry vision or fluctuating vision might be caused by poor optical quality due to a lower BUT (Koh et al., 2008a; Rae and Price, 2009; Liu et al., 2010; Szczesna-Iskander, Alonso-Caneiro and Iskander, 2016; García-Montero et al., 2019c; Gouvea et al., 2019). Moreover, the evaporation of the pre-lens tear film can expose the surface of the contact lens after tear break-up, decreasing optical quality (Szczesna-Iskander, Alonso-Caneiro and Iskander, 2016; Willcox et al., 2017; García-Marqués et al., 2021b). Likewise, areas of break-up have an increased osmolarity, which might also cause fluctuation in the refractive index of the lens and affect vision (Liu et al., 2009; Liu et al., 2010). Due to the link between lens dehydration and optical quality, the measurement of light disturbance might help in the assessment of contact lens in-vivo wettability and optical quality related to the tear film in contact lens wearers, providing non-invasive, and functional information about the quality of vision.

Both contact lenses caused more tear film instability when compared to naked eye assessment when subjects blinked naturally without artificial tears and every 12 seconds. Likewise, the dual-focus contact lens induced greater tear film instability than the single-vision contact lens and naked eye condition. Despite no differences were found in auto Tear Break-Up Time between the single-vision contact lens and the naked eye; these differences are clinically significant since there is a huge difference

between both conditions that could affect clinically. Previous works also found lower pre-lens tear film stability after contact lens fitting (Nichols and Sinnot, 2006; Szczesna-Iskander, 2014; García-Montero et al., 2019c; García-Marqués et al., 2021b). Moreover, when subjects blinked every 6 seconds, no changes were found between the naked eye and single-vision for TFSQ and TFSQ area, suggesting that blinking with more frequency can prevent the tear film from drying out and becoming unstable with a single-vision contact lens.

For the delayed blinking, statistically significant differences were found in light disturbance size between all paired conditions (naked eye, single-vision contact lens and dual-focus contact lens) since during suppressed blinking in contact lens wearers the pre-lens tear film dynamics lose their stability and induce dewetting, causing the loss of the tear film and optical quality (Szczesna-Iskander, Alonso-Caneiro and Iskander, 2016). Higher light disturbance size was found in the dual-focus contact lens than in the naked eye and single-vision contact lens when subjects blink naturally and every 6 seconds. Thus, light disturbance was higher in the single-vision contact lens when subjects blink every 12 seconds but no differences in light disturbance were found between the naked eye and the single-vision contact lens when subjects blink naturally and in 6 seconds interval conditions. This suggests that blinking with more frequency can prevent the ocular surface from light disturbance with a single-vision contact lens since light disturbance was not different from the naked eye condition (without contact lens). When artificial tears were instilled, tear stability and light disturbance size and irregularity improved in the naked eye and single-vision contact lens in comparison with the dual-focus contact lens. Thus, despite the fact that

artificial tears instillation improved tear film stability and light disturbance in the dual focus contact lens, the dual-focus design still showed worse values than the naked eye and the single-vision contact lens.

This study has some limitations to consider. First, the sample was young adults while the target population for the dual-focus contact lens is young children and adolescents. Second, short-term results of the contact lenses were shown. Thus, light disturbance and tear film stability might be worse after more hours of wear. Although some studies (Efron et al., 1987; Brennan et al., 1990; Paugh et al., 2001; Nichols and King-Smith, 2003) reported that this period is adequate to assess the short-term performance of contact lenses because the tear film changes in the first 20 minutes of contact lens wear, other studies (Little and Bruce, 1994; Nichols and King-Smith, 2004) claimed that the pre-lens tear film thinned over the first 30 minutes. Therefore, there is still controversy on this topic. This issue is not expected to influence the comparison between conditions after the same time and after the same washout period. Moreover, Efron et al. (1987) argued that the majority of dehydration takes place within the first 5 minutes of wear.

Conditions were assessed in a random order to avoid bias but artificial tears instillation was always evaluated at the end of the visit to prevent altering the tear film. Besides, subjects were not classified as healthy or DED. Finally, it is also important to comment that not only pre-lens tear film may be altered by the dual-focus design of contact lens, but the Medmont system might be very sensitive and detect non-tear film-related changes on the dual-focus surface.

Overall, low blinking frequency caused higher size and shape light disturbance when subjects were wearing contact lenses. Nonetheless, light disturbance and tear stability improved after artificial tears instillation, suggesting that artificial tears instillation can improve tear film stability and optical quality in subjects with a delayed blinking pattern. Nevertheless, despite artificial tears instillation improved tear film stability and light disturbance in the dual-focus contact lens, the dual-focus contact lens still showed worse values than the naked eye and the single-vision contact lens. Monitoring blinking to blink with more frequency or using artificial tears might decrease the light disturbance and could be an option to manage subjects with short BUT. The measurement of light disturbance might help in the assessment, grading the severity and managing DED subjects, increasing clinicians' knowledge on the impact of DED on visual quality. Moreover, it might be also used as a quick and non-invasive tool to monitor the quality of the tear film over a contact lens and to assess in-vivo the wettability of the lens. Thus, these new metrics could be included in a battery of clinical tests to improve the assessment and monitoring of DED. Further research is needed to assess the performance of light disturbance metrics in subjects diagnosed with DED or MGD, and to study the repeatability of these measurements to assess optical quality related to tear film changes.

CHAPTER 9.4: Assessment of meibomian gland drop-out and visibility through a new quantitative method in scleral lens wearers: A one year follow-up study

9.4 ASSESSMENT OF MEIBOMIAN GLAND DROP-OUT AND VISIBILITY THROUGH A NEW QUANTITATIVE METHOD IN SCLERAL LENS WEARERS: A ONE-YEAR FOLLOW-UP STUDY

In this chapter, the method developed in *Chapter 8.1* will be applied to scleral lens wearers to assess the meibomian gland drop-out and visibility after one year of lens wear.

9.4.1 Introduction

Scleral lenses are large-diameter contact lenses that rest on the bulbar conjunctiva overlying the sclera. As scleral lenses are inserted with liquid (preservative-free saline solution), they create a tear reservoir that keeps the cornea moistened. This characteristic along with correcting anterior corneal aberrations allows these devices to often deliver clear as well as minimize dry eye-related symptoms in patients with irregular corneas and/or severe ocular surface disease (Pullum and Buckley, 1997; Rosenthal and Cotter, 2003; Schornack, Pyle and Patel, 2014; van der Worp et al., 2014; Gemoules, 2015; Porcar et al., 2017; Macedo-de-Araújo et al., 2019; Montalt et al., 2019; Macedo-de-Araújo et al., 2020; Barnett et al., 2021).

Nevertheless, despite the use of scleral lenses is increasing little is known about their effect on meibomian gland structure and function (Walker, Schornack and Vincent, 2021). Some studies concluded that soft and rigid contact lens wear may potentiate meibomian gland drop-out, alter gland morphology such as length and width, alter meibum expressibility and quality, and induce dry eye symptoms,

ultimately classified as MGD (Arita et al., 2008; Alghamdi et al., 2016; Arita, Fukuoka and Morishige, 2017d; Gu et al., 2020b; Llorens-Quintana, Garaszczuk and Szczesna-Iskander, 2020; Iqbal, Thomas and Mahadevan, 2021; Harbiyeli et al., 2022).

A new method based on the visibility of meibomian glands has been validated for Keratograph 5M in *Chapter 8.1* (García-Marqués et al., 2021a). This method is similar to the meibomian gland contrast measurement (Yeh and Lin, 2018). It was proven that, as meibomian glands are lighter than the background in a meibography, the visibility of meibomian glands could be used as a feature to aid in the assessment of those secretory structures. As previously defined in *Chapter 8.1* (García-Marqués et al., 2021a; García-Marqués et al., 2021c), visibility is defined as the grade in which meibomian glands are seen. Thus, in a subject with high gland drop-out, the glands have totally lost their visibility. With this premise, a new method was developed, based on image analysis, to objectively assess the visibility of meibomian glands. It was also demonstrated in *Chapter 8.1* that gland visibility metrics are different from gland drop-out since gland visibility was different in subjects with similar gland drop-out percentages (García-Marqués et al., 2021a). Thus, these metrics were useful to grade the level of visibility of the glands. Moreover, *in Chapter 8.1* (García-Marqués et al., 2021c), it has been found that meibomian gland visibility metrics have good sensitivity and specificity to diagnose MGD, having higher diagnostic capability than current diagnostic metrics such as meibomian gland drop-out. Moreover, gland visibility metrics are correlated with gland expressibility, tear film stability, TMH and bulbar redness.

There is no previous study assessing the effect of scleral lenses on meibomian gland drop-out. Moreover, it has been recognized the need for assessing meibomian glands in subjects fitted with these lenses (Stapleton et al., 2017). Since scleral lenses are usually fitted in subjects with irregular corneas, namely patients with keratoconus who are more likely to suffer from DED and MGD (Carracedo et al., 2014; Mostovoy et al., 2018; Mohamed-Mostafa et al., 2019; Macedo-de-Araújo, van der Worp and González-Méijome, 2020), understanding their effect on meibomian glands is clinically relevant. The present study has two main aims: The first one is to validate a previously developed method based on the visibility of meibomian glands with a commercial fundus camera, which might help to further validate this method, suggesting that it is not instrument-specific. The second aim is to assess dry eye symptoms and meibomian gland alterations in scleral lens wearers after one year of lens wear. The hypothesis is that as both eyelids and the tear film interact directly with scleral lenses, they might be affected by scleral lens wear (Walker, Schornack and Vincent, 2011).

9.4.2 Methodology

Validation of an objective method to quantify meibomian gland visibility

The data from forty-three subjects participating in a prospective clinical study involving scleral lens fitting (Macedo-de-Araújo et al., 2019; Macedo-de-Araújo et al., 2020; Macedo-de-Araújo, van der Worp and González-Méijome, 2020) was also used in the present study. The mean age of the participants was 34.2 ± 10.1 years old (ranging between 18 and 65 years). Subjects were not required to be previous soft or rigid contact lens wearers. No exclusion based on the state of the meibomian glands of

subjects was made. A random eye was chosen for the analysis. Written consent of each subject was obtained after the explanation of the study purpose and clinical protocol. The study procedures were approved by the Ethics Subcommittee for Life and Health Sciences of the University of Minho and following the tenets of the Declaration of Helsinki.

Measurements

Non-contact infrared meibography of the upper eyelid was obtained using the Cobra fundus camera (CSO, Scandicci, Firenze, Italy) by the same experienced and masked researcher, as explained in *Chapter 3 General Methodology*. Meibographies were obtained in the same laboratory under constant conditions of illumination. Illuminance was measured using an illuminance meter (T-10*,* Minolta *Sensing* Inc, Tokyo, Japan). The varying daylight was removed using black-out curtains. The illuminance was 254.65 ± 8.19 lux.

Method validation for the measurement of meibomian gland visibility

Meibographies were subjectively classified into 3 groups (*Figure 9.4.1*), by a masked researcher, as follows: Group 1 = Patients with good subjective glands visibility and an Image J gland drop-out percentage less than one-third of the total area of meibomian glands; Group 2 = Patients with low subjective glands visibility and an Image J gland drop-out percentage lower than one-third of the total area; and Group 3 = Patients with low subjective glands visibility and an Image J gland drop-out percentage higher than one-third of the total area. This classification into groups is not

based on any previous criterion, but subjects were classified into groups to validate the method. However, the cut-off value of 1/3 of gland drop-out is similar to Arita's scale (Arita et al., 2008).

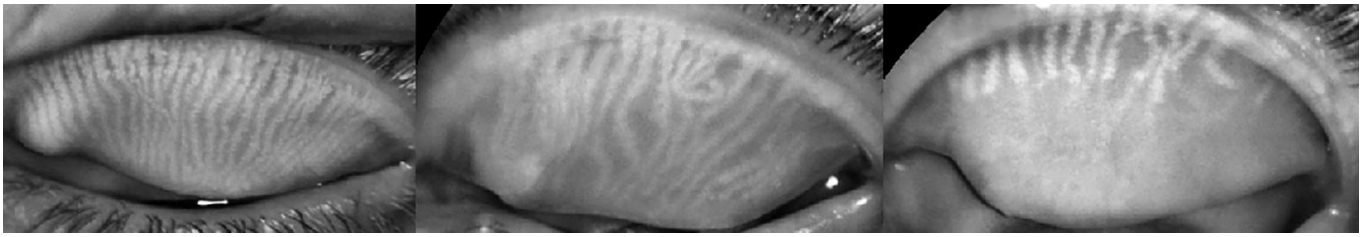

Fig. 9.4.1. *Examples of the 3 meibography groups. From left to right: Group 1, Group 2 and Group 3.*

Once meibographies were classified into these 3 groups, they were analysed using the developed method based on the grey level intensity of pixels. Examiner was masked to the study group allocation of meibographies during image processing analysis. The present method was developed using Matlab© R2018a software (MathWorks, Natick, MA) as explained in *Chapter 8.1* (García-Marqués et al., 2021a) for Keratograph 5M. Meibographies obtained with Cobra fundus camera were lighter than ones obtained with Keratograph 5M. Therefore, in this case, the method included a reduction of 50% in the brightness of the meibography to avoid pixels saturation in the image processing.

Effect of scleral lenses on ocular surface symptoms, gland drop-out and visibility

Out of 43 subjects, data from 29 of them (25.6 ± 11.03 years old, ranging from 18 until 65 years) was available to assess the effect of scleral lens wear after one year. Thus, meibographies were again obtained and analysed with Image J and the

developed method to assess differences in meibomian gland drop-out and visibility after one year of scleral lens wear. Ocular surface symptoms were also assessed at baseline and after one year of scleral lens wear using the OSDI questionnaire.

All volunteers were fitted with Senso MiniScleral lenses from Procornea (Eerbeek, The Netherlands) made of Boston XO material (DK 100 ISO/Fatt). Lenses were fitted by an experienced practitioner using a diagnostic fitting set. Other technical characteristics of the lenses and fitting procedure were previously described (Macedo-de-Araújo, van der Worp and González-Méijome, 2018; Macedo-de-Araújo et al., 2019; Macedo-de-Araújo et al., 2020; Macedo-de-Araújo, van der Worp and González-Méijome, 2020). The lens should align evenly with the conjunctival surface and vault the entire corneal surface and limbus. If the fit was not satisfactory, another diagnostic lens was applied. When the best diagnostic lens fitting was achieved, participants were asked to continue with the diagnostic lens for another 90 min and then to return for a new assessment and to perform over-refraction. After the final assessment, minor adjustments were made and the final lenses were ordered (Macedo-de-Araújo, van der Worp and González-Méijome, 2019).

Statistical analysis

Statistical analysis was performed using SPSS v26.0 for Windows (IBM Corp, Armonk, New York, USA). Results were displayed as the mean ± SD and Shapiro-Wilk test was used to check the normality distribution for each group.

Differences between meibography groups for each metric were assessed using the Kruskal-Wallis test, while the Bonferroni test was used to evaluate the post-hoc differences between paired groups and p-values were shown according to the Bonferroni correction. A p-value less than 0.05 was defined as statistically significant.

Correlations between each gland visibility metric and meibomian gland drop-out percentage were assessed by means of the Rho Spearman test; with the entire sample and after excluding group 2 from the analysis to not take into account the cases in which low visibility was not related to high gland drop-out. Thus, group 2 was excluded to further prove that not only was the method measuring gland drop-out, but it also measured the visibility of the glands.

Since the method was semiautomatic, the repeatability of the method to calculate each metric was obtained by analyzing each meibography three times with the developed method. S_w, CoV and CoR were calculated to assess the repeatability of each new metric, as explained in *Chapter 3 General Methodology*. Finally, either paired t-test or Wilcoxon test were used to assess the effect of scleral lenses in meibomian glands and ocular surface symptoms after one year of wear.

9.4.3 Results

Validation of the method in Cobra fundus camera (CSO)

The new method was applied to forty-three meibographies from the eyes of 43 subjects. Twenty were female (46.5 %) and 23 male (53.5 %), while the mean age was 34.2 ± 10.1 years (ranging from 18 to 65 years). From the total sample, 24 volunteers

were classified in group 1 (34.3 ± 12.0 years), 12 in group 2 (34.2 ± 7.1 years) and 7 in group 3 (34.0 ± 6.7 years). No statistically significant differences in age were found between groups (p = 0.998). *Table 9.4.1* shows the main results obtained for each metric per group and the statistical comparison between them. The method performed properly in all meibographies.

Table 9.4.1. *Mean values for each group and comparison between them.*

Metric	Group	Mean±SD	Significance level (p-value)	Comparison between groups (p-value)
Gland drop-out percentage (%)	Group 1	25.51±7.09	<0.001[1]*	1-2= 0.464
	Group 2	27.03±5.80		1-3= <0.001*
	Group 3	60.19±20.57		2-3= 0.004*
Relative energy	Group 1	0.34±0.07	<0.001[1]*	1-2= 0.008*
	Group 2	0.24±0.05		1-3= <0.001*
	Group 3	0.12±0.10		2-3= 0.522
Energy	Group 1	226.79±9.93	<0.001[1]*	1-2= 0.047*
	Group 2	210.57±7.92		1-3= <0.001*
	Group 3	187.22±12.89		2-3= 0.296
SD Irregularity	Group 1	0.28±0.08	<0.001[1]*	1-2= 0.006*
	Group 2	0.17±0.05		1-3= <0.001*
	Group 3	0.09±0.10		2-3= 0.573
Mean ROI pixels intensity	Group 1	95.77±14.30	<0.001[1]*	1-2= 0.006*
	Group 2	77.03±9.62		1-3= <0.001*
	Group 3	49.07±21.85		2-3= 0.573
SD ROI pixels intensity	Group 1	81.67±5.99	<0.001[1]*	1-2= 0.012*
	Group 2	72.74±6.95		1-3= <0.001*
	Group 3	53.69±15.62		2-3= 0.600
Median ROI pixels intensity	Group 1	72.08±20.72	<0.001[1]*	1-2= 0.013*
	Group 2	49.50±10.13		1-3= <0.001*
	Group 3	28.43±16.72		2-3= 0.339
Kurtosis	Group 1	0.0107±0.0010	<0.001[1]*	1-2= 0.015*
	Group 2	0.0120±0.0009		1-3= <0.001*
	Group 3	0.0167±0.0029		2-3= 0.455
Skewness	Group 1	0.105±0.006	<0.001[1]*	1-2= 0.016*
	Group 2	0.112±0.004		1-3= <0.001*
	Group 3	0.133±0.014		2-3= 0.443

(Where ROI: Region of Interest; SD: Standard Deviation; Group 1: Patients with good subjective gland visibility and gland drop-out less than one-third of the total

*meibomian gland area; Group 2: Patients with low subjective gland visibility and gland drop-out less than one-third of the total meibomian gland area; Group 3: patients with low subjective gland visibility and gland drop-out higher than one-third of the total meibomian gland area; [1]Kruskal-Wallis Test; *Statistically significant values)*

Meibomian gland visibility metrics did not reveal statistically significant differences in gland drop-out percentage between groups 1 and 2. Nevertheless, meibographies of group 1 showed higher grey pixel intensity values than the other groups, which is reflected in relative energy, energy, SD irregularity, mean, SD, median, kurtosis and skewness. This suggests that the method can distinguish between different types of meibographies.

Statistically significant correlations were found between the meibomian gland visibility metrics, based on grey level intensity pixels of meibographies, and gland drop-out percentage with the entire sample and after excluding group 2 (*Table 9.4.2*). Moreover, correlations were stronger after excluding group 2. Group 2 was excluded from the analysis to further prove that the software was not only measuring gland drop-out, but also able to detect differences in gland visibility.

All metrics showed moderate-acceptable repeatability since S_w and CoR values were low and the variability between the three measurements was not high, CoV achieving values between 0.52 and 3.18 (*Table 9.4.3*).

Table 9.4.2. *Rho Spearman correlations between the developed metrics based on grey intensity pixels of meibographies and gland drop-out percentage with the entire sample and after excluding group 2.*

Metric	Groups	Spearman's correlation coefficient (r)	Significance level (p-value)
Relative energy	All the sample	-0.606	<0.001*
	Without group 2	-0.682	<0.001*
Energy	All the sample	-0.564	<0.001*
	Without group 2	-0.602	<0.001*
SD Irregularity	All the sample	-0.589	<0.001*
	Without group 2	-0.663	<0.001*
Mean ROI pixels intensity	All the sample	-0.594	<0.001*
	Without group 2	-0.674	<0.001*
SD ROI pixels intensity	All the sample	-0.502	0.001*
	Without group 2	-0.538	0.002*
Median ROI pixels intensity	All the sample	-0.620	<0.001*
	Without group 2	-0.714	<0.001*
Kurtosis	All the sample	0.605	<0.001*
	Without group 2	0.674	<0.001*
Skewness	All the sample	0.603	<0.001*
	Without group 2	0.668	<0.001*

*(Where ROI: Region of Interest; SD: Standard Deviation; Group 2: Patients with low subjective gland visibility and gland drop-out less than one-third of the total meibomian gland area; *Statistically significant values)*

Table 9.4.3. *Repeatability of each metric.*

Metric	Sw	CoR	CoV (%)
Relative energy	0.006	0.017	2.04
Energy	1.35	3.74	0.63
SD Irregularity	0.006	0.017	2.63
Mean ROI pixels intensity	1.29	3.56	1.46
SD ROI pixels intensity	0.54	1.5	0.70
Median ROI pixels intensity	2.04	5.65	3.18
Kurtosis	0.00012	0.0003	1.02
Skewness	0.0006	0.002	0.52

(Where CoR: Repeatability Coefficient; CoV: Coefficient of Variation; ROI: Region of Interest; SD: Standard Deviation; Sw: Within-subject standard deviation)

Differences in ocular surface symptoms and meibomian glands after 1 year of scleral lens wear

Twenty-nine subjects were fitted with scleral lenses and meibographies were assessed at baseline and after one year of scleral lens wear. The mean age was 25.6 ± 11.03, ranging from 18 to 65 years old. Fifteen were female (51.7 %) and fourteen were male (48.3 %). One eye of each patient was randomly chosen for the meibomian gland evaluation before fitting and 1 year after lens wear: Eighteen eyes had keratoconus (62.1%), four eyes with healthy cornea but high refractive error (13.8 %), four eyes had undergone penetrating keratoplasty (13.8 %) and three eyes had post-Laser Assisted In-Situ Keratomileusis ectasia (10.3 %).

No statistically significant differences were found in meibomian gland drop-out percentage and gland visibility metrics between baseline and after one year of scleral lens wear (*Table 9.4.4*). Nevertheless, an average improvement in OSDI of 24.5 was found after one year of scleral lens wear. Thus, this might suggest that scleral lens wear appears to not adversely affect the meibomian gland drop-out and visibility while promoting comfortable wear.

Table 9.4.4. *Comparison of OSDI, gland drop-out and gland visibility in baseline and after one year of scleral lens fitting.*

Metric	Groups	Mean±SD	Significance level (p-value)
Gland drop-out percentage (%)	Pre	29.29±12.10	0.157[2]
	Post	30.44±11.84	
Relative energy	Pre	0.30±0.10	0.525[1]
	Post	0.29±0.10	
Energy	Pre	213.88±12.73	0.217[1]
	Post	211.05±12.59	
SD Irregularity	Pre	0.25±0.10	0.411[1]
	Post	0.23±0.09	
Mean ROI pixels intensity	Pre	89.09±19.82	0.369[1]
	Post	85.12±20.34	
SD ROI pixels intensity	Pre	78.13±10.54	0.539[2]
	Post	76.57±9.70	
Median ROI pixels intensity	Pre	64.62±23.93	0.539[1]
	Post	60.97±25.84	
Kurtosis	Pre	0.0114±0.0020	0.539[2]
	Post	0.0117±0.0022	
Skewness	Pre	0.108±0.010	0.569[2]
	Post	0.109±0.010	
OSDI	Pre	50.17±22.40	<0.001[2]*
	Post	25.69±14.34	

*(Where OSDI: Ocular Surface Disease Index; ROI: Region of Interest; SD: Standard Deviation; [1]Paired T-test; [2]Wilcoxon Test; *Statistically significant values)*

9.4.4 Discussion

Validation of the method in Cobra fundus camera (CSO)

In the present study, an objective, semiautomatic method based on the analysis of the visibility of meibomian glands, which was previously developed for Keratograph 5M, was validated for a commercial fundus camera. Meibomian gland visibility assessment could be relevant because the link between gland drop-out and gland function is not clear (Llorens-Quintana et al., 2019b).

The results in this study were similar to those found in *Chapter 8.1* (García-Marqués et al., 2021a) in the Keratograph 5M, suggesting that the method is not instrument-dependent. The only modification performed was a reduction of 50% in the brightness of the meibography to avoid pixels saturation since meibographies obtained with the Cobra fundus camera were lighter. As in *Chapter 8.1* (García-Marqués et al., 2021a), results showed lower pixel intensity values for group 2, which had lower gland visibility than group 1 but similar gland drop-out. This evidences that the method was not only able to detect gland drop-out, but it can also objectively assess meibomian gland visibility. Moreover, this was even more evident when correlations between gland visibility metrics and gland drop-out percentage were stronger after excluding group 2 from the analysis. As reported in *Chapter 8.1.2* (García-Marqués et al., 2021c), gland visibility metrics had higher diagnostic ability than current metrics such as meibomian gland drop-out and were correlated with different ocular surface metrics.

Despite the method being semiautomatic - since the region of interest of glands needs to be manually delimited -, repeatability of gland visibility metrics showed to be moderate-acceptable because S_w, CoR and CoV indicate good repeatability when its values are near zero (Bland and Altman, 2010; Cerviño et al., 2015; Martínez-Albert et al., 2018; McAlinden, Khadka and Pesudovs, 2015).

Effect of scleral lenses on ocular surface symptoms, gland drop-out and visibility

Visual rehabilitation of subjects with irregular corneas is usually achieved with scleral lenses. Both eyelids and the tear film interact directly with scleral lenses and

they might be affected by scleral lens wear (Walker, Schornack and Vincent, 2021). For instance, changes in meibomian gland secretion could increase deposits on the anterior surface of scleral lenses (Walker, Schornack and Vincent, 2021). Also, scleral lenses might increase the mechanical interaction with the tarsal structures on repeated blinking due to the thickness and space that occupy. However, few studies assessed the effect of scleral lenses on the tear film and meibomian glands (Romero-Rangel et al., 2000; La Porta Weber et al., 2016; Walker, Schornack and Vincent, 2021). The sample of this study represented irregular corneas, except for four of them. Since scleral lenses are usually fitted in subjects with irregular corneas, who are more likely to suffer from DED (Carracedo et al., 2014; Mostovoy et al., 2018; Mohamed-Mostafa et al., 2019), assessing the effect of these lenses on meibomian glands is vital. Thus, a recent review confirmed that there is a need for prospective evaluation of meibomian gland appearance and function during scleral lens wear (Walker, Schornack and Vincent, 2021).

To my knowledge, only one study (La Porta Weber et al., 2016) attempted to measure some features related to meibomian glands after scleral lens wearing. The authors did not find statistically significant differences in meibum expression after 1 year of scleral lens wear in moderate-severe DED subjects. These results are aligned with ones found in the present study since no statistically significant differences were found in meibomian gland drop-out and meibomian gland visibility after one year of scleral lens wearing. This is the first study evaluating the effect of scleral lenses on the structural aspects of MGD evaluated objectively.

Regarding ocular surface symptoms, it was already shown that scleral lenses can improve OSDI scores compared to other treatment options and that this improvement was maintained over 12 months of lens wear (Macedo-de-Araújo et al., 2019). In the present study a clinically and statistically significant reduction from 50.17 ± 22.40 to 25.69 ± 14.34 was found between Baseline (prior scleral lens fitting) and after 1 year of scleral lens wear ($p < 0.001$). Furthermore, these results are also in agreement with previous studies that claimed that tear film stability, tear film volume, tear film osmolarity, dry eye symptoms, tear film temperature and volume are not altered or are even improved after scleral lens fitting (Romero-Rangel et al., 2000; La Porta Weber et al., 2016; Walker, Schornack and Vincent, 2021).

The present study had some limitations that must be taken into accounts such as the sample size and the lack of a control group. No control group was included in the study and results were only compared with the baseline. Three cases could have happened if a control group was included. First, no differences in the control and scleral lens group would mean that scleral lens did not affect positively and negatively meibomian glands. Second, the control group showed a negative impact on meibomian glands whilst the scleral group did not show changes would mean that scleral lenses prevent the alteration of meibomian glands. Third, the control group improved meibomian glands while the scleral lens group did not show changes would mean that scleral lenses negatively impacted meibomian glands. Nonetheless, this last case might be improbable since it is not expected that meibomian glands improved in the control group without any treatment.

As there is no control group, it cannot be concluded whether the meibomian glands improved after scleral lens wear. Nevertheless, what it can be claimed is that scleral lenses did not affect negatively the structure and visibility of meibomian glands. Future research with a larger sample, with a longer follow-up and with a control group would be required in aged subjects in order to confirm these findings. This work represents the first step in the study of meibomian glands linked to scleral lens wear and further studies with a control group should confirm these preliminary results. In any case, the results of the present study allow a hypothesis to be built for testing in future studies.

Another limitation was that this study focused on the anatomical characteristics of meibomian glands rather than their function. Nevertheless, it has been previously reported (in *Chapter 8.1.2*) that meibomian gland visibility is correlated with gland expressiveness, tear film stability, TMH and bulbar redness (García-Marqués et al., 2021c). Moreover, in this study, the DED status was not taken into account. The procedure was semiautomatic since the clinician still has to manually eliminate the reflexes and delineate the region of interest of glands. However, despite it being semiautomatic, repeatability was moderate-acceptable. Besides, this study was only focused on meibographies of the upper eyelids because it was easier to capture a uniformly focused image of the tarsal plate (Koh et al., 2012).

Overall, the new method based on grey level intensity pixels of meibographies is also able to assess meibomian gland visibility in an objective and repeatable way in the Cobra fundus camera. This might suggest that the method is not instrument-specific.

Moreover, gland visibility metrics might help to assess the follow-up of meibomian glands after scleral lens wear. The present work adds valuable information regarding the effect of scleral lenses on meibomian gland drop-out and visibility. Scleral lens wear appears to not adversely affect meibomian gland drop-out and visibility while promoting comfortable wear and might improve dry eye symptoms after one year of lens wear. All of this may suggest that scleral lenses are not only preferable for visual rehabilitation of subjects with irregular cornea (86.2 % of the sample) but might also benefit their ocular surface comfort as these patients may be predisposed to DED and MGD. Further studies are needed to confirm this preliminary results with a control group and to assess the effect of scleral lenses on meibomian glands depending on DED diagnosis, in different age groups and with longer follow-up periods.

CHAPTER 9.5: The effects of soft contact lens wear on the tear film and meibomian gland drop-out and visibility

9.5 THE EFFECTS OF SOFT CONTACT LENS WEAR ON THE TEAR FILM AND MEIBOMIAN GLAND DROP-OUT AND VISIBILITY

Due to the effect of contact lenses on the tear film and the ocular surface (Korb, Greiner and Glonek, 1996), in this chapter, the effect of soft contact lens wear and duration on the tear film and meibomian glands will be assessed. Thus, the method developed in the *Chapter 8.1* will be applied to soft contact lens wearers to assess the meibomian gland drop-out and visibility. Likewise, it will be studied whether this new method based on the analysis of the visibility of meibomian glands is able to assess changes in glands between contact lens wearers and non-wearers.

9.5.1 Introduction

As explained in *Chapter 1 Introduction*, contact lens use has been acknowledged as a consistent risk factor for DED according to the TFOS DEWS II Epidemiology Report (Stapleton et al., 2017). The alteration of meibomian glands is a possible cause of contact lens-related dry eye (Arita et al., 2009a; Pucker and Tichenor, 2020). Some studies have assessed the effects of contact lens wear on meibomian glands and have reported lid margin abnormalities, gland obstruction, meibum abnormalities, and morphological and functional alterations of meibomian glands with contact lens wear, consequently leading to an increase in ocular symptoms (Korb and Henriquez, 1980; Henriquez and Korb, 1981; Arita et al., 2009a; Machalińska et al., 2015; Alghamdi et al., 2016; Arita, Fukuoka and Morishige, 2017d). Nevertheless, other studies have found

no association between contact lens wear and meibomian glands (Marren, 1994; Ong, 1996; Schaumberg et al., 2011; Nichols et al., 2013a).

Likewise, the association between MGD and contact lens wear is still controversial and demonstrating a relationship between contact lens discomfort and MGD is challenging (Ong, 1996; Nichols et al., 2013a; Machalińska et al., 2015; Arita, Fukuoka and Morishige, 2017d; Pucker et al., 2019b). In this way, the effect of contact lenses on meibomian glands, the tear film and the ocular surface is still unclear and some controversy remains. Moreover, it is not completely clear how the duration of contact lens wear impacts the ocular surface (Dumbleton et al., 2013a; Stapleton et al., 2017; Pucker et al., 2019b). Overall, further studies are required to clarify this topic (Dumbleton et al., 2013a; Stapleton et al., 2017; Kojima, 2018).

A new objective image-based method based on the visibility of meibomian glands has been developed in *Chapter 8.1* (García-Marqués et al., 2021a). Gland visibility has been proven to be used as a feature to aid in meibomian gland assessment. This method is based on the analysis of the grey intensity pixels of meibographies. As meibomian glands are lighter than the background, visibility is defined as the grade in which meibomian glands are seen, being low in individuals with high gland drop-out since glands have lost totally their visibility. Nevertheless, it has been demonstrated in *Chapter 8.1.1* that meibomian gland visibility is not the same as meibomian gland drop-out since the authors of a recent study found different gland visibilities in groups with similar gland drop-out (García-Marqués et al., 2021a). Thus, not only are gland

visibility metrics useful in detecting gland drop-out, but they also grade the level of gland visibility in individuals that have similar gland drop-out.

As found in *Chaper 8.1.2*, gland visibility metrics are significantly correlated with gland expressibility, tear film stability, tear meniscus and bulbar redness (García-Marqués et al., 2021c). Moreover, in *Chapter 8.1.2* (García-Marqués et al., 2021c), it was also found that meibomian gland visibility metrics have good diagnostic capability to diagnose MGD, being higher than current diagnostic metrics such as meibomian gland drop-out. The present study goes one step further by analyzing, for the first time, the effect of soft contact lenses on meibomian gland visibility. It is hypothesized that these new metrics could be used as an objective and complementary tool to assess the effect of contact lenses on meibomian glands.

Due to the effect of contact lenses on the tear film and the ocular surface (Korb, Greiner and Glonek, 1996), the relevance of the tear film in contact lens fitting (Foulks et al., 2013) and the controversy found in the effect of contact lenses on meibomian glands (Dumbleton et al., 2013a; Stapleton et al., 2017; Pucker et al., 2019b), the present study aims to assess the effect of soft contact lens wear and duration on meibomian glands, the tear film and ocular surface parameters. Furthermore, it will be studied whether a new method based on the analysis of the visibility of meibomian glands is able to assess changes in glands between contact lens wearers and non-wearers.

9.5.2 Methodology

Thirty healthy, non-contact lens wearers ranging in age between 18 to 30 years (22.5 ± 2.3 years) and twenty-four healthy, long-term soft contact lens wearers, with a duration of contact lens wear of at least 3 years, and ranging in age between 19 to 27 years (23.8 ± 2.2) participated in this study. Participants who had never worn contact lenses made up the control group. No exclusion based on the tear film or meibomian gland parameters was made to assess different ocular surface and tear film status. Participants with ocular surface complications in the last 6 months were excluded from the study (Uçakhan and Arslanturk-Eren, 2019). Contact lens wearers were instructed to remove their contact lenses on the night before the study and to attend the visit without wearing their contact lenses (Machalińska et al., 2015; Pucker et al., 2015; Alghamdi et al., 2016; Uçakhan and Arslanturk-Eren, 2019; Harbiyeli et al., 2022). Only the right eye of each participant was assessed to avoid data bias (Arita et al., 2009a; Harbiyeli et al., 2022). The study was carried out following the tenets of the Declaration of Helsinki and was approved by the Ethics Committee of the University of Valencia. Written consent from each participant was obtained after a verbal explanation of the protocol, nature and possible consequences of the study.

Measurements

The ocular surface of participants was assessed using the Oculus Keratograph 5M (K5 M; Oculus GmbH, Wetzlar, Germany) by the same experienced examiner within a single visit, as explained in *Chapter 3 General Methodology*. Examiner was masked as to the group each participant belonged to. Measurements were performed following

the guidelines of the TFOS DEWS II Diagnostic Methodology Report, to avoid the destabilization of the tear film, in the following order (Wolffsohn et al., 2017): OSDI, DEQ-5, total bulbar redness, TMH, NIKBUT and upper eyelid meibography. All measurements were performed at the same time of the day to avoid the influence of diurnal variations (Gu et al., 2020a) and the temperature and humidity of the room were maintained at 24.4 ± 1.5 °C and 44.8 ± 4.3 %, respectively.

Contact lens users were surveyed on their wearing habits, including years of contact lens wear and days per week and hours per day of contact lens wear on average. The hours of contact lens wear per week was calculated by multiplying days per week and hours per day.

Meibomian gland visibility was assessed using the validated method in *Chapter 8.1* (*Figure 9.5.1*) (García-Marqués et al., 2021a; García-Marqués et al., 2021c). The mentioned method was developed using Matlab© R2018a software (MathWorks, Natick, MA) and different metrics based on the grey level intensity of pixel of meibographies were calculated: Relative energy, energy, entropy, SD irregularity, mean pixels intensity, SD pixels intensity, median pixels intensity, kurtosis and skewness. Further details on these parameters and their rationale can be found in *Chapter 8.1* (García-Marqués et al., 2021a; García-Marqués et al., 2021c). Examiner was masked to the study group allocation of meibographies during analysis.

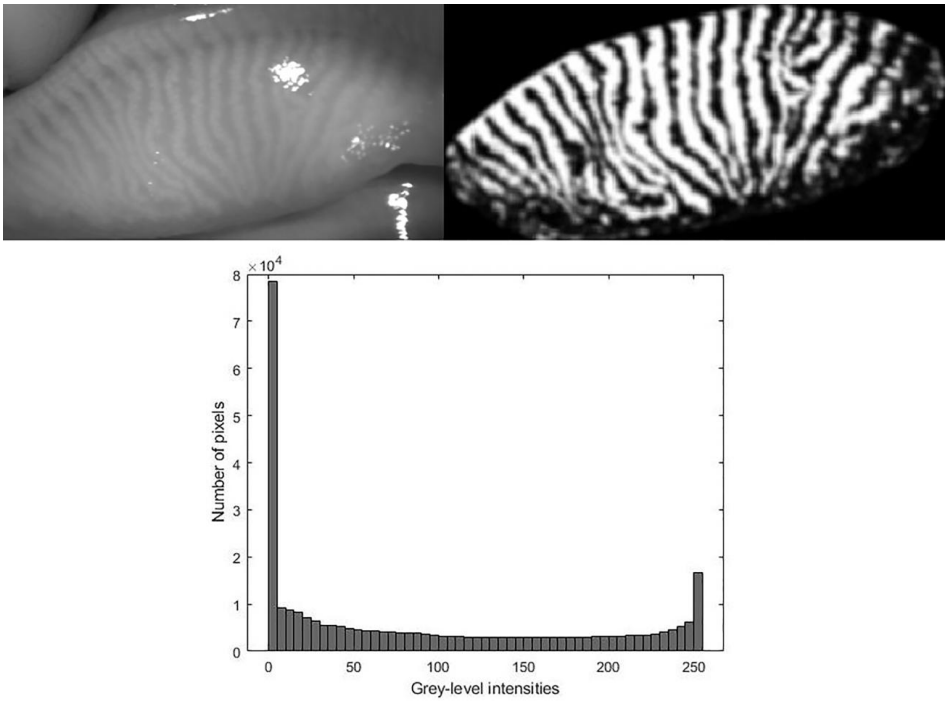

Fig. 9.5.1. *Meibography without image processing (top left), meibography after image processing (top right) and histogram of grey level intensity pixels of the processed meibography (down).*

Statistical analysis

Statistical analysis was performed using SPSS v26.0 for Windows (IBM Corp, Armonk, New York, USA). Results are shown as the mean ± SD. Normality distribution for each group and the total sample were assessed through the Shapiro-Wilk test. Differences in ocular surface parameters between groups (contact lens wearers and controls) were assessed by means of T-Test for independent samples or Mann-Whitney U test, depending on sample distribution. Sex differences between groups were evaluated using the Chi-square test. Moreover, participants with a gland drop-out higher than one-third of the total meibomian gland area (Arita et al., 2008) were

excluded from the analysis to prove whether differences in gland visibility metrics were a consequence of gland drop-out.

Furthermore, univariate logistic regression was initially performed to identify potential predictors of contact lens wear. Parameters with a p-value less than 0.15 were incorporated into the multivariate logistic regression analysis (Wang et al., 2020; Wang et al., 2021). Collinearity assumption was checked among variables. In the case that some variables achieved a p-value < 0.15 but did not follow the assumption of collinearity, the parameter with the lowest p-value was included in the multivariate logistic regression analysis.

Correlations between ocular surface signs and symptoms and hours of contact lens use per week and years of contact lens use were analyzed using Pearson or Rho Spearman correlations for the contact lens group.

Contact lens group was also divided into two groups depending on the years of contact lens wear and the hours of contact lens use per week. The median value was used as the cut-off value to divide the sample into two groups. The cut-off value for years of contact lens wear was 8 years, and the cut-off value for hours of contact lens use per week was 60 hours. Differences in ocular surface parameters between groups (high use of contact lenses or low use of contact lenses) were assessed by means of T-Test for independent samples or Mann-Whitney U test, depending on sample distribution. Sex differences between groups were evaluated using the Chi-square test. Finally, binomial logistic regression was performed to assess the predictability of ocular

surface parameters to the duration of contact lens use. A p-value less than 0.05 was defined as statistically significant.

9.5.3 Results

Thirty non-contact lens wearers (21 females and 9 males) and twenty-four long-term soft contact lens wearers (14 females and 10 males) were assessed in the present study. Mean age was 22.5 ± 2.3 years (ranging from 18 to 30 years old) and 23.8 ± 2.2 years (ranging from 19 to 27 years old) for the control and contact lens groups, respectively. No statistically significant differences in age or sex were found between groups ($p = 0.254$ and $p = 0.650$, respectively).

Differences between contact lens and non-contact lens wearers

Table 9.5.1 shows the main results obtained for each group. The contact lens group showed statistically and clinically higher gland drop-out and lower values in gland visibility metrics, except for SD irregularity and SD of ROI grey pixels intensity. Nevertheless, contact lens use had no impact on dry eye symptoms, TMH, bulbar redness and NIKBUT ($p > 0.005$).

Table 9.5.1. *Mean values for each group and comparison between them.*

Metric	Control group (Mean±SD)	Contact lens group (Mean±SD)	Significance level (p-value)
OSDI	14.89±12.62	18.30±16.70	0.978[2]
DEQ-5	6.21±5.10	7.14±4.41	0.687[1]
TMH (mm)	0.22±0.053	0.20±0.07	0.292[1]
Bulbar redness	0.50±0.24	0.60±0.26	0.381[2]
NIKBUT (seconds)	14.87±8.01	16.87±8.47	0.526[2]
Drop-out percentage (%)	25.50±6.77	37.74±11.42	<0.001[1]*
Relative energy	0.38±0.06	0.30±0.09	<0.001[1]*
Energy	245.07±4.93	238.60±7.32	0.012[1]*
Entropy	3.8×10^{-5}±9.2×10^{-6}	4.6×10^{-5}±1.0×10^{-5}	0.022[2]*
SD Irregularity	0.28±0.07	0.23±0.08	0.069[1]
Mean ROI pixels intensity	109.39±11.76	95.66±17.25	0.004[1]*
SD ROI pixels intensity	76.43±5.72	74.36±8.41	0.283[1]
Median ROI pixels intensity	92.36±17.84	72.17±21.43	<0.001[1]*
Kurtosis	0.0103±0.0006	0.0116±0.019	0.001[1]*
Skewness	0.103±0.004	0.109±0.009	0.001[1]*

*(Where DEQ-5: 5-item Dry Eye Questionnaire; NIKBUT: Non-Invasive Keratograph Break-Up Time; OSDI: Ocular Surface Disease Index; ROI: Region of Interest; SD: Standard Deviation; TMH: Tear Meniscus Height; [1]T-Test.; [2]Mann-Whitney U test; *Statistically significant values)*

Differences between groups without participants with high gland drop-out

Twelve participants in the contact lens group and two in the control group had a gland drop-out higher than one third. The Chi-square test revealed that the proportion of participants with high gland drop-out was higher in the contact lens group than in the control (p = 0.008). No statistically significant differences were found in age between groups (p = 0.241).

Table 9.5.2 shows the mean values for each group and the comparison between them after excluding participants with high gland drop-out. No statistically significant

differences were found between groups in any parameter ($p > 0.05$), suggesting that differences in gland visibility between groups were due to the higher gland drop-out in contact lens wearers.

Table 9.5.2. *Mean values for the control and the contact lens groups and comparison between them after excluding participants with a gland-out higher than one-third of the total meibomian gland area.*

Metric	Control group (Mean±SD)	Contact lens group (Mean±SD)	Significance level (p-value)
Age (years)	22.5 ± 2.4	23.7 ± 3.1	0.241[1]
OSDI	14.90±12.62	10.03±9.35	0.398[2]
DEQ-5	6.21±5.10	4.75±3.59	0.602[1]
TMH (mm)	0.22±0.05	0.18±0.06	0.109[1]
Bulbar redness	0.50±0.23	0.53±0.0.22	0.752[1]
NIKBUT (seconds)	14.28±8.06	13.94±9.27	0.887[2]
Drop-out percentage (%)	24.52±6.11	28.82±4.86	0.124[1]
Relative energy	0.39±0.60	0.36±0.67	0.313[1]
Energy	245.02±5.15	242.98±9.70	0.482[1]
Entropy	$4.5 \times 10^{-5} \pm 9.6 \times 10^{-6}$	$4.3 \times 10^{-5} \pm 8.2 \times 10^{-6}$	0.606[1]
SD Irregularity	0.28±0.08	0.27±0.08	0.670[1]
Mean ROI pixels intensity	109.85±12.17	104.65±13.67	0.371[1]
SD ROI pixels intensity	76.13±5.76	76.56±6.51	0.874[1]
Median ROI pixels intensity	93.70±17.90	85.00±19.81	0.308[1]
Kurtosis	0.0102±0.0006	0.0107±0.0012	0.216[1]
Skewness	0.103±0.003	0.105±0.005	0.249[1]

(Where DEQ-5: 5-item Dry Eye Questionnaire; NIKBUT: Non-Invasive Keratograph Break-Up Time; OSDI: Ocular Surface Disease Index; ROI: Region of Interest; SD: Standard Deviation; TMH: Tear Meniscus Height; [1]T-Test; [2]Mann-Whitney U test)

Binomial logistic regression

Table 9.5.3 shows the univariate and multivariate-adjusted logistic regression analysis, along with the odds ratios of contact lens use for each parameter. Univariate

logistic regression identified the following parameters as potential predictors of contact lens wear: gland drop-out, relative energy, energy, entropy, SD irregularity, mean pixels intensity, median pixels intensity, kurtosis and skewness. The interaction between them in the multivariate logistic regression revealed that gland drop-out percentage was independently associated with the use of contact lenses (p = 0.006). When gland drop-out was excluded from the analysis (*Table 9.5.4*), relative energy showed an independent association with contact lens wear (p = 0.005).

Table 9.5.3. *Univariate and multivariate logistic regressions and odds ratios of contact lens wear for demographic and clinical characteristics.*

Characteristic	Univariate logistic regression				Multivariate logistic regression			
	Odd ratio	Lower CI	Upper CI	p-value	Odd ratio	Lower CI	Upper CI	p-value
Age	1.054	0.995	1.029	0.284				
Sex	1.050	0.164	6.724	0.959				
OSDI	1.018	0.960	1.080	0.553				
DEQ-5	1.043	0.860	1.264	0.669				
TMH (mm)	0.001	0.000	326.650	0.284				
Bulbar redness	4.779	0.274	83.313	0.283				
NIKBUT (seconds)	1.032	0.945	1.127	0.486				
Drop-out percentage (%)	**1.203**	**1.051**	**1.376**	**0.007***	1.207	1.053	1.382	0.006*
Relative energy	**0.000**	**0.000**	**0.029**	**0.013***	0.000	0.000	5.235	0.521
Energy	0.829	0.823	1.049	0.029*				
Entropy	**1.182**	**1.094**	**2.084**	**0.015***	1.152	1.052	1.810	0.282
SD Irregularity	0.000	0.000	3.321	0.081				
Mean ROI pixels intensity	0.927	0.869	0.989	0.022*				
SD ROI pixels intensity	0.954	0.860	1.058	0.375				
Median ROI pixels intensity	0.944	0.902	0.988	0.014*				
Kurtosis	1.782	1.098	8.698	0.022*				
Skewness	1.487	1.424	1.553	0.024*				

(Where DEQ-5: 5-item Dry Eye Questionnaire; NIKBUT: Non-Invasive Keratograph Break-Up Time; OSDI: Ocular Surface Disease Index; ROI: Region of Interest; SD: Standard Deviation; TMH: Tear Meniscus Height; CI: 95 % Confidence Interval;

**Statistically significant values; Bold: Variables included in the multivariate analysis (p < 0.15))*

Table 9.5.4. *Multivariate logistic regressions and odds ratios of contact lens use after excluding gland drop-out percentage.*

	Multivariate logistic regression			
	Odd ratio	Lower CI	Upper CI	p-value
Relative energy	0.000	0.000	0.021	0.005*
Entropy	1.224	1.119	1.523	0.213

*(Where CI: 95 % Confidence Interval. *Statistically significant values)*

Relationship between ocular surface parameters and duration of contact lens wear

Table 9.5.5 shows the correlations between ocular surface parameters and hours of contact lens wear per week and years of contact lens wear, respectively. Statistically significant correlations were found between hours of contact lens wear and DEQ-5 score, TMH and entropy of grey pixels intensity. Likewise, years of contact lens wear was positively correlated with the entropy of grey pixels intensity and negatively with NIKBUT. No other significant correlation was found with other ocular surface parameters.

Table 9.5.5. *Correlations between ocular surface parameters and hours of contact lens wear per week and years of contact lens wear.*

	Metric	Correlation coefficient (r)	Significance level (p-value)
Hours of contact lens use per week	OSDI	0.292	0.111[2]
	DEQ-5	0.387	0.031[1]*
	TMH (mm)	-0.357	0.049[2]*
	Bulbar redness	0.182	0.328[1]
	NIKBUT (seconds)	-0.254	0.169[2]
	Drop-out percentage (%)	0.053	0.778[1]
	Relative energy	-0.203	0.274[1]
	Energy	-0.176	0.345[2]
	Entropy	0.436	0.014[2]*
	SD Irregularity	-0.213	0.251[1]
	Mean ROI pixels intensity	-0.235	0.203[1]
	SD ROI pixels intensity	-0.272	0.138[1]
	Median ROI pixels intensity	-0.212	0.253[1]
	Kurtosis	0.254	0.168[1]
	Skewness	0.248	0.179[1]
Years wearing contact lenses	OSDI	0.269	0.144[2]
	DEQ-5	0.089	0.635[2]
	TMH (mm)	-0.069	0.710[2]
	Bulbar redness	0.038	0.838[2]
	NIKBUT (seconds)	-0.355	0.045[2]*
	Drop-out percentage (%)	0.037	0.842[2]
	Relative energy	-0.073	0.697[2]
	Energy	-0.210	0.258[2]
	Entropy	0.382	0.034[2]*
	SD Irregularity	-0.116	0.533[2]
	Mean ROI pixels intensity	-0.120	0.521[2]
	SD ROI pixels intensity	-0.161	0.387[2]
	Median ROI pixels intensity	-0.008	0.965[2]
	Kurtosis	0.016	0.934[2]
	Skewness	0.032	0.865[2]

*(Where DEQ-5: 5-item Dry Eye Questionnaire; NIKBUT: Non-Invasive Keratograph Break-Up Time; OSDI: Ocular Surface Disease Index; ROI: Region of Interest; SD: Standard Deviation; TMH: Tear Meniscus Height; [1]Pearson coefficient; [2]Spearman coefficient; *Statistically significant values)*

Participants were also classified depending on the years of contact lens wear (*Table 9.5.6*). Twelve participants (7 females and 5 males) were classified into the group of contact lens wear < 60 hours per week and twelve (7 females and 5 males) in the group of contact lens wear ≥ 60 hours per week. Mean age was 23.6 ± 2.2 and 23.9 ± 2.4 years old for participants wearing contact lenses < 60 hours per week and ≥ 60 hours per week, respectively ($p = 0.720$). Moreover, eleven participants (6 females and 5 males) were classified into the group of contact lens wear < 8 years and thirteen (8 females and 5 males) in the group of contact lens wear ≥ 8 years. Mean age was 23.4 ± 2.4 and 24.0 ± 2.3 years old for participants wearing contact lenses < 8 years and ≥ 8 years, respectively ($p = 0.654$). The Chi-square test did not reveal statistically significant differences in sex between groups for hours per week ($p = 0.685$) and years of contact lens wear ($p = 0.625$).

Participants wearing contact lenses for more hours per week showed higher DEQ-5 and entropy values; whilst participants wearing contact lenses more years had higher OSDI and entropy and lower NIKBUT. No statistically significant differences were found for the rest of the parameters assessed.

Table 9.5.6. *Comparison of ocular surface parameters depending on hours of contact lens wear per week and years of contact lens wear.*

Metric	< 60 hours per week (Mean±SD)	≥ 60 hours per week (Mean±SD)	Significance level (p-value)
Weekly hours wearing contact lenses	29.07±17.24	77.19±13.00	<0.001[2]*
OSDI	12.87±10.84	19.89±21.03	0.423[2]
DEQ-5	5.27±3.51	8.31±3.59	0.028[1]*
TMH (mm)	0.22±0.06	0.18±0.06	0.167[1]
Bulbar redness	0.62±0.27	0.65±0.34	0.758[1]
NIKBUT (seconds)	16.58±5.50	15.03±5.27	0.379[2]
Drop-out percentage (%)	35.10±9.39	37.40±10.24	0.095[1]
Relative energy	0.34±0.06	0.30±0.08	0.105[1]
Energy	239.04±2.93	237.47±5.12	0.626[2]
Entropy	$3.8 \times 10^{-5} \pm 6.0 \times 10^{-6}$	$4.6 \times 10^{-5} \pm 1.2 \times 10^{-5}$	0.027[2]*
SD Irregularity	0.23±0.08	0.21±0.09	0.142[1]
Mean ROI pixels intensity	99.00±11.70	90.91±15.32	0.108[1]
SD ROI pixels intensity	74.91±6.03	74.50±5.35	0.251[1]
Median ROI pixels intensity	78.69±16.74	70.67±23.14	0.082[1]
Kurtosis	0.0113±0.0018	0.0116±0.0019	0.051[1]
Skewness	0.106±0.004	0.109±0.008	0.057[1]
Metric	< 8 years of contact lens wear (Mean±SD)	≥ 8 years of contact lens wear (Mean±SD)	Significance level (p-value)
Years wearing contact lenses	5.0±1.0	11.9±2.5	<0.001[1]*
OSDI	18.60±17.86	26.35±13.85	0.048[2]*
DEQ-5	7.57±2.85	7.88±4.53	0.852[1]
TMH (mm)	0.20±0.09	0.19±0.07	0.544[2]
Bulbar redness	0.62±0.27	0.65±0.34	0.732[1]
NIKBUT (seconds)	17.00±6.10	10.07±2.42	0.008[1]*
Drop-out percentage (%)	36.68±10.73	37.62±10.83	0.729[1]
Relative energy	0.30±0.08	0.29±0.07	0.728[1]
Energy	238.49±3.06	238.02±5.29	0.570[2]
Entropy	$3.9 \times 10^{-5} \pm 1.0 \times 10^{-5}$	$4.6 \times 10^{-5} \pm 1.0 \times 10^{-5}$	0.039[2]*
SD Irregularity	0.23±0.09	0.21±0.09	0.523[1]
Mean ROI pixels intensity	96.26±17.75	94.12±16.72	0.679[1]
SD ROI pixels intensity	76.30±7.67	73.25±6.93	0.450[1]
Median ROI pixels intensity	75.29±23.24	70.65±19.31	0.832[1]
Kurtosis	0.0116±0.0018	0.0116±0.0019	0.940[1]
Skewness	0.109±0.008	0.109±0.009	0.897[1]

(Where DEQ-5: 5-item Dry Eye Questionnaire; NIKBUT: Non-Invasive Keratograph Break-Up Time; OSDI: Ocular Surface Disease Index; ROI: Region of Interest; SD:

*Standard Deviation; TMH: Tear Meniscus Height; [1]T-Test; [2]Mann-Whitney U test; *Statistically significant values)*

Table 9.5.7 shows the univariate and multivariate-adjusted logistic regression analysis, along with the odds ratios of ≥ 60 hours of contact lens use per week and ≥ 8 years of contact lens use. Univariate logistic regression identified the following parameters as potential predictors of ≥ 60 hours of contact lens use per week: DEQ-5, gland drop-out percentage, relative energy, entropy, SD irregularity, mean pixels intensity, median pixels intensity, kurtosis and skewness. The interaction between them in the multivariate logistic regression revealed that DEQ-5 and entropy were independently associated with the use of contact lenses ≥ 60 hours per week ($p < 0.029$).

Univariate logistic regression identified the following parameters as potential predictors of ≥ 8 years of contact lens use: OSDI, NIKBUT and entropy. The interaction between them in the multivariate logistic regression revealed that NIKBUT was independently associated with the use of contact lenses ≥ 8 years ($p = 0.030$).

Table 9.5.7. *Univariate and multivariate logistic regressions and odds ratios of contact lens use ≥ 60 hours per week and of contact lens use ≥ 8 years for demographic and clinical characteristics.*

Contact lens use ≥ 60 hours								
Characteristic	Univariate logistic regression				Multivariate logistic regression			
	Odd ratio	Lower CI	Upper CI	p-value	Odd ratio	Lower CI	Upper CI	p-value
Age	1.074	0.894	1.292	0.446				
Sex	1.818	0.350	9.455	0.477				
OSDI	1.017	0.922	1.098	0.197				
DEQ-5	**1.027**	**1.012**	**1.595**	**0.039***	1.330	1.028	1.718	0.029*
TMH (mm)	0.001	0.000	28.250	0.176				
Bulbar redness	1.477	0.136	16.130	0.749				
NIKBUT (seconds)	0.944	0.822	1.085	0.418				
Drop-out percentage (%)	**1.100**	**0.980**	**1.234**	**0.105**	1.044	0.789	1.382	0.762
Relative energy	0.000	0.000	8.264	0.111				
Energy	0.905	0.752	1.091	0.296				
Entropy	**2.837**	**1.390**	**57.890**	**0.044***	1.298	1.194	2.857	0.042*
SD Irregularity	0.000	0.000	9.524	0.105				
Mean ROI pixels intensity	0.955	0.902	1.011	0.113				
SD ROI pixels intensity	0.888	0.728	1.085	0.244				
Median ROI pixels intensity	0.966	0.929	1.006	0.092				
Kurtosis	**1.182**	**1.088**	**6.698**	**0.064**	1.222	0.935	1.423	0.188
Skewness	1.492	1.399	6.501	0.068				
Contact lens use ≥ 8 years								
Characteristic	Univariate logistic regression				Multivariate logistic regression			
	Odd ratio	Lower CI	Upper CI	p-value	Odd ratio	Lower CI	Upper CI	p-value
Age	1.135	0.934	1.379	0.204				
Sex	1.152	0.958	8.480	0.421				
OSDI	**1.223**	**0.976**	**1.973**	**0.123**	1.012	0.959	1.068	0.662
DEQ-5	1.023	0.846	1.236	0.818				
TMH (mm)	0.027	0.000	442.450	0.466				
Bulbar redness	1.546	0.142	16.949	0.721				
NIKBUT (seconds)	**0.766**	**0.607**	**0.967**	**0.025***	0.745	0.570	0.972	0.030*
Drop-out percentage (%)	1.019	0.921	1.128	0.718				
Relative energy	0.152	0.000	4094.118	0.718				
Energy	0.972	0.817	1.156	0.748				
Entropy	**1.481**	**1.290**	**3.210**	**0.089**	1.431	1.105	1.673	0.216
SD Irregularity	0.059	0.000	260.172	0.508				
Mean ROI pixels intensity	0.989	0.939	1.041	0.668				

(continuation)								
Contact lens use ≥ 8 years								
Characteristic	Univariate logistic regression				Multivariate logistic regression			
	Odd ratio	Lower CI	Upper CI	p-value	Odd ratio	Lower CI	Upper CI	p-value
SD ROI pixels intensity	0.926	0.763	1.124	0.436				
Median ROI pixels intensity	0.996	0.962	1.031	0.825				
Kurtosis	1.186	1.018	1.526	0.937				
Skewness	1.158	1.025	1.516	0.892				

*(Where DEQ-5: 5-item Dry Eye Questionnaire; NIKBUT: Non-Invasive Keratograph Break-Up Time; OSDI: Ocular Surface Disease Index; ROI: Region of Interest; SD: Standard Deviation; TMH: Tear Meniscus Height; CI: 95 % Confidence Interval; *Statistically significant values; Bold = Variables included in the multivariate analysis (p < 0.15))*

9.5.4 Discussion

Ocular surface and contact lens wear

To the authors' knowledge, this is the first study that objectively assessed meibomian gland visibility in contact lens wearers as well as its relationship with the time of contact lens wear and other ocular surface parameters. In the present study, meibomian gland drop-out was higher in the contact lens group. These results are in line with previous research that found alterations in meibomian glands in contact lens wearers (Arita et al., 2009a; Machalińska et al., 2015; Kojima, 2018; Siddireddy et al., 2018a; Pucker et al., 2019a; Pucker et al., 2019b; Uçakhan and Arslanturk-Eren, 2019; Gu et al., 2020a; Llorens-Quintana, Garaszczuk and Szczesna-Iskander, 2020; Harbiyeli et al., 2022). Moreover, as meibomian gland drop-out is linked with meibomian gland visibility (*Chapter 8.1*) (García-Marqués et al., 2021a; García-Marqués et al., 2021c),

lower gland visibility was also found in contact lens wearers. When participants with a gland drop-out higher than one-third were excluded from the analysis, it was proved that the low gland visibility found in contact lens wearers was a consequence of the gland drop-out in these participants, since no differences were found between groups.

Multivariate logistic regression revealed that gland drop-out percentage was independently associated with the use of contact lenses. Each additional percentage of gland drop-out increased the probability of being in the contact lens group by 1.2 times. As changes in gland visibility were a consequence of gland drop-out in contact lens wearers, gland drop-out was excluded to assess whether gland visibility metrics were independently associated with the use of contact lenses. When gland drop-out was excluded from the analysis, relative energy was independently associated with the use of contact lenses. In another work (Pucker et al., 2015), authors found that a higher meiboscore was independently associated with being a contact lens wearer, but not gland atrophy percentage.

This does not mean that gland drop-out is a more powerful metric than gland visibility metrics, but that gland visibility does not change independently of gland drop-out in contact lens wearers. Nevertheless, not only are gland visibility metrics useful to detect gland drop-out, but they also measure the visibility of glands. According to *Chapter 8.1*, gland visibility metrics are different from gland drop-out because gland visibility could achieve different values depending on the visibility of glands in participants with similar gland drop-out (García-Marqués et al., 2021a). Moreover, meibomian gland visibility metrics have good sensitivity and specificity to diagnose

MGD, having higher diagnostic capability than current diagnostic metrics such as meibomian gland drop-out (García-Marqués et al., 2021c). Results of the present study suggest that new metrics based on the visibility of meibomian glands can detect changes in the meibomian glands of contat lens wearers. However, despite gland visibility being different from gland drop-out (as found in *Chapter 8.1*) (García-Marqués et al., 2021a), the changes in gland visibility in the present study are attributed to gland drop-out. Thus, gland visibility does not change independently of gland drop-out in contact lens wearers. Despite this, gland visibility metrics can detect alterations in meibomian glands in contact lens wearers and they might be used in the follow-up of meibomian glands in these individuals as a quick, patient-friendly and objective method.

Dry eye symptoms, TMH, bulbar redness and NIKBUT showed a tendency to be worse in contact lens wearers but the difference was not statistically significant between groups. Therefore, in the present study, contact lens wear did not cause changes in these parameters. This is in opposition with the results found in previous studies, which found lower tear meniscus (Alghamdi et al., 2016; Gu et al., 2020b) and more dry eye symptoms (Muselier-Mathieu et al., 2013; Uçakhan and Arslanturk-Eren, 2019; Gu et al., 2020a; Gu et al., 2020b; Harbiyeli et al., 2022), bulbar redness (Machalińska et al., 2015) and tear film instability (Arita et al., 2009a; Muselier-Mathieu et al., 2013; Alghamdi et al., 2016; Siddireddy et al., 2018a; Uçakhan and Arslanturk-Eren, 2019; Gu et al., 2020a; Gu et al., 2020b) in contact lens wearers as compared to non-wearers. In agreement with the results found in the present study, Arita et al. (2009a), Machalińska et al. (2015) and Iqbal, Thomas and Mahadevan

(2021) did not find differences in tear volume between contact lens and non-contact lens wearers. Likewise, other authors did not find statistically significant differences between contact lens and non-contact lens wearers for OSDI (Machalińska et al., 2015), break-up time (Machalińska et al., 2015; Pucker et al., 2015; Iqbal, Thomas and Mahadevan, 2021; Harbiyeli et al., 2022), TMH, bulbar redness and tear osmolarity (Pucker et al., 2015). Differences between studies might be caused by differences in the methodological procedure since in some studies measurements were taken only a few hours after contact lens removal, which could have caused changes in ocular surface parameters. Moreover, there are also differences in the minimum period of years of contact lens wear to include a subject in the contact lens group. In the present work, contact lens wearers used contact lenses for at least 3 years and were instructed to remove their contact lenses on the night before the examination, following the methodology of previous works (Machalińska et al., 2015; Pucker et al., 2015; Alghamdi et al., 2016; Uçakhan and Arslanturk-Eren, 2019; Harbiyeli et al., 2022).

Relationship between ocular surface parameters and duration of contact lens wear

The effect of the duration of contact lens wear on meibomian glands and tear film has also some controversy (Arita et al., 2009a; Schaumberg et al., 2011; Alghamdi et al., 2016; Pucker et al., 2019b). In the present work, hours of contact lens wear per week was positively correlated with DEQ-5 and entropy, and negatively correlated with TMH. Thus, participants who used contact lenses for more hours per week had less TMH and higher dry eye symptoms and entropy in meibomian glands. Years of contact lens wear was also negatively correlated with NIKBUT and positively correlated with

entropy. Entropy measures the randomness of the grey level distribution (Haralick, 1979; Alonso-Caneiro et al., 2013), which might be useful for the analysis of parameters related to meibography arrangement such as tortuosity of glands (García-Marqués et al., 2021a). This might suggest that participants that used contact lenses for more hours per week and for more years had higher tortuosity in meibomian glands. A previous work (Siddireddy et al., 2018a) also found morphological irregularities in meibomian glands in symptomatic contact lens wearers.

In the present study, no association was found between contact lens duration and gland drop-out and visibility. In agreement with the results of this study, other authors (Alghamdi et al., 2016; Llorens-Quintana, Garaszczuk and Szczesna-Iskander, 2020) found that alterations in meibomian glands are either long-term or take place in an early phase of contact lens wear. Thus, Alghamdi et al. (2016) found changes in meibomian glands during the first 2 years of contact lens wear, but prolonged exposure to contact lens beyond this point was not associated with further changes in meibomian glands. This might be explained by some adaptive mechanism in the eyelid tissues (Alghamdi et al., 2016). Therefore, this might explain why no differences were found in gland drop-out in this study. As contact lens wearers in the present study reported using contact lenses for at least 3 years, meibomian gland drop-out might have taken place in the first years of contact lens wear, being stable after that early phase of contact lens use. On the other hand, these results suggest that gland tortuosity might increase with contact lens duration since the entropy of glands increased.

This is in opposition with the results of some authors that found that meibomian glands function and morphology is related to the duration of contact lens wear (Arita et al., 2009a; Machalińska et al., 2015; Uçakhan and Arslanturk-Eren, 2019; gu et al., 2020b; Harbiyeli et al., 2022). For instance, Arita et al. (2009a) found a significant positive correlation between meiboscore and the duration of contact lens wear. Nevertheless, both soft and rigid contact lens wearers were included in the study and participants with at least 1 year of contact lens wear were included, which is lower than the minimum years of lens wear in the present study. In another work (Uçakhan and Arslanturk-Eren, 2019), authors claimed that the meibomian glands of contact lens wearers deteriorate after 6 years of wear, but remain stable thereafter. Harbiyeli et al. (2022) also found that the hours of soft contact lens use was associated with the loss of meibomian glands in multivariate analysis. However, the duration of contact lens use was less than 5 years in more than half of the sample and they mixed soft and rigid contact lens wearers, the latter being more likely to experience more pronounced MGD. Therefore, this study might also confirm that changes in meibomian gland drop-out take place in the first years of contact lens use, which is in agreement with the results found in the present work. Moreover, the present study adds that the duration of contact lens wear might be related to gland tortuosity.

In the present work, the median of pixel intensity, kurtosis and skewness were almost statistically significant and showed a tendency to be worse in the group with more ≥ 60 hours of contact lens use per week. Thus, despite contact lens wearers having higher gland drop-out and lower gland visibility, no relationship was found between the time of contact lens use and gland drop-out and gland visibility, except

for entropy. This suggests that from three years of contact lens use, no changes in gland drop-out and gland visibility occur. Nevertheless, gland drop-out and kurtosis were identified as potential predictors of using contact lenses for ≥ 60 hours per week. Multivariate logistic regression revealed that DEQ-5 score and entropy were independently associated with the use of contact lenses for ≥ 60 hours per week. Each additional score in DEQ-5 and entropy increased the probability of being in the group with high contact lens use by 1.33 and 1.30 times, respectively.

Moreover, OSDI score, NIKBUT and entropy were identified as potential predictors of being a contact lens wearer for ≥ 8 years. A previous work (Uçakhan and Arslanturk-Eren, 2019) also found a higher OSDI score in individuals wearing contact lenses for more than 7 years and a lower break-up time in those wearing contact lenses for more than 7 years and between 3 and 7 years in comparison with a control group. Furthermore, tear film break-up time also worsened after 3 years of wear but seemed to remain stable after 6 years. In the present study, multivariate logistic regression revealed that NIKBUT was independently associated with being a contact lens wearer for ≥ 8 years. Every one second decrease in NIKBUT, increased the probability of being in the group with the high use of contact lenses 1.34 times.

The present study had some limitations to consider. First, participants were instructed to remove their contact lenses the night before the study and to attend the visit without wearing their contact lenses (Machalińska et al., 2015; Pucker et al., 2015; Alghamdi et al., 2016; Uçakhan and Arslanturk-Eren, 2019; Harbiyeli et al., 2022). This could have caused no statistically significant differences between groups in some

parameters such as NIKBUT, TMH or bulbar redness. Moreover, studies with different methodological procedures are not directly comparable. In addition, the method to measure gland visibility is semiautomatic and the clinician still has to manually eliminate reflexes and delineate the area of the glands. Nevertheless, the method is not instrument-specific and despite being semiautomatic, the repeatability was found to be acceptable (in *Chapter 8.1*) (García-Marqués et al., 2021a). Furthermore, only the upper eyelids were assessed since it was easier to capture an uniformly focused image of the tarsal plate (Koh et al., 2012). Arita et al. (2009a) found that the meiboscore in the upper eyelid was higher than in the lower eyelid in contact lens wearers. This might be because the upper eyelid becomes more irritated as it makes longer movements during blinking (Arita et al., 2009a). In another study (Uçakhan and Arslanturk-Eren, 2019), authors found that contact lenses influence upper eyelids in the early years of contact lens wear, but both eyelids were equally affected after 3 years. Therefore, in the present study, no differences between upper and lower eyelids are expected since all participants were contact lens wearers for at least 3 years. The present work was limited to soft contact lens wearers and differences with other contact lens designs or materials were not assessed, which might be studied in future studies. Finally, meibomian gland expressibility and lid margin abnormalities were not assessed in this work. However, in *Chapter 8.1*, gland visibility metrics were reported to be correlated with gland expressibility (García-Marqués et al., 2021c).

Overall, the present work adds valuable information regarding the effect of soft contact lens wear on the tear film, meibomian gland drop-out and meibomian gland visibility. Gland drop-out was higher and gland visibility lower in long-term soft contact

lens wearers in comparison to controls. Nevertheless, gland visibility changed in contact lens wearers as a consequence of gland drop-out. Prolonged hours of contact lens wear is associated with higher dry eye symptoms and entropy of meibomian glands, which might be a measurement of gland tortuosity; whilst more years of contact lens use is related to a reduction in NIKBUT. Therefore, contact lens wear might aggravate dryness and the alterations in meibomian glands that take place in advanced ages even more. Clinicians should assess the ocular surface in contact lens wearers and educate them to use contact lenses properly to maintain healthy meibomian glands and ocular surface. New gland visibility metrics might help to assess the follow-up of meibomian glands in soft contact lens wearers in a quick and objective way. Further studies are needed to confirm these preliminary results and to assess the effect of different soft contact lenses with other materials and designs on meibomian glands depending on DED diagnosis, in different age groups and with longer follow-up periods. A prospective, longitudinal study is required to understand associations between meibomian glands alterations and contact lens wear.

CHAPTER 9.6: Assessment of condition induced changes on the ocular surface using novel methods to assess the tear film dynamics and the lipid layer

9.6 ASSESSMENT OF CONDITION INDUCED CHANGES ON THE OCULAR SURFACE USING NOVEL METHODS TO ASSESS THE TEAR FILM DYNAMICS AND THE LIPID LAYER

In this chapter, the effect of computer use, contact lens wear and artificial tears on new metrics developed in *Chapters 8.2 and 8.3* and current ones will be assessed. Digital devices and contact lenses have been identified as potential risk factors for DED according to the TFOS DEWS II Epidemiology Report (Stapleton et al., 2017). Moreover, the instillation of artificial tears is generally accepted as one of the main management strategies for DED (Jones et al., 2017). Thus, it will be studied whether these new metrics are able to detect changes in the tear film and the ocular surface in a non-invasive and objective way, which might help to further validate these metrics and find clinical applications for them.

9.6.1 Introduction

As explained in *Chapter 2 Justification*, the TFOS DEWS II Diagnostic Methodology Report acknowledged the need of developing new, non-invasive and objective metrics to assess the tear film (Abdelfattah et al., 2015; Ji et al., 2017; Wolffsohn et al., 2017; King-Smith, Begley and Braun, 2018). Two methods have been validated in *Chapters 8.2 and 8.3* to non-invasively assess the tear film in an objective manner (García-Marqués et al., 2021d; García-Marqués et al., 2021e). The first method tried to overcome the issues of the NIKBUT procedure. NIKBUT does not allow the assessment of the tear film under completely natural conditions because subjects must keep their eyes open forcefully and this might cause reflex tearing (King-Smith, Begley and Braun,

2018; Lai et al., 2019). Thus, a method to assess tear film-dynamic in natural conditions was developed. As explained in *Chapter 8.2*, the method is based on the in vivo measurement of the speed of tear film particles post-blink (García-Marqués et al., 2021d). These particles are a combination of eroded epithelial corneal cells, tarsal conjunctival cells, mucin-contaminated lipid particles and small air bubbles (Owens and Phillips, 2001; Khanal and Millar, 2010; Varikooty, Keir and Simpson, 2012; Lai et al., 2019). In *Chapter 8.2*, it was found to provide emerging homeostasis parameters for assessing indirectly the tear film quality in natural conditions with acceptable repeatability (García-Marqués et al., 2021d).

On the other hand, the method developed in *Chapter 8.3*, attempted to measure the lipid layer thickness in an objective way without the need for an interferometer through the analysis of the grey intensity values obtained from the Placido disk pattern reflected onto the tear film. In *Chapter 8.3*, it was found that it can be used as an objective tool to measure the lipid layer thickness with acceptable repeatability, accuracy and diagnostic capability (García-Marqués et al., 2021e).

The present work goes one step further by assessing the effect of computer use, contact lens wear and artificial tears on these new metrics and current ones. It is widely known that the tear film and ocular surface parameters are affected by the use of digital devices (Stapleton et al., 2017; Talens-Estarelles et al., 2020; Talens-Estarelles et al., 2021a) and contact lenses (Gomes et al., 2017; Stapleton et al., 2017). Thus, both have been identified as potential risk factors for DED according to the TFOS DEWS II Epidemiology Report (Stapleton et al., 2017). Moreover, the instillation of artificial

tears is generally accepted as one of the main management strategies for DED (Jones et al., 2017).

The present study aims to assess the effect of computer use, contact lenses and artificial tears on the newly developed metrics and current ones. The hypothesis is that new metrics are able to detect changes in the tear film and the ocular surface in a non-invasive and objective way. The present study might help to further validate these metrics and find clinical applications for them such as the assessment of the ocular surface in contact lens wearers, computer users or in subjects under artificial tears treatment.

9.6.2 Methodology

Eighty-four healthy volunteers ranging in age from 18 to 27 years (22.4 ± 2.6 years) participated in this study. Participants had no prior history of ocular disease or injury in the last three months. Refraction and visual acuity were obtained and participants with an astigmatism > 0.75 dioptres or with a monocular or binocular near and distance visual acuity > 0.00 logMAR were excluded from the study. Contact lens users were instructed not to wear their contact lenses within a day before the first visit. Only the right eye of participants was measured to avoid data duplication. The study was performed following the tenets of the Declaration of Helsinki and was approved by the Ethics Committee of the University of Valencia. Written consent of each participant was obtained after a verbal explanation of the study protocol.

Experimental design

Figure 9.6.1 summarizes the experimental design of the study in both visits.

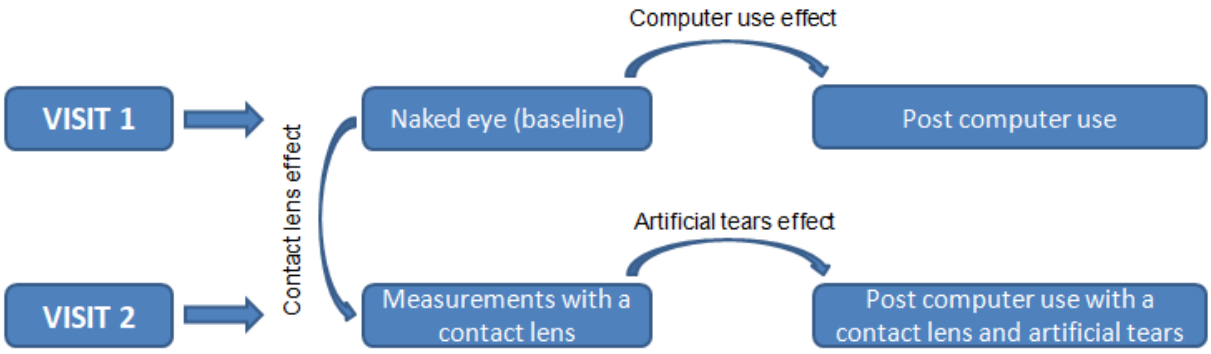

Fig. 9.6.1. *Experimental design of the study.*

The ocular surface and tear film of participants were assessed at (1) baseline, (2) after reading on a modern laptop computer for 20 minutes, (3) after the insertion of a contact lens and (4) after reading on a computer with contact lenses and initial artificial tears instillation. Participants completed a total of two visits. In the first visit, the participants' ocular surface and tear film were assessed at baseline. To minimize the effects of outdoor conditions on the way to the laboratory, a 15-minute acclimatization period was left between the entry into the room of the participants and the measurements. Then participants performed a reading task on a modern laptop computer for 20 minutes. After the 20-minute reading task, the battery of standard clinical tests was repeated. After the visit, contact lens wearers were fitted with contact lenses and were instructed to put in the contact lenses 1 hour previous to the second visit. In the second visit, measurements were repeated (with the contact lenses). Next, participants were instructed to read on the computer for 20 minutes

while wearing the contact lenses. One drop of Systane® Ultra (Alcon SL, Geneva, Switzerland) single-dose artificial tears were instilled on each eye, 2 minutes before the reading. Finally, after the 20-minute reading task, the ocular surface and the tear film were assessed for one last time. Participants were instructed not to use other digital devices 30 minutes previous to the visits. A rest period of 7 days between sessions was established. The approximate duration of each session was 45 minutes. Moreover, each session was performed at the same time of the day and the same day of the week.

The text material was Allan Poe's full stories, displayed using Kindle (2021) reading application (Amazon Inc., Seattle, WA). The font style was Georgia with black letters on a white background, with a 0.15 logMAR visual acuity, angular line spacing, a limited number of words per line and page, page angular width of 25° width, and the text was left-justified. The display was a MacBook Air Retina 2020 laptop computer (Apple Inc., Cupertino, CA) with a 13-inch screen, a resolution of 227 pixels per inch, a refresh rate of 60 Hz and a contrast ratio of 1350:1. The device was placed at 60 cm and a 10º angle below the eyes since it is the usual distance to work with a computer. Participants performed the task with the head fixed in a chin and forehead to minimize head movements. The illuminance, temperature and humidity of the room were maintained at 200 lux, 24.4 ± 1.3 °C and 44.7 ± 5.2 %, respectively.

Contact lenses

After the first visit, participants who were contact lens wearers were binocularly fitted with a daily-disposable contact lens (Dailies Total One®, Alcon Laboratories Inc.

Fort Worth TX, USA), according to the manufacturer's guidelines for the initial lens selection. These contact lenses are made of Delefilcon A with a water content of 33 % in the nucleus and > 80 % in the surface. After a set period of 5 minutes, distance and near logMAR visual acuity was assessed and contact lens correct movement and centration were checked using a slit-lamp.

Measurements

The ocular surface was assessed using Oculus Keratograph 5M (K5 M; Oculus GmbH, Wetzlar, Germany), as explained in *Chapter 3 General Methodology*. Measurements were obtained by the same masked and experienced examiner following the guidelines of the TFOS DEWS II Diagnostic Methodology Report (Wolffsohn et al., 2017) in the following order to prevent the tear film from destabilization: OSDI, DEQ-5, total bulbar redness, TMH, tear film-dynamic and NIKBUT.

Metrics related to the tear film dynamics were developed using Matlab R2018a® (MathWorks, Natick, MA). The method was explained in *Chapter 8.2*. *Figure 9.6.2* shows one video frame with the light particles spreading after a blink. In *Chapter 8.2*, it was reported that these metrics can be used as emerging homeostasis parameters for the indirect assessment of the tear film quality in natural conditions with acceptable repeatability (García-Marqués et al., 2021d). Further details on these parameters and their rationale can be found in *Chapter 8.2* (García-Marqués et al., 2021d).

The first NIKBUT of the tear film was measured three consecutive times and the mean value was calculated (Markoulli et al., 2017; Wolffsohn et al., 2017; Dutta et al., 2019; Rico-del-Viejo et al., 2019). The Keratograph 5M was also used to record a video of the NIKBUT at 32 frames per second with a spatial resolution of 680 x 512 pixels. The video was analysed through a developed software, in *Chapter 8.3*, using Matlab R2019a. *Figure 9.6.3* shows the distribution of Placido disk pixels intensity in one frame. Different metrics were calculated: minimum pixel intensity, energy, relative energy, entropy, SD irregularity of pixels intensity, mean pixels intensity, SD pixels intensity, median pixels intensity, mode pixels intensity, kurtosis, skewness and the total area under the pixel intensity three-dimensional curve of the image was calculated and divided by the number of pixels in the region of interest. In *Chapter 8.3*, it was found that metrics at 5.33 seconds after blinking were correlated with lipid layer thickness and achieved a good diagnostic capability to assess the lipid layer thickness in an easy, repeatable, objective and accessible way without the need for an interferometer (García-Marqués et al., 2021e). Further details on these parameters and their rationale can be found in *Chapter 8.3* (García-Marqués et al., 2021e).

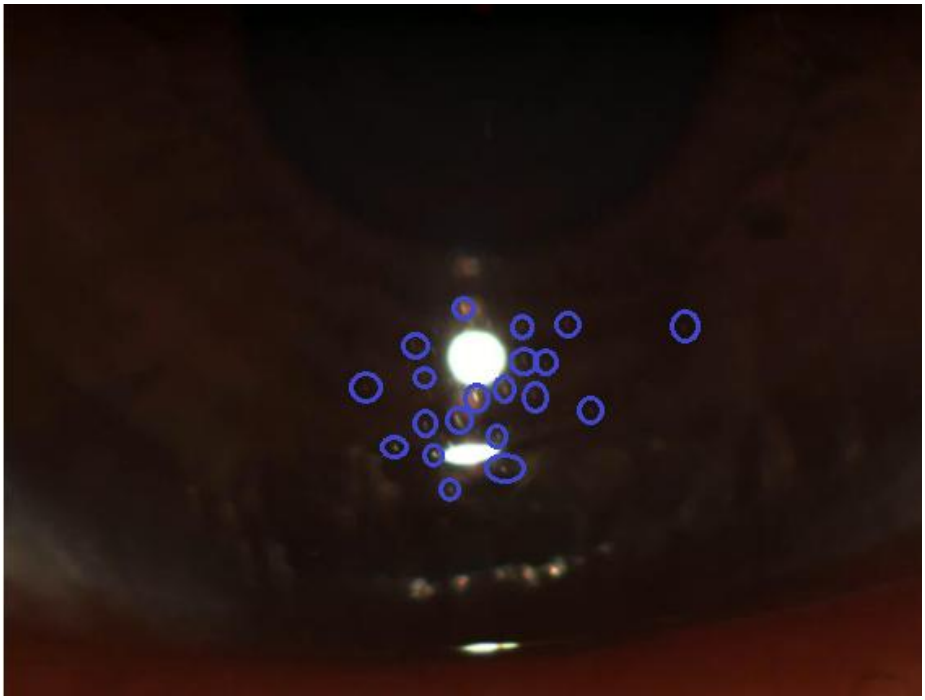

Fig. 9.6.2. *Particles spread after blinking in one frame. Light particles spreading over the cornea (blue circles).*

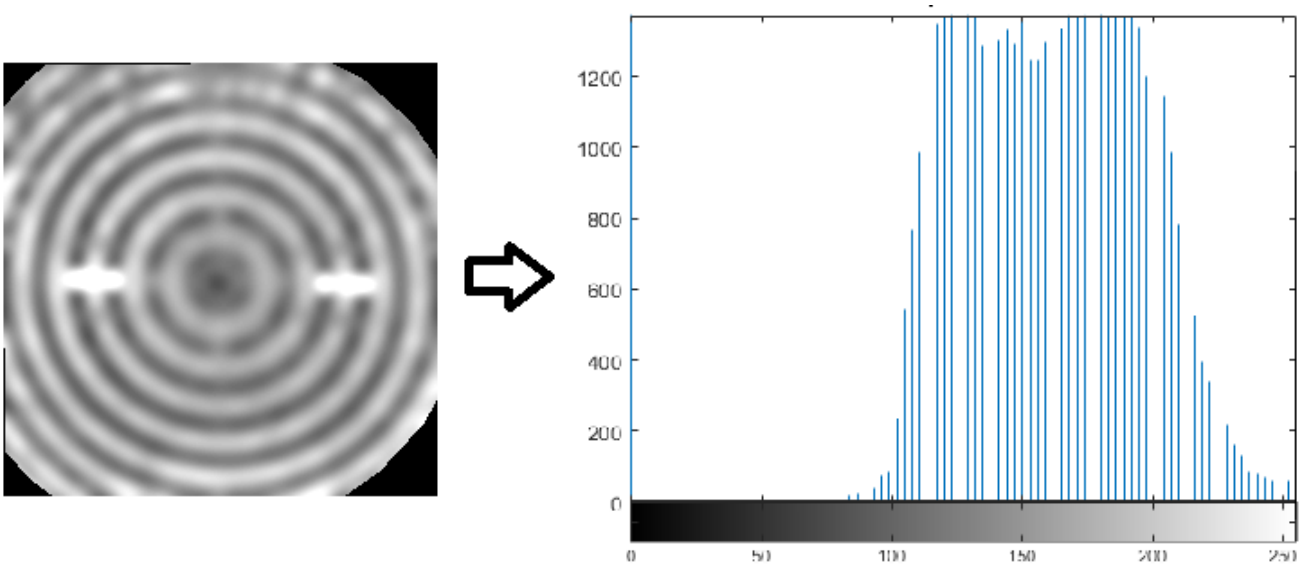

Fig. 9.6.3. *Histogram of the distribution of Placido disk pixels intensity in one frame. In the histogram, axe "x" represents the grey level intensities (0-255), while axe "y" shows the number of pixels*

Statistical analysis

Statistical analysis was performed using SPSS v26.0 for Windows (IBM Corp, Armonk, New York, USA). Results were reported as mean ± SD. Normality distribution was checked by means of the Kolmogorov-Smirnov or Shapiro-Wilk test depending on the sample.

Differences in parameters between before and after reading with a computer were assessed with the paired t-test or Wilcoxon signed-rank test, depending on sample distribution. Moreover, the effect of the contact lenses on ocular surface parameters was also assessed through the aforementioned statistical tests. Finally, mixed ANOVA was performed to evidence which parameters improved after the use of artificial tears while performing the computer task, without taking into account differences in pre-task measurements due to the effect of the contact lens. A p-value less than 0.05 was defined as statistically significant.

9.6.3 Results

Eighty-four right eyes from 84 participants were included in this study, out of which 52 were females (61.9 %) and 32 males (38.1 %). The mean age was 22.4 ± 2.6 years, ranging in age from 18 to 27 years.

Computer use

All participants complied with the instructions of the computer reading task. *Table 9.6.1* shows the mean values for the pre-computer task, post-computer task and the difference between them for the dry eye questionnaires and ocular surface metrics.

Statistical analysis revealed an increase in dry eye symptoms, TMH and bulbar redness; and a decrease in metrics related to the intensity of the reflected Placido disk pattern and in metrics related to particle speed after blinking, except for maximum particle speed and particle speed at 0.25 and 0.50 seconds. This suggests that computer use decreased lipid layer thickness and altered the distribution of the tear film after blinking.

Contact lens wear

Out of the total sample, 30 participants were contact lens wearers (22.8 ± 2.4 years, ranging in age from 18 to 26 years). In the second visit, contact lens wearers were fitted with contact lenses. Contact lenses had a correct movement, centration and coverage in all participants. *Table 9.6.2* shows the comparison between the pre-task of the first visit (naked eye) and the pre-task of the second visit (with the contact lens). Statistical analysis revealed that contact lens use causes lower values of TMH, NIKBUT, mode pixel intensity, minimum pixel intensity of the reflected Placido disk pattern, and particle speed metrics, except for maximum particle speed. Likewise, contact lens use increased entropy of the reflected Placido disk pattern. This suggests that contact lens wear decreased the lipid layer thickness and altered the dynamics and distribution of the tear film across the ocular surface.

Table 9.6.1. *Mean values and statistical comparison for the pre-computer task, post-computer task and the difference between them.*

Metric	Pre-task (Mean±SD)	Post-task (Mean±SD)	Difference post-task – pre-task	Significance level (p-value)
OSDI	6.95±9.62	15.55±15.67	8.60±11.97	<0.001[2]*
DEQ-5	3.83±4.54	6.90±5.37	3.07±5.02	<0.001[2]*
TMH (mm)	0.23±0.06	0.28±0.12	0.06±0.10	<0.001[2]*
Bulbar redness	0.50±0.27	0.57±0.34	0.07±0.19	0.031[2]*
NIKBUT (seconds)	15.67±8.02	14.87±7.53	-0.80±5.83	0.144[2]
Total area	122.02±5.19	116.76±6.02	-5.26±5.73	<0.001[2]*
Minimum pixel intensity	77.96±14.81	60.75±11.84	-17.21±15.19	<0.001[2]*
Energy	254.54±2.08	244.52±15.18	-10.02±9.26	<0.001[2]*
Relative energy	0.78±0.20	0.50±0.19	-0.28±0.20	<0.001[2]*
Entropy	$1.5 \times 10^{-4} \pm 4.5 \times 10^{-5}$	$1.5 \times 10^{-4} \pm 3.9 \times 10^{-5}$	$-6.2 \times 10^{-6} \pm 2.9 \times 10^{-5}$	0.008[2]*
SD irregularity	0.15±0.15	0.06±0.05	-0.09±0.13	<0.001[2]*
Mean pixels intensity	158.39±25.60	132.17±18.80	-26.22±22.68	<0.001[2]*
SD pixels intensity	31.76±4.74	28.34±3.26	-3.42±3.80	<0.001[2]*
Median pixels intensity	159.40±26.54	131.32±12.13	-28.08±23.56	<0.001[2]*
Mode pixels intensity	174.37±47.87	140.18±30.67	-34.19±42.26	<0.001[2]*
Kurtosis	0.013±0.002	0.015±0.002	0.002±0.002	<0.001[2]*
Skewness	0.122±0.013	0.130±0.010	0.008±0.010	<0.001[2]*
Particle speed at 0.25 seconds (mm/second)	2.84±1.21	2.70±1.52	-0.14±1.32	0.619[1]
Particle speed at 0.50 seconds (mm/second)	1.96±0.72	1.66±0.79	-0.3±0.73	0.054[1]
Particle speed at 0.75 seconds (mm/second)	1.52±0.55	1.28±0.58	-0.24±0.56	0.036[1]*
Particle speed at 1.00 second (mm/second)	1.16±0.44	0.96±0.34	-0.2±0.39	0.004[1]*
Particle speed at 1.25 seconds (mm/second)	0.94±0.44	0.79±0.30	-0.15±0.35	0.012[1]*
Particle speed at 1.50 seconds (mm/second)	0.80±0.34	0.67±0.29	-0.13±0.31	0.002[2]*
Particle speed at 1.75 seconds (mm/second)	0.72±0.32	0.58±0.25	-0.14±0.29	0.006[1]*
Mean particle speed (mm/second)	1.39±0.43	1.22±0.46	-0.17±0.44	0.019[1]*
Median particle speed (mm/second)	1.12±0.43	0.92±0.36	-0.2±0.38	0.004[1]*
Maximum particle speed(mm/second)	3.48±1.69	3.50±2.24	0.02±1.92	0.941[2]
Minimum particle speed (mm/second)	0.64±0.29	0.53±0.25	-0.11±0.27	0.008[1]*
Time for particle speed to decrease to < 1.20 mm/second (seconds)	1.09±0.38	0.80±0.39	-0.29±0.38	<0.001[1]*

*(Where DEQ-5: 5-item Dry Eye Questionnaire; NIKBUT: Non-Invasive Keratograph Break-Up Time; OSDI: Ocular Surface Disease Index; SD: Standard Deviation; TMH: Tear Meniscus Height; [1]T-Test; [2]Wilcoxon Signed-Rank test; *Statistically significant values)*

Table 9.6.2. *Comparison between pre-task of the first visit (naked eye) and pre-task of the second visit (with the contact lens).*

Metric	Contact lens effect Difference pre-task (Mean±SD)	Significance level (p-value)
OSDI	-0.92±7.22	0.656[2]
DEQ-5	-0.83±4.79	0.185[2]
TMH (mm)	-0.04±0.05	0.009[2]*
Bulbar redness	-0.04±0.19	0.088[2]
NIKBUT (seconds)	-5.71±7.70	0.001[2]*
Total area	-0.40±4.59	0.191[2]
Minimum pixel intensity	-9.34±16.04	0.028[2]*
Energy	-4.00±2.56	0.119[1]
Relative energy	-0.10±0.15	0.117[1]
Entropy	$2.1 \times 10^{-5} \pm 5.4 \times 10^{-5}$	0.010[2]*
SD irregularity	-0.002±0.009	0.101[2]
Mean pixels intensity	-3.74±19.25	0.112[2]
SD pixels intensity	-1.22±4.26	0.551[2]
Median pixels intensity	-7.19±19.70	0.074[2]
Mode pixels intensity	-12.66±31.72	0.001[2]*
Kurtosis	0.0003±0.0021	0.112[2]
Skewness	0.001±0.015	0.101[2]
Particle speed at 0.25 seconds (mm/second)	-1.11±1.23	0.018[2]*
Particle speed at 0.50 seconds (mm/second)	-0.72±0.84	0.040[2]*
Particle speed at 0.75 seconds (mm/second)	-0.63±0.57	0.007[2]*
Particle speed at 1.00 second (mm/second)	-0.47±0.46	0.003[2]*
Particle speed at 1.25 seconds (mm/second)	-0.26±0.45	0.042[2]*
Particle speed at 1.50 seconds (mm/second)	-0.24±0.36	0.019[2]*
Particle speed at 1.75 seconds (mm/second)	-0.17±0.35	0.044[2]*
Mean particle speed (mm/second)	-0.47±0.44	0.006[2]*
Median particle speed (mm/second)	-0.4±0.42	0.014[2]*
Maximum particle speed(mm/second)	-0.98±1.74	0.106[2]
Minimum particle speed (mm/second)	-0.28±0.29	0.004[2]*
Time for particle speed to decrease to < 1.20 mm/second (seconds)	-0.56±0.42	0.002[2]*

*(Where DEQ-5: 5-item Dry Eye Questionnaire; NIKBUT: Non-Invasive Keratograph Break-Up Time; OSDI: Ocular Surface Disease Index; SD: Standard Deviation; TMH: Tear Meniscus Height; [1]T-Test; [2]Wilcoxon Signed Rank test; *Statistically significant values)*

Computer use, contact lens and artificial tears

Table 9.6.3 shows the mean values for the pre-computer task (with the contact lens), post-computer task (with the contact lens and artificial tears) and the difference between them for the dry eye questionnaires and ocular surface metrics. Statistical analysis revealed an increase in TMH and in metrics related to particle speed after blinking. This suggests that after computer use with a contact lens and artificial tears, lipid layer thickness did not decrease and the distribution of the tear film after blinking improved. Moreover, dry eye symptoms and the rest of the ocular surface parameters remained unaltered, which might be caused by the use of artificial tears.

Computer use and artificial tears

Mixed ANOVA analysis (*Table 9.6.4*) was performed to evidence which parameters improved after the use of artificial tears while performing the computer task, without taking into account differences in pre-task measurements due to the effect of the contact lens. It showed statistically significant differences between conditions (computer versus computer + contact lens + artificial tears) for all ocular surface parameters except for bulbar redness, the entropy of the reflected Placido disk pattern, minimum particle speed and particle speed at 0.75, 1.00, 1.25, 1.50 and 1.75 seconds. However, some parameters had differences in pre-task measurements due to the contact lens.

Table 9.6.3. *Mean values and statistical comparison for the pre-computer task (with the contact lens), post-computer task (with the contact lens and artificial tears) and the difference between them.*

Metric	Pre-task (Mean±SD)	Post-task (Mean±SD)	Difference post-task – pre-task	Significance level (p-value)
OSDI	6.03±9.44	6.47±9.34	0.44±4.98	0.683[2]
DEQ-5	3.00±3.92	2.97±3.75	-0.03±2.55	0.865[2]
TMH (mm)	0.19±0.04	0.23±0.05	0.04±0.05	<0.001[2]*
Bulbar redness	0.46±0.18	0.46±0.24	-0.003±0.124	0.773[2]
NIKBUT (seconds)	9.96±6.27	11.44±6.24	1.48±4.19	0.052[2]
Total area	121.62±8.45	124.30±6.39	2.68±6.93	0.620[2]
Minimum pixel intensity	68.62±13.85	69.27±11.85	0.65±12.36	0.284[1]
Energy	250.54±3.92	254.64±3.16	4.10±3.54	0.829[1]
Relative energy	0.68±0.18	0.73±0.16	0.05±0.16	0.834[1]
Entropy	$1.5 \times 10^{-4} \pm 6.9 \times 10^{-5}$	$1.5 \times 10^{-4} \pm 5.6 \times 10^{-5}$	$-4.9 \times 10^{-6} \pm 4.6 \times 10^{-5}$	0.367[2]
SD irregularity	0.15±0.02	0.15±0.02	-0.003±0.016	0.657[2]
Mean pixels intensity	154.65±15.59	154.51±12.37	-0.14±13.24	0.957[1]
SD pixels intensity	30.54±2.83	30.46±2.58	-0.08±2.62	0.880[1]
Median pixels intensity	152.21±15.7	152.88±12.91	0.67±13.13	0.965[1]
Mode pixels intensity	161.77±26.03	160.92±21.45	-0.85±24.33	0.811[1]
Kurtosis	0.013±0.002	0.013±0.003	0.0009±0.0028	0.124[2]
Skewness	0.123±0.011	0.125±0.015	0.002±0.013	0.086[2]
Particle speed at 0.25 seconds (mm/second)	1.73±1.24	2.10±1.13	0.37±1.17	0.170[2]
Particle speed at 0.50 seconds (mm/second)	1.24±0.93	1.82±0.98	0.58±0.95	0.024[2]*
Particle speed at 0.75 seconds (mm/second)	0.89±0.57	1.53±0.94	0.64±0.77	0.006[2]*
Particle speed at 1.00 second (mm/second)	0.69±0.46	1.17±0.55	0.48±0.52	0.002[2]*
Particle speed at 1.25 seconds (mm/second)	0.68±0.46	0.90±0.35	0.22±0.39	0.020[2]*
Particle speed at 1.50 seconds (mm/second)	0.56±0.38	0.80±0.30	0.24±0.33	0.003[2]*
Particle speed at 1.75 seconds (mm/second)	0.55±0.37	0.72±0.26	0.17±0.32	0.004[2]*
Mean particle speed (mm/second)	0.92±0.46	1.28±0.46	0.36±0.45	0.005[2]*
Median particle speed (mm/second)	0.72±0.40	1.08±0.40	0.36±0.40	0.005[2]*
Maximum particle speed(mm/second)	2.50±1.82	3.05±1.40	0.55±1.63	0.033[2]*
Minimum particle speed (mm/second)	0.36±0.29	0.60±0.30	0.24±0.30	0.007[2]*
Time for particle speed to decrease to < 1.20 mm/second (seconds)	0.53±0.44	0.94±0.45	0.41±0.45	0.003[2]*

*(Where DEQ-5: 5-item Dry Eye Questionnaire; NIKBUT: Non-Invasive Keratograph Break-Up Time; OSDI: Ocular Surface Disease Index; SD: Standard Deviation; TMH: Tear Meniscus Height; [1]T-Test; [2]Wilcoxon Signed-Rank test; *Statistically significant values)*

The interaction between conditions (computer versus computer + contact lens + artificial tears) and the time (pre and post-task) had a significant effect on OSDI, DEQ-5, NIKBUT, the total area of pixels intensity, minimum pixel intensity, energy, relative energy, SD irregularity of pixel intensity, mean pixel intensity, SD pixel intensity, median pixel intensity, mode pixel intensity, mean particle speed, median particle speed, minimum particle speed, time for particle speed to decrease to < 1.20 mm/second and particle speed at 0.50, 0.75, 1.00, 1.25, 1.50 and 1.75 seconds. This suggests that artificial tears help in ameliorating the deterioration of these ocular surface parameters after reading with a computer.

Table 9.6.4. *Analysis of the interaction between the time (pre-task versus post-task) and the condition (computer versus computer + contact lens + artificial tears) for each dependent variable through a mixed ANOVA.*

	Within-Subjects Effects	Between-Subjects Effects
Measurement	Interaction between time (pre versus post-task) and the condition (computer versus computer + contact lens + artificial tears) (Significance level)	Differences between conditions (computer versus computer + contact lens + artificial tears) (Significance level)
OSDI	<0.001*	0.026*
DEQ-5	0.001*	0.005*
TMH (mm)	0.343	0.001*
Bulbar redness	0.182	0.142
NIKBUT (seconds)	0.033*	0.001*
Total area	<0.001*	<0.001*
Minimum pixel intensity	<0.001*	<0.001*
Energy	<0.001*	<0.001*
Relative energy	<0.001*	<0.001*
Entropy	0.831	0.070
SD irregularity	0.003*	0.001*
Mean pixels intensity	<0.001*	<0.001*

(continuation)		
	Within-Subjects Effects	Between-Subjects Effects
Measurement	Interaction between time (pre versus post-task) and the condition (computer versus computer + contact lens + artificial tears) (Significance level)	Differences between conditions (computer versus computer + contact lens + artificial tears) (Significance level)
SD pixels intensity	<0.001*	0.001*
Median pixels intensity	<0.001*	<0.001*
Mode pixels intensity	<0.001*	<0.001*
Kurtosis	0.147	<0.001*
Skewness	0.066	<0.001*
Particle speed at 0.25 seconds (mm/second)	0.184	<0.001*
Particle speed at 0.50 seconds (mm/second)	0.004*	0.049*
Particle speed at 0.75 seconds (mm/second)	<0.001*	0.134
Particle speed at 1.00 second (mm/second)	<0.001*	0.150
Particle speed at 1.25 seconds (mm/second)	0.002*	0.270
Particle speed at 1.50 seconds (mm/second)	<0.001*	0.343
Particle speed at 1.75 seconds (mm/second)	<0.001*	0.664
Mean particle speed (mm/second)	<0.001*	0.019*
Median particle speed (mm/second)	<0.001*	0.042*
Maximum particle speed(mm/second)	0.172	0.023*
Minimum particle speed (mm/second)	<0.001*	0.086
Time for particle speed to decrease to < 1.20 mm/second (seconds)	<0.001*	0.012*

*(Where DEQ-5: 5-item Dry Eye Questionnaire; NIKBUT: Non-Invasive Keratograph Break-Up Time; OSDI: Ocular Surface Disease Index; SD: Standard Deviation; TMH: Tear Meniscus Height; *Statistically significant values)*

9.6.4 Discussion

The use of digital displays and contact lens wear have been previously found to increase dry eye signs and symptoms (Viso, Rodríguez-Ares and Gude, 2009; Paulsen et al., 2014; Yazici et al., 2014; Ribelles et al., 2015; Tan et al., 2015b; Stapleton et al., 2017; Talens-Estarelles et al., 2020; Talens-Estarelles et al., 2021a; Talens-Estarelles et al., 2021b). The present work confirmed these previous findings and included new

objective and non-invasive methods in the analysis that might be used to assess the variations in the tear film induced by several condition induced changes.

Computer use

In this work, reading with a computer for 20 minutes increased dry eye symptoms, TMH and bulbar redness, indicating tear film alterations and ocular surface stress. Furthermore, the intensity of the reflected Placido disk pattern and the speed of particles after blink decreased. Nevertheless, NIKBUT was not statistically altered. As the intensity of the reflected Placido disk pattern can be used to objectively assess the lipid layer thickness (*Chapter 8.3*) (García-Marqués et al., 2021e), these results suggest that computer use decreased lipid layer thickness and altered the dynamics of the tear film after blinking. Aligned with these results, Talens-Esterelles et al. (2020) also found differences in OSDI, TMH and bulbar redness after a 15 minutes task with a computer; however, they found a decrease in NIKBUT.

According to this work, previous studies reported ocular surface and tear film alterations such as reduced tear stability, changes in tear volume and tear composition, oxidative stress, ocular surface inflammation and meibomian gland abnormalities in computer users (Wu et al., 2014a; Yazici et al., 2014; Ribelles et al., 2015; Choi et al., 2018; Talens-Estarelles et al., 2020; Talens-Estarelles et al., 2021b).

The lower value found in entropy after the computer task might be attributable to the higher value found in bulbar redness, TMH and OSDI since, in *Chapter 8.3*, it was reported that entropy was inversely correlated with these parameters (García-

Marqués et al., 2021e). In addition, TMH increased in this study probably due to it was reported a compensatory burst of blinks right after a digital display task (Nielsen et al., 2008). This might be a compensation phenomenon to wet the ocular surface after the oppression of blinking during the task, which could explain the higher TMH found after the computer task in the present study. Conversely, some authors previously reported lower TMH and Schirmer test values in long-term office workers while others found no difference (Cardona et al., 2011; Choi et al., 2018; Talens-Estarelles et al., 2020).

Contact lens wear

Contact lens wear impacts ocular surface homeostasis (Stapleton et al., 2017). When a contact lens is inserted into the eye, tear film destabilizes because the contact lens divides the tear film into two layers: pre-lens and post-lens tear film (Korb, Greiner and Glonek, 1996). Approximately, 50 % of contact lens wearers suffer from dryness and ocular discomfort, both problems being the major causes of contact lens intolerance (Doughty et al., 1997; Gomes et al., 2017). Thus, it has been found that contact lens wear causes a reduction in tear volume (Chen et al., 2011; Del Águila-Carrasco et al., 2015), lipid layer thickness and alterations in tear spreading (Yokoi et al., 2008); and higher tear film instability (Santodomingo-Rubido, Wolffsohn and Gilmartin, 2006b) and tear osmolarity (Hori, 2018).

Delefilcon A daily disposable water gradient contact lenses have high oxygen transmissibility with a lubricious surface and a low coefficient of friction, providing higher levels of comfort (Pérez-Gómez and Giles, 2014). Despite these optimal properties, in the present study, contact lens wear decreased TMH, NIKBUT, minimum

pixel intensity, mode pixels intensity and particle speed after blinking, whilst entropy increased. Despite some metrics related to the intensity of the Placido disk pattern not being statistically significant, they show a tendency to decrease after contact lens wear. Therefore, contact lens wear also affected lipid layer thickness and the dynamics of the tear film after blinking. Results of the present study are aligned with previous ones that also found a relationship between contact lens wear and alterations in the tear film and the ocular surface (Doughty et al., 1997; Uchino et al., 2008; Yang et al., 2015; Rico-del-Viejo et al., 2018; García-Marqués et al., 2021b).

The higher entropy found with contact lens use might be a consequence of the lower TMH since entropy and TMH are inversely correlated (as found in *Chapter 8.3)* (García-Marqués et al., 2021e). Besides, it was previously found that tear volume decreased 20 minutes after the insertion of soft contact lenses (Wang, Cox and Reindel, 2009). In this way, contact lenses with high-water content absorb tear fluid into the contact lens, causing a lower TMH (Kojima, 2018). Nevertheless, dry eye symptoms did not increase after contact lens wear, which might be explained as discomfort and lens dryness usually occur late in the day (Chalmers and Begley, 2006). Thus, the results of this study represent the short-term effects of a daily disposable lens on the ocular surface. Likewise, in the present work, participants were fitted with the same daily disposable contact lens, deleting the possibility that the maintenance of the contact lenses caused alterations.

Computer use, contact lens wear and artificial tears

Artificial tears are an effective strategy to ameliorate dry eye symptoms and signs (Acosta, Gallar and Belmonte, 1999; Jones et al., 2017). In this regard, sodium hyaluronate artificial tears have a prolonged resident time in the eye and have been reported to significantly increase TMH, improve tear film stability and decrease higher-order aberrations 30 minutes after instillation (Montés-Micó, 2007; Montés-Micó et al., 2010b; Calvão-Santos et al., 2011; Diaz-Valle et al., 2012; Igarashi et al., 2015; Kobashi et al., 2015; Schafer et al., 2018; Vandermeer, Chamy and Pisella, 2018).

Moreover, previous studies with the same artificial tears as in the present one found that they were effective for ameliorating symptoms of dryness and increasing tear film stability (Kading, 2010; Benelli, 2011; McDonald et al., 2014; Gokul, Wang and Craig, 2018; Belalcázar-Rey et al., 2021). Although in this study and in previous ones both contact lens wear and the use of digital display increases dry eye signs and symptoms, the use of artificial tears prevent it since no increase was found in dry eye symptoms and bulbar redness after the computer task. NIKBUT increased after the task but the magnitude was not statistically significant. Likewise, lipid layer thickness did not decrease after the task given that metrics related to the intensity of the reflected Placido disk pattern were unaltered. This might be caused by the use of artificial tears before the computer use. Moreover, TMH increased probably due to the instillation of artificial tears and particle speed increased after the task, suggesting that not only does the use of artificial tears prevent the increase of dry eye signs and

symptoms after computer use but it also improves the tear film dynamics after blinking.

Mixed ANOVA was performed to evidence which parameters improved after the use of artificial tears while performing the computer task, without taking into account differences in pre-task measurements due to the effect of the contact lens. The analysis confirmed that artificial tears help in ameliorating the deterioration of dry eye signs and symptoms after reading with a computer. In opposition to these results, Talens-Estarelles et al. (2020) did not find an improvement of ocular surface parameters after the instillation of artificial tears.

The present study had some limitations to consider. First, the lipid layer thickness was not directly measured. Nevertheless, it was previously reported in *Chapter 8.3* that the measurement of the intensity of the reflected Placido disk pattern can be used as an objective method to measure the lipid layer thickness with acceptable repeatability and accuracy (García-Marqués et al., 2021e). In addition, the novel methods are semiautomatic but the repeatability was found to be acceptable (in *Chapters 8.2* and *8.3*) (García-Marqués et al., 2021d; García-Marqués et al., 2021e). Furthermore, no control group was used to assess the effect of the contact lenses. In this case, the condition pre-task of both visits was compared and some variability could exist between visits. Therefore, these results should be confirmed in future studies with a control group to find whether new metrics are able to detect changes in the ocular surface due to the contact lens. In any case, the present study allows a hypothesis to be built for testing in future studies.

Overall, the present work adds valuable information regarding the effect of computer use, contact lens wear and artificial tears use on the ocular surface. Computer use and contact lens wear worsened dry eye signs and symptoms, including lipid layer thickness and tear film dynamics. Moreover, artificial tears help in ameliorating the deterioration of these ocular surface parameters after reading with a computer and they are an effective strategy for preventing the impact of display use on the ocular surface. Newly developed methods can serve as a tool to detect changes in the tear film triggered by different ocular surface-disturbing conditions. In this way, the present work helps to further validate these novel methods as a reliable tool to quickly, non-invasively and objectively assess the changes in the tear film induced by different conditions. Therefore, they could be easily included in a battery of tests to improve the detection and monitoring of DED and meibomian gland dysfunction in the clinical practice. Further research is needed to make methods fully automatic and to assess the performance of these metrics in participants diagnosed with DED or meibomian gland dysfunction.

CHAPTER 10: General conclusions and future work

10. GENERAL CONCLUSIONS AND FUTURE WORK

10.1 General conclusions

Despite many techniques being available to assess the tear film, some of them have limited repeatability, sensitivity and specificity. Moreover, some of them are non-objective or invasive, which makes the assessment of the tear film challenging and the diagnosis of DED difficult. Additionally, there is a lack of agreement between current clinical tests and there is no gold standard test available. Non-invasive imaging techniques should be considered to assess the tear film and the ocular surface and should prevail over invasive ones to achieve greater diagnostic capability and better management of individuals with DED. Non-invasive imaging techniques allow clinicians to assess the tear film under more natural conditions, avoiding reflex tearing and tear film destabilization. Accordingly, non-invasive imaging techniques tend to be more accurate, repeatable and objective than invasive ones.

The main conclusions of the present thesis, after the different studies performed, are:

- The multifactorial aetiology of DED also makes its diagnosis challenging. DED is associated with systemic, environmental and lifestyle risk factors. The present work demonstrated that DED is associated with fewer hours of sleep per day, menopause and the use of anxiolytics. These findings are useful to identify potentially modifiable risk factors, in addition to conventional treatments for DED.
- The NIKBUT measurement has low intraexaminer repeatability even when considering sex, age and DED diagnosis. Nevertheless, this low repeatability is

not only due to the device itself but mainly to the intrinsic variability of the tear film. Despite the NIKBUT procedure being non-invasive, it does not allow the assessment of the tear film under completely natural conditions, since subjects must keep their eyes open forcefully, potentially leading to reflex tearing.

- Bulbar redness metrics measured with the Keratograph 5M provided objective values with acceptable repeatability, which might help clinicians in the assessment of some diseases related to ocular surface inflammation, such as DED.

- The Keratograph 5M might be a useful tool in the follow-up of some treatments. After the application of thermal bags, dry eye-related symptoms improved, while NIKBUT and lipid layer thickness only improved in young subjects.

- Newly developed metrics can help assess the tear film and the ocular surface in a non-invasive, objective and repeatable manner. These new metrics could be included in a battery of clinical tests as easy, repeatable and objective methods to improve the assessment of the tear film, which could enhance the detection and monitoring of DED and MGD.

    -The method developed in the present thesis to assess meibomian glands is able to assess meibomian gland visibility in an objective and repeatable manner. These metrics were correlated with meibomian gland drop-out, NIKBUT, bulbar redness, meibomian gland expressibility score and TMH. Accordingly, higher intensity values were related to a greater healthiness

of the meibomian glands. Moreover, meibomian gland visibility metrics are more powerful to diagnose MGD than current single metrics and can serve as a complementary tool for supporting the diagnosis of MGD.

-Tear film-dynamic metrics are able to predict NIKBUT. Higher particle speed is associated with a longer NIKBUT and might, therefore, help assess tear film stability under more natural conditions than NIKBUT, since subjects are not required to suppress blinking. Newly developed metrics can be emerging homeostasis parameters for indirectly assessing the tear film quality in natural conditions with acceptable repeatability.

-The analysis of grey intensity values in videokeratography can be used as an objective and repeatable tool with acceptable sensitivity and specificity to assess the lipid layer thickness.

- The dual-focus contact lens assessed in the present study decreased the pre-lens tear film stability and the psychophysical and psychometric visual quality scores in the short-term under dim-light conditions when compared to a single-vision contact lens. Nevertheless, visual acuity and stereopsis were not affected by lens design.
- When the influence of the central diameter of two dual-focus contact lenses was studied, it was found that both contact lenses provided acceptable visual performance under photopic conditions. However, the lens with the medium central diameter offered better contrast sensitivity at high frequencies and lower light disturbance size. On the other hand, the smaller central diameter contact lens led to lower levels of higher-order aberrations. Despite these differences, subjective visual comfort was not affected.

- The measurement of light disturbance might help in the assessment and management of subjects with symptoms of DED. Thus, delayed blinking and contact lens wear increased light disturbance due to tear film instability. Blink monitoring or artificial tears use might decrease the light disturbance and could be an option to manage subjects with short BUTs or with a low blink rate.

- The methods developed in the present thesis are capable of assessing the changes in the ocular surface and the tear film due to contact lens wear. Therefore, the newly developed metrics can be useful tools for the follow-up of the ocular surface and the tear film in contact lens wearers in a quick, repeatable and objective manner.

    -Scleral lens wear did not adversely affect meibomian gland drop-out and visibility while dry eye symptoms improved after one year of lens wear. However, these preliminary results should be confirmed with a control group.

    -Meibomian gland drop-out was higher and gland visibility was lower in long-term soft contact lens wearers in comparison with non-contact lens wearers.

    -Computer use and contact lens wear worsened dry eye signs and symptoms, including metrics related to the speed of the tear film particles post-blink and the measurement of the lipid layer thickness obtained from the intensity of the reflected Placido disk. Artificial tears help in

ameliorating the effects of contact lens wear and computer use on current and novel metrics.

10.2 Future work

- Although newly developed metrics are able to assess the tear film and the ocular surface; this is the first step in developing these metrics. Further research is needed to assess the performance of these metrics in subjects diagnosed with DED or MGD, and to establish cut-off values based on the age of the subjects. Nonetheless, although these results are preliminary, they are highly encouraging, and this study could be the basis for future works. Overall, this is a field that needs further research and has a high potential to be explored.
- Specifically, both eyelids could be included in the analysis of meibomian glands visibility. The method based on the analysis of the grey intensity values of the Placido disk pattern could be further developed to distinguish between grades 3 and 4 of lipid layer thickness. In addition, the diagnostic capability of metrics related to the speed of the tear film particles post-blink and the measurement of the lipid layer thickness obtained from the intensity of the reflected Placido disk could be assessed in further research. Likewise, the methods should be further developed to be fully automatic. Finally, a prospective, longitudinal study is required to understand the associations between meibomian gland alterations and contact lens wear. Also, newly developed metrics could be applied to other contact lens designs and materials and after longer wearing times.

APPENDICES

APPENDIX A: OSDI questionnaire

Sujeto n˚:

Cuestionarios

Instrucciones: Marque la casilla que mejor represente su respuesta.

¿Ha experimentado alguna de las siguientes alteraciones durante la última semana?

	En todo momento	Casi en todo momento	El 50% del tiempo	Casi en ningun momento	En ningún momento	No sé
1. Sensibilidad a la luz	4	3	2	1	0	**N/S**
2. Sensación de arenilla en los ojos	4	3	2	1	0	**N/S**
3. Dolor de ojos	4	3	2	1	0	**N/S**
4. Visión borrosa	4	3	2	1	0	**N/S**
5. Mala visión	4	3	2	1	0	**N/S**

¿Ha tenido problemas en los ojos que le han limitado o impedido realizar alguna de las siguientes acciones durante la última semana?

6. Leer	4	3	2	1	0	**N/S**
7. Conducir de noche	4	3	2	1	0	**N/S**
8. Trabajar con un ordenador o utilizar un cajero automático	4	3	2	1	0	**N/S**
9. Ver la televisión	4	3	2	1	0	**N/S**

¿Ha sentido incomodidad en los ojos en alguna de las siguientes situaciones durante la última semana?

10. Viento	4	3	2	1	0	**N/S**
11. Lugares con baja humedad (muy secos)	4	3	2	1	0	**N/S**
12. Zona con aire acondicionado	4	3	2	1	0	**N/S**

APPENDIX B: DEQ-5 questionnaire

1 Pregunta sobre DISCONFORT OCULAR:					
a. Durante un día normal del mes pasado, **¿con qué frecuencia** sintió disconfort ocular?	**0 Nunca**	**1 Rara vez**	**2 A veces**	**3 A menudo**	**4 Constantemente**
b. En caso de sentir disconfort ocular, ¿**cómo de intensa** fue esta sensación al final del día (dos horas antes de dormir)?	**Nunca Lo he experimentado**	**Nada Intenso**			**Muy Intenso**
	0	**1**	**2**	**3**	**4** **5**
2 Pregunta sobre SEQUEDAD OCULAR					
a. Durante un día normal del mes pasado, ¿**con qué frecuencia** sintió sequedad ocular	**0 Nunca**	**1 Rara vez**	**2 A veces**	**3 A menudo**	**4 Constantemente**
b. En caso de sentir sequedad ocular, ¿**cómo de intensa** fue esta sensación al final del día (dos horas antes de dormir)?	**Nunca lo he experimentado**	**Nada Intenso**			**Muy Intenso**
	0	**1**	**2**	**3**	**4** **5**
3 Pregunta sobre LAGRIMEO:					
Durante un día normal del mes pasado, ¿**con qué frecuencia** experimentó lagrimeo?	**0 Nunca**	**1 Rara vez**	**2 A veces**	**3 A menudo**	**4 Constantemente**
4 Pregunta sobre IRRITACION OCULAR:					
Durante un día normal del mes pasado, ¿**con qué frecuencia** sintió irritación ocular?	**0 Nunca**	**1 Rara vez**	**2 A veces**	**3 A menudo**	**4 Constantemente**

¿Ha recibido previamente un diagnóstico clínico de ojo seco? Sí ☐ No ☐

APPENDIX C: QoV questionnaire

ANEXO 1. Inquérito QoV McAlinden (7 e 15 dias)

Nome:_____

Este questionário é composto por 10 itens, cada um com três perguntas sobre a frequência, intensidade e incómodo relativos à sua visão. Compare cada sensação com a explicação gráfica das imagens que lhe serão disponibilizadas.

1. Quantas vezes sente que vê brilhos à volta das luzes?

Nunca ☐ Ocasionalmente ☐ Frequentemente ☐ Muitas vezes ☐

>>Se respondeu "Nunca" passe para a pergunta 2 >>

1.1 Qual a intensidade desses brilhos?

Nenhuma ☐ Leve ☐ Moderada ☐ Forte ☐

1.2 Quanto incómodo lhe produzem os brilhos?

Nenhum ☐ Algum ☐ Bastante ☐ Muito ☐

2. Quantas vezes sente que vê "halos" à volta das luzes?

Nunca ☐ Ocasionalmente ☐ Frequentemente ☐ Muitas vezes ☐

>>Se respondeu "Nunca" passe para a pergunta 3 >>

2.1 Qual a intensidade desses "halos"?

Nenhuma ☐ Leve ☐ Moderada ☐ Forte ☐

2.2 Quanto incómodo lhe produzem os "halos"?

Nenhum ☐ Algum ☐ Bastante ☐ Muito ☐

3. Quantas vezes vê "riscos estrelados" nas luzes?

Nunca ☐ Ocasionalmente ☐ Frequentemente ☐ Muitas vezes ☐

>>Se respondeu "Nunca" passe para a pergunta 4 >>

3.1 Qual a intensidade desses "riscos estrelados"?

Nenhuma ☐ Leve ☐ Moderada ☐ Forte ☐

3.2 Quanto incómodo lhe produzem os "riscos estrelados"?

Nenhuma ☐ Leve ☐ Moderada ☐ Forte ☐

4. Quantas vezes sente a visão enevoada?

Nunca ☐ Ocasionalmente ☐ Frequentemente ☐ Muitas vezes ☐

>>Se respondeu "Nunca" passe para a pergunta 5>>

4.1 Qual a intensidade dessa visão enevoada?

Nenhuma ☐ Leve ☐ Moderada ☐ Forte ☐

4.2 Quanto incómodo lhe produz a visão enevoada?

Nenhum ☐ Algum ☐ Bastante ☐ Muito ☐

5. Quantas vezes sente a visão desfocada?

Nunca ☐ Ocasionalmente ☐ Frequentemente ☐ Muitas vezes ☐

>>Se respondeu "Nunca" passe para a pergunta 6 >>

5.1 Qual a intensidade dessa visão desfocada?

Nenhuma ☐ Leve ☐ Moderada ☐ Forte ☐

5.2 Quanto incómodo lhe produz a visão desfocada?

Nenhum ☐ Algum ☐ Bastante ☐ Muito ☐

6. Quantas vezes sente visão distorcida?

Nunca ☐ Ocasionalmente ☐ Frequentemente ☐ Muitas vezes ☐

>>Se respondeu "Nunca" passe para a pergunta 7 >>

6.1 Qual a intensidade dessa distorção?

Nenhuma ☐ Leve ☐ Moderada ☐ Forte ☐

6.2 Quanto incómodo lhe produz a distorção?

Nenhum ☐ Algum ☐ Bastante ☐ Muito ☐

7. Quantas vezes vê imagens duplas ou múltiplas?

Nunca ☐ Ocasionalmente ☐ Frequentemente ☐ Muitas vezes ☐

>>Se respondeu "Nunca" passe para a pergunta 8 >>

7.1 Qual a intensidade das imagens duplas ou múltiplas?

Nenhuma ☐ Leve ☐ Moderada ☐ Forte ☐

7.2 Quanto incómodo lhe produzem as imagens duplas ou múltiplas?

Nenhum ☐ Algum ☐ Bastante ☐ Muito ☐

8. Quantas vezes sente flutuações na sua visão?

Nunca ☐ Ocasionalmente ☐ Frequentemente ☐ Muitas vezes ☐

>>Se respondeu "Nunca" passe para a pergunta 9 >>

8.1 Qual a intensidade dessas flutuações?

Nenhuma ☐ Leve ☐ Moderada ☐ Forte ☐

8.2 Quanto incómodo lhe produzem as flutuações?

Nenhum ☐ Algum ☐ Bastante ☐ Muito ☐

9. Quantas vezes sente dificuldades em focar?

Nunca ☐ Ocasionalmente ☐ Frequentemente ☐ Muitas vezes ☐

>>Se respondeu "Nunca" passe para a pergunta 10 >>

9.1 Qual a intensidade dessas dificuldades em focar?

Nenhuma ☐ Leve ☐ Moderada ☐ Forte ☐

9.2 Quanto incómodo lhe produzem as dificuldades em focar?

Nenhum ☐ Algum ☐ Bastante ☐ Muito ☐

10. Quantas vezes sente dificuldade na percepção de distância ou profundidade?

Nunca ☐ Ocasionalmente ☐ Frequentemente ☐ Muitas vezes ☐

10.1 Qual a intensidade provocada pela dificuldade de percepção da distância ouprofundidade?

Nenhuma ☐ Leve ☐ Moderada ☐ Forte ☐

10.2 Quanto incómodo lhe produz a dificuldade de percepção da distância ouprofundidade?

Nenhum ☐ Algum ☐ Bastante ☐ Muito☐

REFERENCES

REFERENCES

Abdelfattah, N., Dastiridou, A., Sadda, S. and Lee, O., 2015. Noninvasive Imaging of Tear Film Dynamics in Eyes With Ocular Surface Disease. *Cornea*, 34(Supplement 10), pp.S48-S52.

Abelson, M., Lane, K. and Maffei, C., 2010. Code Red: The Key Features of Hyperemia. *Rev Ophthalmol*, 17, pp.92-94.

Abreau, K., Callan, C., Kottaiyan, R., Zhang, A., Yoon, G., Aquavella, J., Zavislan, J. and Hindman, H., 2016. Temperatures of the Ocular Surface, Lid, and Periorbital Regions of Sjögren's, Evaporative, and Aqueous-Deficient Dry Eyes Relative to Normals. *The Ocular Surface*, 14(1), pp.64-73.

Acosta, M., Gallar, J. and Belmonte, C., 1999. The Influence of Eye Solutions on Blinking and Ocular Comfort at Rest and During Work at Video Display Terminals. *Experimental Eye Research*, 68(6), pp.663-669.

Adil, M., Xiao, J., Olafsson, J., Chen, X., Lagali, N., Ræder, S., Utheim, Ø., Dartt, D. and Utheim, T., 2019. Meibomian Gland Morphology Is a Sensitive Early Indicator of Meibomian Gland Dysfunction. *American Journal of Ophthalmology*, 200, pp.16-25.

Agero, U., Monken, C., Ropert, C., Gazzinelli, R. and Mesquita, O., 2003. Cell surface fluctuations studied with defocusing microscopy. *Physical Review E*, 67(5), p.051904.

Aggarwal, S., Kheirkhah, A., Cavalcanti, B., Cruzat, A., Jamali, A. and Hamrah, P., 2021. Correlation of corneal immune cell changes with clinical severity in dry eye disease: An in vivo confocal microscopy study. *The Ocular Surface*, 19, pp.183-189.

Ağın, A., Kocabeyoğlu, S., Çolak, D. and İrkeç, M., 2019. Ocular Surface, Meibomian Gland Alterations, and In Vivo Confocal Microscopy Characteristics of Corneas in Chronic Cigarette Smokers. *Graefe's Archive for Clinical and Experimental Ophthalmology*, 258(4), pp.835-841.

Agnifili, L., Brescia, L., Oddone, F., Sacchi, M., D'Ugo, E., Di Marzio, G., Perna, F., Costagliola, C. and Mastropasqua, R., 2019. The ocular surface after successful glaucoma filtration surgery: a clinical, in vivo confocal microscopy, and immune-cytology study. *Scientific Reports*, 9(1), p.11299.

Agnifili, L., Fasanella, V., Costagliola, C., Ciabattoni, C., Mastropasqua, R., Frezzotti, P. and Mastropasqua, L., 2013. In vivo confocal microscopy of meibomian glands in glaucoma. *British Journal of Ophthalmology*, 97(3), pp.343-349.

Agnifili, L., Mastropasqua, R., Fasanella, V., Brescia, L., Scatena, B., Oddone, F. and Mastropasqua, L., 2018. Meibomian Gland Features and Conjunctival Goblet Cell Density in Glaucomatous Patients Controlled With Prostaglandin/Timolol Fixed Combinations: A Case Control, Cross-sectional Study. *Journal of Glaucoma*, 27(4), pp.364-370.

Ahn, J., Lee, S., Rim, T., Park, R., Yang, H., Kim, T., Yoon, K. and Seo, K., 2014. Prevalence of and Risk Factors Associated With Dry Eye: The Korea National Health and Nutrition Examination Survey 2010–2011. *American Journal of Ophthalmology*, 158(6), pp.1205-1214.e7.

Akiyama, R., Usui, T. and Yamagami, S., 2015. Diagnosis of Dry Eye by Tear Meniscus Measurements Using Anterior Segment Swept Source Optical Coherence Tomography. *Cornea*, 34(Supplement 11), pp.S115-S120.

Albietz, J. and Schmid, K., 2018. Intense pulsed light treatment and meibomian gland expression for moderate to advanced meibomian gland dysfunction. *Clinical and Experimental Optometry*, 101(1), pp.23-33.

Alex, A., Edwards, A., Hays, J., Kerkstra, M., Shih, A., de Paiva, C. and Pflugfelder, S., 2013. Factors Predicting the Ocular Surface Response to Desiccating Environmental Stress. *Investigative Opthalmology & Visual Science*, 54(5), pp.3325-3332.

Alghamdi, W., Markoulli, M., Holden, B. and Papas, E., 2016. Impact of duration of contact lens wear on the structure and function of the meibomian glands. *Ophthalmic and Physiological Optics*, 36(2), pp.120-131.

Alghamdi, W., Markoulli, M. and Papas, E., 2020. The relationship between tear film MMP-9 and meibomian gland changes during soft contact lens wear. *Contact Lens and Anterior Eye*, 43(2), pp.154-158.

Al-Hayouti, H., Daniel, M., Hingorani, M., Calder, V. and Dahlmann-Noor, A., 2019. Meibography and corneal volume optical coherence tomography to quantify damage to ocular structures in children with blepharokeratoconjunctivitis. *Acta Ophthalmologica*, 97(7), pp.e981-e986.

Aller, T., Liu, M. and Wildsoet, C., 2016. Myopia Control with Bifocal Contact Lenses. *Optometry and Vision Science*, 93(4), pp.344-352.

Alonso-Caneiro, D., Iskander, D. and Collins, M., 2009. Assessment of Tear Film Surface Quality Using Dynamic-Area High-Speed Videokeratoscopy. *IEEE Transactions on Biomedical Engineering*, 56(5), pp.1473-1481.

Alonso-Caneiro, D., Szczesna-Iskander, D., Iskander, D., Read, S. and Collins, M., 2013. Application of texture analysis in tear film surface assessment based on videokeratoscopy. *Journal of Optometry*, 6(4), pp.185-193.

Alshammeri, S., Madden, L., Hagan, S. and Pearce, E., 2019. Strip meniscometry tube: a rapid method for assessing aqueous deficient dry eye. *Clinical and Experimental Optometry*, 103(4), pp.469-473.

Altin Ekin, M., Karadeniz Ugurlu, S. and Kahraman, H., 2020. Meibomian Gland Dysfunction and Its Association With Ocular Discomfort in Patients With Ocular Prosthesis. *Eye & Contact Lens: Science & Clinical Practice*, 46(5), pp.285-290.

Alzahrani, Y., Holguin, L., Pritchard, N. and Efron, N., 2018. Longitudinal changes in Langerhans cell density of the cornea and conjunctiva in contact lens-induced dry eye. *Contact Lens and Anterior Eye*, 41, p.S88.

Amorim-de-Sousa, A., Macedo-de-Araújo, R., Fernandes, P., Queirós, A. and González-Méijome, J., 2019. Impact of Defocus and High-Order Aberrations on Light Disturbance Measurements. *Journal of Ophthalmology*, 2019, pp.1-8.

Amparo, F., Wang, H., Emami-Naeini, P., Karimian, P. and Dana, R., 2013. The Ocular Redness Index: A Novel Automated Method for Measuring Ocular Injection. *Investigative Opthalmology & Visual Science*, 54(7), pp.4821-4826.

Anstice, N. and Phillips, J., 2011. Effect of Dual-Focus Soft Contact Lens Wear on Axial Myopia Progression in Children. *Ophthalmology*, 118(6), pp.1152-1161.

Aragona, E., Rania, L., Postorino, E., Interdonato, A., Giuffrida, R., Cannavò, S., Puzzolo, D. and Aragona, P., 2017. Tear film and ocular surface assessment in psoriasis. *British Journal of Ophthalmology*, 102(3), pp.302-308.

Arita, R. and Fukuoka, S., 2020. Efficacy of Azithromycin Eyedrops for Individuals With Meibomian Gland Dysfunction–Associated Posterior Blepharitis. *Eye & Contact Lens: Science & Clinical Practice*, 47(1), pp.54-59.

Arita, R., Fukuoka, S., Mizoguchi, T. and Morishige, N., 2020. Multicenter Study of Intense Pulsed Light for Patients with Refractory Aqueous-Deficient Dry Eye Accompanied by Mild Meibomian Gland Dysfunction. *Journal of Clinical Medicine*, 9(11), p.3467.

Arita, R., Fukuoka, S. and Morishige, N., 2017a. Functional Morphology of the Lipid Layer of the Tear Film. *Cornea*, 36(1), pp.S60-S66.

Arita, R., Fukuoka, S. and Morishige, N., 2017b. New Insights Into the Lipid Layer of the Tear Film and Meibomian Glands. *Eye & Contact Lens: Science & Clinical Practice*, 43(6), pp.335-339.

Arita, R., Fukuoka, S. and Morishige, N., 2017c. New insights into the morphology and function of meibomian glands. *Experimental Eye Research*, 163, pp.64-71.

Arita, R., Fukuoka, S. and Morishige, N., 2017d. Meibomian Gland Dysfunction and Contact Lens Discomfort. *Eye & Contact Lens: Science & Clinical Practice*, 43(1), pp.17-22.

Arita, R., Itoh, K., Inoue, K. and Amano, S., 2008. Noncontact Infrared Meibography to Document Age-Related Changes of the Meibomian Glands in a Normal Population. *Ophthalmology*, 115(5), pp.911-915.

Arita, R., Itoh, K., Inoue, K., Kuchiba, A., Yamaguchi, T. and Amano, S., 2009a. Contact Lens Wear Is Associated with Decrease of Meibomian Glands. *Ophthalmology*, 116(3), pp.379-384.

Arita, R., Itoh, K., Maeda, S., Maeda, K., Furuta, A., Fukuoka, S., Tomidokoro, A. and Amano, S., 2009b. Proposed Diagnostic Criteria for Obstructive Meibomian Gland Dysfunction. *Ophthalmology*, 116(11), pp.2058-2063.e1.

Arita, R., Mizoguchi, T., Fukuoka, S. and Morishige, N., 2018. Multicenter Study of Intense Pulsed Light Therapy for Patients With Refractory Meibomian Gland Dysfunction. *Cornea*, 37, pp.1566-71.

Arita, R., Morishige, N., Shirakawa, R., Sato, Y. and Amano, S., 2015. Effects of Eyelid Warming Devices on Tear Film Parameters in Normal Subjects and Patients with Meibomian Gland Dysfunction. *The Ocular Surface*, 13(4), pp.321-330.

Arita, R., Suehiro, J., Haraguchi, T., Shirakawa, R., Tokoro, H. and Amano, S., 2013. Objective image analysis of the meibomian gland area. *British Journal of Ophthalmology*, 98(6), pp.746-755.

Arita, R., Yabusaki, K., Hirono, T., Yamauchi, T., Ichihashi, T., Fukuoka, S. and Morishige, N., 2019. Automated Measurement of Tear Meniscus Height with the Kowa DR-1α Tear Interferometer in Both Healthy Subjects and Dry Eye Patients. *Investigative Opthalmology & Visual Science*, 60(6), pp.2092-2101.

Arntz-Bustos, A. and Durán-de-la-Colina, J., 2004. *Anatomía funcional de la superficie ocular*. Madrid: Sociedad Española de Oftalmología.

Arriola-Villalobos, P., Fernández-Vigo, J., Díaz-Valle, D., Almendral-Gómez, J., Fernández-Pérez, C. and Benítez-del-Castillo, J., 2017. Lower Tear Meniscus Measurements Using a New Anterior Segment Swept-Source Optical Coherence Tomography and Agreement With Fourier-Domain Optical Coherence Tomography. *Cornea*, 36(2), pp.183-188.

Arriola-Villalobos, P., Fernández-Vigo, J., Díaz-Valle, D., Peraza-Nieves, J., Fernández-Pérez, C. and Benítez-del-Castillo, J., 2015. Assessment of lower tear meniscus measurements obtained with Keratograph and agreement with Fourier-domain optical-coherence tomography. *British Journal of Ophthalmology*, 99(8), pp.1120-1125.

Asena, L., Altınörs, D., Cezairlioğlu, Ş. and Bölük, S., 2017. Effect of dry eye on Scheimpflug imaging of the cornea and elevation data. *Canadian Journal of Ophthalmology*, 52(3), pp.313-317.

Asharlous, A., Jafarzadehpur, E., Mirzajani, A. and Khabazkhoob, M., 2015. Comparing Tear Film Stability Prolongation Evaluated by Javal–Schiotz Keratometer and Slitlamp. *Eye & Contact Lens: Science & Clinical Practice*, 41(2), pp.101-106.

Asiedu, K., Kyei, S., Boampong, F. and Ocansey, S., 2017. Symptomatic Dry Eye and Its Associated Factors: A Study of University Undergraduate Students in Ghana. *Eye & Contact Lens: Science & Clinical Practice*, 43(4), pp.262-266.

Azzam, D., Nag, N., Tran, J., Chen, L., Visnagra, K., Marshall, K. and Wade, M., 2020. A Novel Epidemiological Approach to Geographically Mapping Population Dry Eye Disease in the United States Through Google Trends. *Cornea*, 40(3), pp.282-291.

Baek, J., Doh, S. and Chung, S., 2015. Comparison of Tear Meniscus Height Measurements Obtained With the Keratograph and Fourier Domain Optical Coherence Tomography in Dry Eye. *Cornea*, 34(10), pp.1209-1213.

Bai, Y., Ngo, W. and Nichols, J., 2019. Characterization of the thickness of the tear film lipid layer using high resolution microscopy. *The Ocular Surface*, 17(2), pp.356-359.

Bai, Y. and Nichols, J., 2017. Advances in thickness measurements and dynamic visualization of the tear film using non-invasive optical approaches. *Progress in Retinal and Eye Research*, 58, pp.28-44.

Bai, Y. and Nichols, J., 2019. In vivo thickness measurement of the lipid layer and the overall tear film by interferometry. *Optics Letters*, 44(10), pp.2410-2413.

Ban, Y., Ogawa, Y., Ibrahim, O., Tatematsu, Y., Kamoi, M., Uchino, M., Yaguchi, S., Dogru, M. and Tsubota, K., 2011. Morphologic evaluation of meibomian glands in chronic graft-versus-host disease using in vivo laser confocal microscopy. *Mol vis*, 17, pp.2533-2543.

Bandlitz, S., Peter, B., Pflugi, T., Jaeger, K., Anwar, A., Bikhu, P., Nosch, D. and Wolffsohn, J., 2019a. Agreement and repeatability of four different devices to measure non-invasive tear breakup time (NIBUT). *Contact Lens and Anterior Eye*, 43(6), pp.507-511.

Bandlitz, S., Purslow, C., Murphy, P. and Pult, H., 2019b. Lid-parallel conjunctival fold (LIPCOF) morphology imaged by optical coherence tomography and its relationship to LIPCOF grade. *Contact Lens and Anterior Eye*, 42(3), pp.299-303.

Barnett, M., Courey, C., Fadel, D., Lee, K., Michaud, L., Montani, G., van der Worp, E., Vincent, S., Walker, M., Bilkhu, P. and Morgan, P., 2021. BCLA CLEAR - Scleral lenses. *Contact Lens and Anterior Eye*, 44(2), pp.270-288.

Bartlett, J., Keith, M., Sudharshan, L. and Snedecor, S., 2015. Associations between signs and symptoms of dry eye disease: a systematic review. *Clinical Ophthalmology*, pp.1719-1730.

Baudouin, C., Barton, K., Cucherat, M. and Traverso, C., 2015. The Measurement of Bulbar Hyperemia: Challenges and Pitfalls. *European Journal of Ophthalmology*, 25(4), pp.273-279.

Baudouin, C., Irkeç, M., Messmer, E., Benítez-del-Castillo, J., Bonini, S., Figueiredo, F., Geerling, G., Labetoulle, M., Lemp, M., Rolando, M., Van Setten, G. and Aragona, P., 2017. Clinical impact of inflammation in dry eye disease: proceedings of the ODISSEY group meeting. *Acta Ophthalmologica*, 96(2), pp.111-119.

Begley, C., Caffery, B., Chalmers, R. and Mitchell, G., 2002. Use of the Dry Eye Questionnaire to Measure Symptoms of Ocular Irritation in Patients With Aqueous Tear Deficient Dry Eye. *Cornea*, 21(7), pp.664-670.

Begley, C., Caffery, B., Nichols, K. and Chalmers, R., 2000. Responses of Contact Lens Wearers to a Dry Eye Survey. *Optometry and Vision Science*, 77(1), pp.40-46.

Begley, C., Chalmers, R., Mitchell, G., Nichols, K., Caffery, B., Simpson, T., DuToit, R., Portello, J. and Davis, L., 2001. Characterization of Ocular Surface Symptoms From Optometric Practices in North America. *Cornea*, 20(6), pp.610-618.

Belalcázar-Rey, S., Sánchez Huerta, V., Ochoa-Tabares, J., Altamirano Vallejo, S., Soto-Gómez, A., Suárez-Velasco, R., García-Félix, F., Baiza-Durán, L., Olvera-Montaño, O. and Muñoz-Villegas, P., 2021. Efficacy and Safety of Sodium Hyaluronate/chondroitin Sulfate Preservative-free Ophthalmic Solution in the Treatment of Dry Eye: A Clinical Trial. *Current Eye Research*, 46(7), pp.919-929.

Belmonte, C., Nichols, J., Cox, S., Brock, J., Begley, C., Bereiter, D., Dartt, D., Galor, A., Hamrah, P., Ivanusic, J., Jacobs, D., McNamara, N., Rosenblatt, M., Stapleton, F. and Wolffsohn, J., 2017. TFOS DEWS II pain and sensation report. *The Ocular Surface*, 15(3), pp.404-437.

Benelli, U., 2011. Systane lubricant eye drops in the management of ocular dryness. *Clinical Ophthalmology*, 5(1), pp.783-790.

Benítez-del-Castillo, J., Labetoulle, M., Baudouin, C., Rolando, M., Akova, Y., Aragona, P., Geerling, G., Merayo-Lloves, J., Messmer, E. and Boboridis, K., 2017. Visual acuity and quality of life in dry eye disease: Proceedings of the OCEAN group meeting. *The Ocular Surface*, 15(2), pp.169-178.

Benito, A., Bueno, J., Pérez, G. and Artal, P., 2019. Tear-film dynamics by combining double-pass images, pupil retro-illumination, and contrast sensitivity. *Journal of the Optical Society of America A*, 36(4), pp.138-142.

Benito, A., Pérez, G., Mirabet, S., Vilaseca, M., Pujol, J., Marín, J. and Artal, P., 2011. Objective optical assessment of tear-film quality dynamics in normal and mildly symptomatic dry eyes. *Journal of Cataract and Refractive Surgery*, 37(8), pp.1481-1487.

Berger, R. and Corrsin, S., 1974. A surface tension gradient mechanism for driving the pre-corneal tear film after a blink. *Journal of Biomechanics*, 7(3), pp.225-238.

Berger, J., Head, K. and Salmon, T., 2009. Comparison of two artificial tear formulations using aberrometry. *Clinical and Experimental Optometry*, 92(3), pp.206-211.

Beshtawi, I., Qaddomi, J., Khuffash, H., El-Titi, S., Ghannam, M. and Otaibi, R., 2019. Ocular surface response and subjective symptoms associated to lens care solutions in Palestine. *Journal of Optometry*, 12(4), pp.248-255.

Best, N., Drury, L. and Wolffsohn, J., 2012. Clinical evaluation of the Oculus Keratograph. *Contact Lens and Anterior Eye*, 35(4), pp.171-174.

Bettach, E., Zadok, D., Abulafia, A., Shoshani, A., Ghebali, R., Weill, Y. and Smadja, D., 2021. Influence of Reading on Smartphone Screens on Visual Optical Quality Metrics and Tear Film Stability. *Cornea*, 40(10), pp.1309-1315.

Bhandari, V., Reddy, J., Relekar, K., Ingawale, A. and Shah, N., 2016. Non-invasive assessment of tear film stability with a novel corneal topographer in Indian subjects. *International Ophthalmology*, 36(6), pp.781-790.

Bhargava, R., Kumar, P., Phogat, H., Kaur, A. and Kumar, M., 2015. Oral omega-3 fatty acids treatment in computer vision syndrome related dry eye. *Contact Lens and Anterior Eye*, 38(3), pp.206-210.

Bilkhu, P., Naroo, S. and Wolffsohn, J., 2014a. Effect of a Commercially Available Warm Compress on Eyelid Temperature and Tear Film in Healthy Eyes. *Optometry and Vision Science*, 91(2), pp.163-170.

Bilkhu, P., Naroo, S. and Wolffsohn, J., 2014b. Randomised masked clinical trial of the MGDRx eyebag for the treatment of meibomian gland dysfunction-related evaporative dry eye. *British Journal of Ophthalmology*, 98(12), pp.1707-1711.

Bilkhu, P., Vidal-Rohr, M., Trave-Huarte, S. and Wolffsohn, J., 2021. Effect of meibomian gland morphology on functionality with applied treatment. *Contact Lens and Anterior Eye*, p.101402.

Bitton, E., Lacroix, Z. and Léger, S., 2016. In-vivo heat retention comparison of eyelid warming masks. *Contact Lens and Anterior Eye*, 39(4), pp.311-315.

Blalock, T., Spurr-Michaud, S., Tisdale, A., Heimer, S., Gilmore, M., Ramesh, V. and Gipson, I., 2007. Functions of MUC16 in Corneal Epithelial Cells. *Investigative Opthalmology & Visual Science*, 48(10), p.4509.

Bland, J. and Altman, D., 2010. Statistical methods for assessing agreement between two methods of clinical measurement. *International Journal of Nursing Studies*, 47(8), pp.931-936.

Bobek, L. and Situ, H., 2003. MUC7 20-Mer: Investigation of Antimicrobial Activity, Secondary Structure, and Possible Mechanism of Antifungal Action. *Antimicrobial Agents and Chemotherapy*, 47(2), pp.643-652.

Bonaccorsi, I., De Pasquale, C., Campana, S., Barberi, C., Cavaliere, R., Benedetto, F. and Ferlazzo, G., 2015. Natural killer cells in the innate immunity network of atherosclerosis. *Immunology Letters*, 168(1), pp.51-57.

Borchman, D., Yappert, M. and Foulks, G., 2010. Changes in human meibum lipid with meibomian gland dysfunction using principal component analysis. *Experimental Eye Research*, 91(2), pp.246-256.

Bradley, A., Nam, J., Xu, R., Harman, L. and Thibos, L., 2014. Impact of contact lens zone geometry and ocular optics on bifocal retinal image quality. *Ophthalmic and Physiological Optics*, 34(3), pp.331-345.

Braun, R., King-Smith, P., Begley, C., Li, L. and Gewecke, N., 2015. Dynamics and function of the tear film in relation to the blink cycle. *Progress in Retinal and Eye Research*, 45, pp.132-164.

Brennan, N., Lowe, R., Efron, N. and Harris, M., 1990. In Vivo Dehydration of Disposable (Acuvue) Contact Lenses. *Optometry and Vision Science*, 67(3), pp.201-203.

Brito, P., Salgado-Borges, J., Neves, H., Gonzalez-Meijome, J. and Monteiro, M., 2015. Light-distortion analysis as a possible indicator of visual quality after refractive lens exchange with diffractive multifocal intraocular lenses. *Journal of Cataract and Refractive Surgery*, 41(3), pp.613-622.

Bron, A., 2015 *The definition and classification of dry eye disease.* In: C. Chan, ed. 2015. Dry Eye: A practical approach. Springer.

Bron, A., Benjamin, L. and Snibson, G., 1991. Meibomian gland disease. Classification and grading of lid changes. *Eye*, 5(4), pp.395-411.

Bron, A., de Paiva, C., Chauhan, S., Bonini, S., Gabison, E., Jain, S., Knop, E., Markoulli, M., Ogawa, Y., Perez, V., Uchino, Y., Yokoi, N., Zoukhri, D. and Sullivan, D., 2017. TFOS DEWS II pathophysiology report. *The Ocular Surface*, 15(3), pp.438-510.

Bron, A. and Tiffany, J., 1998. The meibomian glands and tear film lipids. Structure, function and control. *Advances in experimental medicine and biology*, 438, pp.281-95.

Bron, A. and Tiffany, J., 2004. The Contribution of Meibomian Disease to Dry Eye. *The Ocular Surface*, 2(2), pp.149-164.

Bron, A., Tiffany, J., Gouveia, S., Yokoi, N. and Voon, L., 2004. Functional aspects of the tear film lipid layer. *Experimental Eye Research*, 78(3), pp.347-360.

Brown, M., 2009. Value-Based Medicine, Comparative Effectiveness, and Cost-effectiveness Analysis of Topical Cyclosporine for the Treatment of Dry Eye Syndrome. *Archives of Ophthalmology*, 127(2), pp.146-152.

Calvão-Santos, G., Borges, C., Nunes, S., Salgado-Borges, J. and Duarte, L., 2011. Efficacy of 3 Different Artificial Tears for the Treatment of Dry Eye in Frequent Computer Users and/or Contact Lens Users. *European Journal of Ophthalmology*, 21(5), pp.538-544.

Canan, H., Altan-Yaycioglu, R., Ulas, B., Sizmaz, S. and Coban-Karatas, M., 2014. Interexaminer Reproducibility of Optical Coherence Tomography for Measuring the Tear Film Meniscus. *Current Eye Research*, 39(12), pp.1145-1150.

Cardigos, J., Barcelos, F., Carvalho, H., Hipólito, D., Crisóstomo, S., Vaz-Patto, J. and Alves, N., 2018. Tear Meniscus and Corneal Sub-basal Nerve Plexus Assessment in Primary Sjögren Syndrome and Sicca Syndrome Patients. *Cornea*, 38(2), pp.221-228.

Cardona, G. and López, S., 2016. Pupil diameter, working distance and illumination during habitual tasks. Implications for simultaneous vision contact lenses for presbyopia. *Journal of Optometry*, 9(2), pp.78-84.

Cardona, G., García, C., Serés, C., Vilaseca, M. and Gispets, J., 2011. Blink Rate, Blink Amplitude, and Tear Film Integrity during Dynamic Visual Display Terminal Tasks. *Current Eye Research*, 36(3), pp.190-197.

Carracedo, G., Pastrana, C., Serramito, M. and Rodriguez-Pomar, C., 2018. Evaluation of tear meniscus by optical coherence tomography after different sodium hyaluronate eyedrops instillation. *Acta Ophthalmologica*, 97(2), pp.e162-e169.

Carracedo, G., Recchioni, A., Alejandre-Alba, N., Martin-Gil, A., Crooke, A., Morote, I. and Pintor, J., 2014. Signs and Symptoms of Dry Eye in Keratoconus Patients: A Pilot Study. *Current Eye Research*, 40(11), pp.1088-1094.

Cavanagh, H., Robertson, D., Petroll, W. and Jester, J., 2010. Castroviejo Lecture 2009: 40 Years in Search of the Perfect Contact Lens. *Cornea*, 29(10), pp.1075-1085.

Celik, T., Lee, H., Petznick, A. and Tong, L., 2013. Bioimage informatics approach to automated meibomian gland analysis in infrared images of meibography. *Journal of Optometry*, 6(4), pp.194-204.

Cerviño, A., Dominguez-Vicent, A., Ferrer-Blasco, T., García-Lázaro, S. and Albarrán-Diego, C., 2015. Intrasubject repeatability of corneal power, thickness, and wavefront aberrations with a new version of a dual rotating Scheimpflug–Placido system. *Journal of Cataract and Refractive Surgery*, 41(1), pp.186-192.

Cerviño, A., García Lázaro, S. and Montés-Micó, R., 2011. Evaluación del segmento anterior. In: R. Montés-Micó, ed. 2011. *Optometría. Principios básicos y aplicación clínica.* Barcelona:Elsevier. pp.157-184.

Chalmers, R., 2014. Overview of factors that affect comfort with modern soft contact lenses. *Contact Lens and Anterior Eye*, 37(2), pp.65-76.

Chalmers, R. and Begley, C., 2006. Dryness symptoms among an unselected clinical population with and without contact lens wear. *Contact Lens and Anterior Eye*, 29(1), pp.25-30.

Chalmers, R., Begley, C. and Caffery, B., 2010. Validation of the 5-Item Dry Eye Questionnaire (DEQ-5): Discrimination across self-assessed severity and aqueous tear deficient dry eye diagnoses. *Contact Lens and Anterior Eye*, 33(2), pp.55-60.

Chamberlain, P., Lazon de la Jara, P., Arumugam, B. and Bullimore, M., 2021. Axial length targets for myopia control. *Ophthalmic and Physiological Optics*, 41(3), pp.523-531.

Chamberlain, P., Peixoto-de-Matos, S., Logan, N., Ngo, C., Jones, D. and Young, G., 2019. A 3-year Randomized Clinical Trial of MiSight Lenses for Myopia Control. *Optometry and Vision Science*, 96(8), pp.556-567.

Chan, H., Zhao, Y., Tun, T. and Tong, L., 2015. Repeatability of tear meniscus evaluation using spectral-domain Cirrus® HD-OCT and time-domain Visante® OCT. *Contact Lens and Anterior Eye*, 38(5), pp.368-372.

Chan, T., Chow, S., Wan, K. and Yuen, H., 2019. Update on the association between dry eye disease and meibomian gland dysfunction. *Hong Kong Medical Journal*, 25, pp.38-47.

Chan, T., Wan, K., Shih, K. and Jhanji, V., 2017. Advances in dry eye imaging: the present and beyond. *British Journal of Ophthalmology*, 102(3), pp.295-301.

Chang, K., Oh, J., In, Y., Kim, M., Shin, K., Wee, W., Lee, J. and Park, M., 2009. Preliminary Effects of Oral Uridine on the Ocular Surface in Dry Eye Patients. *Journal of Korean Medical Science*, 24(4), pp.701-707.

Chen, Q., Wang, J., Shen, M., Cui, L., Cai, C., Li, M., Li, K. and Lu, F., 2011. Tear Menisci and Ocular Discomfort during Daily Contact Lens Wear in Symptomatic Wearers. *Investigative Opthalmology & Visual Science*, 52(5), pp.2175-2180.

Chen, Q., Wang, J., Tao, A., Shen, M., Jiao, S. and Lu, F., 2010. Ultrahigh-Resolution Measurement by Optical Coherence Tomography of Dynamic Tear Film Changes on Contact Lenses. *Investigative Opthalmology & Visual Science*, 51(4), p.1988.

Chen, W., Xu, Z., Jiang, H., Zhou, J., Wang, L. and Wang, J., 2017. Altered Bulbar Conjunctival Microcirculation in Response to Contact Lens Wear. *Eye & Contact Lens: Science & Clinical Practice*, 43(2), pp.95-99.

Chen, Y., Chauhan, S., Saban, D., Sadrai, Z., Okanobo, A. and Dana, R., 2011b. Interferon-γ-secreting NK cells promote induction of dry eye disease. *Journal of Leukocyte Biology*, 89(6), pp.965-972.

Chen, Y., Li, J., Wu, Y., Lin, X., Deng, X. and Yun-e, Z., 2021. Comparative Evaluation in Intense Pulsed Light Therapy Combined with or without Meibomian Gland Expression for the Treatment of Meibomian Gland Dysfunction. *Current Eye Research*, pp.1-7.

Cheng, J., Yang, Y., Kong, X., Zeng, L., Chen, Z., Xu, J. and Zhang, C., 2020. The Effect of 0.01% Atropine Eye Drops on the Ocular Surface in Children for the Control of Myopia—The Primary Results from a Six-Month Prospective Study. *Therapeutics and Clinical Risk Management*, 16, pp.735-740.

Cheng, S., Zhang, M., Chen, H., Fan, W. and Huang, Y., 2019. The correlation between the microstructure of meibomian glands and ocular Demodex infestation. *Medicine*, 98(19), p.e15595.

Cher, I., 2008. A New Look at Lubrication of the Ocular Surface: Fluid Mechanics Behind the Blinking Eyelids. *The Ocular Surface*, 6(2), pp.79-86.

Chew, C., Jansweijer, C., Tiffany, J., Dikstein, S. and Bron, A., 1993. An instrument for quantifying meibomian lipid on the lid margin: the Meibometer. *Current Eye Research*, 12(3), pp.247-254.

Chhadva, P., Goldhardt, R. and Galor, A., 2017. Meibomian Gland Disease: The Role of Gland Dysfunction in Dry Eye Disease. *Ophthalmology*, 124, pp.S20-S26.

Cho, B., Jee, D., Kim, W., Shin, M., Kim, E., Kim, M. and Hwang, H., 2019. Direct Visualization of Continuous Meibum Secretion From the Orifices of Meibomian Glands to the Tear Film. *Cornea*, 38(10), pp.1245-1252.

Cho, P., Brown, B., Chan, I., Conway, R. and Yap, M., 1992. Reliability of the Tear Break-Up Time Technique of Assessing Tear Stability and the Locations of the Tear Break-Up in Hong Kong Chinese. *Optometry and Vision Science*, 69(11), pp.879-885.

Choi, J., Li, Y., Kim, S., Jin, R., Kim, Y., Choi, W., You, I. and Yoon, K., 2018. The influences of smartphone use on the status of the tear film and ocular surface. *PLOS ONE*, 13(10), p.e0206541.

Chotikavanich, S., de Paiva, C., Li, D., Chen, J., Bian, F., Farley, W. and Pflugfelder, S., 2009. Production and Activity of Matrix Metalloproteinase-9 on the Ocular Surface Increase in Dysfunctional Tear Syndrome. *Investigative Opthalmology & Visual Science*, 50(7), p.3203.

Chou, Y., Fan, N. and Lin, P., 2019. Value of lipid layer thickness and blinking pattern in approaching patients with dry eye symptoms. *Canadian Journal of Ophthalmology*, 54(6), pp.735-740.

Clausi, D., 2002. An analysis of co-occurrence texture statistics as a function of grey level quantization. *Canadian Journal of Remote Sensing*, 28(1), pp.45-62.

Clegg, J., Guest, J., Lehman, A. and Smith, A., 2006. The Annual Cost of Dry Eye Syndrome in France, Germany, Italy, Spain, Sweden and the United Kingdom Among Patients Managed by Ophthalmologists. *Ophthalmic Epidemiology*, 13(4), pp.263-274.

Cohen, J., 1968. Weighted kappa: Nominal scale agreement provision for scaled disagreement or partial credit. *Psychological Bulletin*, 70(4), pp.213-220.

Colorado, L., Alzahrani, Y., Pritchard, N. and Efron, N., 2016. Time Course of Changes in Goblet Cell Density in Symptomatic and Asymptomatic Contact Lens Wearers. *Investigative Opthalmology & Visual Science*, 57(6), pp.2560-2566.

Conners, R., Trivedi, M. and Harlow, C., 1984. Segmentation of a high-resolution urban scene using texture operators. *Computer Vision, Graphics, and Image Processing*, 25(3), pp.273-310.

Coursey, T., Bohat, R., Barbosa, F., Pflugfelder, S. and de Paiva, C., 2014. Desiccating Stress–Induced Chemokine Expression in the Epithelium Is Dependent on Upregulation of NKG2D/RAE-1 and Release of IFN-γ in Experimental Dry Eye. *The Journal of Immunology*, 193(10), pp.5264-5272.

Cox, S., Nichols, K. and Nichols, J., 2015. Agreement between Automated and Traditional Measures of Tear Film Breakup. *Optometry and Vision Science*, 92(9), pp.e257-e263.

Craig, J., Nichols, K., Akpek, E., Caffery, B., Dua, H., Joo, C., Liu, Z., Nelson, J., Nichols, J., Tsubota, K. and Stapleton, F., 2017. TFOS DEWS II Definition and Classification Report. *The Ocular Surface*, 15(3), pp.276-283.

Craig, J. and Tomlinson, A., 1997. Importance of the Lipid Layer in Human Tear Film Stability and Evaporation. *Optometry and Vision Science*, 74(1), pp.8-13.

Cronau, H., Kankanala, R. and Mauger, T., 2010. Diagnosis and management of red eye in primary care. *American Family Physician*, 81(2), pp.137-144.

Cui, X., Wu, Q., Zhai, Z., Yang, Y., Wei, A., Xu, J. and Hong, J., 2020. Comparison of the Meibomian Gland Openings by Optical Coherence Tomography in Obstructive Meibomian Gland Dysfunction and Normal Patients. *Journal of Clinical Medicine*, 9(10), p.3181.

Cwiklik, L., 2016. Tear film lipid layer: A molecular level view. *Biochimica et Biophysica Acta (BBA) - Biomembranes*, 1858(10), pp.2421-2430.

Czajkowski, G., Kaluzny, B., Laudencka, A., Malukiewicz, G. and Kaluzny, J., 2012. Tear Meniscus Measurement by Spectral Optical Coherence Tomography. *Optometry and Vision Science*, 89(3), pp.336-342.

da Cruz, L., Souza, J., de Sousa, J., Santos, A., de Paiva, A., de Almeida, J., Silva, A., Junior, G. and Gattass, M., 2020. Interferometer eye image classification for dry eye categorization using phylogenetic diversity indexes for texture analysis. *Computer Methods and Programs in Biomedicine*, 188, p.105269.

Dang, A., Nayeni, M., Mather, R. and Malvankar-Mehta, M., 2020. Hormone replacement therapy for dry eye disease patients: systematic review and meta-analysis. *Canadian Journal of Ophthalmology*, 55(1), pp.3-11.

Darbà, J. and Ascanio, M., 2020. Economic impact of dry eye disease in Spain: A multicentre retrospective insurance claims database analysis. *European Journal of Ophthalmology*, 31(2), pp.328-333.

Dartt, D., 2002. Regulation of mucin and fluid secretion by conjunctival epithelial cells. *Progress in Retinal and Eye Research*, 21(6), pp.555-576.

Debarun, D. and Wolffsohn, J., 2021. Effect of large diameter and plasma coating on the initial adaptation of gas permeable contact lens fitting for neophytes. *Contact Lens and Anterior Eye*, 44(1), pp.76-80.

de Gracia, P., Dorronsoro, C. and Marcos, S., 2013. Multiple zone multifocal phase designs. *Optics Letters*, 38(18), pp.3526-3529.

Del Águila-Carrasco, A., Ferrer-Blasco, T., García-Lázaro, S., Esteve-Taboada, J. and Montés-Micó, R., 2015. Assessment of corneal thickness and tear meniscus during contact-lens wear. *Contact Lens and Anterior Eye*, 38(3), pp.185-193.

Denoyer, A., Rabut, G. and Baudouin, C., 2012. Tear Film Aberration Dynamics and Vision-Related Quality of Life in Patients with Dry Eye Disease. *Ophthalmology*, 119(9), pp.1811-1818.

Dereli-Can, G. and Kara, Ö., 2019. Noninvasive evaluation of anterior segment and tear film parameters and morphology of meibomian glands in a pediatric population with hypogonadism. *The Ocular Surface*, 17(4), pp.675-682.

Dermer, H., Hwang, J., Mittal, R., Cohen, A. and Galor, A., 2021. Corneal sub-basal nerve plexus microneuromas in individuals with and without dry eye. *British Journal of Ophthalmology*, 0, pp.1-7.

Deschamps, N., Ricaud, X., Rabut, G., Labbé, A., Baudouin, C. and Denoyer, A., 2013. The Impact of Dry Eye Disease on Visual Performance While Driving. *American Journal of Ophthalmology*, 156(1), pp.184-189.e3.

Díaz-Doutón, F., Benito, A., Pujol, J., Arjona, M., Güell, J. and Artal, P., 2006. Comparison of the Retinal Image Quality with a Hartmann-Shack Wavefront Sensor and a Double-Pass Instrument. *Investigative Opthalmology & Visual Science*, 47(4), pp.1710-1716.

Diaz-Valle, D., Arriola-Villalobos, P., García-Vidal, S., Sánchez-Pulgarín, M., Sanz, L., Gegúndez-Fernández, J. and Benitez-del-Castillo, J., 2012. Effect of lubricating eyedrops on ocular light scattering as a measure of vision quality in patients with dry eye. *Journal of Cataract and Refractive Surgery*, 38(7), pp.1192-1197.

Diec, J., Tilia, D. and Thomas, V., 2018. Comparison of Silicone Hydrogel and Hydrogel Daily Disposable Contact Lenses. *Eye & Contact Lens: Science & Clinical Practice*, 44(1), pp.S167-S172.

Dikmetas, O., Kocabeyoglu, S. and Mocan, M., 2021. The Association between Meibomian Gland Atrophy and Corneal Subbasal Nerve Loss in Patients with Chronic Ocular Graft-versus-host Disease. *Current Eye Research*, 46(6), pp.796-801.

Dilly PN., 1994. Structure and function of the tear film. *Advances in Experimental Medicine and Biology*, 350, pp.239-247.

Doane, M., 1981. Blinking and the Mechanics of the Lacrimal Drainage System. *Ophthalmology*, 88(8), pp.844-851.

Dogan, A., Gurdal, C. and Arslan, N., 2018. Corneal confocal microscopy and dry eye findings in contact lens discomfort patients. *Contact Lens and Anterior Eye*, 41(1), pp.101-104.

Doguizi, S., Sekeroglu, M., Inanc, M. and Yılmazbas, P., 2019. Evaluation of tear meniscus dimensions using anterior segment optical coherence tomography in video terminal display workers. *Clinical and Experimental Optometry*, 102(5), pp.478-484.

Dos Santos, V., Schmetterer, L., Gröschl, M., Garhofer, G., Schmidl, D., Kucera, M., Unterhuber, A., Hermand, J., 2015. In vivo tear film thickness measurement and tear film dynamics visualization using spectral domain optical coherence tomography. Opt Express, 23(16): pp.21043-21063.

Dougherty, B., Nichols, J. and Nichols, K., 2011. Rasch Analysis of the Ocular Surface Disease Index (OSDI). *Investigative Opthalmology & Visual Science*, 52(12), pp.8630-8635.

Doughty, M., 2001. Consideration of Three Types of Spontaneous Eyeblink Activity in Normal Humans: during Reading and Video Display Terminal Use, in Primary Gaze, and while in Conversation. *Optometry and Vision Science*, 78(10), pp.712-725.

Doughty, M., Fonn, D., Richter, D., Simpson, T., Caffery, B. and Gordon, K., 1997. A Patient Questionnaire Approach to Estimating the Prevalence of Dry Eye Symptoms in Patients Presenting to Optometric Practices across Canada. *Optometry and Vision Science*, 74(8), pp.624-631.

Doughty, M., Laiquzzaman, M. and Button, N., 2001. Video-assessment of tear meniscus height in elderly Caucasians and its relationship to the exposed ocular surface. *Current Eye Research*, 22(6), pp.420-426.

Downie, L., 2015. Automated Tear Film Surface Quality Breakup Time as a Novel Clinical Marker for Tear Hyperosmolarity in Dry Eye Disease. *Investigative Opthalmology & Visual Science*, 56(12), pp.7260-7268.

Downie, L., Keller, P. and Vingrys, A., 2015. Assessing ocular bulbar redness: a comparison of methods. *Ophthalmic and Physiological Optics*, 36(2), pp.132-139.

D'Souza, S., Annavajjhala, S., Thakur, P., Mullick, R., Tejal, S. and Shetty, N., 2020. Study of tear film optics and its impact on quality of vision. *Indian Journal of Ophthalmology*, 68(12), pp.2899-2902.

Dumbleton, K., Caffery, B., Dogru, M., Hickson-Curran, S., Kern, J., Kojima, T., Morgan, P., Purslow, C., Robertson, D. and Nelson, J., 2013a. The TFOS International Workshop

on Contact Lens Discomfort: Report of the Subcommittee on Epidemiology. *Investigative Opthalmology & Visual Science*, 54(11), pp. 20-36.

Dumbleton, K., Woods, C., Jones, L. and Fonn, D., 2013b. The Impact of Contemporary Contact Lenses on Contact Lens Discontinuation. *Eye & Contact Lens: Science & Clinical Practice*, 39(1), pp.93-99.

Duong, K., McGwin, G., Franklin, Q., Cox, J. and Pucker, A., 2021. Treating Uncomfortable Contact Lens Wear With Orthokeratology. *Eye & Contact Lens: Science & Clinical Practice*, 47, pp.74–80.

Dutta, D., Kim, J., Sarkes, M., Nath, S. and Markoulli, M., 2019. The repeatability of subjective and objective tear ferning assessment and its association with lipid layer thickness, non-invasive tear break-up time and comfort. *Contact Lens and Anterior Eye*, 42(4), pp.420-427.

Efron, N., Brennan, N., Bruce, A., Duldig, D. and Russo, N., 1987. Dehydration of hydrogel lenses under normal wearing conditions. *CLAO J*, 13, pp.152-156.

Efron, N., Brennan, N., Currie, J., Fitzgerald, J. and Hughes, M., 1986. Determinants of the Initial Comfort of Hydrogel Contact Lenses. *Optometry and Vision Science*, 63(10), pp.819-823.

El Ameen, A., Majzoub, S., Vandermeer, G. and Pisella, P., 2018. Influence of cataract surgery on Meibomian gland dysfunction. *Journal Français d'Ophtalmologie*, 41(5), pp.e173-e180.

Eom, Y., Lee, J., Kang, S., Kim, H. and Song, J., 2013. Correlation Between Quantitative Measurements of Tear Film Lipid Layer Thickness and Meibomian Gland Loss in Patients With Obstructive Meibomian Gland Dysfunction and Normal Controls. *American Journal of Ophthalmology*, 155(6), pp.1104-1110.e2.

Erie, J., McLaren, J. and Patel, S., 2009. Confocal Microscopy in Ophthalmology. *American Journal of Ophthalmology*, 148(5), pp.639-646.

Eroglu, F., Karalezli, A. and Dursun, R., 2016. Is optical coherence tomography an effective device for evaluation of tear film meniscus in patients with acne rosacea?. *Eye*, 30(4), pp.545-552.

Escandón-García, S., Ribeiro, F., McAlinden, C., Queirós, A. and González-Méijome, J., 2018. Through-Focus Vision Performance and Light Disturbances of 3 New Intraocular Lenses for Presbyopia Correction. *Journal of Ophthalmology*, 2018, p.6165493.

Esmaeili, M., Dehnavi, A., Rabbani, H. and Hajizadeh, F., 2016. Three-dimensional segmentation of retinal cysts from spectral-domain optical coherence tomography images by the use of three-dimensional curvelet based K-SVD. *Journal of Medical Signals & Sensors*, 6(3), pp.166-171.

Faber, E., Golding, T., Lowe, R. and Brennan, N., 1991. Effect of Hydrogel Lens Wear on Tear Film Stability. *Optometry and Vision Science*, 68(5), pp.380-384.

Fan, Q., Pazo, E., You, Y., Zhang, C., Zhang, C., Xu, L. and He, W., 2020. Subjective Quality of Vision in Evaporative Dry Eye Patients After Intense Pulsed Light. *Photobiomodulation, Photomedicine, and Laser Surgery*, 38(7), pp.444-451.

Faria-Ribeiro, M., Amorim-de-Sousa, A. and González-Méijome, J., 2018. Predicted accommodative response from image quality in young eyes fitted with different dual-focus designs. *Ophthalmic and Physiological Optics*, 38(3), pp.309-316.

Faria-Ribeiro, M. and González-Méijome, J., 2019. Multifocal contact lenses: towards customisation?. *Ophthalmic and Physiological Optics*, 39(1), pp.37-45.

Farrand, K., Fridman, M., Stillman, I. and Schaumberg, D., 2017. Prevalence of Diagnosed Dry Eye Disease in the United States Among Adults Aged 18 Years and Older. *American Journal of Ophthalmology*, 182, pp.90-98.

Farrand, K., Stillman, I., Fridman, M. and Schaumberg, D., 2016. Impact of Dry Eye Disease on Quality of Life, Work Productivity, Daily Activities, and Health Care Resource Use in a Survey of 74,095 American Adults. *Value in Health*, 19(3), p.A127.

Faul, F., Erdfelder, E., Lang, A. and Buchner, A., 2007. G*Power 3: A flexible statistical power analysis program for the social, behavioral, and biomedical sciences. *Behavior Research Methods*, 39(2), pp.175-191.

Fedtke, C., Bakaraju, R., Ehrmann, K., Chung, J., Thomas, V. and Holden, B., 2016a. Visual performance of single vision and multifocal contact lenses in non-presbyopic myopic eyes. *Contact Lens and Anterior Eye*, 39(1), pp.38-46.

Fedtke, C., Ehrmann, K. and Bakaraju, R., 2020. Peripheral refraction and spherical aberration profiles with single vision, bifocal and multifocal soft contact lenses. *Journal of Optometry*, 13(1), pp.15-28.

Fedtke, C., Ehrmann, K., Thomas, V. and Bakaraju, R., 2016b. Visual performance with multifocal soft contact lenses in non-presbyopic myopic eyes during an adaptation period. *Clinical Optometry*, 8, pp.37-46.

Fedtke, C., Sha, J., Thomas, V., Ehrmann, K. and Bakaraju, R., 2017. Impact of Spherical Aberration Terms on Multifocal Contact Lens Performance. *Optometry and Vision Science*, 94(2), pp.197-207.

Fernandes, P., Amorim-de-Sousa, A., Queirós, A., Escandón-Garcia, S., McAlinden, C. and González-Méijome, J., 2018. Light disturbance with multifocal contact lens and monovision for presbyopia. *Contact Lens and Anterior Eye*, 41(4), pp.393-399.

Fernández, J., Rodríguez-Vallejo, M., Martínez, J., Tauste, A., García-Montesinos, J. and Piñero, D., 2018. Agreement and repeatability of objective systems for assessment of

the tear film. *Graefe's Archive for Clinical and Experimental Ophthalmology*, 256(8), pp.1535-1541.

Ferreira-Neves, H., Macedo-de-Araújo, R., Rico-del-Viejo, L., da-Silva, A., Queirós, A. and González-Méijome, J., 2015. Validation of a method to measure light distortion surrounding a source of glare. *Journal of Biomedical Optics*, 20(7), p.075002.

Ferrer-Blasco, T., García-Lázaro, S., Montés-Micó, R., Cerviño, A. and González-Méijome, J., 2009. Dynamic changes in the air–tear film interface modulation transfer function. *Graefe's Archive for Clinical and Experimental Ophthalmology*, 248(1), pp.127-132.

Ferrero, A., Alassane, S., Binquet, C., Bretillon, L., Acar, N., Arnould, L., Muselier-Mathieu, A., Delcourt, C., Bron, A. and Creuzot-Garcher, C., 2018. Dry eye disease in the elderly in a French population-based study (the Montrachet study: Maculopathy, Optic Nerve, nuTRition, neurovAsCular and HEarT diseases): Prevalence and associated factors. *The Ocular Surface*, 16(1), pp.112-119.

Fieguth, P. and Simpson, T., 2002. Automated measurement of bulbar redness. *Investigative Ophthalmology and Visual Science*, 43(2), pp.340-347.

Finis, D., Ackermann, P., Pischel, N., König, C., Hayajneh, J., Borrelli, M., Schrader, S. and Geerling, G., 2014. Evaluation of Meibomian Gland Dysfunction and Local Distribution of Meibomian Gland Atrophy by Non-contact Infrared Meibography. *Current Eye Research*, 40(10), pp.982-989.

Finis, D., Pischel, N., Schrader, S. and Geerling, G., 2013. Evaluation of Lipid Layer Thickness Measurement of the Tear Film as a Diagnostic Tool for Meibomian Gland Dysfunction. *Cornea*, 32(12), pp.1549-1553.

Fodor, E., Hagyó, K., Resch, M., Somodi, D. and Németh, J., 2010. Comparison of Tearscope-Plus versus Slit Lamp Measurements of Inferior Tear Meniscus Height in Normal Individuals. *European Journal of Ophthalmology*, 20(5), pp.819-824.

Fonn, D., Peterson, R. and Woods, C., 2010. Corneal Staining as a Response to Contact Lens Wear. *Eye & Contact Lens: Science & Clinical Practice*, 36(5), pp.318-321.

Foulks, G., 2007. The Correlation Between the Tear Film Lipid Layer and Dry Eye Disease. *Survey of Ophthalmology*, 52(4), pp.369-374.

Foulks, G. and Bron, A., 2003. Meibomian Gland Dysfunction: A Clinical Scheme for Description, Diagnosis, Classification, and Grading. *The Ocular Surface*, 1(3), pp.107-126.

Foulks, G. and Pflugfelder, S., 2014. New Testing Options for Diagnosing and Grading Dry Eye Disease. *American Journal of Ophthalmology*, 157(6), pp.1122-1129.

Foulks, G., Chalmers, R., Keir, N., Woods, C., Simpson, T., Lippman, R., Gleason, W., Schaumberg, D., Willcox, M. and Jalbert, I., 2013. The TFOS International Workshop on

Contact Lens Discomfort: Report of the Subcommittee on Clinical Trial Design and Outcomes. *Investigative Opthalmology & Visual Science*, 54(11), pp.157-182.

Friedland, B., Fleming, C., Blackie, C. and Korb, D., 2011. A Novel Thermodynamic Treatment for Meibomian Gland Dysfunction. *Current Eye Research*, 36(2), pp.79-87.

Friedman, J., Hastie, T. and Tibshirani, R., 2000. Additive logistic regression: a statistical view of boosting (With discussion and a rejoinder by the authors). *The Annals of Statistics*, 28(2), pp.337-407.

Fukuda, R., Usui, T., Miyai, T., Yamagami, S. and Amano, S., 2013. Tear Meniscus Evaluation by Anterior Segment Swept-Source Optical Coherence Tomography. *American Journal of Ophthalmology*, 155(4), pp.620-624.e2.

Gad, A., Vingrys, A., Wong, C., Jackson, D. and Downie, L., 2019. Tear film inflammatory cytokine upregulation in contact lens discomfort. *The Ocular Surface*, 17(1), pp.89-97.

Galor, A., Feuer, W., Lee, D., Florez, H., Faler, A., Zann, K. and Perez, V., 2012. Depression, Post-traumatic Stress Disorder, and Dry Eye Syndrome: A Study Utilizing the National United States Veterans Affairs Administrative Database. *American Journal of Ophthalmology*, 154(2), pp.340-346.

Gao, Y., Liu, R., Liu, Y., Ma, B., Yang, T., Hu, C. and Qi, H., 2021. Optical quality in patients with dry eye before and after treatment. *Clinical and Experimental Optometry*, 104(1), pp.101-106.

Garaszczuk, I., Mousavi, M., Cervino Exposito, A., Bartuzel, M., Montes-Micó, R. and Iskander, D., 2018. Evaluating tear clearance rate with optical coherence tomography. *Contact Lens and Anterior Eye*, 41(1), pp.54-59.

Garcia-Alfaro, P., Bergamaschi, L., Marcos, C., Garcia, S. and Rodríguez, I., 2020. Prevalence of ocular surface disease symptoms in peri- and postmenopausal women. *Menopause*, 27(9), pp.993-998.

Garcia-Lázaro, S., Belda-Salmerón, L., Ferrer-Blasco, T., Cerviño, A. and Montés-Micó, R., 2011. Comparison of two artificial tear formulations for dry eye through high-resolution optical coherence tomography. *Clinical and Experimental Optometry*, 94(6), pp.549-556.

García-Lázaro, S., Ferrer-Blasco, T., Madrid-Costa, D., Albarrán-Diego, C. and Montés-Micó, R., 2015. Visual Performance of Four Simultaneous-Image Multifocal Contact Lenses Under Dim and Glare Conditions. *Eye & Contact Lens: Science & Clinical Practice*, 41(1), pp.19-24.

Garcia-Lázaro, S., Madrid-Costa, D., Ferrer-Blasco, T., Montés-Micó, R. and Cerviño, A., 2012. OCT for Assessing Artificial Tears Effectiveness in Contact Lens Wearers. *Optometry and Vision Science*, 89(1), pp.E62-E69.

García-Marqués, J., Cerviño, A., Esteve-Taboada, J., Ferrer-Blasco, T. and Montés-Micó, R., 2016. Applications of an adaptive optics visual system. *J Emmetropia*, 3, pp.167-176.

García-Marqués, J., García-Lázaro, S., Martínez-Albert, N. and Cerviño, A., 2021a. Meibomian glands visibility assessment through a new quantitative method. *Graefe's Archive for Clinical and Experimental Ophthalmology*, 259(5), pp.1323-1331.

García-Marqués, J., García-Lázaro, S., Talens-Estarelles, C., Martínez-Albert, N. and Cerviño, A., 2021c. Diagnostic Capability of a New Objective Method to Assess Meibomian Gland Visibility. *Optometry and Vision Science*, 98(9), pp.1045-1055.

García-Marqués, J., Macedo-De-Araújo, R., Cerviño, A., García-Lázaro, S., McAlinden, C. and González-Méijome, J., 2020. Comparison of short-term light disturbance, optical and visual performance outcomes between a myopia control contact lens and a single-vision contact lens. *Ophthalmic and Physiological Optics*, 40(6), pp.718-727.

García-Marqués, J., Macedo-de-Araújo, R., Lopes-Ferreira, D., Cerviño, A., García-Lázaro, S. and González-Méijome, J., 2021b. Tear film stability over a myopia control contact lens compared to a monofocal design. *Clinical and Experimental Optometry*, 105(1), pp.41-47.

García-Marqués, J., Talens-Estarelles, C., Martínez-Albert, N., García-Lázaro, S. and Cerviño, A., 2021d. An Emerging Method to Assess Tear Film Spread and Dynamics as Possible Tear Film Homeostasis Markers. *Current Eye Research*, 46(9), pp.1291-1298.

García-Marqués, J., Talens-Estarelles, C., García-Lázaro, S. and Cerviño, A., 2021e. Validation of a new objective method to assess lipid layer thickness without the need of an interferometer. *Graefe's Archive for Clinical and Experimental Ophthalmology*, 260(2), pp.655-676.

García-Montero, M., Rico-del-Viejo, L., Llorens-Quintana, C., Lorente-Velázquez, A., Hernández-Verdejo, J. and Madrid-Costa, D., 2019a. Randomized crossover trial of silicone hydrogel contact lenses. *Contact Lens and Anterior Eye*, 42(5), pp.475-481.

García-Montero, M., Rico-del-Viejo, L., Lorente-Velázquez, A., Martínez-Alberquilla, I., Hernández-Verdejo, J. and Madrid-Costa, D., 2019b. Repeatability of Noninvasive Keratograph 5M Measurements Associated With Contact Lens Wear. *Eye & Contact Lens: Science & Clinical Practice*, 45(6), pp.377-381.

García-Montero, M., Rico-del-Viejo, L., Martínez-Alberquilla, I., Hernández-Verdejo, J., Lorente-Velázquez, A. and Madrid-Costa, D., 2019c. Effects of Blink Rate on Tear Film Optical Quality Dynamics with Different Soft Contact Lenses. *Journal of Ophthalmology*, 2019, pp.1-8.

García-Porta, N., Gantes-Nuñez, F., Tabernero, J. and Pardhan, S., 2019. Characterization of the ocular surface temperature dynamics in glaucoma subjects

using long-wave infrared thermal imaging. *Journal of the Optical Society of America A*, 36(6), p.1015.

García-Resúa, C., Fernández, M., González Penedo, M., Calvo, D., Penas, M. and Yebra-Pimentel, E., 2013. New Software Application for Clarifying Tear Film Lipid Layer Patterns. *Cornea*, 32(4), pp.538-546.

García-Resúa, C., Pena-Verdeal, H., Miñones, M., Giráldez, M. and Yebra-Pimentel, E., 2014. Interobserver and intraobserver repeatability of lipid layer pattern evaluation by two experienced observers. *Contact Lens and Anterior Eye*, 37(6), pp.431-437.

García-Resúa, C., Santodomingo-Rubido, J., Lira, M., Giraldez, M. and Vilar, E., 2009. Clinical assessment of the lower tear meniscus height. *Ophthalmic and Physiological Optics*, 29(5), pp.526-534.

Garduño, F., Salinas, A., Contreras, K., Rios, Y., García, N., Quintanilla, P., Mendoza, C. and Garza Leon, M., 2020. Comparative Study of Two Infrared Meibographers in Evaporative Dry Eye Versus Nondry Eye Patients. *Eye & Contact Lens: Science & Clinical Practice*, 47(6), pp.335-340.

Garg, P., Gupta, A., Tandon, N. and Raj, P., 2020. Dry Eye Disease after Cataract Surgery: Study of its Determinants and Risk Factors. *Turkish Journal of Ophthalmology*, 50(3), pp.133-142.

Garza-Leon, M., Gonzalez-Dibildox, A., Ramos-Betancourt, N. and Hernandez-Quintela, E., 2020. Comparison of meibomian gland loss area measurements between two computer programs and intra–inter-observer agreement. *International Ophthalmology*, 40(5), pp.1261-1267.

Garzón., S., López-Alemany, A. and Gené-Sampedro, A., 2019. Correlation between type 2 diabetes, dry eye and Meibomian glands dysfunction. *Journal of Optometry*, 12(4), pp.256-262.

Ge, J., Liu, N., Wang, X., Du, Y., Wang, C., Li, Z., Li, J. and Wang, L., 2020. Evaluation of the efficacy of optimal pulsed technology treatment in patients with cataract and Meibomian gland dysfunction in the perioperative period. *BMC Ophthalmology*, 20(1), p.111.

Geerling, G., Baudouin, C., Aragona, P., Rolando, M., Boboridis, K., Benítez-del-Castillo, J., Akova, Y., Merayo-Lloves, J., Labetoulle, M., Steinhoff, M. and Messmer, E., 2017. Emerging strategies for the diagnosis and treatment of meibomian gland dysfunction: Proceedings of the OCEAN group meeting. *The Ocular Surface*, 15(2), pp.179-192.

Geerling, G., Tauber, J., Baudouin, C., Goto, E., Matsumoto, Y., O'Brien, T., Rolando, M., Tsubota, K. and Nichols, K., 2011. The International Workshop on Meibomian Gland Dysfunction: Report of the Subcommittee on Management and Treatment of Meibomian Gland Dysfunction. *Investigative Opthalmology & Visual Science*, 52(4), pp.2050-2064.

Gemoules, G., 2005. Therapeutic Effects of Contact Lenses After Refractive Surgery. *Eye & Contact Lens: Science & Clinical Practice*, 31(1), pp.12-22.

Giannaccare, G., Vigo, L., Pellegrini, M., Sebastiani, S. and Carones, F., 2018. Ocular Surface Workup With Automated Noninvasive Measurements for the Diagnosis of Meibomian Gland Dysfunction. *Cornea*, 37(6), pp.740-745.

Gilbard, J., Gray, K. and Rossi, S., 1986. A Proposed Mechanism for Increased Tear-Film Osmolarity in Contact Lens Wearers. *American Journal of Ophthalmology*, 102(4), pp.505-507.

Ginsburg, A., 1984. A New Contrast Sensitivity Vision Test Chart. *Optometry and Vision Science*, 61(6), pp.403-407.

Gipson, I., 2007. The Ocular Surface: The Challenge to Enable and Protect Vision. *Investigative Opthalmology & Visual Science*, 48(10), p.4391.Harriet, D. and Kuonen, V., 2004. The tear film and ocular mucins. *Veterinary Ophthalmology*, 7(2), pp.71-77.

Gipson, I., Hori, Y. and Argüeso, P., 2004. Character of Ocular Surface Mucins and Their Alteration in Dry Eye Disease. *The Ocular Surface*, 2(2), pp.131-148.

Gjerdrum, B., Gundersen, K., Lundmark, P., Potvin, R. and Aakre, B., 2020. Prevalence of Signs and Symptoms of Dry Eye Disease 5 to 15 After Refractive Surgery. *Clinical Ophthalmology*, 14, pp.269-279.

Glasgow, B., 2019. Ellipsometry of human tears. *The Ocular Surface*, 17(2), pp.341-346.

Gokul, A., Wang, M. and Craig, J., 2018. Tear lipid supplement prophylaxis against dry eye in adverse environments. *Contact Lens and Anterior Eye*, 41(1), pp.97-100.

Golebiowski, B., Long, J., Harrison, K., Lee, A., Chidi-Egboka, N. and Asper, L., 2019. Smartphone Use and Effects on Tear Film, Blinking and Binocular Vision. *Current Eye Research*, 45(4), pp.428-434.

Gomes, J., Azar, D., Baudouin, C., Efron, N., Hirayama, M., Horwath-Winter, J., Kim, T., Mehta, J., Messmer, E., Pepose, J., Sangwan, V., Weiner, A., Wilson, S. and Wolffsohn, J., 2017. TFOS DEWS II iatrogenic report. *The Ocular Surface*, 15(3), pp.511-538.

González-Méijome, J., Peixoto-de-Matos, S., Faria-Ribeiro, M., Lopes-Ferreira, D., Jorge, J., Legerton, J. and Queiros, A., 2016. Strategies to Regulate Myopia Progression With Contact Lenses. *Eye & Contact Lens: Science & Clinical Practice*, 42(1), pp.24-34.

Goto, E. and Tseng, S., 2003. Kinetic Analysis of Tear Interference Images in Aqueous Tear Deficiency Dry Eye before and after Punctal Occlusion. *Investigative Opthalmology & Visual Science*, 44(5), pp.1897-1905.

Goto, T., Zheng, X., Klyce, S., Kataoka, H., Uno, T., Yamaguchi, M., Karon, M., Hirano, S., Okamoto, S. and Ohashi, Y., 2004a. Evaluation of the tear film stability after laser in situ keratomileusis using the tear film stability analysis system. *American Journal of Ophthalmology*, 137(1), pp.116-120.

Goto, T., Zheng, X., Okamoto, S. and Ohashi, Y., 2004b. Tear Film Stability Analysis System: Introducing a New Application for Videokeratography. *Cornea*, 23(8), pp.S65-S70.

Gouvea, L., Waring, G., Brundrett, A., Crouse, M. and Rocha, K., 2019. Objective assessment of optical quality in dry eye disease using a double-pass imaging system. *Clinical Ophthalmology*, 13, pp.1991-1996.

Govindarajan, B. and Gipson, I., 2010. Membrane-tethered mucins have multiple functions on the ocular surface. *Experimental Eye Research*, 90(6), pp.655-663.

Gu, T., Du, B., Bi, H., Zhou, L., Liu, G., Jin, N., Liu, Z., Zhang, B. and Wei, R., 2020a. Meibomian Gland Dropout, not Distortion, Can Distinguish Dry Eyes from Normal Eyes in Contact Lens Wearers. *Current Eye Research*, 45(8), pp.897-903.

Gu, T., Zhao, L., Liu, Z., Zhao, S., Nian, H. and Wei, R., 2020b. Evaluation of tear film and the morphological changes of meibomian glands in young Asian soft contact lens wearers and non-wearers. *BMC Ophthalmology*, 20(1), p.84.

Guarnieri, A., Carnero, E., Bleau, A., Alfonso-Bartolozzi, B. and Moreno-Montañés, J., 2019. Relationship between OSDI questionnaire and ocular surface changes in glaucomatous patients. *International Ophthalmology*, 40(3), pp.741-751.

Guillon, J., 1998a. Non-invasive tearscope plus routine for contact lens fitting. *Contact Lens and Anterior Eye*, 21, pp.S31-S40.

Guillon, J., 1998b. Use of the tearscope plus and attachments in the routine examination of the marginal dry eye contact lens patient. In: Guillon. JP, ed., *Advances in Experimental Medicine and Biology*. pp.859-867.

Guillon, M., Dumbleton, K., Theodoratos, P., Patel, T., Karkkainen, T. and Moody, K., 2018. Objective Assessment of Ocular Surface Response to Contact Lens Wear in Presbyopic Contact Lens Wearers of Asian Descent. *Eye & Contact Lens: Science & Clinical Practice*, 44(3), pp.182-189.

Guillon, M., Dumbleton, K., Theodoratos, P., Wong, S., Patel, K., Banks, G. and Patel, T., 2016. Association Between Contact Lens Discomfort and Pre-lens Tear Film Kinetics. *Optometry and Vision Science*, 93(8), pp.881-891.

Guillon, M. and Maissa, C., 2008. Contact Lens Wear Affects Tear Film Evaporation. *Eye & Contact Lens: Science & Clinical Practice*, 34(6), pp.326-330.

Guillon, M., Patel, T., Patel, K., Gupta, R. and Maissa, C., 2019a. Quantification of contact lens wettability after prolonged visual device use under low humidity conditions. *Contact Lens and Anterior Eye*, 42(4), pp.386-391.

Guillon, M., Styles, E., Guillon, J., Maïssa, C. and Guillon, M., 1997. Preocular Tear Film Characteristics of Nonwearers and Soft Contact Lens Wearers. *Optometry and Vision Science*, 74(5), pp.273-279.

Guillon, M., Theodoratos, P., Patel, K., Gupta, R. and Patel, T., 2019b. Pre-contact lens and pre-corneal tear film kinetics. *Contact Lens and Anterior Eye*, 42(3), pp.246-252.

Guirao, A. and Artal, P., 2000. Corneal wave aberration from videokeratography: accuracy and limitations of the procedure. *Journal of the Optical Society of America A*, 17(6), pp.955-965.

Gumus, K., Crockett, C., Rao, K., Yeu, E., Weikert, M., Shirayama, M., Hada, S. and Pflugfelder, S., 2011. Noninvasive Assessment of Tear Stability with the Tear Stability Analysis System in Tear Dysfunction Patients. *Investigative Opthalmology & Visual Science*, 52(1), pp.456-461.

Gumus, K. and Pflugfelder, S., 2013. Increasing Prevalence and Severity of Conjunctivochalasis With Aging Detected by Anterior Segment Optical Coherence Tomography. *American Journal of Ophthalmology*, 155(2), pp.238-242.e2.

Gumus, K. and Pflugfelder, S., 2017. Anterior Segment Optical Coherence Tomography (AS-OCT) in the Management of Dry Eye. *International Ophthalmology Clinics*, 57(2), pp.13-22.

Gumus, K. and Pflugfelder, S., 2021. Conjunctivochalasis and Tear Osmolarity Are Associated With Reduced Conjunctival Epithelial Thickness in Dry Eye. *American Journal of Ophthalmology*, 227, pp.35-44.

Guo, Y., Ha, J., Piao, H., Sung, M. and Park, S., 2020. The protective effect of 3% diquafosol on meibomian gland morphology in glaucoma patients treated with prostaglandin analogs: a 12-month follow-up study. *BMC Ophthalmology*, 20(1), p.277.

Gupta, A., Monroy, D., Ji, Z., Yoshino, K., Huang, A. and Pflugfelder, S., 1996. Transforming growth factor beta-1 and beta-2 in human tear fluid. *Current Eye Research*, 15(6), pp.605-614.

Gupta, N., Prasad, I., Himashree, G. and D'Souza, P., 2008. Prevalence of Dry Eye at High Altitude: A Case Controlled Comparative Study. *High Altitude Medicine & Biology*, 9(4), pp.327-334.

Ha, M., Kim, J., Hong, S., Chang, D., Whang, W., Na, K., Kim, E., Kim, H. and Hwang, H., 2021. Relationship between eyelid margin irregularity and meibomian gland dropout. *The Ocular Surface*, 19, pp.31-37.

Habay, T., Majzoub, S., Perrault, O., Rousseau, C. and Pisella, P., 2014. Évaluation objective de l'impact fonctionnel de la sévérité de la sécheresse oculaire sur la qualité de vision par aberrométrie double passage. *Journal Français d'Ophtalmologie*, 37(3), pp.188-194.

Hallak, J., Tibrewal, S. and Jain, S., 2015. Depressive Symptoms in Patients With Dry Eye Disease. *Cornea*, 34(12), pp.1545-1550.

Han, S., Hyon, J., Woo, S., Lee, J., Kim, T. and Kim, K., 2011. Prevalence of Dry Eye Disease in an Elderly Korean Population. *Archives of Ophthalmology*, 129(5), pp.633-638.

Haralick, R., 1979. Statistical and structural approaches to texture. *Proceedings of the IEEE*, 67(5), pp.786-804.

Harbiyeli, I., Bozkurt, B., Erdem, E., Ozcan, H., Cam, B., Sertdemir, Y. and Yagmur, M., 2022. Associations with meibomian gland loss in soft and rigid contact lens wearers. *Contact Lens and Anterior Eye*, 45(1), p.101400.

He, F., Zhao, Z., Liu, Y., Lu, L. and Fu, Y., 2018. Assessment of Ocular Surface Damage during the Course of Type 2 Diabetes Mellitus. *Journal of Ophthalmology*, 2018, pp.1-8.

Henriquez, A. and Korb, D., 1981. Meibomian glands and contact lens wear. *British Journal of Ophthalmology*, 65(2), pp.108-111.

Herbaut, A., Liang, H., Rabut, G., Trinh, L., Kessal, K., Baudouin, C. and Labbé, A., 2018. Impact of Dry Eye Disease on Vision Quality: An Optical Quality Analysis System Study. *Translational Vision Science & Technology*, 7(4), p.5.

Higginbotham, E., Feldman, R., Stiles, M. and Dubiner, H., 2002. Latanoprost and Timolol Combination Therapy vs Monotherapy: One-year randomized trial. *Archives of Ophthalmology*, 120(7), pp.915-922.

Himebaugh, N., Wright, A., Bradley, A., Begley, C. and Thibos, L., 2003. Use of Retroillumination to Visualize Optical Aberrations Caused by Tear Film Break-Up. *Optometry and Vision Science*, 80(1), pp.69-78.

Hiraoka, T., Daito, M., Okamoto, F., Kiuchi, T. and Oshika, T., 2010. Contrast Sensitivity and Optical Quality of the Eye after Instillation of Timolol Maleate Gel-Forming Solution and Brinzolamide Ophthalmic Suspension. *Ophthalmology*, 117(11), pp.2080-2087.

Holly, F. and Lemp, M., 1977. Tear physiology and dry eyes. *Survey of Ophthalmology*, 22(2), pp.69-87.

Hong, J., Sun, X., Wei, A., Cui, X., Li, Y., Qian, T., Wang, W. and Xu, J., 2013. Assessment of Tear Film Stability in Dry Eye With a Newly Developed Keratograph. *Cornea*, 32(5), pp.716-721.

Hori, Y., 2018. Secreted Mucins on the Ocular Surface. *Investigative Opthalmology & Visual Science*, 59(14), pp.DES151-DES156.

Hosaka, E., Kawamorita, T., Ogasawara, Y., Nakayama, N., Uozato, H., Shimizu, K., Dogru, M., Tsubota, K. and Goto, E., 2011. Interferometry in the Evaluation of Precorneal Tear Film Thickness in Dry Eye. *American Journal of Ophthalmology*, 151(1), pp.18-23.e1.

Hosmer, D. and Lemesbow, S., 1980. Goodness of fit tests for the multiple logistic regression model. *Communications in Statistics - Theory and Methods*, 9(10), pp.1043-1069.

Hosmer, D., Lemeshow, S. and Sturdivant, R., 2013. *Applied Logistic Regression*. 3rd ed. New Jersey, p.2013.

Hovanesian, J., Epitropoulos, A., Donnenfeld, E. and Holladay, J., 2019. The Effect Of Lifitegrast On Refractive Accuracy And Symptoms In Dry Eye Patients Undergoing Cataract Surgery. *Clinical Ophthalmology*, 2020(14), pp.2709-2716.

Hughes, R., Vincent, S., Read, S. and Collins, M., 2020. Higher order aberrations, refractive error development and myopia control: a review. *Clinical and Experimental Optometry*, 103(1), pp.68-85.

Hwang, J., Lee, J. and Chung, S., 2019. Comparison of Meibomian Gland Imaging Findings and Lipid Layer Thickness between Primary Sjögren Syndrome and Non-Sjögren Syndrome Dry Eyes. *Ocular Immunology and Inflammation*, 28(2), pp.182-187.

Hwang, H., Jeon, H., Yow, K., Hwang, H. and Chung, E., 2017. Image-based quantitative analysis of tear film lipid layer thickness for meibomian gland evaluation. *BioMedical Engineering OnLine*, 16(1), p.135.

Hwang, H., Shin, J., Lee, B., Eom, T. and Joo, C., 2013. In Vivo 3D Meibography of the Human Eyelid Using Real Time Imaging Fourier-Domain OCT. *PLoS ONE*, 8(6), p.e67143.

Ibrahim, O., Dogru, M., Takano, Y., Satake, Y., Wakamatsu, T., Fukagawa, K., Tsubota, K. and Fujishima, H., 2010a. Application of Visante Optical Coherence Tomography Tear Meniscus Height Measurement in the Diagnosis of Dry Eye Disease. *Ophthalmology*, 117(10), pp.1923-1929.

Ibrahim, O., Matsumoto, Y., Dogru, M., Adan, E., Wakamatsu, T., Goto, T., Negishi, K. and Tsubota, K., 2010b. The Efficacy, Sensitivity, and Specificity of In Vivo Laser Confocal Microscopy in the Diagnosis of Meibomian Gland Dysfunction. *Ophthalmology*, 117(4), pp.665-672.

Ibrahim, O., Matsumoto, Y., Dogru, M., Adan, E., Wakamatsu, T., Shimazaki, J., Fujishima, H. and Tsubota, K., 2012. In Vivo Confocal Microscopy Evaluation of Meibomian Gland Dysfunction in Atopic-Keratoconjunctivitis Patients. *Ophthalmology*, 119(10), pp.1961-1968.

Igarashi, A., Kamiya, K., Kobashi, H. and Shimizu, K., 2015. Effect of Rebamipide Ophthalmic Suspension on Intraocular Light Scattering for Dry Eye After Corneal Refractive Surgery. *Cornea*, 34(8), pp.895-900.

Imamura, H., Tabuchi, H., Nakakura, S., Nagasato, D., Baba, H. and Kiuchi, Y., 2017. Usability and reproducibility of tear meniscus values generated via swept-source optical coherence tomography and the slit lamp with a graticule method. *International Ophthalmology*, 38(2), pp.679-686.

Iqbal, A., Thomas, R. and Mahadevan, R., 2021. Impact of modulus of elasticity of silicone hydrogel contact lenses on meibomian glands morphology and function. *Clinical and Experimental Optometry*, 104(7), pp.760-766.

Isenberg, S., Del Signore, M., Chen, A., Wei, J. and Guillon, J., 2003. The lipid layer and stability of the preocular tear film in newborns and infants. *Ophthalmology*, 110(7), pp.1408-1411.

Itokawa, T., Okajima, Y., Suzuki, T., Kakisu, K., Iwashita, H., Murakami, Y. and Hori, Y., 2018. Association Between Ocular Surface Temperature and Tear Film Stability in Soft Contact Lens Wearers. *Investigative Opthalmology & Visual Science*, 59(2), pp.771-775.

Itokawa, T., Suzuki, T., Iwashita, H., Hori, Y., 2020. Comparison and evaluation of prelens tear film stability by different noninvasive in vivo methods. *Clinical Ophthalmology*, 14, pp.4459-4468.

Jeon, J. and Park, S., 2021. Comparison of the efficacy of eyelid warming masks and artificial tears for dry eye symptoms in contact lens wearers. *Contact Lens and Anterior Eye*, 44(1), pp.30-34.

Ji, Q., Yoo, Y., Alam, H. and Yoon, G., 2018. Through-focus optical characteristics of monofocal and bifocal soft contact lenses across the peripheral visual field. *Ophthalmic and Physiological Optics*, 38(3), pp.326-336.

Ji, Y., Lee, J., Lee, H., Seo, K., Kim, E. and Kim, T., 2017. Automated Measurement of Tear Film Dynamics and Lipid Layer Thickness for Assessment of Non-Sjögren Dry Eye Syndrome With Meibomian Gland Dysfunction. *Cornea*, 36(2), pp.176-182.

Jiang, Y., Ye, H., Xu, J. and Lu, Y., 2014. Noninvasive Keratograph assessment of tear film break-up time and location in patients with age-related cataracts and dry eye syndrome. *Journal of International Medical Research*, 42(2), pp.494-502.

Jie, Y., Sella, R., Feng, J., Gomez, M. and Afshari, N., 2019. Evaluation of incomplete blinking as a measurement of dry eye disease. *The Ocular Surface*, 17(3), pp.440-446.

Jiménez, R., Perez, M., Garcia, J. and Gonzalez, M., 2004. Statistical normal values of visual parameters that characterize binocular function in children. *Ophthalmic and Physiological Optics*, 24(6), pp.528-542.

Johnson, M. and Murphy, P., 2005. The Agreement and Repeatability of Tear Meniscus Height Measurement Methods. *Optometry and Vision Science*, 82(12), pp.1030-1037.

Johnson, M. and Murphy, P., 2006. Temporal changes in the tear menisci following a blink. *Experimental Eye Research*, 83(3), pp.517-525.

Jones, S. and Nischal, K., 2013. The non-invasive tear film break-up time in normal children. *British Journal of Ophthalmology*, 97(9), pp.1129-1133.

Jones, L., Downie, L., Korb, D., Benitez-del-Castillo, J., Dana, R., Deng, S., Dong, P., Geerling, G., Hida, R., Liu, Y., Seo, K., Tauber, J., Wakamatsu, T., Xu, J., Wolffsohn, J. and Craig, J., 2017. TFOS DEWS II Management and Therapy Report. *The Ocular Surface*, 15(3), pp.575-628.

Jumblatt, M., McKenzie, R., Steele, P., Emberts, C. and Jumblatt, J., 2003. MUC7 Expression in the Human Lacrimal Gland and Conjunctiva. *Cornea*, 22(1), pp.41-45.

Kading, D., 2010. A two-week clinical evaluation of the safety of Systane Ultra in contact lens-wearing patients. *Clinical Ophthalmology*, 4(1), pp.27-32.

Kaido, M., Kawashima, M., Ishida, R. and Tsubota, K., 2020. Tear Film Dynamics of Soft Contact Lens-Induced Dry Eye. *Current Eye Research*, 45(7), pp.782-788.

Kamao, T., Yamaguchi, M., Kawasaki, S., Mizoue, S., Shiraishi, A. and Ohashi, Y., 2011. Screening for Dry Eye With Newly Developed Ocular Surface Thermographer. *American Journal of Ophthalmology*, 151(5), pp.782-791.

Kang, D., Lee, Y., Hwang, K., Koh, K., Kwon, Y., Kim, B., Song, S. and Kim, K., 2019. Changes of tear film lipid layer thickness by 3% diquafosol ophthalmic solutions in patients with dry eye syndrome. *International Journal of Ophthalmology*, 12(10), pp.1555-1560.

Kang, M., Shin, J., Kwon, J., Huh, J. and Lee, J., 2021. Efficacy of 0.05% cyclosporine A on the lipid layer and meibomian glands after cataract surgery: A randomized, double-masked study. *PLOS ONE*, 16(1), p.e0245329.

Kang, P., McAlinden, C. and Wildsoet, C., 2016. Effects of multifocal soft contact lenses used to slow myopia progression on quality of vision in young adults. *Acta Ophthalmologica*, 95(1), pp.e43-e53.

Kang, Y., Lee, H., Li, Y., Choi, W. and Yoon, K., 2017. Manifestation of meibomian gland dysfunction in patients with Sjögren's syndrome, non-Sjögren's dry eye, and non-dry eye controls. *International Ophthalmology*, 38(3), pp.1161-1167.

Karaca, E., Özek, D. and Evren Kemer, Ö., 2020. Comparison study of two different topical lubricants on tear meniscus and tear osmolarity in dry eye. *Contact Lens and Anterior Eye*, 43(4), pp.373-377.

Karaca, I., Yagci, A., Palamar, M., Tasbakan, M. and Basoglu, O., 2019. Ocular surface assessment and morphological alterations in meibomian glands with meibography in obstructive sleep apnea Syndrome. *The Ocular Surface*, 17(4), pp.771-776.

Karadenız Ugurlu, S., Altın Ekın, M. and Aytogan, H., 2019. Assessment of tear meniscus by optical coherence tomography in patients with canalicular laceration repair. *International Ophthalmology*, 40(1), pp.13-18.

Karaiskos, D., Mavragani, C., Makaroni, S., Zinzaras, E., Voulgarelis, M., Rabavilas, A. and Moutsopoulos, H., 2008. Stress, coping strategies and social support in patients with primary Sjögren's syndrome prior to disease onset: a retrospective case–control study. *Annals of the Rheumatic Diseases*, 68(1), pp.40-46.

Kawali, A., 2013. Thermography in ocular inflammation. *Indian Journal of Radiology and Imaging*, 23(03), pp.281-283.

Keech, A., Flanagan, J., Simpson, T. and Jones, L., 2009. Tear Meniscus Height Determination Using the OCT2 and the RTVue-100. *Optometry and Vision Science*, 86(10), pp.1154-1159.

Khanal, S. and Millar, T., 2010. Nanoscale phase dynamics of the normal tear film. *Nanomedicine: Nanotechnology, Biology and Medicine*, 6(6), pp.707-713.

Kheirkhah, A., Coco, G., Satitpitakul, V. and Dana, R., 2018. Subtarsal Fibrosis Is Associated With Ocular Surface Epitheliopathy in Graft-Versus-Host Disease. *American Journal of Ophthalmology*, 189, pp.102-110.

Kheirkhah, A., Coco, G., Satitpitakul, V., Pham, T. and Dana, R., 2019. Limbal and Conjunctival Epithelial Thickness in Ocular Graft-Versus-Host Disease. *Cornea*, 38(10), pp.1286-1290.

Kilduff, C. and Luis, C., 2016. Red eyes and red-flags: improving ophthalmic assessment and referral in primary care. *BMJ Quality Improvement Reports*, 5(1), pp.1-8.

Kim, A., Muntz, A., Lee, J., Wang, M. and Craig, J., 2020. Therapeutic benefits of blinking exercises in dry eye disease. *Contact Lens and Anterior Eye*.

Kim, J., Kim, J., Seo, K., Kim, T., Chin, H. and Jung, J., 2019. Location and pattern of non-invasive keratographic tear film break-up according to dry eye disease subtypes. *Acta Ophthalmologica*, 97(8), pp.1089-1097.

Kim, J., Lee, H., Choi, S., Kim, E., Seo, K. and Kim, T., 2016. Assessment of the Tear Film Lipid Layer Thickness after Cataract Surgery. *Seminars in Ophthalmology*, 33:2, pp.231-236.

Kim, A., Muntz, A., Lee, J., Wang, M. and Craig, J., 2021. Therapeutic benefits of blinking exercises in dry eye disease. *Contact Lens and Anterior Eye*, 44(3), p.101329.

Kim, Y., Kwak, A., Lee, S., Yoon, J. and Jang, S., 2015. Meibomian gland dysfunction in Graves' orbitopathy. *Canadian Journal of Ophthalmology*, 50(4), pp.278-282.

King-Smith, E., Fink, B., Fogt, N., Nichols, K., Hill, R. and Wilson, G., 2000. The thickness of the human precorneal tear film: evidence from reflection spectra. *Investigative Ophthalmology & Visual Science*, 41, pp.3348-59.

King-Smith, E., Fink, B., Hill, R., Koelling, K. and Tiffany, J., 2004. The thickness of the tear film. *Current Eye Research*, 29(4-5), pp.357-368.

King-Smith, P., Begley, C. and Braun, R., 2018. Mechanisms, imaging and structure of tear film breakup. *The Ocular Surface*, 16(1), pp.4-30.

King-Smith, P., Fink, B., Nichols, J., Nichols, K., Braun, R. and McFadden, G., 2009. The Contribution of Lipid Layer Movement to Tear Film Thinning and Breakup. *Investigative Opthalmology & Visual Science*, 50(6), p.2747.

King-Smith, P., Hinel, E. and Nichols, J., 2010. Application of a Novel Interferometric Method to Investigate the Relation between Lipid Layer Thickness and Tear Film Thinning. *Investigative Opthalmology & Visual Science*, 51(5), p.2418.

King-Smith, P., Reuter, K., Braun, R., Nichols, J. and Nichols, K., 2013. Tear Film Breakup and Structure Studied by Simultaneous Video Recording of Fluorescence and Tear Film Lipid Layer Images. *Investigative Opthalmology & Visual Science*, 54(7), pp.4900-4909.

Klein, B., Klein, R., Lee, K. and Cruickshanks, K., 1998. Performance-based and self-assessed measures of visual function as related to history of falls, hip fractures, and measured gait time. *Ophthalmology*, 105(1), pp.160-164.

Knop, E., Knop, N., Millar, T., Obata, H. and Sullivan, D., 2011. The International Workshop on Meibomian Gland Dysfunction: Report of the Subcommittee on Anatomy, Physiology, and Pathophysiology of the Meibomian Gland. *Investigative Opthalmology & Visual Science*, 52(4), pp.1938-1978.

Kobayashi, A., Yoshita, T. and Sugiyama, K., 2005. In Vivo Findings of the Bulbar/Palpebral Conjunctiva and Presumed Meibomian Glands by Laser Scanning Confocal Microscopy. *Cornea*, 24(8), pp.985-988.

Kobashi, H., Kamiya, K., Igarashi, A., Miyake, T. and Shimizu, K., 2015. Intraocular Scattering after Instillation of Diquafosol Ophthalmic Solution. *Optometry and Vision Science*, 92(9), pp.e303-e309.

Kobashi, H., Kamiya, K., Yanome, K., Igarashi, A. and Shimizu, K., 2013. Longitudinal Assessment of Optical Quality and Intraocular Scattering Using the Double-Pass Instrument in Normal Eyes and Eyes with Short Tear Breakup Time. *PLoS ONE*, 8(12), pp.824-827.

Kobia-Acquah, E., Akowuah, P., Antwi-Adjei, E., Forkuo, P., Koomson, N., Odotei, S., Alabi, E. and Donkor, R., 2021a. Contact lens complications among wearers in Ghana. *Contact Lens and Anterior Eye*, 44, pp.67-71.

Kobia-Acquah, E., Ankamah-Lomotey, S., Owusu, E., Forfoe, S., Bannor, J., Koomson, J., Opoku, M., Dzikpo, D., Mensah, D., Amonoo, J. and Akowuah, P., 2021b. Prevalence and associated risk factors of symptomatic dry eye in Ghana: A cross-sectional population-based study. *Contact Lens and Anterior Eye*, 44(6), p.101404.

Koh, S., 2016. Mechanisms of Visual Disturbance in Dry Eye. *Cornea*, 35(Supplement 1), pp.S83-S88.

Koh, S., 2020. Contact Lens Wear and Dry Eye: Beyond the Known. *Asia-Pacific Journal of Ophthalmology*, 9(6), pp.498-504.

Koh, S., Higashiura, R. and Maeda, N., 2016. Overview of Objective Methods for Assessing Dynamic Changes in Optical Quality. *Eye & Contact Lens: Science & Clinical Practice*, 42(5), pp.333-338.

Koh, S., Ikeda, C., Fujimoto, H., Oie, Y., Soma, T., Maeda, N. and Nishida, K., 2016. Regional Differences in Tear Film Stability and Meibomian Glands in Patients With Aqueous-Deficient Dry Eye. *Eye & Contact Lens: Science & Clinical Practice*, 42(4), pp.250-255.

Koh, S., Ikeda, C., Watanabe, S., Oie, Y., Soma, T., Watanabe, H., Maeda, N. and Nishida, K., 2014a. Effect of non-invasive tear stability assessment on tear meniscus height. *Acta Ophthalmologica*, 93(2), pp.e135-e139.

Koh, S., Inoue, Y., Sugmimoto, T., Maeda, N. and Nishida, K., 2013a. Effect of Rebamipide Ophthalmic Suspension on Optical Quality in the Short Break-up Time Type of Dry Eye. *Cornea*, 32(9), pp.1219-1223.

Koh, S. and Maeda, N., 2007. Wavefront Sensing and the Dynamics of Tear Film. *Cornea*, 26(Supplement 1), pp.S41-S45.

Koh, S., Maeda, N., Hamano, T., Hirohara, Y., Mihashi, T., Hori, Y., Hosohata, J., Fujikado, T. and Tano, Y., 2008a. Effect of Internal Lubricating Agents of Disposable Soft Contact Lenses on Higher-Order Aberrations After Blinking. *Eye & Contact Lens: Science & Clinical Practice*, 34(2), pp.100-105.

Koh, S., Maeda, N., Hirohara, Y., Mihashi, T., Bessho, K., Hori, Y., Inoue, T., Watanabe, H., Fujikado, T. and Tano, Y., 2008b. Serial Measurements of Higher-Order Aberrations after Blinking in Patients with Dry Eye. *Investigative Opthalmology & Visual Science*, 49(1), pp.133-138.

Koh, S., Maeda, N., Hori, Y., Inoue, T., Watanabe, H., Hirohara, Y., Mihashi, T., Fujikado, T. and Tano, Y., 2008c. Effects of Suppression of Blinking on Quality of Vision in Borderline Cases of Evaporative Dry Eye. *Cornea*, 27(3), pp.275-278.

Koh, S., Maeda, N., Ikeda, C., Asonuma, S., Mitamura, H., Oie, Y., Soma, T., Tsujikawa, M., Kawasaki, S. and Nishida, K., 2014b. Ocular Forward Light Scattering and Corneal Backward Light Scattering in Patients With Dry Eye. *Investigative Opthalmology & Visual Science*, 55(10), pp.6601-6606.

Koh, S., Maeda, N., Ikeda, C., Takai, Y., Fujimoto, H., Oie, Y., Soma, T., Tsujikawa, M. and Nishida, K., 2013b. Effect of Instillation of Eyedrops for Dry Eye on Optical Quality. *Investigative Opthalmology & Visual Science*, 54(7), pp.4927-4933.

Koh, S., Maeda, N., Kuroda, T., Hori, Y., Watanabe, H., Fujikado, T., Tano, Y., Hirohara, Y. and Mihashi, T., 2002. Effect of tear film break-up on higher-order aberrations measured with wavefront sensor. *American Journal of Ophthalmology*, 134(1), pp.115-117.

Koh, S., Tung, C., Aquavella, J., Yadav, R., Zavislan, J. and Yoon, G., 2010. Simultaneous Measurement of Tear Film Dynamics Using Wavefront Sensor and Optical Coherence Tomography. *Investigative Opthalmology & Visual Science*, 51(7), pp.3441-3448.

Koh, S., Tung, C., Inoue, Y. and Jhanji, V., 2018. Effects of tear film dynamics on quality of vision. *British Journal of Ophthalmology*, 102(12), pp.1615-1620.

Koh, Y., Celik, T., Lee, H., Petznick, A. and Tong, L., 2012. Detection of meibomian glands and classification of meibography images. *Journal of Biomedical Optics*, 17(8), p.086008.

Kojima, T., 2018. Contact Lens-Associated Dry Eye Disease: Recent Advances Worldwide and in Japan. *Investigative Opthalmology & Visual Science*, 59(14), pp.102-108.

Kojima, T., Ibrahim, O., Wakamatsu, T., Tsuyama, A., Ogawa, J., Matsumoto, Y., Dogru, M. and Tsubota, K., 2011. The Impact of Contact Lens Wear and Visual Display Terminal Work on Ocular Surface and Tear Functions in Office Workers. *American Journal of Ophthalmology*, 152(6), pp.933-940.e2.

Kojima, T., Matsumoto, Y., Dogru, M. and Tsubota, K., 2010. The application of in vivo laser scanning confocal microscopy as a tool of conjunctival in vivo cytology in the diagnosis of dry eye disease. *Mol Vis*, 16, pp.2457-64.

Kolbe, O., Zimmermann, F., Marx, S. and Sickenberger, W., 2019. Introducing a novel in vivo method to access visual performance during dewetting process of contact lens surface. *Contact Lens and Anterior Eye*, 42(6), pp.359-365.

Kollbaum, P., Jansen, M., Tan, J., Meyer, D. and Rickert, M., 2013. Vision Performance With a Contact Lens Designed to Slow Myopia Progression. *Optometry and Vision Science*, 90(3), pp.205-214.

Konieczka, K., Koch, S., Hauenstein, D., Chackathayil, T., Binggeli, T., Schoetzau, A. and Flammer, J., 2019. Effects of the Glaucoma Drugs Latanoprost and Brimonidine on Corneal Temperature. *Translational Vision Science & Technology*, 8(3), p.47.

Konieczka, K., Schoetzau, A., Koch, S., Hauenstein, D. and Flammer, J., 2018. Cornea Thermography: Optimal Evaluation of the Outcome and the Resulting Reproducibility. *Translational Vision Science & Technology*, 7(3), p.14.

Koprowski, R., Tian, L. and Olczyk, P., 2017. A clinical utility assessment of the automatic measurement method of the quality of Meibomian glands. *BioMedical Engineering OnLine*, 16(1), p.82.

Koprowski, R., Wilczyński, S., Olczyk, P., Nowińska, A., Węglarz, B. and Wylęgała, E., 2016. A quantitative method for assessing the quality of meibomian glands. *Computers in Biology and Medicine*, 75, pp.130-138.

Korb D., 2002. The tear film: Structure, function and clinical evaluation Butterworth-Heinemman, editor. Londres: Butterworth-Heinemman.

Korb, D., Greiner, J. and Glonek, T., 1996. Tear Film Lipid Layer Formation: Implications for Contact Lens Wear. *Optometry and Vision Science*, 73(3), pp.189-192.

Korb, D. and Henriquez, A., 1980. Meibomian gland dysfunction and contact lens intolerance. *Journal of the American Optometric Association*, 51(3), pp.243-251.

Korb, D., Herman, J., Greiner, J., Scaffidi, R., Finnemore, V., Exford, J., Blackie, C. and Douglass, T., 2005. Lid Wiper Epitheliopathy and Dry Eye Symptoms. *Eye & Contact Lens: Science & Clinical Practice*, 31(1), pp.2-8.

Kottaiyan, R., Yoon, G., Wang, Q., Yadav, R., Zavislan, J. and Aquavella, J., 2012. Integrated Multimodal Metrology for Objective and Noninvasive Tear Evaluation. *The Ocular Surface*, 10(1), pp.43-50.

Kremers, I., Hohberger, B. and Bergua, A., 2020. Infrared thermography: different options of thermal eyelid warming. *Graefe's Archive for Clinical and Experimental Ophthalmology*, 258(7), pp.1515-1522.

Kunnen, C., Brown, S., de la Jara, P., Holden, B., Blanksby, S., Mitchell, T. and Papas, E., 2016. Influence of Meibomian Gland Expression Methods on Human Lipid Analysis Results. *The Ocular Surface*, 14(1), pp.49-55.

Kwon, K., Shipley, R., Edirisinghe, M., Ezra, D., Rose, G., Best, S. and Cameron, R., 2013. High-speed camera characterization of voluntary eye blinking kinematics. *Journal of The Royal Society Interface*, 10(85), p.20130227.

Labbé, A., Wang, Y., Jie, Y., Baudouin, C., Jonas, J. and Xu, L., 2013. Dry eye disease, dry eye symptoms and depression: the Beijing Eye Study. *British Journal of Ophthalmology*, 97(11), pp.1399-1403.

Labetoulle, M., Baudouin, C., Calonge, M., Merayo-Lloves, J., Boboridis, K., Akova, Y., Aragona, P., Geerling, G., Messmer, E. and Benítez-del-Castillo, J., 2018. Role of corneal nerves in ocular surface homeostasis and disease. *Acta Ophthalmologica*, 97(2), pp.137-145.

Lafosse, E., Martínez-Albert, N., Wolffsohn, J., Cerviño, A. and García-Lázaro, S., 2019. Response of the Aging Eye to First Day of Modern Material Contact Lens Wear. *Eye & Contact Lens: Science & Clinical Practice*, 45(1), pp.40-45.

Lafosse, E., Romín, D., Esteve-Taboada, J., Wolffsohn, J., Talens-Estarelles, C. and García-Lázaro, S., 2018. Comparison of the influence of corneo-scleral and scleral lenses on ocular surface and tear film metrics in a presbyopic population. *Contact Lens and Anterior Eye*, 41(1), pp.122-127.

Lai, H., Kuo, M., Fang, P., Lin, C., Chien, C., Cho, W., Chen, A. and Lai, I., 2019. Tracking the Reflective Light Particles Spreading on the Cornea: An Emerging Assessment for Tear Film Homeostasis. *Translational Vision Science & Technology*, 8(3), p.32.

Lam, A., Tai, S., Chan, J. and Ng, R., 2019. Lower Tear Meniscus Height Measurements Using Keratography and Swept-Source Optical Coherence Tomography and Effect of Fluorescein Instillation Methods. *Current Eye Research*, 44(11), pp.1203-1208.

Lam, C., Tang, W., Tse, D., Tang, Y. and To, C., 2013. Defocus Incorporated Soft Contact (DISC) lens slows myopia progression in Hong Kong Chinese schoolchildren: a 2-year randomised clinical trial. *British Journal of Ophthalmology*, 98(1), pp.40-45.

Lan, W., Lin, L., Yang, X. and Yu, M., 2014. Automatic Noninvasive Tear Breakup Time (TBUT) and Conventional Fluorescent TBUT. *Optometry and Vision Science*, 91(12), pp.1412-1418.

Landis, J. and Koch, G., 1977. The Measurement of Observer Agreement for Categorical Data. *Biometrics*, 33(1), pp.159-174.

Lane, S., DuBiner, H., Epstein, R., Ernest, P., Greiner, J., Hardten, D., Holland, E., Lemp, M., McDonald, J., Silbert, D., Blackie, C., Stevens, C. and Bedi, R., 2012. A New System, the LipiFlow, for the Treatment of Meibomian Gland Dysfunction. *Cornea*, 31(4), pp.396-404.

La Porta Weber, S., Becco de Souza, R., Gomes, J. and Hofling-Lima, A., 2016. The Use of the Esclera Scleral Contact Lens in the Treatment of Moderate to Severe Dry Eye Disease. *American Journal of Ophthalmology*, 163, pp.167-173.e1.

Latifi, G., Banafshe Afshan, A., Houshang Beheshtnejad, A., Zarei-Ghanavati, M., Mohammadi, N., Ghaffari, R., Ghassemi, H., Mohammadi, S. and Kheirkhah, A., 2020. Changes in Corneal Subbasal Nerves after Punctal Occlusion in Dry Eye Disease. *Current Eye Research*, 46(6), pp.777-783.

Lazón- de la Jara, P., Papas, E., Diec, J., Naduvilath, T., Willcox, M. and Holden, B., 2013. Effect of Lens Care Systems on the Clinical Performance of a Contact Lens. *Optometry and Vision Science*, 90(4), pp.344-350.

Leat, S. and Wegmann, D., 2004. Clinical Testing of Contrast Sensitivity in Children: Age-related Norms and Validity. *Optometry and Vision Science*, 81(4), pp.245-254.

Lee, J., Jeon, Y., Kim, K., Hwang, K., Kwon, Y. and Koh, K., 2020a. Ocular surface analysis: A comparison between the LipiView® II and IDRA®. *European Journal of Ophthalmology*, 31(5), pp.2300-2306.

Lee, J., Jun, I., Kim, E., Seo, K. and Kim, T., 2020b. Clinical Accuracy of an Advanced Corneal Topographer with Tear-Film Analysis in Functional and Structural Evaluation of Dry Eye Disease. *Seminars in Ophthalmology*, 35(2), pp.134-140.

Lee, J., Kim, C., Choe, C. and Choi, T., 2020c. Correlation Analysis between Ocular Surface Parameters with Subjective Symptom Severity in Dry Eye Disease. *Korean Journal of Ophthalmology*, 34(3), pp.203-209.

Lee, O., Tepelus, T., Huang, J., Irvine, A., Irvine, C., Chiu, G. and Sadda, S., 2018. Evaluation of the corneal epithelium in non-Sjögren's and Sjögren's dry eyes: an in vivo confocal microscopy study using HRT III RCM. *BMC Ophthalmology*, 18(1), p.309.

Lee, S., Lee, J., Kim, S., Jung, J. and Shin, J., 2019. Effect of topical glaucoma medication on tear lipid layer thickness in patients with unilateral glaucoma. *Indian Journal of Ophthalmology*, 67(8), pp.1297-302.

Lee, S., Petznick, A. and Tong, L., 2012. Associations of systemic diseases, smoking and contact lens wear with severity of dry eye. *Ophthalmic and Physiological Optics*, 32(6), pp.518-526.

Lee, Y., Hyon, J. and Jeon, H., 2021. Characteristics of dry eye patients with thick tear film lipid layers evaluated by a LipiView II interferometer. *Graefe's Archive for Clinical and Experimental Ophthalmology*, 259(5), pp.1235-1241.

Lekhanont, K., Jongkhajornpong, P., Sontichai, V., Anothaisintawee, T. and Nijvipakul, S., 2019. Evaluating Dry Eye and Meibomian Gland Dysfunction With Meibography in Patients With Stevens–Johnson Syndrome. *Cornea*, 38(12), pp.1489-1494.

Lema, I., Sobrino, T., Duran, J., Brea, D. and Diez-Feijoo, E., 2009. Subclinical keratoconus and inflammatory molecules from tears. *British Journal of Ophthalmology*, 93(6), pp.820-824.

Lemp, M., 2008. Advances in Understanding and Managing Dry Eye Disease. *American Journal of Ophthalmology*, 146(3), pp.350-356.e1.

Li, B., Fu, H., Liu, T. and Xu, M., 2020a. Comparison of the therapeutic effect of Meibomian Thermal Pulsation LipiFlow® on obstructive and hyposecretory meibomian gland dysfunction patients. *International Ophthalmology*, 40(12), pp.3469-3479.

Li, D., Lokeshwar, B., Solomon, A., Monroy, D., Ji, Z. and Pflugfelder, S., 2001. Regulation of MMP-9 Production by Human Corneal Epithelial Cells. *Experimental Eye Research*, 73(4), pp.449-459.

Li, D., Luo, L., Chen, Z., Kim, H., Song, X. and Pflugfelder, S., 2006. JNK and ERK MAP kinases mediate induction of IL-1β, TNF-α and IL-8 following hyperosmolar stress in human limbal epithelial cells. *Experimental Eye Research*, 82(4), pp.588-596..

Li, J., Ma, J., Hu, M., Yu, J. and Zhao, Y., 2020b. Assessment of tear film lipid layer thickness in patients with Meibomian gland dysfunction at different ages. *BMC Ophthalmology*, 20(1), pp.394.

Li, J., Li, D., Zhou, N., Qi, M., Luo, Y. and Wang, Y., 2020c. Effects of chalazion and its treatments on the meibomian glands: a nonrandomized, prospective observation clinical study. *BMC Ophthalmology*, 20(1), p.278

Li, L., Braun, R., Driscoll, T., Henshaw, W., Banks, J. and King-Smith, P., 2015a. Computed tear film and osmolarity dynamics on an eye-shaped domain. *Mathematical Medicine and Biology*, 33(2), pp.123-157.

Li, N., Wang, T., Wang, R. and Duan, X., 2019. Tear Film Instability and Meibomian Gland Dysfunction Correlate with the Pterygium Size and Thickness Pre- and Postexcision in Patients with Pterygium. *Journal of Ophthalmology*, 2019, pp.1-9.

Li, S., Kang, M., Wu, S., Meng, B., Sun, Y., Wei, S., Liu, L., Peng, X., Chen, Z., Zhang, F. and Wang, N., 2016. Studies using concentric ring bifocal and peripheral add multifocal contact lenses to slow myopia progression in school-aged children: a meta-analysis. *Ophthalmic and Physiological Optics*, 37(1), pp.51-59.

Li, W., Graham, A., Selvin, S. and Lin, M., 2015b. Ocular Surface Cooling Corresponds to Tear Film Thinning and Breakup. *Optometry and Vision Science*, 92(9), pp.e248-e256.

Li, W., Sun, X., Wang, Z. and Zhang, Y., 2018. A survey of contact lens-related complications in a tertiary hospital in China. *Contact Lens and Anterior Eye*, 41(2), pp.201-204.

Liang, Q., Pan, Z., Zhou, M., Zhang, Y., Wang, N., Li, B., Baudouin, C. and Labbé, A., 2015. Evaluation of Optical Coherence Tomography Meibography in Patients With Obstructive Meibomian Gland Dysfunction. *Cornea*, 34(10), pp.1193-1199.

Lim, P., Han, T. and Tong, L., 2020. Short-Term Changes in Tear Lipid Layer Thickness After Instillation of Lipid Containing Eye Drops. *Translational Vision Science & Technology*, 9(8), p.29.

Lin, H. and Yiu, S., 2014. Dry eye disease: A review of diagnostic approaches and treatments. *Saudi Journal of Ophthalmology*, 28(3), pp.173-181.

Lin, X., Wu, Y., Chen, Y., Zhao, Y., Xiang, L., Dai, Q., Fu, Y., Zhao, Y. and Zhao, Y., 2020. Characterization of Meibomian Gland Atrophy and the Potential Risk Factors for Middle Aged to Elderly Patients With Cataracts. *Translational Vision Science & Technology*, 9(7), p.48.

Linhares, J., Neves, H., Lopes-Ferreira, D., Faria-Ribeiro, M., Peixoto-de-Matos, S. and Gonzalez-Meijome, J., 2013. Radiometric characterization of a novel LED array system for visual assessment. *Journal of Modern Optics*, 60(14), pp.1136-1144.

Little, S. and Bruce, A., 1994. Hydrogel (Acuvue) Lens Movement is Influenced by the Postlens Tear Film. *Optometry and Vision Science*, 71(6), pp.364-370.

Liu, H., Begley, C., Chen, M., Bradley, A., Bonanno, J., McNamara, N., Nelson, J. and Simpson, T., 2009. A Link between Tear Instability and Hyperosmolarity in Dry Eye. *Investigative Opthalmology & Visual Science*, 50(8), pp.3671-3679.

Liu, H., Thibos, L., Begley, C. and Bradley, A., 2010. Measurement of the Time Course of Optical Quality and Visual Deterioration during Tear Break-Up. *Investigative Opthalmology & Visual Science*, 51(6), pp.3318-3326.

Liu, J., Dong, Y. and Wang, Y., 2020. Vitamin D deficiency is associated with dry eye syndrome: a systematic review and meta-analysis. *Acta Ophthalmologica*, 98(8), pp.749-754.

Liu, Q., Xu, Z., Xu, Y., Zhang, J., Li, Y., Xia, J., Wang, Y., He, X., Qu, J. and Hu, L., 2020. Changes in Corneal Dendritic Cell and Sub-basal Nerve in Long-Term Contact Lens Wearers With Dry Eye. *Eye & Contact Lens: Science & Clinical Practice*, 46(4), pp.238-244.

Liu, Y., Chou, Y., Dong, X., Liu, Z., Jiang, X., Hao, R. and Li, X., 2017. Corneal Subbasal Nerve Analysis Using In Vivo Confocal Microscopy in Patients With Dry Eye: Analysis and Clinical Correlations. *Cornea*, 38(10), pp.1253-1258.

Llorens-Quintana, C., Garaszczuk, I. and Szczesna-Iskander, D., 2020. Meibomian glands structure in daily disposable soft contact lens wearers: a one-year follow-up study. *Ophthalmic and Physiological Optics*, 40(5), pp.607-616.

Llorens-Quintana, C., Mousavi, M., Szczesna-Iskander, D. and Iskander, D., 2018. Non-invasive pre-lens tear film assessment with high-speed videokeratoscopy. *Contact Lens and Anterior Eye*, 41(1), pp.18-22.

Llorens-Quintana, C., Rico-del-Viejo, L., Syga, P., Madrid-Costa, D. and Iskander, D., 2019a. A Novel Automated Approach for Infrared-Based Assessment of Meibomian Gland Morphology. *Translational Vision Science & Technology*, 8(4), p.17.

Llorens-Quintana, C., Rico-del-Viejo, L., Syga, P., Madrid-Costa, D. and Iskander, D., 2019b. Meibomian Gland Morphology: The Influence of Structural Variations on Gland Function and Ocular Surface Parameters. *Cornea*, 38(12), pp.1506-1512.

Llorens-Quintana, C., Szczesna-Iskander, D. and Iskander, D., 2019. Supporting Dry Eye Diagnosis with a New Method for Noninvasive Tear Film Quality Assessment. *Optometry and Vision Science*, 96(2), pp.103-110.

Lopes-Ferreira, D., Fernandes, P., Queirós, A. and González-Meijome, J., 2018. Combined Effect of Ocular and Multifocal Contact Lens Induced Aberrations on Visual Performance: Center-Distance Versus Center-Near Design. *Eye & Contact Lenses*, 44(1), pp.S131-S137.

Lopes-Ferreira, D., Neves, H., Queiros, A., Faria-Ribeiro, M., Peixoto-de-Matos, S. and González-Méijome, J., 2013. Ocular Dominance and Visual Function Testing. *BioMed Research International*, 2013, p.238943.

Lopes-Ferreira, D., Ribeiro, C., Maia, R., García-Porta, N., Queirós, A., Villa-Collar, C. and González-Méijome, J., 2011. Peripheral myopization using a dominant design multifocal contact lens. *Journal of Optometry*, 4(1), pp.14-21.

López-De La Rosa, A., Alghamdi, W., Kunnen, C., Lazon de la Jara, P., González-García, M., Markoulli, M. and Papas, E., 2019a. Changes in the tarsal conjunctiva viewed by in vivo confocal microscopy are associated with ocular symptoms and contact lens wear. *Ophthalmic and Physiological Optics*, 39(5), pp.328-336.

López-De La Rosa, A., Arroyo-Del Arroyo, C., Cañadas, P., López-Miguel, A., Calonge, M., Enríquez-De-Salamanca, A. and González-García, M., 2017. Are Contact Lens Discomfort or Soft Contact Lens Material Properties Associated with Alterations in the Corneal Sub-Basal Nerve Plexus?. *Current Eye Research*, 43(4), pp.487-492.

López-De La Rosa, A., Arroyo-del Arroyo, C., Enríquez-de-Salamanca, A., Pinto-Fraga, J., López-Miguel, A. and González-García, M., 2019b. The ability of the Contact Lens Dry Eye Questionnaire (CLDEQ)-8 to detect ocular surface alterations in contact lens wearers. *Contact Lens and Anterior Eye*, 42(3), pp.273-277.

López-García, J., García-Lozano, I. and Martínez-Garchitorena, J., 2003. Measure of the fatty layer thickness of precorneal tear film by interference colours in different types of dry eye. *Archivos de la Sociedad Española de Oftalmología*, 78(5), pp.257-264.

López-Gil, N., Castejón-Mochón, J., Benito, A., Marín, J., Lo-a-Foe, G., Marin, G., Fermigier, B., Renard, D., Joyeux, D., Château, N. and Artal, P., 2002. Aberration Generation by Contact Lenses With Aspheric and Asymmetric Surfaces. *Journal of Refractive Surgery*, 18(5), pp.S603-609.

López-Miguel, A., Tesón, M., Martín-Montañez, V., Enríquez-de-Salamanca, A., Stern, M., Calonge, M. and González-García, M., 2014. Dry Eye Exacerbation in Patients Exposed to Desiccating Stress under Controlled Environmental Conditions. *American Journal of Ophthalmology*, 157(4), pp.788-798.e2.

Lorente-Velázquez, A., García-Montero, M., Gómez-Sanz, F., Rico-del-Viejo, L., Hernández-Verdejo, J. and Madrid-Costa, D., 2019. Comparison of the impact of nesofilcon A hydrogel contact lens on the ocular surface and the comfort of presbyopic and non-presbyopic wearers. *International Journal of Ophthalmology*, 12(4), pp.640-646.

Lu, H., Wang, M., Wang, J. and Shen, M., 2014. Tear film measurement by optical reflectometry technique. *Journal of Biomedical Optics*, 19(2), p.027001.

Lyu, Y., Zeng, X., Li, F. and Zhao, S., 2019. The effect of the duration of diabetes on dry eye and corneal nerves. *Contact Lens and Anterior Eye*, 42(4), pp.380-385.

Ma, J., Wang, L., Weikert, M., Montes de Oca, I. and Koch, D., 2018. Evaluation of the Repeatability and Reproducibility of Corneal Epithelial Thickness Mapping for a 9-mm Zone Using Optical Coherence Tomography. *Cornea*, 38(1), pp.67-73.

Ma, J., Wei, S., Jiang, X., Chou, Y., Wang, Y., Hao, R., Yang, J. and Li, X., 2020. Evaluation of objective visual quality in dry eye disease and corneal nerve changes. *International Ophthalmology*, 40(11), pp.2995-3004.

Macchi, I., Bunya, V., Massaro-Giordano, M., Stone, R., Maguire, M., Zheng, Y., Chen, M., Gee, J., Smith, E. and Daniel, E., 2018. A new scale for the assessment of conjunctival bulbar redness. *The Ocular Surface*, 16(4), pp.436-440.

Macedo-de-Araújo, R., Amorim-de-Sousa, A., van der Worp, E. and González-Méijome, J., 2019. Clinical Findings and Ocular Symptoms Over 1 Year in a Sample of Scleral Lens Wearers. *Eye & Contact Lens: Science & Clinical Practice*, 46(6), pp.e40-e55.

Macedo-de-Araújo, R., Faria-Ribeiro, M., McAlinden, C., van der Worp, E. and González-Méijome, J., 2020. Optical Quality and Visual Performance for One Year in a Sample of Scleral Lens Wearers. *Optometry and Vision Science*, 97(9), pp.775-789.

Macedo-de-Araújo, R., Ferreira-Neves, H., Rico-del-Viejo, L., Peixoto-de-Matos, S. and González-Méijome, J., 2016. Light distortion and spherical aberration for the accommodating and nonaccommodating eye. *Journal of Biomedical Optics*, 21(7), p.075003.

Macedo-de-Araújo, R., van der Worp, E. and González-Méijome, J., 2018. On-eye breakage and recovery of mini-scleral contact lens without compromise for the ocular surface. *Contact Lens and Anterior Eye*, 41(3), pp.311-314.

Macedo-de-Araújo, R., van der Worp, E. and González-Méijome, J., 2019. Practitioner Learning Curve in Fitting Scleral Lenses in Irregular and Regular Corneas Using a Fitting Trial. *BioMed Research International*, 2019, pp.1-11.

Macedo-de-Araújo, R., van der Worp, E. and González-Méijome, J., 2020. A one-year prospective study on scleral lens wear success. *Contact Lens and Anterior Eye*, 43(6), pp.553-561.

Machalińska, A., Zakrzewska, A., Adamek, B., Safranow, K., Wiszniewska, B., Parafiniuk, M. and Machaliński, B., 2015. Comparison of Morphological and Functional Meibomian Gland Characteristics Between Daily Contact Lens Wearers and Nonwearers. *Cornea*, 34(9), pp.1098-1104.

Machowicz, A., de Pablo, P., Rauz, S., Richards, A., Higham, J., Poveda-Gallego, A., Imamura, F., Bowman, S., Barone, F. and Fisher, B., 2020. Mediterranean diet and risk of Sjögren's syndrome. *Clinical Experimental Rheumatology*, 38, pp.216-221.

Madrid-Costa, D., García-Lázaro, S., Albarrán-Diego, C., Ferrer-Blasco, T. and Montés-Micó, R., 2012. Visual performance of two simultaneous vision multifocal contact lenses. *Ophthalmic and Physiological Optics*, 33(1), pp.51-56.

Madrid-Costa, D., Ruiz-Alcocer, J., García-Lázaro, S., Ferrer-Blasco, T. and Montés-Micó, R., 2015. Optical power distribution of refractive and aspheric multifocal contact lenses: Effect of pupil size. *Contact Lens and Anterior Eye*, 38(5), pp.317-321.

Mainstone, J., Bruce, A. and Golding, T., 1996. Tear meniscus measurement in the diagnosis of dry eye. *Current Eye Research*, 15(6), pp.653-661.

Makrynioti, D., Zagoriti, Z., Koutsojannis, C., Morgan, P. and Lagoumintzis, G., 2020. Ocular conditions and dry eye due to traditional and new forms of smoking: A review. *Contact Lens and Anterior Eye*, 43(3), pp.277-284.

Malet, F., Le Goff, M., Colin, J., Schweitzer, C., Delyfer, M., Korobelnik, J., Rougier, M., Radeau, T., Dartigues, J. and Delcourt, C., 2013. Dry eye disease in French elderly subjects: the Alienor Study. *Acta Ophthalmologica*, 92(6), pp.e429-e436.

Mann, A. and Tighe, B., 2013. Contact lens interactions with the tear film. *Experimental Eye Research*, 117, pp.88-98.

Mann, A., Campbell, D., Mirza, Z., Hunt, O., Wolffsohn, J. and Tighe, B., 2019. Clinical and biochemical analysis of the ageing tear film. *British Journal of Ophthalmology*, 104(7), pp.1028-1032.

Mantelli, F. and Argüeso, P., 2008. Functions of ocular surface mucins in health and disease. *Current Opinion in Allergy & Clinical Immunology*, 8(5), pp.477-483.

Markoulli, M., Duong, T., Lin, M. and Papas, E., 2017. Imaging the Tear Film: A Comparison Between the Subjective Keeler Tearscope-Plus™ and the Objective Oculus® Keratograph 5M and LipiView® Interferometer. *Current Eye Research*, 43(2), pp.155-162.

Markoulli, M. and Kolanu, S., 2017. Contact lens wear and dry eyes: challenges and solutions. *Clinical Optometry*, Volume 9, pp.41-48.

Markoulli, M., Sobbizadeh, A., Tan, J., Briggs, N. and Coroneo, M., 2018. The Effect of Optive and Optive Advanced Artificial Tears on the Healthy Tear Film. *Current Eye Research*, 43(5), pp.588-594.

Marren, S., 1994. Contact Lens Wear, Use of Eye Cosmetics, and Meibomian Gland Dysfunction. *Optometry and Vision Science*, 71(1), pp.60-62.

Martin, D., 1995. Water transport in dehydrating hydrogel contact lenses: Implications for corneal desiccation. *Journal of Biomedical Materials Research*, 29(7), pp.857-865.

Martin, J. and Roorda, A., 2003. Predicting and Assessing Visual Performance with Multizone Bifocal Contact Lenses. *Optometry and Vision Science*, 80(12), pp.812-819.

Martínez-Alberquilla, I., García-Montero, M., Ruiz-Alcocer, J., Crooke, A. and Madrid-Costa, D., 2020. Visual function, ocular surface integrity and symptomatology of a new extended depth-of-focus and a conventional multifocal contact lens. *Contact Lens and Anterior Eye*.

Martínez-Albert, N., Esteve-Taboada, J. and Montés-Micó, R., 2018. Repeatability assessment of anterior segment biometric measurements under accommodative and nonaccommodative conditions using an anterior segment OCT. *Graefe's Archive for Clinical and Experimental Ophthalmology*, 256(1), pp.113-123.

Martínez-Albert, N., Esteve-Taboada, J., Montés-Micó, R., Fernández-Vega-Cueto, L. and Ferrer-Blasco, T., 2018. Repeatability assessment of biometric measurements with different refractive states and age using a swept-source biometer. *Expert Review of Medical Devices*, 16(1), pp.63-69.

Martins, C., Amorim-De-Sousa, A., Faria-Ribeiro, M., Pauné, J., González-Méijome, J. and Queirós, A., 2019. Visual Performance and High-Order Aberrations with Different Contact Lens Prototypes with Potential for Myopia Control. *Current Eye Research*, 45(1), pp.24-30.

Marx, S., Eckstein, J. and Sickenberger, W., 2020. Objective Analysis of Pre-Lens Tear Film Stability of Daily Disposable Contact Lenses Using Ring Mire Projection. *Clinical Optometry*, 12, pp.203-211.

Mathers, W., Daley, T. and Verdick, R., 1994. Video Imaging of the Meibomian Gland. *Archives of Ophthalmology*, 112(4), pp.448-449.

Matsumoto, Y., Dogru, M., Goto, E., Sasaki, Y., Inoue, H., Saito, I., Shimazaki, J. and Tsubota, K., 2008. Alterations of the tear film and ocular surface health in chronic smokers. *Eye*, 22(7), pp.961-968.

Matsumoto, Y. and Ibrahim, O., 2018. Application of In Vivo Confocal Microscopy in Dry Eye Disease. *Investigative Opthalmology & Visual Science*, 59(14), pp.41-47.

Matsumoto, Y., Ibrahim, O., Kojima, T., Dogru, M., Shimazaki, J. and Tsubota, K., 2020. Corneal In Vivo Laser-Scanning Confocal Microscopy Findings in Dry Eye Patients with Sjögren's Syndrome. *Diagnostics*, 10(7), p.497.

Matsumoto, Y., Shigeno, Y., Sato, E., Ibrahim, O., Saiki, M., Negishi, K., Ogawa, Y., Dogru, M. and Tsubota, K., 2009. The evaluation of the treatment response in obstructive meibomian gland disease by in vivo laser confocal microscopy. *Graefe's Archive for Clinical and Experimental Ophthalmology*, 247(6), pp.821-829.

Matteoli, S., Favuzza, E., Mazzantini, L., Aragona, P., Cappelli, S., Corvi, A. and Mencucci, R., 2017. Ocular surface temperature in patients with evaporative and aqueous-deficient dry eyes: a thermographic approach. *Physiological Measurement*, 38(8), pp.1503-1512.

Matteoli, S., Vannetti, F., Sodi, A. and Corvi, A., 2020. Infrared thermographic investigation on the ocular surface temperature of normal subjects. *Physiological Measurement*, 41(4), p.045003.

McAlinden, C., Khadka, J. and Pesudovs, K., 2011. Statistical methods for conducting agreement (comparison of clinical tests) and precision (repeatability or reproducibility) studies in optometry and ophthalmology. *Ophthalmic and Physiological Optics*, 31(4), pp.330-338.

McAlinden, C., Khadka, J. and Pesudovs, K., 2015. Precision (repeatability and reproducibility) studies and sample-size calculation. *Journal of Cataract and Refractive Surgery*, 41(12), pp.2598-2604.

McAlinden, C., McCartney, M. and Moore, J., 2011. Mathematics of Zernike polynomials: a review. *Clinical & Experimental Ophthalmology*, 39(8), pp.820-827.

McAlinden, C., Pesudovs, K. and Moore, J., 2010. The Development of an Instrument to Measure Quality of Vision: The Quality of Vision (QoV) Questionnaire. *Investigative Opthalmology & Visual Science*, 51(11), pp.5537-5545.

McDonald, J., 1969. Surface Phenomena of the Tear Film. *American Journal of Ophthalmology*, 67(1), pp.56-64.

McDonald, M., Patel, D., Keith, M. and Snedecor, S., 2016. Economic and Humanistic Burden of Dry Eye Disease in Europe, North America, and Asia: A Systematic Literature Review. *The Ocular Surface*, 14(2), pp.144-167.

McDonald, M., Schachet, J., Lievens, C. and Kern, J., 2014. Systane® Ultra Lubricant Eye Drops for Treatment of Contact Lens–Related Dryness. *Eye & Contact Lens: Science & Clinical Practice*, 40(2), pp.106-110.

McGinnigle, S., Eperjesi, F. and Naroo, S., 2014. A preliminary investigation into the effects of ocular lubricants on higher order aberrations in normal and dry eye subjects. *Contact Lens and Anterior Eye*, 37(2), pp.106-110.

McGinnigle, S., Naroo, S. and Eperjesi, F., 2012. Evaluation of Dry Eye. *Survey of Ophthalmology*, 57(4), pp.293-316.

McMonnies, C., 2009. Mechanisms of Rubbing-Related Corneal Trauma in Keratoconus. *Cornea*, 28(6), pp.607-615.

McMonnies, C., 2018. An Amplifying Cascade of Contact Lens-Related End-of-Day Hyperaemia and Dryness Symptoms. *Current Eye Research*, 43(7), pp.839-847.

McMonnies, C., Korb, D. and Blackie, C., 2012. The role of heat in rubbing and massage-related corneal deformation. *Contact Lens and Anterior Eye*, 35(4), pp.148-154.

Mencucci, R., Favuzza, E., Scali, G., Vignapiano, R. and Cennamo, M., 2020. Protecting the Ocular Surface at the Time of Cataract Surgery: Intracameral Mydriatic and Anaesthetic Combination Versus A Standard Topical Protocol. *Ophthalmology and Therapy*, 9(4), pp.1055-1067.

Mengher, L., Bron, A., Tonge, S. and Gilbert, D., 1985. A non-invasive instrument for clinical assessment of the pre-corneal tear film stability. *Current Eye Research*, 4(1), pp.1-7.

Menzies, K., Srinivasan, S., Prokopich, C. and Jones, L., 2015. Infrared Imaging of Meibomian Glands and Evaluation of the Lipid Layer in Sjogren's Syndrome Patients and Nondry Eye Controls. *Investigative Ophthalmology & Visual Science*, 56(2), pp.836-841.

Mertzanis, P., Abetz, L., Rajagopalan, K., Espindle, D., Chalmers, R., Snyder, C., Caffery, B., Edrington, T., Simpson, T., Nelson, J. and Begley, C., 2005. The Relative Burden of Dry Eye in Patients' Lives: Comparisons to a U.S. Normative Sample. *Investigative Opthalmology & Visual Science*, 46(1), pp.46-50.

Mihashi, T., Hirohara, Y., Koh, S., Ninomiya, S., Maeda, N. and Fujikado, T., 2006. Tear Film Break-up Time Evaluated by Real-Time Hartmann-Shack Wavefront Sensing. *Japanese Journal of Ophthalmology*, 50(2), pp.85-89.

Millán, A., Viso, E., Gude, F., Parafita-Fernández, A., Moraña, N. and Rodríguez-Ares, M., 2018. Incidence and Risk Factors of Dry Eye in a Spanish Adult Population: 11-Year Follow-Up From the Salnés Eye Study. *Cornea*, 37(12), pp.1527-1534.

Millar, T. and Schuett, B., 2015. The real reason for having a meibomian lipid layer covering the outer surface of the tear film – A review. *Experimental Eye Research*, 137, pp.125-138.

Miller, D., 1969. Measurement of the Surface Tension of Tears. *Archives of Ophthalmology*, 82(3), pp.368-371.

Minatel-Riguetto, C., Minicucci, W., Moura Neto, A., Tambascia, M. and Zantut-Wittmann, D., 2019. Value of Infrared Thermography Camera Attached to a Smartphone for Evaluation and Follow-up of Patients with Graves' Ophthalmopathy. *International Journal of Endocrinology*, 2019, pp.1-9.

Minsky, M., 1988. Memoir on inventing the confocal scanning microscope. *Scanning*, 10(4), pp.128-138.

Mishima, S. and Maurice, D., 1961. The oily layer of the tear film and evaporation from the corneal surface. *Experimental Eye Research*, 1(1), pp.39-45.

Mizuno, Y., Yamada, M. and Shigeyasu, 2012. Annual direct cost of dry eye in Japan. *Clinical Ophthalmology*, 6, p.755.

Mohamed-Mostafa, E., Abdellah, M., Elhawary, A. and Mounir, A., 2019. Noncontact Meibography in Patients with Keratoconus. *Journal of Ophthalmology*, 2019, pp.1-6.

Molinari, J. and Tapie, R., 1982. Color photography of meibomian glands. *Optometry and Vision Science*, 59(9), pp.758-759.

Monaco, G. and Casalino, G., 2020. Superficial keratectomy followed by intense pulsed light for Salzmann's nodular degeneration and coexisting meibomian gland dysfunction. *European Journal of Ophthalmology*, pp.1-4.

Monsálvez-Romín, D., González-Méijome, J., Esteve-Taboada, J., García-Lázaro, S. and Cerviño, A., 2020. Light distortion of soft multifocal contact lenses with different pupil size and shape. *Contact Lens and Anterior Eye*, 43(2), pp.130-136.

Montalt, J., Porcar, E., España-Gregori, E. and Peris-Martínez, C., 2019. Visual quality with corneo-scleral contact lenses after intracorneal ring segment (ICRS) implantation for keratoconus management. *Contact Lens and Anterior Eye*, 42(1), pp.111-116.

Montani, G., Murphy, P. and Patel, S., 2018. Immediate effect of a tear enhancer and meibomian gland expression on the corneal surface and whole eye higher order aberrations. *Journal of Optometry*, 11(4), pp.223-231.

Montés-Micó, R., 2007. Role of the tear film in the optical quality of the human eye. *Journal of Cataract and Refractive Surgery*, 33(9), pp.1631-1635.

Montés-Micó, R., 2011. *Optometría.Principios básicos y aplicación clínica*. Barcelona (España): Elsevier.

Montés-Micó, R., Alió, J. and Charman, W., 2005a. Dynamic Changes in the Tear Film in Dry Eyes. *Investigative Opthalmology & Visual Science*, 46(5), pp.1615-1619.

Montés-Micó, R., Alió, J. and Charman, W., 2005b. Postblink Changes in the Ocular Modulation Transfer Function Measured by a Double-Pass Method. *Investigative Opthalmology & Visual Science*, 46(12), pp.4468-4473.

Montés-Micó, R., Alió, J., Muñoz, G. and Charman, W., 2004. Temporal Changes in Optical Quality of Air–Tear Film Interface at Anterior Cornea after Blink. *Investigative Opthalmology & Visual Science*, 45(6), pp.1752-1757.

Montés-Micó, R., Cervino, A., Ferrer-Blasco, T., García-Lázaro, S. and Madrid-Costa, D., 2010a. The Tear Film and the optical Quality of the Eye. *The Ocular Surface*, 8(4), pp.185-192.

Montés-Micó, R., Cerviño, A., Ferrer-Blasco, T., García-Lázaro, S. and Ortí-Navarro, S., 2010b. Optical quality after instillation of eyedrops in dry-eye syndrome. *Journal of Cataract and Refractive Surgery*, 36(6), pp.935-940.

Montés-Micó, R., Madrid-Costa, D., Domínguez-Vicent, A., Belda-Salmerón, L. and Ferrer-Blasco, T., 2014. In vitro power profiles of multifocal simultaneous vision contact lenses. *Contact Lens and Anterior Eye*, 37(3), pp.162-167.

Mooi, J., Wang, M., Lim, J., Müller, A. and Craig, J., 2017. Minimising instilled volume reduces the impact of fluorescein on clinical measurements of tear film stability. *Contact Lens and Anterior Eye*, 40(3), pp.170-174.

Morgan, P., Murphy, P., Gifford, K., Gifford, P., Golebiowski, B., Johnson, L., Makrynioti, D., Moezzi, A., Moody, K., Navascues-Cornago, M., Schweizer, H., Swiderska, K., Young, G. and Willcox, M., 2021. BCLA CLEAR - Effect of contact lens materials and designs on the anatomy and physiology of the eye. *Contact Lens and Anterior Eye*, 44(2), pp.192-219.

Moro, A., Fagnola, M., Picarazzi, S., Di Dio, A., Pastori, V., Lecchi, M. and Tavazzi, S., 2018. Hydrogen-peroxide and silicone-hydrogel contact lenses: Worsening of external eye condition and tear film instability. *Contact Lens and Anterior Eye*, 41(2), pp.157-161.

Moss, S., Klein, R. and Klein, B., 2008. Long-term Incidence of Dry Eye in an Older Population. *Optometry and Vision Science*, 85(8), pp.668-674.

Mostovoy, D., Vinker, S., Mimouni, M., Goldich, Y., Levartovsky, S. and Kaiserman, I., 2018. The association of keratoconus with blepharitis. *Clinical and Experimental Optometry*, 101(3), pp.339-344.

Mousavi, M., Jesus, D., Garaszczuk, I., Szczesna-Iskander, D. and Iskander, D., 2018. The utility of measuring tear film break-up time for prescribing contact lenses. *Contact Lens and Anterior Eye*, 41(1), pp.105-109.

Muntz, A., Subbaraman, L., Craig, J. and Jones, L., 2020. Cytomorphological assessment of the lid margin in relation to symptoms, contact lens wear and lid wiper epitheliopathy. *The Ocular Surface*, 18(2), pp.214-220.

Murakami, D., Blackie, C. and Korb, D., 2015. All Warm Compresses Are Not Equally Efficacious. *Optometry and Vision Science*, 92(9), pp.e327-e333.

Murphy, P., Lau, J., Sim, M. and Woods, R., 2006. How red is a white eye? Clinical grading of normal conjunctival hyperaemia. *Eye*, 21(5), pp.633-638.

Murphy, O., O' Dwyer, V. and Lloyd-Mckernan, A., 2019. The Efficacy of Warm Compresses in the Treatment of Meibomian Gland Dysfunction and Demodex Folliculorum Blepharitis. *Current Eye Research*, 45(5), pp.563-575.

Murube, J., 2008. REM Sleep: Tear Secretion and Dreams. *The Ocular Surface*, 6(1), pp.2-8.

Muselier-Mathieu, A., Bron, A., Mathieu, B., Souchier, M., Brignole-Baudouin, F., Acar, N., Brétillon, L. and Creuzot-Garcher, C., 2013. Ocular surface assessment in soft

contact lens wearers; the contribution of tear osmolarity among other tests. *Acta Ophthalmologica*, 92(4), pp.364-369.

Mylla-Bosso, A., Gasperi, E., Fernandes, L., Paulino-Costa, V. and Alves, M., 2020. Impact of Ocular Surface Disease Treatment in Patients with Glaucoma. *Clinical Ophthalmology*, 14, pp.103-111.

Na, K., Han, K., Park, Y., Na, C. and Joo, C., 2015. Depression, Stress, Quality of Life, and Dry Eye Disease in Korean Women. *Cornea*, 34(7), pp.733-738.

Nakamori, K., Odawara, M., Nakajima, T., Mizutani, T. and Tsubota, K., 1997. Blinking Is Controlled Primarily by Ocular Surface Conditions. *American Journal of Ophthalmology*, 124(1), pp.24-30.

Nakamura, Y., Matsuda, J., Suzuki, K., Toyoda, H., Hakamata, N., Shimamoto, T. and Kinoshita, S., 2008. Measurement of spontaneous blinks with a high-speed blink analyzing system. *Nihon Ganka Gakkai Zasshi*, 112(12), pp.1059-1067.

Nelson, J., Shimazaki, J., Benitez-del-Castillo, J., Craig, J., McCulley, J., Den, S. and Foulks, G., 2011. The International Workshop on Meibomian Gland Dysfunction: Report of the Definition and Classification Subcommittee. *Investigative Opthalmology & Visual Science*, 52(4), pp.1930-1937.

Németh, J., Erdélyi, B. and Csákány, B., 2001. Corneal topography changes after a 15 second pause in blinking. *Journal of Cataract and Refractive Surgery*, 27(4), pp.589-592.

Németh, O., Langenbucher, A., Eppig, T., Lepper, S., Milioti, G., Abdin, A., Nagy, Z., Seitz, B. and Szentmáry, N., 2020. Ocular Surface Disease Index and Ocular Thermography in Keratoconus Patients. *Journal of Ophthalmology*, 2020, pp.1-8.

Ngo, W., Gann, D. and Nichols, J., 2020. Impact of the 2011 International Workshop on Meibomian Gland Dysfunction on clinical trial attributes for meibomian gland dysfunction. *The Ocular Surface*, 18(1), pp.27-30.

Ngo, W., Srinivasan, S. and Jones, L., 2019. An Eyelid Warming Device for the Management of Meibomian Gland Dysfunction. *Journal of Optometry*, 12(2), pp.120-130.

Nichols, B., Chiappino, M. and Dawson, C., 1985. Demonstration of the mucous layer of the tear film by electron microscopy. Investigative Ophthalmology & Visual Science, 26, pp.464-73.

Nichols, J., Berntsen, D., Mitchell, G. and Nichols, K., 2005. An Assessment of Grading Scales for Meibography Images. *Cornea*, 24(4), pp.382-388.

Nichols, J. and King-Smith, P., 2003. Thickness of the Pre- and Post–Contact Lens Tear Film Measured In Vivo by Interferometry. *Investigative Opthalmology & Visual Science*, 44(1), pp.68-77.

Nichols, J. and King-Smith, P., 2004. The Impact of Hydrogel Lens Settling on the Thickness of the Tears and Contact Lens. *Investigative Opthalmology & Visual Science*, 45(8), pp.2549-2554.

Nichols, J., Mitchell, G. and King-Smith, P., 2005. Thinning Rate of the Precorneal and Prelens Tear Films. *Investigative Opthalmology & Visual Science*, 46(7), p.2353.

Nichols, J., Mitchell, G., Nichols, K., Chalmers, R. and Begley, C., 2002a. The Performance of the Contact Lens Dry Eye Questionnaire as a Screening Survey for Contact Lens-related Dry Eye. *Cornea*, 21(5), pp.469-475.

Nichols, J., Nichols, K., Puent, B., Saracino, M. and Mitchell, G., 2002b. Evaluation of Tear Film Interference Patterns and Measures of Tear Break-Up Time. *Optometry and Vision Science*, 79(6), pp.363-369.

Nichols, J. and Sinnott, L., 2006. Tear Film, Contact Lens, and Patient-Related Factors Associated with Contact Lens–Related Dry Eye. *Investigative Opthalmology & Visual Science*, 47(4), pp.1319-1328.

Nichols, J., Willcox, M., Bron, A., Belmonte, C., Ciolino, J., Craig, J., Dogru, M., Foulks, G., Jones, L., Nelson, J., Nichols, K., Purslow, C., Schaumberg, D., Stapleton, F. and Sullivan, D., 2013a. The TFOS International Workshop on Contact Lens Discomfort: Executive Summary. *Investigative Opthalmology & Visual Science*, 54(11), pp.TFOS7-TFOS13.

Nichols, K., Foulks, G., Bron, A., Glasgow, B., Dogru, M., Tsubota, K., Lemp, M. and Sullivan, D., 2011. The International Workshop on Meibomian Gland Dysfunction: Executive Summary. *Investigative Opthalmology & Visual Science*, 52(4), pp.1922-1929.

Nichols, K., Mitchell, G. and Zadnik, K., 2004. The Repeatability of Clinical Measurements of Dry Eye. *Cornea*, 23(3), pp.272-285.

Nichols, K., Redfern, R., Jacob, J., Nelson, J., Fonn, D., Forstot, S., Huang, J., Holden, B. and Nichols, J., 2013b. The TFOS International Workshop on Contact Lens Discomfort: Report of the Definition and Classification Subcommittee. *Investigative Opthalmology & Visual Science*, 54(11), pp.14-19.

Nielsen, P., Søgaard, K., Skotte, J. and Wolkoff, P., 2008. Ocular surface area and human eye blink frequency during VDU work: the effect of monitor position and task. *European Journal of Applied Physiology*, 103(1), pp.1-7.

Nikolov, A., Wasan, D., Chengara, A., Koczo, K., Policello, G. and Kolossvary, I., 2002. Superspreading driven by Marangoni flow. *Advances in Colloid and Interface Science*, 96(1-3), pp.325-338.

Norn, M., 1969. Dessication of the precorneal film I. Corneal wetting-time. *Acta Ophthalmologica*, 47(4), pp.865-880.

Nosch, D., Joos, R. and Job, M., 2020. Prospective randomized study to evaluate the efficacy and tolerability of Ectoin® containing Eye Spray (EES09) and comparison to the liposomal Eye Spray Tears Again® (TA) in the treatment of dry eye disease. *Contact Lens and Anterior Eye*.

Nosch, D., Pult, H., Albon, J., Purslow, C. and Murphy, P., 2016. Relationship between Corneal Sensation, Blinking, and Tear Film Quality. *Optometry and Vision Science*, 93(5), pp.471-481.

Novaes, P., Hilário do Nascimento Saldiva, P., Matsuda, M., Macchione, M., Peres Rangel, M., Kara-José, N. and Berra, A., 2010. The effects of chronic exposure to traffic derived air pollution on the ocular surface. *Environmental Research*, 110(4), pp.372-374.

Oguz, H., Yokoi, N. and Kinoshita, S., 2000. The Height and Radius of the Tear Meniscus and Methods for Examining These Parameters. *Cornea*, 19(4), pp.497-500.

Ong, B., 1996. Relation between Contact Lens Wear and Meibomian Gland Dysfunction. *Optometry and Vision Science*, 73(3), pp.208-210.

Ong, B. and Larke, J., 1990. Meibomian gland dysfunction: some clinical, biochemical and physical observations. *Ophthalmic and Physiological Optics*, 10(2), pp.144-148.

Onwubiko, S., Eze, B., Udeh, N., Arinze, O., Onwasigwe, E. and Umeh, R., 2014. Dry eye disease: Prevalence, distribution and determinants in a hospital-based population. *Contact Lens and Anterior Eye*, 37(3), pp.157-161.

Ortiz, S., Siedlecki, D., Pérez-Merino, P., Chia, N., de Castro, A., Szkulmowski, M., Wojtkowski, M. and Marcos, S., 2011. Corneal topography from spectral optical coherence tomography (sOCT). *Biomedical Optics Express*, 2(12), p.3232.

Ousler, G., Hagberg, K., Schindelar, M., Welch, D. and Abelson, M., 2008. The Ocular Protection Index. *Cornea*, 27(5), pp.509-513.

Owens, H. and Phillips, J., 2001. Spreading of the Tears After a Blink. *Cornea*, 20(5), pp.484-487.

Özcura, F., Aydin, S. and Helvaci, M., 2007. Ocular Surface Disease Index for the Diagnosis of Dry Eye Syndrome. *Ocular Immunology and Inflammation*, 15(5), pp.389-393.

Ozek, D., Karaca, E. and Evren Kemer, O., 2020. The effect of conjunctivochalasis detected by anterior segment optical coherence tomography on tear function in an elderly population. *Therapeutic Advances in Ophthalmology*, 12, pp.1-8.

Ozulken, K., Aksoy Aydemir, G., Tekin, K. and Mumcuoğlu, T., 2020. Correlation of Non-invasive Tear Break-Up Time with Tear Osmolarity and Other Invasive Tear Function Tests. *Seminars in Ophthalmology*, 35(1), pp.78-85.

Palakuru, J., Wang, J. and Aquavella, J., 2007. Effect of Blinking on Tear Dynamics. *Investigative Opthalmology & Visual Science*, 48(7), pp.3032-3037.

Palakuru, J., Wang, J. and Aquavella, J., 2008. Effect of Blinking on Tear Volume After Instillation of Midviscosity Artificial Tears. *American Journal of Ophthalmology*, 146(6), pp.920-924.

Papadatou, E., Del Águila-Carrasco, A., Esteve-Taboada, J., Madrid-Costa, D. and Cerviño-Expósito, A., 2017. Objective assessment of the effect of pupil size upon the power distribution of multifocal contact lenses. *International Journal of Ophthalmology*, 10(1), pp.103-108.

Papas, E., 2000. Key factors in the subjective and objective assessment of conjunctival erythema. *Investig Ophthalmol Vis Sci*, 41(3), pp.687-691.

Papas, E., Vajdic, C., Austen, R. and Holden, B., 1997. High-oxygen-transmissibility soft contact lenses do not induce limbal hyperaemia. *Current Eye Research*, 16(9), pp.942-948.

Park, J. and Baek, S., 2018. Dry eye syndrome in thyroid eye disease patients: The role of increased incomplete blinking and Meibomian gland loss. *Acta Ophthalmologica*, 97(5), pp.e800-e806.

Park, J., Kim, J. and Baek, S., 2018. Clinical features and treatment outcomes of patients with tearing after chemotherapy. *Eye*, 33(5), pp.746-753.

Park, J., Kim, J., Lee, H., Park, M. and Baek, S., 2018. Functional and structural evaluation of the meibomian gland using a LipiView interferometer in thyroid eye disease. *Canadian Journal of Ophthalmology*, 53(4), pp.373-379.

Passi, S., Brooks, C., Thompson, A. and Gupta, P., 2020. Optical Quality and Tear Film Analysis Before and After Intranasal Stimulation in Patients with Dry Eye Syndrome. *Clinical Ophthalmology*, 14, pp.1987-1992.

Passing, H. and Bablok, W., 1983. A New Biometrical Procedure for Testing the Equality of Measurements from Two Different Analytical Methods. Application of linear regression procedures for method comparison studies in Clinical Chemistry, Part I. *Clinical Chemistry and Laboratory Medicine*, 21(11), pp.709-720.

Patel, S., Hwang, J., Mehra, D. and Galor, A., 2021. Corneal Nerve Abnormalities in Ocular and Systemic Diseases. *Experimental Eye Research*, 202, p.108284.

Patel, S., Murray, D., McKenzie, A., Shearer, D. and McGrath, B., 1985. Effects of Fluorescein on Tear Breakup Time and on Tear Thinning Time. *Optometry and Vision Science*, 62(3), pp.188-190.

Paugh, J., Stapleton, F., Keay, L. and Ho, A., 2001. Tear exchange under hydrogel contact lenses: Methodological considerations. *Investigative Ophthalmology & Visual Science*, 42, pp.2813-2820.

Paulsen, A., Cruickshanks, K., Fischer, M., Huang, G., Klein, B., Klein, R. and Dalton, D., 2014. Dry Eye in the Beaver Dam Offspring Study: Prevalence, Risk Factors, and Health-Related Quality of Life. *American Journal of Ophthalmology*, 157(4), pp.799-806.

Pauné, J., Morales, H., Armengol, J., Quevedo, L., Faria-Ribeiro, M. and González-Méijome, J., 2015. Myopia Control with a Novel Peripheral Gradient Soft Lens and Orthokeratology: A 2-Year Clinical Trial. *BioMed Research International*, 2015, pp.1-10.

Pauné, J., Queiros, A., Quevedo, L., Neves, H., Lopes-Ferreira, D. and González-Méijome, J., 2014. Peripheral myopization and visual performance with experimental rigid gas permeable and soft contact lens design. *Contact Lens and Anterior Eye*, 37(6), pp.455-460.

Pena-Verdeal, H., Garcia-Resua, C., Barreira, N., Giraldez, M. and Yebra-Pimentel, E., 2016. Interobserver variability of an open-source software for tear meniscus height measurement. *Contact Lens and Anterior Eye*, 39(4), pp.249-256.

Peng, C., Cerretani, C., Braun, R. and Radke, C., 2014a. Evaporation-driven instability of the precorneal tear film. *Advances in Colloid and Interface Science*, 206, pp.250-264.

Peng, C., Cerretani, C., Li, Y., Bowers, S., Shahsavarani, S., Lin, M. and Radke, C., 2014b. Flow Evaporimeter To Assess Evaporative Resistance of Human Tear-Film Lipid Layer. *Industrial & Engineering Chemistry Research*, 53(47), pp.18130-18139.

Pérez-Bartolomé, F., Martínez de la Casa, J., Arriola Villalobos, P., Fernández Pérez, C., Polo, V., Sánchez Jean, R. and García Feijoó, J., 2017. Ocular Redness Measured with the Keratograph 5M in Patients Using Anti-Glaucoma Eye Drops. *Seminars in Ophthalmology*, 33(5), pp.643-650.

Pérez-Bartolomé, F., Sanz-Pozo, C., Martínez-de la Casa, J., Arriola-Villalobos, P., Fernández-Pérez, C. and García-Feijoó, J., 2018. Assessment of ocular redness measurements obtained with keratograph 5M and correlation with subjective grading scales. *Journal Français d'Ophtalmologie*, 41(9), pp.836-846.

Pérez-Gómez, I. and Giles, T., 2014. European survey of contact lens wearers and eye care professionals on satisfaction with a new water gradient daily disposable contact lens. *Clinical Optometry*, 6, pp.17-23.

Pesudovs, K., 2004. The usefulness of Vistech and FACT contrast sensitivity charts for cataract and refractive surgery outcomes research. *British Journal of Ophthalmology*, 88(1), pp.11-16.

Peteiro-Barral, D., Remeseiro, B., Méndez, R. and Penedo, M., 2016. Evaluation of an automatic dry eye test using MCDM methods and rank correlation. *Medical & Biological Engineering & Computing*, 55(4), pp.527-536.

Peterson, R. and Wolffsohn, J., 2007. Sensitivity and reliability of objective image analysis compared to subjective grading of bulbar hyperaemia. *British Journal of Ophthalmology*, 91(11), pp.1464-1466.

Peterson, R. and Wolffsohn, J., 2009. Objective Grading of The Anterior Eye. *Optometry and Vision Science*, 86(3), pp.273-278.

Peterson, R., Wolffsohn, J. and Fowler, C., 2006. Optimization of Anterior Eye Fluorescein Viewing. *American Journal of Ophthalmology*, 142(4), pp.572-575.e2.

Peterson, R., Wolffsohn, J., Nick, J., Winterton, L. and Lally, J., 2006. Clinical performance of daily disposable soft contact lenses using sustained release technology. *Contact Lens and Anterior Eye*, 29(3), pp.127-134.

Pili, K., Kastelan, S., Karabatic, M., Kasun, B. and Culig, B., 2014. Dry eye in contact lens wearers as a growing public health problem. *Psychiatr Danub*, 26(3), pp.528-532.

Pisella, P., Malet, F., Lejeune, S., Brignole, F., Debbasch, C., Bara, J., Rat, P., Colin, J. and Baudouin, C., 2001. Ocular Surface Changes Induced by Contact Lens Wear. *Cornea*, 20(8), pp.820-825.

Poh, S., Lee, R., Gao, J., Tan, C., Gupta, P., Sabanayagam, C., Cheng, C., Wong, T. and Tong, L., 2017. Factors that influence tear meniscus area and conjunctivochalasis: The Singapore Indian eye study. *Ophthalmic Epidemiology*, 25(1), pp.70-78.

Pondelis, N., Dieckmann, G., Jamali, A., Kataguiri, P., Senchyna, M. and Hamrah, P., 2020. Infrared meibography allows detection of dimensional changes in meibomian glands following intranasal neurostimulation. *The Ocular Surface*, 18(3), pp.511-516.

Porcar, E., España, E., Montalt, J., Benlloch-Fornés, J. and Peris-Martínez, C., 2017. Post-LASIK Visual Quality With a Corneoscleral Contact Lens to Treat Irregular Corneas. *Eye & Contact Lens: Science & Clinical Practice*, 43(1), pp.46-50.

Portela, R., Fares, N., Machado, L., São Leão, A., de Freitas, D., Paranhos, A., Prata, T. and Gracitelli, C., 2018. Evaluation of Ocular Surface Disease in Patients With Glaucoma: Clinical Parameters, Self-report Assessment, and Keratograph Analysis. *Journal of Glaucoma*, 27(9), pp.794-801.

Przekoracka, K., Michalak, K., Olszewski, J., Zeri, F., Michalski, A., Paluch, J. and Przekoracka-Krawczyk, A., 2020. Contrast sensitivity and visual acuity in subjects wearing multifocal contact lenses with high additions designed for myopia progression control. *Contact Lens and Anterior Eye*, 43(1), pp.33-39.

Pucker, A. and Tichenor, A., 2020. A Review of Contact Lens Dropout. *Clinical Optometry*, 12, pp.85-94.

Pucker, A., Jones-Jordan, L., Kunnen, C., Marx, S., Powell, D., Kwan, J., Srinivasan, S., Sickenberger, W. and Jones, L., 2019a. Impact of meibomian gland width on successful contact lens use. *Contact Lens and Anterior Eye*, 42(6), pp.646-651.

Pucker, A., Jones-Jordan, L., Li, W., Kwan, J., Lin, M., Sickenberger, W., Marx, S., Srinivasan, S. and Jones, L., 2015. Associations with Meibomian Gland Atrophy in Daily Contact Lens Wearers. *Optometry and Vision Science*, 92(9), pp.e206-e213.

Pucker, A., Jones-Jordan, L., Marx, S., Powell, D., Kwan, J., Srinivasan, S., Sickenberger, W. and Jones, L., 2019b. Clinical factors associated with contact lens dropout. *Contact Lens and Anterior Eye*, 42(3), pp.318-324.

Pullum, K. and Buckley, R., 1997. A Study of 530 Patients Referred for Rigid Gas Permeable Scleral Contact Lens Assessment. *Cornea*, 16(6), pp.612-622.

Pult, H., Murphy, P. and Purslow, C., 2009. A Novel Method to Predict the Dry Eye Symptoms in New Contact Lens Wearers. *Optometry and Vision Science*, 86(9), pp.E1042-E1050.

Pult, H., Murphy, P., Purslow, C., Nyman, J. and Woods, R., 2008a. Limbal and Bulbar Hyperaemia in Normal Eyes. *Ophthalmic and Physiological Optics*, 28(1), pp.13-20.

Pult, H. and Nichols, J., 2012. A Review of Meibography. *Optometry and Vision Science*, 89(5), pp.E760-E769.

Pult, H., Purslow, C., Berry, M. and Murphy, P., 2008b. Clinical Tests for Successful Contact Lens Wear: Relationship and Predictive Potential. *Optometry and Vision Science*, 85(10), pp.E924-E929.

Pult, H., Purslow, C. and Murphy, P., 2011. The relationship between clinical signs and dry eye symptoms. *Eye*, 25(4), pp.502-510.

Pult, H. and Riede-Pult, B., 2011a. Non-contact Meibography: keep it simple but effective. *Contact Lens and Anterior Eye*, 34, pp.S12-S13.

Pult, H. and Riede-Pult, B., 2011b. The new “TF-Scan” application for video keratography: its repeatability and usefulness in tear film break-up time analysis. *Contact Lens and Anterior Eye*, 34, p.S14.

Pult, H. and Riede-Pult, B., 2012a. A new modified fluorescein strip: Its repeatability and usefulness in tear film break-up time analysis. *Contact Lens and Anterior Eye*, 35(1), pp.35-38.

Pult, H. and Riede-Pult, B., 2012b. Non-contact Meibography: keep it simple but effective. *Contact Lens and Anterior Eye*, 35, pp.77-80.

Pult, H. and Riede-Pult, B., 2013. Comparison of subjective grading and objective assessment in meibography. *Contact Lens and Anterior Eye*, 36(1), pp.22-27.

Pult, H., Riede-Pult, B. and Nichols, J., 2012. Relation Between Upper and Lower Lids' Meibomian Gland Morphology, Tear Film, and Dry Eye. *Optometry and Vision Science*, 89(3), pp.E310-E315.

Pult, H., Tosatti, S., Spencer, N., Asfour, J., Ebenhoch, M. and Murphy, P., 2015. Spontaneous Blinking from a Tribological Viewpoint. *The Ocular Surface*, 13(3), pp.236-249.

Purslow, C., 2013. Evaluation of the ocular tolerance of a novel eyelid-warming device used for meibomian gland dysfunction. *Contact Lens and Anterior Eye*, 36(5), pp.226-231.

Qazi, Y., Kheirkhah, A., Blackie, C., Trinidad, M., Williams, C., Cruzat, A., Korb, D. and Hamrah, P., 2018. Clinically Relevant Immune-Cellular Metrics of Inflammation in Meibomian Gland Dysfunction. *Investigative Opthalmology & Visual Science*, 59(15), pp.6111-6123.

Qi, Y., Zhang, C., Zhao, S., Huang, Y. and Yang, R., 2017. A novel noninvasive ocular surface analyzer for the assessment of dry eye with Meibomian gland dysfunction. *Experimental and Therapeutic Medicine*, 13(6), pp.2983-2988.

Qiao, J. and Yan, X., 2013. Emerging treatment options for meibomian gland dysfunction. *Clinical Ophthalmology*, 7, pp.1797-1803.

Qiu, X., Gong, L., Lu, Y., Jin, H. and Robitaille, M., 2012. The diagnostic significance of Fourier-domain optical coherence tomography in Sjögren syndrome, aqueous tear deficiency and lipid tear deficiency patients. *Acta Ophthalmologica*, 90(5), pp.e359-e366.

Rae, S. and Price, H., 2009. The effect of soft contact lens wear and time from blink on wavefront aberration measurement variation. *Clinical and Experimental Optometry*, 92(3), pp.274-282.

Raj, A., Dhasmana, R. and Nagpal, R., 2016. Anterior Segment Optical Coherence Tomography for Tear Meniscus Evaluation and its Correlation with other Tear Variables in Healthy Individuals. *Journal of Clinical and Diagnostic Research*, 10(5), pp.NC01-NC04.

Ramos, L., Barreira, N., Mosquera, A., Penedo, M., Yebra-Pimentel, E. and García-Resúa, C., 2014. Analysis of parameters for the automatic computation of the tear film break-up time test based on CCLRU standards. *Computer Methods and Programs in Biomedicine*, 113(3), pp.715-724.

Ramos, L., Barreira, N., Pena-Verdeal, H., Giráldez, M. and Yebra-Pimentel, E., 2015. Computational approach for tear film assessment based on break-up dynamics. *Biosystems Engineering*, 138, pp.90-103.

Randon, M., Aragno, V., Abbas, R., Liang, H., Labbé, A. and Baudouin, C., 2018. In vivo confocal microscopy classification in the diagnosis of meibomian gland dysfunction. *Eye*, 33(5), pp.754-760.

Read, M., Navascues-Cornago, M., Keir, N., Maldonado-Codina, C. and Morgan, P., 2020. The impact of contact lens wear on ocular surface mucins using a novel clinical fluorescence imaging system. *Contact Lens and Anterior Eye*, 43(4), pp.378-388.

Recchioni, A., Sisó-Fuertes, I., Hartwig, A., Hamid, A., Shortt, A., Morris, R., Vaswani, S., Dermott, J., Cerviño, A., Wolffsohn, J. and O'Donnell, C., 2020. Short-Term Impact of

FS-LASIK and SMILE on Dry Eye Metrics and Corneal Nerve Morphology. *Cornea*, 39(7), pp.851-857.

Remeseiro, B., Barreira, N., García-Resúa, C., Lira, M., Giráldez, M., Yebra-Pimentel, E. and Penedo, M., 2016. iDEAS: A web-based system for dry eye assessment. *Computer Methods and Programs in Biomedicine*, 130, pp.186-197.

Remeseiro, B., Bolon-Canedo, V., Peteiro-Barral, D., Alonso-Betanzos, A., Guijarro-Berdinas, B., Mosquera, A., Penedo, M. and Sanchez-Marono, N., 2014a. A Methodology for Improving Tear Film Lipid Layer Classification. *IEEE Journal of Biomedical and Health Informatics*, 18(4), pp.1485-1493.

Remeseiro, B., Oliver, K., Tomlinson, A., Martin, E., Barreira, N. and Mosquera, A., 2014c. Automatic grading system for human tear films. *Pattern Analysis and Applications*, 18(3), pp.677-694.

Remeseiro, B., Penas, M., Barreira, N., Mosquera, A., Novo, J. and García-Resúa, C., 2013. Automatic classification of the interferential tear film lipid layer using colour texture analysis. *Computer Methods and Programs in Biomedicine*, 111(1), pp.93-103.

Remeseiro, B., Penedo, M., García-Resúa, C., Yebra-Pimentel, E. and Mosquera, A., 2014b. *Ophthalmological Imaging and Applications: Dry eye characterization by analyzing tear film images*. 1st ed. pp.449-175.

Remón, L., Pérez-Merino, P., Macedo-de-Araújo, R., Amorim-de-Sousa, A. and González-Méijome, J., 2020. Bifocal and Multifocal Contact Lenses for Presbyopia and Myopia Control. *Journal of Ophthalmology*, 27, p.8067657.

Ren, Y., Chen, J., Zheng, Q. and Chen, W., 2018. Short-term effect of a developed warming moist chamber goggle for video display terminal-associated dry eye. *BMC Ophthalmology*, 18(1), p.33.

Ribelles, A., Galbis-Estrada, C., Parras, M., Vivar-Llopis, B., Marco-Ramírez, C. and Diaz-Llopis, M., 2015. Ocular Surface and Tear Film Changes in Older Women Working with Computers. *BioMed Research International*, 2015, pp.1-10.

Rico-del-Viejo, L., Benítez-del-Castillo, J., Gómez-Sanz, F., García-Montero, M., Llorens-Quintana, C. and Madrid-Costa, D., 2019. The influence of meibomian gland loss on ocular surface clinical parameters. *Contact Lens and Anterior Eye*, 42(5), pp.562-568.

Rico-del-Viejo, L., Lorente-Velázquez, A., Hernández-Verdejo, J., García-Mata, R., Benítez-del-Castillo, J. and Madrid-Costa, D., 2018. The effect of ageing on the ocular surface parameters. *Contact Lens and Anterior Eye*, 41(1), pp.5-12.

Ridder, W., Lamotte, J., Ngo, L. and Fermin, J., 2005. Short-term Effects of Artificial Tears on Visual Performance in Normal Subjects. *Optometry and Vision Science*, 82(5), pp.370-377.

Ring, M., Rabensteiner, D., Horwath-Winter, J., Boldin, I., Schrödl, F., Reitsamer, H. and Haslwanter, T., 2015. Non invasive assessment of the human tear film dynamics. *Annals of Anatomy - Anatomischer Anzeiger*, 202, pp.61-70.

Robin, M., Liang, H., Rabut, G., Augstburger, E., Baudouin, C. and Labbé, A., 2019. The Role of Meibography in the Diagnosis of Meibomian Gland Dysfunction in Ocular Surface Diseases. *Translational Vision Science & Technology*, 8(6), pp.1-9.

Rocha-de-Lossada, C., Sánchez-González, J., Zamorano-Martín, F., Rachwani-Anil, R., Torras-Sanvicens, J. and Peraza-Nieves, J., 2020. Influence of Sodium Hyaluronate Concentration in Tear Meniscus Height. *Eye & Contact Lens: Science & Clinical Practice*, 00, pp.1-5.

Rodriguez, J., Johnston, P., Ousler III, G., Abelson, M. and Smith, 2013. Automated grading system for evaluation of ocular redness associated with dry eye. *Clinical Ophthalmology*, 7, pp.1197-1204.

Roh, H., Lee, J., Kim, M., Oh, J., Chang, M., Chuck, R. and Park, C., 2016. Systemic comorbidities of dry eye syndrome: The Korean national health and nutrition examination survey V, 2010 to 2012. *Cornea*, 35(2), pp.187-192.

Rohit, A., Willcox, M., Brown, S., Mitchell, T. and Stapleton, F., 2014. Clinical and Biochemical Tear Lipid Parameters in Contact Lens Wearers. *Optometry and Vision Science*, 91(12), pp.1384-1390.

Rohit, A., Willcox, M. and Stapleton, F., 2017. Lipid Supplements and Clinical Aspects of Tear Film in Habitual Lens Wearers. *Optometry and Vision Science*, 94(2), pp.174-182.

Romero-Rangel, T., Stavrou, P., Cotter, J., Rosenthal, P., Baltatzis, S. and Foster, C., 2000. Gas-permeable scleral contact lens therapy in ocular surface disease. *American Journal of Ophthalmology*, 130(1), pp.25-32.

Rosenfield, G. and Fitzpatrick-Lins, K., 1986. A coefficient of agreement as a measure of thematic classification accuracy. *Photogramm Eng Remote Sens*, 52, pp.223-227.

Rosenthal, P. and Cotter, J., 2003. The Boston Scleral Lens in the management of severe ocular surface disease. *Ophthalmology Clinics of North America*, 16(1), pp.89-93.

Ruan, F., Zang, Y., Sella, R., Lu, H., Li, S., Yang, K., Jin, T., Afshari, N., Pan, Z. and Jie, Y., 2019. Intense Pulsed Light Therapy with Optimal Pulse Technology as an Adjunct Therapy for Moderate to Severe Blepharitis-Associated Keratoconjunctivitis. *Journal of Ophthalmology*, 2019, pp.1-10.

Ruiz-Alcocer, J., Monsálvez-Romín, D., García-Lázaro, S., Albarrán-Diego, C., Hernández-Verdejo, J. and Madrid-Costa, D., 2018. Impact of contact lens material and design on the ocular surface. *Clinical and Experimental Optometry*, 101(2), pp.188-192.

Ruiz-Pomeda, A., Fernandes, P., Amorim-de-Sousa, A., González-Méijome, J., Prieto-Garrido, F., Pérez-Sánchez, B. and Villa-Collar, C., 2019. Light disturbance analysis in the controlled randomized clinical trial MiSight® Assessment Study Spain (MASS). *Contact Lens and Anterior Eye*, 42(2), pp.200-205.

Ruiz-Pomeda, A., Pérez-Sánchez, B., Prieto-Garrido, F., Gutiérrez-Ortega, R. and Villa-Collar, C., 2018a. MiSight Assessment Study Spain: Adverse Events, Tear Film Osmolarity, and Discontinuations. *Eye & Contact Lens: Science & Clinical Practice*, 44(2), pp.180-186.

Ruiz-Pomeda, A., Pérez-Sánchez, B., Valls, I., Prieto-Garrido, F., Gutiérrez-Ortega, R. and Villa-Collar, C., 2018b. MiSight Assessment Study Spain (MASS). A 2-year randomized clinical trial. *Graefe's Archive for Clinical and Experimental Ophthalmology*, 256(5), pp.1011-1021.

Ruiz-Pomeda, A., Pérez-Sánchez, B., Cañadas, P., Prieto-Garrido, F., Gutiérrez-Ortega, R. and Villa-Collar, C., 2018c. Binocular and accommodative function in the controlled randomized clinical trial MiSight® Assessment Study Spain (MASS). *Graefe's Archive for Clinical and Experimental Ophthalmology*, 257(1), pp.207-215.

Ruiz-Pomeda, A., Pérez-Sánchez, B., Cañadas Suárez, M., Prieto Garrido, F., Gutiérrez-Ortega, R. and Villa-Collar, C., 2018d. MiSight Assessment Study Spain: A Comparison of Vision-Related Quality-of-Life Measures Between MiSight Contact Lenses and Single-Vision Spectacles. *Eye & Contact Lens: Science & Clinical Practice*, 44(2), pp.S99-S104.

Russo, P., Bouchard, C. and Galasso, J., 2007. Extended-Wear Silicone Hydrogel Soft Contact Lenses in the Management of Moderate to Severe Dry Eye Signs and Symptoms Secondary to Graft-Versus-Host Disease. *Eye & Contact Lens: Science & Clinical Practice*, 33(3), pp.144-147.

Sambhi, R., Sambhi, G., Mather, R. and Malvankar-Mehta, M., 2020. Dry eye after refractive surgery: a meta-analysis. *Canadian Journal of Ophthalmology*, 55(2), pp.99-106.

Sánchez, I., Ortiz-Toquero, S., Blanco, M. and Martin, R., 2018. A new method to analyse the effect of multifocal contact lenses on visual function. *Contact Lens and Anterior Eye*, 41(2), pp.169-174.

Sánchez-Brea, L., Barreira-Rodríguez, N., Mosquera-González, A., Pena-Verdeal, H. and Yebra-Pimentel Vilar, E., 2017. Precise segmentation of the bulbar conjunctiva for hyperaemia images. *Pattern Analysis and Applications*, 21(2), pp.563-577.

Sánchez-Pavón, I., Cañadas, P. and Martin, R., 2020. Repeatability and agreement of intraocular pressure measurement among three tonometers. *Clinical and Experimental Optometry*, 103(6), pp.808-812.

Sano, K., Kawashima, M., Takechi, S., Mimura, M. and Tsubota, K., 2018. Exercise program improved subjective dry eye symptoms for office workers. *Clinical Ophthalmology*, Volume 12, pp.307-311.

Santodomingo-Rubido, J., Barrado-Navascués, E. and Rubido-Crespo, M., 2010. Ocular Surface Comfort During the Day Assessed by Instant Reporting in Different Types of Contact and Non–Contact Lens Wearers. *Eye & Contact Lens: Science & Clinical Practice*, 36(2), pp.96-100.

Santodomingo-Rubido, J., Wolffsohn, J. and Gilmartin, B., 2006a. Comparison between graticule and image capture assessment of lower tear film meniscus height. *Contact Lens and Anterior Eye*, 29(4), pp.169-173.

Santodomingo-Rubido, J., Wolffsohn, J. and Gilmartin, B., 2006b. Changes in Ocular Physiology, Tear Film Characteristics, and Symptomatology With 18 Months Silicone Hydrogel Contact Lens Wear. *Optometry and Vision Science*, 83(2), pp.73-81.

Sapkota, K., Franco, S. and Lira, M., 2018. Daily versus monthly disposable contact lens: Which is better for ocular surface physiology and comfort?. *Contact Lens and Anterior Eye*, 41(3), pp.252-257.

Savini, G., 2008. The challenge of dry eye diagnosis. *Clinical Ophthalmology*, p.31.

Savini, G., Barboni, P. and Zanini, M., 2006. Tear Meniscus Evaluation by Optical Coherence Tomography. *Ophthalmic Surgery, Lasers and Imaging Retina*, 37(2), pp.112-118.

Savini, G., Goto, E., Carbonelli, M., Barboni, P. and Huang, D., 2009. Agreement Between Stratus and Visante Optical Coherence Tomography Systems in Tear Meniscus Measurements. *Cornea*, 28(2), pp.148-151.

Schafer, J., Reindel, W., Steffen, R., Mosehauer, G. and Chinn, J., 2018. Use of a novel extended blink test to evaluate the performance of two polyvinylpyrrolidone-containing, silicone hydrogel contact lenses. *Clinical Ophthalmology*, Volume 12, pp.819-825.

Schaumberg, D., Nichols, J., Papas, E., Tong, L., Uchino, M. and Nichols, K., 2011. The International Workshop on Meibomian Gland Dysfunction: Report of the Subcommittee on the Epidemiology of, and Associated Risk Factors for, MGD. *Investigative Opthalmology & Visual Science*, 52(4), pp.1994-2005.

Schaumberg, D., Sullivan, D., Buring, J. and Dana, M., 2003. Prevalence of dry eye syndrome among US women. *American Journal of Ophthalmology*, 136(2), pp.318-326.

Schiffman, R., 2000. Reliability and Validity of the Ocular Surface Disease Index. *Archives of Ophthalmology*, 118(5), pp.615-621.

Schornack, M., Pyle, J. and Patel, S., 2014. Scleral Lenses in the Management of Ocular Surface Disease. *Ophthalmology*, 121(7), pp.1398-1405.

Schulze, M., Hutchings, N. and Simpson, T., 2011. Grading Bulbar Redness Using Cross-Calibrated Clinical Grading Scales. *Investigative Opthalmology & Visual Science*, 52(8), pp.5812-5817.

Schulze, M., Ng, A., Yang, M., Panjwani, F., Srinivasan, S., Jones, L. and Senchyna, M., 2021. Bulbar Redness and Dry Eye Disease: Comparison of a Validated Subjective Grading Scale and an Objective Automated Method. *Optometry and Vision Science*, 98(2), pp.113-120.

Sella, R., Zangwill, L., Weinreb, R. and Afshari, N., 2019. Repeatability and Reproducibility of Corneal Epithelial Thickness Mapping With Spectral-Domain Optical Coherence Tomography in Normal and Diseased Cornea Eyes. *American Journal of Ophthalmology*, 197, pp.88-97.

Seo, K., Kang, S., Ha, D., Chin, H. and Jung, J., 2018. Long-term effects of intense pulsed light treatment on the ocular surface in patients with rosacea-associated meibomian gland dysfunction. *Contact Lens and Anterior Eye*, 41(5), pp.430-435.

Sha, J., Bakaraju, R., Tilia, D., Chung, J., Delaney, S., Munro, A., Ehrmann, K., Thomas, V. and Holden, B., 2015. Short-term visual performance of soft multifocal contact lenses for presbyopia. *Arquivos Brasileiros de Oftalmologia*, 79(2), pp.73-77.

Sha, J., Tilia, D., Diec, J., Fedtke, C., Yeotikar, N., Jong, M., Thomas, V. and Bakaraju, R., 2018. Visual performance of myopia control soft contact lenses in non-presbyopic myopes. *Clinical Optometry*, Volume 10, pp.75-86.

Shaaban, Y. and Badran, T., 2018. Tear meniscus evaluation after microkeratome laser in situ keratomileusis, femtosecond laser and femtosmile laser techniques using anterior segment optical coherence tomography. *Clinical Ophthalmology*, Volume 12, pp.1337-1345.

Shaheen, B., Bakir, M. and Jain, S., 2014. Corneal nerves in health and disease. *Survey of Ophthalmology*, 59(3), pp.263-285.

Sharma, N. and Oliver, K., 2018. Subjective and objective interpretation of tear film interferometry images. *International Journal of Research in Medical Sciences*, 6(9), p.2923.

Shehadeh-Mashor, R., Mimouni, M., Shapira, Y., Sela, T., Munzer, G. and Kaiserman, I., 2019. Risk Factors for Dry Eye After Refractive Surgery. *Cornea*, 38(12), pp.1495-1499.

Shehzad, D., Gorcuyeva, S., Dag, T. and Bozkurt, B., 2019. Novel Application Software for the Semi-Automated Analysis of Infrared Meibography Images. *Cornea*, 38(11), pp.1456-1464.

Shimazaki, J., Goto, E., Ono, M., Shimmura, S. and Tsubota, K., 1998. Meibomian gland dysfunction in patients with Sjögren syndrome. *Ophthalmology*, 105(8), pp.1485-1488.

Shimazaki, J., Sakata, M. and Tsubota, K., 1995. Ocular Surface Changes and Discomfort in Patients With Meibomian Gland Dysfunction. *Archives of Ophthalmology*, 113(10), pp.1266-1270.

Shinzawa, M., Dogru, M., Miyasaka, K., Shimazaki, J. and Sekiryu, T., 2018. Application of CASIA SS-1000 Optical Coherence Tomography Tear Meniscus Imaging in Testing the Efficacy of New Strip Meniscometry in Dry Eye Diagnosis. *Eye & Contact Lens: Science & Clinical Practice*, 44(1), pp.S44-S49.

Shrestha, T., Moon, H., Choi, W., Yoon, H., Ji, Y., Ueta, M. and Yoon, K., 2019. Characteristics of meibomian gland dysfunction in patients with Stevens–Johnson syndrome. *Medicine*, 98(26), p.e16155.

Siddireddy, J., Vijay, A., Tan, J. and Willcox, M., 2018a. The eyelids and tear film in contact lens discomfort. *Contact Lens and Anterior Eye*, 41(2), pp.144-153.

Siddireddy, J., Tan, J., Vijay, A. and Willcox, M., 2018b. Predictive Potential of Eyelids and Tear Film in Determining Symptoms in Contact Lens Wearers. *Optometry and Vision Science*, 95(11), pp.1035-1045.

Sim, H., Petznick, A., Barbier, S., Tan, J., Acharya, U., Yeo, S. and Tong, L., 2014. A Randomized, Controlled Treatment Trial of Eyelid-Warming Therapies in Meibomian Gland Dysfunction. *Ophthalmology and Therapy*, 3(1-2), pp.37-48.

Simpson, T., Situ, P., Jones, L. and Fonn, D., 2008. Dry Eye Symptoms Assessed by Four Questionnaires. *Optometry and Vision Science*, 85(8), pp.E692-E699.

Simsek, C., Kojima, T., Dogru, M., Tanaka, M., Takano, Y., Wakamatsu, T., Ibrahim, O., Toda, I., Negishi, K. and Tsubota, K., 2020. The Early Effects of Alcohol Consumption on Functional Visual Acuity, Tear Functions, and the Ocular Surface. *Eye & Contact Lens: Science & Clinical Practice*, 47(1), pp.20-26.

Singh, A., Vanathi, M., Kishore, A., Gupta, N. and Tandon, R., 2019. Evaluation of strip meniscometry, tear meniscus height and depth in the diagnosis of dry eye disease in asian Indian eyes. *The Ocular Surface*, 17(4), pp.747-752.

Situ, P., Simpson, T., Begley, C. and Keir, N., 2020. Role of diurnal variation of corneal sensory processing in contact lens discomfort. *The Ocular Surface*, 18(4), pp.770-776.

Sokolova, M., Japkowicz, N. and Szpakowicz, S., 2006. Beyond accuracy, F-score and ROC: A family of discriminant measures for performance evaluation. *In: AAAI Workshop - Technical Report*, pp.24-29.

Solomon, A., Dursun, D., Liu, Z., Xie, Y., Macri, A. and Pflugfelder, S., 2001. Pro- and anti-inflammatory forms of interleukin-1 in the tear fluid and conjunctiva of patients with dry-eye disease. *Investig Ophthalmol Vis Sci*, 42, pp.2283-2292.

Sorbara, L., Maram, J., Simpson, T. and Hutchings, N., 2018. Corneal, Conjunctival effects and blood flow changes related to silicone hydrogel lens wear and their

correlations with end of day comfort. *Contact Lens and Anterior Eye*, 41(2), pp.193-200.

Srinivasan, S., Joyce, E., Senchyna, M., Simpson, T. and Jones, L., 2008. Clinical signs and symptoms in post-menopausal females with symptoms of dry eye. *Ophthalmic and Physiological Optics*, 28(4), pp.365-372.

Srinivasan, S., Menzies, K., Sorbara, L. and Jones, L., 2012. Infrared Imaging of Meibomian Gland Structure Using a Novel Keratograph. *Optometry and Vision Science*, 89(5), pp.788-794.

Stahl, U. and Jalbert, I., 2018. Exploring the links between contact lens comfort, osmolarity and lid wiper staining. *Contact Lens and Anterior Eye*, 41(1), pp.110-116.

Stapleton, F., Alves, M., Bunya, V., Jalbert, I., Lekhanont, K., Malet, F., Na, K., Schaumberg, D., Uchino, M., Vehof, J., Viso, E., Vitale, S. and Jones, L., 2017. TFOS DEWS II Epidemiology Report. *The Ocular Surface*, 15(3), pp.334-365.

Stapleton, F., Keay, L., Jalbert, I. and Cole, N., 2007. The Epidemiology of Contact Lens Related Infiltrates. *Optometry and Vision Science*, 84(4), pp.257-272.

Stapleton, F., Stretton, S., Papas, E., Skotnitsky, C. and Sweeney, D., 2006. Silicone Hydrogel Contact Lenses and the Ocular Surface. *The Ocular Surface*, 4(1), pp.24-43.

Stephens, D. and McNamara, N., 2015. Altered Mucin and Glycoprotein Expression in Dry Eye Disease. *Optometry and Vision Science*, 92(9), pp.931-938.

Stern, M., Beuerman, R., Fox, R., Gao, J., Mircheff, A. and Pflugfelder, S., 1998. The Pathology of Dry Eye. *Cornea*, 17(6), p.584.

Stern, M., Gao, J., Siemasko, K., Beuerman, R. and Pflugfelder, S., 2004. The role of the lacrimal functional unit in the pathophysiology of dry eye. *Experimental Eye Research*, 78(3), pp.409-416.

Stern, M., Schaumburg, C. and Pflugfelder, S., 2013. Dry Eye as a Mucosal Autoimmune Disease. *International Reviews of Immunology*, 32(1), pp.19-41.

Stevenson, D., Tauber, J. and Reis, B., 2000. Efficacy and safety of cyclosporin a ophthalmic emulsion in the treatment of moderate-to-severe dry eye disease. *Ophthalmology*, 107(5), pp.967-974.

Su, T. and Chang, S., 2021. Normalized ocular surface temperature models for tear film characteristics and dry eye disease evaluation. *The Ocular Surface*, 19, pp.74-82.

Su, T., Ho, W., Chang, S. and Chiang, H., 2016. Thermographic evaluation of tear film break-up time to study tear film stability. *International Journal of Thermal Sciences*, 99, pp.36-40.

Su, T., Ho, W., Chiang, S., Lu, C., Chiang, H. and Chang, S., 2017. Infrared thermography in the evaluation of meibomian gland dysfunction. *Journal of the Formosan Medical Association*, 116(7), pp.554-559.

Su, T., Hwa, C., Liu, P., Wu, M., Chang, D., Su, P., Chang, S. and Chiang, H., 2011. Noncontact detection of dry eye using a custom designed infrared thermal image system. *Journal of Biomedical Optics*, 16(4), p.046009.

Sullivan, B., 2014. Challenges in Using Signs and Symptoms to Evaluate New Biomarkers of Dry Eye Disease. *The Ocular Surface*, 12(1), pp.2-9.

Sullivan, B., Crews, L., Messmer, E., Foulks, G., Nichols, K., Baenninger, P., Geerling, G., Figueiredo, F. and Lemp, M., 2012a. Correlations between commonly used objective signs and symptoms for the diagnosis of dry eye disease: clinical implications. *Acta Ophthalmologica*, 92(2), pp.161-166.

Sullivan, B., Crews, L., Sönmez, B., de la Paz, M., Comert, E., Charoenrook, V., de Araujo, A., Pepose, J., Berg, M., Kosheleff, V. and Lemp, M., 2012b. Clinical Utility of Objective Tests for Dry Eye Disease. *Cornea*, 31(9), pp.1000-1008.

Sullivan, D., Hammitt, K., Schaumberg, D., Sullivan, B., Begley, C., Gjorstrup, P., Garrigue, J., Nakamura, M., Quentric, Y., Barabino, S., Dalton, M. and Novack, G., 2012. Report of the TFOS/ARVO Symposium on Global Treatments for Dry Eye Disease: An Unmet Need. *The Ocular Surface*, 10(2), pp.108-116.

Sullivan, D., Rocha, E., Aragona, P., Clayton, J., Ding, J., Golebiowski, B., Hampel, U., McDermott, A., Schaumberg, D., Srinivasan, S., Versura, P. and Willcox, M., 2017. TFOS DEWS II Sex, Gender, and Hormones Report. *The Ocular Surface*, 15(3), pp.284-333.

Sweeney, D., Millar, T. and Raju, S., 2013. Tear film stability: A review. *Experimental Eye Research*, 117, pp.28-38.

Szczesna, D., 2011. Assessing Tear Film on Soft Contact Lenses With Lateral Shearing Interferometry. *Eye & Contact Lens: Science & Clinical Practice*, 37(6), pp.342-347.

Szczesna-Iskander, D., 2014. Comparison of Tear Film Surface Quality Measured In Vivo on Water Gradient Silicone Hydrogel and Hydrogel Contact Lenses. *Eye & Contact Lens: Science & Clinical Practice*, 40(1), pp.23-27.

Szczesna-Iskander, D., 2018. Post-blink tear film dynamics in healthy and dry eyes during spontaneous blinking. *The Ocular Surface*, 16(1), pp.93-100.

Szczesna-Iskander, D., Alonso-Caneiro, D. and Iskander, D., 2016. Objective Measures of Pre-lens Tear Film Dynamics versus Visual Responses. *Optometry and Vision Science*, 93(8), pp.872-880.

Szczesna-Iskander, D. and Iskander, D., 2014. Tear Film Dynamics on Soft Contact Lenses. *Optometry and Vision Science*, 91(12), pp.1406-1411.

Szczesna-Iskander, D., Iskander, D., Read, S. and Alonso-Caneiro, D., 2012. Noninvasive In Vivo Assessment of Soft Contact Lens Type on Tear Film Surface Quality. *Investigative Opthalmology & Visual Science*, 53(1), pp.525-531.

Szegedi, S., Scheschy, U., Schmidl, D., Aranha dos Santos, V., Stegmann, H., Adzhemian, N., Fondi, K., Bata, A., Werkmeister, R., Couderc, C., Schmetterer, L. and Garhofer, G., 2018. Effect of Single Instillation of Two Hyaluronic Acid-Based Topical Lubricants on Tear Film Thickness in Patients with Dry Eye Syndrome. *Journal of Ocular Pharmacology and Therapeutics*, 34(9), pp.605-611.

Talens-Estarelles, C., García-Del Valle, A. and García-Lázaro, S., 2022. Impact of the pupil size – central optical zone diameter relationship on visual performance in aspheric multifocal contact lenses. *Contact Lens and Anterior Eye*, 45(2), p.101440.

Talens-Estarelles, C., García-Marqués, J., Cervino, A. and García-Lázaro, S., 2021a. Use of digital displays and ocular surface alterations: A review. *The Ocular Surface*, 19, pp.252-265.

Talens-Estarelles, C., García-Marqués, J., Cervino, A. and García-Lázaro, S., 2021b. Online Vs In-person Education: Evaluating the Potential Influence of Teaching Modality on Dry Eye Symptoms and Risk Factors During the COVID-19 Pandemic. *Eye & Contact Lens: Science & Clinical Practice*, 47(10), pp.565-572.

Talens-Estarelles, C., Sanchis-Jurado, V., Esteve-Taboada, J., Pons, Á. and García-Lázaro, S., 2020. How Do Different Digital Displays Affect the Ocular Surface?. *Optometry and Vision Science*, 97(12), pp.1070-1079.

Tan, C., Labbé, A., Liang, Q., Qiao, L., Baudouin, C., Wan, X. and Wang, N., 2015a. Dynamic Change of Optical Quality in Patients With Dry Eye Disease. *Investigative Opthalmology & Visual Science*, 56(5), pp.2848-2854.

Tan, J., Ho, L., Wong, K., La, A., Lee, S., Park, S., Tran, L. and Stapleton, F., 2018. The effects of a hydrating mask compared to traditional warm compresses on tear film properties in meibomian gland dysfunction. *Contact Lens and Anterior Eye*, 41(1), pp.83-87.

Tan, J., Ng, E. and Acharya U, R., 2011. An Efficient Automated Algorithm to Detect Ocular Surface Temperature on Sequence of Thermograms Using Snake and Target Tracing Function. *Journal of Medical Systems*, 35(5), pp.949-958.

Tan, L., Morgan, P., Cai, Z. and Straughan, R., 2015b. Prevalence of and risk factors for symptomatic dry eye disease in Singapore. *Clinical and Experimental Optometry*, 98(1), pp.45-53.

Tan, L., Sanjay, S. and Morgan, P., 2016a. Repeatability of infrared ocular thermography in assessing healthy and dry eyes. *Contact Lens and Anterior Eye*, 39(4), pp.284-292.

Tan, L., Sanjay, S. and Morgan, P., 2016b. Screening for dry eye disease using infrared ocular thermography. *Contact Lens and Anterior Eye*, 39(6), pp.442-449.

Tao, A., Shen, M., Wang, J., Chen, Q. and Lu, F., 2010. Upper and Lower Tear Menisci After Laser In Situ Keratomileusis. *Eye & Contact Lens: Science & Clinical Practice*, 36(2), pp.81-85.

Tauste, A., Ronda, E., Baste, V., Bråtveit, M., Moen, B. and Seguí Crespo, M., 2017. Ocular surface and tear film status among contact lens wearers and non-wearers who use VDT at work: comparing three different lens types. *International Archives of Occupational and Environmental Health*, 91(3), pp.327-335.

Tesón, M., González-García, M., López-Miguel, A., Enríquez-de-Salamanca, A., Martín-Montañez, V., Benito, M., Mateo, M., Stern, M. and Calonge, M., 2013. Influence of a Controlled Environment Simulating an In-Flight Airplane Cabin on Dry Eye Disease. *Investigative Opthalmology & Visual Science*, 54(3), p.2093-2099.

Tesón, M., López-Miguel, A., Neves, H., Calonge, M., González-García, M. and González-Méijome, J., 2015. Influence of Climate on Clinical Diagnostic Dry Eye Tests. *Optometry and Vision Science*, 92(9), pp.e284-e289.

Thibos, L. and Hong, X., 1999. Clinical Applications of the Shack-Hartmann Aberrometer. *Optometry and Vision Science*, 76(12), pp.817-825.

Thulasi, P. and Djalilian, A., 2017. Update in Current Diagnostics and Therapeutics of Dry Eye Disease. *Ophthalmology*, 124(11), pp.S27-S33.

Tian, L., Qu, J., Zhang, X. and Sun, X., 2016. Repeatability and Reproducibility of Noninvasive Keratograph 5M Measurements in Patients with Dry Eye Disease. *Journal of Ophthalmology*, 2016, pp.1-6.

Tiffany, J., 2006. Surface Tension in Tears. Archivos de la Sociedad Española de Oftalmología, 29, pp.169-173

Tiffany, J., Todd, B., Baker, M., 1998. Computer-assisted calculation of exposed area of the human eye. *Advances in Experimental Medicine and Biology*, 438, pp.433-439.

Tittler, E., Bujak, M., Nguyen, P., Zhang, X., Li, Y., Yiu, S. and Huang, D., 2011. Between-Grader Repeatability of Tear Meniscus Measurements Using Fourier-Domain OCT in Patients With Dry Eye. *Ophthalmic Surgery, Lasers, and Imaging*, 42(5), pp.423-427.

Tomlinson, A., Bron, A., Korb, D., Amano, S., Paugh, J., Pearce, E., Yee, R., Yokoi, N., Arita, R. and Dogru, M., 2011. The International Workshop on Meibomian Gland Dysfunction: Report of the Diagnosis Subcommittee. *Investigative Opthalmology & Visual Science*, 52(4), pp.2006-2049.

Tomlinson, A., Khanal, S., Ramaesh, K., Diaper, C. and McFadyen, A., 2006. Tear Film Osmolarity: Determination of a Referent for Dry Eye Diagnosis. *Investigative Opthalmology & Visual Science*, 47(10), pp.4309-4315.

Tong, L. and Teng, L., 2018. Review of Literature on Measurements of Non-invasive Break Up Times, Lipid Morphology and Tear Meniscal Height Using Commercially Available Hand-held Instruments. *Current Eye Research*, 43(5), pp.567-575.

Tong, L., Teo, C. and Lee, R., 2019. Spatial Distribution of Noninvasive Break Up Times and Clinical Relevance in Healthy Participants and Mild Dry Eye. *Translational Vision Science & Technology*, 8(5), p.30.

Tongg, L., Saw, S., Lamoureux, E., Wang, J., Rosman, M., Tan, D. and Wong, T., 2009. A Questionnaire-Based Assessment of Symptoms Associated with Tear Film Dysfunction and Lid Margin Disease in an Asian Population. *Ophthalmic Epidemiology*, 16(1), pp.31-37.

Tsubota, K., 1996. Quantitative Videographic Analysis of Blinking in Normal Subjects and Patients With Dry Eye. *Archives of Ophthalmology*, 114(6), pp.715-720.

Tukenmez-Dikmen, N., Yildiz, E., Imamoglu, S., Turan-Vural, E. and Sevim, M., 2016. Correlation of Dry Eye Workshop Dry Eye Severity Grading System With Tear Meniscus Measurement by Optical Coherence Tomography and Tear Osmolarity. *Eye & Contact Lens: Science & Clinical Practice*, 42(3), pp.153-157.

Tung, C., Kottaiyan, R., Koh, S., Wang, Q., Yoon, G., Zavislan, J., Davio, S. and Aquavella, J., 2012. Noninvasive, Objective, Multimodal Tear Dynamics Evaluation of 5 Over-the-Counter Tear Drops in a Randomized Controlled Trial. *Cornea*, 31(2), pp.108-114.

Tutt, R., Bradley, A., Begley, C., Thibos, LN., 2000. Optical and visual impact of tear break-up in human eyes. *Investigative Opthalmology & Visual Science*, 41(13), pp.4117-4123.

Tyagi, G., Alonso-Caneiro, D., Collins, M. and Read, S., 2012. Tear Film Surface Quality With Rigid and Soft Contact Lenses. *Eye & Contact Lens: Science & Clinical Practice*, 38(3), pp.171-178.

Ubels, J., Gipson, I., Spurr-Michaud, S., Tisdale, A., Van Dyken, R. and Hatton, M., 2012. Gene Expression in Human Accessory Lacrimal Glands of Wolfring. *Investigative Opthalmology & Visual Science*, 53(11), p.6738.

Uchida, A., Uchino, M., Goto, E., Hosaka, E., Kasuya, Y., Fukagawa, K., Dogru, M., Ogawa, Y. and Tsubota, K., 2007. Noninvasive Interference Tear Meniscometry in Dry Eye Patients With Sjögren Syndrome. *American Journal of Ophthalmology*, 144(2), pp.232-237.e1.

Uchino, M., Nishiwaki, Y., Michikawa, T., Shirakawa, K., Kuwahara, E., Yamada, M., Dogru, M., Schaumberg, D., Kawakita, T., Takebayashi, T. and Tsubota, K., 2011. Prevalence and Risk Factors of Dry Eye Disease in Japan: Koumi Study. *Ophthalmology*, 118(12), pp.2361-2367.

Uchino, M., Schaumberg, D., Dogru, M., Uchino, Y., Fukagawa, K., Shimmura, S., Satoh, T., Takebayashi, T. and Tsubota, K., 2008. Prevalence of Dry Eye Disease among Japanese Visual Display Terminal Users. *Ophthalmology*, 115(11), pp.1982-1988.

Uchino, M., Uchino, Y., Dogru, M., Kawashima, M., Yokoi, N., Komuro, A., Sonomura, Y., Kato, H., Kinoshita, S., Schaumberg, D. and Tsubota, K., 2014. Dry Eye Disease and Work Productivity Loss in Visual Display Users: The Osaka Study. *American Journal of Ophthalmology*, 157(2), pp.294-300.

Uchino, M., Yokoi, N., Uchino, Y., Dogru, M., Kawashima, M., Komuro, A., Sonomura, Y., Kato, H., Kinoshita, S., Schaumberg, D. and Tsubota, K., 2013. Prevalence of Dry Eye Disease and its Risk Factors in Visual Display Terminal Users: The Osaka Study. *American Journal of Ophthalmology*, 156(4), pp.759-766.

Uçakhan, Ö. and Arslanturk-Eren, M., 2019. The Role of Soft Contact Lens Wear on Meibomian Gland Morphology and Function. *Eye & Contact Lens: Science & Clinical Practice*, 45(5), pp.292-300.

Ulusoy, M., Işık-Ulusoy, S. and Kıvanç, S., 2019. Evaluation of dry eye disease in newly diagnosed anxiety and depression patients using anterior segment optical coherence tomography. *Eye and Vision*, 6(1).

Vagge, A., Bernabei, F., Del Noce, C., Pellegrini, M., Giannaccare, G., Senni, C., Scotto, R. and Traverso, C., 2020. In Vivo Confocal Microscopy Morphometric Analysis of Meibomian Glands in Patients With Graves Ophthalmopathy. *Cornea*, 00, pp.1-5.

Vandermeer, G., Chamy, Y. and Pisella, P., 2018. Comparison of objective optical quality measured by double-pass aberrometry in patients with moderate dry eye: Normal saline vs. artificial tears: A pilot study. *Journal Français d'Ophtalmologie*, 41(2), pp.e51-e57.

Van der Vaart, R., Weaver, M., Lefebvre, C. and Davis, R., 2015. The Association Between Dry Eye Disease and Depression and Anxiety in a Large Population-Based Study. *American Journal of Ophthalmology*, 159(3), pp.470-474.

van der Worp, E., Bornman, D., Ferreira, D., Faria-Ribeiro, M., Garcia-Porta, N. and González-Meijome, J., 2014. Modern scleral contact lenses: A review. *Contact Lens and Anterior Eye*, 37(4), pp.240-250.

Varikooty, J., Keir, N. and Simpson, T., 2012. Estimating Tear Film Spread and Stability Through Tear Hydrodynamics. *Optometry and Vision Science*, 89(8), pp.E1119-E1124.

Vehof, J., Hysi, P. and Hammond, C., 2017. A Metabolome-Wide Study of Dry Eye Disease Reveals Serum Androgens as Biomarkers. *Ophthalmology*, 124(4), pp.505-511.

Vehof, J., Kozareva, D., Hysi, P. and Hammond, C., 2014. Prevalence and risk factors of dry eye disease in a British female cohort. *British Journal of Ophthalmology*, 98(12), pp.1712-1717.

Vehof, J., Utheim, T., Bootsma, H. and Hammond, C., 2021. Advances, Limitations and Future Perspectives in the Diagnosis and Management of Dry Eye in Sjögren's Syndrome. *Clinical and Experimental Rheumatology*, 38, pp.S301-S309.

Versura, P., Giannaccare, G., Fresina, M. and Campos, E., 2015. Subjective Discomfort Symptoms Are Related to Low Corneal Temperature in Patients With Evaporative Dry Eye. *Cornea*, 34(9), pp.1079-1085.

Vidal-Rohr, M., Wolffsohn, J., Davies, L. and Cerviño, A., 2018. Effect of contact lens surface properties on comfort, tear stability and ocular physiology. *Contact Lens and Anterior Eye*, 41(1), pp.117-121.

Viera, A. and Garrett, J., 2005. Understanding interobserver agreement: The kappa statistic. *Fam Med*, 37, pp.360-363.

Villa, C., Gutierrez, R., Jimenez, J. and Gonzalez-Meijome, J., 2007. Night vision disturbances after successful LASIK surgery. *British Journal of Ophthalmology*, 91(8), pp.1031-1037.

Villani, E., Beretta, S., De Capitani, M., Galimberti, D., Viola, F. and Ratiglia, R., 2011a. In Vivo Confocal Microscopy of Meibomian Glands in Sjögren's Syndrome. *Investigative Opthalmology & Visual Science*, 52(2), pp.933-999.

Villani, E. and Arita, R., 2019. Imaging of meibomian glands: from bench to bedside and back. *Eye*, 33(5), pp.695-697

Villani, E., Canton, V., Magnani, F., Viola, F., Nucci, P. and Ratiglia, R., 2013a. The Aging Meibomian Gland: An In Vivo Confocal Study. *Investigative Opthalmology & Visual Science*, 54(7), pp.4735-4740.

Villani, E., Ceresara, G., Beretta, S., Magnani, F., Viola, F. and Ratiglia, R., 2011b. In Vivo Confocal Microscopy of Meibomian Glands in Contact Lens Wearers. *Investigative Opthalmology & Visual Science*, 52(8), pp.5212-5219.

Villani, E., Galimberti, D., Viola, F., Mapelli, C. and Ratiglia, R., 2007. The Cornea in Sjögren's Syndrome: An In Vivo Confocal Study. *Investigative Opthalmology & Visual Science*, 48(5), pp.2017-2022.

Villani, E., Garoli, E., Canton, V., Pichi, F., Nucci, P. and Ratiglia, R., 2015. Evaluation of a novel eyelid-warming device in meibomian gland dysfunction unresponsive to traditional warm compress treatment: an in vivo confocal study. *International Ophthalmology*, 35(3), pp.319-323.

Villani, E., Magnani, F., Viola, F., Santaniello, A., Scorza, R., Nucci, P. and Ratiglia, R., 2013b. In Vivo Confocal Evaluation of the Ocular Surface Morpho-Functional Unit in Dry Eye. *Optometry and Vision Science*, 90(6), pp.576-586.

Villani, E., Marelli, L., Dellavalle, A., Serafino, M. and Nucci, P., 2020. Latest evidences on meibomian gland dysfunction diagnosis and management. *The Ocular Surface*, 18(4), pp.871-892.

Viso, E., Gude, F. and Rodríguez-Ares, M., 2011. The Association of Meibomian Gland Dysfunction and Other Common Ocular Diseases With Dry Eye: A Population-Based Study in Spain. *Cornea*, 30(1), pp.1-6.

Viso, E., Rodríguez-Ares, M. and Gude, F., 2009. Prevalence of and Associated Factors for Dry Eye in a Spanish Adult Population (The Salnes Eye Study). *Ophthalmic Epidemiology*, 16(1), pp.15-21.

Wahl, S., Fornoff, L., Ochakovski, G. and Ohlendorf, A., 2018. Disability glare in soft multifocal contact lenses. *Contact Lens and Anterior Eye*, 41(2), pp.175-179.

Wakamatsu, T., Okada, N., Kojima, T., Matsumoto, Y., Ibrahim, O., Dogru, M., Adan, E., Fukagawa, K., Katakami, C., Tsubota, K., Shimazaki, J. and Fujishima, H., 2009. Evaluation of conjunctival inflammatory status by confocal scanning laser microscopy and conjunctival brush cytology in patients with atopic keratoconjunctivitis (AKC). *Molecular vision*, 15, pp.1611-1619.

Wakamatsu, T., Sato, E., Matsumoto, Y., Ibrahim, O., Dogru, M., Kaido, M., Ishida, R. and Tsubota, K., 2010. Conjunctival In Vivo Confocal Scanning Laser Microscopy in Patients with Sjögren Syndrome. *Investigative Opthalmology & Visual Science*, 51(1), pp.144-150.

Walker, M., Schornack, M. and Vincent, S., 2021. Anatomical and physiological considerations in scleral lens wear: Eyelids and tear film. *Contact Lens and Anterior Eye*, 44(5), p.101407.

Walline, J., Greiner, K., McVey, M. and Jones-Jordan, L., 2013. Multifocal Contact Lens Myopia Control. *Optometry and Vision Science*, 90(11), pp.1207-1214.

Walt, JG., Rowe, MM. and Stern, KL., 1997. Evaluating the functional impact of dry eye: the Ocular Surface Disease Index. *Drug Inf J*. pp. 311436.

Walther, H., Subbaraman, L. and Jones, L., 2019. Novel in vitro method to determine pre-lens tear break-up time of hydrogel and silicone hydrogel contact lenses. *Contact Lens and Anterior Eye*, 42(2), pp.178-184.

Wang, A., Gu, Z., Liao, R. and Shuai, Z., 2019c. Dry Eye Indexes Estimated by Keratograph 5M of Systemic Lupus Erythematosus Patients without Secondary Sjögren's Syndrome Correlate with Lupus Activity. *Journal of Ophthalmology*, 2019, pp.1-8.

Wang, J., Aquavella, J., Palakuru, J., Chung, S. and Feng, C., 2006. Relationships between Central Tear Film Thickness and Tear Menisci of the Upper and Lower Eyelids. *Investigative Ophthalmology & Visual Science*, 47(10), pp.4349-4355.

Wang, J., Cox, I. and Reindel, W., 2009. Upper and Lower Tear Menisci on Contact Lenses. *Investigative Opthalmology & Visual Science*, 50(3), pp.1106-11.

Wang, J., Jiao, S., Ruggeri, M., Shousha, M. and Chen, Q., 2009. In Situ Visualization of Tears on Contact Lens Using Ultra High Resolution Optical Coherence Tomography. *Eye & Contact Lens: Science & Clinical Practice*, 35(2), pp.44-49.

Wang, J., Palakuru, J. and Aquavella, J., 2008. Correlations Among Upper and Lower Tear Menisci, Noninvasive Tear Break-up Time, and the Schirmer Test. *American Journal of Ophthalmology*, 145(5), pp.795-800.e1.

Wang, M. and Craig, J., 2018. Comparative Evaluation of Clinical Methods of Tear Film Stability Assessment. *JAMA Ophthalmology*, 136(3), p.291.

Wang, M. and Craig, J., 2019. Natural history of dry eye disease: Perspectives from inter-ethnic comparison studies. *The Ocular Surface*, 17(3), pp.424-433.

Wang, M., Feng, J., Wong, J., Turnbull, P. and Craig, J., 2019d. Randomised trial of the clinical utility of an eyelid massage device for the management of meibomian gland dysfunction. *Contact Lens and Anterior Eye*, 42(6), pp.620-624.

Wang, M., Gokul, A. and Craig, J., 2015. Temperature profiles of patient-applied eyelid warming therapies. *Contact Lens and Anterior Eye*, 38(6), pp.430-434.

Wang, M., Jaitley, Z., Lord, S. and Craig, J., 2015. Comparison of Self-applied Heat Therapy for Meibomian Gland Dysfunction. *Optometry and Vision Science*, 92(9), pp.e321-e326.

Wang, M., Muntz, A., Mamidi, B., Wolffsohn, J. and Craig, J., 2021. Modifiable lifestyle risk factors for dry eye disease. *Contact Lens and Anterior Eye*, 44(6), p.101409.

Wang, M., Murphy, P., Blades, K. and Craig, J., 2017. Comparison of non-invasive tear film stability measurement techniques. *Clinical and Experimental Optometry*, 101(1), pp.13-17.

Wang, M., Vidal-Rohr, M., Muntz, A., Diprose, W., Ormonde, S., Wolffsohn, J. and Craig, J., 2020. Systemic risk factors of dry eye disease subtypes: A New Zealand cross-sectional study. *The Ocular Surface*, 18(3), pp.374-380.

Wang, X., Li, J., Zhang, R., Li, N., Pang, Y., Zhang, Y. and Wei, R., 2019a. The Influence of Overnight Orthokeratology on Ocular Surface and Meibomian Gland Dysfunction in Teenagers with Myopia. *Journal of Ophthalmology*, 2019, pp.1-6.

Wang, X., Lu, X., Yang, J., Wei, R., Yang, L., Zhao, S. and Wang, X., 2016. Evaluation of Dry Eye and Meibomian Gland Dysfunction in Teenagers with Myopia through Noninvasive Keratograph. *Journal of Ophthalmology*, 2016, pp.1-5.

Wang, Y., Qin, Q., Liu, B., Fu, Y., Lin, L., Huang, X. and Jin, X., 2019b. Clinical Analysis: Aqueous-Deficient and Meibomian Gland Dysfunction in Patients With Primary Sjogren's Syndrome. *Frontiers in Medicine*, 6.

Wei, S., Ren, X., Wang, Y., Chou, Y. and Li, X., 2020. Therapeutic Effect of Intense Pulsed Light (IPL) Combined with Meibomian Gland Expression (MGX) on Meibomian Gland Dysfunction (MGD). *Journal of Ophthalmology*, 2020, pp.1-7.

Weng, H., Ho, W., Chiu, C., Tsai, T. and Chang, S., 2021. Characteristics of tear film lipid layer in young dry eye patients. *Journal of the Formosan Medical Association*, 120(7), pp.1478-1484.

Werkmeister, R., Alex, A., Kaya, S., Unterhuber, A., Hofer, B., Riedl, J., Bronhagl, M., Vietauer, M., Schmidl, D., Schmoll, T., Garhöfer, G., Drexler, W., Leitgeb, R., Groeschl, M. and Schmetterer, L., 2013. Measurement of Tear Film Thickness Using Ultrahigh-Resolution Optical Coherence Tomography. *Investigative Opthalmology & Visual Science*, 54(8), p.5578.

Whitcher, J., Shiboski, C., Shiboski, S., Heidenreich, A., Kitagawa, K., Zhang, S., Hamann, S., Larkin, G., McNamara, N., Greenspan, J. and Daniels, T., 2010. A Simplified Quantitative Method for Assessing Keratoconjunctivitis Sicca From the Sjögren's Syndrome International Registry. *American Journal of Ophthalmology*, 149(3), pp.405-415.

Willcox, M., 2019. Tear film, contact lenses and tear biomarkers. *Clinical and Experimental Optometry*, 102(4), pp.350-363.

Willcox, M., Argüeso, P., Georgiev, G., Holopainen, J., Laurie, G., Millar, T., Papas, E., Rolland, J., Schmidt, T., Stahl, U., Suarez, T., Subbaraman, L., Uçakhan, O. and Jones, L., 2017. TFOS DEWS II Tear Film Report. *The Ocular Surface*, 15(3), pp.366-403.

Wolffsohn, J., 2004. Incremental nature of anterior eye grading scales determined by objective image analysis. *British Journal of Ophthalmology*, 88(11), pp.1434-1438.

Wolffsohn, J., Arita, R., Chalmers, R., Djalilian, A., Dogru, M., Dumbleton, K., Gupta, P., Karpecki, P., Lazreg, S., Pult, H., Sullivan, B., Tomlinson, A., Tong, L., Villani, E., Yoon, K., Jones, L. and Craig, J., 2017. TFOS DEWS II Diagnostic Methodology report. *The Ocular Surface*, 15(3), pp.539-574.

Wolffsohn, J. and Davies, L., 2019. Presbyopia: Effectiveness of correction strategies. *Progress in Retinal and Eye Research*, 68, pp.124-143.

Wolffsohn, J., Flitcroft, D., Gifford, K., Jong, M., Jones, L., Klaver, C., Logan, N., Naidoo, K., Resnikoff, S., Sankaridurg, P., Smith, E., Troilo, D. and Wildsoet, C., 2019. IMI – Myopia Control Reports Overview and Introduction. *Investigative Opthalmology & Visual Science*, 60(3), pp.M1-M19.

Wolffsohn, J. and Purslow, C., 2003. Clinical monitoring of ocular physiology using digital image analysis. *Contact Lens and Anterior Eye*, 26(1), pp.27-35.

Wong, K., Flanagan, J., Jalbert, I. and Tan, J., 2019a. The effect of Blephadex™ Eyelid Wipes on Demodex mites, ocular microbiota, bacterial lipase and comfort: a pilot study. *Contact Lens and Anterior Eye*, 42(6), pp.652-657.

Wong, S., Srinivasan, S., Murphy, P. and Jones, L., 2019b. Comparison of meibomian gland dropout using two infrared imaging devices. *Contact Lens and Anterior Eye*, 42(3), pp.311-317.

Wu, D., Boyer, K., Nichols, J. and King-Smith, P., 2008. Texture based prelens tear film segmentation in interferometry images. *Machine Vision and Applications*, 21(3), pp.253-259.

Wu, H., Wang, Y., Dong, N., Yang, F., Lin, Z., Shang, X. and Li, C., 2014a. Meibomian Gland Dysfunction Determines the Severity of the Dry Eye Conditions in Visual Display Terminal Workers. *PLoS ONE*, 9(8), p.e105575.

Wu, M., Gao, H., Zhao, L., Chen, H. and Huang, Y., 2020a. Real dynamic assessment of tear film optical quality for monitoring and early prevention of dry eye. *Medicine*, 99(31), p.e21494.

Wu, S., Hong, J., Tian, L., Cui, X., Sun, X. and Xu, J., 2015. Assessment of Bulbar Redness with a Newly Developed Keratograph. *Optometry and Vision Science*, 92(8), pp.892-899.

Wu, Y., Li, J., Hu, M., Zhao, Y., Lin, X., Chen, Y., Li, L. and Zhao, Y., 2020b. Comparison of two intense pulsed light patterns for treating patients with meibomian gland dysfunction. *International Ophthalmology*, 40(7), pp.1695-1705.

Wu, Z., Begley, C., Situ, P. and Simpson, T., 2014b. The Effects of Increasing Ocular Surface Stimulation on Blinking and Sensation. *Investigative Opthalmology & Visual Science*, 55(3), p.1555.

Xi, L., Qin, J. and Bao, Y., 2019. Assessment of tear film optical quality in a young short tear break-up time dry eye. *Medicine*, 98(40), pp.1-6.

Xiao, J., Adil, M., Chen, X., Utheim, Ø., Ræder, S., Tønseth, K., Lagali, N., Dartt, D. and Utheim, T., 2020. Functional and Morphological Evaluation of Meibomian Glands in the Assessment of Meibomian Gland Dysfunction Subtype and Severity. *American Journal of Ophthalmology*, 209, pp.160-167.

Xie, W., Zhang, X., Xu, Y. and Yao, Y., 2018. Assessment of Tear Film and Bulbar Redness by Keratograph 5M in Pediatric Patients After Orthokeratology. *Eye & Contact Lens: Science & Clinical Practice*, 44(2), pp.S382-S386.

Yazici, A., Sari, E., Sahin, G., Kilic, A., Cakmak, H., Ayar, O. and Ermis, S., 2014. Change in Tear Film Characteristics in Visual Display Terminal Users. *European Journal of Ophthalmology*, 25(2), pp.85-89.

Yamaguchi, M., Sakane, Y., Kamao, T., Zheng, X., Goto, T., Shiraishi, A. and Ohashi, Y., 2016. Noninvasive Dry Eye Assessment Using High-Technology Ophthalmic Examination Devices. *Cornea*, 35(Supplement 1), pp.S38-S48.

Yang, L., Pazo, E., Zhang, Q., Wu, Y., Song, Y., Qin, G., Zhang, H., Li, J., Xu, L. and He, W., 2022. Treatment of contact lens related dry eye with intense pulsed light. *Contact Lens and Anterior Eye*, 45(2), p.101449.

Yang, M., Kim, N., Choung, H. and In Khwarg, S., 2019. Effect of topical steroids on recently developed incomplete nasolacrimal duct obstruction: optical coherence tomography study. *Graefe's Archive for Clinical and Experimental Ophthalmology*, 257(10), pp.2315-2322.

Yang, W., Yang, Y., Cao, J., Man, Z., Yuan, J., Xiao, X. and Xing, Y., 2015. Risk Factors for Dry Eye Syndrome. *Optometry and Vision Science*, 92(9), pp.e199-e205.

Yao, W., Davidson, R., Durairaj, V. and Gelston, C., 2011. Dry Eye Syndrome: An Update in Office Management. *The American Journal of Medicine*, 124(11), pp.1016-1018.

Ye, F., Jiang, F., Lu, Y., Xue, C., Zhu, X., Wu, Y. and Huang, Z., 2019. Objective optical assessment of tear-film quality dynamics in patients with meibomian gland dysfunction and aqueous-deficient dry eye optical quality changes in different dry eye subtypes. *Indian Journal of Ophthalmology*, 67(5), pp.599-603.

Yeh, T., Graham, A. and Lin, M., 2015. Relationships among Tear Film Stability, Osmolarity, and Dryness Symptoms. *Optometry and Vision Science*, 92(9), pp.e264-e272.

Yeh, T. and Lin, M., 2018. Repeatability of Meibomian Gland Contrast, a Potential Indicator of Meibomian Gland Function. *Cornea*, 38(2), pp.256-261.

Yeter, V., Koçak, N. and Eser-Ozturk, H., 2020. Changes in corneal thickness, upper and lower tear film in seasonal allergic conjunctivitis by steroid treatment: anterior segment optical coherence tomography study. *International Ophthalmology*, 40(9), pp.2275-2281.

Yildirim, Y., Ozsaygili, C. and Kucuk, B., 2020. The short term effect of trehalose and different doses of sodium hyaluronate on anterior corneal aberrations in dry eye patients. *Cutaneous and Ocular Toxicology*, 40(1), pp.14-20.

Yin, Y. and Gong, L., 2019. The quantitative measuring method of meibomian gland vagueness and diagnostic efficacy of meibomian gland index combination. *Acta Ophthalmologica*, 97(3), pp.e403-e409.

Yin, Y., Liu, N., Gong, L. and Song, N., 2017. Changes in the Meibomian Gland After Exposure to Intense Pulsed Light in Meibomian Gland Dysfunction (MGD) Patients. *Current Eye Research*, 43(3), pp.308-313.

Yokoi, N., Bron, A., Tiffany, J., Brown, N., Hsuan, J. and Fowler, C., 1999. Reflective meniscometry: a non-invasive method to measure tear meniscus curvature. *British Journal of Ophthalmology*, 83(1), pp.92-97.

Yokoi, N., Bron, A., Tiffany, J., Maruyama, K., Komuro, A., Kinoshita, S., 2004. Relationship Between Tear Volume and Tear Meniscus Curvature. *Archives of Ophthalmology*, 122(9), p.1265-1269.

Yokoi, N., Georgiev, G., Kato, H., Komuro, A., Sonomura, Y., Sotozono, C., Tsubota, K. and Kinoshita, S., 2017. Classification of Fluorescein Breakup Patterns: A Novel Method of Differential Diagnosis for Dry Eye. *American Journal of Ophthalmology*, 180, pp.72-85.

Yokoi, N., Komuro, A., Yamada, H., Maruyama, K. and Kinoshita, S., 2007. A Newly Developed Video-Meibography System Featuring a Newly Designed Probe. *Japanese Journal of Ophthalmology*, 51(1), pp.53-56.

Yokoi, N., Takehisa, Y. and Kinoshita, S., 1996. Correlation of Tear Lipid Layer Interference Patterns With the Diagnosis and Severity of Dry Eye. *American Journal of Ophthalmology*, 122(6), pp.818-824.

Yokoi, N., Yamada, H., Mizukusa, Y., Bron, A., Tiffany, J., Kato, T. and Kinoshita, S., 2008. Rheology of Tear Film Lipid Layer Spread in Normal and Aqueous Tear–Deficient Dry Eyes. *Investigative Opthalmology & Visual Science*, 49(12), pp.5319-5324.

Yoo, Y., Na, K., Byun, Y., Shin, J., Lee, B., Yoon, G., Eom, T. and Joo, C., 2017a. Examination of Gland Dropout Detected on Infrared Meibography by Using Optical Coherence Tomography Meibography. *The Ocular Surface*, 15(1), pp.130-138.e1.

Yoo, Y., Na, K., Kim, D., Yang, S. and Joo, C., 2017b. Morphological evaluation for diagnosis of dry eye related to meibomian gland dysfunction. *Experimental Eye Research*, 163, pp.72-77.

Young, G., 1996. Evaluation of Soft Contact Lens Fitting Characteristics. *Optometry and Vision Science*, 73(4), pp.247-254.

Young, G., Chalmers, R., Napier, L., Kern, J., Hunt, C. and Dumbleton, K., 2012. Soft Contact Lens-Related Dryness with and without Clinical Signs. *Optometry and Vision Science*, 89(8), pp.1125-1132.

Young, G., Veys, J., Pritchard, N. and Coleman, S., 2002. A multi-centre study of lapsed contact lens wearers. *Ophthalmic and Physiological Optics*, 22(6), pp.516-527.

Yu, J., Asche, C. and Fairchild, C., 2011. The Economic Burden of Dry Eye Disease in the United States: A Decision Tree Analysis. *Cornea*, 30(4), pp.379-387.

Yu, A., Lu, T., Pan, A., Lin, D., Xu, C., Huang, J. and Bao, F., 2016. Assessment of Tear Film Optical Quality Dynamics. *Investigative Opthalmology & Visual Science*, 57(8), pp.3821-3827.

Yu, T., 2019. Morphological and cytological changes of meibomian glands in patients with type 2 diabetes mellitus. *International Journal of Ophthalmology*, 12(9), pp.1415-1419.

Yuan, K., Zhu, H., Mou, Y., Wu, Y., He, J., Huang, X. and Jin, X., 2020. Effects on the ocular surface from reading on different smartphone screens: A prospective randomized controlled study. *Clinical and Translational Science*.

Yuan, Y., Wang, J., Chen, Q., Tao, A., Shen, M. and Shousha, M., 2010. Reduced Tear Meniscus Dynamics in Dry Eye Patients With Aqueous Tear Deficiency. *American Journal of Ophthalmology*, 149(6), pp.932-938.e1.

Yucekul, B., Mocan, M., Kocabeyoglu, S., Tan, C. and Irkec, M., 2019. Evaluation of Long-Term Silicone Hydrogel Use on Ocular Surface Inflammation and Tear Function in Patients With and Without Meibomian Gland Dysfunction. *Eye & Contact Lens: Science & Clinical Practice*, 45(1), pp.61-66.

Yüksel, B., Bozdağ, B., Acar, M. and TopaloğLu, E., 2010. Evaluation of the Effect of Topical Cyclosporine a with Impression Cytology in Dry Eye Patients. *European Journal of Ophthalmology*, 20(4), pp.675-679.

Zaman, M., Doughty, M. and Button, N., 1998. The Exposed Ocular Surface and its Relationship to Spontaneous Eyeblink Rate in Elderly Caucasians. *Experimental Eye Research*, 67(6), pp.681-686.

Zang, S., Cui, Y., Cui, Y. and Fei, W., 2018. Meibomian gland dropout in Sjögren's syndrome and non-Sjögren's dry eye patients. *Eye*, 32(11), pp.1681-1687.

Zhang, A., Maki, K., Salahura, G., Kottaiyan, R., Yoon, G., Hindman, H., Aquavella, J. and Zavislan, J., 2015. Thermal analysis of dry eye subjects and the thermal impulse perturbation model of ocular surface. *Experimental Eye Research*, 132, pp.231-239.

Zhang, J., Wu, Z., Sun, L. and Liu, X., 2020a. Function and Morphology of the Meibomian Glands Using a LipiView Interferometer in Rotating Shift Medical Staff. *Journal of Ophthalmology*, 2020, pp.1-6.

Zhang, K., Zhang, S., Yu, J., Lu, Y. and Zhu, X., 2020. Changes of the tear film lipid layer thickness after cataract surgery in patients with diabetes mellitus. *Acta Ophthalmologica*, 99(2), pp.1-7.

Zhang, X., Chen, Q., Chen, W., Cui, L., Ma, H. and Lu, F., 2011. Tear Dynamics and Corneal Confocal Microscopy of Subjects with Mild Self-Reported Office Dry Eye. *Ophthalmology*, 118(5), pp.902-907.

Zhang, X., Volpe, E., Gandhi, N., Schaumburg, C., Siemasko, K., Pangelinan, S., Kelly, S., Hayday, A., Li, D., Stern, M., Niederkorn, J., Pflugfelder, S. and De Paiva, C., 2012. NK Cells Promote Th-17 Mediated Corneal Barrier Disruption in Dry Eye. *PLoS ONE*, 7(5), p.e36822.

Zhao, Y., Tan, C. and Tong, L., 2015. Intra-observer and inter-observer repeatability of ocular surface interferometer in measuring lipid layer thickness. *BMC Ophthalmology*, 15(1), p.53.

Zhong, S., Zhou, H., Chen, X., Zhang, W. and Yi, L., 2018. Influence of glaucoma surgery on the ocular surface using oculus keratograph. *International Ophthalmology*, 39(4), pp.745-752.

Zhou, S. and Robertson, D., 2018. Wide-Field In Vivo Confocal Microscopy of Meibomian Gland Acini and Rete Ridges in the Eyelid Margin. *Investigative Opthalmology & Visual Science*, 59(10), pp.4249-4257.

Zhou, S., Li, Y., Lu, A., Liu, P., Tang, M., Yiu, S. and Huang, D., 2009. Reproducibility of Tear Meniscus Measurement by Fourier-Domain Optical Coherence Tomography: A Pilot Study. *Ophthalmic Surgery, Lasers, and Imaging*, 40(5), pp.442-447.

PUBLICATIONS

PUBLICATIONS

Journal publications

1. García-Marqués, J., García-Lázaro, S., Martínez-Albert, N. and Cerviño, A., 2021a. Meibomian glands visibility assessment through a new quantitative method. *Graefe's Archive for Clinical and Experimental Ophthalmology*, 259(5), pp.1323-1331.
2. García-Marqués, J., García-Lázaro, S., Talens-Estarelles, C., Martínez-Albert, N. and Cerviño, A., 2021b. Diagnostic Capability of a New Objective Method to Assess Meibomian Gland Visibility. *Optometry and Vision Science*, 98(9), pp.1045-1055.
3. García-Marqués, J., Macedo-De-Araújo, R., Cerviño, A., García-Lázaro, S. and González-Méijome, J., 2022. Assessment of meibomian gland drop-out and visibility through a new quantitative method in scleral lens wearers: A one-year follow-up study. *Contact Lens and Anterior Eye*, p.101571.
4. García-Marqués, J., Macedo-De-Araújo, R., Cerviño, A., García-Lázaro, S., McAlinden, C. and González-Méijome, J., 2020. Comparison of short-term light disturbance, optical and visual performance outcomes between a myopia control contact lens and a single-vision contact lens. *Ophthalmic and Physiological Optics*, 40(6), pp.718-727.
5. García-Marqués, J., Macedo-de-Araújo, R., Lopes-Ferreira, D., Cerviño, A., García-Lázaro, S. and González-Méijome, J., 2021c. Tear film stability over a myopia control contact lens compared to a monofocal design. *Clinical and Experimental Optometry*, 105(1), pp.41-47.

6. García-Marqués, J., Martínez-Albert, N., Talens-Estarelles, C., García-Lázaro, S. and Cerviño, A., 2021. Repeatability of Non-invasive Keratograph Break-Up Time measurements obtained using Oculus Keratograph 5M. *International Ophthalmology*, 41(7), pp.2473-2483.
7. García-Marqués, J., Talens-Estarelles, C., García-Lázaro, S. and Cerviño, A., 2021e. Validation of a new objective method to assess lipid layer thickness without the need of an interferometer. *Graefe's Archive for Clinical and Experimental Ophthalmology*, 260(2), pp.655-676.
8. García-Marqués, J., Talens-Estarelles, C., Martínez-Albert, N., García-Lázaro, S. and Cerviño, A., 2021d. An Emerging Method to Assess Tear Film Spread and Dynamics as Possible Tear Film Homeostasis Markers. *Current Eye Research*, 46(9), pp.1291-1298.
9. García-Marqués, J., Talens-Estarelles, C., García-Lázaro, S., Wolffsohn, J. and Cerviño, A., 2021. Systemic, environmental and lifestyle risk factors for dry eye disease in a mediterranean caucasian population. *Contact Lens and Anterior Eye*, p.101539.
10. García-Marqués, J., Talens-Estarelles, C., Martínez-Albert, N., García-Lázaro, S. and Cerviño, A., 2022. Evaluation of the MGDRx eyebag treatment in young and older subjects with dry eye symptoms. *Journal Français d'Ophtalmologie*, 45(1), pp.20-27.

Conference contributions

1. García-Marqués, J., Talens-Estarelles, C., Martínez-Albert, N., García-Lázaro, S. and Cerviño, A. 2021. Evaluación de la velocidad de propagación post-parpadeo de las partículas en suspensión en la película lagrimal (Estudio piloto). 5º Congreso Internacional Online de Jóvenes Optometristas SIYO 2020. On-line.
2. García-Marqués, J., Talens-Estarelles, C., Martínez-Albert, N., García-Lázaro, S. and Cerviño, A. 2021. Comparación de cuatro cuestionarios para la evaluación de la sintomatología asociada a la sequedad ocular. 5º Congreso Internacional Online de Jóvenes Optometristas SIYO 2020. On-line.
3. García-Marqués, J., Martínez-Albert, N., Cerviño, A. and García-Lázaro, S., 2021. Evaluación de distintas variables en función de la nueva definición de síndrome del ojo seco. 26º Congreso Internacional de Optometría, Contactología y Óptica Oftálmica OPTOM 2021. On-line.
4. Cerviño, A., García-Marqués, J., Martínez-Albert, N., and García-Lázaro, S., 2021. Efecto del tratamiento con bolsas térmicas en pacientes portadores de lentes de contacto sintomáticos. 26º Congreso Internacional de Optometría, Contactología y Óptica Oftálmica OPTOM 2021. On-line.
5. García-Marqués, J., Martínez-Albert, N., Cerviño, A. and García-Lázaro, S., 2021. Evaluación de la actividad de las glándulas de meibomio a través de un nuevo método cuantitativo (Estudio piloto). 26º Congreso Internacional de Optometría, Contactología y Óptica Oftálmica OPTOM 2021. On-line.
6. García-Marqués, J., Talens-Estarelles, C., García-Lázaro, S. and Cerviño, A. 2022. Influence of soft contact lens wear on meibomian gland drop-out and visibility. The International Society for Contact Lens Research Meeting. Porto. Accepted

Book chapters

1. García-Marqués, J., Talens-Estarelles, C., Martínez-Albert, N., García-Lázaro, S. and Cerviño, A., 2021. Evaluación de la velocidad de propagación post-parpadeo de las partículas en suspensión en la película lagrimal (Estudio piloto). In: A. Gené-Sampedro, I. Bueno-Gimeno, M. Luque-Cobija, M. Díez-Ajenjo, M. García-Domene, J. Esteve-Taboada and R. Hernández-Andrés, ed., *Temas actuales en optometría*, 1st ed. Valencia: Obrapropia, pp.325-332.
2. García-Marqués, J., Talens-Estarelles, C., Martínez-Albert, N., García-Lázaro, S. and Cerviño, A., 2021. Comparación de cuatro cuestionarios para la evaluación de la sintomatología asociada a la sequedad ocular In: A. Gené-Sampedro, I. Bueno-Gimeno, M. Luque-Cobija, M. Díez-Ajenjo, M. García-Domene, J. Esteve-Taboada and R. Hernández-Andrés, ed., *Temas actuales en optometría*, 1st ed. Valencia: Obrapropia, pp.373-380.